



## NICKEL-CATALYZED REDUCTIVE CARBOXYLATION AND AMIDATION OF ORGANIC MATTER

Andreu Tortajada Navarro

**ADVERTIMENT.** L'accés als continguts d'aquesta tesi doctoral i la seva utilització ha de respectar els drets de la persona autora. Pot ser utilitzada per a consulta o estudi personal, així com en activitats o materials d'investigació i docència en els termes establerts a l'art. 32 del Text Refós de la Llei de Propietat Intel·lectual (RDL 1/1996). Per altres utilitzacions es requereix l'autorització prèvia i expressa de la persona autora. En qualsevol cas, en la utilització dels seus continguts caldrà indicar de forma clara el nom i cognoms de la persona autora i el títol de la tesi doctoral. No s'autoritza la seva reproducció o altres formes d'explotació efectuades amb finalitats de lucre ni la seva comunicació pública des d'un lloc aliè al servei TDX. Tampoc s'autoritza la presentació del seu contingut en una finestra o marc aliè a TDX (framing). Aquesta reserva de drets afecta tant als continguts de la tesi com als seus resums i índexs.

**ADVERTENCIA.** El acceso a los contenidos de esta tesis doctoral y su utilización debe respetar los derechos de la persona autora. Puede ser utilizada para consulta o estudio personal, así como en actividades o materiales de investigación y docencia en los términos establecidos en el art. 32 del Texto Refundido de la Ley de Propiedad Intelectual (RDL 1/1996). Para otros usos se requiere la autorización previa y expresa de la persona autora. En cualquier caso, en la utilización de sus contenidos se deberá indicar de forma clara el nombre y apellidos de la persona autora y el título de la tesis doctoral. No se autoriza su reproducción u otras formas de explotación efectuadas con fines lucrativos ni su comunicación pública desde un sitio ajeno al servicio TDR. Tampoco se autoriza la presentación de su contenido en una ventana o marco ajeno a TDR (framing). Esta reserva de derechos afecta tanto al contenido de la tesis como a sus resúmenes e índices.

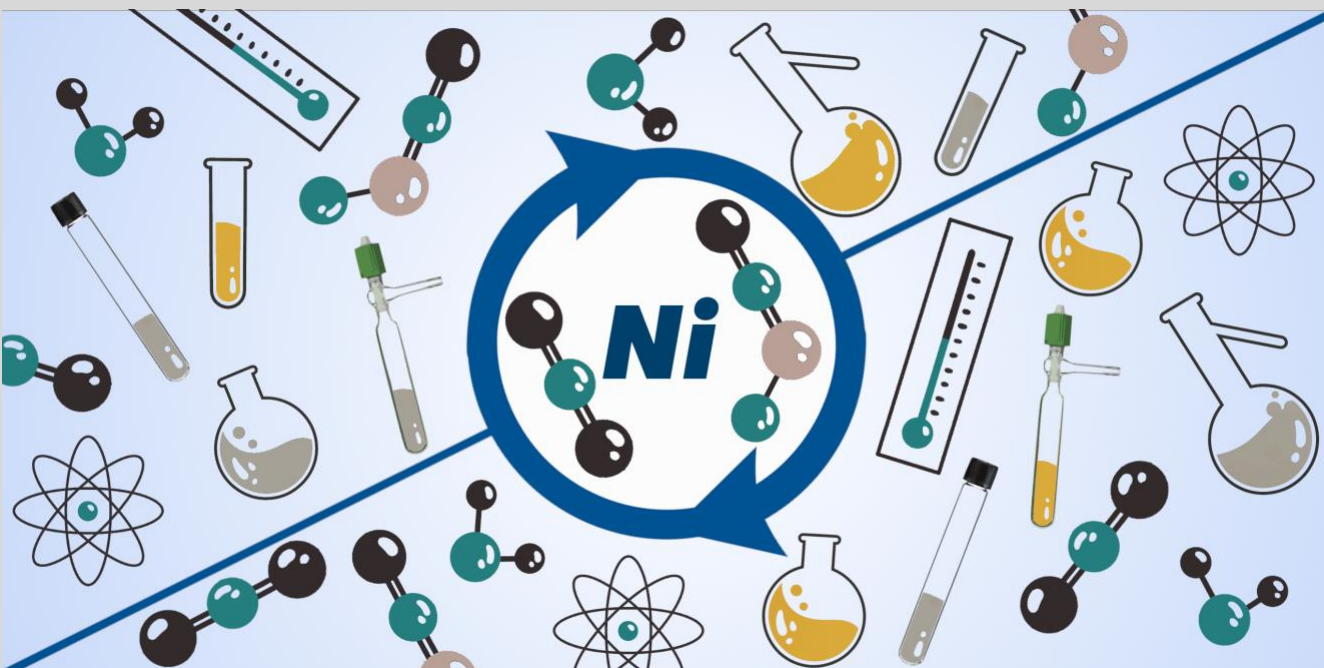
**WARNING.** Access to the contents of this doctoral thesis and its use must respect the rights of the author. It can be used for reference or private study, as well as research and learning activities or materials in the terms established by the 32nd article of the Spanish Consolidated Copyright Act (RDL 1/1996). Express and previous authorization of the author is required for any other uses. In any case, when using its content, full name of the author and title of the thesis must be clearly indicated. Reproduction or other forms of for profit use or public communication from outside TDX service is not allowed. Presentation of its content in a window or frame external to TDX (framing) is not authorized either. These rights affect both the content of the thesis and its abstracts and indexes.



UNIVERSITAT  
ROVIRA i VIRGILI

# Nickel-Catalyzed Reductive Carboxylation and Amidation of Organic Matter

ANDREU TORTAJADA NAVARRO



DOCTORAL THESIS  
2020





# Nickel-Catalyzed Reductive Carboxylation and Amidation of Organic Matter

**Andreu Tortajada Navarro**

Doctoral Thesis

**Supervised by Prof. Ruben Martin Romo**

Institut Català d'Investigació Química (ICIQ)

Universitat Rovira i Virgili (URV)

Department of Analytical Chemistry and Organic Chemistry





'Life is like riding a bicycle. To keep your balance you must keep moving'  
***Albert Einstein***

'The good thing about science is that it's true whether or not you believe in it'  
***Neil deGrasse Tyson***







Prof. Ruben Martin Romo, Group Leader at the Institute of Chemical Research of Catalonia (ICIQ) and Research Professor of the Catalan Institution for Research and Advanced Studies (ICREA),

STATES that the present study, entitled “Nickel-Catalyzed Reductive Carboxylation and Amidation of Organic Matter”, developed by Andreu Tortajada Navarro for the award of the degree of Doctor, has been carried out under his supervision at the Institute of Chemical Research of Catalonia (ICIQ).

Tarragona, October 1<sup>st</sup>, 2020

Doctoral Thesis Supervisor

Prof. Ruben Martin Romo



## Table of Contents

Acknowledgements .....	7
Preface .....	11
List of publications.....	13
Abstract.....	15
Chapter 1. General Introduction .....	17
1.1. Reductive Cross-Electrophile Couplings.....	19
1.2. Nickel catalysis general characteristics (vs group 10 metals).....	21
1.3. CO <sub>2</sub> reactivity and functionalization.....	23
1.4. Cross-Electrophile Couplings for the synthesis of carboxylic acids.....	26
1.4.1. Carboxylation of (pseudo)alkyl-halides.....	26
1.4.2. Catalytic reductive carboxylation of C-O electrophiles.....	37
1.5. Carboxylation of alkynes and alkenes.....	42
1.5.1. Catalytic carboxylation of alkynes.....	42
1.5.2. Catalytic carboxylation of alkenes.....	49
General Objectives of this Doctoral Thesis.....	57
Chapter 2. Site-Selective Catalytic Carboxylation of Allylic Alcohols with CO <sub>2</sub> .....	69
2.1. Introduction.....	71
2.1.1. Metal-catalyzed cross-couplings of activated allyl electrophiles.....	69
2.1.2. Metal-catalyzed cross-coupling of allylic alcohols.....	71
2.1.3. Transition Metal-catalyzed cross-coupling of allylic alcohols.....	72
2.1.4. CO <sub>2</sub> as an activating reagent for allylic alcohols.....	76
2.2. General Objective of the Project.....	78
2.3. Site-Selective Catalytic Carboxylation of Allylic Alcohols with CO <sub>2</sub> .....	80
2.3.1. Optimization of the reaction conditions (linear carboxylic acids).....	80
2.3.2. Optimization of the reaction conditions ( $\alpha$ -branched carboxylic acids).....	86
2.3.3. Preparative substrate scope.....	92
2.4. Mechanistic studies.....	96
2.5. Proposed reaction mechanisms.....	99
2.6. Conclusions.....	102
2.7. Experimental section.....	103
Chapter 3. Ni-Catalyzed Site-Selective Dicarboxylation of 1,3-Dienes with CO <sub>2</sub> .....	157
3.1. Introduction.....	159
3.2. General Objective of the Project.....	165
3.3. Nickel catalyzed dicarboxylation of 1,3-dienes with CO <sub>2</sub> .....	166
3.3.1. Optimization of the reaction conditions.....	166
3.3.2. Preparative substrate scope.....	176
3.4. Mechanistic investigations.....	180
3.5. Conclusions.....	184
3.6. Experimental section.....	185

<b>Chapter 4. Catalytic Decarboxylation/Carboxylation Platform for Accessing Isotopically Labeled Carboxylic Acids.....</b>	<b>253</b>
<b>4.1. Introduction.....</b>	<b>255</b>
<b>4.1.1. Isotopic labeling and drug metabolism in drug discovery .....</b>	<b>255</b>
<b>4.1.2. CO<sub>2</sub> as a source of isotopically labeled carbon.....</b>	<b>256</b>
<b>4.1.3. Carboxylation reactions with isotopically labeled CO<sub>2</sub>.....</b>	<b>259</b>
<b>4.2. General Objective of the Project.....</b>	<b>263</b>
<b>4.3. Catalytic Decarboxylation/Carboxylation of carboxylic acids.....</b>	<b>264</b>
<b>4.3.1. Isotope carbon exchange with <i>N</i>-hydroxyphthalimide esters.....</b>	<b>264</b>
<b>4.3.2. Isotope carbon exchange with alkyl halides.....</b>	<b>273</b>
<b>4.4. Conclusions.....</b>	<b>276</b>
<b>4.5. Experimental section.....</b>	<b>277</b>
<b>Chapter 5. Regiodivergent Ligand-Controlled Ni-Catalyzed Reductive Amidation of Unactivated Secondary Alkyl Bromides.....</b>	<b>397</b>
<b>5.1. Introduction.....</b>	<b>399</b>
<b>5.1.1. Isocyanates as Amide Synthons.....</b>	<b>399</b>
<b>5.1.2. Metal-Catalyzed Functionalization of Unactivated Secondary Alkyl Halides.....</b>	<b>402</b>
<b>5.1.3. Metal Chain-Walking, a Strategy for Remote <i>sp</i><sup>3</sup> C-H Functionalization.....</b>	<b>402</b>
<b>5.1.4. Ni-Catalyzed Chain-Walking Functionalization.....</b>	<b>403</b>
<b>5.2. General Aim of the Project.....</b>	<b>405</b>
<b>5.3. Regiodivergent Reductive amidation of Unactivated Secondary Alkyl bromides with Isocyanates.....</b>	<b>406</b>
<b>5.3.1. Optimization of the reaction conditions.....</b>	<b>406</b>
<b>5.3.2. Preparative substrate scope.....</b>	<b>410</b>
<b>5.4. Mechanistic investigations.....</b>	<b>414</b>
<b>5.5. Conclusions.....</b>	<b>418</b>
<b>5.6. Experimental section.....</b>	<b>419</b>
<b>Chapter 6. General Conclusions.....</b>	<b>495</b>

## ***Acknowledgements***

First of all, I would like to thank my supervisor **Prof. Ruben Martin** for taking me as a Master and PhD student in his research group. His guidance, motivation and support along these years have helped me develop as a passionate chemist and taught me the importance of quality and excellent day-to-day work. Thank you very much for trusting me when I arrived as a summer fellow and for guiding me to the end of the doctoral studies.

During the past five years I had the chance to meet a lot of people from all over the world. When I arrived into the lab 2.7, I worked with many excellent chemists that are no longer in the research group. Thanks to **Xue, Masaki, Miriam, Yiting, YangYang, Manuel, Toni, Morgane, Caye, Eloisa, Daniel, Reddy** and **Francisco** for helping me when I arrived to the group and teaching me how a lab can work in an efficient and very friendly way at the same time. I want to specially thank **Morgane**, my mentor during my master and my first fume hood partner in the group, for teaching me how to do an optimization and how to do a proper chromatography column. Moreover, I would like to thank **Caye** for being always keen to help with anything and giving me advice when I was looking for a group to do my research stay.

After I started many new people arrived to the group, some to stay others for a short period of time. Thanks to **Lily, Tim, Keisho, Kentaro, Tomoyuki, Riccardo, Antonio, Johanes, Georgios, Yutaka, Liang and Isabel** for being a nice labmates during your visit. Specially thanks to the people I had the chance to work with: **Ryo** for joining me with the diene carboxylation project, **Georgios** for making a fantastic work on the isotopic labeling of carboxylic acids (and being a fantastic friend in and outside the lab) and **Isabel** for starting a new carboxylation collaboration.

Regarding all the people that I will leave behind or that recently have left the group, **Rosie**, you were the light of inorganic chemistry in our lab, one of the kindest person that I have met and a really positive and helpful person, thanks for all the help and good moments we shared. **Marino**, our machino from Graná, with who I have spent so many hours working in the lab, have discussed about our projects and have partied in Tarragona, I am grateful for having shared this experience with you. **Raúl**, our other R. Martin, my 'brosito', which always has a nice outing plan in mind or is ready to dance in the lab with the music, thanks for becoming a great friend and supporting me through all the PhD. **Alicia**, you came to the lab and brought your cheerful attitude and good atmosphere, becoming a very important member of the group. Thanks for working with me trying to finish the amidation project and for all the good moments we had in and outside the lab. **Shang-Zheng**, one of the kindest people in the lab, thanks for sharing all the goodies you brought from China and for

having an awesome lunch time every day. I want to thank as well **Cris**, for sharing with us lunch time almost every day and becoming a good friend. **Bradley**, thanks for always being willing to help and bring you positive vibe to the group. **Yaya** and **Hongfei**, thanks for all the help and advice during the last years of my PhD. **Jessica**, thanks for bringing your energy to lab 2.7 and for always be willing to discuss about our projects. **Craig** and **Fei**, thank you for actively be involved in some of the research in this thesis and be good 2.7 labmates. **Laura** and **Carlota**, one of the last incorporations to the group, thanks for the good times we shared after I came back from the US. I want to thank as well to the rest of the group, **Jacob, Ciro, Victoria, Chris, Bafa, Thomas, Xinyang, Dmitry, Wen- Jun** and **Jesús** for creating the nice atmosphere we have now in our group. Finally, I want to thank as well to the people that has been in the shadows, making sure that everything was functioning, thanks to **Miriam, Sope, David** and **Ingrid** for your support in the day-to-day functioning of the lab.

I want to thank the **Chirik group** for welcoming me to Princeton University to do some exciting iron chemistry. I would like to thank **Prof. Paul Chirik** for said opportunity and for his advice and support during the six months I was there. I want to thank also all the people in the group: **Jon, Rose, Rebeca, Megan, Jake, Sam, Yoonsu, Aaron, Sangmin, Boran, Tyler, Peter, Paul, Carli, Lauren, Connor** and **Javier** for the great time I had with them in and outside the lab.

Por supuesto, quiero agradecer a los que han sido mi segunda familia en el ICIQ y fuera de él aquí en Tarragona. Gracias por haber creado este grupo de “pavipollos” (quién me habría dicho que el trivial nos daría tan buenos recuerdos) y por haber estado en los buenos y en los malos momentos. Todo empezó con **Nuria**, cuando en los primeros días de máster me recogió en la rotonda de avenida Catalunya para venir al ICIQ juntos con su mini naranja y piso tras piso y año tras año acabó convirtiéndose en una de las personas más importantes aquí en Tarragona. Gracias por viajar al otro lado del océano conmigo, aguantar un confinamiento y compartir una escritura de tesis codo con codo en el salón de casa. Creo que después de esto ya nada va a poder con nuestra amistad. A partir de aquí tuve la oportunidad de conocer al lab Vidal, con lo que se unieron Alicia y Ester. **Alicia**, gracias por acercarnos un trocito de Albacete hasta Tarragona (¡los Miguelitos de todos los sabores!), por compartir tantos buenos momentos de conciertos y festivales y estar siempre dispuesta a ayudar. **Ester**, nuestra terremoto de la Cope, ha sido un placer compartir estos años en Tarragona contigo, gracias por todos los buenos y malos momentos que hemos vivido (primeras visitas al cine, fiestas de cumple, santa Tecla, charlas en las escaleras del Cau,...) y espero que sigamos compartiéndolos durante mucho tiempo. Junto con las chicas Vidal, vino también **Cris** y con el tiempo **Victoria**. Gracias por compartir con nosotros todos estos buenos momentos. Ha sido un placer

celebrar nuestro cumple a la vez todos estos años, salir de fiesta hasta cerrar los bares y poder ver a tu chiqui crecer. Entonces llegaron Jesús y Miguel, así como en un pack indivisible. **Jesús**, desde el primer concierto de Izal en Camp de Mart hasta el que vivimos esta santa Tecla extraña a causa de la COVID, gracias por todos los momentos que hemos compartido siempre rodeados de cerveza y comida, ha sido un placer vivirlos contigo bro. **Miguel**, nuestra representación asturiana, gracias por introducirnos en el mundo de la sidra, el cachopo y la cultura asturiana en general! Me llevo un montón de palabras nuevas y de momentos que recordaré siempre. Tendremos siempre una cerveza y una revancha a les ovelles pendiente. En ese momento me crucé con Kike del lab 2.6, y empezó nuestra andanza en la calle Reding juntamente con Chuchi. **Kike**, fue un placer vivir juntos en la calle Reding, viendo a tu Real Madrid ganar (y también perder a veces), verte cocinar esos maravillosos filetes que te hacías para cenar, hablar de química y jugar a juegos de mesa o a la play después de cenar. **Chuchi**, gracias por aportar un poco de calma al piso, enseñarnos y compartir tu pasión por la cocina con nosotros, aguantarnos a Kike y a mi hablar de química orgánica día si y día también y por aportar tu granito de arena a nuestra cultura cinéfila y musical. Gracias a los dos por hacer del piso una fantástica experiencia. Ese mismo año se unió al 2.7 **Raúl**, mi bro, que se unió rápido a este grupo. Gracias por compartir conmigo tu conocimiento en los comienzos del gimnasio, por todos los viajes que hemos hecho (congresos, Tromsø, tu curso inmersión en valenciano, ...), por estar ahí siempre que lo he necesitado y por todos los buenos momentos. Al tiempo, se unió **Alicia Monleón** (nuestra segunda Alicia), con quien he compartido muchos viajes a Valencia los fines de semana y muchas horas en el laboratorio, en el gym y fuera de él. Gracias por siempre estar dispuesta a ayudar en todo y por esos momentos de compartir nuestra cultura valenciana con el resto! Hace poco **Alba**, nuestra segunda manchega vino al grupo para quedarse. Gracias por dejarte llevar al lado oscuro del step, por todas las cerves (o nesteas) que hemos compartido y por ser tan espontánea y alegre. Por último, estos meses **Ana** se unió a la crue del step y a todas las celebraciones, que pese a la pandemia hemos podido ir haciendo. Ha sido un placer haber vivido estos cinco años con vosotros.

També m'agradaria mencionar als amics que vaig deixar a València, però que cada vegada que vaig estan ahí per a quedar amb ells i posar-nos al dia. **Sole, Rubén, Valle, Sandra i Raquel**, compis de la carrera i que encara que solament ens veiem un cop a l'any (o ho intentem!) sembla que el temps no haja passat quan ho fem. I els meus amics de Benaguasil, que tant al poble com a les diferents vegades que m'han visitat a Tarragona segueixen estan ahí sempre, gràcies **Kevin, Bast, Edu, Melanie, Vero, Fran, Jordi i Cynthia**.

Per últim, m'agradaria agrair a la meva familia, qui sempre ha estat recolzant-me en cada desició que he prés, i que cada vegada que vaig a casa están disposats a

celebrar-ho amb un dinar. Especialment als meus tios i cosins, **Raquel, Marcos, Enri, Jose, Maica, Marc, Raquel, Javier, Mireia i Josep** que estiguin a prop o molt lluny, sempre els he sentit que han estat al meu costat aquí a Tarragona. I per últim, als **meus pares, Pepa i Vicent**, qui sempre m'han animat a seguir el camí que jo he cregut seria millor per a mi, encara que això significués que estaria a molts quilòmetres de distància que haurien de fer en un viatge de més de dotze hores per terra, mar i aire per visitar-me uns dies. Gràcies per sempre cuidar de mi, per preparar-me els tuffers i totes les fruites i verdures per vindre carregat a Tarragona i per tota l'estima que em doneu dia a dia. Aquesta tesi no hauria pogut ser possible sense el vostre suport.



## Preface

The work presented in this dissertation has been performed at the Catalan Institute of Chemical Research (ICIQ) during the period of September 2016 to September 2020 under the supervision of Professor Ruben Martin. The present manuscript is divided into six main parts: a general introduction, four research chapters, and a final chapter in which general conclusions of the work are presented. Each of the research chapters consists of an introduction and a summary of the aims of the project, followed by a discussion of the experimental results, and finally an experimental section. The numeration of each chapter has been done independently for an easier understanding, and therefore some structure might be named with a different number in different chapters.

In chapter 1, the principles of reductive cross-electrophile coupling are presented alongside of nickel catalytic systems that are relevant to this work. This is followed by an overview of the existing transition metal-catalyzed carboxylation with CO<sub>2</sub>. This final section has been the subject of a review, published in *Angew. Chem. Int. Ed.* **2018**, *57* (49), 15948 (10.1002/anie.201803186).

In the second chapter, '*Switchable Site-Selective Catalytic Carboxylation of Allylic Alcohols with CO<sub>2</sub>*' the synthesis of linear and branched β,γ-unsaturated carboxylic acids from allylic alcohols and CO<sub>2</sub> is described, in which CO<sub>2</sub> is used with dual roles, both facilitating C–OH cleavage and as a C<sub>1</sub> source. This methodology is characterized by its mild reaction conditions, absence of stoichiometric amounts of organometallic reagents, broad scope, and exquisite selectivity which can be modulated by the type of ligand employed. It was performed in collaboration with Dr. Manuel van Gemmeren, Marino Börjesson, Shang-Zheng Sun and Keisho Okura, being my contribution focused on the development of the reaction conditions for the α-branched carboxylation of allylic alcohols and the preparation of the substrate scope. It was published in *Angew. Chem. Int. Ed.* **2017**, *56*, 6556 (10.1002/anie.201702857).

The third chapter, '*Ni-Catalyzed Site-Selective Dicarboxylation of 1,3-Dienes with CO<sub>2</sub>*', a site-selective catalytic incorporation of multiple CO<sub>2</sub> molecules into 1,3-dienes *en route* to adipic acids is described. This protocol is characterized by its mild conditions, excellent chemo- and regioselectivity and ease of execution under CO<sub>2</sub> (1 atm), including the use of bulk butadiene and/or isoprene feedstocks. It was performed in collaboration with Ryo Ninokata and it was published in *J. Am. Chem. Soc.* **2018**, *140*, 2050 (10.1021/jacs.7b13220).

The fourth chapter, entitled '*Catalytic Decarboxylation/Carboxylation Platform for Accessing Isotopically Labeled Carboxylic Acids*', describes a procedure for exchanging carbon isotopes by effectively converting a variety of carboxylic acids into their labeled analogues by means of nickel catalysis. This methodology allows an easy and direct isotopic labeling of organic molecules, which represents an essential task in drug development. The work described was carried out in collaboration with Georgios Toupalas (NHP optimization), Dr. Yaya Duan, Dr. Basudev Sahoo and Fei Cong (preparative scope) and the group of Prof. Davide Audisio ( $^{14}\text{C}$  labeling). It was published in *ACS Catalysis* **2019**, 9, 5897 (10.1021/acscatal.9b01921).

The last research chapter, '*Regiodivergent Ligand-Controlled Ni-Catalyzed Reductive Amidation of Unactivated Secondary Alkyl Bromides*' describes a procedure for the preparation of aliphatic primary and secondary amides from secondary alkyl bromides and isocyanates. This methodology allows the selective functionalization of the alkyl bromide in the initial C-Br bond or in the primary terminal C-H bond by simply changing the ligand employed, selectively enabling or suppressing  $\beta$ -hydride elimination of the nucleophilic alkyl-nickel intermediates to obtain the corresponding amides after isocyanate insertion. The work described in this chapter was accomplished in collaboration with Eloisa Serrano, Dr. Alicia Monleón, Dr. Tiago Menezes and Alberto Tampieri (optimization and substrate scope), Craig Day (mechanistic investigations) and Dr. Francisco Juliá-Hernández (initial discoveries).

### List of publications:

The following articles have been published during the realization of this doctoral thesis:

- 'Switchable Site-Selective Catalytic Carboxylation of Allylic Alcohols with CO<sub>2</sub>' M. van Gemmeren<sup>+</sup>, M. Börjesson<sup>+</sup>, A. Tortajada<sup>+</sup>, S.-Z. Sun<sup>+</sup>, K. Okura, R. Martin\* *Angew. Chem. Int. Ed.* **2017**, *56*, 6556. <sup>+</sup>Equal contribution.
- 'Transition Metal-Catalyzed Carboxylation Reactions with Carbon Dioxide' A. Tortajada, F. Juliá-Hernández, M. Börjesson, T. Moragas, R. Martin\* *Angew. Chem. Int. Ed.* **2018**, *57* (49), 15948 (Review article).
- 'Ni-Catalyzed Site-Selective Dicarboxylation of 1,3-Dienes with CO<sub>2</sub>' A. Tortajada, R. Ninokata, R. Martin\*, *J. Am. Chem. Soc.* **2018**, *140*, 2050.
- 'N-Containing Heterocycles on Demand by Merging Ni Catalysis and Photoredox PCET' M. Börjesson<sup>+</sup>, A. Tortajada<sup>+</sup>, R. Martin\*, *Chem* **2019**, *5* (2), 254 (Highlight article). <sup>+</sup>Equal contribution
- 'Catalytic Decarboxylation/Carboxylation Platform for Accessing Isotopically Labeled Carboxylic Acids' A. Tortajada, Y. Duan, B. Sahoo, F. Cong, G. Toupalas, A. Sallustrau, O. Loreau, D. Audisio, R. Martin\* *ACS Catalysis* **2019**, *9*, 5897.

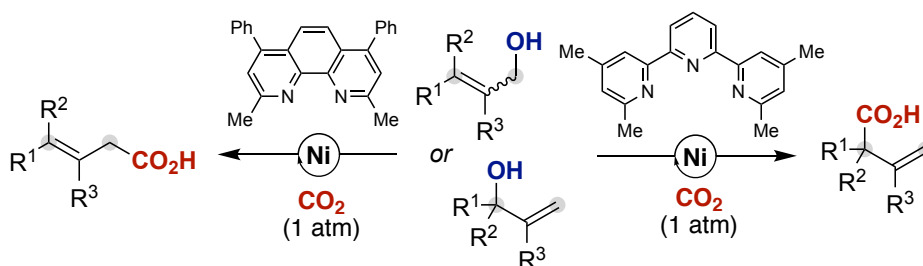


## Abstract

In recent years, reductive cross-electrophile couplings have become a powerful alternative to classical cross-coupling reactions for the formation of both C–C and C–X bonds. The use of two electrophiles instead of an electrophile and a nucleophile offers numerous advantages. For example, the absence of strongly basic reagents allows these reactions to occur under milder conditions, resulting in a broader functional group tolerance. Moreover, the use of readily available starting materials circumvents the need to prepare air- and moisture-sensitive organometallic reagents, offering a more practical set-up. Within these methods, nickel catalysis has become a valuable tool for the selective cross-coupling of two electrophiles in the presence of a metallic or organic reductant, via two-electron or single-electron transfer processes.

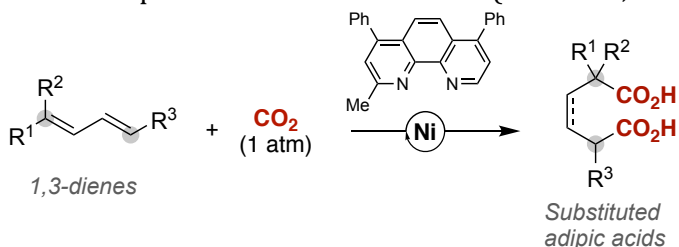
From the different electrophiles for C–C bond formation, our group has had a special interest in carbon dioxide, CO<sub>2</sub>, because it is considered an abundant, inexpensive and renewable C1 synthon. However, the number of chemicals directly available from CO<sub>2</sub> still remains very narrow compared to those derived from currently available petrochemicals, thus encouraging the development of novel methods using CO<sub>2</sub>. From all the different moieties that can be prepared from it, the synthesis of carboxylic acids constitutes an ideal target since these compounds are privileged motifs in a wide number of natural products, agrochemicals and pharmaceutically relevant compounds. This doctoral dissertation has focused on the development and understanding of new, simple and practical reductive carboxylation reaction to produce carboxylic acids from inexpensive and abundant electrophiles by means of Ni catalysis. In parallel, the use of isoelectronic isocyanates for the preparation of amides was also investigated.

In this doctoral thesis our efforts have been focused first into the development of a site-selective carboxylation of unprotected allylic alcohols with CO<sub>2</sub>, since alcohols are the simplest and the most abundant C–O counterparts. This methodology is able to deliver  $\beta,\gamma$ -unsaturated carboxylic acids with excellent control of the selectivity obtained by varying the ligand employed in the nickel center (Scheme 1, Chapter 2).



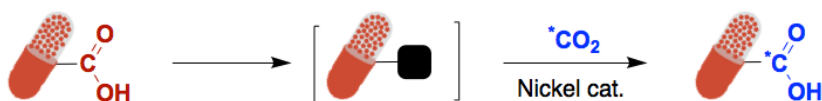
**Scheme 1.** Ni-Catalyzed carboxylation of allylic alcohols with CO<sub>2</sub>.

After achieving this goal, we decided to investigate the carboxylation of unsaturated hydrocarbons, which can be obtained in bulk from the petrochemical industry or biomass sources. Thus, we envisaged that the combination of 1,3-dienes with carbon dioxide could form by a double insertion of CO<sub>2</sub> substituted adipic acids, compounds that can be of potential industrial interest (Scheme 2, Chapter 3).



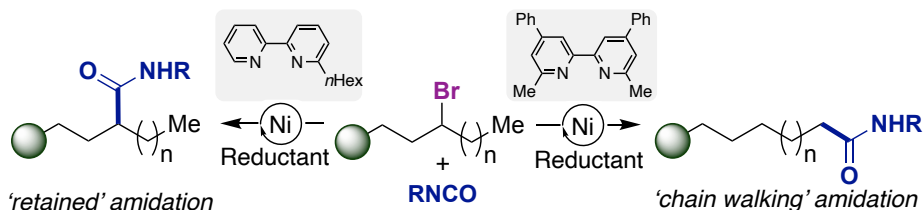
**Scheme 2.** Ni-Catalyzed dicarboxylation of 1,3-dienes with CO<sub>2</sub>.

Based on the importance of isotopically labeled compounds for the pharmaceutical industry we envisioned to use all the knowledge that our group has gained about the catalytic carboxylation of organic substrates with CO<sub>2</sub> to develop a new protocol to perform a late-stage isotopic labeling using isotopically enriched CO<sub>2</sub>. This transformation would avoid the conversion of isotopically enriched CO<sub>2</sub> into other compounds such as carbonates or cyanide salts, resulting in a shorter and more direct route to isotopically labeled compounds. Herein, we have found a 2-step sequence to prepare isotopically labeled carboxylic acids using directly labeled carbon dioxide by means of nickel catalysis. This methodology represents a direct use of CO<sub>2</sub> in late-stage or advanced intermediates for isotopic labeling, without the need of its derivatization to secondary synthons (Scheme 3, Chapter 4).



**Scheme 3.** Isotopic labeling with CO<sub>2</sub>.

Finally, the use of isoelectronic isocyanates as amide synthons was investigated. Its combinations with secondary alkyl bromides allowed us the study of different ligands that promoted or suppressed  $\beta$ -hydride elimination from the alkyl-nickel intermediates, delivering a regiodivergent transformation to obtain the corresponding amide in the initial or in a remote position (Scheme 4, Chapter 5).



**Scheme 4.** Regiodivergent amidation of secondary alkyl bromides.

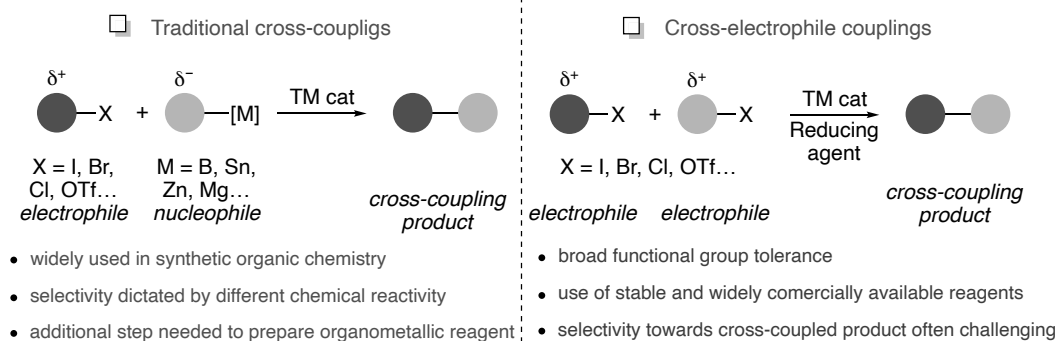
**Chapter 1:**  
***General Introduction***





## 1. Reductive Cross-Electrophile Couplings.

Metal-catalyzed cross-coupling reactions have undoubtedly brought a revolution to the landscape of organic synthesis.<sup>1</sup> These technologies allow for the design of innovative ways of building C–C and C–heteroatom bonds in organic compounds and have found immediate application in the preparation of agrochemicals, polymers and pharmaceuticals, among others.<sup>2</sup> These transformations are based on the utilization of an organic electrophile in combination with a nucleophilic reagent that are coupled together via the formation of C–metal bonds (Scheme 1). The electrophilic partner is commonly an organohalide or pseudohalide, whereas the nucleophilic partner is typically an alkene, an alkyne or a heteroatom- or carbon-based nucleophile (e.g. an organometallic reagent). The mild conditions, broad functional group tolerance and high efficiency that characterize these transformations have promoted their widespread use in organic chemistry, both in industry and in academic laboratories. The importance of the field was recognized by the 2010 Nobel Prize in Chemistry awarded to Professors Richard F. Heck, Ei-ichi Negishi and Akira Suzuki, for the discoveries in Pd-catalyzed cross-coupling reactions for the formation of C–C bonds.<sup>3</sup>



**Scheme 1.** Traditional cross-coupling and reductive cross-coupling reactions.

Despite the excellent preparative advances of cross-coupling reactions with organometallic reagents, it is worth noting that the latter reagents need to be prepared from the corresponding (pseudo)halides by classical metalation reactions, thus adding an additional synthetic step on the reaction sequence. In addition, the sensitivity of a non-negligible number of organometallic species requires rigorous exclusion of moisture and oxygen whereas the high nucleophilicity of these species might reduce the potential applicability of these processes in complex settings, i.e. in the presence of densely functionalized backbones. These observations prompted the development of catalytic reductive cross-coupling reactions where the organometallic reagent can be replaced by a simple electrophilic source in the

presence of stoichiometric amounts of a reducing agent.<sup>4</sup> This approach has the advantages of its experimental simplicity, the wide commercial availability of organic halides compared to organometallic reagents and the enhanced chemoselectivity that arises from the mild reaction conditions provided by the in situ formation of a transient organometallic intermediate.

The first reports of reductive cross-couplings can be traced back to the discovery of sodium-mediated dimerization reactions of alkyl halides by Wurtz in 1855,<sup>5</sup> the cross-coupling of aryl halides and alkyl halides discovered by Fittig,<sup>6</sup> and the Ullmann coupling, a copper mediated biaryl formation pioneered by the scientist of the same name.<sup>7</sup> These conceptions were taken in the 1970's for designing Ni-catalyzed Nozaki-Hiyama-Kishi reactions with Mn as stoichiometric reductant<sup>8,9</sup> and more recently within the context of electrochemical settings.<sup>10-13</sup> Still, however, the requirement for special equipment in the latter and the necessary use of sacrificial anodes has hampered its routine use and further development of these protocols until recently.<sup>14-17</sup> In these transformations, a reducing agent is needed to provide the necessary electrons to balance the redox equation of the reaction. Specifically, these reagents are believed to be involved in the reduction of the transient catalytic metal-species within the catalytic cycle prior to the targeted bond-forming event. Common reducing agents employed in these transformations are Mn, Zn or Mg, as well as organic reductants such as  $B_2pin_2$ <sup>18</sup> or TDAE (Tetrakis(dimethylamino)ethylene),<sup>19</sup> among others.<sup>20-22</sup> From a mechanistic standpoint, however, the employment of metallic reductants might also involve the generation of organometallic reagents via direct metal insertion into the corresponding C-X (typically X = halide). Note, however, that coining such a process as reductive cross-coupling reaction is questionable.<sup>4</sup>




While the selective formation of cross-coupled products in traditional, redox-neutral, metal-catalyzed cross-coupling reactions relies on the different chemical nature of the nucleophile and electrophile employed, the coupling partners used in cross-electrophile couplings have similar reactivities, which often lead to undesired homocoupling reactions instead of the formation of the targeted cross-coupled product. Reaching high levels of selectivity in cross-electrophile couplings is therefore one of the major challenges to be surpassed. Different strategies to increase the selectivity in these protocols include: the addition of an excess of one reagent, the electronic differentiation of the starting materials, catalyst-substrate steric matching and the development of reactions that couple substrates for which oxidative addition occurs via two different mechanisms, such as two-electron or one-electron manifolds.<sup>23</sup> The study and understanding of the mechanisms by which cross-electrophile couplings operate has not only contributed to advances within the field, but has also inspired the design of novel transformations,

particularly of dual nickel/photoredox systems in which the photoredox cycle replaces the reducing agent by a terminal organic electron donor.

In recent years, our research group has contributed to the field of reductive carboxylation reactions using CO<sub>2</sub> as a C1-synthon as a mean to access valuable carboxylic acids from simple electrophilic coupling partners.<sup>24</sup> These processes fall into the category of cross-electrophile coupling reactions, in which a reducing agent is required to drive the reaction forward. The efforts carried out by our group have allowed to couple CO<sub>2</sub> with aryl halides, benzylic electrophiles, alkyl halides, allylic acetates and unsaturated hydrocarbons, among others by using, in most instances, nickel catalysts in combination with phosphine or nitrogen-containing ligands in the presence of metal reductants.

## 2. Nickel catalysis general characteristics (vs group 10 metals).

Nickel belongs to the group 10 metals of the periodic table, and it is the 24<sup>th</sup> most abundant element in the Earth's crust, being more abundant than Cu, Zn or Pb. The use of nickel as a catalyst in organic transformations was pioneered by the Nobel Laureate Paul Sabatier for his work on the catalytic hydrogenation of ethylene. Since that report, the development of organonickel chemistry has led to the discovery of several powerful applications, such as the alkene polymerization or cross-coupling reactions of electrophiles with carbon nucleophiles (organometallic compounds). Different organometallic compounds were successfully employed in the Kumada-Corriu (magnesium), Suzuki-Miyaura (boron), Negishi (zinc) and Hiyama (silicon) reactions.<sup>1</sup> However, further progress in the field was overshadowed by rapid developments in Pd chemistry, perhaps due to the difficulties associated with the nature of organonickel species, which also contributed to the false impression that nickel was not suitable for synthetic applications.<sup>25</sup> A renewed interest in nickel catalysts within the last decades, however, has led to the design of novel chemical transformations that exploit the versatility of earth-abundant nickel salts.<sup>26</sup> Important advancements have been accomplished during the last years, especially in the Mizoroki-Heck reaction,<sup>27</sup> reductive cross-coupling reactions, C–O,<sup>28</sup> C–N<sup>29</sup> and C–H<sup>30</sup> bond functionalizations, asymmetric couplings,<sup>31</sup> and metallaphotoredox reactions,<sup>32</sup> among others. The utility of nickel-catalyzed transformations has been demonstrated as well in industrial applications such as the Shell Higher Olefin Process (SHOP) for the production of  $\alpha$ -olefins and DuPont's hydrocyanation of butadiene for adiponitrile synthesis.

			
Covalent radius (Å)	1.24	1.39	1.36
Pauling Electro Negativity	1.91	2.20	2.28
Usual Oxidation States	<b>0, +1, +2, +3</b>	<b>0, +2, +4</b>	<b>0, +2, +4</b>

□ Bond Dissociation Energies (kcal mol<sup>-1</sup>)

C–C	<b>Ni–C</b>	<b>Pd–C</b>	<b>Pt–C</b>
87.4	38.0–51.1	48.3–55.2	60.8–66.5

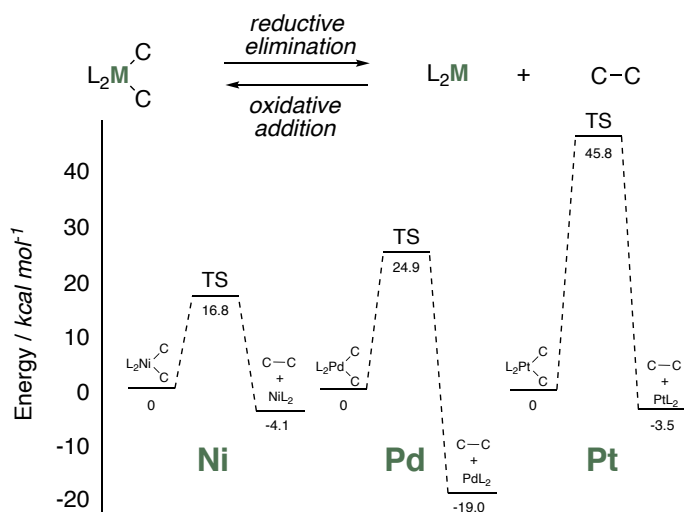
**Scheme 2.** Group 10 metal characteristics.

The construction of molecular frameworks requires flexible tools for the formation and cleavage of carbon–carbon bonds, which is difficult to achieve because of the high strength of the C–C bond (Scheme 2). Weaker M–C bonding provides the necessary fundamental basis for catalytic transformations, favoring the reductive elimination to forge the targeted C–C bond. Comparison between the group 10 metals (Scheme 2 and 3) shows that, indeed, nickel complexes should be the most reactive in both directions. Palladium is perfectly suited for C–C bond formation, whereas platinum should form the least reactive and most stable complexes. A similar reactivity trend was observed for C–N and C–O bond formation.<sup>33</sup> At the same time, Pd–alkyl complexes are more prone to  $\beta$ -hydride elimination than Ni–alkyl species due to a better agostic interaction resulting from the more effective  $\sigma$ -donation of the C–H $_{\beta}$  *s*-bond to the lower-lying empty *d* orbital of the metal, which weakens the C–H bond.<sup>34,35</sup> The reverse reaction, migratory insertion, is therefore more favored with Ni. Homolytic bond cleavage shows the following trend: Ni–C>Pd–C>Pt–C, in which the reactivity decreases from nickel to palladium and then to platinum. Therefore, among the group 10 metals, the contribution of radical processes via one electron processes is most probable for nickel species.<sup>36</sup> For nickel, the M<sup>I</sup> and M<sup>III</sup> oxidation states are much more accessible than for palladium and platinum complexes, whereas M<sup>0</sup>, M<sup>II</sup>, and M<sup>IV</sup> oxidation states are more common in the latter. These characteristic gives nickel a particular reactivity, in which often radical and single electron transfer pathways come into play.

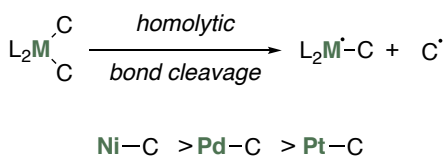
Finally, if we consider the coordination of unsaturated compounds to the metal center, the binding of alkene and alkyne units to nickel complexes is exceptionally strong:  $\Delta E = 34.3$  and  $41.6$  kcal/mol (Scheme 3).<sup>25</sup> In contrast, the binding of double and triple carbon–carbon bonds to palladium and platinum is less energetically favored,  $\Delta E = 16.1$ – $23.7$  kcal/mol. This marked difference explains the great

reactivity of nickel catalysts with  $\pi$ -systems in cyclization and cycloisomerization reactions and polymerization events.

□ Activation and Reaction Energies for C-C bond formation



□ Homolytic cleavage



□ Binding Energies of Alkyne and Alkene ( $\text{kcal mol}^{-1}$ )

Metal	Alkyne	Alkene
Ni	34.3	41.6
Pd	16.1	17.9
Pt	19.6	23.7

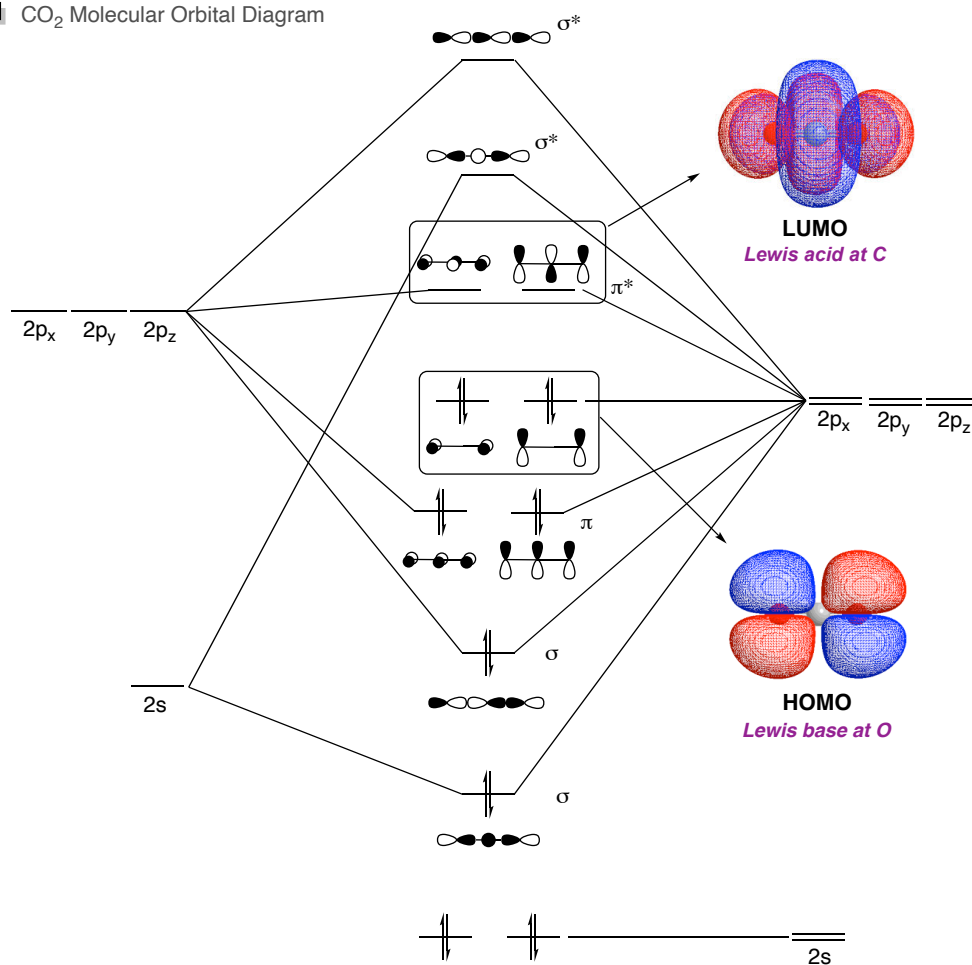
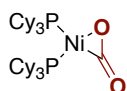
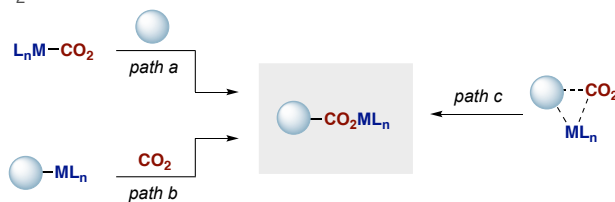
**Scheme 3.** Reactivity of Group 10 metal species.

### 3. CO<sub>2</sub> reactivity and functionalization.

CO<sub>2</sub> is an abundant, inexpensive and renewable synthon that could be potentially used as a C1 building block. Indeed, CO<sub>2</sub> functionalization into valuable products holds great promise for revolutionizing the field of organic synthesis, in particular when preparing high value-added chemicals, thus offering new applications in the immediate future.<sup>37</sup> In fact, close to 110 Mt CO<sub>2</sub>/y are converted into urea, inorganic carbonates or used as additives to carbon monoxide (CO) in the synthesis of methanol.<sup>38</sup> Other chemicals such as salicylic acid and propylene carbonate cover a minor share of the market. However, the number of chemicals directly available from CO<sub>2</sub> still remains very narrow compared to those derived from currently available petrochemicals, thus encouraging the design of novel methods using CO<sub>2</sub>.

Taking into consideration that catalytic CO<sub>2</sub> fixation technologies typically involve the coordination of CO<sub>2</sub> to a metal center, it is particularly important to understand the basic features associated to the molecule of CO<sub>2</sub> and its binding modes to transition metals. In its ground state, CO<sub>2</sub> is a linear triatomic molecule with D<sub>∞h</sub> symmetry in which the central carbon atom possesses *sp* hybridization. It has two dipole moments opposite each other, making CO<sub>2</sub> a non-polar molecule that shows a remarkable kinetic and thermodynamic stability. The main molecular orbitals (MO) that are primarily responsible for the reactivity of CO<sub>2</sub> are the 1<sub>πg</sub>-occupied MO (HOMO) and 2<sub>πu</sub>-unoccupied MO (LUMO).<sup>39</sup> While the former is centered on the oxygen atoms, the latter preferentially lies on the carbon atom. These characteristics confer an ambiphilic character to CO<sub>2</sub>, exhibiting Lewis basic character at oxygen and Lewis acidic character at carbon (Scheme 4). These features govern the binding of CO<sub>2</sub> to transition metals; in particular, metals in low oxidation states typically bind CO<sub>2</sub> by the carbon atom, whereas highly oxidized metals predominantly interact with the oxygen atoms.

The binding of the metal center to CO<sub>2</sub> causes in most cases a significant deviation of the O–C–O angle from linearity. This observation explains the fact that the binding significantly lowers down the activation energy required for CO<sub>2</sub> activation, thus setting the basis for promoting the targeted C–C bond-forming event. It can be seen for example in the first transition metal complex that could be structurally characterized containing a coordinated CO<sub>2</sub> to a nickel center, reported by Aresta and co-workers (Cy<sub>3</sub>P)<sub>2</sub>Ni(CO<sub>2</sub>) (Scheme 4, *bottom left*).<sup>40</sup> In this complex, the Ni atom adopts a planar geometry, with CO<sub>2</sub> possessing two nonequivalent C–O bonds (1.17 and 1.22 Å) that slightly deviate from free CO<sub>2</sub> (1.16 Å). Although other pathways are potentially conceivable, the conversion of CO<sub>2</sub> into the targeted carboxylic acid can formally be explained via three different pathways (Scheme 4, *bottom right*): (a) initial coordination of the metal center to CO<sub>2</sub> followed by reaction with the substrate; (b) interaction of the substrate to the metal center prior to CO<sub>2</sub> binding or insertion; (c) dual coordination of the substrate and CO<sub>2</sub> to the metal center. In any case, it is inevitable to establish a connection between the Aresta complex and the recent popularity gained by Ni catalysts.

CO<sub>2</sub> Molecular Orbital Diagram

 Aresta's complex

 CO<sub>2</sub> functionalization


**Scheme 4.** CO<sub>2</sub> Molecular Orbital Diagram, CO<sub>2</sub> Functionalization and Aresta's complex.

#### 4. Cross-Electrophile Couplings for the synthesis of carboxylic acids.

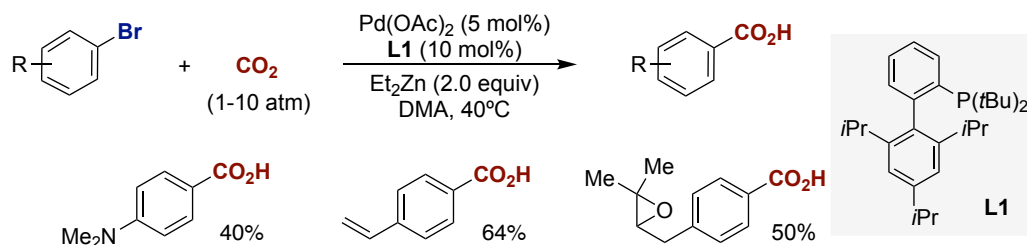
The synthesis of carboxylic acids constitutes an ideal target for CO<sub>2</sub> utilization since these compounds are privileged motifs in a wide number of natural products, agrochemicals and pharmaceutically relevant compounds.<sup>41</sup> From an ideal standpoint, carboxylic acids could derive from abundant and inexpensive CO<sub>2</sub>, thus following the principles of sustainability by using renewable feedstock to produce high-value added chemicals.<sup>38</sup> At present, the current state-of-the-art for preparing carboxylic acids from CO<sub>2</sub> relies on the use of very reactive and well-defined, stoichiometric and, in many instances, organometallic species such as organolithium or Grignard reagents. Unfortunately, the reliability of obtaining these organometallic species from the corresponding aryl or alkyl halides,<sup>42</sup> their low chemoselectivity profile and the requirement for special techniques for handling these compounds reinforce a change in strategy to the development of novel reductive carboxylation reactions, coupling CO<sub>2</sub> with other electrophiles.

##### 4.1. Carboxylation of (pseudo)alkyl-halides.

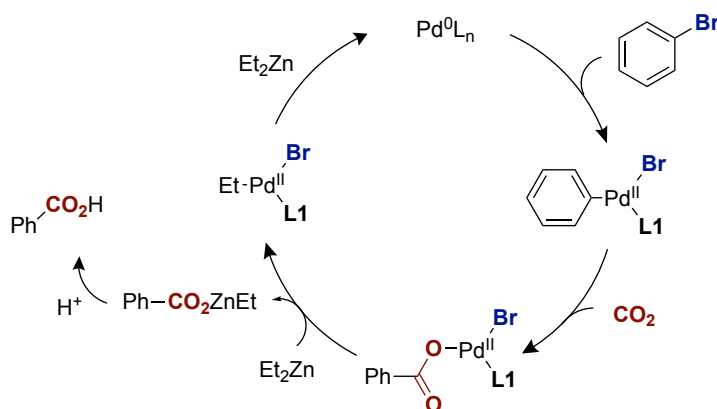
In 1994, pioneering studies by Osakada and Yamamoto demonstrated that stoichiometric amounts of PhNiBr(bpy), readily prepared by simple exposure of PhBr to Ni(COD)<sub>2</sub> and bipyridine, could effectively react with CO<sub>2</sub> at low pressure to afford benzoic acid in moderate yield.<sup>43</sup> This experiment confirmed not only the unique ability of nickel complexes to trigger CO<sub>2</sub> insertion into putative oxidative addition complexes, but also establishing the basis for designing a catalytic procedure for preparing carboxylic acids from simple organic halides. Osakada's findings found little echo and the field remained dormant until 2009, when our group reported the first catalytic carboxylation of aryl bromides with CO<sub>2</sub> (1-10 atm) by using Et<sub>2</sub>Zn as terminal reductant (Scheme 5).<sup>44</sup> Particularly important was the observation that bulky and electron-rich phosphine (*t*BuXPhos) was critical for success, minimizing Negishi-type cross-coupling reaction as well as unproductive reduction pathways. Preliminary mechanistic experiments ruled out the intervention of intermediate organozinc species, thus suggesting a direct CO<sub>2</sub> insertion into the corresponding ArPd(II)Br oxidative addition species.



■ Pd-catalyzed carboxylation of aryl bromides



■ mechanistic rationale



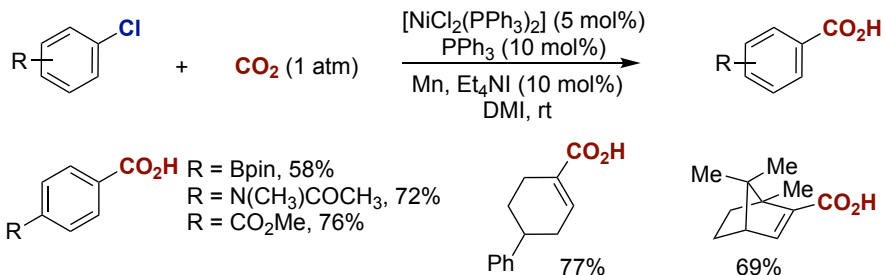
**Scheme 5.** Pd-catalyzed carboxylation of aryl bromides.

While this method constituted the genesis of catalytic reductive carboxylation of organic halides with  $\text{CO}_2$ , the need for relatively high pressures, a pyrophoric reducing agent ( $\text{Et}_2\text{Zn}$ ) and the limitation to aryl bromide counterparts were important drawbacks to be overcome. In 2012, the group of Tsuji and Fujihara extended the scope of catalytic carboxylations to the more challenging and readily available aryl and vinyl chlorides at low pressure of  $\text{CO}_2$  (Scheme 6).<sup>45</sup> It was shown that a mild and air-stable reducing agent (Mn) in combination with ammonium salts ( $\text{Et}_4\text{NI}$ ) as additives were critical for success. The role of the reducing agent and the ammonium salt was recently investigated by the Hazari group.<sup>20</sup> They found that manganese acts as reducing agent and as a Lewis acid after oxidation to  $\text{MnCl}_2$ , increasing the rate of  $\text{CO}_2$  insertion into the Ni(I) aryl complex to generate the carboxylic acid group. In contrast, the ammonium salt undergoes a ligand-exchange reaction and facilitates reduction of the proposed Ni(I) carboxylate. As it will become apparent in the following sections, the use of additives has not only been critical for achieving reactivity in the reductive carboxylation field, but also for establishing site-selective protocols. These observations were corroborated by Hazari on the Ni-catalyzed carboxylation of aryl chlorides with different organic reductants. The addition of an ammonium halide boosted the yield when Mn or  $\text{Cp}_2\text{Co}$  were used as

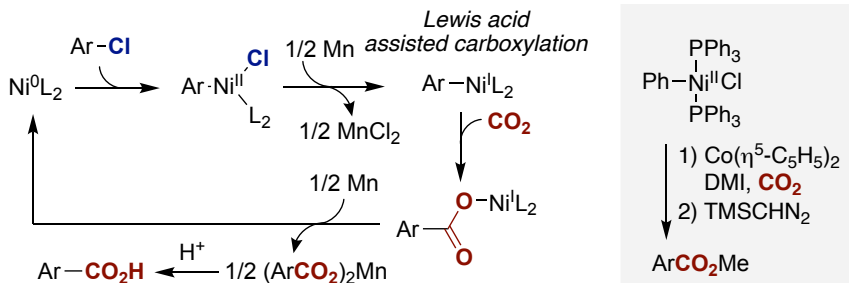
## Chapter 1

a reducing agent, whereas the addition of  $\text{MnCl}_2$  improved the yield of the reductants with a sufficient potential to reduce  $\text{Ni(II)}$  to  $\text{Ni(0)}$  (as shown in Scheme 6, TDAE is not able to perform said reduction in this catalytic system). Theoretical calculations supported a  $\text{CO}_2$  insertion pathway into the  $\text{Ar-Ni(I)(PPh}_3)_2$ ,<sup>46</sup> which can be generated upon Mn-mediated single electron transfer (SET).<sup>47</sup>

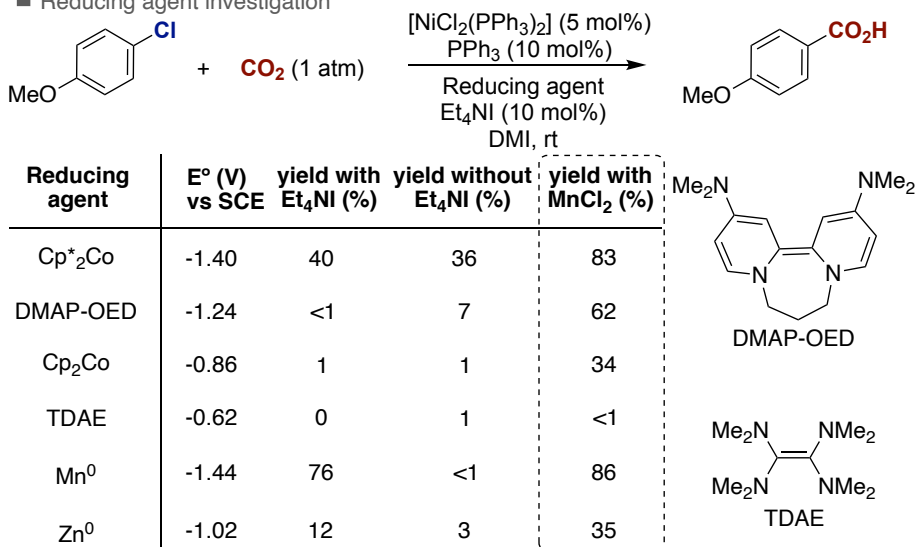
### ■ Ni-catalyzed carboxylation of aryl and vinyl chlorides



### ■ Mechanistic rationale



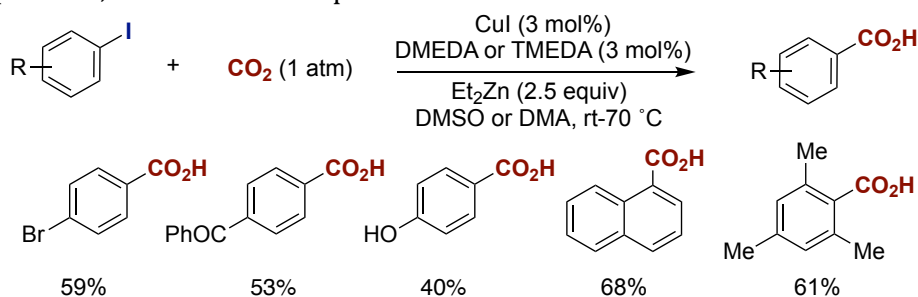
### ■ Reducing agent investigation



DMI: 1,3-dimethyl-2-imidazolidinone, SCE: Saturated Calomel Electrode

**Scheme 6.** Ni-catalyzed carboxylation of aryl chlorides.

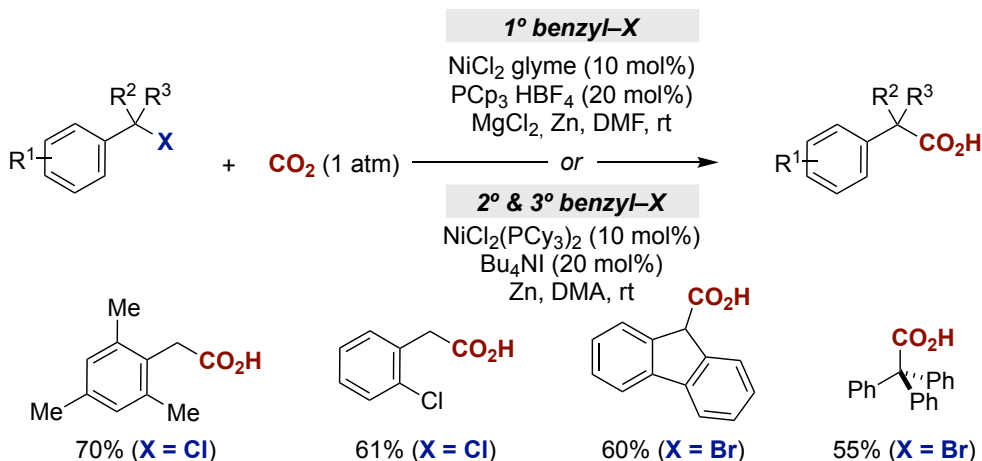
In 2013, Daugulis reported the Cu-catalyzed reductive carboxylation of aryl iodides using a CuI/TMEDA or CuI/DMEDA regime when combined with Et<sub>2</sub>Zn as reducing agent (Scheme 7).<sup>48</sup> In contrast to previous catalytic carboxylations of aryl halides, the presence of particularly sterically hindered substrate combinations did not pose any problem, even at room temperature.



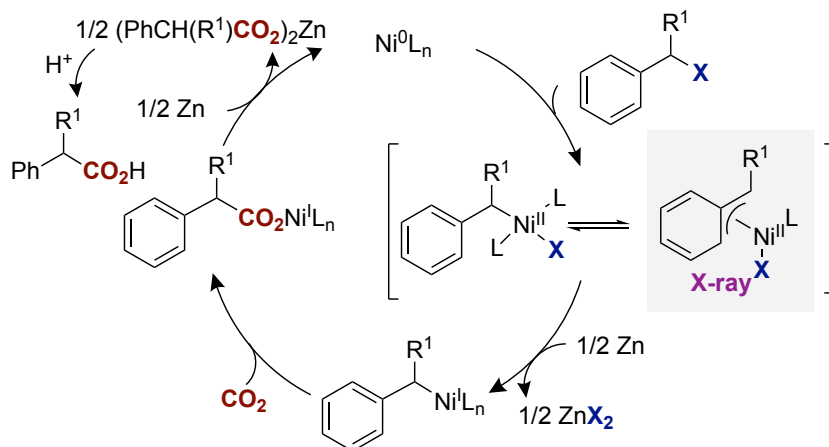
**Scheme 7.** Cu-catalyzed carboxylation of aryl iodides.

Aiming to expand the catalytic reductive carboxylation portfolio beyond the utilization of aryl halides, our group described a Ni-catalyzed protocol of primary, secondary or even tertiary benzyl halides with CO<sub>2</sub> at 1 atmosphere of pressure (Scheme 8).<sup>49</sup> In this case, highly electron-rich phosphines such as PCp<sub>3</sub> and PCy<sub>3</sub> were found to be critical in the presence of Zn as reducing agent. Although not yet fully understood, the presence of additives was found to play a profound influence on reactivity; while the presence of MgCl<sub>2</sub> mediated the coupling of primary benzyl halides, the addition of TBAI (tetrabutylammonium iodide) proved particularly useful for secondary and tertiary benzyl halides. Control experiments argued against a mechanism consisting of the intermediacy of benzyl zinc reagents or styrene derivatives obtained via β-hydride elimination and suggested a one-electron reduction of in situ generated η<sup>3</sup>-benzylnickel(II) complexes mediated by either Zn or comproportionation with Ni(0)L<sub>2</sub>, resulting in Ni(I) intermediates that would subsequently insert CO<sub>2</sub> at the sp<sup>3</sup> C–Ni bond.<sup>50</sup> Although not conclusive, an initial SET was proposed based on the inhibition found in the presence of radical scavengers as well as the observed racemization if an enantiopure benzyl bromide was used as substrate. In 2014, a detailed DFT study suggested that the addition of MgCl<sub>2</sub> might accelerate CO<sub>2</sub> insertion while favoring SET-type processes.<sup>51</sup>

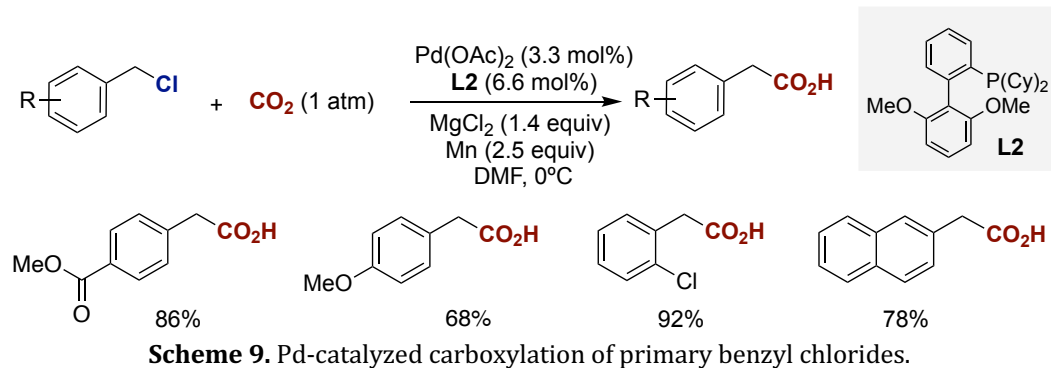
■ Ni-catalyzed carboxylation of benzyl bromides and chlorides



■ mechanistic rationale



In line with the ability of electron-rich and bulky phosphines to mediate the Pd-catalyzed carboxylation of aryl bromides,<sup>44</sup> He reported the catalytic carboxylation of primary benzyl chlorides using a Pd precatalyst and SPhos as ligand (Scheme 9).<sup>52</sup> Once again, the addition of MgCl<sub>2</sub> turned out to be important, improving the overall catalytic efficiency of the reaction. In this case, however, DFT calculations favored a pathway consisting of a Lewis acid coordination to CO<sub>2</sub>, thus lowering down its activation energy and setting up the stage for a CO<sub>2</sub> insertion into the sp<sup>2</sup> C–Pd<sup>II</sup> bond.

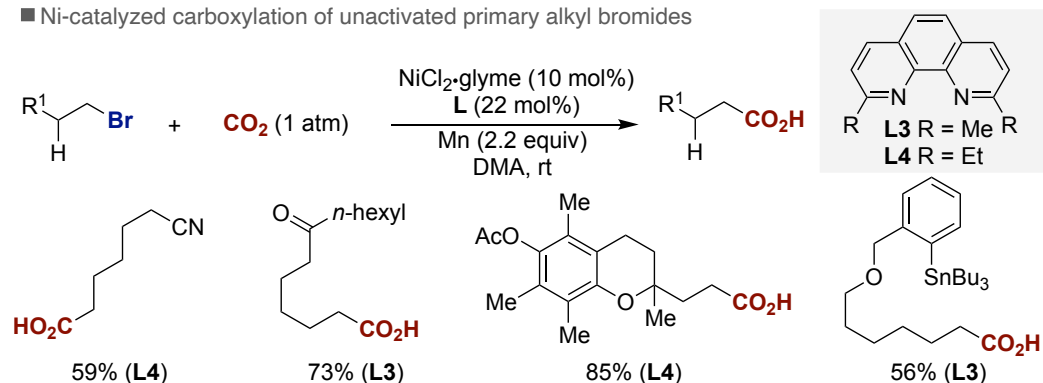


By 2014, metal-catalyzed reductive carboxylations remained confined to the utilization of aryl, benzyl or allyl (pseudo)halides as coupling partners. This observation indirectly suggested that extending the scope of these technologies beyond substrates that easily undergo oxidative addition might be more problematic than initially anticipated. Despite the advances realized in metal-catalyzed cross-coupling reactions of unactivated alkyl halides,<sup>53</sup> the vast majority of these technologies made use of particularly reactive, in many instances homogenous, precursors that can effectively intercept the in situ generated alkyl metal species. Unfortunately, CO<sub>2</sub> is thermodynamically stable, kinetically inert and not particularly soluble in the classical solvents required for effecting cross-coupling reactions. Therefore, it was anticipated that the direct carboxylation of unactivated alkyl halides would be hampered by the particularly low concentration of CO<sub>2</sub> in solution, thus making particularly difficult to intercept the in situ generated alkyl metal species with CO<sub>2</sub> prior unproductive β-hydride elimination and/or homodimerization pathways.

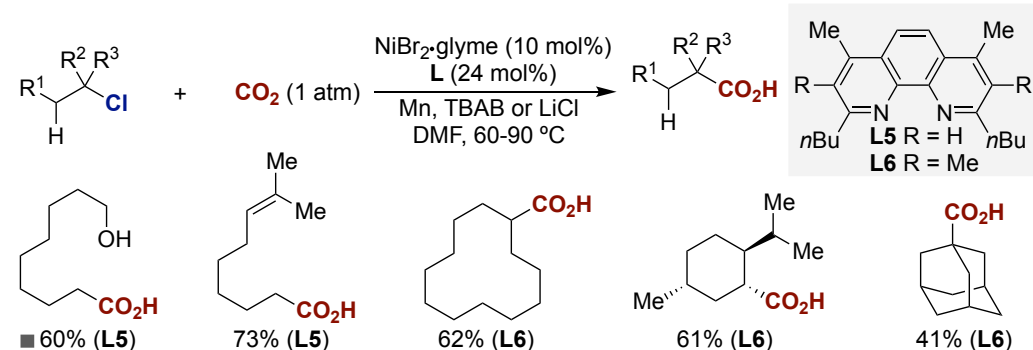
Our group offered a solution to this challenge by utilizing 1,10-phenanthroline ligands possessing substituents adjacent to the nitrogen atom (Scheme 10, *top*).<sup>54</sup> While a full rationale behind these results will likely require future efforts, it was suggested that the presence of such substituents prevented parasitic β-hydride elimination while favoring the formation of alkyl-Ni(I) intermediates prior to CO<sub>2</sub> insertion. The insertion of CO<sub>2</sub> into those Ni(I) intermediates was confirmed recently by our group with this family of ligands, shedding light on the mechanism of unactivated alkyl halides carboxylation.<sup>55</sup> Although the reaction exhibited a remarkable functional group tolerance, this technique did not include either the coupling of secondary (or tertiary) alkyl bromides nor the more accessible unactivated alkyl chlorides. These limitations were overcome in 2016 in a new Ni-catalyzed carboxylation of primary, secondary or even tertiary alkyl chlorides (Scheme 10, *bottom*),<sup>56</sup> constituting the first time that such coupling partners could be employed in catalytic reductive cross-couplings. As anticipated, a more electron-

rich ligand was expected to accelerate the oxidative addition whereas the inclusion of *ortho*-substituents would prevent decomposition reaction pathways prior to CO<sub>2</sub> insertion into the alkyl C–metal bond. As for other carboxylation reactions, the addition of additives turned out to be essential for the reaction to occur, with a mixture based on *n*Bu<sub>4</sub>NBr (TBAB) or LiCl providing the best results. Although not fully understood, the former might facilitate SET processes, whereas the later could significantly enhance the nucleophilicity of the transient alkyl nickel intermediates. Aiming at extending the scope of catalytic carboxylation reactions, our group described as well the use of cyclopropyl motifs in these endeavours.<sup>57</sup>

■ Ni-catalyzed carboxylation of unactivated primary alkyl bromides



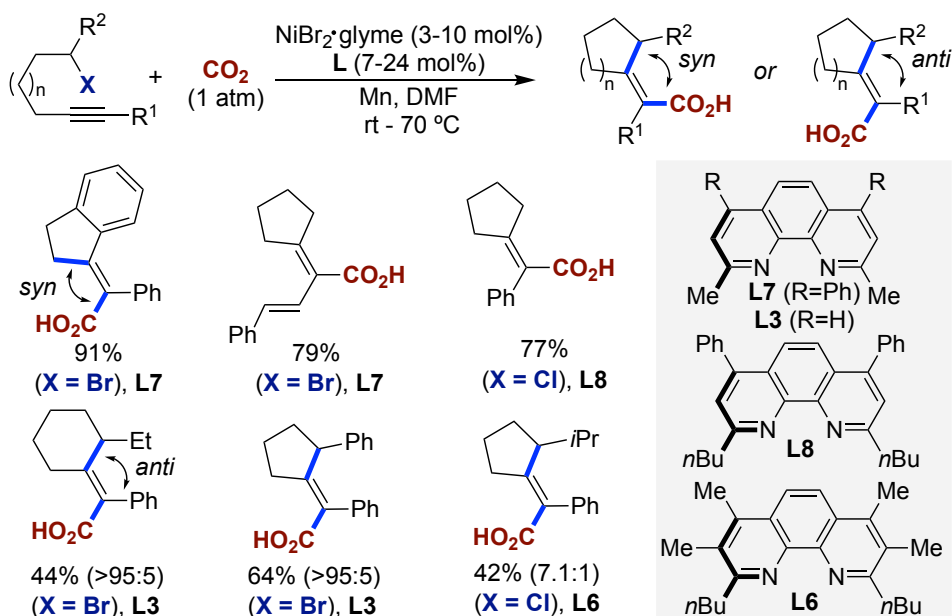
■ Ni-catalyzed carboxylation of primary, secondary and tertiary alkyl chlorides



**Scheme 10.** Ni-catalyzed carboxylation of unactivated alkyl halides.

Although one might argue that the loss of stereochemical integrity observed in carboxylation reactions via SET processes might inherently limit the application profile of these technologies, these a priori undesired pathways can be turned into a strategic advantage. Our group reported a cyclization/carboxylation of unactivated alkyl halides possessing an alkyne on the side chain, resulting in polycyclic carboxylic skeletons. The rationale behind such reactivity was attributed to an initial SET, triggering a rapid 5-*exo*-trig cyclization prior recombination with the Ni(I) complex, delivering a vinyl-Ni(II) intermediate that can subsequently be intercepted

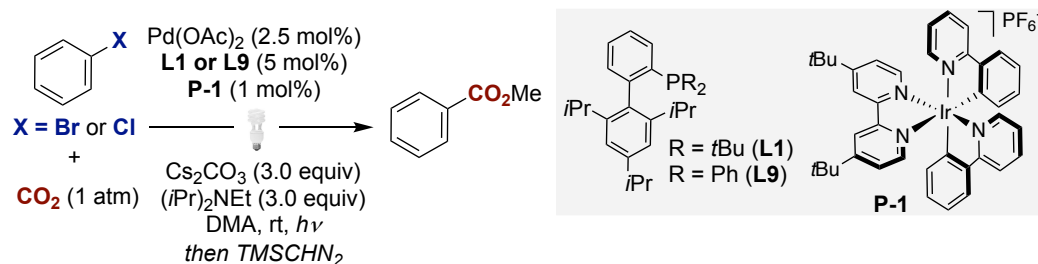
with CO<sub>2</sub> (Scheme 11).<sup>56,58</sup> While primary alkyl halides rendered the *syn*-product exclusively, *anti*-products were predominantly observed with secondary alkyl halides. The nature of the ligand and the substrate profoundly influenced such site-selectivity.



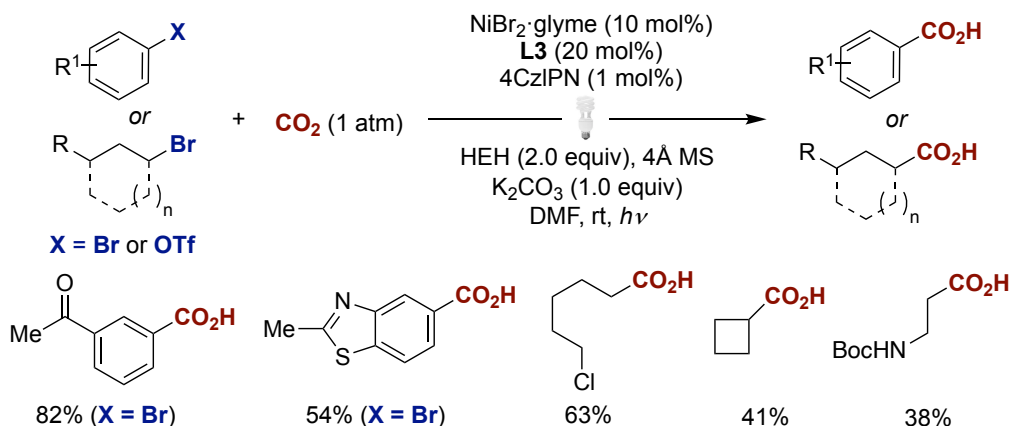
**Scheme 11.** Ni-catalyzed cyclization/carboxylation of unactivated alkyl halides.

Over the recent years, visible light photoredox catalysis has emerged as a powerful tool for building up molecular complexity under remarkably mild reaction conditions.<sup>59</sup> Driven by the ability to generate transient radical intermediates via non-invasive outer-sphere SET processes, photoredox catalysis might open new vistas in catalytic reductive carboxylation reactions by avoiding the need for stoichiometric amounts of metallic single-electron reductants. Recently, Iwasawa described the merger of Pd and photoredox catalysis for the direct carboxylation of aryl bromides and chlorides (Scheme 12).<sup>60</sup> As initially anticipated from previous Pd-catalyzed carboxylations, a particularly bulky and electron-rich phosphine (*t*BuXPhos) was found to be well-suited for the carboxylation of aryl chlorides, whereas PhXPhos proved to be superior when coupling aryl bromides. Preliminary mechanistic studies showed a mismatch between the reduction potentials of PhPdBr(XPhos) (-2.28 V vs Fc/Fc<sup>+</sup>) and the photocatalyst utilized (-1.87 V vs Fc/Fc<sup>+</sup>). Interestingly, however, CV measurements in CO<sub>2</sub> atmosphere (1 bar) indicated a way lower reduction potential for the oxidative addition complex (-1.4 V). Although tentative, this result suggested that the coordination of CO<sub>2</sub> to the Pd(II)

center might facilitate a subsequent single-electron transfer *en route* to a Ar-Pd(I)XPhos intermediate prior to CO<sub>2</sub> insertion into the *sp*<sup>2</sup> C-Pd bond.



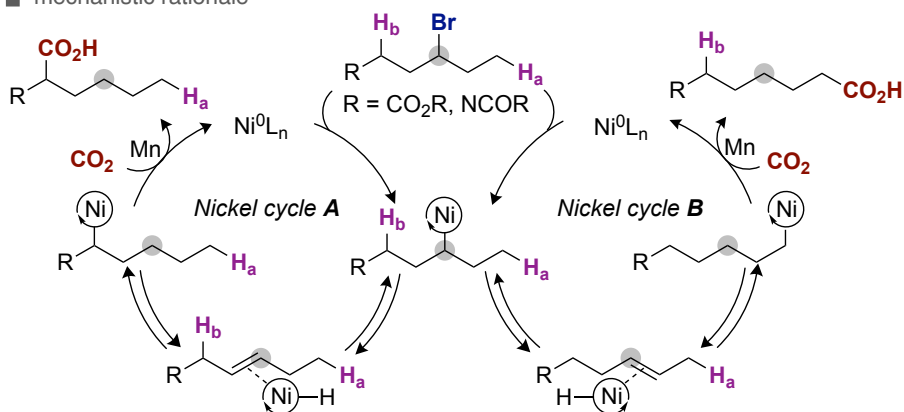
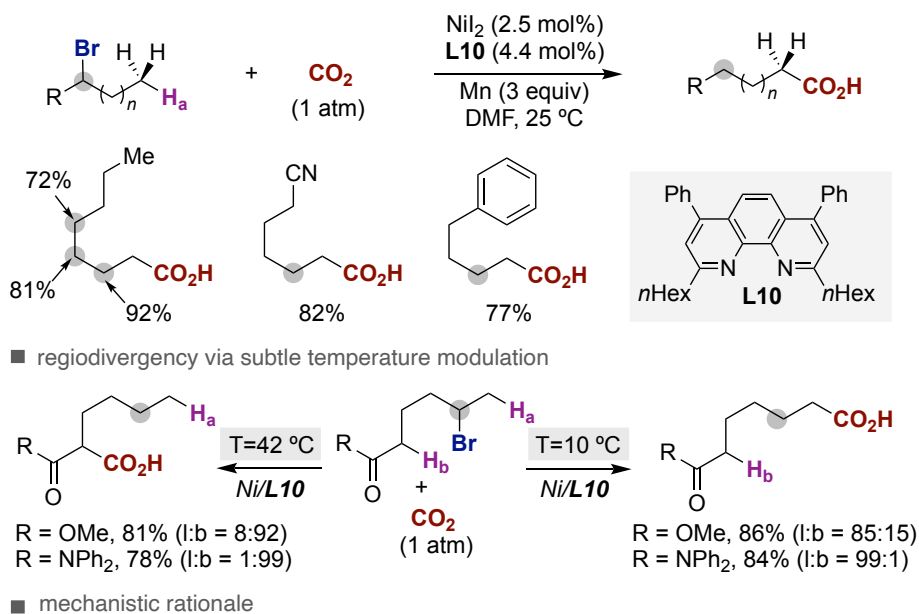
In the same direction, the König group described the merger of Ni catalysis within the photoredox arena for the carboxylation of aryl and alkyl bromides (Scheme 13).<sup>61</sup> Unlike the iridium polypyridyl sensitizers used in the Pd/photoredox couple, an organic photosensitizer (4CzIPN) turned out to be particularly useful when combined with Hantzsch ester (HEH) as sacrificial reductants and K<sub>2</sub>CO<sub>3</sub> as the inorganic base. As for previous carboxylation reactions, the employment of *ortho*-substituted 1,10-phenanthrolines was key for success. Electrochemical experiments suggested that both oxidative and reductive quenching of the excited state of 4CzIPN may be operating, although the latter was expected to be considerably faster than the former.



Although metal-catalyzed cross-couplings of unactivated alkyl halides have enabled new paradigms for introducing saturated hydrocarbon chains into organic motifs, these processes require prefunctionalization at the initial reaction site. In 2017, our group designed a method by which unactivated alkyl halides can be used as vehicles for promoting remote carboxylation events at distal *sp*<sup>3</sup> C-H reaction sites (Scheme 14).<sup>62</sup> Such a design principle is based on the ability of an *in situ*

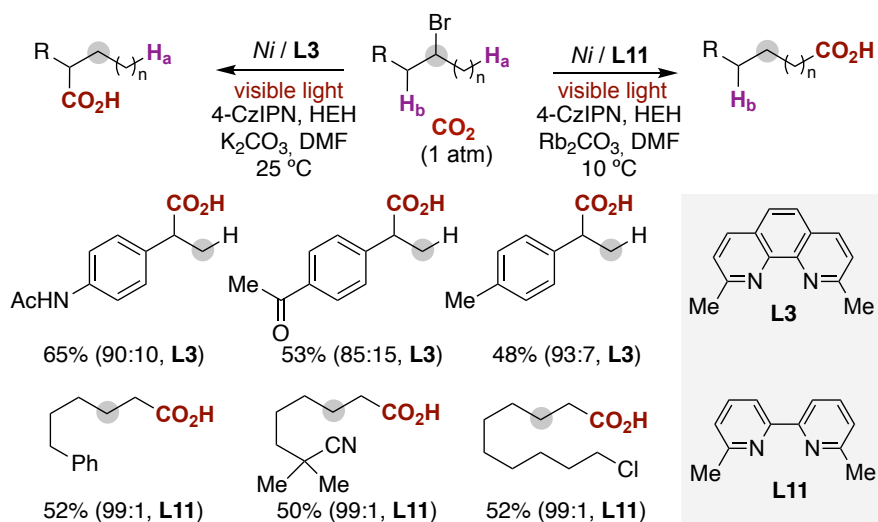


generated alkyl-Ni intermediate to accelerate  $\beta$ -hydride elimination while preventing  $\text{CO}_2$  insertion at the initial reaction site. A key contributory factor for success was the design of a 1,10-phenanthroline ligand possessing big *ortho*-substituents and arene motifs at C4 & C7. While the former likely favors halide dissociation and triggers a fast  $\beta$ -hydride elimination, the latter enhances the electrophilicity at the Ni(II) center, facilitating the binding of the intermediate alkene. These features result in a “chain-walking” via iterative  $\beta$ -hydride elimination/migratory insertion sequence, thus setting the basis for a  $\text{CO}_2$  insertion at distal sites. As the selectivity is controlled by the “chain-walking” motion, similar reactivity was observed regardless of the location of the halide function within the alkyl chain. This concept was used for converting alkanes or unrefined mixtures of olefins into fatty acids by a two-step sequence consisting of bromination/“chain-walking” carboxylation. Notably, a bidirectional motion could be established by a subtle temperature modulation, enabling the regiochemical discrimination between multiple  $sp^3$  C-H bonds within an alkyl chain. It is worth noting that substrates containing pre-existing stereogenic centers substantially preserved their chiral integrity, suggesting that the Ni catalyst remains bound to the olefin during the “chain-walking” event.<sup>63</sup>



**Scheme 14.** Ni-catalyzed remote carboxylation of halogenated hydrocarbons.

A recent collaboration by König and our group found that the combination of this strategy within the context of photoredox catalysis allowed the use of inexpensive Hantzsch esters as a terminal reductants, achieving the carboxylation at the benzylic position or at the terminal position by modification of the ligand and the reaction conditions (Scheme 15).<sup>64</sup>



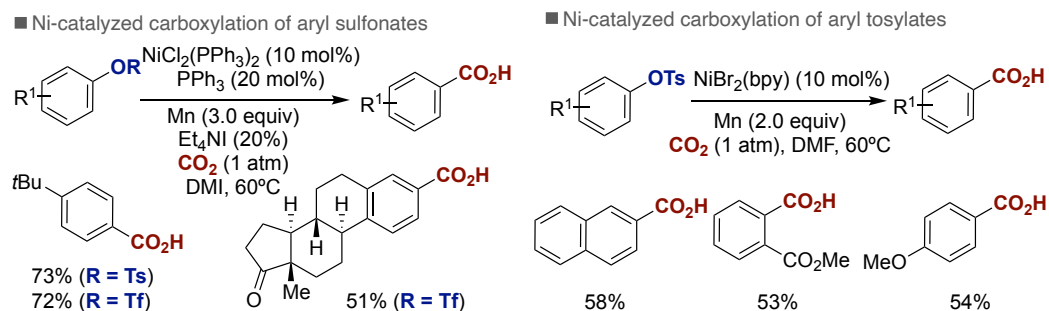
**Scheme 15.** Metallaphotoredox site-selective remote  $sp^3$  C-H carboxylation.

## 4.2 Catalytic reductive carboxylation of C–O electrophiles.

Prompted by the ready availability and natural abundance of phenols and aliphatic alcohols, the utilization of C–O electrophiles as organic halides surrogates in cross-coupling reactions has gained considerable momentum.<sup>65</sup> Practicality and accessibility aside, these technologies offer the advantage of lower toxicity as well as the opportunity to design orthogonal techniques in the presence of aryl halides. Unlike cross-coupling reactions with aryl halides that are typically conducted with Pd catalysts, the higher activation energy required for C–O cleavage is commonly achieved with Ni catalysts. These favorable attributes have been adopted within the carboxylation field. In particular, Tsuji and Fujihara reported the catalytic carboxylation of activated aryl sulfonates under otherwise similar conditions to that shown for aryl chlorides based on  $PPh_3$  as the ligand (Scheme 16, *left*).<sup>45</sup>

In 2016, Durandetti showed that the carboxylation of aryl tosylates could be conducted with  $NiBr_2(bpy)$  as precatalyst without the need for neither ammonium salts nor phosphine ligands (Scheme 16, *right*).<sup>66</sup> Although the transformation afforded moderate yields, it is worth noting that the coupling of *ortho*-substituted aryl tosylates was equally effective. Extensions to more sterically hindered substrates or vinyl triflates could be applied recently with either a Ni or Co regime.<sup>67</sup>

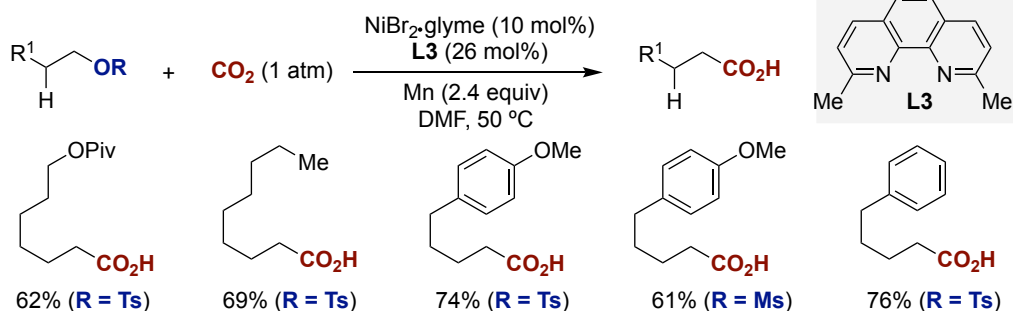
## Chapter 1



**Scheme 16.** Ni-catalyzed carboxylation of aryl sulfonates.

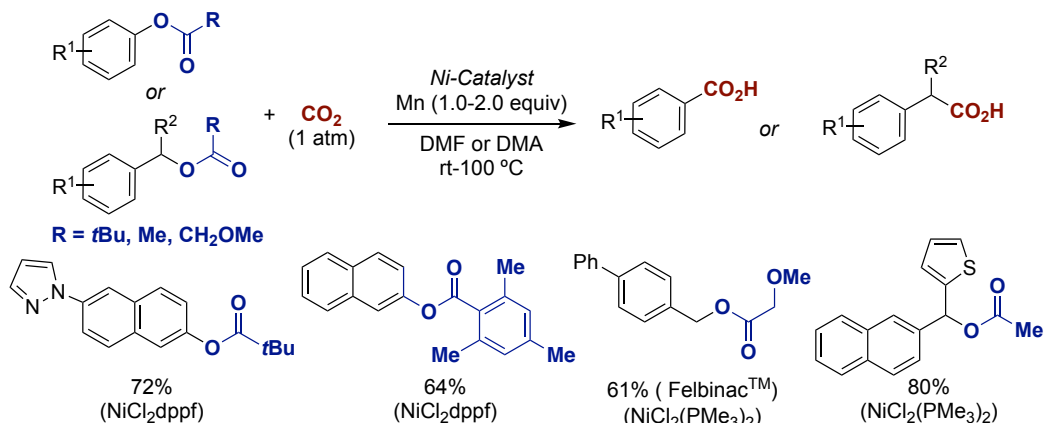
Our group extended these processes to the utilization of unactivated alkyl mesylates and tosylates (Scheme 17).<sup>54</sup> As expected, it was found that a slight increase in temperature when compared to the utilization of alkyl bromides was necessary for the reaction to occur. The loss of the stereochemical integrity when employing  $\alpha,\beta$ -bisdeuterated alkyl tosylates suggested the involvement of single-electron transfer processes.

■ Ni-catalyzed carboxylation of unactivated alkyl sulfonates



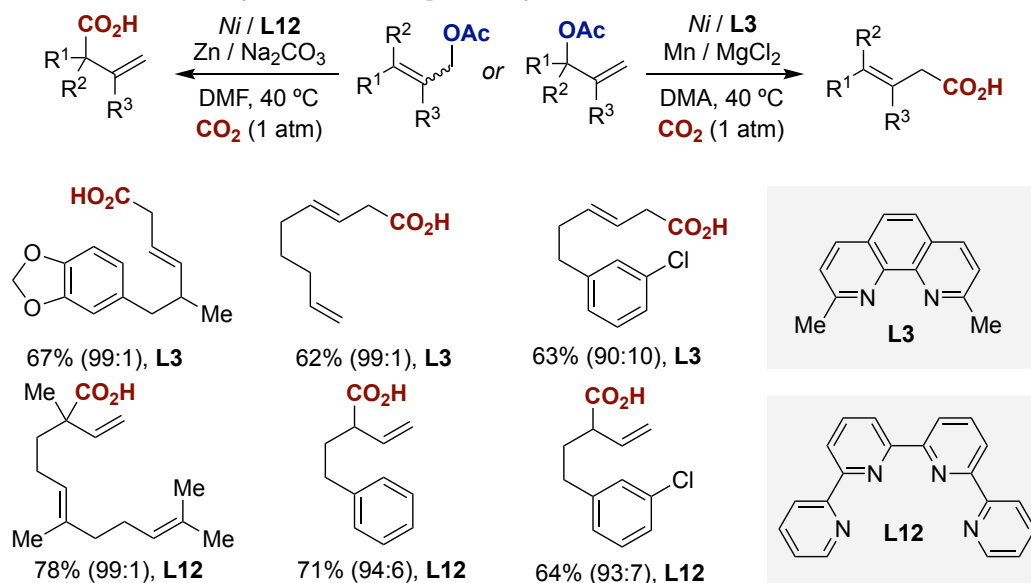
**Scheme 17.** Ni-catalyzed carboxylation of aliphatic tosylates.

Unlike activated organic sulfonates, less-attention has been devoted to simpler ester derivatives as C–O counterparts. Despite the high activation energy required for C–O scission and propensity for acyl C–O cleavage, our group designed a reductive carboxylation of aryl and benzyl ester derivatives (Scheme 18).<sup>68</sup> As expected, the choice of the ligand exerted a profound effect on the reactivity, with dppf being particularly suited for the carboxylation of aryl pivalates and  $\text{PMe}_3$  for the corresponding benzyl esters. Although non- $\pi$ -extended aryl or benzyl esters failed to furnish the targeted carboxylic acids, this limitation could be partially alleviated by using hemilabile groups, enabling a faster oxidative addition into the C–O bond while opening up vacant coordination sites for  $\text{CO}_2$  binding at the Ni center.



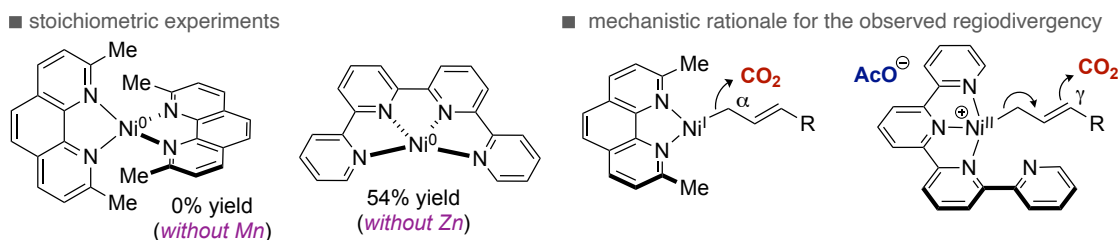
**Scheme 18.** Ni-catalyzed carboxylation of C(sp<sup>2</sup>)- and C(sp<sup>3</sup>)-O bonds.

In 2014, a Ni-catalyzed regiodivergent reductive carboxylation of allyl acetates with CO<sub>2</sub> was reported by our group, with site-selectivity dictated by the coordination geometry of the ligand utilized (Scheme 19).<sup>69</sup> In this manner, both  $\alpha$ -branched or linear carboxylic acids could be accessed regardless of the allyl acetate regioisomer utilized. While not fully understood, the reactivity could also be modulated by the appropriate selection of both reductant and additive, with Mn/MgCl<sub>2</sub> and Zn/Na<sub>2</sub>CO<sub>3</sub> being particularly suited for the carboxylation of linear and  $\alpha$ -branched allyl acetates, respectively.



**Scheme 19.** Ni-catalyzed regiodivergent carboxylation of allyl acetates

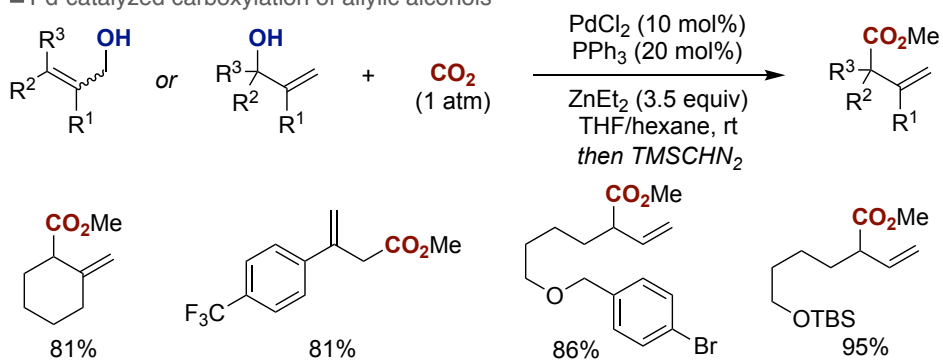
Stoichiometric experiments with Ni(0)(**L3**)<sub>2</sub> and Ni(0)**L12**, both of which characterized by X-ray diffraction, were particularly illustrative (Scheme 20). While the former necessarily required Mn for the reaction to occur, non-negligible yields of  $\alpha$ -branched product were observed with the latter in the absence of Zn. These results suggested a linear carboxylation via Ni(I) intermediates with **L3**, whereas a CO<sub>2</sub> insertion at the  $\gamma$ -position of well-defined alkyl-Ni(II) intermediates seems the most plausible avenue for **L12**, an interpretation that gains credence when comparing with the reactivity found by Hazari<sup>70</sup> and Iwasawa<sup>71,72</sup> with  $\sigma$ -bound Pd(II) pincer complexes.



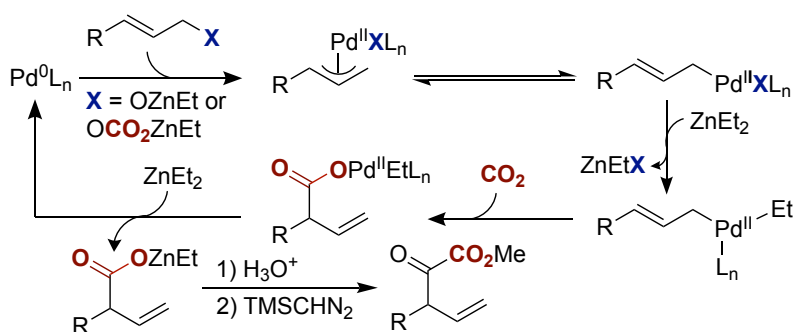
**Scheme 20.** Ni-catalyzed regiodivergent carboxylation of allyl acetates.

Given that C–O electrophiles ultimately derive from the corresponding alcohols, one could envision the possibility for effecting a direct carboxylation of these counterparts. However, the high polarizability of the O–H bond, together with the high activation energy required for effecting  $sp^3$  C–OH cleavage left a reasonable doubt that such a transformation would be viable. Mita and Sato described the first efforts towards this goal, culminating in a Pd-catalyzed carboxylation of allylic alcohols with Et<sub>2</sub>Zn as reducing agent, affording  $\alpha$ -branched carboxylic acids regardless of the regioisomer of the allylic alcohol utilized (Scheme 21).<sup>73</sup> It was proposed that the high Lewis acidity of the Zn(II) reagent triggered the formation of an alkoxylate that reacts reversibly with CO<sub>2</sub>, lowering down the activation energy for C–OH cleavage. The observed selectivity is indicative of  $\pi$ -allyl Pd(II) species that are in equilibrium with  $\eta^1$ -allyl Pd(II), setting the stage for a CO<sub>2</sub> insertion at the  $\gamma$ -position of the alkene.

■ Pd-catalyzed carboxylation of allylic alcohols



■ mechanistic rationale



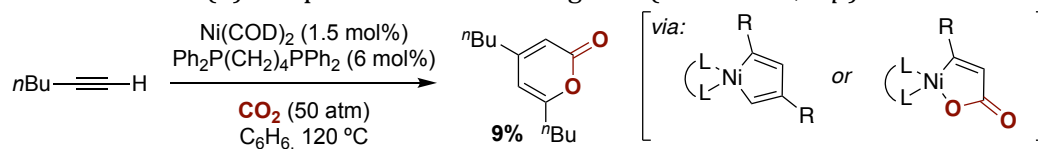
**Scheme 21.** Pd-catalyzed carboxylation of allylic alcohols.

## 5. Carboxylation of alkynes and alkenes.

The development of catalytic cross-coupling reactions of organometallic reagents and organic (pseudo)halides with CO<sub>2</sub> has led to a wide variety of synthetic alternatives to prepare valuable carboxylic acid derivatives via C–C bond-formation. Although robust and efficient protocols, the need for well-defined, stoichiometric organometallic reagents or pre-functionalized organic (pseudo)halides might hamper the application profile of these procedures. From a synthetic standpoint, the direct carboxylation of non-polarized substrates would be particularly advantageous. To such end, the use of simple unsaturated hydrocarbons is particularly attractive, constituting an opportunity to combine two chemical feedstocks towards valuable carboxylic acids.

### 5.1. Catalytic carboxylation of alkynes

The first studies on the catalytic carboxylation of alkynes with CO<sub>2</sub> were reported by Inoue in the late 70's.<sup>74–76</sup> Specifically, it was found that Ni and Co catalysts supported by phosphine ligands triggered a cycloaddition of CO<sub>2</sub> with terminal or internal alkynes, resulting in 2-pyrone derivatives in low to moderate yields (Scheme 22). The initial mechanistic proposal involved the formation of nickelacyclopentadienes via oxidative cyclization of two alkynes with the Ni(0) catalyst prior to CO<sub>2</sub> insertion. Mechanistic investigations by Walther, however, revealed the formation of oxanickelacyclopentene via the coupling of alkyne and CO<sub>2</sub> with Ni(0) active species.<sup>77,78</sup> Shortly after Inoue's work and contemporary to the discovery of nickelalactones with alkenes and CO<sub>2</sub>, Hoberg and co-workers first isolated oxanickelacyclopentene derivatives via the oxidative cyclization of alkynes and CO<sub>2</sub> with Ni(0) complexes and diamine ligands (Scheme 23, *top*).<sup>79–81</sup>



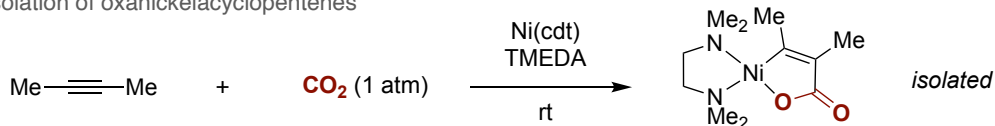
**Scheme 22.** Catalytic formation of 2-pyrone derivatives.

Oxanickelacyclopentenes are particularly stable compounds with versatile reactivity (Scheme 23, *bottom*). While direct protonolysis leads to the formation of acrylic acid derivatives, the coupling with CO and other aliphatic unsaturated compounds affords the preparation of products with different molecular complexity. Recently, oxanickelacyclopentenes<sup>82</sup> or structurally-related oxazirconacyclopentenes<sup>83</sup> have shown to react with alkyl electrophiles to afford fully substituted acrylic acids. The formation of oxanickelacyclopentenes was

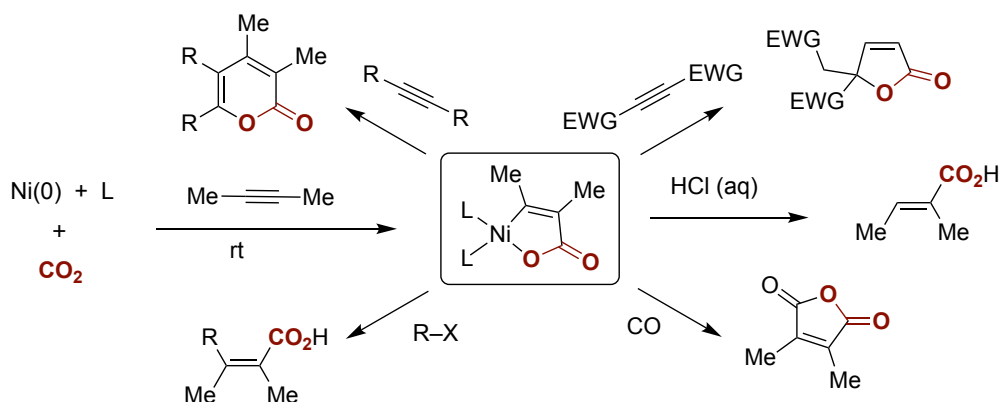


studied by DFT calculations, and indicated that unlike the coupling of alkenes and CO<sub>2</sub>, the reaction proceeds through an associative mechanism, involving the coordination of both alkyne and CO<sub>2</sub> to the Ni(0) complex prior to the cyclization.<sup>84-87</sup>

■ isolation of oxanickelacyclopentenones



■ reactivity of oxanickelacyclopentenones

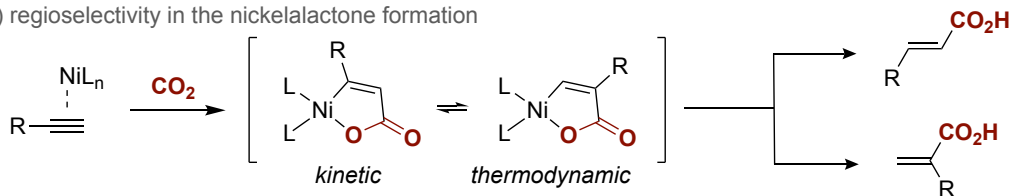


**Scheme 23.** Oxanickelacyclopentenones formation and reactivity (cdt = cyclododecatriene).

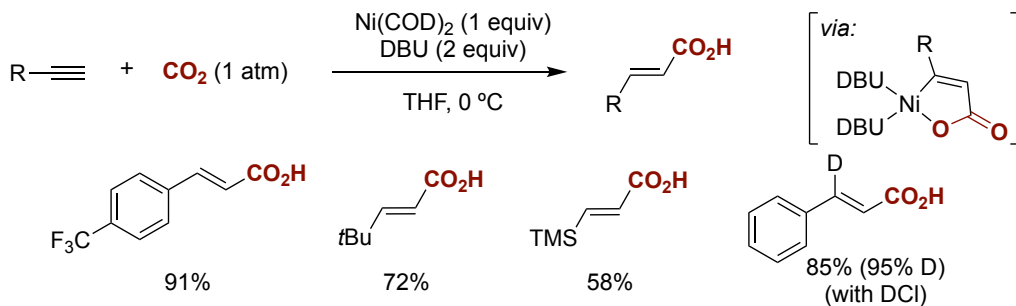
In 1999, Saito and Yamamoto reported the preparation of  $\beta$ -substituted acrylic acids from the cross-coupling of terminal alkynes with CO<sub>2</sub> via protonolysis of oxanickelacyclopentenones (Scheme 24, *a*).<sup>88</sup> Regardless the electronic nature of the substrates, almost exclusive formation of the  $\beta$ -substituted isomer was observed. The regioselectivity was later rationalized by DFT calculations, suggesting a subtle thermodynamic vs kinetic control. Specifically, formation of oxanickelacyclopentene resulting from CO<sub>2</sub> attack to the substituted carbon is thermodynamically favoured, whereas the insertion at a distal position is kinetically preferred due to a markedly lower energy barrier (Scheme 24, *b*). As for other cross-coupling reactions, Iwasawa demonstrated that the nature of the ligand might dictate the regioselectivity pattern in Ni-mediated carboxylation reactions of terminal alkynes (Scheme 24, *c*).<sup>89</sup> In particular, methylene-substituted bis(amidine)ligands selectively afforded  $\beta$ -substituted acrylic acids whereas less-sterically encumbered ligands resulted in a regioselectivity switch, giving rise to  $\alpha$ -substituted acrylic acids in lower yields.

## Chapter 1

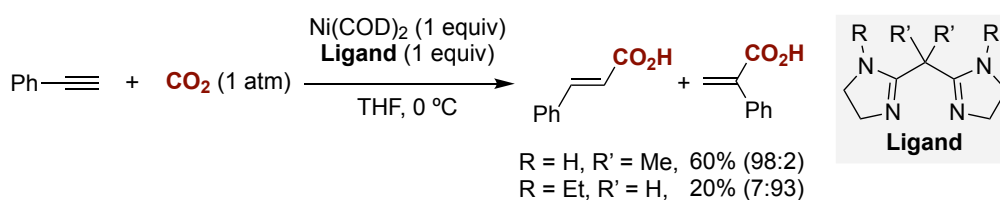
a) regioselectivity in the nickelalactone formation



b) hydrocarboxylation of terminal alkynes

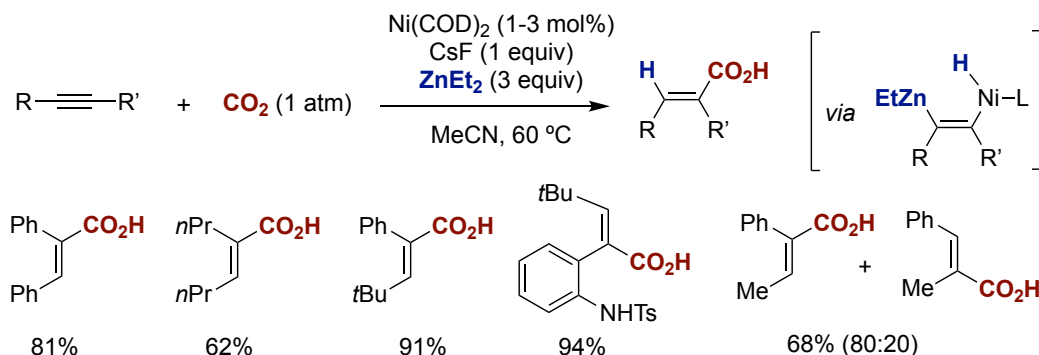


c) Iwasawa's regioselectivity switch



**Scheme 24.** Stoichiometric hydrocarboxylation of alkynes.

In retrospect, it is evident that these stoichiometric experiments set the standards for designing catalytic carboxylation of alkynes with  $\text{CO}_2$ . Among these, considerable research has been devoted to the implementation of hydrocarboxylation reactions, as it might constitute a rapid entry to acrylic acids, and an alternative to the existent oxidative coupling of olefins with  $\text{CO}_2$  that remain primarily restricted to the coupling of ethylene as coupling partner.<sup>90</sup> In 2011, Ma disclosed a catalytic hydrocarboxylation of alkynes using  $\text{Ni}(0)$  catalysts and  $\text{Et}_2\text{Zn}$  as reducing agent (Scheme 25).<sup>91</sup> If unsymmetrically substituted alkynes were utilized,  $\text{CO}_2$  insertion occurred adjacent to the aromatic substituent. This observation is consistent with a formal Markovnikov hydrozincation, where the metal center is adjacent to the aromatic motif, prior to  $\text{CO}_2$  insertion. Similarly, the same authors later reported a methyl-carboxylation of homopropargylic alcohols under similar reaction conditions.<sup>92</sup> Independently, Tsuji and Fujihara described a  $\text{Cu}$ -catalyzed hydrocarboxylation of alkynes with similar yields and regioselectivities as Ma's protocol.<sup>93</sup>

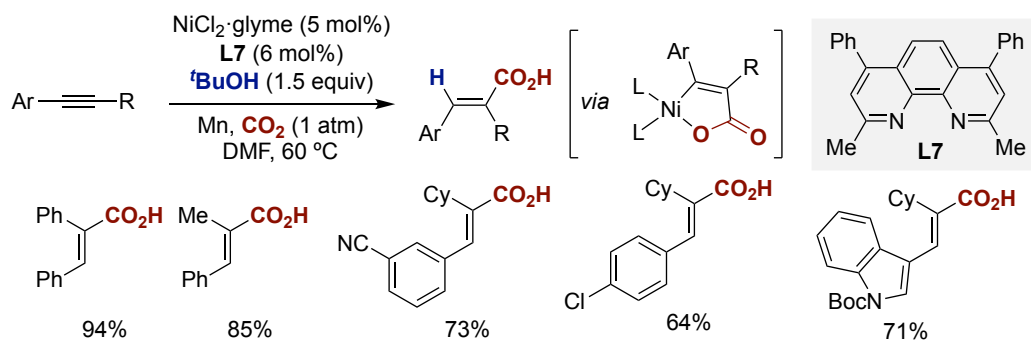


**Scheme 25.** Catalytic hydrocarboxylation of alkynes with well-defined hydrides.

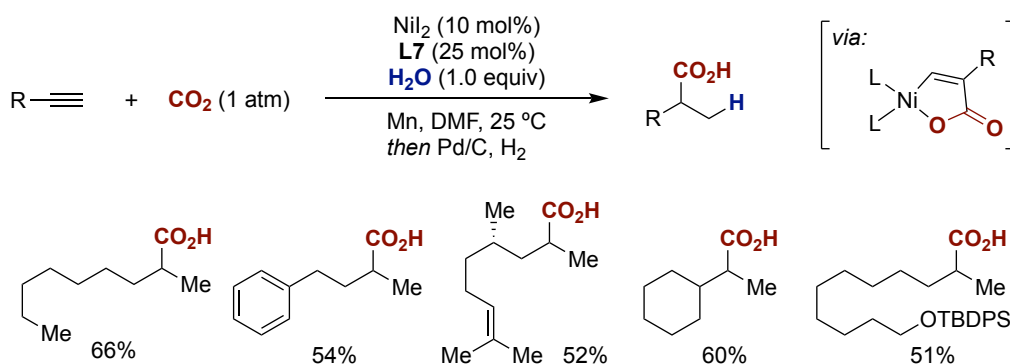
Challenged by the need for either well-defined organometallic reagents or high-molecular silanes as formal hydride precursors, our group described two Ni-catalyzed hydrocarboxylation protocols using more available and benign hydride sources. In 2015, it was found that simple alcohols can be used as formal hydride sources in a mild Ni-catalyzed regioselective hydrocarboxylation of alkynes, a finding that allowed to expand significantly the functional group tolerance of these protocols (Scheme 26, *top*).<sup>94</sup> CO<sub>2</sub> insertion took place exclusively at a distal position to the aromatic site, independently of the substitution pattern at the alkyne terminus. Such an intriguing regioselectivity profile can be attributed to the formation of two electronically and sterically-differentiated oxanickelacyclopentene intermediates that might be in rapid equilibrium prior selective protonation with the alcohol motif. A final reduction event with Mn recovers back the active Ni(0)L<sub>n</sub> species. Following a similar mechanistic rationale, aliphatic terminal and internal alkynes could also be employed as counterparts, using water as the formal hydride source, ultimately generating α-branched aliphatic carboxylic acids (Scheme 26, *bottom*).<sup>95</sup> Such outcome is consistent with the formation of an intermediate oxanickelacyclopentene that locates the metal catalyst at the less-hindered site followed by reductive protonation with water and Mn as the terminal reductant. Subsequent reduction with H<sub>2</sub> over Pd/C delivers the targeted carboxylic acid. More recently, Sato reported the hydrocarboxylation of ynamides with water and Zn as reducing agent.<sup>96</sup>

## Chapter 1

### ■ Catalytic hydrocarboxylation of aromatic alkynes with *t*BuOH



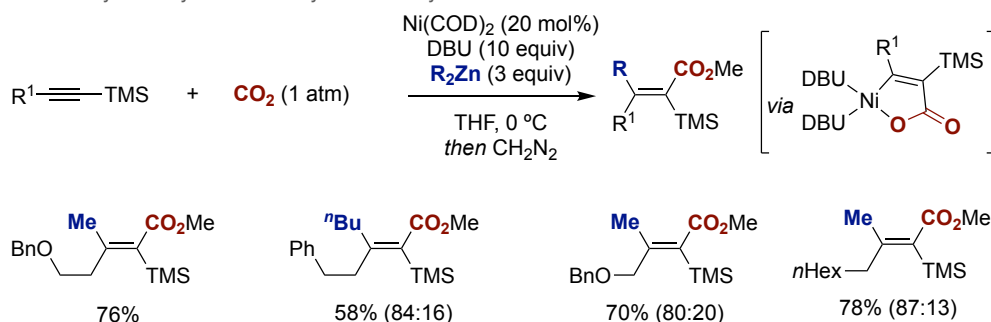
### ■ Catalytic hydrocarboxylation of aliphatic alkynes with H<sub>2</sub>O



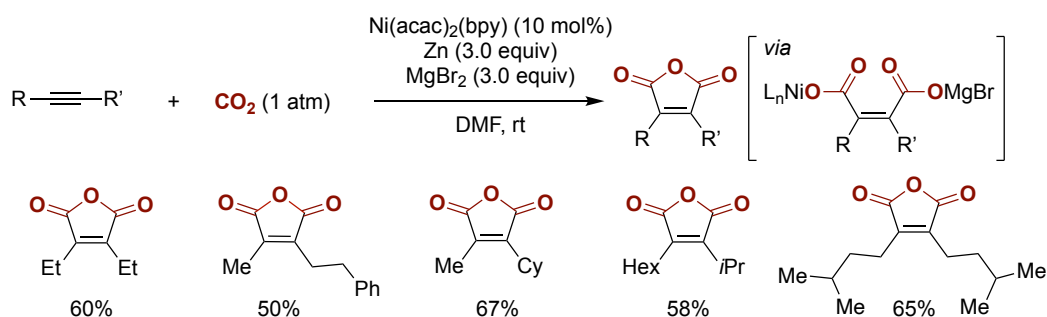
**Scheme 26.** Catalytic hydrocarboxylation of alkynes using alcohols and water.

The site-selective controllable addition of a both carbon synthon and CO<sub>2</sub> across an alkyne would be a particularly attractive endeavor in the carboxylation field. To such end, Mori reported a Ni-catalyzed alkylative carboxylation of silyl-substituted alkynes using organozinc reagents as nucleophilic partners (Scheme 27, *top*).<sup>97</sup> The method allows rapid access to tetrasubstituted acrylic acids, likely via nickelalactone intermediates, in which the nickel catalyst is located distal to the silyl group due to both electronic and steric effects. Such interpretation was later corroborated by theoretical calculations. The regioselectivity pattern was controlled by a preferential *syn*-carboxylation across the alkyne, with CO<sub>2</sub> insertion occurring adjacent to the amine moiety. Tsuji and Fujihara demonstrated the feasibility of triggering multiple CO<sub>2</sub> insertions across the alkyne, obtaining the corresponding maleic anhydrides with Zn as reducing agent (Scheme 27, *bottom*).<sup>98</sup> The presence of Lewis acidic MgBr<sub>2</sub> was essential for the second carboxylation to occur, suggesting that the Lewis acid might facilitate the ring opening of the oxanickelacyclopentene intermediate prior CO<sub>2</sub> insertion into the Ni-C bond.

■ Ni-catalyzed alkylative carboxylation of alkynes



■ Ni-catalyzed double carboxylation of alkynes

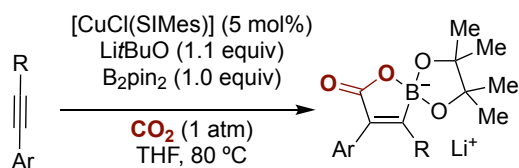


**Scheme 27.** Catalytic alkylative carboxylation of alkynes.

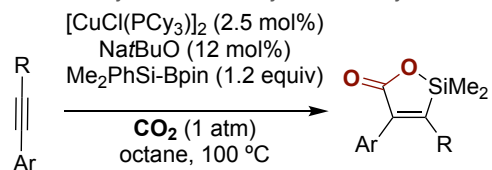
While nickel catalysts proved to be particularly competent for hydrocarboxylations and dicarbofunctionalizations of alkynes with  $CO_2$ , copper catalysts turned out to be suited for effecting heterocarboxylation reactions. In 2012, Hou developed a Cu-catalyzed boracarboxylation of internal alkynes with  $B_2pin_2$  under basic conditions, resulting in the preparation of a variety of  $\alpha,\beta$ -unsaturated  $\beta$ -boralactone derivatives (Scheme 28, *left*).<sup>99</sup> Shortly after, Tsuji and Fujihara disclosed a structurally-related Cu-catalyzed silacarboxylation of alkynes with  $PhMe_2SiBpin$  en route to  $\alpha,\beta$ -unsaturated  $\beta$ -silalactones (Scheme 28, *right*).<sup>100</sup> Both reactions are believed to proceed via similar pathways in which the presence of the base mediates the formation of either Cu-Bpin or Cu-SiMe<sub>2</sub>Ph species which are added across the alkyne prior to  $CO_2$  insertion. As anticipated, the regioselectivity can be interpreted on the basis of a preferential boryl or silyl cupration in which the Cu atom is located adjacent to the arene or a  $\pi$ -component, invariably leading to the targeted carboxylic acid by  $CO_2$  insertion into the C-Cu bond.

## Chapter 1

### ■ Cu-catalyzed boracarboxylation of alkynes



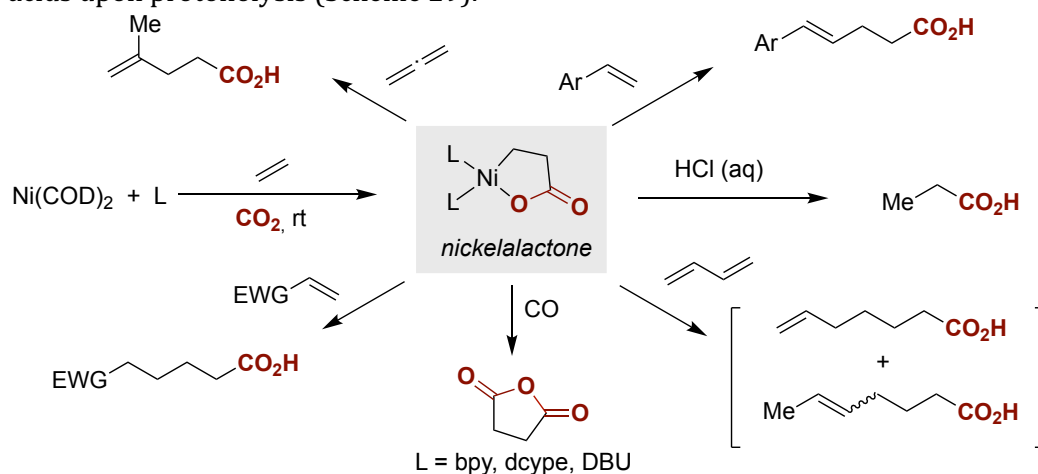
### ■ Cu-catalyzed silacarboxylation of alkynes



**Scheme 28.** Cu-catalyzed bora- and silacarboxylation of alkynes.

## 5.2. Catalytic carboxylation of alkenes

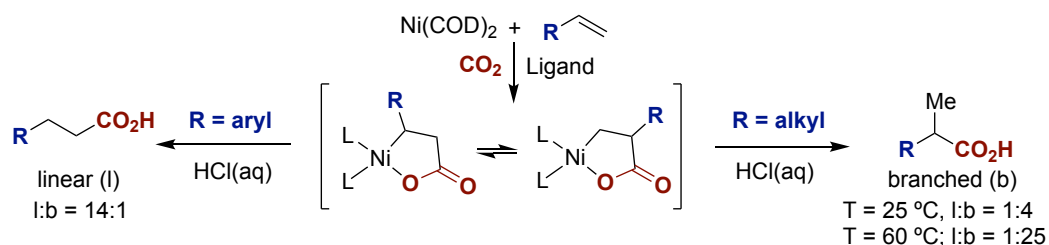
The first catalytic procedure for incorporating CO<sub>2</sub> into alkenes was reported in 1978 by Lapidus and co-workers.<sup>101</sup> Specifically, the authors demonstrated the feasibility of a previously considered inaccessible transformation, allowing to access propionic acid from ethylene and CO<sub>2</sub> by using Rh and Pd heterogeneous catalysts. This discovery fueled a revolution, setting the basis for new developments in this area. For instance, Höberg showed that electron-rich Ni(0) complexes could be engaged in an oxidative cyclization of olefins with CO<sub>2</sub> in the presence of imine, diimine and phosphine ligands, giving rise to nickelalactones that afforded propionic acids upon protonolysis (Scheme 29).<sup>102-104</sup>



**Scheme 29.** Nickelalactone formation and reactivity.

Nickelalactones turned out to be superb reaction intermediates, resulting in a formal homologation reaction that allowed to access high-ordered carboxylic acids by coupling with styrenes, 1,3-dienes, allenes or carbon monoxide, among others (Scheme 29).<sup>105</sup> Although regioselectivity issues might arise when using monosubstituted olefins, the site-selectivity could be controlled by a subtle temperature modulation and/or the electronic features of the alkene (Scheme 30).<sup>106</sup> For example, styrenes form preferentially nickelalactones with the metal center located at the most stable benzylic position. In sharp contrast,  $\alpha$ -olefins give rise to a mixture of nickelalactones at room temperature that are in dynamic equilibrium. A seemingly trivial raise in temperature favors the formation of the less-sterically congested nickelalactone. As anticipated, the ligand played a crucial role on site-selectivity. Specifically, good yields could be obtained with phosphines and electron-rich imines whereas disproportionation of CO<sub>2</sub> to form CO was observed when using bipyridine ligands. More recently, an improved site-selectivity

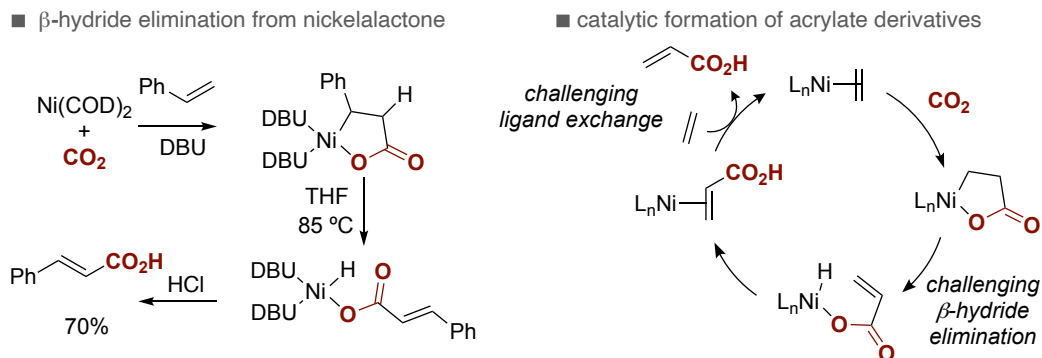
with aliphatic olefins was observed with more sophisticated pyridyl-phosphine ligands,<sup>107,108</sup> and even the rather elusive trisubstituted alkenes could be within reach as well.<sup>109</sup> The formation of nickelalactones via oxidative cyclization has also been investigated by DFT calculations, concluding that the metallacycle is formed by an ethylene-coordinated Ni(0) intermediate.<sup>110-113</sup> Subsequently, CO<sub>2</sub> formally attacks the olefin followed by an outer sphere pathway in which previous coordination of CO<sub>2</sub> to the metal center is not indispensable for the nickelalactone formation.<sup>114</sup> The formation of five-membered metallalactones should by no means be limited to the oxidative cyclization of unsaturated hydrocarbons with Ni(0) species. Indeed, Ti(II),<sup>115</sup> Zr(II)<sup>116</sup> and Fe(0)<sup>117</sup> complexes have shown to be competent for the formation of oxametallacyclopentanones with ethylene and CO<sub>2</sub> as coupling partners.



**Scheme 30.** Substrate-controlled regioselectivity in the formation of nickelalactones.

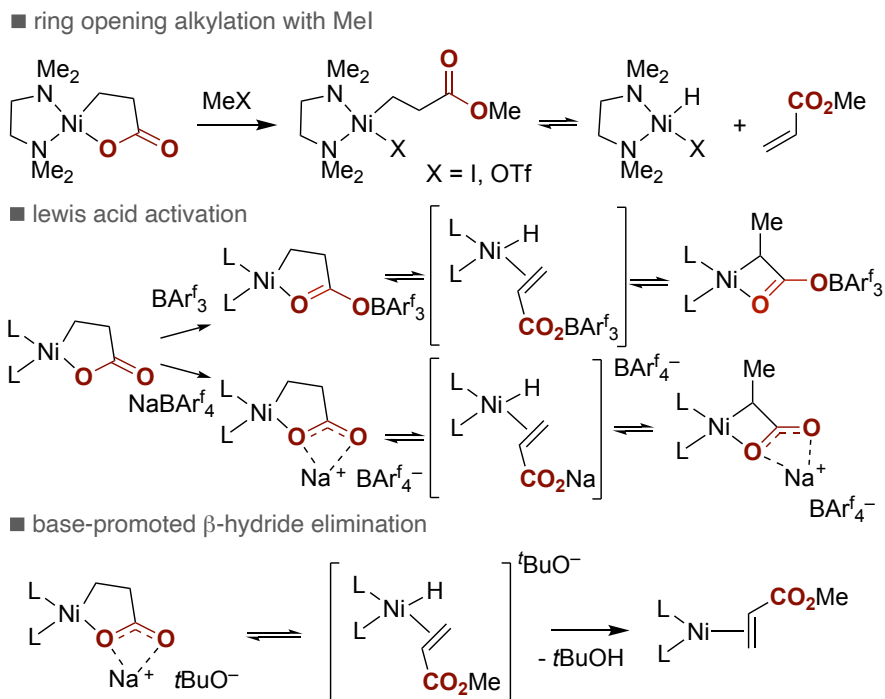
The cross-coupling reaction of ethylene and CO<sub>2</sub> for the preparation of acrylic acid, a building block of utmost relevance in industry, ranks amongst the most studied reactions in both academic and industrial laboratories. Although important milestones have been achieved during the last 30 years, the oftentimes denominated ‘dream reaction’ is still considered a rather challenging process.<sup>118</sup> The origin of such interest can be traced back from the pioneering studies reported by Hoberg, that observed the formation of  $\alpha,\beta$ -unsaturated carboxylic acids from nickelalactones upon raising the temperature to 85 °C (Scheme 31, *left*).<sup>104</sup> This result demonstrated the feasibility for promoting a  $\beta$ -hydride elimination from nickelalactones, a rather intriguing observation taking into consideration that such a complex might not easily establish the required syn conformation required for  $\beta$ -elimination events. Driven by these precedents, one could easily envision a catalytic cycle for preparing acrylic acid from CO<sub>2</sub> and ethylene (Scheme 31 *right*). However, the implementation of a catalytic route for the preparation of acrylic acid from ethylene is considerably more complicated than one might anticipate. This is due to the fact that (a) the overall transformation is highly endothermic;<sup>119</sup> (b) the kinetic barrier for  $\beta$ -hydride elimination is particularly high and (c) the ethylene/acrylic acid ligand exchange that recovers back the active Ni(0) species is not trivial to say the least.





**Scheme 31.** Acrylate formation from ethylene and CO<sub>2</sub>.

In 2006, Walther studied the formation of acrylate from nickelalactones in the presence of bidentate ligands.<sup>120</sup> Interestingly, the presence of acrylate was detected with bis(diphenylphosphino)methane, resulting in the formation of a rather stable Ni(I)–Ni(I) dimer. Encouraged by these empirical evidences, theoretical calculations were carried out to shed light on the critical features that assist the  $\beta$ -hydride elimination step.<sup>121</sup> As anticipated, DFT studies confirmed that the agostic Ni–H interaction in the corresponding nickelalactone is energetically uphill due to a considerable ring strain. Consequently, it was predicted that an elongation of the Ni–O bond would facilitate  $\beta$ -hydride elimination, thus serving as an inspiration for designing a catalytic route for producing acrylic acids from CO<sub>2</sub>. Riecker and Kühn showed that  $\beta$ -hydride elimination could be affected by exposure to a methylating agent (MeI), delivering the corresponding methyl acrylate (Scheme 32, *top*).<sup>122,123</sup> Bernskoetter and co-workers devised a different strategy consisting of ring-opening of the nickelalactone intermediate by Lewis acids (Scheme 32, *middle*).<sup>124</sup> Subsequent theoretical investigations disclosed that the addition of a base was also effective to capture the Ni hydride intermediate and deliver the desired acrylate (Scheme 32, *bottom*).<sup>125</sup>

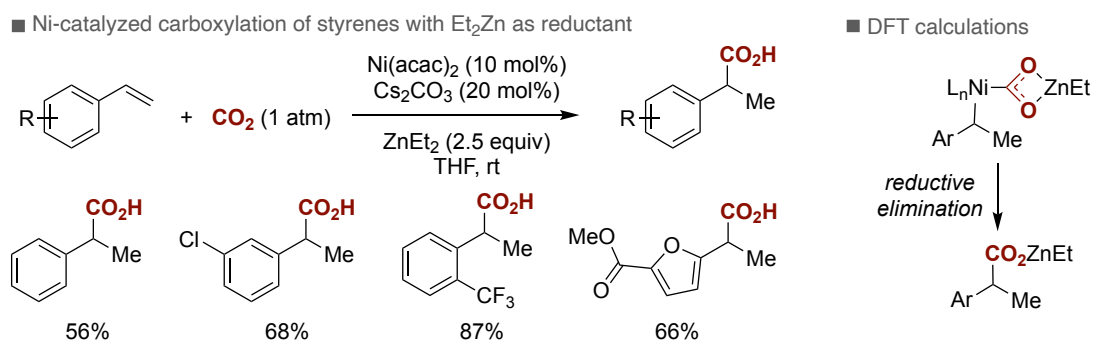


**Scheme 32.** Strategies to promote  $\beta$ -hydride elimination in nickelalactones.

In 2012, Limbach and co-workers put together all these stoichiometric investigations and attempted the first catalytic carboxylation of ethylene with  $\text{CO}_2$  using a bidentate phosphine ligand and  $\text{Na}^t\text{BuO}$  as the exogenous base.<sup>126</sup> It became quickly apparent that a subtle balance of all of the elementary steps within the catalytic cycle would be critical for success. For example, while nickelalactone formation typically proceed at high pressures of  $\text{CO}_2$ , the subsequent steps needed to be carried out at lower pressures of  $\text{CO}_2$  due to the formation of carbonic acid esters with the base. Although other reaction conditions were reported, including the use of metal alkoxides as bases,<sup>127</sup> the following investigations were directed to find a base with a subtle balance of nucleophilicity and basicity, which could be compatible with all of the individual steps within the catalytic cycle. In this context, Schaub and Limbach found that the use of substituted metal phenoxides efficiently promote the formation of the acrylate  $\text{Ni}(0)$  complex in the presence of  $\text{CO}_2$ , allowing to obtain the targeted metal acrylates from ethylene and  $\text{CO}_2$  in up to 107 TONs.<sup>128,129</sup> Following a different strategy, Vogt and co-workers tackled the critical  $\beta$ -hydride elimination step by using a strong Lewis acid such as lithium iodide in the presence of trimethylamine as base, obtaining the corresponding lithium acrylates.<sup>130</sup> Despite the advances realized, there is ample consensus that these protocols are still far from

being implemented at an industrial scale, suggesting that more research should be conducted for a more efficient production of acrylic acid from CO<sub>2</sub>.

Prompted by the stoichiometric studies by Höberg, the chemical community has been challenged to devise catalytic carboxylations of alkenes other than ethylene. In 2008, Rovis reported the Ni-catalyzed hydrocarboxylation of styrenes by using Et<sub>2</sub>Zn as reducing agent, resulting in the corresponding phenyl acetic acids (Scheme 33).<sup>131</sup> The authors excluded the intermediacy of nickelalactones, favoring a mechanism consisting of putative nickel hydride intermediates generated upon transmetalation/ $\beta$ -hydride elimination with Et<sub>2</sub>Zn. Such interpretation gained credence by deuterium labelling experiments, thus ruling out a mechanism consisting of an initial oxidative cyclization. DFT calculations by Lin and Yuan subsequently revealed that while the generation of nickelalactone was thermodynamically favored, the involvement of nickel hydrides was kinetically driven.<sup>132</sup> Moreover, theoretical calculations confirmed a dual role for Et<sub>2</sub>Zn, acting both as hydride source and as Lewis acid that might facilitate the reaction of the transient benzyl nickel(II) intermediate with CO<sub>2</sub>.

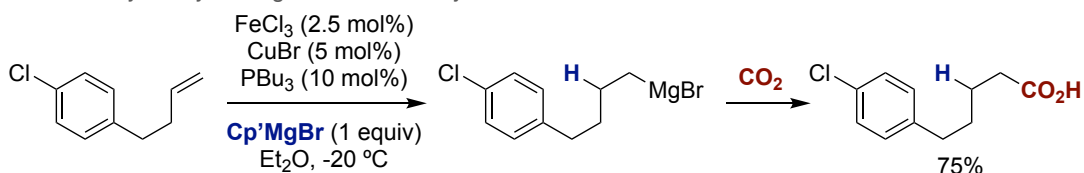


**Scheme 33.** Rovis' hydrocarboxylation of styrenes.

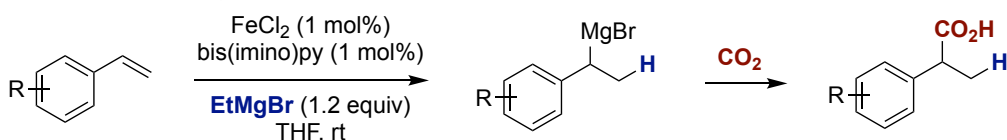
In 2012, Hayashi and Shirakawa reported an Fe/Cu-catalyzed tandem hydromagnesiation/carboxylation of a variety of alkenes via iron hydride intermediates.<sup>133</sup> Of particular relevance was the ability to use unactivated alkenes as substrates, resulting in the corresponding primary alkyl Grignard reagents that ultimately generate, upon exposure to CO<sub>2</sub>, the targeted linear carboxylic acids with excellent levels of regioselectivity (Scheme 34, *top*). Prompted by these studies, Thomas reported a similar approach towards phenyl acetic acids from electron-rich styrenes using an Fe/(bis)imino-pyridine couple and Grignard reagents as hydride sources (Scheme 34, *middle*).<sup>134</sup> The use of EtMgBr resulted in preferential formation of branched carboxylic acids. Intriguingly, a linear selectivity was predominantly observed with cyclopentyl magnesium bromide, revealing the non-innocent character of the hydride source on site-selectivity. While the authors did not include

a rationale behind these results, one might argue that this finding is likely due to the binding of the cyclopentene to the iron intermediate, increasing the steric hindrance of the hydride entity and favoring the hydrometalation at the homobenzylic position. Prompted by these precedents, Xi showed that titanium precatalysts could be used in an alkene hydromagnesiation followed by carboxylation in the presence of Grignard reagents (Scheme 34, *bottom*).<sup>135</sup> As for Hayashi and Shirakawa, the utilization of terminal olefins gave rise to the corresponding linear carboxylic acids.

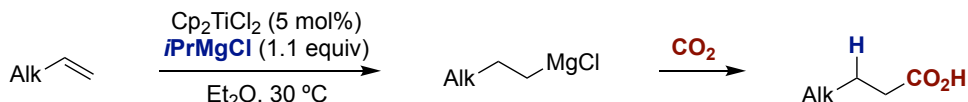
■ Fe/Cu-catalyzed hydromagnesiation/carboxylation of alkenes



■ Fe-catalyzed hydromagnesiation/carboxylation of styrenes



■ Ti-catalyzed hydromagnesiation/carboxylation of olefins

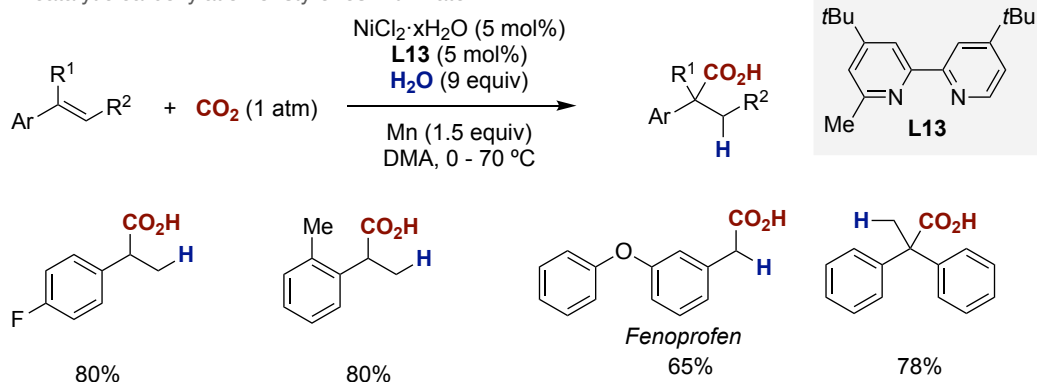


**Scheme 34.** Catalytic hydromagnesiation/carboxylation reactions.

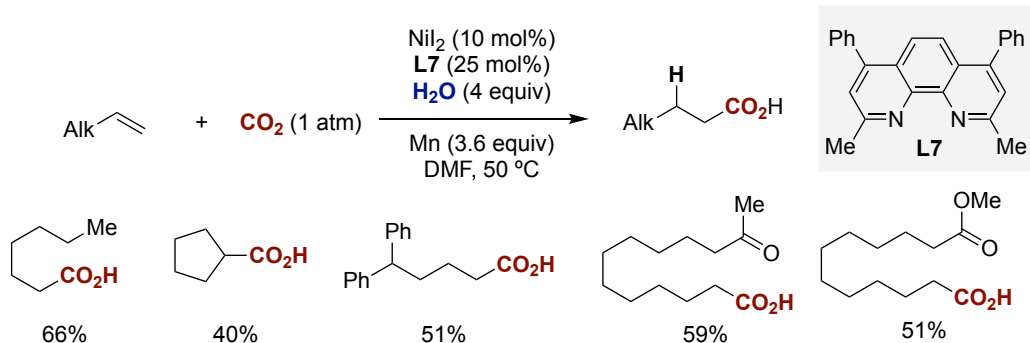
Aimed at fundamentally alter the effective discrimination of  $\text{CO}_2$  incorporation across an alkene backbone in the absence of either organometallic reagents or hazardous  $\text{CO}$ , our group has recently described the ability of harnessing water as an inexpensive hydride source in catalytic hydrocarboxylation of a wide range of alkene derivatives with  $\text{CO}_2$  at atmospheric pressure (Scheme 35, *top*).<sup>95</sup> The mild conditions achieved could be translated into a high chemoselectivity profile in the presence of multiple number of functional groups. This protocol could be extended to unactivated olefins, compounds produced in bulk from the ethylene oligomerization, providing an opportunity to repurpose three chemical feedstocks ( $\text{H}_2\text{O}$ , alkene and  $\text{CO}_2$ ) in a controllable fashion (Scheme 35, *middle*). In a formal sense, this method is complementary to that shown for the hydrocarboxylation of terminal alkynes in which branched carboxylic acids were exclusively obtained under otherwise similar conditions.<sup>95</sup> As alkynes and alkenes can be easily interconverted by common chemical methods, these results constitute a formal regiodivergent scenario by which either linear or branched carboxylic acids can be

accessed from simple unsaturated hydrocarbons. This technique could be extended to the coupling of ethylene, the largest volume chemical produced annually, thus affording propionic acid, albeit with low TONs. Mixtures of internal olefins could also be carboxylated under otherwise identical reaction conditions, obtaining exclusively the linear carboxylic acid (Scheme 35, *bottom*). This result arises from a “chain-walking” migration of the Ni catalyst throughout the aliphatic chain prior to the carboxylation step, suggesting that water can be used in lieu of commonly-employed stoichiometric organometallic reagents or high-molecular weight silanes as hydride sources in chain-walking scenarios.<sup>136</sup>

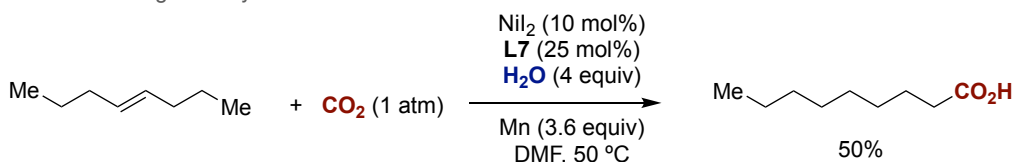
■ catalytic carboxylation of styrenes with water



■ catalytic carboxylation of unactivated terminal olefins with water

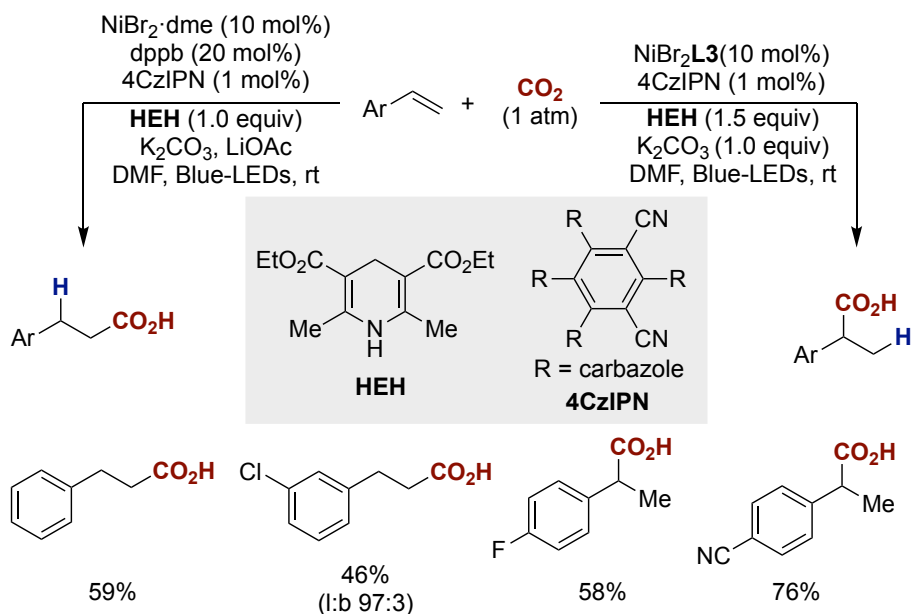


■ chain walking carboxylation of internal olefins to linear acids



**Scheme 35.** Ni-catalyzed hydrocarboxylation of olefins with CO<sub>2</sub> and H<sub>2</sub>O.

Recently, the König group described the merger of transition metal catalysis and photocatalysis for the hydrocarboxylation of styrenes and electrondeficient alkenes. Specifically, they found that a protocol based on Hantzsch ester as terminal reductant and 4CzIPN as photosensitizer provided the best results under high-intensity Blue-LED irradiation when combined with a cocktail of inorganic bases such as  $K_2CO_3$  and LiOAc (Scheme 36).<sup>137</sup> Apart from providing a powerful alternative to classical carboxylation technologies based on the utilization of metal reductants, the authors found that regiodivergency can be dictated by the ligand employed; while bidentate phosphines provided access to linear carboxylic acids, 1,10-phenanthrolines possessing *ortho*-substituents (**L3**) afforded phenyl acetic acids instead. While the requirement for 4CzIPN, Hantzsch ester as well as the combination of  $K_2CO_3$  and LiOAc is not yet fully understood, the observed outcome is consistent with a dual pathway by which nickel hydride species are obtained with a **L3** regime whereas the intermediacy of nickelalactones are the most plausible scenario with dppb.



**Scheme 36.** Photocatalyzed hydrocarboxylation of styrenes and electrondeficient alkenes with  $CO_2$ .

**General Objectives of this Doctoral Thesis:**

The ubiquity and importance of carboxylic acids in peptides, pharmaceuticals, agrochemicals and synthetical materials encourages the development of novel carboxylation methods. A particular interest is given to the design of new and alternative chemical transformations that complement and expand the scope of traditional carboxylic acid formation, which occurs via the oxidation of alcohols or aldehydes, the hydrolysis of nitriles or more recently by the utilization of toxic carbon monoxide with transition metal catalysis or CO<sub>2</sub> with high polar organometallics. In this regard, the discovery of atom-economical catalytic carboxylation protocols with CO<sub>2</sub> that display high chemoselectivity represents a worthwhile endeavor.

One of the main interests of our research group has been the development of novel nickel-catalyzed reductive cross-coupling reactions. In the last years we have focused our efforts towards the utilization of CO<sub>2</sub> and the isoelectronic isocyanates, for the synthesis of carboxylic acids and amides. These methodologies were extended to more challenging unactivated electrophiles and readily available olefins, as described above.

The general objective of the work presented in this dissertation is to develop new nickel-catalyzed carboxylation methods, opening new opportunities for the use of CO<sub>2</sub> in combination with available and abundant allylic alcohols or 1,3-dienes. We also explored the use of other heteroallenes (isocyanates) in reductive cross-coupling regimes, in particular its combination with alkyl bromides in the presence and absence of “chain walking” scenarios. Furthermore, we sought to contribute to the understanding of the mechanisms of these transformations, with the aim of building up new knowledge in the area of Ni-catalyzed reductive cross-coupling reactions. That being set, we envisioned the development of new radiolabeling techniques to prepare labeled carboxylic acids with isotopically enriched CO<sub>2</sub>, shortening and providing a direct access for labeled drugs and pharmaceuticals.

**Bibliography**

- (1) *Metal-Catalyzed Cross-Coupling Reactions and More: DeMeijere/Metal-Catalyzed Cross-Coupling Reactions and More*; de Meijere, A., Bräse, S., Oestreich, M., Eds.; Wiley-VCH Verlag GmbH & Co. KGaA: Weinheim, Germany, 2014. <https://doi.org/10.1002/9783527655588>.
- (2) *Metal-Catalyzed Cross-Coupling Reactions*, 1st ed.; de Meijere, A., Diederich, F., Eds.; Wiley, 2004. <https://doi.org/10.1002/9783527619535>.
- (3) The Nobel Prize in Chemistry 2010 <https://www.nobelprize.org/prizes/chemistry/2010/summary/> (accessed May 15, 2020).
- (4) Knappke, C. E. I.; Grupe, S.; Gärtner, D.; Corpet, M.; Gosmini, C.; Jacobi von Wangelin, A. Reductive Cross-Coupling Reactions between Two Electrophiles. *Chemistry – A European Journal* **2014**, *20* (23), 6828–6842. <https://doi.org/10.1002/chem.201402302>.
- (5) Wurtz, A. Ueber eine neue Klasse organischer Radicale. *Ann. Chem. Pharm.* **1855**, *96*(3), 364–375. <https://doi.org/10.1002/jlac.18550960310>.
- (6) Tollens, B.; Fittig, R. Ueber Die Synthese Der Kohlenwasserstoffe Der Benzolreihe. *Justus Liebigs Annalen der Chemie* **1864**, *131* (3), 303–323. <https://doi.org/10.1002/jlac.18641310307>.
- (7) Ullmann, F.; Bielecki, J. Ueber Synthesen in Der Biphenylreihe. *Berichte der deutschen chemischen Gesellschaft* **1901**, *34* (2), 2174–2185. <https://doi.org/10.1002/cber.190103402141>.
- (8) Okude, Y.; Hirano, S.; Hiyama, T.; Nozaki, H. Grignard-Type Carbonyl Addition of Allyl Halides by Means of Chromous Salt. A Chemospecific Synthesis of Homoallyl Alcohols. *J. Am. Chem. Soc.* **1977**, *99* (9), 3179–3181. <https://doi.org/10.1021/ja00451a061>.
- (9) Jin, Haolun.; Uenishi, Junichi.; Christ, W. J.; Kishi, Yoshito. Catalytic Effect of Nickel(II) Chloride and Palladium(II) Acetate on Chromium(II)-Mediated Coupling Reaction of Iodo Olefins with Aldehydes. *J. Am. Chem. Soc.* **1986**, *108* (18), 5644–5646. <https://doi.org/10.1021/ja00278a057>.
- (10) Schiavon, G.; Bontempelli, G.; Corain, B. Coupling of Organic Halides Electrocatalyzed by the Ni(II)/Ni(I)/Ni(0)-PPh<sub>3</sub> System. A Mechanistic Study Based on an Electroanalytical Approach. *J. Chem. Soc., Dalton Trans.* **1981**, No. 5, 1074–1081. <https://doi.org/10.1039/DT9810001074>.
- (11) Amatore, Christian.; Jutand, Anny. Rates and Mechanism of Biphenyl Synthesis Catalyzed by Electrogenerated Coordinatively Unsaturated Nickel Complexes. *Organometallics* **1988**, *7* (10), 2203–2214. <https://doi.org/10.1021/om00100a019>.
- (12) Amatore, C.; Jutand, A. Activation of Carbon Dioxide by Electron Transfer and Transition Metals. Mechanism of Nickel-Catalyzed Electrocarboxylation of Aromatic Halides. *J. Am. Chem. Soc.* **1991**, *113* (8), 2819–2825. <https://doi.org/10.1021/ja00008a003>.
- (13) Durandetti, M.; Nédélec, J.-Y.; Périchon, J. Nickel-Catalyzed Direct Electrochemical Cross-Coupling between Aryl Halides and Activated Alkyl Halides. *J. Org. Chem.* **1996**, *61* (5), 1748–1755. <https://doi.org/10.1021/jo9518314>.
- (14) Perkins, R. J.; Pedro, D. J.; Hansen, E. C. Electrochemical Nickel Catalysis for Sp<sup>2</sup>-Sp<sup>3</sup> Cross-Electrophile Coupling Reactions of Unactivated Alkyl Halides. *Org. Lett.* **2017**, *19* (14), 3755–3758. <https://doi.org/10.1021/acs.orglett.7b01598>.
- (15) Perkins, R. J.; Hughes, A. J.; Weix, D. J.; Hansen, E. C. Metal-Reductant-Free Electrochemical Nickel-Catalyzed Couplings of Aryl and Alkyl Bromides in Acetonitrile. *Org. Process Res. Dev.* **2019**, *23* (8), 1746–1751. <https://doi.org/10.1021/acs.oprd.9b00232>.
- (16) Sengmany, S.; Vitu-Thiebaud, A.; Le Gall, E.; Condon, S.; Léonel, E.; Thobie-Gautier, C.;



- Pipelier, M.; Lebreton, J.; Dubreuil, D. An Electrochemical Nickel-Catalyzed Arylation of 3-Amino-6-Chloropyridazines. *J. Org. Chem.* **2013**, *78* (2), 370–379. <https://doi.org/10.1021/jo3022428>.
- (17) Kumar, G. S.; Peshkov, A.; Brzozowska, A.; Nikolaienko, P.; Zhu, C.; Rueping, M. Nickel-Catalyzed Chain-Walking Cross-Electrophile Coupling of Alkyl and Aryl Halides and Olefin Hydroarylation Enabled by Electrochemical Reduction. *Angew. Chem. Int. Ed.* **2020**, *59* (16), 6513–6519. <https://doi.org/10.1002/anie.201915418>.
- (18) Xu, H.; Zhao, C.; Qian, Q.; Deng, W.; Gong, H. Nickel-Catalyzed Cross-Coupling of Unactivated Alkyl Halides Using Bis(Pinacolato)Diboron as Reductant. *Chem. Sci.* **2013**, *4*(10), 4022–4029. <https://doi.org/10.1039/C3SC51098K>.
- (19) Anka-Lufford, L. L.; Huihui, K. M. M.; Gower, N. J.; Ackerman, L. K. G.; Weix, D. J. Nickel-Catalyzed Cross-Electrophile Coupling with Organic Reductants in Non-Amide Solvents. *Chem. Eur. J.* **2016**, *22* (33), 11564–11567. <https://doi.org/10.1002/chem.201602668>.
- (20) Charboneau, D. J.; Brudvig, G. W.; Hazari, N.; Lant, H. M. C.; Saydjari, A. K. Development of an Improved System for the Carboxylation of Aryl Halides through Mechanistic Studies. *ACS Catal.* **2019**, *9* (4), 3228–3241. <https://doi.org/10.1021/acscatal.9b00566>.
- (21) Yurino, T.; Ueda, Y.; Shimizu, Y.; Tanaka, S.; Nishiyama, H.; Tsurugi, H.; Sato, K.; Mashima, K. Salt-Free Reduction of Nonprecious Transition-Metal Compounds: Generation of Amorphous Ni Nanoparticles for Catalytic C–C Bond Formation. *Angew. Chem. Int. Ed.* **2015**, *54* (48), 14437–14441. <https://doi.org/10.1002/anie.201507902>.
- (22) Ueda, Y.; Tsujimoto, N.; Yurino, T.; Tsurugi, H.; Mashima, K. Nickel-Catalyzed Cyanation of Aryl Halides and Triflates Using Acetonitrile via C–CN Bond Cleavage Assisted by 1,4-Bis(Trimethylsilyl)-2,3,5,6-Tetramethyl-1,4-Dihydropyrazine. *Chem. Sci.* **2019**, *10* (4), 994–999. <https://doi.org/10.1039/C8SC04437F>.
- (23) Everson, D. A.; Weix, D. J. Cross-Electrophile Coupling: Principles of Reactivity and Selectivity. *J. Org. Chem.* **2014**, *79* (11), 4793–4798. <https://doi.org/10.1021/jo500507s>.
- (24) Tortajada, A.; Juliá-Hernández, F.; Börjesson, M.; Moragas, T.; Martin, R. Transition-Metal-Catalyzed Carboxylation Reactions with Carbon Dioxide. *Angew. Chem. Int. Ed.* **2018**, *57* (49), 15948–15982. <https://doi.org/10.1002/anie.201803186>.
- (25) Ananikov, V. P. Nickel: The “Spirited Horse” of Transition Metal Catalysis. *ACS Catal.* **2015**, *5* (3), 1964–1971. <https://doi.org/10.1021/acscatal.5b00072>.
- (26) Tasker, S. Z.; Standley, E. A.; Jamison, T. F. Recent Advances in Homogeneous Nickel Catalysis. *Nature* **2014**, *509* (7500), 299–309. <https://doi.org/10.1038/nature13274>.
- (27) Ackermann, L.; Born, R. Mizoroki–Heck Reactions with Metals Other than Palladium. In *The Mizoroki–Heck Reaction*; John Wiley & Sons, Ltd, 2009; pp 383–403. <https://doi.org/10.1002/9780470716076.ch10>.
- (28) Rosen, B. M.; Quasdorf, K. W.; Wilson, D. A.; Zhang, N.; Resmerita, A.-M.; Garg, N. K.; Percec, V. Nickel-Catalyzed Cross-Couplings Involving Carbon–Oxygen Bonds. *Chem. Rev.* **2011**, *111* (3), 1346–1416. <https://doi.org/10.1021/cr100259t>.
- (29) Dander, J. E.; Garg, N. K. Breaking Amides Using Nickel Catalysis. *ACS Catal.* **2017**, *7*(2), 1413–1423. <https://doi.org/10.1021/acscatal.6b03277>.
- (30) Harry, N. A.; Saranya, S.; Ujwaldev, S. M.; Anilkumar, G. Recent Advances and Prospects in Nickel-Catalyzed C–H Activation. *Catal. Sci. Technol.* **2019**, *9* (8), 1726–1743. <https://doi.org/10.1039/C9CY00009G>.
- (31) Cherney, A. H.; Kadunce, N. T.; Reisman, S. E. Enantioselective and Enantiospecific Transition-Metal-Catalyzed Cross-Coupling Reactions of Organometallic Reagents To Construct C–C Bonds. *Chem. Rev.* **2015**, *115* (17), 9587–9652.

<https://doi.org/10.1021/acs.chemrev.5b00162>.

(32) Twilton, J.; Le, C. (Chip); Zhang, P.; Shaw, M. H.; Evans, R. W.; MacMillan, D. W. C. The Merger of Transition Metal and Photocatalysis. *Nat Rev Chem* **2017**, *1* (7), 1–19. <https://doi.org/10.1038/s41570-017-0052>.

(33) Macgregor, S. A.; Neave, G. W.; Smith, C. Theoretical Studies on C–Heteroatom Bond Formation via Reductive Elimination from Group 10  $M(\text{PH}_3)_2(\text{CH}_3)(\text{X})$  Species ( $\text{X} = \text{CH}_3, \text{NH}_2, \text{OH}, \text{SH}$ ) and the Determination of Metal–X Bond Strengths Using Density Functional Theory. *Faraday Discuss.* **2003**, *124*, 111–127. <https://doi.org/10.1039/B212309F>.

(34) Koga, N.; Obara, S.; Kitaura, K.; Morokuma, K. Role of Agostic Interaction in  $\beta$ -Elimination of Palladium and Nickel Complexes. An Ab Initio MO Study. *J. Am. Chem. Soc.* **1985**, *107* (24), 7109–7116. <https://doi.org/10.1021/ja00310a059>.

(35) Strömberg, S.; Zetterberg, K.; Siegbahn, P. E. M. Trends within a Triad: Comparison between  $\sigma$ -Alkyl Complexes of Nickel, Palladium and Platinum with Respect to Association of Ethylene, Migratory Insertion and  $\beta$ -Hydride Elimination. A Theoretical Study. *J. Chem. Soc., Dalton Trans.* **1997**, No. 22, 4147–4152. <https://doi.org/10.1039/A704584K>.

(36) Wilke, G. Contributions to Organo-Nickel Chemistry. *Angew. Chem. Int. Ed.* **1988**, *27*(1), 185–206. <https://doi.org/10.1002/anie.198801851>.

(37) Assen, N. von der; Voll, P.; Peters, M.; Bardow, A. Life Cycle Assessment of  $\text{CO}_2$  Capture and Utilization: A Tutorial Review. *Chem. Soc. Rev.* **2014**, *43* (23), 7982–7994. <https://doi.org/10.1039/C3CS60373C>.

(38) Aresta, M.; *Carbon Dioxide Recovery and Utilization*; Ed.; Springer Netherlands, 2003. <https://doi.org/10.1007/978-94-017-0245-4>.

(39) Aresta, M.; Dibenedetto, A.; Quaranta, E. *Reaction Mechanisms in Carbon Dioxide Conversion*; Springer Berlin Heidelberg: Berlin, Heidelberg, 2016. <https://doi.org/10.1007/978-3-662-46831-9>.

(40) Aresta, M.; Nobile, C. F.; Albano, V. G.; Forni, E.; Manassero, M. New Nickel–Carbon Dioxide Complex: Synthesis, Properties, and Crystallographic Characterization of (Carbon Dioxide)-Bis(Tricyclohexylphosphine)Nickel. *J. Chem. Soc., Chem. Commun.* **1975**, No. 15, 636–637. <https://doi.org/10.1039/C39750000636>.

(41) Maag, H. Prodrugs of Carboxylic Acids. In *Prodrugs: Challenges and Rewards Part 1*; Stella, V. J., Borchardt, R. T., Hageman, M. J., Oliyai, R., Maag, H., Tilley, J. W., Eds.; Biotechnology: Pharmaceutical Aspects; Springer: New York, NY, 2007; pp 703–729. [https://doi.org/10.1007/978-0-387-49785-3\\_20](https://doi.org/10.1007/978-0-387-49785-3_20).

(42) Seyferth, D. Alkyl and Aryl Derivatives of the Alkali Metals: Useful Synthetic Reagents as Strong Bases and Potent Nucleophiles. 1. Conversion of Organic Halides to Organoalkali-Metal Compounds. *Organometallics* **2006**, *25* (1), 2–24. <https://doi.org/10.1021/om058054a>.

(43) Osakada, K.; Sato, R.; Yamamoto, T. Nickel-Complex-Promoted Carboxylation of Haloarenes Involving Insertion of  $\text{CO}_2$  into NiII–C Bonds. *Organometallics* **1994**, *13* (11), 4645–4647. <https://doi.org/10.1021/om00023a078>.

(44) Correa, A.; Martín, R. Palladium-Catalyzed Direct Carboxylation of Aryl Bromides with Carbon Dioxide. *J. Am. Chem. Soc.* **2009**, *131* (44), 15974–15975. <https://doi.org/10.1021/ja905264a>.

(45) Fujihara, T.; Nogi, K.; Xu, T.; Terao, J.; Tsuji, Y. Nickel-Catalyzed Carboxylation of Aryl and Vinyl Chlorides Employing Carbon Dioxide. *J. Am. Chem. Soc.* **2012**, *134* (22), 9106–9109. <https://doi.org/10.1021/ja303514b>.

(46) Sayyed, F. B.; Tsuji, Y.; Sakaki, S. The Crucial Role of a Ni(I) Intermediate in Ni-Catalyzed Carboxylation of Aryl Chloride with  $\text{CO}_2$ : A Theoretical Study. *Chem. Commun.*

**2013**, 49 (91), 10715–10717. <https://doi.org/10.1039/C3CC45836A>.

(47) Iyoda, M.; Otsuka, H.; Sato, K.; Nisato, N.; Oda, M. Homocoupling of Aryl Halides Using Nickel(II) Complex and Zinc in the Presence of Et<sub>4</sub>Ni. An Efficient Method for the Synthesis of Biaryls and Bipyridines. *Bull. Chem. Soc. Jpn.* **1990**, 63 (1), 80–87. <https://doi.org/10.1246/bcsj.63.80>.

(48) Tran-Vu, H.; Daugulis, O. Copper-Catalyzed Carboxylation of Aryl Iodides with Carbon Dioxide. *ACS Catal.* **2013**, 3 (10), 2417–2420. <https://doi.org/10.1021/cs400443p>.

(49) León, T.; Correa, A.; Martin, R. Ni-Catalyzed Direct Carboxylation of Benzyl Halides with CO<sub>2</sub>. *J. Am. Chem. Soc.* **2013**, 135 (4), 1221–1224. <https://doi.org/10.1021/ja311045f>.

(50) Menges, F. S.; Craig, S. M.; Tötsch, N.; Bloomfield, A.; Ghosh, S.; Krüger, H.-J.; Johnson, M. A. Capture of CO<sub>2</sub> by a Cationic Nickel(I) Complex in the Gas Phase and Characterization of the Bound, Activated CO<sub>2</sub> Molecule by Cryogenic Ion Vibrational Predissociation Spectroscopy. *Angew. Chem. Int. Ed.* **2016**, 55 (4), 1282–1285. <https://doi.org/10.1002/anie.201507965>.

(51) Sayyed, F. B.; Sakaki, S. The Crucial Roles of MgCl<sub>2</sub> as a Non-Innocent Additive in the Ni-Catalyzed Carboxylation of Benzyl Halide with CO<sub>2</sub>. *Chem. Commun.* **2014**, 50 (86), 13026–13029. <https://doi.org/10.1039/C4CC04962D>.

(52) Zhang, S.; Chen, W.-Q.; Yu, A.; He, L.-N. Palladium-Catalyzed Carboxylation of Benzyl Chlorides with Atmospheric Carbon Dioxide in Combination with Manganese/Magnesium Chloride. *ChemCatChem* **2015**, 7 (23), 3972–3977. <https://doi.org/10.1002/cctc.201500724>.

(53) Choi, J.; Fu, G. C. Transition Metal-Catalyzed Alkyl-Alkyl Bond Formation: Another Dimension in Cross-Coupling Chemistry. *Science* **2017**, 356 (6334). <https://doi.org/10.1126/science.aaf7230>.

(54) Liu, Y.; Cornella, J.; Martin, R. Ni-Catalyzed Carboxylation of Unactivated Primary Alkyl Bromides and Sulfonates with CO<sub>2</sub>. *J. Am. Chem. Soc.* **2014**, 136 (32), 11212–11215. <https://doi.org/10.1021/ja5064586>.

(54) Somerville, R. J.; Odena, C.; Obst, M. F.; Hazari, N.; Hopmann, K. H.; Martin, R. Ni(I)-Alkyl Complexes Bearing Phenanthroline Ligands: Experimental Evidence for CO<sub>2</sub> Insertion at Ni(I) Centers. *J. Am. Chem. Soc.* **2020**, 142 (25), 10936–10941. <https://doi.org/10.1021/jacs.0c04695>.

(56) Börjesson, M.; Moragas, T.; Martin, R. Ni-Catalyzed Carboxylation of Unactivated Alkyl Chlorides with CO<sub>2</sub>. *J. Am. Chem. Soc.* **2016**, 138 (24), 7504–7507. <https://doi.org/10.1021/jacs.6b04088>.

(57) Moragas, T.; Martin, R. Nickel-Catalyzed Reductive Carboxylation of Cyclopropyl Motifs with Carbon Dioxide. *Synthesis* **2016**, 48 (17), 2816–2822. <https://doi.org/10.1055/s-0035-1560439>.

(58) Wang, X.; Liu, Y.; Martin, R. Ni-Catalyzed Divergent Cyclization/Carboxylation of Unactivated Primary and Secondary Alkyl Halides with CO<sub>2</sub>. *J. Am. Chem. Soc.* **2015**, 137 (20), 6476–6479. <https://doi.org/10.1021/jacs.5b03340>.

(59) Romero, N. A.; Nicewicz, D. A. Organic Photoredox Catalysis. *Chem. Rev.* **2016**, 116 (17), 10075–10166. <https://doi.org/10.1021/acs.chemrev.6b00057>.

(60) Shimomaki, K.; Murata, K.; Martin, R.; Iwasawa, N. Visible-Light-Driven Carboxylation of Aryl Halides by the Combined Use of Palladium and Photoredox Catalysts. *J. Am. Chem. Soc.* **2017**, 139 (28), 9467–9470. <https://doi.org/10.1021/jacs.7b04838>.

(61) Meng, Q.-Y.; Wang, S.; König, B. Carboxylation of Aromatic and Aliphatic Bromides and Triflates with CO<sub>2</sub> by Dual Visible-Light-Nickel Catalysis. *Angew. Chem. Int. Ed.* **2017**, 56 (43), 13426–13430. <https://doi.org/10.1002/anie.201706724>.

- (62) Juliá-Hernández, F.; Moragas, T.; Cornella, J.; Martin, R. Remote Carboxylation of Halogenated Aliphatic Hydrocarbons with Carbon Dioxide. *Nature* **2017**, *545* (7652), 84–88. <https://doi.org/10.1038/nature22316>.
- (63) Mei, T.-S.; Patel, H. H.; Sigman, M. S. Enantioselective Construction of Remote Quaternary Stereocentres. *Nature* **2014**, *508* (7496), 340–344. <https://doi.org/10.1038/nature13231>.
- (64) Sahoo, B.; Bellotti, P.; Juliá-Hernández, F.; Meng, Q.-Y.; Crespi, S.; König, B.; Martin, R. Site-Selective, Remote Sp<sup>3</sup> C–H Carboxylation Enabled by the Merger of Photoredox and Nickel Catalysis. *Chem. Eur. J.* **2019**, *25* (38), 9001–9005. <https://doi.org/10.1002/chem.201902095>.
- (65) Zarate, C.; van Gemmeren, M.; Somerville, R. J.; Martin, R. Chapter Four - Phenol Derivatives: Modern Electrophiles in Cross-Coupling Reactions. In *Advances in Organometallic Chemistry*; Pérez, P. J., Ed.; Academic Press, 2016; Vol. 66, pp 143–222. <https://doi.org/10.1016/bs.adomc.2016.07.001>.
- (66) Rebih, F.; Andreini, M.; Moncomble, A.; Harrison-Marchand, A.; Maddaluno, J.; Durandetti, M. Direct Carboxylation of Aryl Tosylates by CO<sub>2</sub> Catalyzed by In Situ-Generated Ni(0). *Chem. Eur. J.* **2016**, *22* (11), 3758–3763. <https://doi.org/10.1002/chem.201503926>.
- (67) Nogi, K.; Fujihara, T.; Terao, J.; Tsuji, Y. Cobalt- and Nickel-Catalyzed Carboxylation of Alkenyl and Sterically Hindered Aryl Triflates Utilizing CO<sub>2</sub>. *J. Org. Chem.* **2015**, *80* (22), 11618–11623. <https://doi.org/10.1021/acs.joc.5b02307>.
- (68) Correa, A.; León, T.; Martin, R. Ni-Catalyzed Carboxylation of C(sp<sup>2</sup>)– and C(sp<sup>3</sup>)–O Bonds with CO<sub>2</sub>. *J. Am. Chem. Soc.* **2014**, *136* (3), 1062–1069. <https://doi.org/10.1021/ja410883p>.
- (69) Moragas, T.; Cornella, J.; Martin, R. Ligand-Controlled Regiodivergent Ni-Catalyzed Reductive Carboxylation of Allyl Esters with CO<sub>2</sub>. *J. Am. Chem. Soc.* **2014**, *136* (51), 17702–17705. <https://doi.org/10.1021/ja509077a>.
- (70) Suh, H.-W.; Guard, L. M.; Hazari, N. A Mechanistic Study of Allene Carboxylation with CO<sub>2</sub> Resulting in the Development of a Pd(II) Pincer Complex for the Catalytic Hydroboration of CO<sub>2</sub>. *Chem. Sci.* **2014**, *5* (10), 3859–3872. <https://doi.org/10.1039/C4SC01110D>.
- (71) Takaya, J.; Iwasawa, N. Hydrocarboxylation of Allenes with CO<sub>2</sub> Catalyzed by Silyl Pincer-Type Palladium Complex. *J. Am. Chem. Soc.* **2008**, *130* (46), 15254–15255. <https://doi.org/10.1021/ja806677w>.
- (72) Takaya, J.; Sasano, K.; Iwasawa, N. Efficient One-to-One Coupling of Easily Available 1,3-Dienes with Carbon Dioxide. *Org. Lett.* **2011**, *13* (7), 1698–1701. <https://doi.org/10.1021/ol2002094>.
- (73) Mita, T.; Higuchi, Y.; Sato, Y. Highly Regioselective Palladium-Catalyzed Carboxylation of Allylic Alcohols with CO<sub>2</sub>. *Chem. Eur. J.* **2015**, *21* (46), 16391–16394. <https://doi.org/10.1002/chem.201503359>.
- (74) Inoue, Y.; Itoh, Y.; Hashimoto, H. Incorporation of Carbon Dioxide in Alkyne Oligomerization Catalyzed by Nickel(0) Complexes. Formation of Substituted 2-Pyrones. *Chem. Lett.* **1977**, *6* (8), 855–856. <https://doi.org/10.1246/cl.1977.855>.
- (75) Inoue, Y.; Itoh, Y.; Hashimoto, H. Oligomerization of 3-Hexyne by Nickel(0) Complexes under CO<sub>2</sub>. Incorporation of CO<sub>2</sub> and Novel Cyclotrimerization. *Chem. Lett.* **1978**, *7* (6), 633–634. <https://doi.org/10.1246/cl.1978.633>.
- (76) Inoue, Y.; Itoh, Y.; Kazama, H.; Hashimoto, H. Reaction of Dialkyl-Substituted Alkynes with Carbon Dioxide Catalyzed by Nickel(0) Complexes. Incorporation of Carbon Dioxide in Alkyne Dimers and Novel Cyclotrimerization of the Alkynes. *Bull. Chem. Soc. Jpn.* **1980**, *53* (11), 3329–3333. <https://doi.org/10.1246/bcsj.53.3329>.

- (77) Walther, D.; Schönberg, H.; Dinjus, E.; Sieler, J. Aktivierung von Kohlendioxid an Übergangsmetallzentren: Selektive Cooligomerisation mit Hexin(-3) durch das Katalysatorsystem Acetonitril/Trialkylphosphan/Nickel(0) und Struktur eines Nickel(0)-Komplexes mit side-on gebundenem Acetonitril. *Journal of Organometallic Chemistry* **1987**, 334 (3), 377–388. [https://doi.org/10.1016/0022-328X\(87\)80100-6](https://doi.org/10.1016/0022-328X(87)80100-6).
- (78) Walther, D.; Bräunlich, G.; Kempe, R.; Sieler, J. Aktivierung von CO<sub>2</sub> an Übergangsmetallzentren: Zum Ablauf der homogen-katalytischen Bildung von 2-Pyron aus Kohlendioxid und Hex-3-in an Nickel(0)-Fragmenten. *Journal of Organometallic Chemistry* **1992**, 436 (1), 109–119. [https://doi.org/10.1016/0022-328X\(92\)85032-R](https://doi.org/10.1016/0022-328X(92)85032-R).
- (79) Hoberg, H.; Schaefer, D. Modellkomplexe Des Nickels Für Die [2+2+2']-Cycloaddition von Alkinen Mit Kohlendioxid. *Journal of Organometallic Chemistry* **1982**, 238 (4), 383–387. [https://doi.org/10.1016/S0022-328X\(00\)83800-0](https://doi.org/10.1016/S0022-328X(00)83800-0).
- (80) Hoberg, H.; Schaefer, D.; Burkhart, G. Oxanickelacyclopenten-Derivate, Ein Neuer Typ Vielseitig Verwendbarer Synthone. *Journal of Organometallic Chemistry* **1982**, 228 (1), C21–C24. [https://doi.org/10.1016/S0022-328X\(00\)86783-2](https://doi.org/10.1016/S0022-328X(00)86783-2).
- (81) Burkhart, G.; Hoberg, H. Oxanickelacyclopentene Derivatives from Nickel(0), Carbon Dioxide, and Alkynes. *Angew. Chem. Int. Ed.* **1982**, 21 (1), 76–76. <https://doi.org/10.1002/anie.198200762>.
- (82) Langer, J.; Gärtner, M.; Görls, H.; Walther, D. Five- and Six-Membered Nickelacyclic Carboxylates as Reagents for the Facile Synthesis of  $\delta$ -Ketocarboxylic Acids, Isocoumarins, and 1,3-Dicarbonyl Derivatives- of Benzoic Acid. *Synthesis* **2006**, 2006 (16), 2697–2706. <https://doi.org/10.1055/s-2006-942507>.
- (83) Yamashita, K.; Chatani, N. Cp<sub>2</sub>ZrCl<sub>2</sub>-Mediated Three-Component Coupling Reactions of CO<sub>2</sub>, Ethylene (or Alkynes), and Electrophiles Leading to Carboxylic Acid Derivatives. *Synlett* **2005**, 2005 (6), 919–922. <https://doi.org/10.1055/s-2005-864807>.
- (84) Sakaki, S.; Mine, K.; Taguchi, D.; Arai, T. Formation of the Oxanickelacyclopentene Complex from Nickel(0), Carbon Dioxide, and Alkyne. An Ab Initio MO/SD-CI Study. *Bull. Chem. Soc. Jpn.* **1993**, 66 (11), 3289–3299. <https://doi.org/10.1246/bcsj.66.3289>.
- (85) Sakaki, S.; Mine, K.; Hamada, T.; Arai, T. Formation of the Oxanickelacyclopentene Complex from Nickel(0), Carbon Dioxide, and Alkyne. An Ab Initio MO/SD-CI Study. Part II. Reactivity and Regioselectivity of Hydroxyacetylene. *Bull. Chem. Soc. Jpn.* **1995**, 68 (7), 1873–1882. <https://doi.org/10.1246/bcsj.68.1873>.
- (86) Graham, D. C.; Bruce, M. I.; Metha, G. F.; Bowie, J. H.; Buntine, M. A. Regioselective Control of the Nickel-Mediated Coupling of Acetylene and Carbon Dioxide – A DFT Study. *Journal of Organometallic Chemistry* **2008**, 693 (16), 2703–2710. <https://doi.org/10.1016/j.jorganchem.2008.05.015>.
- (87) Li, J.; Jia, G.; Lin, Z. Theoretical Studies on Coupling Reactions of Carbon Dioxide with Alkynes Mediated by Nickel(0) Complexes. *Organometallics* **2008**, 27 (15), 3892–3900. <https://doi.org/10.1021/om8002224>.
- (88) Saito, S.; Nakagawa, S.; Koizumi, T.; Hirayama, K.; Yamamoto, Y. Nickel-Mediated Regio- and Chemoselective Carboxylation of Alkynes in the Presence of Carbon Dioxide. *J. Org. Chem.* **1999**, 64 (11), 3975–3978. <https://doi.org/10.1021/jo982443f>.
- (89) Aoki, M.; Kaneko, M.; Izumi, S.; Ukai, K.; Iwasawa, N. Bidentate Amidine Ligands for Nickel(0)-Mediated Coupling of Carbon Dioxide with Unsaturated Hydrocarbons. *Chem. Commun.* **2004**, No. 22, 2568–2569. <https://doi.org/10.1039/B411802B>.
- (90) Wang, X.; Wang, H.; Sun, Y. Synthesis of Acrylic Acid Derivatives from CO<sub>2</sub> and Ethylene. *Chem* **2017**, 3 (2), 211–228. <https://doi.org/10.1016/j.chempr.2017.07.006>.
- (91) Li, S.; Yuan, W.; Ma, S. Highly Regio- and Stereoselective Three-Component Nickel-

Catalyzed Syn-Hydrocarboxylation of Alkynes with Diethyl Zinc and Carbon Dioxide. *Angew. Chem. Int. Ed.* **2011**, *50* (11), 2578–2582. <https://doi.org/10.1002/anie.201007128>.

(92) Li, S.; Ma, S. Highly Selective Nickel-Catalyzed Methyl-Carboxylation of Homopropargylic Alcohols for  $\alpha$ -Alkylidene- $\gamma$ -Butyrolactones. *Org. Lett.* **2011**, *13* (22), 6046–6049. <https://doi.org/10.1021/ol202520x>.

(93) Fujihara, T.; Xu, T.; Semba, K.; Terao, J.; Tsuji, Y. Copper-Catalyzed Hydrocarboxylation of Alkynes Using Carbon Dioxide and Hydrosilanes. *Angew. Chem. Int. Ed.* **2011**, *50* (2), 523–527. <https://doi.org/10.1002/anie.201006292>.

(94) Wang, X.; Nakajima, M.; Martin, R. Ni-Catalyzed Regioselective Hydrocarboxylation of Alkynes with CO<sub>2</sub> by Using Simple Alcohols as Proton Sources. *J. Am. Chem. Soc.* **2015**, *137* (28), 8924–8927. <https://doi.org/10.1021/jacs.5b05513>.

(95) Gaydou, M.; Moragas, T.; Juliá-Hernández, F.; Martin, R. Site-Selective Catalytic Carboxylation of Unsaturated Hydrocarbons with CO<sub>2</sub> and Water. *J. Am. Chem. Soc.* **2017**, *139* (35), 12161–12164. <https://doi.org/10.1021/jacs.7b07637>.

(96) Doi, R.; Abdullah, I.; Taniguchi, T.; Saito, N.; Sato, Y. Nickel-Catalyzed Hydrocarboxylation of Ynamides with CO<sub>2</sub> and H<sub>2</sub>O: Observation of Unexpected Regioselectivity. *Chem. Commun.* **2017**, *53* (55), 7720–7723. <https://doi.org/10.1039/C7CC03127K>.

(97) Shimizu, K.; Takimoto, M.; Sato, Y.; Mori, M. Nickel-Catalyzed Regioselective Synthesis of Tetrasubstituted Alkene Using Alkylative Carboxylation of Disubstituted Alkyne. *Org. Lett.* **2005**, *7* (2), 195–197. <https://doi.org/10.1021/ol047912g>.

(98) Fujihara, T.; Horimoto, Y.; Mizoe, T.; Sayyed, F. B.; Tani, Y.; Terao, J.; Sakaki, S.; Tsuji, Y. Nickel-Catalyzed Double Carboxylation of Alkynes Employing Carbon Dioxide. *Org. Lett.* **2014**, *16* (18), 4960–4963. <https://doi.org/10.1021/ol502538r>.

(99) Zhang, L.; Cheng, J.; Carry, B.; Hou, Z. Catalytic Boracarboxylation of Alkynes with Diborane and Carbon Dioxide by an N-Heterocyclic Carbene Copper Catalyst. *J. Am. Chem. Soc.* **2012**, *134* (35), 14314–14317. <https://doi.org/10.1021/ja3063474>.

(100) Fujihara, T.; Tani, Y.; Semba, K.; Terao, J.; Tsuji, Y. Copper-Catalyzed Silacarboxylation of Internal Alkynes by Employing Carbon Dioxide and Silylboranes. *Angew. Chem. Int. Ed.* **2012**, *51* (46), 11487–11490. <https://doi.org/10.1002/anie.201207148>.

(101) Lapidus, A. L.; Pirozhkov, S. D.; Koryakin, A. A. Catalytic Synthesis of Propionic Acid by Carboxylation of Ethylene with Carbon Dioxide. *Russ Chem Bull* **1978**, *27* (12), 2513–2515. <https://doi.org/10.1007/BF00941114>.

(102) Hoberg, H.; Schaefer, D. Nickel(0)-induzierte c—c-verknüpfung zwischen alkenen und kohlendioxid. *Journal of Organometallic Chemistry* **1982**, *236* (1), C28–C30. [https://doi.org/10.1016/S0022-328X\(00\)86765-0](https://doi.org/10.1016/S0022-328X(00)86765-0).

(103) Hoberg, H.; Schaefer, D. Nickel(0)-Induzierte C-C-Verknüpfung Zwischen Kohlendioxid Und Ethylen Sowie Mono- Oder Di-Substituierten Alkenen. *Journal of Organometallic Chemistry* **1983**, *251* (3), c51–c53. [https://doi.org/10.1016/S0022-328X\(00\)98789-8](https://doi.org/10.1016/S0022-328X(00)98789-8).

(104) Hoberg, H.; Peres, Y.; Milchereit, A. C–C-Verknüpfung von alkenen mit CO<sub>2</sub> an nickel(0); herstellung von zimtsäure aus styrol. *Journal of Organometallic Chemistry* **1986**, *307* (2), C38–C40. [https://doi.org/10.1016/0022-328X\(86\)80487-9](https://doi.org/10.1016/0022-328X(86)80487-9).

(105) Hoberg, H.; Peres, Y.; Krüger, C.; Tsay, Y.-H. A 1-Oxa-2-Nickela-5-Cyclopentanone from Ethene and Carbon Dioxide: Preparation, Structure, and Reactivity. *Angew. Chem. Int. Ed.* **1987**, *26* (8), 771–773. <https://doi.org/10.1002/anie.198707711>.

(106) Hoberg, H.; Schaefer, D.; Burkhart, G.; Krüger, C.; Romão, M. J. Nickel(0)-induzierte C–C-verknüpfung zwischen kohlendioxid und alkenen sowie alkenen. *Journal of*

- Organometallic Chemistry* **1984**, 266 (2), 203–224. [https://doi.org/10.1016/0022328X\(84\)80129-1](https://doi.org/10.1016/0022328X(84)80129-1).
- (107) Hoberg, H.; Ballesteros, A.; Sigan, A.; Jégat, C.; Bärhausen, D.; Milchereit, A. Ligandgesteuerte Ringkontraktion von Nickela-Fünf- in Vierringkomplexe—Neuartige Startsysteme Für Die Präparative Chemie. *Journal of Organometallic Chemistry* **1991**, 407 (3), C23–C29. [https://doi.org/10.1016/0022-328X\(91\)86320-P](https://doi.org/10.1016/0022-328X(91)86320-P).
- (108) Greenburg, Z. R.; Jin, D.; Williard, P. G.; Bernskoetter, W. H. Nickel Promoted Functionalization of CO<sub>2</sub> to Anhydrides and Ketoacids. *Dalton Trans.* **2014**, 43 (42), 15990–15996. <https://doi.org/10.1039/C4DT01221F>.
- (109) Murakami, M.; Ishida, N.; Miura, T. Solvent and Ligand Partition Reaction Pathways in Nickel-Mediated Carboxylation of Methylenecyclopropanes. *Chem. Commun.* **2006**, No. 6, 643–645. <https://doi.org/10.1039/B515684J>.
- (110) Aresta, M.; Quaranta, E.; Tommasi, I. Reduction of Co-Ordinated Carbon Dioxide to Carbon Monoxide via Protonation by Thiols and Other Brønsted Acids Promoted by Ni-Systems: A Contribution to the Understanding of the Mode of Action of the Enzyme Carbon Monoxide Dehydrogenase. *J. Chem. Soc., Chem. Commun.* **1988**, No. 7, 450–452. <https://doi.org/10.1039/C39880000450>.
- (111) Aresta, M.; Gobetto, R.; Quaranta, E.; Tommasi, I. A Bonding-Reactivity Relationship for (Carbon Dioxide)Bis(Tricyclohexylphosphine)Nickel: A Comparative Solid-State-Solution Nuclear Magnetic Resonance Study (Phosphorus-31, Carbon-13) as a Diagnostic Tool to Determine the Mode of Bonding of Carbon Dioxide to a Metal Center. *Inorg. Chem.* **1992**, 31 (21), 4286–4290. <https://doi.org/10.1021/ic00047a015>.
- (112) Pápai, I.; Schubert, G.; Mayer, I.; Besenyi, G.; Aresta, M. Mechanistic Details of Nickel(0)-Assisted Oxidative Coupling of CO<sub>2</sub> with C<sub>2</sub>H<sub>4</sub>. *Organometallics* **2004**, 23 (22), 5252–5259. <https://doi.org/10.1021/om049496+>.
- (113) Yang, G.; Schäffner, B.; Blug, M.; Hensen, E. J. M.; Pidko, E. A. A Mechanistic Study of Ni-Catalyzed Carbon Dioxide Coupling with Ethylene towards the Manufacture of Acrylic Acid. *ChemCatChem* **2014**, 6 (3), 800–807. <https://doi.org/10.1002/cctc.201301051>.
- (114) Plessow, P. N.; Schäfer, A.; Limbach, M.; Hofmann, P. Acrylate Formation from CO<sub>2</sub> and Ethylene Mediated by Nickel Complexes: A Theoretical Study. *Organometallics* **2014**, 33(14), 3657–3668. <https://doi.org/10.1021/om500151h>.
- (115) Cohen, S. A.; Bercaw, J. E. Titanacycles Derived from Reductive Coupling of Nitriles, Alkynes, Acetaldehyde, and Carbon Dioxide with Bis(Pentamethylcyclopentadienyl)(Ethylene)Titanium(II). *Organometallics* **1985**, 4 (6), 1006–1014. <https://doi.org/10.1021/om00125a008>.
- (116) Alt, H. G.; Denner, C. E. Metallacyclen des zirkonocens. *Journal of Organometallic Chemistry* **1990**, 390 (1), 53–60. [https://doi.org/10.1016/0022-328X\(90\)85081-9](https://doi.org/10.1016/0022-328X(90)85081-9).
- (117) Hoberg, H.; Jenni, K.; Angermund, K.; Krüger, C. CC-Linkages of Ethene with CO<sub>2</sub> on an Iron(0) Complex—Synthesis and Crystal Structure Analysis of [(PEt<sub>3</sub>)<sub>2</sub>Fe(C<sub>2</sub>H<sub>4</sub>)<sub>2</sub>]. *Angew. Chem. Int. Ed.* **1987**, 26 (2), 153–155. <https://doi.org/10.1002/anie.198701531>.
- (118) Limbach, M. Chapter Four - Acrylates from Alkenes and CO<sub>2</sub>, the Stuff That Dreams Are Made Of. In *Advances in Organometallic Chemistry*; Pérez, P. J., Ed.; Academic Press, 2015; Vol. 63, pp 175–202. <https://doi.org/10.1016/bs.adomc.2015.03.001>.
- (119) Kirillov, E.; Carpentier, J.-F.; Bunel, E. Carboxylic Acid Derivatives via Catalytic Carboxylation of Unsaturated Hydrocarbons: Whether the Nature of a Reductant May Determine the Mechanism of CO<sub>2</sub> Incorporation? *Dalton Trans.* **2015**, 44 (37), 16212–16223. <https://doi.org/10.1039/C5DT02350E>.
- (120) Fischer, R.; Langer, J.; Malassa, A.; Walther, D.; Görls, H.; Vaughan, G. A Key Step in

the Formation of Acrylic Acid from CO<sub>2</sub> and Ethylene: The Transformation of a Nickelalactone into a Nickel-Acrylate Complex. *Chem. Commun.* **2006**, No. 23, 2510–2512. <https://doi.org/10.1039/B603540J>.

(121) Graham, D. C.; Mitchell, C.; Bruce, M. I.; Metha, G. F.; Bowie, J. H.; Buntine, M. A. Production of Acrylic Acid through Nickel-Mediated Coupling of Ethylene and Carbon Dioxide—A DFT Study. *Organometallics* **2007**, 26 (27), 6784–6792. <https://doi.org/10.1021/om700592w>.

(122) Bruckmeier, C.; Lehenmeier, M. W.; Reichardt, R.; Vagin, S.; Rieger, B. Formation of Methyl Acrylate from CO<sub>2</sub> and Ethylene via Methylation of Nickelalactones. *Organometallics* **2010**, 29 (10), 2199–2202. <https://doi.org/10.1021/om100060y>.

(123) Lee, S. Y. T.; Cokoja, M.; Drees, M.; Li, Y.; Mink, J.; Herrmann, W. A.; Kühn, F. E. Transformation of Nickelalactones to Methyl Acrylate: On the Way to a Catalytic Conversion of Carbon Dioxide. *ChemSusChem* **2011**, 4 (9), 1275–1279. <https://doi.org/10.1002/cssc.201000445>.

(124) Jin, D.; Schmeier, T. J.; Williard, P. G.; Hazari, N.; Bernskoetter, W. H. Lewis Acid Induced  $\beta$ -Elimination from a Nickelalactone: Efforts toward Acrylate Production from CO<sub>2</sub> and Ethylene. *Organometallics* **2013**, 32 (7), 2152–2159. <https://doi.org/10.1021/om400025h>.

(125) Guo, W.; Michel, C.; Schwiedernoch, R.; Wischert, R.; Xu, X.; Sautet, P. Formation of Acrylates from Ethylene and CO<sub>2</sub> on Ni Complexes: A Mechanistic Viewpoint from a Hybrid DFT Approach. *Organometallics* **2014**, 33 (22), 6369–6380. <https://doi.org/10.1021/om5006808>.

(126) Lejkowski, M. L.; Lindner, R.; Kageyama, T.; Bódizs, G. É.; Plessow, P. N.; Müller, I. B.; Schäfer, A.; Rominger, F.; Hofmann, P.; Futter, C.; Schunk, S. A.; Limbach, M. The First Catalytic Synthesis of an Acrylate from CO<sub>2</sub> and an Alkene—A Rational Approach. *Chem. Eur. J.* **2012**, 18 (44), 14017–14025. <https://doi.org/10.1002/chem.201201757>.

(127) Manzini, S.; Huguet, N.; Trapp, O.; Paciello, R. A.; Schaub, T. Synthesis of Acrylates from Olefins and CO<sub>2</sub> Using Sodium Alkoxides as Bases. *Catalysis Today* **2017**, 281, 379–386. <https://doi.org/10.1016/j.cattod.2016.03.025>.

(128) Huguet, N.; Jevtovikj, I.; Gordillo, A.; Lejkowski, M. L.; Lindner, R.; Bru, M.; Khalimon, A. Y.; Rominger, F.; Schunk, S. A.; Hofmann, P.; Limbach, M. Nickel-Catalyzed Direct Carboxylation of Olefins with CO<sub>2</sub>: One-Pot Synthesis of  $\alpha,\beta$ -Unsaturated Carboxylic Acid Salts. *Chem. Eur. J.* **2014**, 20 (51), 16858–16862. <https://doi.org/10.1002/chem.201405528>.

(129) Jevtovikj, I.; Manzini, S.; Hanauer, M.; Rominger, F.; Schaub, T. Investigations on the Catalytic Carboxylation of Olefins with CO<sub>2</sub> towards  $\alpha,\beta$ -Unsaturated Carboxylic Acid Salts: Characterization of Intermediates and Ligands as Well as Substrate Effects. *Dalton Trans.* **2015**, 44 (24), 11083–11094. <https://doi.org/10.1039/C5DT01040C>.

(130) Hendriksen, C.; Pidko, E. A.; Yang, G.; Schäffner, B.; Vogt, D. Catalytic Formation of Acrylate from Carbon Dioxide and Ethene. *Chem. Eur. J.* **2014**, 20 (38), 12037–12040. <https://doi.org/10.1002/chem.201404082>.

(131) Williams, C. M.; Johnson, J. B.; Rovis, T. Nickel-Catalyzed Reductive Carboxylation of Styrenes Using CO<sub>2</sub>. *J. Am. Chem. Soc.* **2008**, 130 (45), 14936–14937. <https://doi.org/10.1021/ja8062925>.

(132) Yuan, R.; Lin, Z. Computational Insight into the Mechanism of Nickel-Catalyzed Reductive Carboxylation of Styrenes Using CO<sub>2</sub>. *Organometallics* **2014**, 33 (24), 7147–7156. <https://doi.org/10.1021/om500962a>.

(133) Shirakawa, E.; Ikeda, D.; Masui, S.; Yoshida, M.; Hayashi, T. Iron–Copper Cooperative Catalysis in the Reactions of Alkyl Grignard Reagents: Exchange Reaction with Alkenes and



Carbometalation of Alkynes. *J. Am. Chem. Soc.* **2012**, *134* (1), 272–279. <https://doi.org/10.1021/ja206745w>.

(134) Greenhalgh, M. D.; Thomas, S. P. Iron-Catalyzed, Highly Regioselective Synthesis of  $\alpha$ -Aryl Carboxylic Acids from Styrene Derivatives and CO<sub>2</sub>. *J. Am. Chem. Soc.* **2012**, *134* (29), 11900–11903. <https://doi.org/10.1021/ja3045053>.

(135) Shao, P.; Wang, S.; Chen, C.; Xi, C. Cp<sub>2</sub>TiCl<sub>2</sub>-Catalyzed Regioselective Hydrocarboxylation of Alkenes with CO<sub>2</sub>. *Org. Lett.* **2016**, *18* (9), 2050–2053. <https://doi.org/10.1021/acs.orglett.6b00665>.

(136) He, Y.; Cai, Y.; Zhu, S. Mild and Regioselective Benzylic C–H Functionalization: Ni-Catalyzed Reductive Arylation of Remote and Proximal Olefins. *J. Am. Chem. Soc.* **2017**, *139*(3), 1061–1064. <https://doi.org/10.1021/jacs.6b11962>.

(137) Meng, Q.-Y.; Wang, S.; Huff, G. S.; König, B. Ligand-Controlled Regioselective Hydrocarboxylation of Styrenes with CO<sub>2</sub> by Combining Visible Light and Nickel Catalysis. *J. Am. Chem. Soc.* **2018**, *140* (9), 3198–3201. <https://doi.org/10.1021/jacs.7b13448>.



## **Chapter 2: Site-Selective Catalytic Carboxylation of Allylic Alcohols with CO<sub>2</sub>**

*In collaboration with Dr. Manuel van Gemmeren, Dr. Marino Börjesson,  
Shang-Zheng Sun and Keisho Okura*

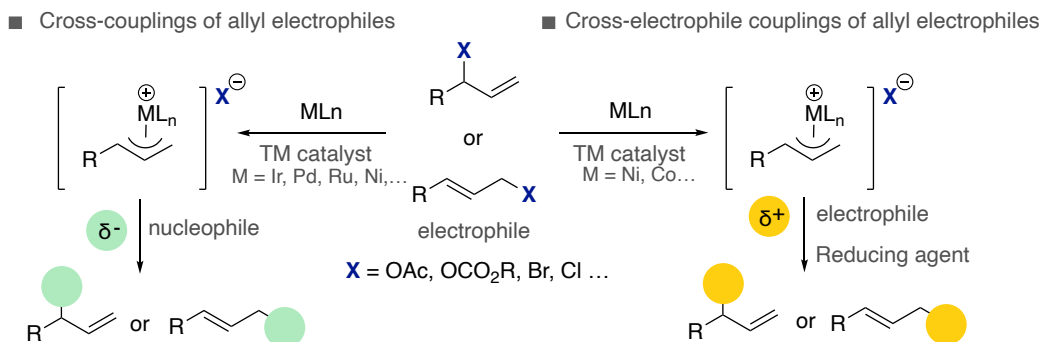


## 1. Introduction

### 1.1 Metal-catalyzed cross-couplings of activated allyl electrophiles

Allyl electrophiles are versatile organic synthons that have been used in a multitude of synthetic organic transformations. Indeed, many of these processes rank amongst the most valuable tools to build-up molecular complexity such as the Pd-catalyzed Tsuji-Trost allylic substitution reaction for forging C–C and C–heteroatom bonds with suitable nucleophilic entities (Scheme 1, *left*).<sup>1–4</sup> Classical organic electrophiles employed in these endeavors are allylic halides and C–O counterparts derived from an allylic alcohol motif. Interestingly, these processes have been applied within the context of asymmetric catalysis by employing chiral ligands, allowing to achieve high levels of regio-, stereo- and enantioselectivity. Not surprisingly, these transformations have rapidly been adopted in both academic and industrial laboratories, particularly in the total synthesis of natural products<sup>5</sup> and molecules of biological significance.<sup>6</sup>

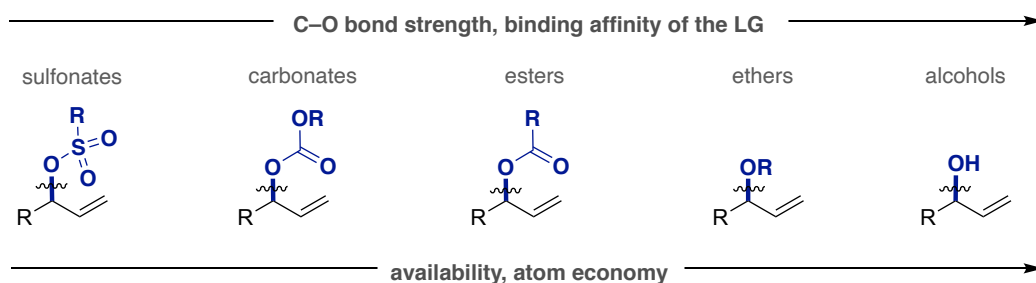
Prompted by the inherent interest in Tsuji-Trost allylation reactions, it comes as no surprise that these methods have been adapted to cross-electrophile coupling processes (Scheme 1, *right*). Unlike classical nucleophile-electrophile regimes, the utilization of two electrophiles limits the number of transition metals that can be employed, as the formed species should be amenable for reduction. In this context, considerable progress has been observed with Ni, and at lower extent with Co catalysts, due to their ability to access non-canonical oxidation states and one-electron processes.<sup>7,8,9</sup>



**Scheme 1.** Metal-catalyzed cross-couplings and cross-electrophile couplings of activated allylic electrophiles

## 1.2 Metal-catalyzed cross-coupling of allylic alcohols

Undoubtedly, a high degree of molecular complexity has been reached in allylation reactions by using activated allyl electrophiles containing appropriate leaving groups, such as halides, esters or carbonates, among others. This is due to the low binding affinity of these leaving groups, enabling a fast generation of catalytically active metal-allylic species upon initial oxidative addition. In contrast, the utilization of allylic alcohols as organic electrophiles have found little echo due to their poor leaving group abilities and high binding affinity of the alcohol R-OH moiety to transition metals (Scheme 2).<sup>10</sup> However, the direct substitution of allylic alcohols by an appropriate building block represents a greener, cheaper and more atom economical alternative to classical cross-coupling reactions for forging C-C, C-N and C-O bonds, as the only generated byproduct is water.<sup>3,4</sup> Although the majority of the transformations using allylic alcohol as electrophiles have been conducted with Pd catalysts ending up in linear compounds,<sup>11,12</sup> significant amount of branched-selective Ru- and Ir-catalyzed transformations have also been described.<sup>13</sup>



**Scheme 2.** General properties of the different C-O allyl-electrophiles.

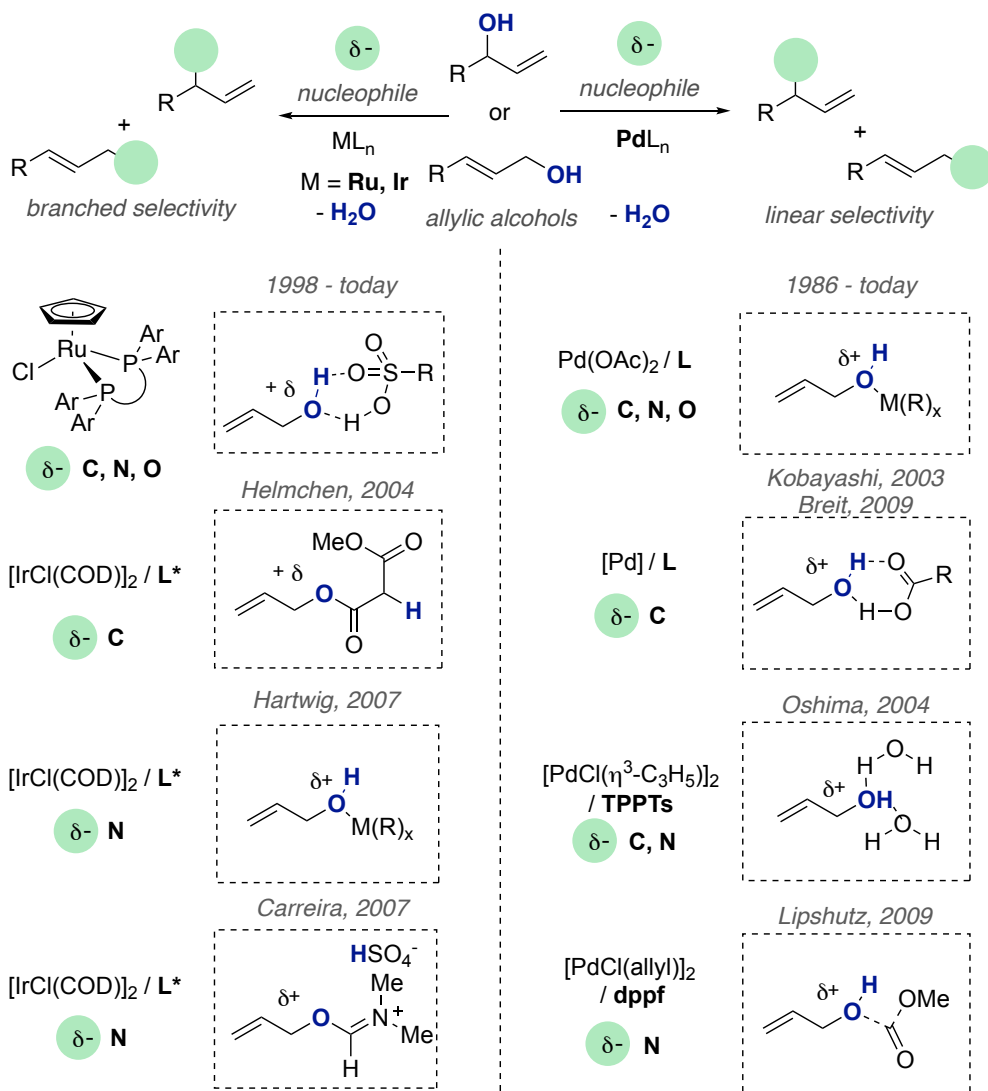
## 1.3. Transition Metal-catalyzed cross-coupling of allylic alcohols

Since the first report describing the use of [RuCl<sub>2</sub>(PPh<sub>3</sub>)<sub>3</sub>] as precatalyst to form allylic ethers from allylic alcohols,<sup>14</sup> a variety of cyclopentadienyl Ru(II)-complexes have been described as efficient catalysts for this transformation.<sup>15</sup> The presence of sulfonic acids have proven to be beneficial for the reaction to occur (Scheme 3).<sup>16,17</sup> These methodologies have been extended to a wide variety of carbon, nitrogen, oxygen and sulfur-type nucleophiles, resulting in the selective formation of branched products,<sup>4</sup> with chiral ligands allowing the development of enantioselective allylic substitution reactions.<sup>18</sup> Undoubtedly, the utilization of Ir catalysts constitute the major breakthrough in enantioselective substitution reactions of allylic alcohols (Scheme 3, *left*). In particular, Helmchen reported the first enantioselective contribution in 2004 describing the coupling of allylic alcohols

with carbon type nucleophiles in high levels of regio- and enantioselectivity through the utilization of [IrCl(COD)]<sub>2</sub> and phosphinooxazoline ligands.<sup>19</sup> Subsequently, Hartwig reported the successful activation of various unsymmetrical allylic alcohols towards allylic amination using iridium complexes bearing phosphoramidite ligand.<sup>20</sup> Stoichiometric amounts of Lewis acids such as titanium tetraalkoxide, or catalytic quantity of BPh<sub>3</sub> served as alcohol activators, achieving excellent levels of regio- and enantiocontrol. Carreira made significant contributions in allylic amination reactions of allylic alcohols through the utilization of sulfamic acid (NH<sub>2</sub>SO<sub>3</sub>H), which acts as both aminating reagent and direct activator of the allylic alcohol.<sup>21,22</sup>

In line with the knowledge acquired in Ru- and Ir-catalyzed allylic substitutions, the presence of stoichiometric metals or acids was crucial for the development of alternative Pd catalyzed protocols. Notably, the utilization of Pd catalysis results in regioselectivity switch, favoring the formation of linear isomers (Scheme 3, *right*). In this context, the utilization of As, B and Ti complexes have proven to be beneficial for activating the O–H motif, thus accelerating the oxidative addition of the C–O electrophile to Pd(0). In 2003 Manabe and Kobayashi reported a carboxylic acid-assisted activation of allylic alcohols under aqueous conditions.<sup>23</sup> The reaction was quite efficient being completed within 10–90 minutes. In 2009, Breit improved this concept simultaneously activating allylic alcohols and carbonyl compounds through the utilization of (*DL*)-proline.<sup>24</sup> While the carboxylic acid of proline could trigger the ionization step of the palladium olefin complex through hydrogen bonding and protonation of the hydroxyl-leaving group, the secondary amine could enolize ketones or aldehydes. Overall, this would result in the formation of a tight ion pair between the enamine nucleophile and the  $\pi$ -allyl palladium electrophile, thus enhancing allylation.

In 2004, Oshima and coworkers demonstrated that the use of water as solvent could play a crucial role in the activation of allylic alcohols.<sup>25</sup> Water was proposed to have a dual role by activating the allylic OH group and by solvating the leaving group. In this manner, the utilization of water-soluble catalytic species generated from [PdCl( $\eta^3$ -C<sub>3</sub>H<sub>5</sub>)]<sub>2</sub> and TPPTS (Tris(3-sulfophenyl)phosphine trisodium salt) resulted in a rate enhancement, allowing to trigger these reactions at room temperature in the absence of any additional activating agent. Subsequently, Lipshutz demonstrated that surfactants could enable the activation of allylic alcohols in water, avoiding the need for water-soluble ligands.<sup>26</sup> While TPS (Tetrapropylenebenzene sulfonate) surfactant generates nanomicellar microreactors where Pd-catalysis can function, methyl formate enables the labilization of the hydroxyl group through the elimination of methanol and formate anion.

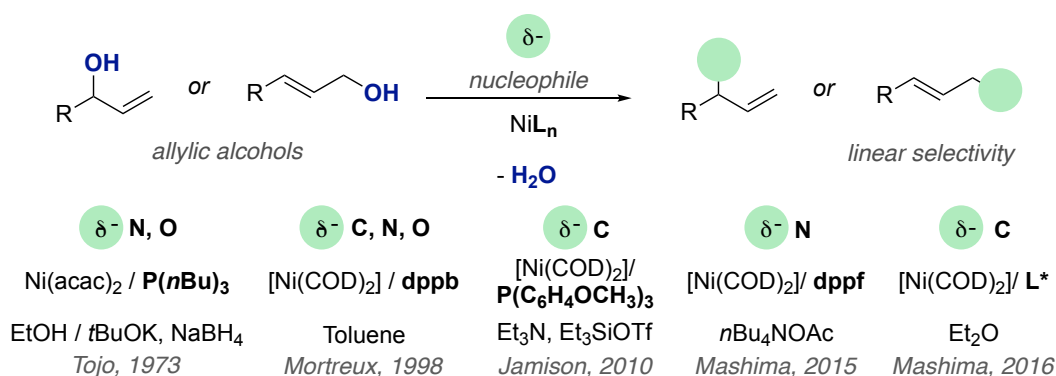


**Scheme 3.** In-situ activation of allylic alcohols and catalysis with TMs.

As judged by the literature data, the utilization of metals other than Pd, Ru or Ir in allylic substitution reactions of allyl alcohols has remained less explored. Among these, the utilization of Ni catalysts has proven to be particularly appealing, either with or without activators (Scheme 4). In particular, Tojo described the first Ni-catalyzed allylic substitution using allylic alcohols early in 1973.<sup>27</sup> Although the strong reducing agent and the harsh reaction conditions resulted in modest reaction yield and selectivity, this publication demonstrated that phosphine ligated Ni-catalyst could be used to effectively activate allylic alcohols in the absence of activating reagents. Surprisingly this approach remained unexplored until 1998,



when Mortreux reported a much more efficient catalytic system based on the utilization of Ni(COD)<sub>2</sub> and bidentate dppb as ligand.<sup>28</sup> Remarkably, it was found that nickel catalysts were much more active than the corresponding Pd analogues, yet more sensitive, and in the absence of activating agents.<sup>29</sup> Surprisingly, the utilization of nickel catalysts remained largely unexplored until 2010, when Jamison reported that cinnamyl alcohol could undergo catalytic substitution with ethylene as nucleophile by using Ni(COD)<sub>2</sub> and P(*ortho*-anisyl)<sub>3</sub> in the presence of Et<sub>3</sub>SiOTf.<sup>30</sup> In 2015 Mashima achieved remarkably low catalyst loadings in an allylic amination through the utilization of *n*Bu<sub>4</sub>NOAc as mild activator.<sup>31</sup> One year later, Mashima developed an enantioselective allylic substitution using carbon-based nucleophiles in which the extruded OH<sup>-</sup> anion serves as base to enolize β-ketoesters.<sup>32</sup>

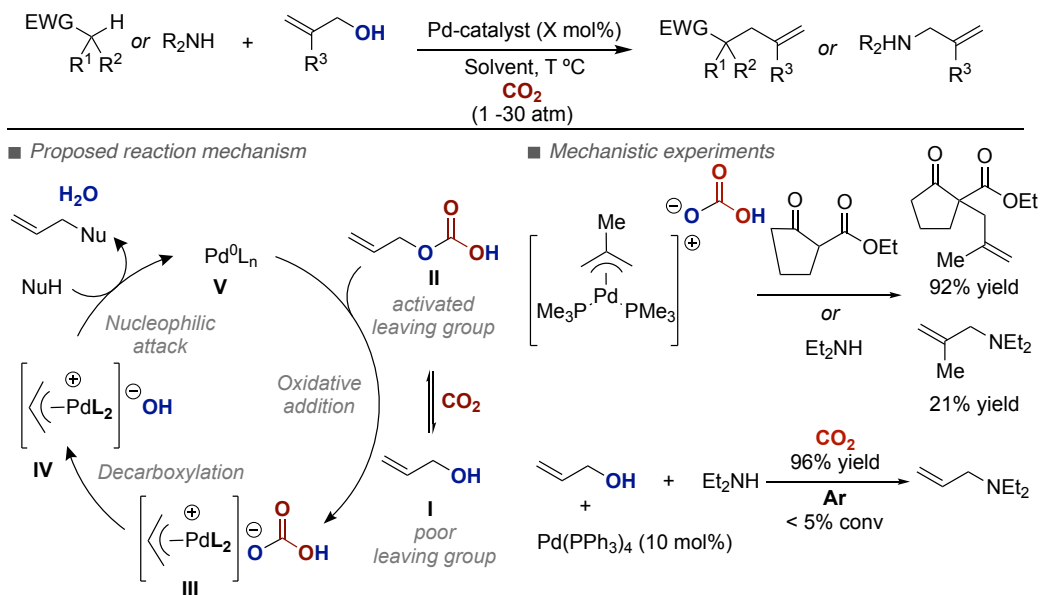


**Scheme 4.** Activation of allylic alcohols and catalysis with Ni-phosphine complexes.

At the outset of this doctoral thesis, a single example was described to promote the cross-coupling of allylic alcohols with CO<sub>2</sub> en route to carboxylic acids (Chapter 1, Scheme 21). This reaction demonstrated to be selective for the formation of branched carboxylic acids, regardless of the regioisomer of the allylic alcohol utilized. However, this protocol was conducted with pyrophoric Et<sub>2</sub>Zn as reducing agent thus lowering down the application profile of this methodology. From a mechanistic standpoint, the authors suggested that C–OH cleavage could be triggered by coordination with the zinc(II) Lewis acidic entity, thus forming a carbonate upon reaction with CO<sub>2</sub>. Although this methodology represented the first reductive carboxylation of allylic alcohols, it is important to remark that these results were published during the course of the studies described in this chapter. In any case, we considered that an approach based on the lack of pyrophoric reagent while controlling the site-selectivity of the transformation would be a particularly interesting endeavor for chemical invention.

### 1.4 CO<sub>2</sub> as an activating reagent for allylic alcohols

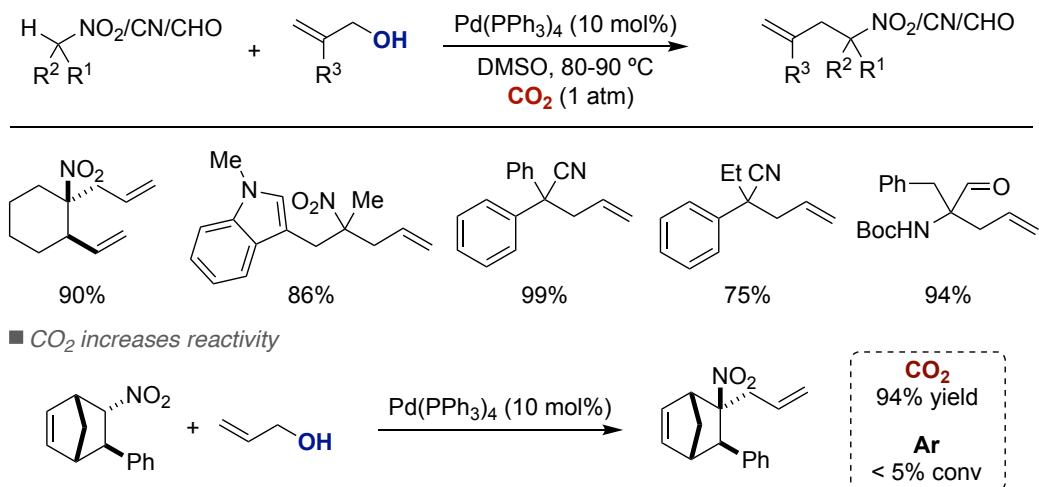
In 1996, Yamamoto described the Pd-catalyzed allylic substitution of allylic alcohols with appropriate nucleophilic entities under CO<sub>2</sub> atmosphere (Scheme 5).<sup>34</sup> The transformation was believed to proceed via the intermediacy of a hydrogenocarbonate (**II**), thus lowering down the bond dissociation energy of the targeted C–O bond en route to a hydrogenocarbonate anion (**III**).<sup>35</sup> Importantly, no reaction was observed under argon. Decarboxylation of the latter may release a hydroxide anion, which is sufficiently basic to abstract a proton from the amine or an active methylene compound, thus generating a nucleophilic entity with concomitant release of water. Direct attack of these nucleophiles to the η<sup>3</sup>-allyl-Pd complexes generates the allylated products and regenerates the active catalytic species **V**.



**Scheme 5.** Activation of allylic alcohols towards allylic substitution using CO<sub>2</sub>

Following Yamamoto's seminal discovery, Tunge reported that allylic alcohols could be activated with weakly acidic pronucleophiles, such as nitroalkanes, nitriles, and aldehydes in the presence of CO<sub>2</sub> (Scheme 6).<sup>36</sup> As previously observed, control experiments revealed that no conversion was observed in the absence of CO<sub>2</sub>, thus pointing towards the intermediacy of carbonic acids. Additionally, the released hydroxide anion was able to deprotonate pronucleophiles having a pK<sub>a</sub> up to 25.

## Site-Selective Catalytic Carboxylation of Allylic Alcohols with CO<sub>2</sub>

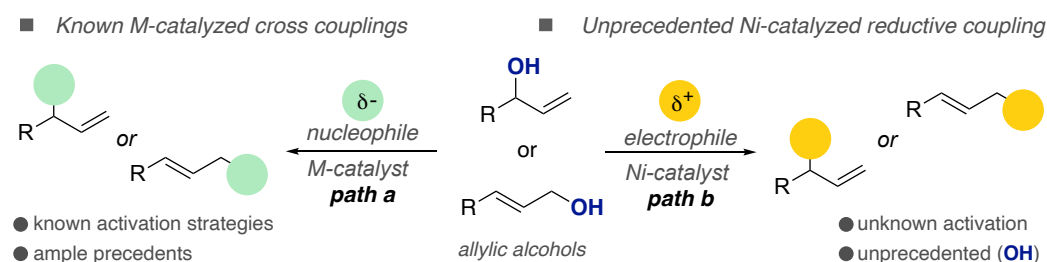


**Scheme 6.** Allylic alcohol activation towards allylic substitution using CO<sub>2</sub>.

From all the strategies that have been used for the activation of allylic alcohols, the utilization of CO<sub>2</sub> as an inert activating reagent probably represents the most atom economical, efficient and cost-effective approach. Indeed, the use of CO<sub>2</sub> and MeOH has already been employed in industrial settings as a strategy for the in-situ generation of a weak Brønsted methyl carbonic acid.<sup>37</sup>

## 2. General Objective of the Project

While redox-neutral metal-catalyzed allylic substitution reactions of allyl alcohols for forging C–C and C–heteroatom bonds have been well-developed (Scheme 7, *path a*),<sup>38</sup> the design of alternative cross-electrophilic regimes is not as commonly practiced as one might initially anticipate (Scheme 7, *path b*). This is largely due to the high polarizability and bond-dissociation energy of the O–H bond, together with the difficulty of trapping the corresponding intermediates with electrophilic rather than nucleophilic entities. We anticipated that the successful realization of this approach would unravel the potential of simple alcohols in cross-electrophile couplings, providing rapid access to important building blocks from one of the simplest and most atom economical allylic precursors.

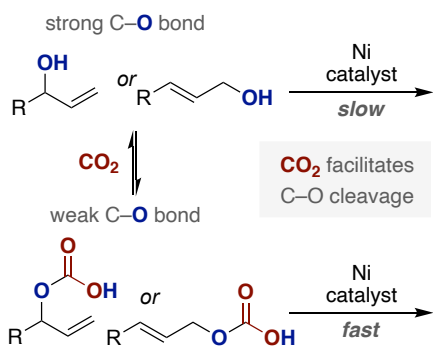


**Scheme 7.** Design principle for a Ni-catalyzed switchable site-selective carboxylation of allylic alcohols with CO<sub>2</sub>.

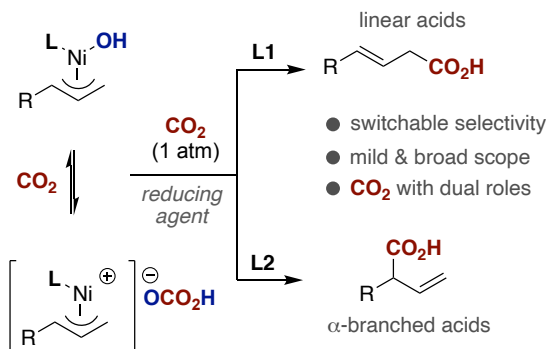
By 2015, the catalytic carboxylation of C–O electrophiles remained confined to activated *sp*<sup>2</sup> C–O bonds (chapter 1). Prompted by these observations, we wondered whether an atom- and step-economical technique could be implemented by promoting the direct carboxylation of allyl alcohols in the absence of stoichiometric amounts of air-sensitive organometallic reagents.<sup>39</sup> We hypothesized that CO<sub>2</sub> could be used with dual roles, both as a C1 source and as an activating group to facilitate C–O bond cleavage given the known propensity of CO<sub>2</sub> to reversibly react with alcohols to form carbonic acids. In this manner, we anticipated that CO<sub>2</sub> might lower the activation energy to promote C–O bond scission, thus accelerating the rate of oxidative addition to Ni(0)L<sub>*n*</sub> species prior to CO<sub>2</sub> insertion. In addition, the formation of a bicarbonate anion upon reversible reaction of the OH group with CO<sub>2</sub> would most likely enable the formation of key cationic π-allyl-Ni intermediates. In line with our knowledge in Ni catalysis, we hoped that site-selectivity at the allyl terminus could be controlled by the ligand used, leading to either linear or branched carboxylic acids from the same allylic precursor (Scheme 8).

## Site-Selective Catalytic Carboxylation of Allylic Alcohols with CO<sub>2</sub>

● CO<sub>2</sub> accelerated oxidative addition



● Ligand controlled site-selectivity

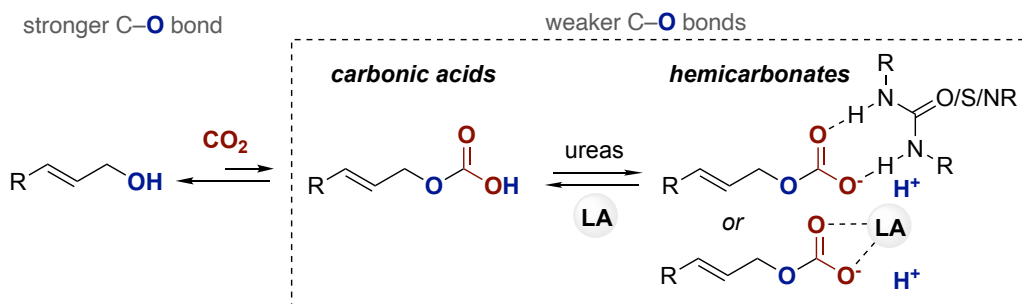


**Scheme 8.** Design principle for Ni-catalyzed switchable site-selective carboxylation of allylic alcohols with CO<sub>2</sub>.

### 3. Switchable Site-Selective Catalytic Carboxylation of Allylic Alcohols with CO<sub>2</sub>

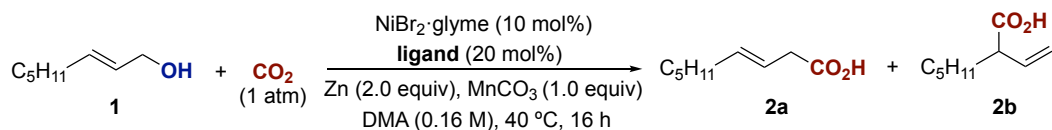
#### 3.1 Optimization of the reaction conditions (linear carboxylic acids)

According to the rationale depicted in Scheme 8, we anticipated that in-situ generated carbonic acids – coexisting in equilibrium with the corresponding alcohols upon reaction with CO<sub>2</sub> – might trigger oxidative addition to Ni(0)L<sub>n</sub>. Therefore, it was deemed necessary to shift the equilibrium towards the formation of such carbonic acid derivatives. To such end, we speculated that the utilization of suitable hydrogen bond donors as guanidinium ion, (thio)ureas or Lewis acids could favorably shift this equilibrium via the formation of hemicarbonates (Scheme 9).<sup>40-46</sup>

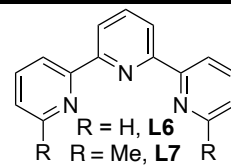
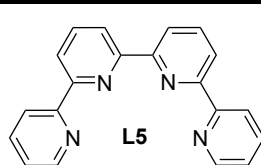
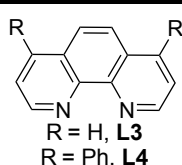
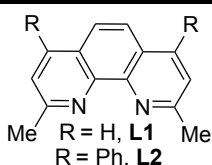


**Scheme 9.** Design principle for the activation of allylic alcohol in the presence of CO<sub>2</sub> and additives.

Initial investigations revealed that small amounts of carboxylic acids **2a/2b** were formed in the presence of MnCO<sub>3</sub> (Table 1). With these preliminary results in hand, we turned our attention to the ligand backbone, as we anticipated that we could establish valuable structure-reactivity relationships and exert site-selectivity principles en route to linear or branched products. Interestingly, tri- and tetradentate pyridine-based ligands provided low conversions, but favoring the formation of  $\alpha$ -branched products (**L5-7**), thus representing a useful entry point for future investigations. In contrast, bidentate phenanthroline ligands were found to preferentially form linear products in low yields (**L1-4**), with *ortho*-substituted **L2** giving the best results (11% yield and 73% conversion).

Site-Selective Catalytic Carboxylation of Allylic Alcohols with CO<sub>2</sub>


Ligand	Conv (%) <sup>a</sup>	Yield 2a + 2b (%) <sup>a</sup>	2a:2b <sup>a</sup>
neocuproine ( <b>L1</b> )	40	8	89:11
<b>bathocuproine (L2)</b>	<b>73</b>	<b>11</b>	<b>94:6</b>
phenantroline ( <b>L3</b> )	27	1	71:29
bathophenanthroline ( <b>L4</b> )	33	1	58:42
quaterpyridine ( <b>L5</b> )	37	1	1:99
terpyridine ( <b>L6</b> )	28	1	1:99
6,6''-dimethylterpyridine ( <b>L7</b> )	33	0	-

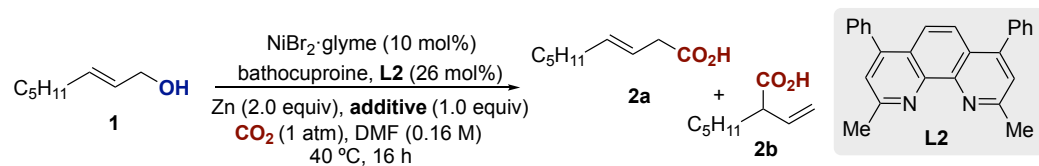


Reaction conditions: **1** (0.25 mmol), CO<sub>2</sub> (1 atm), NiBr<sub>2</sub>·glyme (10 mol%), ligand (20 mol%), Zn (0.5 mmol), MnCO<sub>3</sub> (0.25 mmol), DMA (1.5 mL), 40 °C, 16 h. <sup>a</sup> GC conversion, yield and selectivity determined using anisole as internal standard. The reduction of the starting material to the corresponding olefin accounts for the mass balance as the major side product.

**Table 1.** Screening of ligands.

With these preliminary results in hand, we focused our attention on the stabilization of the carbonic acid adducts formed upon reaction of allylic alcohol with CO<sub>2</sub> (Table 2). First, pyridine was tested with the assumption that this additive might act as weak base enabling a more facile equilibration of alcohol and CO<sub>2</sub> to the required hemicarbonat (entry 1). Arguing that Li-ions could have the capacity of stabilizing the hemicarbonat or carbonic acid adducts, LiCl was tested with no considerable improvement (entry 2). Prompted by the positive effects exerted by ammonium salts in catalytic carboxylation reactions, a number of these additives were also screened (entries 4-6). Although a slight improvement could be observed when using *n*Bu<sub>4</sub>Ni, the yield remained low. H-bond donors, which have demonstrated to accelerate hemicarbonat formation, were tested as well (entries 7 and 8). However, low conversions were obtained, which might suggest that these additives deactivate the catalytically active species by coordination to the nickel center. Turning our attention to the utilization of Lewis acids, it was found that Mg-based halide salts manifested a significant positive effect both on reactivity and

yield, with  $\text{MgCl}_2$  achieving the best results (entry 12). This boost in reactivity could be attributed to either the stabilization of the postulated carbonic acids or hemicarbonates as well as the known ability of magnesium (II) salts to facilitate  $\text{CO}_2$  insertion in Pd- and Ni-catalyzed carboxylation reactions.<sup>47</sup>



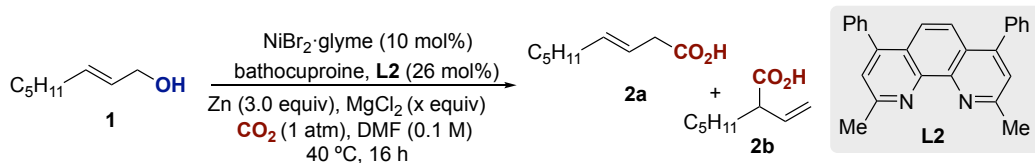
Entry	Additive	Conv (%) <sup>a</sup>	Yield 2a + 2b (%) <sup>a</sup>	2a:2b <sup>a</sup>
1	pyridine	44	6	99:1
2	LiCl	63	15	99:1
3	$\text{AlCl}_3$	74	12	99:1
4	$n\text{Bu}_4\text{NCl}$	38	9	97:3
5	$n\text{Bu}_4\text{NBr}$	43	10	99:1
6	$n\text{Bu}_4\text{NI}$	86	22	99:1
7	guanidine·HCl	28	5	99:1
8	diphenylthiourea	26	8	99:1
9	$\text{MgF}_2$	50	30	98:2
10	$\text{MgBr}_2$	79	52	99:1
11	$\text{MgI}_2$	82	54	98:2
<b>12</b>	<b><math>\text{MgCl}_2</math></b>	<b>95</b>	<b>61</b>	<b>99:1</b>

Reaction conditions: **1** (0.25 mmol),  $\text{CO}_2$  (1 atm),  $\text{NiBr}_2\cdot\text{glyme}$  (10 mol%), bathocuproine **L2** (26 mol%), Zn (0.5 mmol), additive (0.25 mmol), DMF (1.5 mL), 40 °C, 16 h. <sup>a</sup> GC conversion, yield and selectivity determined using anisole as internal standard. <sup>b</sup> DMF (2.5 ml). The reduction of the starting material to the corresponding olefin accounts for the mass balance as the major side product.

**Table 2.** Screening of additives.

Slight improvements could be achieved by increasing the loading of the reductant and diluting the reaction to 0.1 M with 1.2 equivalents of  $\text{MgCl}_2$  (Table 3).



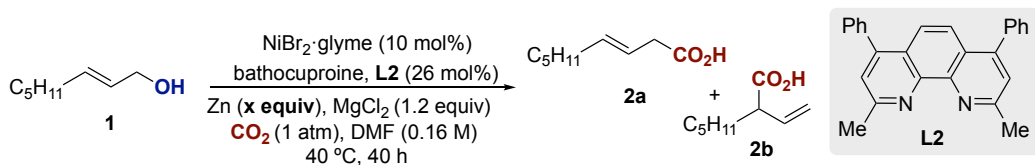
Site-Selective Catalytic Carboxylation of Allylic Alcohols with CO<sub>2</sub>


Entry	Additive equivalents	Conv (%) <sup>a</sup>	Yield <b>2a</b> + <b>2b</b> (%) <sup>a</sup>	<b>2a:2b</b> <sup>a</sup>
1	No MgCl <sub>2</sub>	59	26	99:1
2	MgCl <sub>2</sub> (0.25 equiv)	57	28	99:1
3	MgCl <sub>2</sub> (1.0 equiv)	73	47	99:1
4	<b>MgCl<sub>2</sub> (1.25 equiv)</b>	<b>88</b>	<b>64</b>	<b>99:1</b>
5	MgCl <sub>2</sub> (1.5 equiv)	84	55	99:1

Reaction conditions: **1** (0.25 mmol), CO<sub>2</sub> (1 atm), NiBr<sub>2</sub>·glyme (10 mol%), bathocuproine **L2** (26 mol%), Zn (0.75 mmol), MgCl<sub>2</sub> (x mmol), DMF (2.5 mL), 40 °C, 16 h. <sup>a</sup> GC conversion, yield and selectivity determined using anisole as internal standard. The reduction of the starting material to the corresponding olefin accounts for the mass balance as the major side product.

**Table 3.** Screening of MgCl<sub>2</sub> equivalents.

Even though the utilization of CO<sub>2</sub> in combination with MgCl<sub>2</sub> improved the formation of **2a**, it is noticeable that driving the reaction to full conversion was found to be particularly challenging. Unfortunately, lower chemoselectivities were found by raising the reaction temperature whereas the employment of Lewis acids other than MgCl<sub>2</sub> led to low conversions of **1**. Fine-tuning of the reaction conditions showed that the use of 4.0 equivalents of Zn reductant together with 1.2 equivalents of dry MgCl<sub>2</sub> (previously stored in the glove box), could drive the reaction to completion, giving rise to **2a** in 70% isolated yield with excellent site-selectivity profile (Table 4, entry 4).



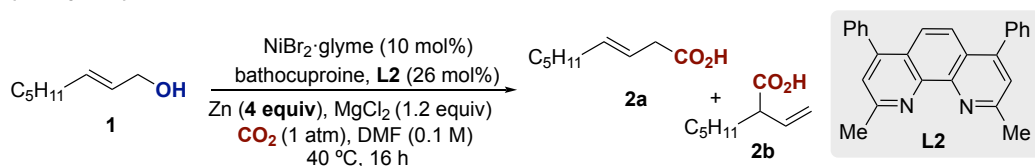
Entry	Ligand (mol%)	Conv (%) <sup>a</sup>	Yield <b>2a</b> + <b>2b</b> (%) <sup>a</sup>	<b>2a:2b</b> <sup>a</sup>
1	Zn (2.0 equiv)	68	37	99:1
2	Zn (2.5 equiv)	77	52	99:1
3	Zn (3.0 equiv)	87	64 (59)	99:1
4	<b>Zn (4.0 equiv)</b>	<b>99</b>	<b>78 (70)</b>	<b>99:1</b>

Reaction conditions: **1** (0.25 mmol), CO<sub>2</sub> (1 atm), NiBr<sub>2</sub>·glyme (10 mol%), bathocuproine **L2** (26 mol%), Zn (x mmol), MgCl<sub>2</sub> (1.25 mmol), DMF (2.5 mL), 40 °C, 40 h. <sup>a</sup> GC conversion, yield

and selectivity determined using anisole as internal standard. The reduction of the starting material to the corresponding olefin accounts for the mass balance as the major side product.

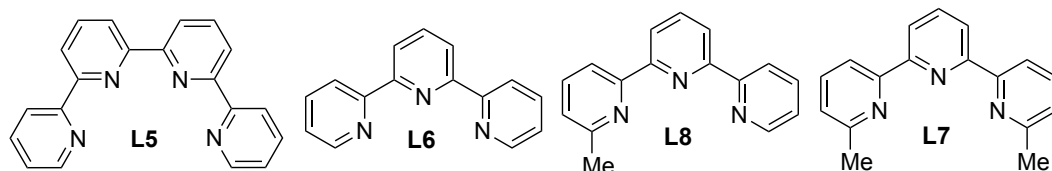
**Table 4.** Screening of zinc equivalents.

As shown in Table 5, the utilization of nickel precatalysts other than NiBr<sub>2</sub>·glyme afforded lower yields of **2a** (Table 5, entries 2-4). Notably, the use of quaterpyridine (entry 5) or terpyridine ligands (entries 6-8) afforded low amounts of carboxylated product, with preferential selectivity for the  $\alpha$ -branched **2b**. As previously shown in other carboxylation reactions, non-amide based solvents afforded very low yields of the desired product (entry 9). MgCl<sub>2</sub> was found to outperform other MgX<sub>2</sub> salts, suggesting that the nature of the halide might have an important role (entries 11 and 12). Interestingly, the utilization of Mn in lieu of Zn led to low yields, an intriguing observation taking into consideration the stronger reduction potential of the former (entry 14).



Entry	Deviation from standard conditions	Conv (%) <sup>a</sup>	Yield 2a + 2b (%) <sup>a</sup>	2a:2b <sup>a</sup>
<b>1</b>	<b>none</b>	<b>99</b>	<b>78 (70)</b>	<b>99:1</b>
2	NiBr <sub>2</sub> instead of NiBr <sub>2</sub> ·glyme	93	64	99:1
3	NiCl <sub>2</sub> ·glyme instead of NiBr <sub>2</sub> ·glyme	80	58	99:1
4	NiCl( <i>o</i> -tolyl)(TMEDA) instead of NiBr <sub>2</sub> ·glyme	99	60	99:1
5	<b>L5</b> instead of <b>L2</b>	22	1	-
6	<b>L6</b> instead of <b>L2</b>	8	0	-
7	<b>L8</b> instead of <b>L2</b>	25	6	38:62
8	<b>L7</b> instead of <b>L2</b>	55	18	23:77
9	THF instead of DMF	94	1	-
10	DMA instead of DMF	72	52	99:1
11	MgF <sub>2</sub> instead of MgCl <sub>2</sub>	50	30	98:2
12	MgI <sub>2</sub> instead of MgCl <sub>2</sub>	82	54	99:1
13	Na <sub>2</sub> CO <sub>3</sub> instead of MgCl <sub>2</sub>	46	32	99:1
14	Mn instead of Zn	10	9	-

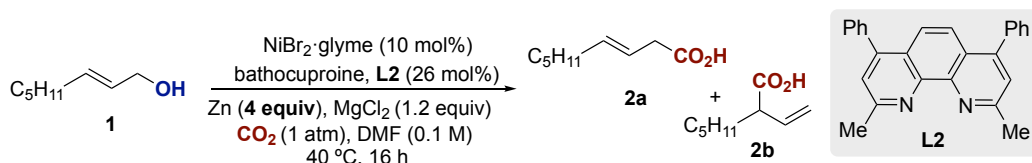
## Site-Selective Catalytic Carboxylation of Allylic Alcohols with CO<sub>2</sub>



Reaction conditions: **1** (0.25 mmol), CO<sub>2</sub> (1 atm), NiBr<sub>2</sub>·glyme (10 mol%), bathocuproine **L2** (26 mol%), Zn (1.0 mmol), MgCl<sub>2</sub> (1.25 mmol), DMF (2.5 mL), 40 °C, 16 h. <sup>a</sup> GC conversion, yield and selectivity determined using anisole as internal standard. The reduction of the starting material to the corresponding olefin accounts for the mass balance as the major side product.

**Table 5.** Deviation from standard conditions.

Control experiments demonstrated that all the reaction parameters were crucial for success. As shown in Table 6, the absence of Ni, ligand or reductant resulted in no conversion to **2a** (entries 2-4). Although significant amounts of product were observed in the absence of MgCl<sub>2</sub>, its presence boosted the reactivity of the carboxylation event. Importantly, significant conversion of **1** was found under argon atmospheres, indicating that direct oxidative addition of the allylic alcohol to the Ni(0) species might be a conceivable pathway.



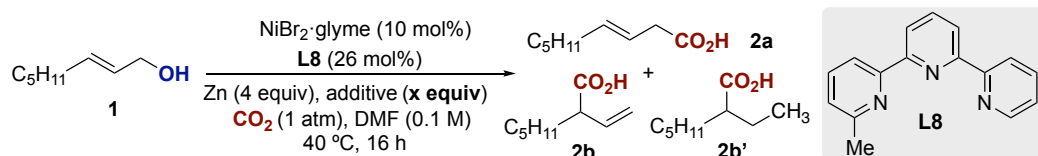
Entry	Deviation from standard conditions	Conv (%) <sup>a</sup>	Yield 2a + 2b (%) <sup>a</sup>	2a:2b <sup>a</sup>
<b>1</b>	<b>40 h</b>	<b>99</b>	<b>78 (70)</b>	<b>99:1</b>
2	no NiBr <sub>2</sub> ·glyme	0	-	-
3	no <b>L2</b>	32	0	-
4	no Zn	0	-	-
5	no MgCl <sub>2</sub>	82	48	99:1
6	no CO <sub>2</sub>	66	0	-

Reaction conditions: **1** (0.25 mmol), CO<sub>2</sub> (1 atm), NiBr<sub>2</sub>·glyme (10 mol%), bathocuproine **L2** (26 mol%), Zn (1.0 mmol), MgCl<sub>2</sub> (1.25 mmol), DMF (2.5 mL), 40 °C, 16 h. <sup>a</sup> GC conversion, yield and selectivity determined using anisole as internal standard. The reduction of the starting material to the corresponding olefin accounts for the mass balance as the major side product.

**Table 6.** Control experiments.

### 3.2. Optimization of the reaction conditions ( $\alpha$ -branched carboxylic acids)

With the aim of developing a regiodivergent system that would allow access to both linear or  $\alpha$ -branched carboxylic acids at will from the same allylic alcohol precursor, we turned our attention to study in detail the influence of the coordination geometry of the ligand employed. Indeed, the utilization of *ortho*-substituted terpyridine **L8** resulted in a site-selectivity switch, leading to  $\alpha$ -branched products, albeit in low yield (Table 7, entry 1). In line with our experience on carboxylation reactions, we anticipated that the nature of the additive employed will be crucial for success. Interestingly, improved results were found by reducing the amount of  $\text{MgCl}_2$  to 0.6 equivalents with 2.4 equivalents of  $n\text{Bu}_4\text{NCl}$  (entry 4). Intriguingly, this effect was only observed when  $n\text{Bu}_4\text{NCl}$  was used in combination with  $\text{MgCl}_2$  (entry 2 vs entries 5-8). These results indicated that both the Mg cation and the chloride anion have important roles in the catalytic activity. Unfortunately, no full conversion was achieved upon raising the temperature or extending the reaction time, suggesting catalyst deactivation. In addition, we identified the formation of the hydrogenated product **2b'** in the crude reaction mixtures, likely via reduction of **2b** with in-situ generated Ni-hydride intermediates.

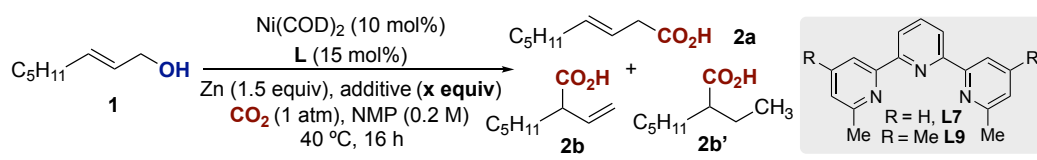


Entry	Additives	Conv (%) <sup>a</sup>	Yield 2a + 2b (%) <sup>a</sup>	2a:2b <sup>a</sup>	2b' (%) <sup>a</sup>
1	$\text{MgCl}_2$ (1.2 equiv)	55	18	1:99	3
2	$n\text{Bu}_4\text{NCl}$ (1.2 equiv)	30	0	-	-
3	$\text{MgCl}_2$ (1.2 eq), $n\text{Bu}_4\text{NCl}$ (1.2 eq)	92	23	2:98	9
4	<b><math>\text{MgCl}_2</math> (0.6 eq), <math>n\text{Bu}_4\text{NCl}</math> (2.4 eq)</b>	<b>53</b>	<b>41</b>	<b>4:96</b>	<b>5</b>
5	$\text{MgCl}_2$ (0.6 eq), $n\text{Bu}_4\text{NBr}$ (2.4 eq)	21	1	1:99	-
6	$\text{MgCl}_2$ (0.6 eq), $n\text{Bu}_4\text{NI}$ (2.4 eq)	7	1	1:99	-
7	$\text{MgCl}_2$ (0.6 eq), $n\text{Bu}_4\text{OTf}$ (2.4 eq)	6	2	1:99	-
8	$\text{MgCl}_2$ (0.6 eq), $\text{LiCl}$ (2.4 eq)	77	45	1:95	4

Reaction conditions: **1** (0.25 mmol),  $\text{CO}_2$  (1 atm),  $\text{NiBr}_2 \cdot \text{glyme}$  (10 mol%), **L8** (26 mol%), Zn (4.0 mmol), DMF (0.1 M),  $40^\circ\text{C}$ , 16 h. <sup>a</sup> GC conversion, yield and selectivity determined using anisole as internal standard. The reduction of the starting material to the corresponding olefin accounts for the mass balance as the major side product. **2b'** is the product resulting from alkene reduction of **2b**.

**Table 7.** Screening of additives.

After extensive experimentation, better reproducibility was obtained when Ni(COD)<sub>2</sub> and NMP were used. We also observed that *n*Bu<sub>4</sub>NOAc<sup>31</sup> afforded **2b** in low yields but with high site-selectivity towards **2b** (Table 8, entry 2). Intriguingly, better results were observed by increasing the number of equivalents of *n*Bu<sub>4</sub>NOAc (entry 3). While the inclusion of more electron-donating terpyridine ligand with two alkyl *para*-substituents (**L9**) was found to be rather beneficial (entry 5), full conversion could not be achieved and significant amounts of **2b'** were inevitably formed in the crude mixture.



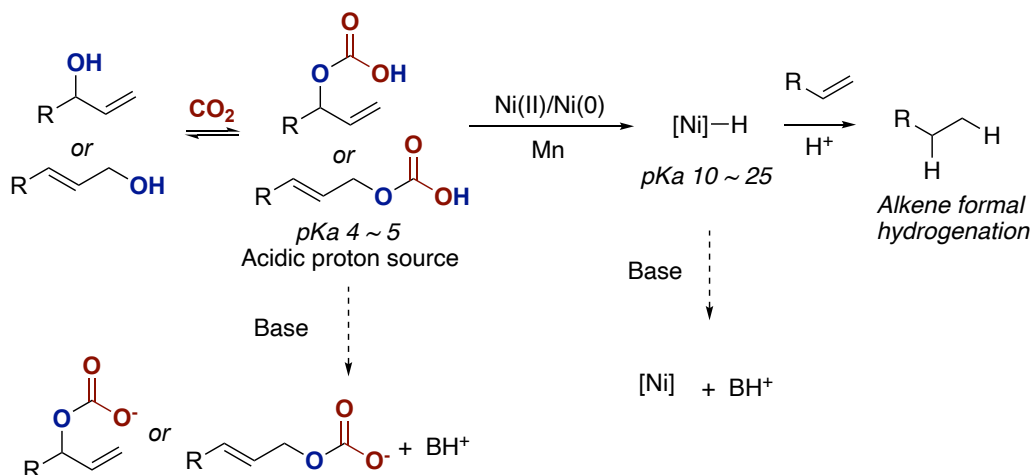
Entry	Additives	Ligand	Conv (%) <sup>a</sup>	Yield 2a + 2b (%) <sup>a</sup>	2a:2b <sup>a</sup>	2b' (%) <sup>a</sup>
1	MgCl <sub>2</sub> (0.6 eq), <i>n</i> Bu <sub>4</sub> NCl (2.4 eq)	L7	67	41	4:96	5
2	<i>n</i> Bu <sub>4</sub> NOAc (1.0 equiv)	L7	36	24	3:97	5
3	<i>n</i> Bu <sub>4</sub> NOAc (2.0 equiv)	L7	60	52	3:97	7
4	<i>n</i> Bu <sub>4</sub> NOAc (2.0 equiv)	L9	70	63 (58)	3:97	7
5	<i>n</i> Bu <sub>4</sub> NOAc (3.0 equiv)	L9	84	76	3:97	8
6	LiOAc (2.0 equiv)	L7	63	26	5:95	22
7	NaOAc (2.0 equiv)	L7	21	2	2:98	5

Reaction conditions: **1** (0.25 mmol), CO<sub>2</sub> (1 atm), Ni(COD)<sub>2</sub> (10 mol%), **LX** (15 mol%), Zn (0.38 mmol), additives (x mmol), NMP (1.25 mL), 40 °C, 16 h. <sup>a</sup> GC conversion, yield and selectivity determined using anisole as internal standard. The reduction of the starting material to the corresponding olefin accounts for the mass balance as the major side product. **2b'** is the product resulting from alkene reduction of **2b**.

**Table 8.** Screening of additives.

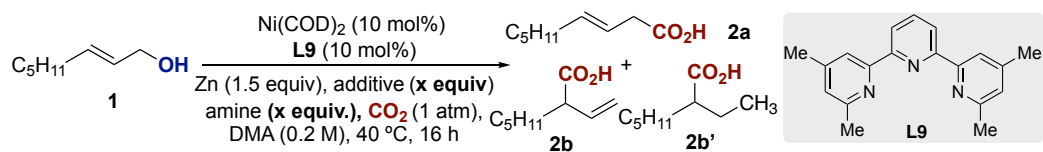
In parallel, we observed that the ligand used could be reduced to 10 mol% without any erosion in yield or selectivity. Due to the difficulty of obtaining anhydrous ammonium acetates, we decided to explore the influence of different Lewis acids in combination with *n*Bu<sub>4</sub>NCl. Particularly noteworthy was the observation that CaCl<sub>2</sub> outperformed MgCl<sub>2</sub> and other Lewis acids when DMA was used as solvent. However, competitive reduction of **2b** was still occurring, although to a lower extent. At this point we realized that the presence of alcohols/water in the media or the transient formation of carbonic acid might be promoting the formation of nickel hydrides, which would reduce partially product **2b**, giving an

inseparable mixture of acids **2b** and **2b'**. Aiming at avoiding the formation of nickel hydrides, we decided to test different bases (Scheme 10). We hypothesized that the base could deprotonate the acidic carbonic acids formed in-situ,<sup>48-49</sup> thus avoiding the formation of nickel hydrides. Alternatively, if the nickel hydride was formed, it could potentially be deprotonated as some nickel hydrides might present a slightly acidic character.<sup>50</sup>



**Scheme 10.** Mechanistic hypothesis for the hydrogenation of double bonds in the reaction conditions.

Importantly, the inclusion of organic bases did not only avoid the formation of **2b'** but also led, for the first time, to full conversion of **1** (Table 9). While tentative, these results could indicate that the addition of a base could avoid catalyst decomposition via the formation of Ni-hydride species. With these results in hand, we wondered whether excess amounts of  $\text{CaCl}_2$  might avoid the utilization of  $n\text{Bu}_4\text{NCl}$ . Gratifyingly, this was indeed the case and we could obtain **2b** in 81% isolated yield with an excellent site-selectivity pattern (entry 9).



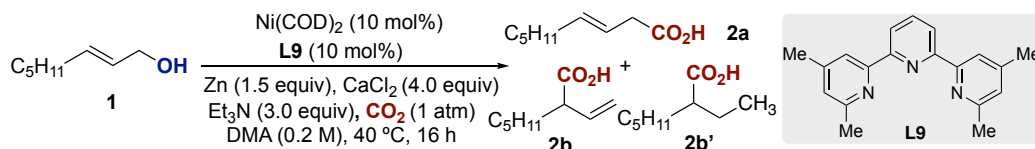
Entry	Additives	Amine	Conv (%) <sup>a</sup>	Yield 2a + 2b (%) <sup>a</sup>	2a:2b <sup>a</sup>	2b' (%) <sup>a</sup>
1	$\text{MgCl}_2$ (0.6 eq), $n\text{Bu}_4\text{NCl}$ (2.4 eq)	-	47	20	3:97	4
2	$\text{CaCl}_2$ (0.6 eq), $n\text{Bu}_4\text{NCl}$ (2.4 eq)	-	69	62	3:97	4

3	ZnCl <sub>2</sub> (0.6 eq), <i>n</i> Bu <sub>4</sub> NCl (2.4 eq)	-	25	14	3:97	2
4	CaCl <sub>2</sub> (2.0 eq), <i>n</i> Bu <sub>4</sub> NCl (1.0 eq)	-	94	49	3:97	4
5	CaCl <sub>2</sub> (2.0 eq), <i>n</i> Bu <sub>4</sub> NCl (1.0 eq)	Cy <sub>2</sub> MeN (1.0 equiv)	99	60	3:97	0
6	CaCl <sub>2</sub> (2.0 eq), <i>n</i> Bu <sub>4</sub> NCl (1.0 eq)	DIPEA (1.0 equiv)	99	56	3:97	0
7	CaCl <sub>2</sub> (2.0 eq), <i>n</i> Bu <sub>4</sub> NCl (1.0 eq)	Et <sub>3</sub> N (1.0 equiv)	99	59	3:97	0
8	CaCl <sub>2</sub> (2.0 eq), <i>n</i> Bu <sub>4</sub> NCl (1.0 eq)	Et <sub>3</sub> N (3.0 equiv)	99	66	3:97	0
9	<b>CaCl<sub>2</sub> (4.0 equiv)</b>	<b>Et<sub>3</sub>N (3.0 equiv)</b>	<b>99</b>	<b>86 (81)</b>	<b>3:97</b>	<b>0</b>

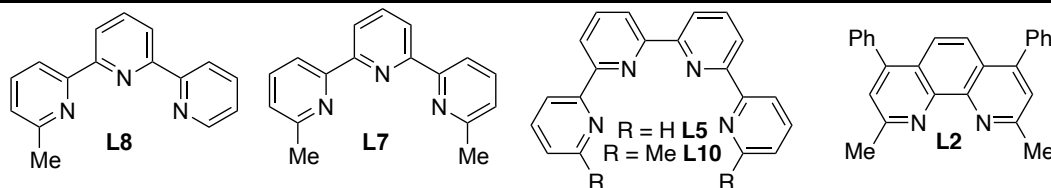
Reaction conditions: **1** (0.25 mmol), CO<sub>2</sub> (1 atm), Ni(COD)<sub>2</sub> (10 mol%), **L9** (10 mol%), Zn (0.38 mmol), additives (*x* mmol), DMA (1.25 mL), 40 °C, 16 h. <sup>a</sup> GC conversion, yield and selectivity determined using anisole as internal standard. The reduction of the starting material to the corresponding olefin accounts for the mass balance as the major side product. **2b'** is the product resulting from alkene reduction of **2b**.

**Table 9.** Screening of additives and amine bases.

Next, we turned our attention to study in detail whether all the reaction parameters were critical for success (Table 10). As expected, the utilization of other Ni(II) sources resulted in lower yield and conversion of the starting material (entries 2-4). Highly substituted **L9** demonstrated to be superior to all other terpyridine and quaterpyridine ligands we tried (entries 5-8). Importantly, these conditions could not be employed to afford **2a** efficiently by using **L2** (entry 9). While the use of other ethereal or amide-base solvents was detrimental for the reaction to occur (entries 10-12). Replacement of CaCl<sub>2</sub> for other Ca-based Lewis acids was found to inhibit the formation of **2b** (entries 14-15). Likewise, low reactivity was found by solely employing *n*Bu<sub>4</sub>NCl (entry 16). As expected, replacement of Et<sub>3</sub>N for other organic or inorganic bases resulted in lower conversion and yields, with significant amounts of **2b'** being formed in the reaction mixtures (entries 17-19). In line with our previous observations, poor results were accomplished by replacing Zn for Mn (entry 20).



Entry	Deviation from standard conditions	Conv (%) <sup>a</sup>	Yield		2a:2b <sup>a</sup>	2b' (%) <sup>a</sup>
			2a + 2b (%) <sup>a</sup>			
1	none	99	86 (81)		3:97	0
2	NiBr <sub>2</sub> ·glyme instead of Ni(COD) <sub>2</sub>	90	62		3:97	0
3	NiCl <sub>2</sub> ·glyme instead of Ni(COD) <sub>2</sub>	90	57		3:97	0
4	Ni(acac) <sub>2</sub> instead of Ni(COD) <sub>2</sub>	87	58		3:97	0
5	<b>L8</b> instead of <b>L9</b>	65	27		4:96	0
6	<b>L7</b> instead of <b>L9</b>	82	47		4:96	0
7	<b>L5</b> instead of <b>L9</b>	72	38		6:94	0
8	<b>L10</b> instead of <b>L9</b>	67	14		15:85	0
9	<b>L2</b> (26 mol%) instead of <b>L9</b>	70	32		90:10	0
10	THF instead of DMA	8	0		-	-
11	DMF instead of DMA	99	35		3:97	0
12	NMP instead of DMA	75	45		3:97	0
13	MgCl <sub>2</sub> instead of CaCl <sub>2</sub>	98	59		3:97	0
14	Ca(OTf) <sub>2</sub> instead of CaCl <sub>2</sub>	32	0		-	-
15	CaI <sub>2</sub> instead of CaCl <sub>2</sub>	22	0		-	-
16	<i>n</i> Bu <sub>4</sub> NCl instead of CaCl <sub>2</sub>	10	7		-	-
17	Na <sub>2</sub> CO <sub>3</sub> instead of Et <sub>3</sub> N	79	31		3:97	3
18	DIPEA instead of Et <sub>3</sub> N	99	67		3:97	0
19	Pyridine instead of Et <sub>3</sub> N	64	16		3:97	1
20	Mn instead of Zn	43	21		-	-

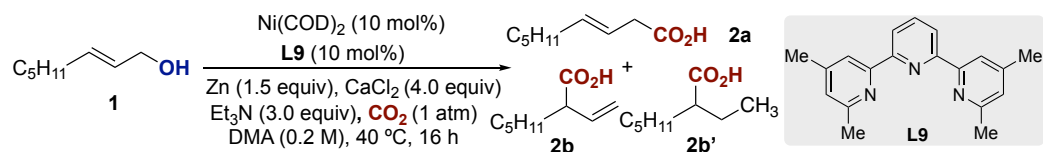


Reaction conditions: **1** (0.25 mmol),  $\text{CO}_2$  (1 atm),  $\text{Ni}(\text{COD})_2$  (10 mol%), **L9** (10 mol%), Zn (0.38 mmol),  $\text{CaCl}_2$  (1.0 mmol),  $\text{Et}_3\text{N}$  (0.75 mmol), DMA (1.25 mL), 40 °C, 16 h.<sup>a</sup> GC conversion, yield and selectivity determined using anisole as internal standard. The reduction of the starting material to the corresponding olefin accounts for the mass balance as the major side product. **2b'** is the product resulting from alkene reduction of **2b**.

**Table 10.** Deviation from standard conditions.



Table 11 shows that the presence of Ni, ligand and Zn was critical for success (entries 2-4). The omission of CaCl<sub>2</sub> resulted in no conversion of the starting material, thus indicating that it has a critical role in mediating one or more steps in the catalytic cycle (entry 5). Furthermore, the absence of Et<sub>3</sub>N resulted in lower yields of **2b** and **2b'**. Notably, olefin byproducts were observed by conducting the reaction under argon atmospheres.



Entry	Deviation from standard conditions	Conv (%) <sup>a</sup>	Yield		
			2a + 2b (%) <sup>a</sup>	2a:2b <sup>a</sup>	2b' (%) <sup>a</sup>
1	none	99	86 (81)	3:97	0
2	no Ni(COD) <sub>2</sub>	0	-	-	-
3	no L9	34	0	-	-
4	no Zn	0	-	-	-
5	no CaCl <sub>2</sub>	0	-	-	-
6	no Et <sub>3</sub> N	99	50	3:97	4
7	no CO <sub>2</sub>	21	-	-	-

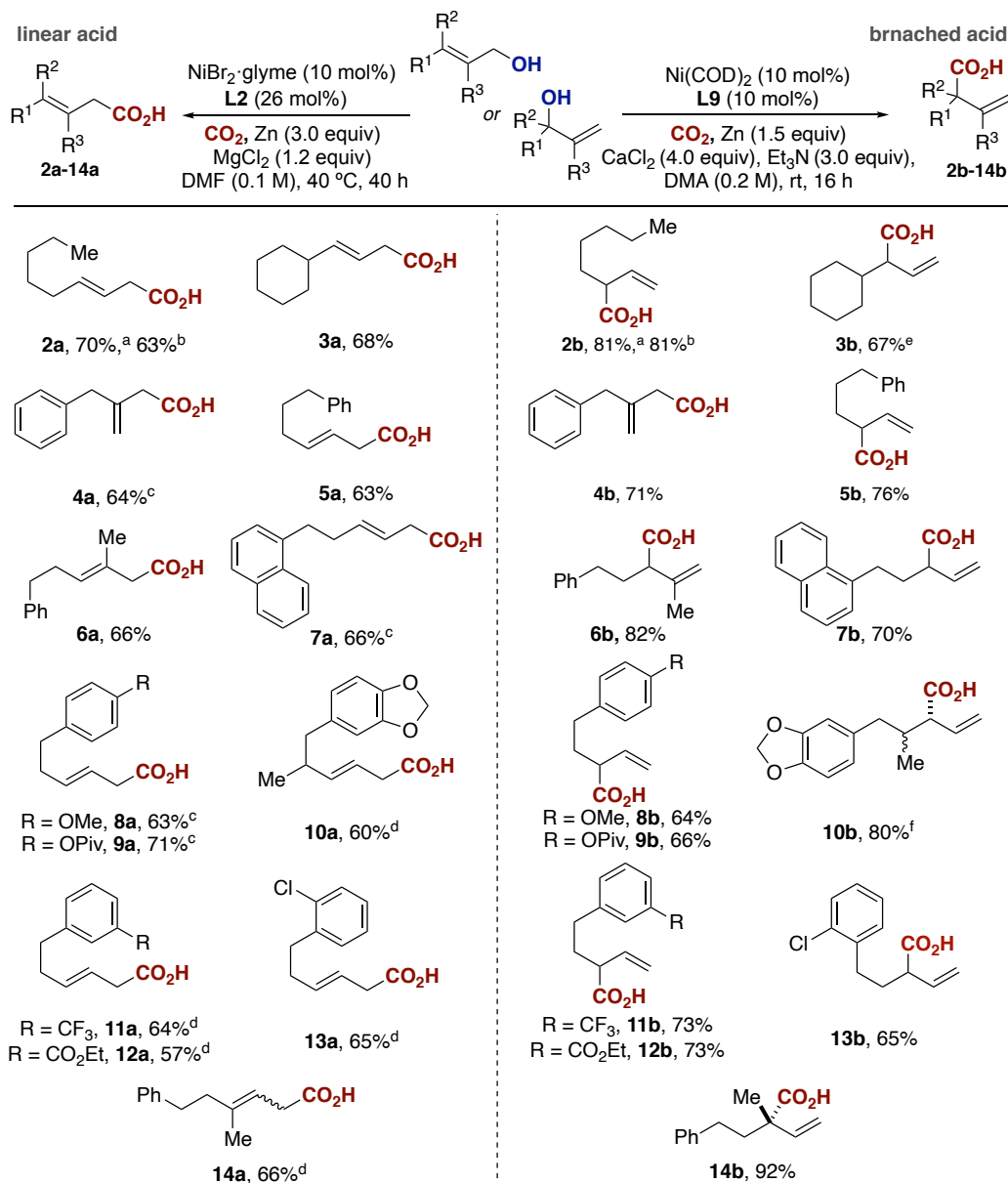
Reaction conditions: **1** (0.25 mmol), CO<sub>2</sub> (1 atm), Ni(COD)<sub>2</sub> (10 mol%), L9 (10 mol%), Zn (0.38 mmol), CaCl<sub>2</sub> (1.0 mmol), Et<sub>3</sub>N (0.75 mmol), DMA (1.25 mL), 40 °C, 16 h. <sup>a</sup> GC conversion, yield and selectivity determined using anisole as internal standard. The reduction of the starting material to the corresponding olefin accounts for the mass balance as the major side product. **2b'** is the product resulting from alkene reduction of **2b**.

**Table 11.** Control experiments.

### 3.3. Preparative substrate scope

Having optimized conditions to access either linear or  $\alpha$ -branched carboxylic acids, we next turned our attention to evaluate the generality of our Ni-catalyzed switchable site-selective carboxylation of allylic alcohols with CO<sub>2</sub> by using a Ni/L2 or Ni/L9 couple (Scheme 11). All the allylic alcohols were used as received or synthesized in one or two steps through vinyl magnesium bromide addition to the corresponding aldehyde. In all the examples we analyzed, an exquisite site-selectivity was observed regardless of whether linear or  $\alpha$ -branched allylic alcohols were employed, thus indicating that substrate-controlled site-selectivity does not come into play. This was demonstrated by the observation that **2a** and **2b** could be either accessed from the primary allyl alcohol or its branched analogue. Additionally, the carboxylation of  $\alpha$ -branched allylic alcohols gave rise to thermodynamically favored (*E*)-configured linear carboxylic acids in more than a 92:8 *E/Z* ratio (**2a-12a**). Not surprisingly, tertiary allyl alcohols provided **14a** as an *E* and *Z* mixture (ratio *E/Z* = 45:55), as two possible nickel  $\pi$ -allyl intermediates with similar energy are formed upon oxidative addition. However, the substitution pattern on the double bond of the allyl terminus had no influence on reactivity or site-selectivity, obtaining predominantly the corresponding linear or  $\alpha$ -branched carboxylic acids with the appropriate nickel/ligand system. In a similar way, the inclusion of substituents in the  $\alpha$ -position of the allyl motif had no influence over the efficiency of the reaction as **3a**, **3b** and **10a**, **10b** were obtained in good yields. Nevertheless, these substituents did have a minor influence over the site-selectivity of **3b** and **10b**, which were obtained in 82:18 and 85:15 branched/linear ratios, respectively. This lower selectivity could indicate that the direct nucleophilic attack of the  $\gamma$ -carbon of the olefin to CO<sub>2</sub> could be partially disfavored due to the steric hindrance of this substituent. Regarding the functional group compatibility of our carboxylation event, the presence of esters (**9a**, **9b**), acetals (**10a**, **10b**) or aryl chlorides (**13a**, **13b**) did not interfere with productive CO<sub>2</sub> insertion, thus providing ample opportunities for further functionalization. Particularly noteworthy was the ability to access quaternary centers (**14b**), as the number of examples of cross-electrophile coupling reactions utilizing tertiary alkyl electrophiles are still scarce.<sup>51-54</sup>

## Site-Selective Catalytic Carboxylation of Allylic Alcohols with CO<sub>2</sub>



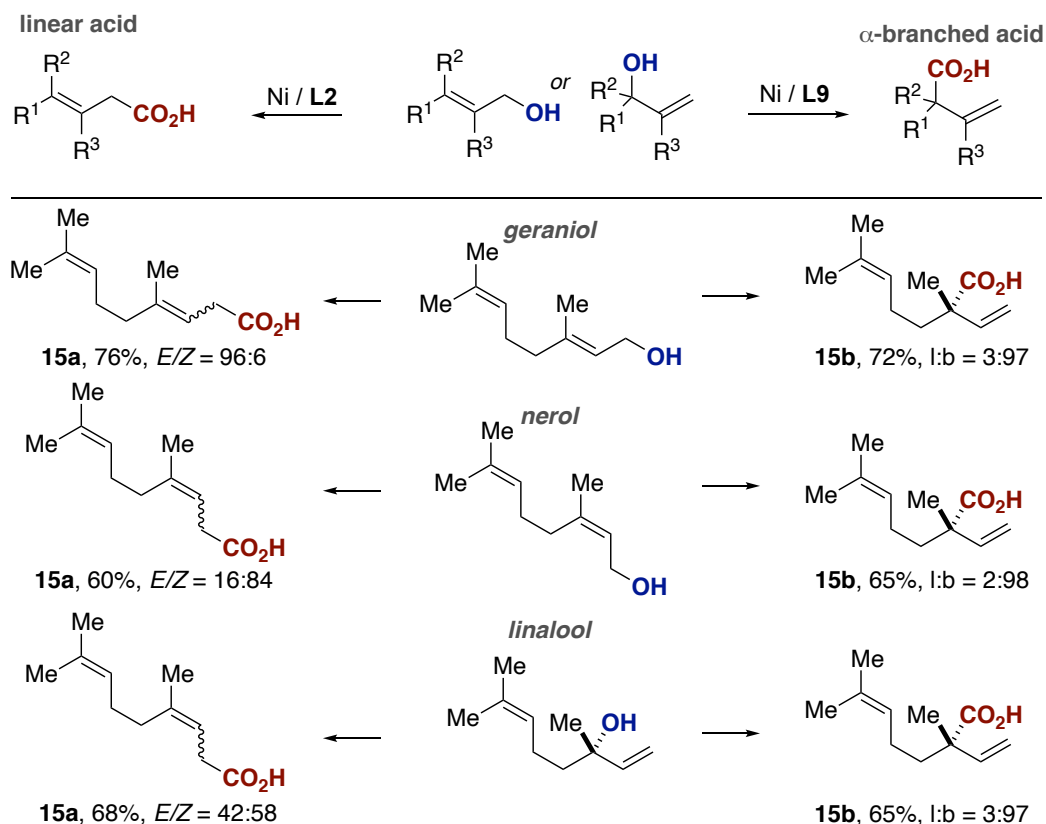
Reaction conditions for linear acids: **1** (0.25 mmol), CO<sub>2</sub> (1 atm), NiBr<sub>2</sub>·glyme (10 mol%), bathocuproine **L2** (26 mol%), Zn (1.0 mmol), MgCl<sub>2</sub> (0.3 mmol), DMF (2.5 mL), 40 °C, 40 h. Yield is that of isolated product, and an average of at least two independent runs. **2a – 15a** were all obtained in 99:1 (linear/branched) ratio. **2a – 13a** were obtained in > 92:8 *E/Z* ratio. <sup>a</sup> From linear alcohol. <sup>b</sup> From a branched alcohol. <sup>c</sup> Zn (2.50 equiv) in DMF (3.5 mL). <sup>d</sup> *E/Z*=45:55. Reaction conditions for α-branched acids: **1** (0.25 mmol), CO<sub>2</sub> (1 atm), Ni(COD)<sub>2</sub> (10 mol%), **L9** (10 mol%), Zn (0.38 mmol), CaCl<sub>2</sub> (1.0 mmol), Et<sub>3</sub>N (0.75 mmol) DMA (1.25 mL), rt, 16 h. Yield is that of isolated product, and an average of at least two Independent

runs. With the exception of 3b and 10b, all products were obtained in > 92:8 (branched/linear) ratio. <sup>e</sup> 82:18 (branched/linear). <sup>f</sup> 85:15 (branched/linear) and 1:1 diastereomeric ratio.

**Scheme 11.** Scope of the switchable site-selective catalytic carboxylation of allylic alcohols with CO<sub>2</sub>.

### 3.3.2. Application to isomeric geraniol, nerol and linalool natural allylic alcohols

After showing the versatility of the carboxylation with a wide variety of allylic alcohols to afford either (*E*)-configured linear or  $\alpha$ -branched carboxylic acids, we next turned our attention to explore the carboxylation of some monoterpenoid allylic alcohol isomers (Scheme 12). While the carboxylation of these substrates would certainly show the applicability of our methodology to naturally abundant allylic alcohols, the different configuration and substitution of the double bond in geraniol, nerol and linalool would provide valuable information about the stereoselectivity of the reaction. Under conditions to afford linear carboxylic acids, we observed a decent degree of stereoretention of the double bond configuration by using (*E*)-configured geraniol and (*Z*)-configured nerol, thus indicating that *E/Z*-isomerization through  $\pi$ -allyl formation does not occur to a large extent under these reaction conditions. This observation in the configuration of the double bond in the allylic alcohol precursor could be due to subtle changes in the hapticities of the intermediate allyl-Ni complex or the known ability of tethered alkenes on the side-chain to act as intramolecular directing groups.<sup>55</sup> As it could be foreseen from previous results, the carboxylation of linalool, which necessarily proceeds through two possible  $\pi$ -allyl intermediate, afforded **15a** as an *E* and *Z* mixture. In contrast, quaternary carboxylic acid **15b** was exclusively obtained from geraniol, nerol or linalool under the Ni/**L9** regime.



Reaction conditions for linear acids: **1** (0.25 mmol), CO<sub>2</sub> (1 atm), NiBr<sub>2</sub>·glyme (10 mol%), bathocuproine **L2** (26 mol%), Zn (1.0 mmol), MgCl<sub>2</sub> (0.3 mmol), DMF (2.5 mL), 40 °C, 16 h. Yield is that of isolated product, and an average of at least two Independent runs. **2a–15a** were all obtained in 99:1 (linear/branched) ratio. Reaction conditions for α-branched acids: **1** (0.25 mmol), CO<sub>2</sub> (1 atm), Ni(COD)<sub>2</sub> (10 mol%), **L9** (10 mol%), Zn (0.38 mmol), CaCl<sub>2</sub> (1.0 mmol), Et<sub>3</sub>N (0.75 mmol) DMA (1.25 mL), rt, 16 h. Yield is that of isolated product, and an average of at least two Independent runs. With the exception of **3b** and **10b**, all products were obtained in > 92:8 (branched/linear) ratio.

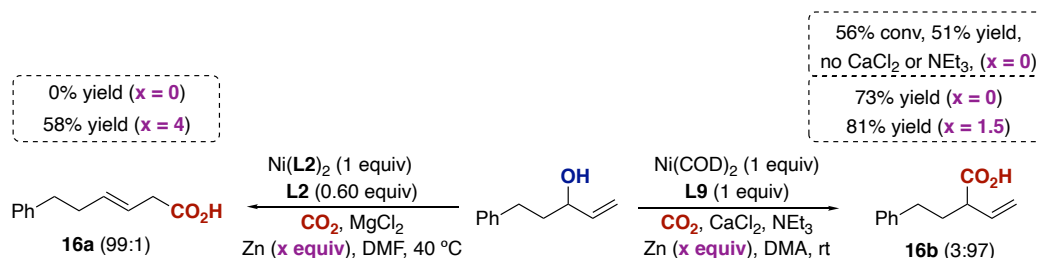
**Scheme 12.** Scope of the catalytic carboxylation using geraniol, nerol and linalool natural products.

## 4. Mechanistic studies

### 4.1. Stoichiometric experiments with Ni(0)(L2)<sub>2</sub> and Ni(COD)<sub>2</sub>/L9

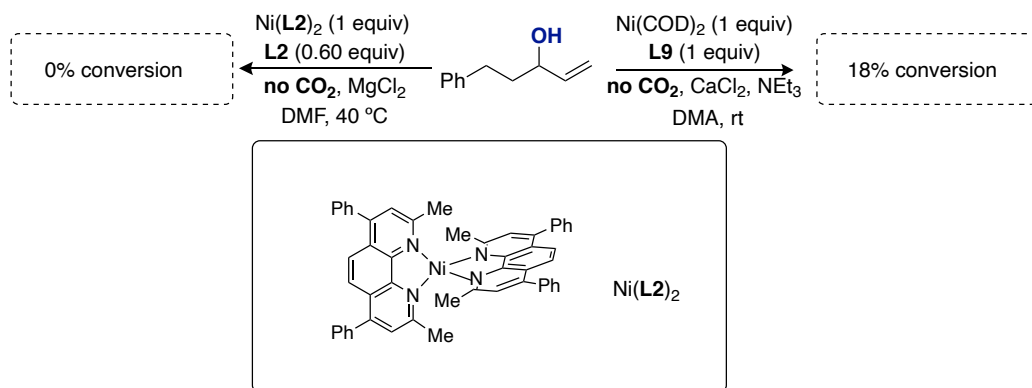
To obtain more mechanistic information, we decided to perform some stoichiometric and catalytic studies with isolated and well-characterized nickel complexes. We attempted the synthesis of nickel(0) complexes starting from Ni(COD)<sub>2</sub>, and while Ni(L2)<sub>2</sub> could be easily synthesized by following a reported literature procedure,<sup>56</sup> the synthesis of Ni(0)(L9) was more challenging as complex reaction mixtures or uncompleted reactions were observed. These results were not surprising considering that most of the known Ni-terpyridine complexes are formally Ni(II)/Ni(I)-halide or Ni(I)-alkyl complexes.<sup>57</sup> Despite the unsuccessful preparation of Ni(0)L9 complex in an analytically pure form, we decided to carry our mechanistic studies by employing Ni(COD)<sub>2</sub>/L9 instead.

Although we do not have a complete understanding on the full mechanistic picture, we turned our attention to gather empirical evidence about the role of the ligand by studying the reactivity of the two Ni(0) species. Firstly, stoichiometric experiments were conducted both in the presence and absence of the metal reductant (Scheme 13). While a Ni(L2)<sub>2</sub> required the presence of Zn to afford **16a**, the corresponding Ni(COD)<sub>2</sub>/L9 couple cleanly produced a 73% yield of **16b** in the absence of reductant, thus evidencing the unique role exerted by the ligand backbone. Although speculative, these results might suggest the intermediacy of in-situ generated  $\eta^1$ -Ni(I) intermediates after reduction by zinc with bidentate L2, in which CO<sub>2</sub> insertion takes place at the  $\alpha$ -carbon (Scheme 13, *left*). In contrast, the high yield observed in the absence of reductant by using tridentate L9 points towards the intermediacy of  $\eta^1$ -Ni(II) species, in which C–C bond-formation occurs through nucleophilic attack of the  $\gamma$ -carbon of the alkene to CO<sub>2</sub> (Scheme 13, *right*). This mechanistic interpretation is somewhat reminiscent of the elegant Pd-catalyzed carboxylation of allenes via  $\eta^1$ -allyl-Pd(II) intermediates possessing structurally related tridentate pincer-type ligands.<sup>58,59</sup> Interestingly, neither CaCl<sub>2</sub> or Et<sub>3</sub>N were found to be indispensable to afford the carboxylation when a stoichiometric amount of Ni(COD)<sub>2</sub>/L9 was employed. However, the absence of these additives did have an impact on the reaction conversion, possibly indicating that the reaction is occurring at a slower rate. These results are in sharp contrast to what was found in the catalytic version, where CaCl<sub>2</sub> was required in order to afford conversion to the targeted carboxylic acid products. Overall, these results suggest CaCl<sub>2</sub> could have a role in accelerating oxidative addition or CO<sub>2</sub> insertion, but it might have a bigger impact in turning over the catalytic cycle.



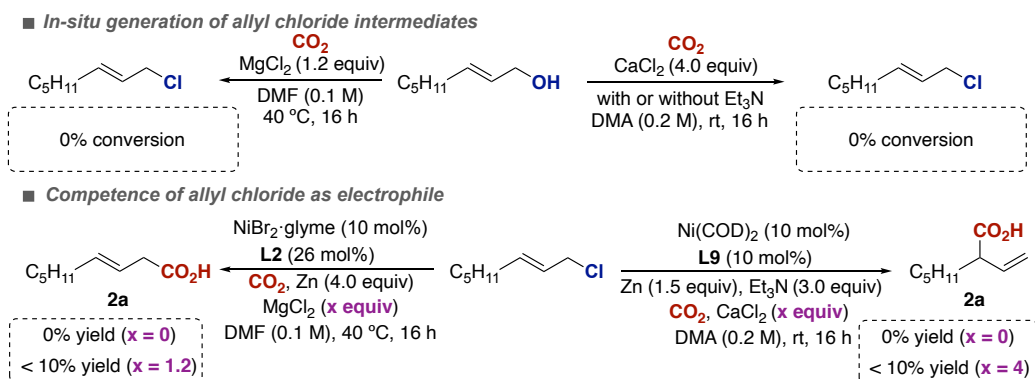
**Scheme 13.** Stoichiometric experiments with Ni(0)(L2)<sub>2</sub> and Ni(COD)<sub>2</sub>/L9 with and without Zn.

In order to shed some light over the possible role of CO<sub>2</sub> mediating oxidative addition through the in-situ formation of hemicarbonates or carbonic acids, we decided to study the conversion of the allylic alcohol when exposed to stoichiometric amounts of Ni(L2)<sub>2</sub> and Ni(COD)<sub>2</sub>/L9 in the absence of CO<sub>2</sub> (Scheme 14). If direct oxidative addition of these Ni(0) complexes to the allyl alcohol would be a fast process, a high conversion towards the corresponding reduced or dimerized products would be expected upon acidic quench of the putative nickel(II) intermediates. In contrast, we observed a complete absence of reactivity when it was exposed to Ni(L2)<sub>2</sub> even in the presence of Lewis acids. Similarly, a modest 18% conversion was observed when Ni(COD)<sub>2</sub>/L9 was used in combination with Et<sub>3</sub>N and CaCl<sub>2</sub>. Although tentative, these results might indicate that the actual reactive species are the proposed CO<sub>2</sub> adducts, which coexist in equilibrium with the corresponding allyl alcohols. Nevertheless, stronger evidence would be required to fully support such assumption. To such end, direct measurement of the equilibrium constants, the isolation and characterization of some of the reactive intermediates or the development of other Ni-catalyzed processes that used CO<sub>2</sub> as an activating reagent would help in determining the actual pathway for oxidative addition.



**Scheme 14.** Stoichiometric experiments with Ni(0)(L2)<sub>2</sub> and Ni(COD)<sub>2</sub>/L9 in the absence of CO<sub>2</sub>.

Although large amounts of MgCl<sub>2</sub> or CaCl<sub>2</sub> might generate an allyl chloride in-situ upon exposure to an allyl alcohol, control experiments ruled out this possibility (Scheme 15, top). Additionally, we demonstrated the corresponding allyl chlorides were not competent electrophiles under the reaction conditions (Scheme 15, bottom). While in the absence of Lewis acids full conversion to dimerized and reduced products was observed, the presence of either MgCl<sub>2</sub> or CaCl<sub>2</sub> allowed the formation of carboxylation products in less than 10% yield. These results could be rationalized by the known ability of these additives in facilitating CO<sub>2</sub> insertion into Ni-alkyl intermediates.



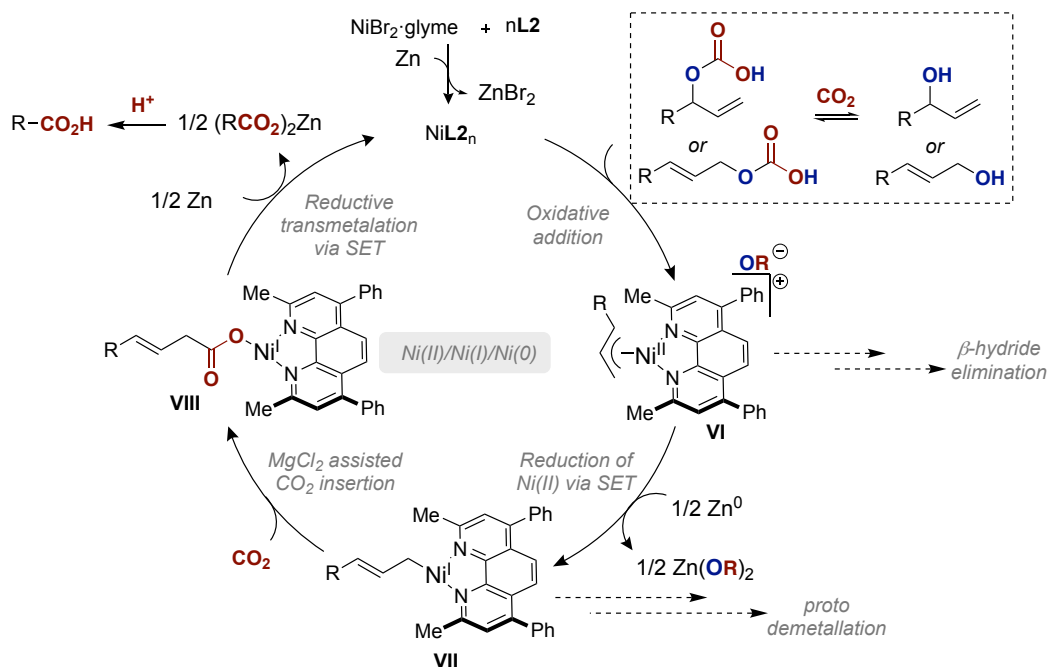
**Scheme 15.** Control experiments with allyl chlorides.



## 5. Proposed reaction mechanisms

### 5.1. Proposed reaction mechanism for the synthesis of linear carboxylic acids

In line with the above-mentioned results, we tentatively propose a catalytic cycle consisting of an initial generation of Ni(L2)<sub>2</sub> through two consecutive SET events mediated by Zn (Scheme 16). Oxidative addition of the more reactive carbonic acid or the corresponding hemicarbonato to Ni(0) should give rise to cationic  $\pi$ -allyl intermediate **VI**, in which the lower binding affinity of the carbonate anion should facilitate its formation. A higher reactivity of these CO<sub>2</sub> bound C–O electrophiles as compared to allylic alcohols is supported by the literature and by the observed negligible conversion when directly exposing allyl alcohols to Ni(0)(L2)<sub>2</sub> in the absence of CO<sub>2</sub> (Scheme 15). Based on the known reactivity of Ni(I)-alkyl complexes towards CO<sub>2</sub> insertion<sup>60,61</sup> and the lack of reactivity of Ni(L2)<sub>2</sub> in the absence of metal reductant, we propose Zn mediated SET might be required in order to promote efficient CO<sub>2</sub> insertion into a more nucleophilic C(sp<sup>3</sup>)-Ni(I) bond. Although two possible alkyl-Ni(I) species could be formed upon reduction of **VI**, the high rigidity of the phenanthroline ligand, and the steric bulk of the *ortho*-substituents would most likely favor the formation of a primary Ni(I)-alkyl complex (**VII**), thus explaining the site-selectivity observed for L2. Subsequently, CO<sub>2</sub> insertion could be assisted by MgCl<sub>2</sub> to afford Ni(I)-carboxylate **VIII**. Considering that the use of MgCl<sub>2</sub> was not absolutely critical for success, we tentatively propose that Zn might directly mediate the final reductive transmetalation of **VIII** to regenerate the catalytically active Ni(0) species with concomitant generation of Zn-carboxylate. Final acidic workup of the reaction should afford the corresponding linear carboxylic acid.

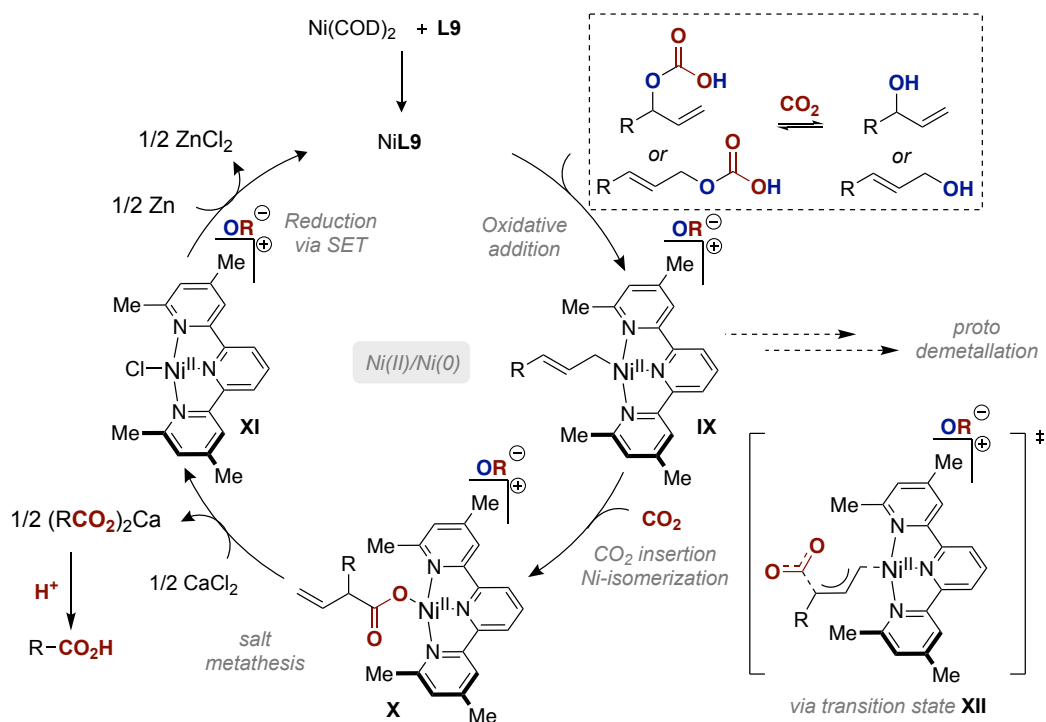


**Scheme 16.** Proposed reaction mechanism via Ni(II)/Ni(I)/Ni(0) for the formation of linear carboxylic acids.

## 5.2. Proposed reaction mechanism for the synthesis of $\alpha$ -branched carboxylic acids

As commented in the case of the linear carboxylation conditions, a more complete mechanistic picture would require further investigation. The basic observations we made throughout the optimization and the conducted mechanistic experiments have helped to propose the catalytic cycle depicted in Scheme 17. The formation of catalytically active Ni(L9) might occur upon L9 coordination to Ni(COD)<sub>2</sub>. In analogy with the linear carboxylation event, oxidative addition of the in-situ formed carbonic acids or hemicarbonates should give rise to Ni(II) intermediate **IX**. In contrast to the use of bidentate phenanthroline ligands, tridentate terpyridine ligands such as L9 would promote the formation of cationic  $\eta^1$ -alkyl-Ni(II)L9 complexes. Additionally, the higher binding affinity of a pyridine ligand as compared to an internal alkene would definitely favor this type of coordination in **IX**, resulting in a nickel center coordinatively saturated. Considering that stoichiometric experiments with Ni(COD)<sub>2</sub>/L9 in the absence of any metal reductant afforded **16b** in 73% yield (Scheme 13, right), we propose CO<sub>2</sub> insertion is directly occurring into **IX** without any prior SET reduction to nickel(I). As it has been proposed in the literature using related Pd-<sup>62,63</sup> and Ni-complexes,<sup>64</sup> CO<sub>2</sub> insertion is most likely occurring via transition state **XII**, in which direct nucleophilic attack of the  $\gamma$ -carbon of the alkene

to CO<sub>2</sub> allows the formation of an alkene coordinated Ni(II) intermediate that rapidly isomerizes to form Ni(II)-carboxylate **X**. Taking into consideration our optimization studies and the control experiments in the absence of CaCl<sub>2</sub> that revealed Lewis acids containing a chloride anion as a requisite for the reaction to occur, we proposed that this additive is likely enabling the regeneration of the active catalyst. Salt metathesis of CaCl<sub>2</sub> with **X**, should generate a Ca-carboxylate and Ni(II)-chloride intermediate **XI**, which presumably could be more easily reduced than the corresponding carboxylate. This hypothesis gains credence when considering that the stoichiometric carboxylation afforded 51% yield of the branched carboxylic acid in the absence of CaCl<sub>2</sub>, thus suggesting that this additive is most probably implicated at the last stages of the catalytic cycle, possibly enabling the regeneration of the active Ni(0) species. Nevertheless, further experimentation with isolated and characterized complexes or DFT calculations would be required to elucidate the actual mechanism of the reaction.



**Scheme 17.** Proposed reaction mechanism via Ni(II)/Ni(0) for the formation of α-branched carboxylic acids.

## 6. Conclusions

In this chapter we have collected the efforts towards the development of a Ni-catalyzed switchable site-selective carboxylation of allylic alcohols with CO<sub>2</sub>. Throughout the optimization we discovered the feasibility of this transformation utilizing pyridine-based ligands in combination with Lewis acids containing chloride anions. Different ligand structures provide access to two different mechanisms for CO<sub>2</sub> insertion, controlling the selectivity of the process to obtain selectively different products. The utilization of MCl<sub>2</sub> Lewis acids seems to be enhancing the overall reactivity of the catalytic cycle, favoring CO<sub>2</sub> insertion or the formation of hemcarbonate/carbonic acids to give an easier C–O cleavage. Additionally, CO<sub>2</sub> is used to enhance the reactivity of allylic alcohols through the in-situ formation of more reactive carbonic acids or hemcarbonate species. Given the mild reaction conditions of these reductive carboxylations, this transformation could be applied to a wide variety of allylic alcohols containing different functional groups. Moreover, the process was characterized by a broad generality allowing the carboxylation of structurally diverse allylic alcohols with high selectivity to form either linear or  $\alpha$ -branched carboxylic acids. Finally, we carried out some preliminary mechanistic investigations using stoichiometric amounts of isolated and characterized Ni(0)-complexes or a combination of Ni(COD)<sub>2</sub> and ligand. These results gave valuable insight about the oxidation state of the Ni-intermediate prior to CO<sub>2</sub> insertion and some hints about the possible role of the additives and the involvement of CO<sub>2</sub> in facilitating oxidative addition. Nevertheless, further mechanistic investigations are required to elucidate the full mechanistic picture of these transformations.

## 7. Experimental Section

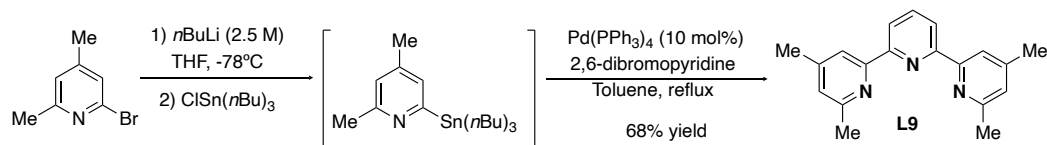
### General considerations

**Reagents.** Commercially available materials were used without further purification. NiBr<sub>2</sub>·glyme (97% purity; a better reproducibility was found when stored in the glovebox), MgCl<sub>2</sub> anhydrous (98% purity), CaCl<sub>2</sub> anhydrous (>92% purity, grinded inside the glovebox), Et<sub>3</sub>N anhydrous, nerol (>97% purity), linalool (>97% purity), and zinc dust (<10 μm, >98%) were purchased from Aldrich. Anhydrous *N,N*-dimethylformamide (DMF, 99.8% purity) and *N,N*-dimethylacetamide (DMA, 99.8% purity) were purchased from Acros Organics. 2-octen-1-ol (>97% purity) was obtained from Alfa Aesar, geraniol (>96% purity) and **L2** (>98% purity) from TCI, **L7** (>98% purity) from HETCAT and Ni(COD)<sub>2</sub> was obtained from Strem Chemicals.

**Analytical methods.** <sup>1</sup>H and <sup>13</sup>C NMR spectra were recorded on a Bruker 300MHz, 400 MHz and 500 MHz at 20 °C. All <sup>1</sup>H NMR spectra are reported in parts per million (ppm) downfield of TMS and were calibrated using the residual solvent peak of CHCl<sub>3</sub> (7.26 ppm), unless otherwise indicated. All <sup>13</sup>C NMR spectra are reported in ppm relative to TMS, were calibrated using the signal of CDCl<sub>3</sub> (77.16 ppm) and were obtained with <sup>1</sup>H decoupling unless otherwise indicated. Coupling constants, *J*, are reported in Hertz. Melting points were measured using open glass capillaries in a Büchi B540 apparatus. Infrared spectra were recorded on a Bruker Tensor 27. Gas chromatographic analyses were performed on Hewlett-Packard 6890 gas chromatography instrument with an FID detector and a Nujol stationary phase. Flash chromatography was performed with EM Science silica gel 60 (230-400 mesh). The yields reported as part of the substrate scope represent an average of at least two independent runs.

### Optimizations details

**General procedure.** An oven-dried schlenk tube containing a stirring bar was charged with Zn dust and the corresponding ligand. Subsequently the Schlenk tube was introduced into the glove box and charged with the corresponding nickel source and additives. The tube was taken out of the glovebox and connected to a vacuum line where it was evacuated and back filled under CO<sub>2</sub> flow for at least 3 times. Allyl alcohol **1** (0.2 mmol), Et<sub>3</sub>N (if applicable) and the solvent were added under CO<sub>2</sub> flow. Once added, the schlenk tube was closed at 1 atm of CO<sub>2</sub> and stirred for 16 hours at 40 °C . The mixture was carefully quenched with 2 M HCl to hydrolyze the resulting carboxylate and diluted with EtOAc. A sample of such obtained solution was analyzed by <sup>1</sup>H NMR spectroscopy using 1,3,5-trimethoxybenzene as internal standard or by gas chromatography analysis (GC) using anisole as internal standard. If needed, the resulting carboxylic acid was purified by column chromatography on silica gel (pentane/Et<sub>2</sub>O 6/1 followed by pentane/Et<sub>2</sub>O 1/1) to deliver the expected product.

**Synthesis of the ligand (L9)**

**Synthesis of 4,4'',6,6''-tetramethyl-2,2':6',2''-terpyridine (L9).** 2-bromo-4,6-dimethylpyridine<sup>65</sup> (9.0 g, 48 mmol) was placed in a dried 500 mL flask under argon. THF (100 mL) was added and the resulting solution was cooled to -78 °C. After stirring for 10 minutes at this temperature, *n*BuLi (2.5 M in hexanes, 21.5 mL, 1.1 equiv) was added dropwise. After the addition was complete, the resulting mixture was stirred at -78 °C for 90 min, followed by a slow addition of *n*Bu<sub>3</sub>SnCl (15.7 mL, 18.6 g, 57.0 mmol, 1.2 equiv). After the addition was complete, the resulting mixture was stirred at the same temperature for 2 h, followed by removal of the cooling bath and further stirring for 1 h. The reaction was quenched by the addition of water and extraction with Et<sub>2</sub>O. The combined organic layers were dried over MgSO<sub>4</sub>, filtered and concentrated. The crude product obtained (22.9 g, mixture of unreacted *n*-Bu<sub>3</sub>SnCl and product) was mixed with 2,6-dibromopyridine (3.8 g, 16.1 mmol), Pd(PPh<sub>3</sub>)<sub>4</sub> (1.86 g, 10 mol%) in toluene (150 mL) and placed in a dried flask under argon and stirred under reflux. After 24 hours the reaction mixture was allowed to cool to room temperature, and the volatiles were removed under reduced pressure. The black tarlike residue was taken up in aq. HCl (6 M, 10 mL) and CH<sub>2</sub>Cl<sub>2</sub> (30 mL). After a time-consuming phase separation, the organic phase was extracted with aq. HCl (6 M, 3 × 10 mL). The aqueous phases were combined and filtered through a plug of cotton. The resulting solution was cooled to 0 °C, and slowly basified with a saturated solution of NaOH. The basic solution was extracted with CH<sub>2</sub>Cl<sub>2</sub> (30 mL) three times, washed with brine, dried over MgSO<sub>4</sub>, filtered and evaporated under reduced pressure. The black residue was purified by flash column chromatography on basic alumina mixed with K<sub>2</sub>CO<sub>3</sub> (10% w/w) using a gradient of hexane:CH<sub>2</sub>Cl<sub>2</sub> (9:1 to 3:1 to pure CH<sub>2</sub>Cl<sub>2</sub>) affording of **L9** as white solid in 68% yield (3.15 g, 10.8 mmol).

**<sup>1</sup>H NMR (300 MHz, CDCl<sub>3</sub>):** δ = 8.43 (d, *J* = 7.8 Hz, 2H), 8.21 (s, 2H), 7.91 (t, *J* = 8.0 Hz, 1H), 7.03 (s, 2H), 2.61 (s, 6H), 2.45 (s, 6H) ppm.

**<sup>13</sup>C NMR (75 MHz, CDCl<sub>3</sub>):** δ = 157.8, 156.0, 155.8, 148.1, 137.8, 124.4, 121.2, 119.2, 24.6, 21.3 ppm.

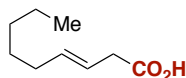
**Melting Point:** 146-147 °C.

**IR (neat, cm<sup>-1</sup>):** 3061, 2955, 2917, 1609, 1563, 1438, 1399, 1373, 1264, 1169, 1078, 911, 858, 821, 7400, 643, 530.

**HRMS (ESI<sup>+</sup>):** calcd. for C<sub>19</sub>H<sub>20</sub>N<sub>3</sub> (M+H): 290.1652, found 290.1652.

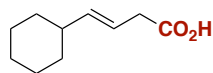
**Ni-catalyzed carboxylation of allyl alcohols using L2**

**General procedure A:** An oven-dried Schlenk tube equipped with a magnetic stirring bar was charged with Zn dust (60 mg, 1.0 mmol, 4.0 equiv) and **L2** (23.4 mg, 0.065 mmol, 26 mol%). Subsequently the Schlenk tube was introduced into the glove box and charged with MgCl<sub>2</sub> (28.2 mg, 0.300 mmol, 1.2 equiv). The Schlenk flask was extracted from the glove box and filled with CO<sub>2</sub> by applying three cycles of evacuation and filling with CO<sub>2</sub>. Subsequently, the allyl alcohol substrate (0.25 mmol) was added by syringe, followed by a stock solution of NiBr<sub>2</sub>·glyme (7.7 mg, 25 μmol, 10 mol%) in DMF (2.5 mL). During the addition of liquids, a continuous flow of CO<sub>2</sub> was maintained. The Schlenk flask was tightly sealed and placed into a pre-heated (40 °C) aluminum block. The reaction mixture was stirred at 40 °C for approx. 40 h, after which it was allowed to cool to room temperature and quenched by careful addition of 2 M aq. HCl sol. The reaction mixture was diluted with water and extracted three times with EtOAc. The combined organic phases were washed with brine, dried over MgSO<sub>4</sub> and filtered. The crude product was concentrated under reduced pressure and subjected to column chromatography (hexanes/EtOAc).



**(E)-3-nonenic acid (2a).** *From (E)-2-octen-1-ol:* Following the general procedure A, using (E)-2-octen-1-ol (38 μL, 0.25 mmol) as starting material, the title compound was obtained (28.6 mg, 73%) as a 94:6 E/Z-mixture (a pale yellow oil). In a separate experiment, 26.3 mg (67%) were obtained, giving an average yield of 70%. *From 1-octen-3-ol:* Following the general procedure A, using 1-octen-3-ol (37 μL, 0.25 mmol) as starting material, the title compound was obtained (24.6 mg, 63%) as a 93:7 E/Z-mixture (a pale yellow oil). In a separate experiment, 24.2 mg (62%) were obtained, giving an average yield of 63%. The observed spectral data are in good agreement with the literature.<sup>66</sup>

**<sup>1</sup>H NMR (500 MHz, CDCl<sub>3</sub>):** δ = 9.64 (brs, 1H), 5.63 – 5.46 (m, 2H), 3.07 (d, J = 5.6 Hz, 2H), 2.03 (td, J = 7.0, 6.6 Hz, 2H), 1.40 – 1.23 (m, 6H), 0.88 (t, J = 7.0 Hz, 3H) ppm.  
**<sup>13</sup>C NMR (125 MHz, CDCl<sub>3</sub>):** δ = 178.6, 135.6, 120.8, 37.9, 32.5, 31.4, 28.9, 22.6, 14.1 ppm.



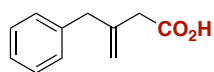
**(E)-4-cyclohexyl-3-butenic acid (3a).** Following the general procedure A, using 1-cyclohexyl-2-propen-1-ol (35 mg, 0.25 mmol) as starting material, the title compound was obtained (29.1 mg, 69%) as an 91:9 E/Z-mixture (a pale yellow oil). In a separate experiment, 27.9 mg (66%) were obtained, giving an average yield of 68%.

**<sup>1</sup>H NMR (500 MHz, CDCl<sub>3</sub>):** δ = 8.62 (brs, 1H), 5.57 – 5.42 (m, 2H), 3.06 (d, J = 6.5 Hz, 2H), 2.00 – 1.91 (m, 1H), 1.76 – 1.60 (m, 5H), 1.31 – 1.01 (m, 5H) ppm.  
**<sup>13</sup>C NMR (126 MHz, CDCl<sub>3</sub>):** δ = 178.3, 141.3, 118.5, 40.7, 38.0, 32.8, 26.2, 26.1 ppm.



**IR (neat, cm<sup>-1</sup>):** 3026, 2922, 2850, 1707, 1448, 1411, 1288, 1219, 967, 934.

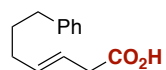
**HRMS (ESI-):** calcd. for C<sub>10</sub>H<sub>15</sub>O<sub>2</sub> (M-H): 167.1078, found 167.1070.



**3-benzyl-3-butenoic acid (4a).** General procedure A with the following changes: Zn (37.5 mg, 2.5 equiv.), DMF (3.5 mL) and a reaction time of 13 h using 2-benzyl-2-propen-1-ol (37.1 mg, 0.25 mmol) as starting material, the title compound was obtained (24.2 mg, 55%). In a separate experiment, 23.3 mg (53%) were obtained, giving an average yield of 54%. The observed spectral data are in good agreement with the ones reported in literature.<sup>67</sup>

**<sup>1</sup>H-NMR (500 MHz, CDCl<sub>3</sub>):** δ = 7.32 – 7.29 (m, 2H), 7.24 – 7.20 (m, 3H), 5.05 (d, *J* = 1.4 Hz, 1H), 5.01 (d, *J* = 1.4 Hz, 1H), 3.49 (s, 2H), 3.03 (s, 2H) ppm.

**<sup>13</sup>C NMR (126 MHz, CDCl<sub>3</sub>):** δ = 177.7, 141.3, 138.6, 129.2, 128.5, 126.5, 116.4, 42.7, 40.7 ppm.



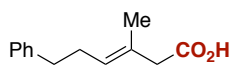
**(E)-7-phenyl-3-heptenoic acid (5a).** A modified form of general procedure A with the following changes: DMF (3.5 mL) and a reaction time of 13h, was followed using 6-phenyl-1-hexen-3-ol (48 mg, 0.25 mmol) as starting material, the title compound was obtained (31.6 mg, 62%) as a 91:9 *E/Z*-mixture (a pale yellow oil). In a separate experiment, 30.5 mg (60%) were obtained, giving an average yield of 61%.

**<sup>1</sup>H NMR (500 MHz, CDCl<sub>3</sub>):** δ = 7.30 – 7.24 (m, 2H), 7.20-7.14 (m, 3H), 5.65 – 5.48 (m, 2H), 3.08 (dd, *J* = 6.8, 1.3 Hz, 2H), 2.61 (t, *J* = 7.7 Hz, 2H), 2.08 (dtd, *J* = 7.5, 6.6, 1.2 Hz, 2H), 1.71 (tt, *J* = 7.7, 6.6 Hz, 2H) ppm.

**<sup>13</sup>C NMR (75 MHz, CDCl<sub>3</sub>):** δ = 178.5, 142.4, 135.0, 128.5, 128.4, 125.8, 121.4, 37.9, 35.4, 32.0, 30.8 ppm.

**IR (neat, cm<sup>-1</sup>):** 2928, 1705, 1412, 1288, 1220, 967, 908, 732, 698.

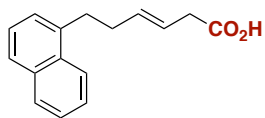
**HRMS (ESI-):** calcd. for C<sub>13</sub>H<sub>15</sub>O<sub>2</sub> (M-H): 203.1078, found 203.1070.



**(E)-3-methyl-6-phenyl-3-hexenoic acid (6a).** General procedure A was followed but employing 15 mol% Ni-source and the corresponding amount of ligand with 40 h of reaction time. Using 2-methyl-5-phenyl-1-penten-3-ol (44 mg, 0.25 mmol) as starting material, the title compound was obtained (29.5 mg, 58%) as a 92:8 *E/Z*-mixture (a pale yellow oil). In two further experiments, 26.0 mg (51%) and 29.4 mg (58%) were obtained, giving an average yield of 56%. The observed spectral data are in good agreement with the ones reported in literature.<sup>64</sup>

**<sup>1</sup>H NMR (400 MHz, CDCl<sub>3</sub>):** δ = 7.34 – 7.28 (m, 2H), 7.24 – 7.19 (m, 3H), 5.44 – 5.37 (m, 1H), 3.06 (s, 2H), 2.73 – 2.67 (m, 2H), 2.39 (q, *J* = 7.5 Hz, 2H) 1.69 (s, 3H) ppm.

**<sup>13</sup>C NMR (101 MHz, CDCl<sub>3</sub>):** δ = 178.3, 142.0, 129.2, 128.54, 128.5, 128.4, 125.9, 44.8, 35.7, 30.1, 16.3 ppm.



**(E)-6-(1-naphthalenyl)-3-hexenoic acid (6a).** General procedure A with the following changes: Zn (37.5 mg, 2.5 equiv.), DMF (3.5 mL) and a reaction time of 13 h, was followed using 5-(1-naphthalenyl)-1-penten-3-ol (53 mg,

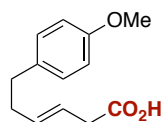
0.25 mmol) as starting material, the title compound was obtained (39.2 mg, 65%) as a 96:4 *E/Z*-mixture (a yellow oil). In a separate experiment, 36.0 mg (60%) were obtained, giving an average yield of 63%.

**<sup>1</sup>H NMR (400 MHz, CDCl<sub>3</sub>):** δ = 8.03 (dd, *J* = 8.1, 1.0 Hz, 1H), 7.86 (dd, *J* = 7.8, 1.6 Hz, 1H), 7.72 (d, *J* = 8.2 Hz, 1H), 7.51 (ddd, *J* = 8.2, 6.8, 1.6 Hz, 1H), 7.47 (ddd, *J* = 7.8, 6.8, 1.3 Hz, 1H), 7.39 (dd, *J* = 8.1, 7.2 Hz, 1H), 7.32 (dd, *J* = 7.2, 1.0 Hz, 1H), 5.74 (dtt, *J* = 15.4, 6.5, 1.2 Hz, 1H), 5.61 (dtt, *J* = 15.4, 6.8, 1.3 Hz, 1H), 3.15 (t, *J* = 7.9 Hz, 2H), 3.11 (dd, *J* = 6.8, 1.2 Hz, 2H), 2.51 (tdd, *J* = 7.9, 6.5, 1.3 Hz, 2H) ppm.

**<sup>13</sup>C NMR (126 MHz, CDCl<sub>3</sub>):** δ = 178.3, 137.8, 134.7, 134.0, 131.9, 128.9, 126.8, 126.1, 125.9, 125.6, 125.5, 123.8, 121.6, 37.8, 33.6, 32.7 ppm.

**IR (neat, cm<sup>-1</sup>):** 2923, 1705, 1397, 1264, 1217, 966, 776, 736.

**HRMS (ESI<sup>-</sup>):** calcd. for C<sub>16</sub>H<sub>15</sub>O<sub>2</sub> (M-H): 239.1078, found 239.1071.



**(E)-6-(4-methoxyphenyl)-3-hexenoic acid (8a).** General procedure A with the following changes: Zn (37.5 mg, 2.5 equiv.), DMF (3.5 mL) and a reaction time of 13 h using 5-(4-methoxyphenyl)-1-penten-3-ol (48 mg, 0.25 mmol) as starting

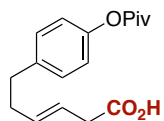
material, the title compound was obtained (35.4 mg, 64%) as a 92:8 *E/Z*-mixture (a yellow oil). In a separate experiment, 34.3 mg (62%) were obtained, giving an average yield of 63%.

**<sup>1</sup>H NMR (500 MHz, CDCl<sub>3</sub>):** δ = 7.11 – 7.06 (m, 2H), 6.85 – 6.80 (m, 2H), 5.64 (dtt, *J* = 15.4, 6.5, 1.2 Hz, 1H), 5.57 (dtt, *J* = 15.4, 6.8, 1.2 Hz, 1H), 3.79 (s, 3H), 3.08 (dd, *J* = 6.8, 1.2 Hz, 2H), 2.64 (t, *J* = 7.8 Hz, 2H), 2.34 (tdd, *J* = 7.8, 6.5, 1.2 Hz, 2H) ppm.

**<sup>13</sup>C NMR (126 MHz, CDCl<sub>3</sub>):** δ = 178.2, 157.9, 134.6, 133.8, 129.4, 121.5, 113.8, 55.3, 37.8, 34.7, 34.6 ppm.

**IR (neat, cm<sup>-1</sup>):** 2928, 1706, 1511, 1299, 1242, 1176, 1035, 967, 909, 823, 731, 518.

**HRMS (ESI<sup>-</sup>):** calcd. for C<sub>13</sub>H<sub>15</sub>O<sub>3</sub> (M-H): 219.1027, found 219.1022.



**(E)-6-(4-(pivaloyloxy)phenyl)-3-hexenoic acid (9a).** General procedure A with the following changes: Zn (37.5 mg, 2.5 equiv.), DMF (3.5 mL) and a reaction time of 13h using 5-(4-(pivaloyloxy)phenyl)-1-penten-3-ol (53 mg, 0.25 mmol) as starting

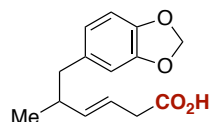
material, the title compound was obtained (52.5 mg, 72%) as a 95:5 *E/Z*-mixture (a pale yellow oil). In a separate experiment, 51.1 mg (70%) were obtained, giving an average yield of 71%.

**<sup>1</sup>H NMR (400 MHz, CDCl<sub>3</sub>):**  $\delta$  = 7.19 – 7.14 (m, 2H), 7.01 – 6.94 (m, 2H), 5.68 – 5.47 (m, 2H), 3.06 (d,  $J$  = 6.5 Hz, 2H), 2.75 – 7.66 (m, 2H), 2.42 – 2.33 (m, 2H), 1.37 (s, 9H) ppm.

**<sup>13</sup>C NMR (126 MHz, CDCl<sub>3</sub>):**  $\delta$  = 177.8, 177.4, 149.2, 139.0, 134.1, 129.4, 121.9, 121.3, 39.1, 37.8, 35.0, 34.3, 27.2 ppm.

**IR (neat, cm<sup>-1</sup>):** 2972, 1743, 1707, 1057, 1398, 1277, 1223, 1192, 1115, 895, 520.

**HRMS (ESI<sup>-</sup>):** calcd. for C<sub>17</sub>H<sub>21</sub>O<sub>4</sub> (M-H): 289.1445, found 289.1444.

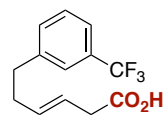


**(E)-6-(benzo[*d*][1,3]dioxol-5-yl)-5-methyl-3-hexenoic acid (10a).** General procedure A with the following changes: Zn (37.5

mg, 2.5 equiv), DMF (3.5 mL) and a reaction time of 13 h using 5-(benzo[*d*][1,3]dioxol-5-yl)-4-methyl-1-penten-3-ol (mixture of diastereoisomers, 55 mg, 0.25 mmol) as starting material, the title compound was obtained (39.3 mg, 63%) as a 97:3 *E/Z*-mixture (a pale yellow oil). In a separate experiment, 33.6 mg (57%) were obtained, giving an average yield of 60%. The observed spectral data are in good agreement with the ones reported in literature.<sup>64</sup>

**<sup>1</sup>H NMR (400 MHz, CDCl<sub>3</sub>):**  $\delta$  = 6.71 (d,  $J$  = 7.9 Hz, 1H), 6.62 (d,  $J$  = 1.7 Hz, 1H), 6.57 (dd,  $J$  = 7.9, 1.7 Hz, 1H), 5.91 (s, 2H), 5.58–5.39 (m, 2H), 3.05 (d,  $J$  = 6.6 Hz, 2H), 2.58 (dd,  $J$  = 12.8, 6.5 Hz, 1H), 2.48 – 2.34 (m, 2H), 0.98 (d,  $J$  = 6.4 Hz, 3H) ppm.

**<sup>13</sup>C NMR (101 MHz, CDCl<sub>3</sub>):**  $\delta$  = 178.3, 147.4, 145.7, 140.2, 134.4, 122.1, 119.7, 109.6, 108.0, 100.8, 43.3, 43.1, 38.5, 37.9, 19.5 ppm.



**(E)-6-(3-(trifluoromethyl)phenyl)-3-hexenoic acid (11a).**

General procedure A with the following changes: Zn (37.5 mg, 2.5 equiv.), DMF (3.5 mL) and a reaction time of 13 h using 5-(3-(trifluoromethyl)phenyl)-1-penten-3-ol (57.5 mg, 0.25 mmol) as starting material, the title compound was obtained (43.3 mg, 67%) as a 94:6 *E/Z*-mixture (a pale yellow oil). In a separate experiment, 39.2 mg (61%) were obtained, giving an average yield of 64%.

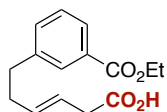
**<sup>1</sup>H-NMR (400 MHz, CDCl<sub>3</sub>):**  $\delta$  = 7.46 – 7.34 (m, 4H), 5.67 – 5.51 (m, 2H), 3.08 (d,  $J$  = 6.5 Hz, 2H), 2.76 (t,  $J$  = 7.7 Hz, 2H), 2.42 – 2.35 (m, 2H) ppm.

**<sup>13</sup>C NMR (101 MHz, CDCl<sub>3</sub>):**  $\delta$  = 178.2, 142.5, 133.7, 131.9, 130.7 (q,  $J$  = 31.9 Hz), 128.8, 125.2 (q,  $J$  = 3.8), 124.3 (q,  $J$  = 272.1 Hz), 122.9 (q,  $J$  = 3.9 Hz), 120.3, 37.7, 35.4, 34.0 ppm.

**<sup>19</sup>F NMR (376 MHz, CDCl<sub>3</sub>):**  $\delta$  –62.69 ppm.

**IR (neat, cm<sup>-1</sup>):** 2933, 1711, 1451, 1407, 1326, 1161, 1118, 1073, 968, 909, 800, 734, 702, 660.

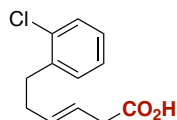
**HRMS (ESI<sup>-</sup>):** calcd. for C<sub>13</sub>H<sub>12</sub>F<sub>3</sub>O<sub>2</sub> (M-H): 257.0793, found 257.0795.

**(E)-6-(3-(ethoxycarbonyl)phenyl)-3-hexenoic acid (12a).**

General procedure A with the following changes: Zn (37.5 mg, 2.5 equiv.), DMF (3.5 mL) and a reaction time of 13h using ethyl 3-(3-hydroxy-4-penten-1-yl)benzoate (58.5 mg, 0.25 mmol) as starting material, the title compound was obtained (37.3 mg, 57%) as a 94:6 *E/Z*-mixture (a pale yellow oil). In a separate experiment, 36.4 mg (56%) were obtained, giving an average yield of 57%. The observed spectral data are in good agreement with the ones reported in literature.<sup>64</sup>

**<sup>1</sup>H NMR (500 MHz, CDCl<sub>3</sub>):**  $\delta$  = 7.89 – 7.85 (m, 2H), 7.37 – 7.33 (m, 2H), 5.67 – 5.51 (m, 2H), 4.37 (q, *J* = 7.1 Hz, 2H), 3.07 (d, *J* = 6.3 Hz, 2H), 2.78 – 2.72 (m, 2H), 2.42 – 2.34 (m, 2H), 1.39 (t, *J* = 7.1 Hz, 3H) ppm.

**<sup>13</sup>C NMR (126 MHz, CDCl<sub>3</sub>):**  $\delta$  = 178.0, 166.9, 141.9, 134.0, 133.1, 130.6, 129.6, 128.4, 127.3, 122.1, 61.0, 37.8, 35.3, 34.1, 14.4 ppm.

**(E)-6-(2-chlorophenyl)-3-hexenoic acid (13a).**

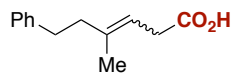
General procedure A with the following changes: Zn (37.5 mg, 2.5 equiv.), DMF (3.5 mL) and a reaction time of 13 h using 5-(2-chlorophenyl)-1-penten-3-ol (49.0 mg, 0.25 mmol) as starting material, the title compound was obtained (37.1 mg, 66%) as an approx. 93:7 (*E/Z*)-mixture (a pale yellow oil). In a separate experiment, 36.0 mg (64%) were obtained, giving an average yield of 65%.

**<sup>1</sup>H NMR (500 MHz, CDCl<sub>3</sub>):**  $\delta$  = 7.35 – 7.31 (m, 1H), 7.21 – 7.10 (m, 3H), 5.70 – 5.52 (m, 2H), 3.08 (dd, *J* = 6.7, 1.2 Hz, 1H), 2.82 (t, *J* = 7.7 Hz, 2H), 2.37 (tdd, *J* = 7.8, 6.4, 0.9 Hz, 1H) ppm.

**<sup>13</sup>C NMR (126 MHz, CDCl<sub>3</sub>):**  $\delta$  = 178.3, 139.2, 134.2, 134.0, 130.5, 129.5, 127.5, 126.8, 121.9, 37.8, 33.3, 32.5 ppm.

**IR (neat, cm<sup>-1</sup>):** 2932, 1703, 1474, 1442, 1295, 1220, 1051, 1033, 966, 748, 676.

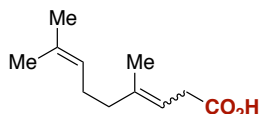
**HRMS (ESI):** calcd. for C<sub>12</sub>H<sub>12</sub>ClO<sub>2</sub> (M-H): 223.0528, found 223.0531.

**4-methyl-6-phenyl-3-hexenoic acid (14a).**

General procedure A was followed with 40 h of reaction time using 3-methyl-5-phenyl-1-penten-3-ol (44 mg, 0.25 mmol) as starting material, the title compound was obtained (34.7 mg, 68%) as a 1:1.2 *E/Z*-mixture (a pale yellow oil). In two further experiments 31.1 mg (61%) and 34.8 (68%) were obtained, giving an average yield of 66%. The observed spectral data are in good agreement with the ones reported in literature.<sup>64</sup>

**<sup>1</sup>H NMR (400 MHz, CDCl<sub>3</sub>):**  $\delta$  = 7.31 – 7.25 (m<sub>A</sub> 2H), 7.23 – 7.15 (m, 3H), 5.34 (tq, *J* = 7.1, 1.4 Hz, 1H), 3.10 (signal for (*E*), dq, *J* = 7.2, 1.0 Hz, 1H), 2.92 (signal for (*Z*), dq, *J* = 7.1, 1.2 Hz, 1H), 2.80 – 2.65 (m, 2H), 2.40 – 2.30 (m, 2H), 1.81 (signal for (*Z*), dt, *J* = 1.3, 1.3 Hz, 3H) 1.71 (signal for (*E*), d, *J* = 1.3 Hz, 3H) ppm.

**<sup>13</sup>C NMR (101 MHz, CDCl<sub>3</sub>):**  $\delta$  = 178.6, 142.1, 141.8, 139.4, 139.0, 128.5, 128.43, 128.40, 128.37, 126.0, 125.9, 116.4, 115.5, 41.5, 34.5, 34.3, 34.1, 33.5, 33.1, 23.5, 16.6 ppm.



**(E)-4,8-dimethylnona-3,7-dienoic acid (15a).** *From geraniol:* Following the general procedure A using geraniol (43  $\mu$ L, 0.25 mmol) as starting material, the title compound was obtained (34.9 mg, 77%) as a 94:6 *E/Z*-mixture (a pale yellow oil). In a separate experiment, 33.6 mg (74%) were obtained, giving an average yield of 76%.

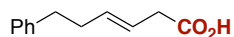
*From nerol:* General procedure A was followed but employing 15 mol% Ni-source and the corresponding amount of ligand. Using nerol (44  $\mu$ L, 0.25 mmol) as starting material, the title compound was obtained (28.5 mg, 63%) as a 16:84 *E/Z*-mixture (a pale yellow oil). In a separate experiment, 26.1 mg (57%) were obtained, giving an average yield of 60%.

*From linalool:* Following the general procedure A using linalool (44  $\mu$ L, 0.25 mmol) as starting material, the title compound was obtained (28.3 mg, 62%) as a 1:1.4 (*E*)/(*Z*)-mixture (a pale yellow oil). In a separate experiment, 27.5 mg (60%) were obtained, giving an average yield of 61%.

The observed spectral data are in good agreement with the literature.<sup>64</sup>

**<sup>1</sup>H NMR (500 MHz, CDCl<sub>3</sub>):**  $\delta$  = 9.23 (br. s, 1 H), 5.35 – 5.23 (d, *J* = 7.1 Hz, 1H), 5.12 – 5.06 (m, 1H), 3.09 (d, *J* = 7.1 Hz, 2H), 2.14-2.01 (m, 4H), 1.77 – 1.75 (signal of *Z*-isomer, m, 3H), 1.68 (brs, 3H), 1.64 (signal of *E*-isomer, br s, 3H), 1.60 (br s, 3H) ppm.

**<sup>13</sup>C NMR (125 MHz, CDCl<sub>3</sub>):** *E*-isomer:  $\delta$  = 178.8, 139.8, 131.8, 124.0, 115.0, 39.6, 33.6, 26.5, 25.8, 17.8, 16.5 ppm. *Z*-isomer:  $\delta$  = 178.8, 139.9, 132.2, 123.8, 115.7, 33.4, 32.2, 26.3, 25.8, 23.5, 17.7 ppm.



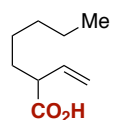
**(E)-6-phenyl-3-hexenoic acid (16a).** General procedure A with the following changes: Zn (37.5 mg, 2.5 equiv.), DMF (3.5 mL) and a reaction time of 13 h using 5-phenyl-1-penten-3-ol (40.5 mg, 0.25 mmol) as starting material, the title compound was obtained (29.9 mg, 63%) as an approx. 92:8 *E/Z*-mixture (incomplete signal separation, a pale yellow oil). In a separate experiment, 28.8 mg (61%) were obtained, giving an average yield of 62%. The observed spectral data are in good agreement with the ones reported in literature:<sup>64</sup>

**<sup>1</sup>H NMR (500 MHz, CDCl<sub>3</sub>):**  $\delta$  = 10.13 (br. s, 1 H), 7.33 – 7.27 (m, 2H), 7.22 – 7.16 (m, 3H), 5.70 – 5.54 (m, 2H), 3.07 (d, *J* = 6.5 Hz, 2H), 2.68 (t, *J* = 7.8 Hz, 2H), 2.36 (td, *J* = 7.8, 7.0 Hz, 2H) ppm.

**<sup>13</sup>C NMR (126 MHz, CDCl<sub>3</sub>):**  $\delta$  = 178.5, 141.7, 134.5, 128.5, 128.4, 125.9, 121.6, 37.9, 35.6, 34.3 ppm.

## Ni-catalyzed carboxylation of allyl alcohols using L9

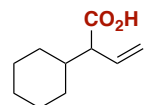
**General procedure B:** An oven-dried Schlenk tube equipped with a magnetic stirring bar was charged with Zn dust (24.5 mg, 0.38 mmol, 1.5 equiv) and 4,4'',6,6''-tetramethyl-2,2':6',2''-terpyridine (7.2 mg, 0.025 mmol, 10 mol%). Subsequently the Schlenk tube was introduced into the glove box and charged with CaCl<sub>2</sub> (111 mg, 1.00 mmol, 4.0 equiv) and Ni(COD)<sub>2</sub> (6.9 mg, 0.025 mmol, 10 mol%). The Schlenk flask was extracted from the glove box and filled with CO<sub>2</sub> by applying three cycles of evacuation and filling with CO<sub>2</sub>. Subsequently, the allyl alcohol substrate (0.25 mmol) was added by syringe, followed by Et<sub>3</sub>N (105 μL, 0.75 mmol, 3.0 equiv) and DMA (1.25 mL) with a constant flow of CO<sub>2</sub>. The Schlenk flask was tightly sealed and stirred at room temperature for 16 hours (otherwise stated) after which it was quenched by careful addition of 2 M aq. HCl sol. The reaction mixture was diluted with water and extracted 3 times with EtOAc. The combined organic phases were washed with brine, dried over MgSO<sub>4</sub> and filtered. The products were purified by flash chromatography (hexanes/EtOAc).



**2-vinylheptanoic acid (2b).** General procedure B was followed using (*E*)-oct-2-en-1-ol (32.1 mg, 0.25 mmol) as starting material provided 32.4 mg (83% yield) of the corresponding carboxylic acid (97:3 **2b:2a** mixture) as a colourless oil. In a separate experiment, 30.8 mg (79%) were obtained, giving an average yield of 81%. General procedure B was followed using oct-1-en-3-ol (32.1 mg, 0.25 mmol) as starting material provided 31.8 mg (81% yield) of the corresponding carboxylic acid (97:3 **2b:2a** mixture) as a colourless oil. In a separate experiment, 32.0 mg (82%) were obtained, giving an average yield of 81%. The observed spectral data are in agreement with the ones reported in literature.<sup>64</sup>

**<sup>1</sup>H NMR (400 MHz, CDCl<sub>3</sub>):** δ = 5.82 (ddd, *J* = 17.0, 10.3, 8.6 Hz, 1H), 5.18 (dd, *J* = 7.7, 1.1 Hz, 1H), 5.15 (s, 1H), 3.02 (3.02 (q, *J* = 7.2 Hz, 1H)), 1.83 – 1.72 (m, 1H), 1.61 – 1.51 (m, 1H), 1.36 – 1.14 (m, 6H), 0.88 (t, *J* = 6.6 Hz, 3H) ppm.

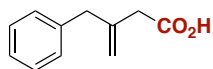
**<sup>13</sup>C NMR (101 MHz, CDCl<sub>3</sub>):** δ = 180.7, 135.7, 117.7, 50.3, 32.1, 31.6, 26.8, 22.6, 14.1 ppm.



**2-cyclohexylbut-3-enoic acid (3b).** General procedure B was followed using 1-cyclohexylprop-2-en-1-ol (35.1mg, 0.25 mmol) as starting material provided 28.9 mg (69% yield) of the corresponding carboxylic acid (82:18 **3b:3a** mixture) as a pale yellow oil. In a separate experiment, 27.2 mg (65%) were obtained, giving an average yield of 67%. The observed spectral data are in agreement with the ones reported in literature.<sup>68</sup>

**<sup>1</sup>H NMR (500 MHz, CDCl<sub>3</sub>):** δ = 5.79 (dt, *J* = 17.0, 9.9 Hz, 1H), 5.17 (dd, *J* = 10.2, 1.5 Hz, 1H), 5.13 (dd, *J* = 17.0, 1.5 Hz, 1H), 2.77 (t, *J* = 8.9 Hz, 1H), 1.91 – 1.57 (m, 6H), 1.37 – 0.83 (m, 5H) ppm.

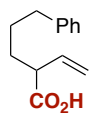
**<sup>13</sup>C NMR (75 MHz, CDCl<sub>3</sub>):** δ = 180.4, 134.7, 118.7, 57.4, 39.9, 31.3, 30.1, 26.3, 26.2, 26.2 ppm.



**3-benzyl-3-butenoic acid (4a).** General procedure B was followed using 2-benzyl-2-propen-1-ol (37.1 mg, 0.25 mmol) as starting material, the title compound was obtained (31.3 mg, 71%) as a pale yellow oil. In a separate experiment, 31.5 mg (71%) were obtained, giving an average yield of 71%. The observed spectral data are in good agreement with the ones reported in literature.<sup>67</sup>

**<sup>1</sup>H NMR (500 MHz, CDCl<sub>3</sub>):** δ = 7.32 – 7.29 (m, 2H), 7.24 – 7.20 (m, 3H), 5.05 (d, *J* = 1.4 Hz, 1H), 5.01 (d, *J* = 1.4 Hz, 1H), 3.49 (s, 2H), 3.03 (s, 2H) ppm.

**<sup>13</sup>C NMR (126 MHz, CDCl<sub>3</sub>):** δ = 177.7, 141.3, 138.6, 129.2, 128.5, 126.5, 116.4, 42.7, 40.7 ppm.



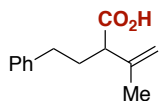
**5-phenyl-2-vinylpentanoic acid (5b).** General procedure B was followed using 6-phenylhex-1-en-3-ol (44.1 mg, 0.25 mmol) as starting material provided 40.5 mg (79% yield) of the corresponding carboxylic acid (95:5 **5b:5a** mixture) as a pale yellow oil. In a separate experiment, 37.5 mg (73%) were obtained, giving an average yield of 76%.

**<sup>1</sup>H NMR (300 MHz, CDCl<sub>3</sub>):** δ = 7.34 – 7.27 (m, 2H), 7.25 – 7.13 (m, 3H), 5.83 (ddd, *J* = 17.1, 9.9, 8.7 Hz, 1H), 5.21 (d, *J* = 3.7 Hz, 1H), 5.18 – 5.15 (m, 1H), 3.13 – 3.00 (m, 1H), 2.71 – 2.61 (m, 2H), 1.92 – 1.78 (m, 1H), 1.75 – 1.53 (m, 3H) ppm.

**<sup>13</sup>C NMR (75 MHz, CDCl<sub>3</sub>):** δ = 180.6, 142.0, 135.4, 128.5, 128.5, 126.0, 118.0, 50.1, 35.7, 31.6, 28.9 ppm.

**IR (neat, cm<sup>-1</sup>):** 3026, 2933, 2861, 1703, 1638, 1496, 1453, 1413, 1286, 1222, 992, 924, 748, 699.

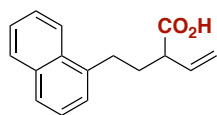
**HRMS (ESI):** calcd. for C<sub>13</sub>H<sub>15</sub>O<sub>2</sub> (M-H): 203.1078, found 203.1083.



**3-methyl-2-phenethylbut-3-enoic acid (6b).** General procedure B was followed using 2-methyl-5-phenylpent-1-en-3-ol (44.1 mg, 0.25 mmol) as starting material provided 41.7 mg (82% yield) of the corresponding carboxylic acid (>99:1 **6b:6a** mixture) as a pale yellow oil. In a separate experiment, 42.5 mg (83%) were obtained, giving an average yield of 82%. The observed spectral data are in agreement with the ones reported in literature.<sup>64</sup>

**<sup>1</sup>H NMR (400 MHz, CDCl<sub>3</sub>):** δ = 7.35 – 7.27 (m, 2H), 7.25 – 7.15 (m, 3H), 5.02 (q, *J* = 1.4 Hz, 1H), 4.98 (s, 1H), 3.11 (t, *J* = 7.5 Hz, 1H), 2.64 (d, *J* = 7.4 Hz, 2H), 2.26 – 2.08 (m, 1H), 2.03 – 1.88 (m, 1H), 1.83 (s, 3H) ppm.

**<sup>13</sup>C NMR (101 MHz, CDCl<sub>3</sub>):**  $\delta$  = 180.0, 141.8, 141.4, 128.6, 128.5, 126.2, 115.0, 52.4, 33.6, 31.6, 20.3 ppm.



**2-(2-(naphthalen-1-yl)ethyl)but-3-enoic acid (7b).** General procedure B was followed using 5-(1-naphthalenyl)-1-penten-3-ol (53 mg, 0.25 mmol) as starting material provided 42.0 mg (67% yield) of the corresponding carboxylic acid (>98:2 **7b**:**7a**

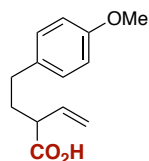
mixture) as a yellow oil. In a separate experiment, 43.6 mg (73% yield) were obtained, giving an average yield of 70%.

**<sup>1</sup>H NMR (400 MHz, CDCl<sub>3</sub>):**  $\delta$  = 8.04 (dq,  $J$  = 8.6, 0.9 Hz, 1H), 7.86 (dd,  $J$  = 7.9, 1.6 Hz, 1H), 7.74 (dt,  $J$  = 8.1, 1.0 Hz, 1H), 7.57 – 7.47 (m, 2H), 7.41 (t,  $J$  = 8.0, 1H), 7.34 (d,  $J$  = 7.0, 1H), 6.02 – 5.87 (m, 1H), 5.31 (d,  $J$  = 6.7 Hz, 1H), 5.27 (d,  $J$  = 0.8 Hz, 1H), 3.22 (q,  $J$  = 7.5 Hz, 1H), 3.17 – 3.11 (m, 2H), 2.37 – 2.26 (m, 1H), 2.09 – 1.98 (m, 1H) ppm.

**<sup>13</sup>C NMR (101 MHz, CDCl<sub>3</sub>):**  $\delta$  = 180.3, 137.5, 135.2, 134.1, 131.9, 128.9, 127.1, 126.3, 126.1, 125.7, 123.7, 118.6, 50.0, 32.9, 30.5 ppm.

**IR (neat, cm<sup>-1</sup>):** 3046, 2931, 1704, 1597, 1510, 1414, 1284, 926, 778.

**HRMS (ESI):** calcd. for C<sub>16</sub>H<sub>15</sub>O<sub>2</sub> (M-H): 239.1078, found 239.1084.



**2-(4-methoxyphenethyl)but-3-enoic acid (8b).** General procedure B was followed using 5-(4-methoxyphenyl)-1-penten-3-ol (48 mg, 0.25 mmol) as starting material provided 35.2 mg (64% yield) of the corresponding carboxylic acid (97:3 **8b**:**8a** mixture) as a pale yellow oil. In a separate experiment, 34.5 mg (63% yield) were obtained,

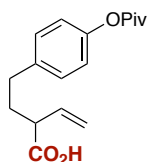
giving an average yield of 64%.

**<sup>1</sup>H NMR (400 MHz, CDCl<sub>3</sub>):**  $\delta$  = 7.10 (d,  $J$  = 8.6 Hz, 2H), 6.83 (d,  $J$  = 8.6 Hz, 2H), 5.86 (ddd,  $J$  = 17.0, 10.4, 8.6 Hz, 1H), 5.26 – 5.15 (m, 2H), 3.79 (s, 3H), 3.06 (q,  $J$  = 7.8 Hz, 1H), 2.70 – 2.52 (m, 2H), 2.16 – 2.05 (m, 1H), 1.89 – 1.79 (m, 1H) ppm.

**<sup>13</sup>C NMR (101 MHz, CDCl<sub>3</sub>):**  $\delta$  180.3, 158.1, 135.3, 133.3, 129.5, 129.5, 118.3, 114.0, 55.4, 49.4, 33.8, 32.3 ppm.

**IR (neat, cm<sup>-1</sup>):** 2932, 2836, 1704, 1512, 1442, 1300, 1245, 1177, 1036, 925, 831.

**HRMS (ESI):** calcd. for C<sub>13</sub>H<sub>15</sub>O<sub>3</sub> (M-H): 219.1027, found 219.1027.



**2-(4-(pivaloyloxy)phenethyl)but-3-enoic acid (9b):.** General procedure B was followed using 5-(4-(pivaloyloxy)phenyl)-1-penten-3-ol (53 mg, 0.25 mmol) as starting material provided 49.8 mg (69% yield) of the corresponding carboxylic acid (97:3 **9b**:**9a** mixture) as a white solid. In a separate experiment, 45.5 mg (63% yield) were

obtained, giving an average yield of 66%.

**<sup>1</sup>H NMR (400 MHz, CDCl<sub>3</sub>):**  $\delta$  = 7.18 (d,  $J$  = 8.5 Hz, 2H), 7.06 – 6.93 (m, 2H), 5.86 (ddd,  $J$  = 17.0, 10.3, 8.6 Hz, 1H), 5.25 – 5.22 (m, 1H), 5.22 – 5.16 (m, 1H), 3.06 (q,  $J$  =



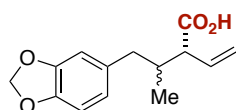
7.7 Hz, 1H), 2.77 – 2.52 (m, 2H), 2.18 – 2.07 (m, 1H), 1.92 – 1.81(m, 1H), 1.35 (s, 9H) ppm.

**<sup>13</sup>C NMR (101 MHz, CDCl<sub>3</sub>):** δ = 180.0, 177.4, 149.5, 138.5, 135.2, 129.4, 121.5, 118.4, 49.4, 39.2, 33.5, 32.6, 27.3 ppm.

**Melting Point:** 85-86 °C.

**IR (neat, cm<sup>-1</sup>):** 2978, 1740, 1699, 1637, 1506, 1456, 1279, 1197, 1165, 1122, 924, 898, 761.

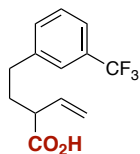
**HRMS (ESI-):** calcd. for C<sub>17</sub>H<sub>21</sub>O<sub>4</sub> (M-H): 289.1445, found 289.1446.



**2-(1-(Benzo[d][1,3]dioxol-6-yl)propan-2-yl)but-3-enoic acid (10b).** General procedure B (reaction time: 40 h) was followed using 5-(benzo[d][1,3]dioxol-5-yl)-4-methylpent-1-en-3-ol (55.1 mg, 0.25 mmol) as starting material provided 48.5 mg (78% yield) of the corresponding carboxylic acid (1:1 *syn:anti*, 85:15 **10b:10a** mixture) as a pale yellow oil. In a separate experiment, 51.1 mg (82%) were obtained, giving an average yield of 80%. The observed spectral data are in agreement with the ones reported in literature.<sup>64</sup> (Mixture of isomers)

**<sup>1</sup>H NMR (400 MHz, CDCl<sub>3</sub>):** δ = 6.77 – 6.51 (m, 3H), 5.97 – 5.78 (m, 3H), 5.33 – 5.14 (m, 2H), 3.11 – 2.79 (m, 2H), 2.73 – 2.06 (m, 2H), 0.90 (d, *J* = 6.0 Hz, 2H), 0.87 (d, *J* = 6.6 Hz, 1H) ppm.

**<sup>13</sup>C NMR (101 MHz, CDCl<sub>3</sub>):** δ = 180.4, 180.0, 147.6, 145.9, 140.3, 134.5, 134.2, 133.9, 133.3, 122.2, 122.2, 119.7, 119.4, 109.7, 109.6, 108.2, 100.9, 56.2, 55.3, 40.9, 39.7, 37.9, 37.3, 17.0, 16.1 ppm.



**2-(3-(trifluoromethyl)phenethyl)but-3-enoic acid (11b).** General procedure B was followed using 5-(3-(trifluoromethyl)phenyl)-1-penten-3-ol (57.5 mg, 0.25 mmol) as starting material provided 46.5 mg (72% yield) of the corresponding carboxylic acid (97:3 **11b:11a** mixture) as a pale yellow oil. In a separate experiment, 47.5 mg (74%

yield) were obtained, giving an average yield of 73%.

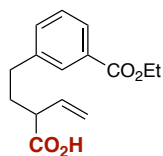
**<sup>1</sup>H NMR (400 MHz, CDCl<sub>3</sub>):** δ = 7.49 – 7.34 (m, 4H), 5.87 (ddd, *J* = 17.1, 10.3, 8.6 Hz, 1H), 5.34 – 5.13 (m, 2H), 3.07 (q, *J* = 7.7 Hz, 1H), 2.80 – 2.64 (m, 2H), 2.21 – 2.10 (m, 1H), 1.96 – 1.85 (m, 1H) ppm.

**<sup>13</sup>C NMR (101 MHz, CDCl<sub>3</sub>):** δ = 180.2, 142.2, 134.9, 132.0, 130.9 (q, *J* = 31.9 Hz), 129.0, 125.3 (q, *J* = 3.8 Hz), 124.3 (q, *J* = 273.0 Hz), 123.2 (q, *J* = 3.8 Hz), 123.0, 118.8, 49.5, 33.3, 33.1 ppm.

**<sup>19</sup>F NMR (376 MHz, CDCl<sub>3</sub>):** δ = -62.71.

**IR (neat, cm<sup>-1</sup>):** 2933, 1706, 1450, 1414, 1328, 1163, 1123, 1074, 927, 802, 703, 660.

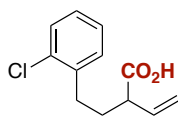
**HRMS (ESI-):** calcd. for C<sub>13</sub>H<sub>12</sub>O<sub>2</sub>F<sub>3</sub> (M-H): 257.0795, found 257.0789.


**2-(3-(ethoxycarbonyl)phenethyl)but-3-enoic acid (12b).**

General procedure B was followed using ethyl 3-(3-hydroxypent-4-en-1-yl)benzoate (58.6 mg, 0.25 mmol) as starting material provided 50.4 mg (77% yield) of the corresponding carboxylic acid (97:3 **12b**:**12a** mixture) as a pale yellow oil. In a separate experiment, 45.2 mg (69%) were obtained, giving an average yield of 73%. The observed spectral data are in agreement with the ones reported in literature.<sup>64</sup>

**<sup>1</sup>H NMR (300 MHz, CDCl<sub>3</sub>):**  $\delta$  = 7.91 – 9.85 (m, 2H), 7.46 – 7.31 (m, 2H), 5.86 (ddd,  $J$  = 16.8, 10.5, 8.6 Hz, 1H), 5.25 (s, 1H), 5.20 (dt,  $J$  = 9.3, 1.0 Hz, 1H), 4.37 (q,  $J$  = 7.1 Hz, 2H), 3.07 (q,  $J$  = 7.7 Hz, 1H), 2.75 – 2.64 (m, 2H), 2.21 – 2.10 (m, 1H), 1.96 – 1.85 (m, 1H), 1.39 (t,  $J$  = 7.1 Hz, 3H) ppm.

**<sup>13</sup>C NMR (75 MHz, CDCl<sub>3</sub>):**  $\delta$  180.0, 166.9, 141.5, 135.1, 133.2, 130.8, 129.6, 128.6, 127.5, 118.6, 61.1, 49.5, 33.4, 33.0, 14.5 ppm.


**2-(2-chlorophenethyl)but-3-enoic acid (13b).**

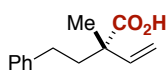
General procedure B was followed using 5-(2-chlorophenyl)-1-penten-3-ol (49.0 mg, 0.25 mmol) as starting material provided 35.4 mg (63% yield) of the corresponding carboxylic acid (97:3 **13b**:**13a**, mixture) as a pale yellow oil. In a separate experiment, 37.7 mg (67% yield) were obtained, giving an average yield of 65%.

**<sup>1</sup>H NMR (400 MHz, CDCl<sub>3</sub>):**  $\delta$  = 7.34 (dd,  $J$  = 7.5, 1.6 Hz, 1H), 7.25 – 7.11 (m, 3H), 5.89 (ddd,  $J$  = 17.4, 9.9, 8.5 Hz, 1H), 5.27 (d,  $J$  = 6.4 Hz, 1H), 5.24 (d,  $J$  = 0.8 Hz, 1H), 3.11 (q,  $J$  = 7.6 Hz, 1H), 2.97 – 2.63 (m, 2H), 2.21 – 2.07 (m, 1H), 1.96 – 1.84 (m, 1H) ppm.

**<sup>13</sup>C NMR (101 MHz, CDCl<sub>3</sub>):**  $\delta$  = 180.3, 139.0, 135.1, 134.1, 130.6, 129.7, 127.7, 127.0, 118.6, 49.7, 31.7, 31.2 ppm.

**IR (neat, cm<sup>-1</sup>):** 3069, 2931, 1702, 1638, 1474, 1443, 1412, 1283, 1219, 1052, 991, 923, 748, 680.

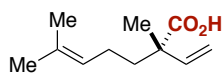
**HRMS (ESI<sup>-</sup>):** calcd. for C<sub>12</sub>H<sub>12</sub>O<sub>2</sub>Cl (M-H): 223.0531, found 223.0528.


**2-methyl-2-phenethylbut-3-enoic acid (14b).**

General procedure B (reaction time: 40 h) was followed using 3-methyl-5-phenylpent-1-en-3-ol (44.1 mg, 0.25 mmol) as starting material provided 47.1 mg (92% yield) of the corresponding carboxylic acid (>99:1 **14b**:**14a** mixture) as a pale yellow oil. In a separate experiment, 47.1 mg (92%) were obtained, giving an average yield of 92%. The observed spectral data are in agreement with the ones reported in literature.<sup>64</sup>

**<sup>1</sup>H NMR (500 MHz, CDCl<sub>3</sub>):**  $\delta$  = 7.33 – 7.26 (m, 2H), 7.24 – 7.16 (m, 3H), 6.13 (ddd,  $J$  = 17.6, 10.7, 1.4 Hz, 1H), 5.25 (d,  $J$  = 3.5 Hz, 1H), 5.23 (d,  $J$  = 3.1 Hz, 1H), 2.68 – 2.63 (m, 2H), 2.14 – 2.05 (m, 1H), 1.99 – 1.92 (m, 1H), 1.42 (d,  $J$  = 1.4 Hz, 3H) ppm.

<sup>13</sup>C NMR (75 MHz, CDCl<sub>3</sub>): δ = 182.5, 142.0, 140.8, 128.5, 128.5, 126.1, 114.7, 48.7, 41.0, 31.2, 20.6 ppm.



**2,6-dimethyl-2-vinylhept-5-enoic acid (15b).** *From linalool:*

General procedure B (reaction time: 40 h) was followed using linalool (38.6 mg, 0.25 mmol) as starting material provided 31.7 mg (69% yield) of the corresponding carboxylic acid (97:3 **15b**:**15a** mixture) as a pale yellow oil. In a separate experiment, 28.1 mg (62%) were obtained, giving an average yield of 65%.

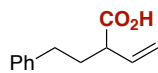
*From geraniol:* General procedure B (reaction time: 40 h) was followed using geraniol (38.6 mg, 0.25 mmol) as starting material provided 33.6 mg (74% yield) of the corresponding carboxylic acid (97:3 **15b**:**15a** mixture) as a pale yellow oil. In a separate experiment, 31.8 mg (70%) were obtained, giving an average yield of 72%.

*From nerol:* General procedure B (reaction time: 40 h) was followed using nerol (38.6 mg, 0.25 mmol) as starting material provided 29.8 mg (65% yield) of the corresponding carboxylic acid (92:8 **15b**:**15a** mixture) as a pale yellow oil. In a separate experiment, 29.7 mg (65%) were obtained, giving an average yield of 65%.

The observed spectral data are in agreement with the ones reported in literature.<sup>64</sup>

<sup>1</sup>H NMR (500 MHz, CDCl<sub>3</sub>): δ = 6.11 – 5.98 (m, 1H), 5.16 (s, 1H), 5.13 (d, *J* = 5.2 Hz, 1H), 5.08 (tt, *J* = 7.2, 1.4 Hz, 1H), 2.03 – 1.89 (m 2H), 1.80 – 1.72 (m, 1H), 1.67 (s, 3H), 1.65 – 1.60 (m, 1H), 1.58 (s, 3H), 1.31 (s, 3H) ppm.

<sup>13</sup>C NMR (75 MHz, CDCl<sub>3</sub>): δ = 182.6, 141.1, 132.3, 123.8, 114.3, 48.5, 39.1, 25.8, 23.4, 20.4, 17.7 ppm.



**2-phenethylbut-3-enoic acid (16b).** General procedure B was

followed using 5-phenyl-1-penten-3-ol (40.5 mg, 0.25 mmol) as starting material provided 37.0 mg (78% yield) of the corresponding carboxylic acid (97:3 **16b**:**16a**, mixture) as a pale yellow oil. In a separate experiment, 39.2 mg (82%) were obtained, giving an average yield of 80%. The observed spectral data are in agreement with the ones reported in literature.<sup>64</sup>

<sup>1</sup>H NMR (400 MHz, CDCl<sub>3</sub>): δ = 7.37 – 7.30 (m, 2H), 7.27 – 7.17 (m, 3H), 5.91 (dd, *J* = 16.9, 10.2 Hz, 1H), 5.28 (dd, *J* = 2.3, 1.2 Hz, 1H), 5.26 – 5.22 (m, 1H), 3.11 (q, *J* = 7.7 Hz, 1H), 2.84 – 2.55 (m, 2H), 2.25 – 2.14 (m, 1H), 1.98 – 1.87 (m, 1H) ppm.

<sup>13</sup>C NMR (101 MHz, CDCl<sub>3</sub>): δ = 180.6, 141.3, 135.2, 128.6, 128.6, 126.2, 118.4, 49.5, 33.5, 33.2 ppm.

**References:**

- (1) Trost, B. M.; Van Vranken, D. L. Asymmetric Transition Metal-Catalyzed Allylic Alkylations. *Chem. Rev.* **1996**, *96* (1), 395–422. <https://doi.org/10.1021/cr9409804>.
- (2) Trost, B. M. Asymmetric Allylic Alkylation, an Enabling Methodology. *J. Org. Chem.* **2004**, *69* (18), 5813–5837. <https://doi.org/10.1021/jo0491004>.
- (3) Sundararaju, B.; Achard, M.; Bruneau, C. Transition Metal Catalyzed Nucleophilic Allylic Substitution: Activation of Allylic Alcohols via  $\pi$ -Allylic Species. *Chem. Soc. Rev.* **2012**, *41* (12), 4467–4483. <https://doi.org/10.1039/C2CS35024F>.
- (4) Butt, N. A.; Zhang, W. Transition Metal-Catalyzed Allylic Substitution Reactions with Unactivated Allylic Substrates. *Chem. Soc. Rev.* **2015**, *44* (22), 7929–7967. <https://doi.org/10.1039/C5CS00144G>.
- (5) Trost, B. M.; Crawley, M. L. Asymmetric Transition-Metal-Catalyzed Allylic Alkylations: Applications in Total Synthesis. *Chem. Rev.* **2003**, *103* (8), 2921–2944. <https://doi.org/10.1021/cr020027w>.
- (6) Yin, J. Selected Applications of Pd- and Cu-Catalyzed Carbon–Heteroatom Cross-Coupling Reactions in the Pharmaceutical Industry. In *Applications of Transition Metal Catalysis in Drug Discovery and Development*; John Wiley & Sons, Ltd, 2012; pp 97–163. <https://doi.org/10.1002/9781118309872.ch3>.
- (7) Wang, X.; Dai, Y.; Gong, H. Nickel-Catalyzed Reductive Couplings. In *Ni- and Fe-Based Cross-Coupling Reactions*; Correa, A., Ed.; Topics in Current Chemistry Collections; Springer International Publishing: Cham, 2017; pp 61–89. [https://doi.org/10.1007/978-3-319-49784-6\\_3](https://doi.org/10.1007/978-3-319-49784-6_3).
- (8) Gomes, P.; Gosmini, C.; Périchon, J. New Chemical Cross-Coupling between Aryl Halides and Allylic Acetates Using a Cobalt Catalyst. *Org. Lett.* **2003**, *5* (7), 1043–1045. <https://doi.org/10.1021/ol0340641>.
- (9) Qian, X.; Auffrant, A.; Felouat, A.; Gosmini, C. Cobalt-Catalyzed Reductive Allylation of Alkyl Halides with Allylic Acetates or Carbonates. *Angew. Chem. Int. Ed.* **2011**, *50* (44), 10402–10405. <https://doi.org/10.1002/anie.201104390>.
- (10) Blanksby, S. J.; Ellison, G. B. Bond Dissociation Energies of Organic Molecules. *Acc. Chem. Res.* **2003**, *36* (4), 255–263. <https://doi.org/10.1021/ar020230d>.
- (11) Muzart, J. Palladium-Catalysed Reactions of Alcohols. Part B: Formation of C–C and C–N Bonds from Unsaturated Alcohols. *Tetrahedron* **2005**, *61* (17), 4179–4212. <https://doi.org/10.1016/j.tet.2005.02.026>.
- (12) Muzart, J. Procedures for and Possible Mechanisms of Pd-Catalyzed Allylations of Primary and Secondary Amines with Allylic Alcohols. *Eur. J. Org. Chem.* **2007**, *2007* (19), 3077–3089. <https://doi.org/10.1002/ejoc.200601050>.
- (13) Bandini, M.; Cera, G.; Chiarucci, M. Catalytic Enantioselective Alkylations with Allylic Alcohols. *Synthesis* **2012**, *44* (4), 504–512. <https://doi.org/10.1055/s-0031-1289681>.
- (14) Wang, D.; Li, C.-J. Mono-Alkylation of Diols Through Ruthenium-Catalyzed Reaction with Homoallyl Alcohols. *Synthetic Communications* **1998**, *28* (3), 507–515. <https://doi.org/10.1080/00397919808005106>.
- (15) van der Drift, R. C.; Vailati, M.; Bouwman, E.; Drent, E. Two Reactions of Allylic Alcohols Catalysed by Ruthenium Cyclopentadienyl Complexes with Didentate Phosphine Ligands: Isomerisation and Ether Formation. *Journal of Molecular Catalysis A: Chemical* **2000**, *159* (2), 163–177. [https://doi.org/10.1016/S1381-1169\(00\)00221-1](https://doi.org/10.1016/S1381-1169(00)00221-1).
- (16) Rijn, J. A. van; Lutz, M.; von Chrzanowski, L. S.; Spek, A. L.; Bouwman, E.; Drent, E. Cationic Ruthenium-Cyclopentadienyl-Diphosphine Complexes as Catalysts for the Allylation of Phenols with Allyl Alcohol; Relation between Structure and Catalytic Performance in O- vs.

C-Allylation. *Adv. Synth. & Cataly* **2009**, *351* (10), 1637–1647. <https://doi.org/10.1002/adsc.200900085>.

(17) van Rijn, J. A.; Siegler, M. A.; Spek, A. L.; Bouwman, E.; Drent, E. Ruthenium-Diphosphine-Catalyzed Allylation of Phenols: A Gem-Dialkyl-Type Effect Induces High Selectivity toward O-Allylation. *Organometallics* **2009**, *28* (24), 7006–7014. <https://doi.org/10.1021/om900832g>.

(18) Tanaka, S.; Seki, T.; Kitamura, M. Asymmetric Dehydrative Cyclization of  $\omega$ -Hydroxy Allyl Alcohols Catalyzed by Ruthenium Complexes. *Angew. Chem. Int. Ed.* **2009**, *48* (47), 8948–8951. <https://doi.org/10.1002/anie.200904671>.

(19) García-Yebra, C.; Janssen, J. P.; Rominger, F.; Helmchen, G. Asymmetric Iridium(I)-Catalyzed Allylic Alkylation of Monosubstituted Allylic Substrates with Phosphinooxazolines as Ligands. Isolation, Characterization, and Reactivity of Chiral (Allyl)Iridium(III) Complexes. *Organometallics* **2004**, *23* (23), 5459–5470. <https://doi.org/10.1021/om0401105>.

(20) Yamashita, Y.; Gopalarathnam, A.; Hartwig, J. F. Iridium-Catalyzed, Asymmetric Amination of Allylic Alcohols Activated by Lewis Acids. *J. Am. Chem. Soc.* **2007**, *129* (24), 7508–7509. <https://doi.org/10.1021/ja0730718>.

(21) Defieber, C.; Ariger, M. A.; Moriel, P.; Carreira, E. M. Iridium-Catalyzed Synthesis of Primary Allylic Amines from Allylic Alcohols: Sulfamic Acid as Ammonia Equivalent. *Angew. Chem. Int. Ed.* **2007**, *46* (17), 3139–3143. <https://doi.org/10.1002/anie.200700159>.

(22) Roggen, M.; Carreira, E. M. Stereospecific Substitution of Allylic Alcohols To Give Optically Active Primary Allylic Amines: Unique Reactivity of a (P,Alkene)Ir Complex Modulated by Iodide. *J. Am. Chem. Soc.* **2010**, *132* (34), 11917–11919. <https://doi.org/10.1021/ja105271z>.

(23) Manabe, K.; Kobayashi, S. Palladium-Catalyzed, Carboxylic Acid-Assisted Allylic Substitution of Carbon Nucleophiles with Allyl Alcohols as Allylating Agents in Water. *Org. Lett.* **2003**, *5* (18), 3241–3244. <https://doi.org/10.1021/ol035126q>.

(24) Usui, I.; Schmidt, S.; Breit, B. Dual Palladium- and Proline-Catalyzed Allylic Alkylation of Enolizable Ketones and Aldehydes with Allylic Alcohols. *Org. Lett.* **2009**, *11* (6), 1453–1456. <https://doi.org/10.1021/ol9001812>.

(25) Kinoshita, H.; Shinokubo, H.; Oshima, K. Water Enables Direct Use of Allyl Alcohol for Tsuji–Trost Reaction without Activators. *Org. Lett.* **2004**, *6* (22), 4085–4088. <https://doi.org/10.1021/ol048207a>.

(26) Nishikata, T.; Lipshutz, B. H. Amination of Allylic Alcohols in Water at Room Temperature. *Org. Lett.* **2009**, *11* (11), 2377–2379. <https://doi.org/10.1021/ol900235s>.

(27) Furukawa, J.; Kiji, J.; Yamamoto, K.; Tojo, T. Nickel-Catalyzed Allyl-Transfer Reactions. *Tetrahedron* **1973**, *29* (20), 3149–3151. [https://doi.org/10.1016/S0040-4020\(01\)93457-X](https://doi.org/10.1016/S0040-4020(01)93457-X).

(28) Bricout, H.; Carpentier, J.-F.; Mortreux, A. Synthetic and Kinetic Aspects of Nickel-Catalysed Amination of Allylic Alcohol Derivatives. *Tetrahedron* **1998**, *54* (7), 1073–1084. [https://doi.org/10.1016/S0040-4020\(97\)10208-3](https://doi.org/10.1016/S0040-4020(97)10208-3).

(29) Bricout, H.; Carpentier, J.-F.; Mortreux, A. Nickel vs. Palladium Catalysts for Coupling Reactions of Allyl Alcohol with Soft Nucleophiles: Activities and Deactivation Processes. *Journal of Molecular Catalysis A: Chemical* **1998**, *136* (3), 243–251. [https://doi.org/10.1016/S1381-1169\(98\)00067-3](https://doi.org/10.1016/S1381-1169(98)00067-3).

(30) Matsubara, R.; Jamison, T. F. Nickel-Catalyzed Allylic Substitution of Simple Alkenes. *J. Am. Chem. Soc.* **2010**, *132* (20), 6880–6881. <https://doi.org/10.1021/ja101186p>.

(31) Kita, Y.; Sakaguchi, H.; Hoshimoto, Y.; Nakauchi, D.; Nakahara, Y.; Carpentier, J.-F.; Ogoshi, S.; Mashima, K. Pentacoordinated Carboxylate  $\pi$ -Allyl Nickel Complexes as Key

Intermediates for the Ni-Catalyzed Direct Amination of Allylic Alcohols. *Chem. Eur. J.* **2015**, *21* (41), 14571–14578. <https://doi.org/10.1002/chem.201502329>.

(32) Kita, Y.; Kavthe, R. D.; Oda, H.; Mashima, K. Asymmetric Allylic Alkylation of  $\beta$ -Ketoesters with Allylic Alcohols by a Nickel/Diphosphine Catalyst. *Angew. Chem. Int. Ed.* **2016**, *55* (3), 1098–1101. <https://doi.org/10.1002/anie.201508757>.

(33) Jia, X.-G.; Guo, P.; Duan, J.; Shu, X.-Z. Dual Nickel and Lewis Acid Catalysis for Cross-Electrophile Coupling: The Allylation of Aryl Halides with Allylic Alcohols. *Chem. Sci.* **2018**, *9* (3), 640–645. <https://doi.org/10.1039/C7SC03140H>.

(34) Sakamoto, M.; Shimizu, I.; Yamamoto, A. Activation of C–O and C–N Bonds in Allylic Alcohols and Amines by Palladium Complexes Promoted by CO<sub>2</sub>. Synthetic Applications to Allylation of Nucleophiles, Carbonylation, and Allylamine Disproportionation. *Bull. Chem. Soc. Jpn.* **1996**, *69* (4), 1065–1078. <https://doi.org/10.1246/bcsj.69.1065>.

(35) Gohres, J. L.; Marin, A. T.; Lu, J.; Liotta, C. L.; Eckert, C. A. Spectroscopic Investigation of Alkylcarbonic Acid Formation and Dissociation in CO<sub>2</sub>-Expanded Alcohols. *Ind. Eng. Chem. Res.* **2009**, *48* (3), 1302–1306. <https://doi.org/10.1021/ie8011227>.

(36) Lang, S. B.; Locascio, T. M.; Tunge, J. A. Activation of Alcohols with Carbon Dioxide: Intermolecular Allylation of Weakly Acidic Pronucleophiles. *Org. Lett.* **2014**, *16* (16), 4308–4311. <https://doi.org/10.1021/ol502023d>.

(37) Xie, X.; Liotta, C. L.; Eckert, C. A. CO<sub>2</sub>-Catalyzed Acetal Formation in CO<sub>2</sub>-Expanded Methanol and Ethylene Glycol. *Ind. Eng. Chem. Res.* **2004**, *43* (11), 2605–2609. <https://doi.org/10.1021/ie034103c>.

(38) Tsuji, Jiro.; Kiji, Jitsuo.; Imamura, Shinzo.; Morikawa, Masanobu. Organic Syntheses by Means of Noble Metal Compounds. VIII.1 Catalytic Carbonylation of Allylic Compounds with Palladium Chloride. *J. Am. Chem. Soc.* **1964**, *86* (20), 4350–4353. <https://doi.org/10.1021/ja01074a023>.

(39) Mita, T.; Higuchi, Y.; Sato, Y. Highly Regioselective Palladium-Catalyzed Carboxylation of Allylic Alcohols with CO<sub>2</sub>. *Chem. Eur. J.* **2015**, *21* (46), 16391–16394. <https://doi.org/10.1002/chem.201503359>.

(40) Best, M. D.; Tobey, S. L.; Anslyn, E. V. Abiotic Guanidinium Containing Receptors for Anionic Species. *Coord. Chem. Rev.* **2003**, *240* (1), 3–15. [https://doi.org/10.1016/S0010-8545\(02\)00256-4](https://doi.org/10.1016/S0010-8545(02)00256-4).

(41) Brooks, S. J.; Gale, P. A.; Light, M. E. Anion-Binding Modes in a Macrocyclic Amidourea. *Chem. Commun.* **2006**, No. 41, 4344–4346. <https://doi.org/10.1039/B610938A>.

(42) Das Neves Gomes, C.; Jacquet, O.; Villiers, C.; Thuéry, P.; Ephritikhine, M.; Cantat, T. A Diagonal Approach to Chemical Recycling of Carbon Dioxide: Organocatalytic Transformation for the Reductive Functionalization of CO<sub>2</sub>. *Angew. Chem. Int. Ed.* **2012**, *51* (1), 187–190. <https://doi.org/10.1002/anie.201105516>.

(43) Gumrukcu, Y.; de Bruin, B.; Reek, J. N. H. Hydrogen-Bond-Assisted Activation of Allylic Alcohols for Palladium-Catalyzed Coupling Reactions. *ChemSusChem* **2014**, *7* (3), 890–896. <https://doi.org/10.1002/cssc.201300723>.

(44) Pramanik, A.; Emami Khansari, M.; Powell, D. R.; Fronczek, F. R.; Hossain, Md. A. Absorption of Atmospheric CO<sub>2</sub> as Carbonate Inside the Molecular Cavity of a New Tripodal Hexaurea Receptor. *Org. Lett.* **2014**, *16* (2), 366–369. <https://doi.org/10.1021/ol403186k>.

(45) Ravikumar, I.; Ghosh, P. Efficient Fixation of Atmospheric CO<sub>2</sub> as Carbonate in a Capsule of a Neutral Receptor and Its Release under Mild Conditions. *Chem. Commun.* **2010**, *46* (7), 1082–1084. <https://doi.org/10.1039/B915661E>.

(46) Krishnamurty, K. V.; McLeod Harris, Gordon.; Sastri, V. S. Chemistry of the Metal Carbonato Complexes. *Chem. Rev.* **1970**, *70* (2), 171–197.

<https://doi.org/10.1021/cr60264a001>.

(47) Charboneau, D. J.; Brudvig, G. W.; Hazari, N.; Lant, H. M. C.; Saydjari, A. K. Development of an Improved System for the Carboxylation of Aryl Halides through Mechanistic Studies. *ACS Catal.* **2019**, *9* (4), 3228–3241. <https://doi.org/10.1021/acscatal.9b00566>.

(48) Gattow, G.; Behrendt, W. Methyl Hydrogen Carbonate. *Angew. Chem. Int. Ed. Engl.* **1972**, *11* (6), 534–535. <https://doi.org/10.1002/anie.197205342>.

(49) Tshepelevitsh, S.; Kütt, A.; Lõkov, M.; Kaljurand, I.; Saame, J.; Heering, A.; Plieger, P. G.; Vianello, R.; Leito, I. On the Basicity of Organic Bases in Different Media. *Eur. J. Org. Chem.* **2019**, *2019* (40), 6735–6748. <https://doi.org/10.1002/ejoc.201900956>.

(50) Eberhardt, N. A.; Guan, H. Nickel Hydride Complexes. *Chem. Rev.* **2016**, *116* (15), 8373–8426. <https://doi.org/10.1021/acs.chemrev.6b00259>.

(51) Zhao, C.; Jia, X.; Wang, X.; Gong, H. Ni-Catalyzed Reductive Coupling of Alkyl Acids with Unactivated Tertiary Alkyl and Glycosyl Halides. *J. Am. Chem. Soc.* **2014**, *136* (50), 17645–17651. <https://doi.org/10.1021/ja510653n>.

(52) Wang, X.; Wang, S.; Xue, W.; Gong, H. Nickel-Catalyzed Reductive Coupling of Aryl Bromides with Tertiary Alkyl Halides. *J. Am. Chem. Soc.* **2015**, *137* (36), 11562–11565. <https://doi.org/10.1021/jacs.5b06255>.

(53) Börjesson, M.; Moragas, T.; Martin, R. Ni-Catalyzed Carboxylation of Unactivated Alkyl Chlorides with CO<sub>2</sub>. *J. Am. Chem. Soc.* **2016**, *138* (24), 7504–7507. <https://doi.org/10.1021/jacs.6b04088>.

(54) Wang, X.; Ma, G.; Peng, Y.; Pitsch, C. E.; Moll, B. J.; Ly, T. D.; Wang, X.; Gong, H. Ni-Catalyzed Reductive Coupling of Electron-Rich Aryl Iodides with Tertiary Alkyl Halides. *J. Am. Chem. Soc.* **2018**, *140* (43), 14490–14497. <https://doi.org/10.1021/jacs.8b09473>.

(55) Miller, K. M.; Jamison, T. F. Ligand-Switchable Directing Effects of Tethered Alkenes in Nickel-Catalyzed Additions to Alkynes. *J. Am. Chem. Soc.* **2004**, *126* (47), 15342–15343. <https://doi.org/10.1021/ja0446799>.

(56) Wang, X.; Liu, Y.; Martin, R. Ni-Catalyzed Divergent Cyclization/Carboxylation of Unactivated Primary and Secondary Alkyl Halides with CO<sub>2</sub>. *J. Am. Chem. Soc.* **2015**, *137* (20), 6476–6479. <https://doi.org/10.1021/jacs.5b03340>.

(57) Budnikova, Y. H.; Vicic, D. A.; Klein, A. Exploring Mechanisms in Ni Terpyridine Catalyzed C–C Cross-Coupling Reactions—A Review. *Inorganics* **2018**, *6* (1), 18. <https://doi.org/10.3390/inorganics6010018>.

(58) Takaya, J.; Iwasawa, N. Hydrocarboxylation of Allenes with CO<sub>2</sub> Catalyzed by Silyl Pincer-Type Palladium Complex. *J. Am. Chem. Soc.* **2008**, *130* (46), 15254–15255. <https://doi.org/10.1021/ja806677w>.

(59) Suh, H.-W.; Guard, L. M.; Hazari, N. A Mechanistic Study of Allene Carboxylation with CO<sub>2</sub> Resulting in the Development of a Pd(II) Pincer Complex for the Catalytic Hydroboration of CO<sub>2</sub>. *Chem. Sci.* **2014**, *5* (10), 3859–3872. <https://doi.org/10.1039/C4SC01110D>.

(60) Diccianni, J. B.; Hu, C. T.; Diao, T. Insertion of CO<sub>2</sub> Mediated by a (Xantphos)Ni(I)–Alkyl Species. *Angew. Chem. Int. Ed.* **2019**, *58* (39), 13865–13868. <https://doi.org/10.1002/anie.201906005>.

(61) Somerville, R. J.; Odena, C.; Obst, M. F.; Hazari, N.; Hopmann, K. H.; Martin, R. Ni(I)–Alkyl Complexes Bearing Phenanthroline Ligands: Experimental Evidence for CO<sub>2</sub> Insertion at Ni(I) Centers. *J. Am. Chem. Soc.* **2020**, *142* (25), 10936–10941. <https://doi.org/10.1021/jacs.0c04695>.

(62) Wu, J.; Green, J. C.; Hazari, N.; Hruszkewycz, D. P.; Incarvito, C. D.; Schmeier, T. J. The Reaction of Carbon Dioxide with Palladium–Allyl Bonds. *Organometallics* **2010**, *29* (23),

6369–6376. <https://doi.org/10.1021/om1007456>.

(63) Johnson, M. T.; Johansson, R.; Kondrashov, M. V.; Steyl, G.; Ahlquist, M. S. G.; Roodt, A.; Wendt, O. F. Mechanisms of the CO<sub>2</sub> Insertion into (PCP) Palladium Allyl and Methyl  $\sigma$ -Bonds. A Kinetic and Computational Study. *Organometallics* **2010**, *29* (16), 3521–3529. <https://doi.org/10.1021/om100325v>.

(64) Moragas, T.; Cornella, J.; Martin, R. Ligand-Controlled Regiodivergent Ni-Catalyzed Reductive Carboxylation of Allyl Esters with CO<sub>2</sub>. *J. Am. Chem. Soc.* **2014**, *136* (51), 17702–17705. <https://doi.org/10.1021/ja509077a>.

(65) Zhang, F.; Zaidi, S.; Haney, K. M.; Kellogg, G. E.; Zhang, Y. Regio- and Stereoselective Syntheses of the Natural Product CCR5 Antagonist Anibamine and Its Three Olefin Isomers. *J. Org. Chem.* **2011**, *76* (19), 7945–7952. <https://doi.org/10.1021/jo2013669>.

(66) Browne, D. M.; Niyomura, O.; Wirth, T. Catalytic Use of Selenium Electrophiles in Cyclizations. *Org. Lett.* **2007**, *9* (16), 3169–3171. <https://doi.org/10.1021/ol071223y>.

(67) Sun, X.; Zhou, L.; Wang, C.-J.; Zhang, X. Rh-Catalyzed Highly Enantioselective Synthesis of 3-Arylbutanoic Acids. *Angew. Chem. Int. Ed.* **2007**, *46* (15), 2623–2626. <https://doi.org/10.1002/anie.200604810>.

(68) Brun, E. M.; Gil, S.; Mestres, R.; Parra, M. Regioselective Alkylation of Lithium Dienediolates of  $\alpha$ ,  $\beta$ -Unsaturated Carboxylic Acids. *Synthesis* **2000**, *2000* (08), 1160–1165.



**<sup>1</sup>H NMR, <sup>13</sup>C NMR and <sup>19</sup>F NMR spectra**



# Site-Selective Catalytic Carboxylation of Allylic Alcohols with CO<sub>2</sub>

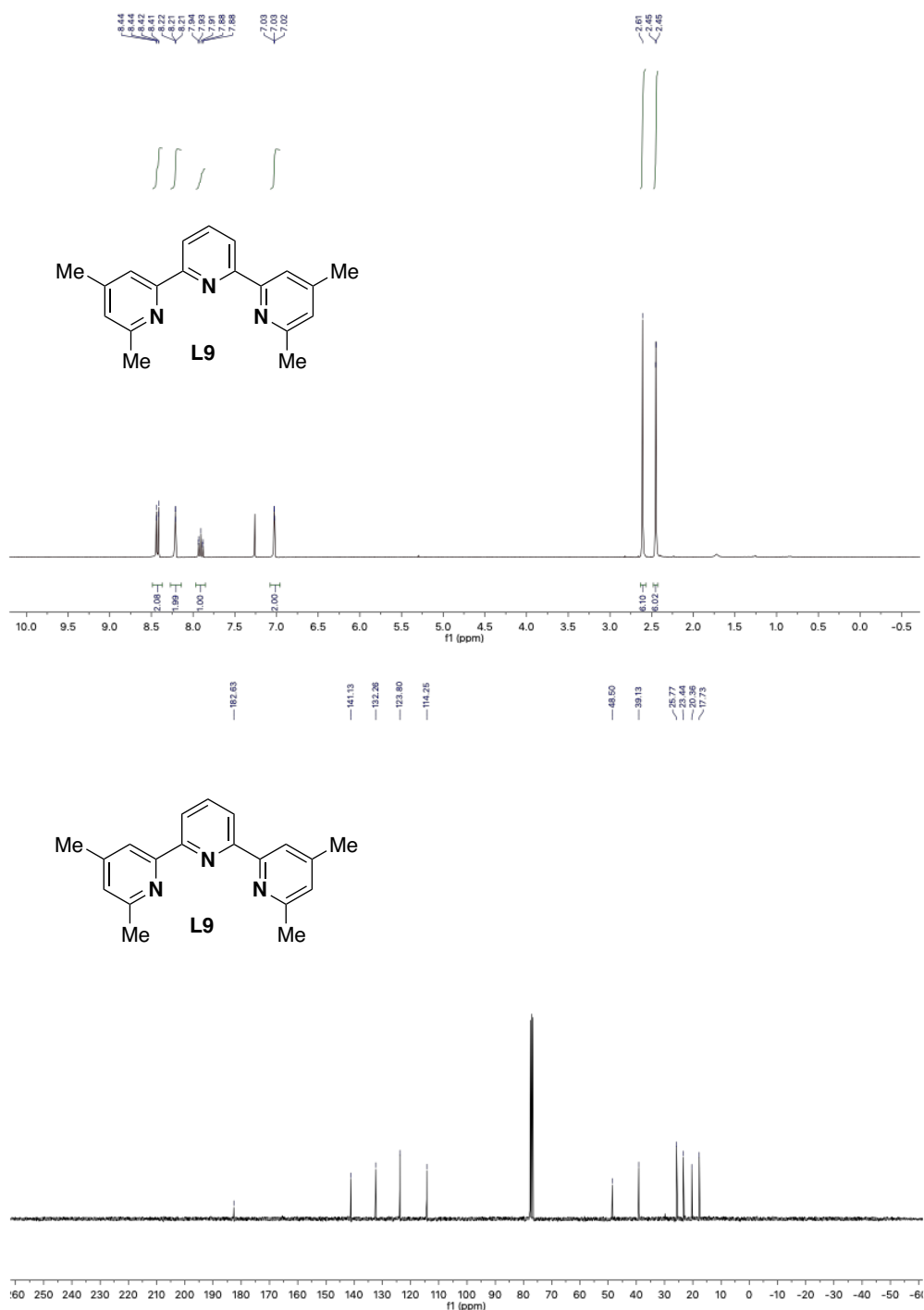


Figure 1. <sup>1</sup>H and <sup>13</sup>C NMR spectra of **L9**.

# Chapter 2

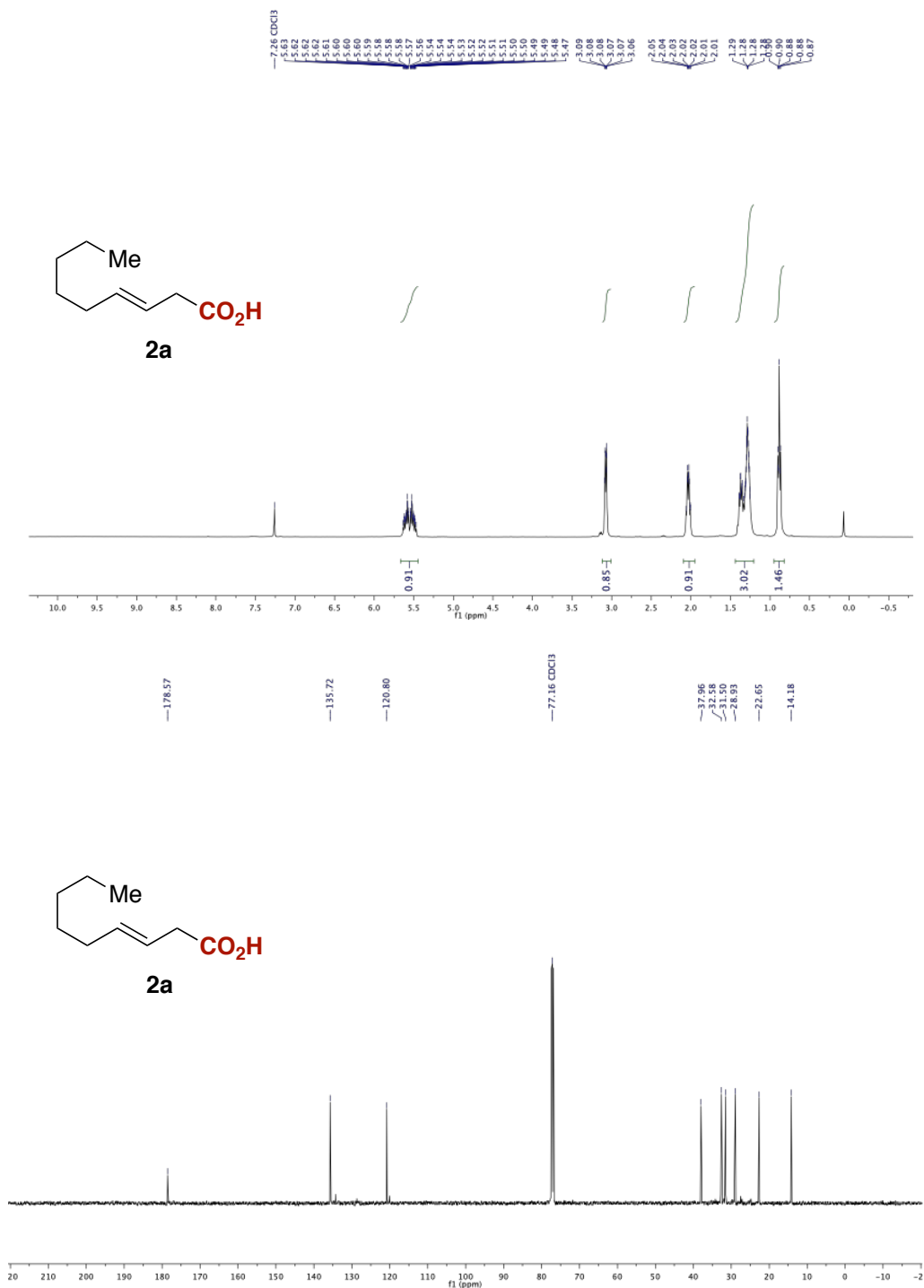


Figure 2. <sup>1</sup>H and <sup>13</sup>C NMR spectra of **2a**.

# Site-Selective Catalytic Carboxylation of Allylic Alcohols with CO<sub>2</sub>

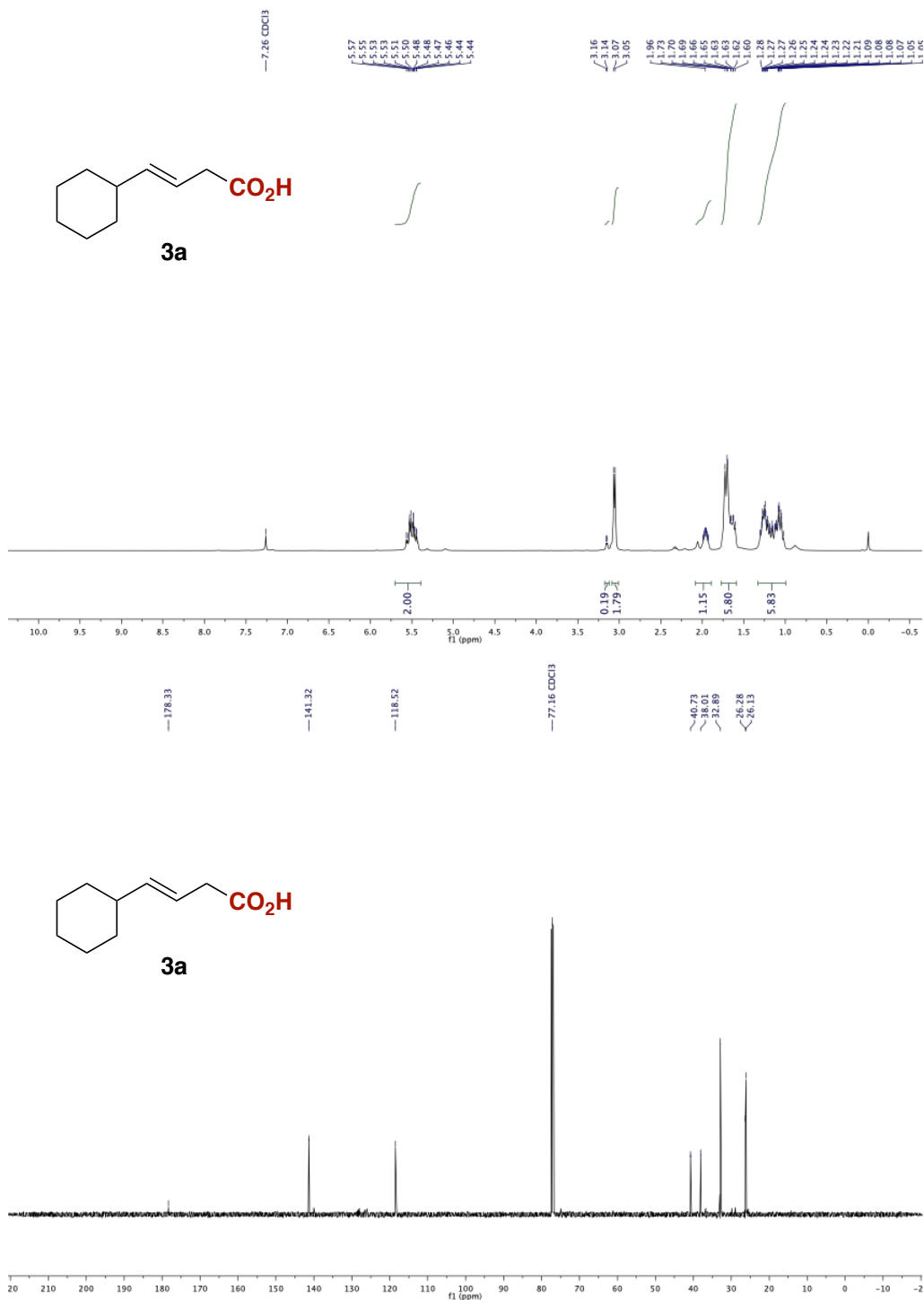


Figure 3. <sup>1</sup>H and <sup>13</sup>C NMR spectra of **3a**.

# Chapter 2

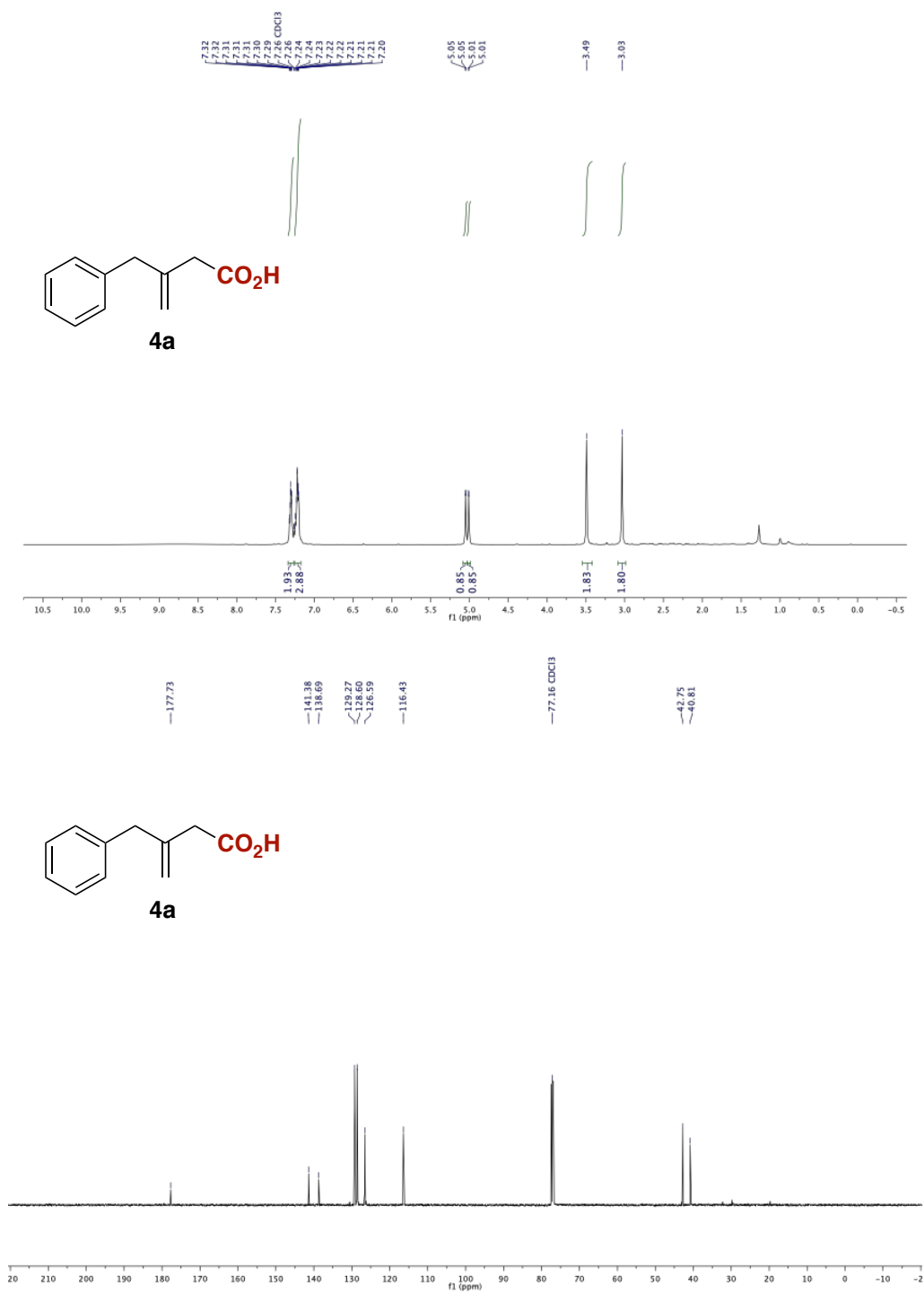


Figure 4. <sup>1</sup>H and <sup>13</sup>C NMR spectra of **4a**.

# Site-Selective Catalytic Carboxylation of Allylic Alcohols with CO<sub>2</sub>

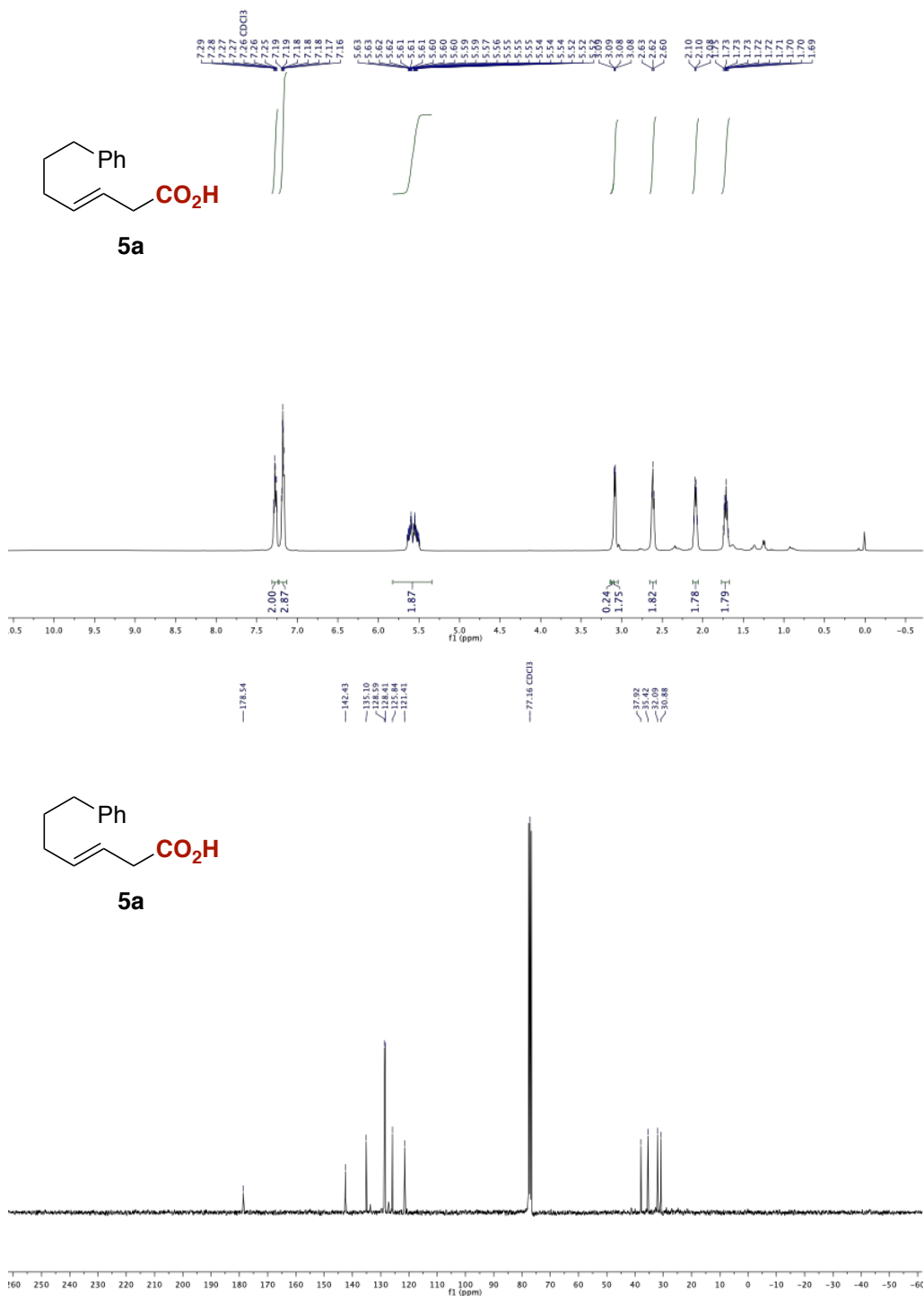


Figure 5. <sup>1</sup>H and <sup>13</sup>C NMR spectra of **5a**.

# Chapter 2

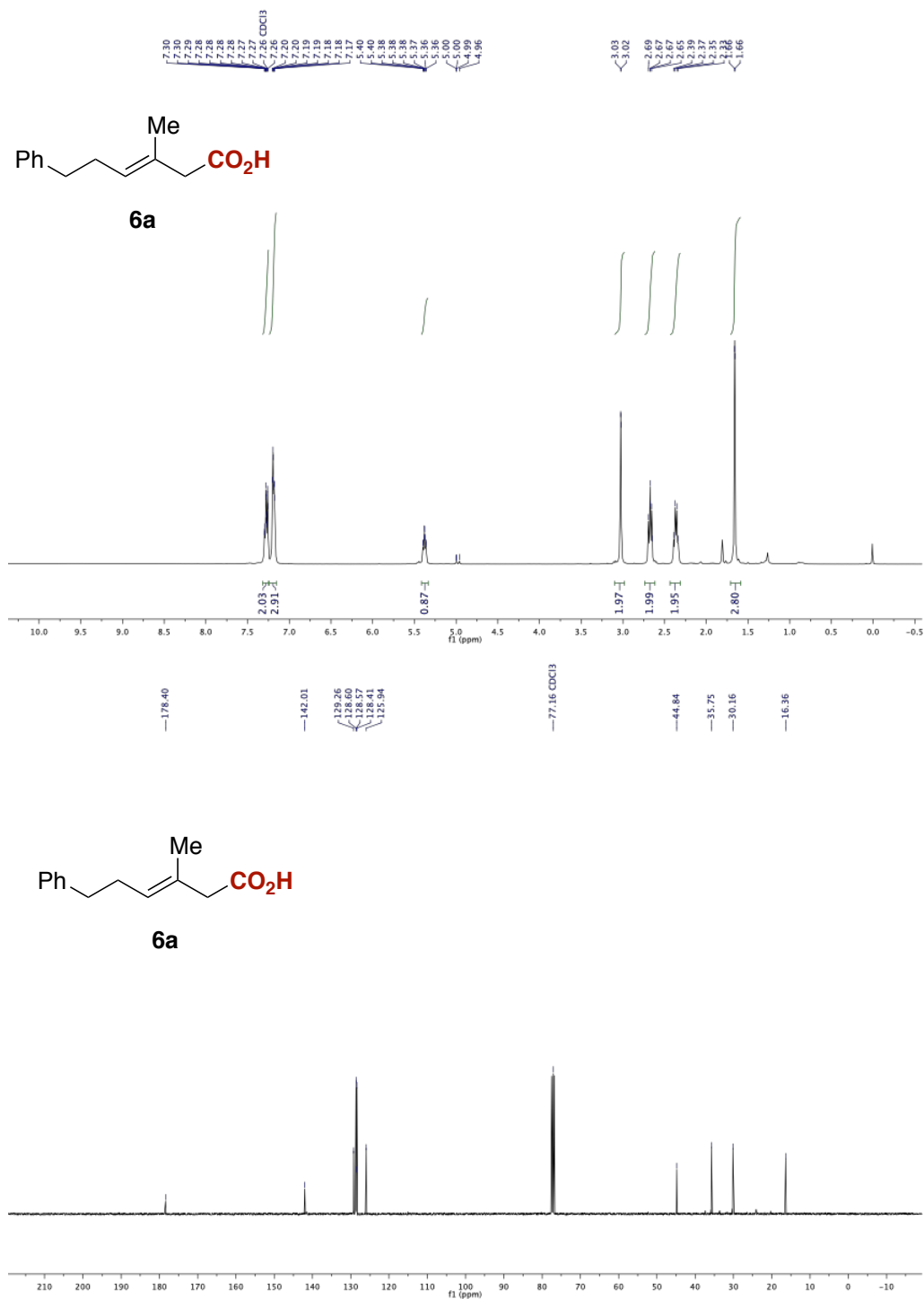


Figure 6. <sup>1</sup>H and <sup>13</sup>C NMR spectra of **6a**.





# Chapter 2

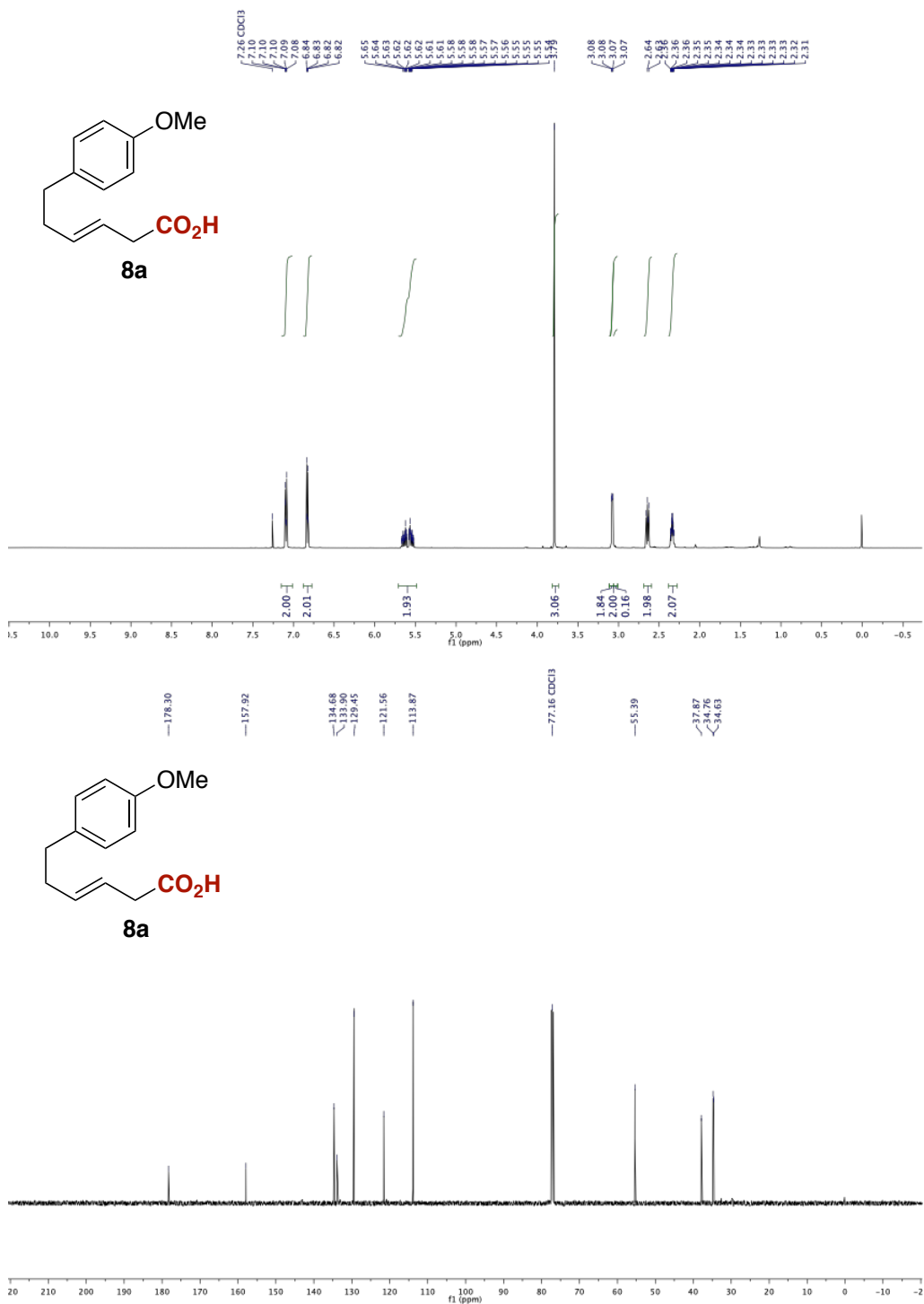


Figure 8. <sup>1</sup>H and <sup>13</sup>C NMR spectra of **8a**.

Site-Selective Catalytic Carboxylation of Allylic Alcohols with CO<sub>2</sub>

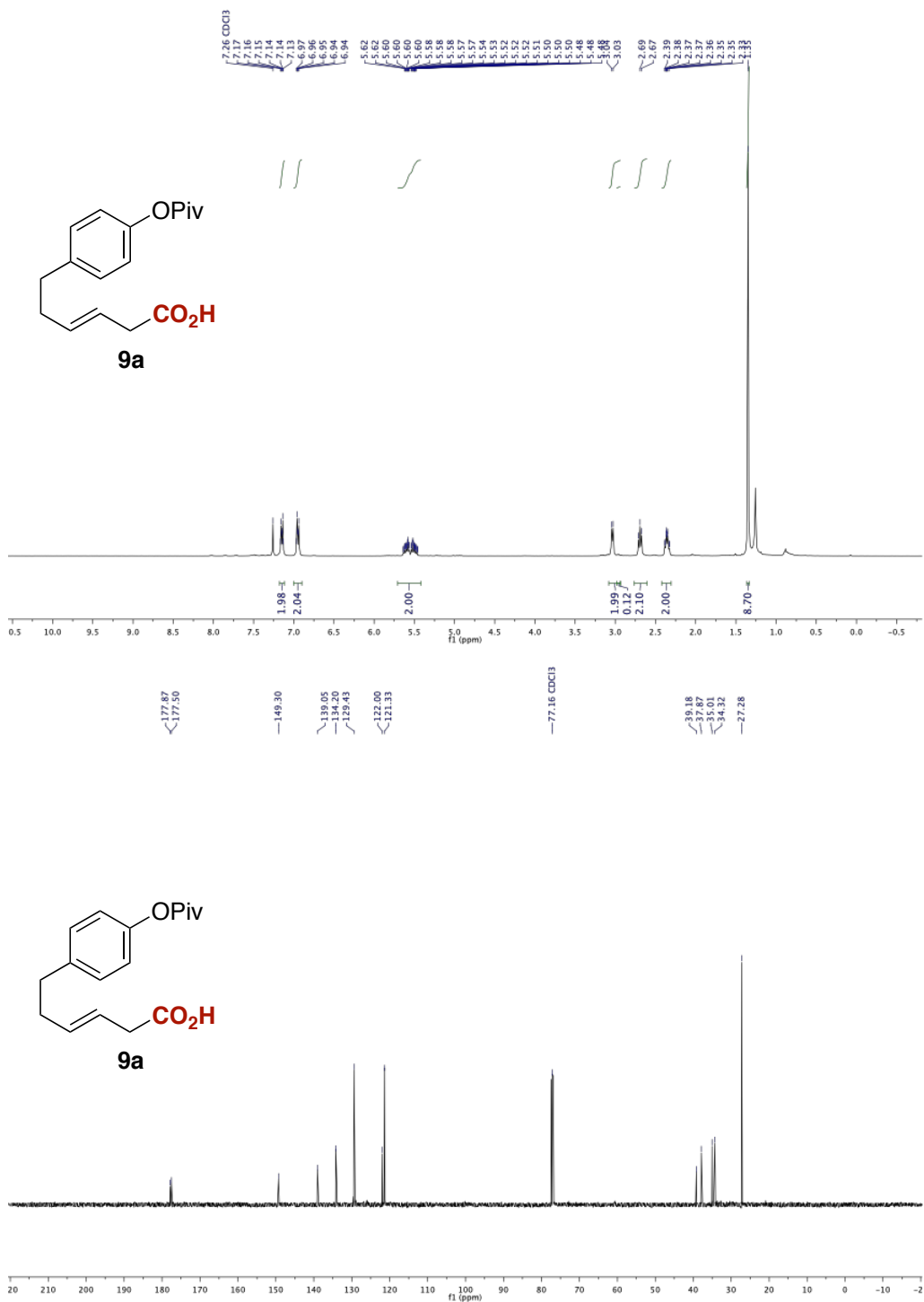


Figure 9. <sup>1</sup>H and <sup>13</sup>C NMR spectra of **9a**.

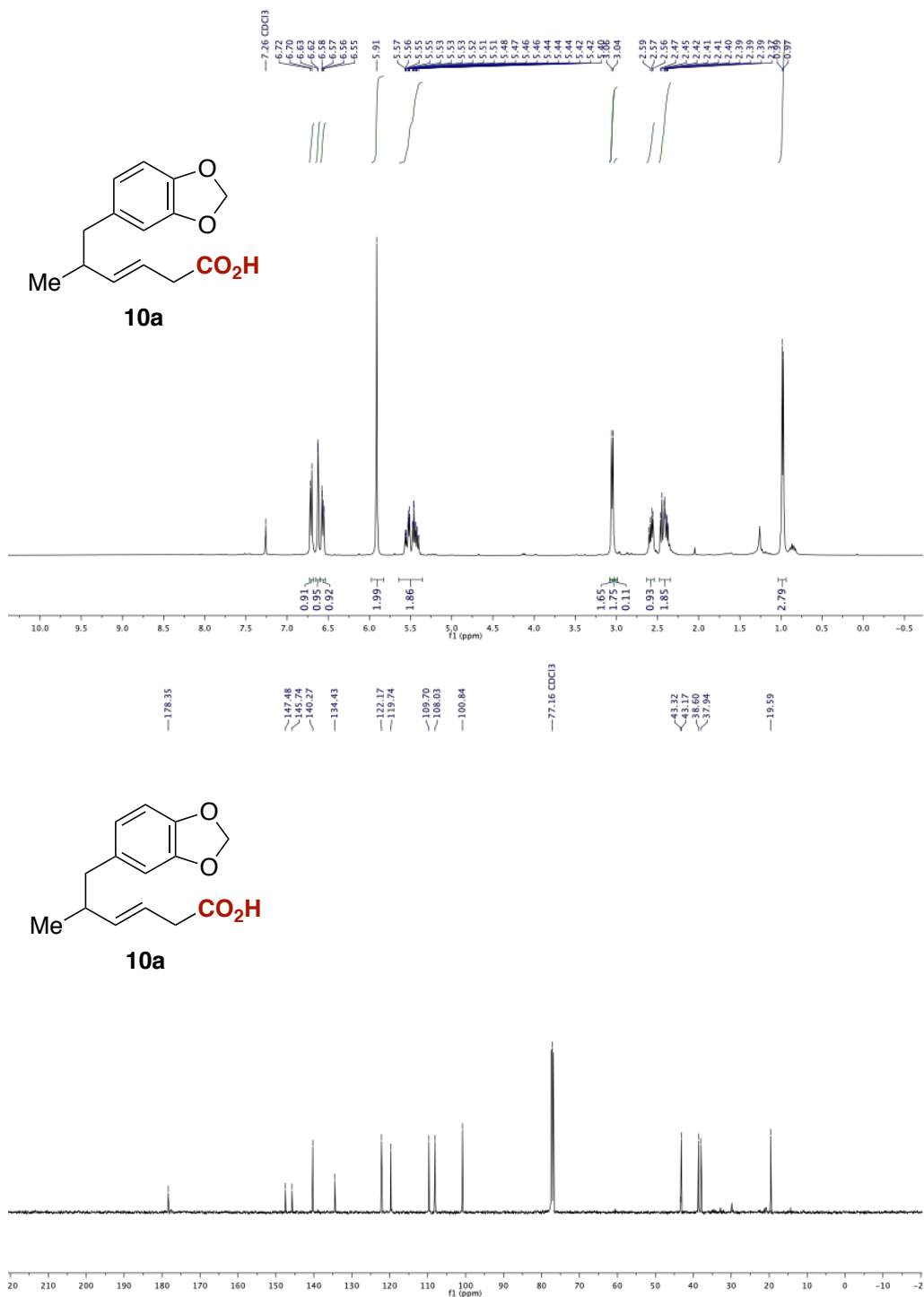
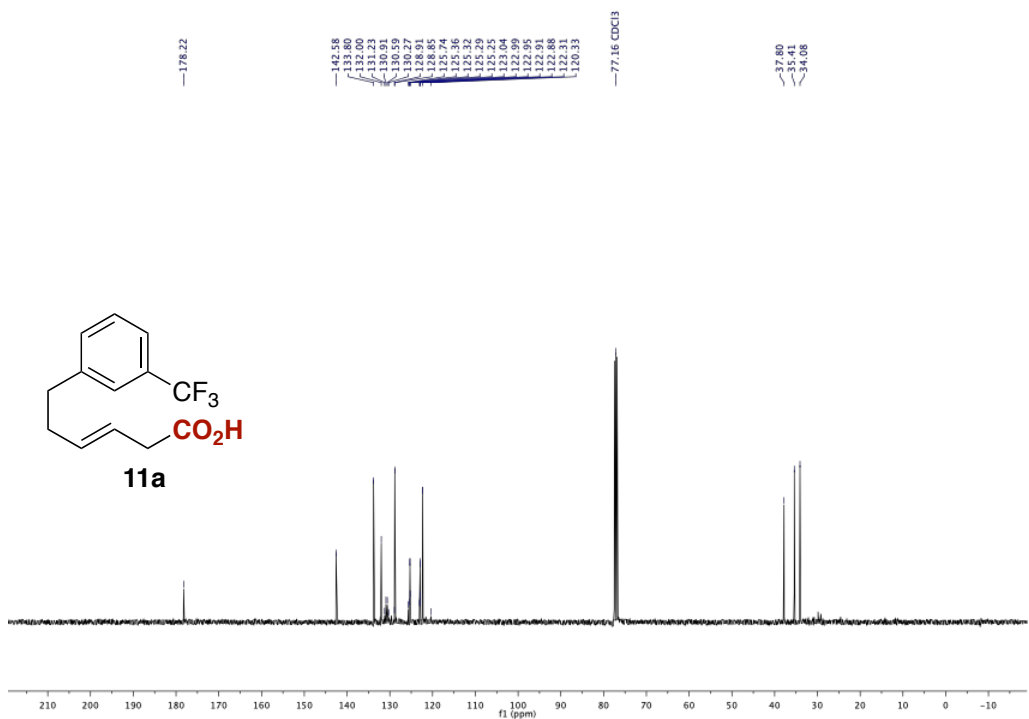
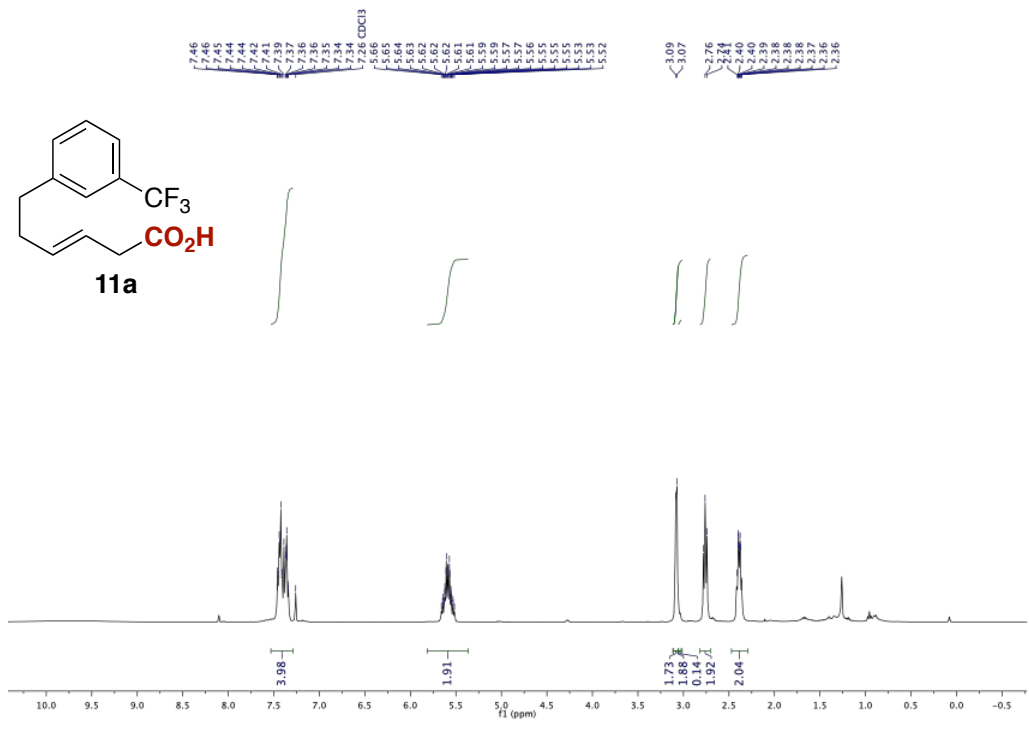


Figure 10.  $^1\text{H}$  and  $^{13}\text{C}$  NMR spectra of **10a**.

# Site-Selective Catalytic Carboxylation of Allylic Alcohols with CO<sub>2</sub>



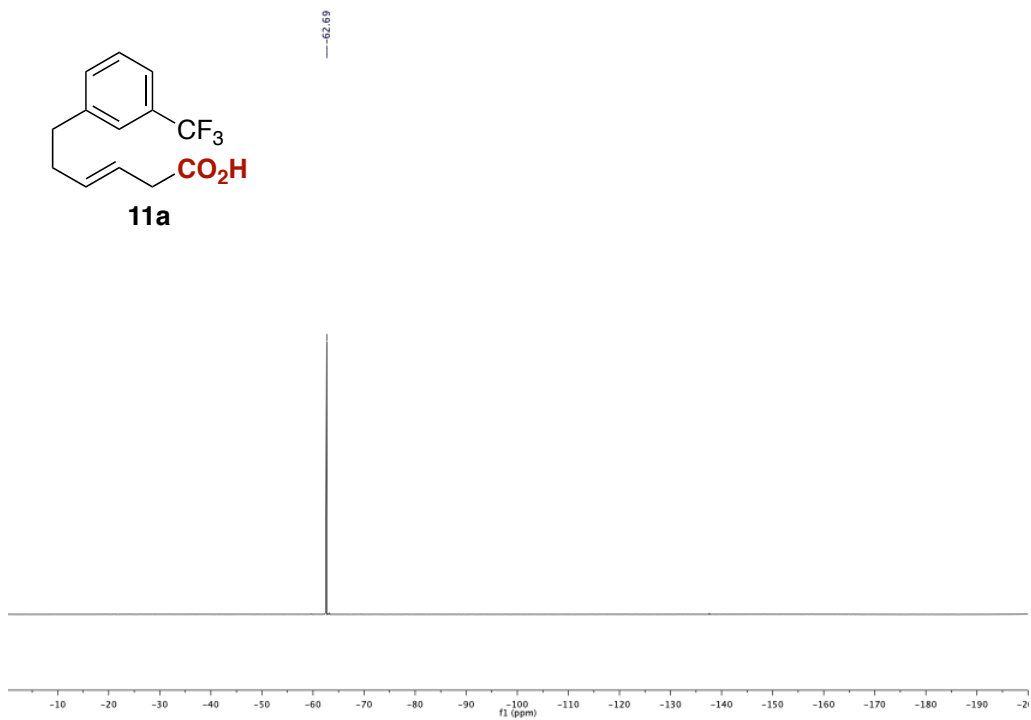


Figure 11.  $^1\text{H}$ ,  $^{13}\text{C}$  and  $^{19}\text{F}$  NMR spectra of **11a**.

# Site-Selective Catalytic Carboxylation of Allylic Alcohols with CO<sub>2</sub>

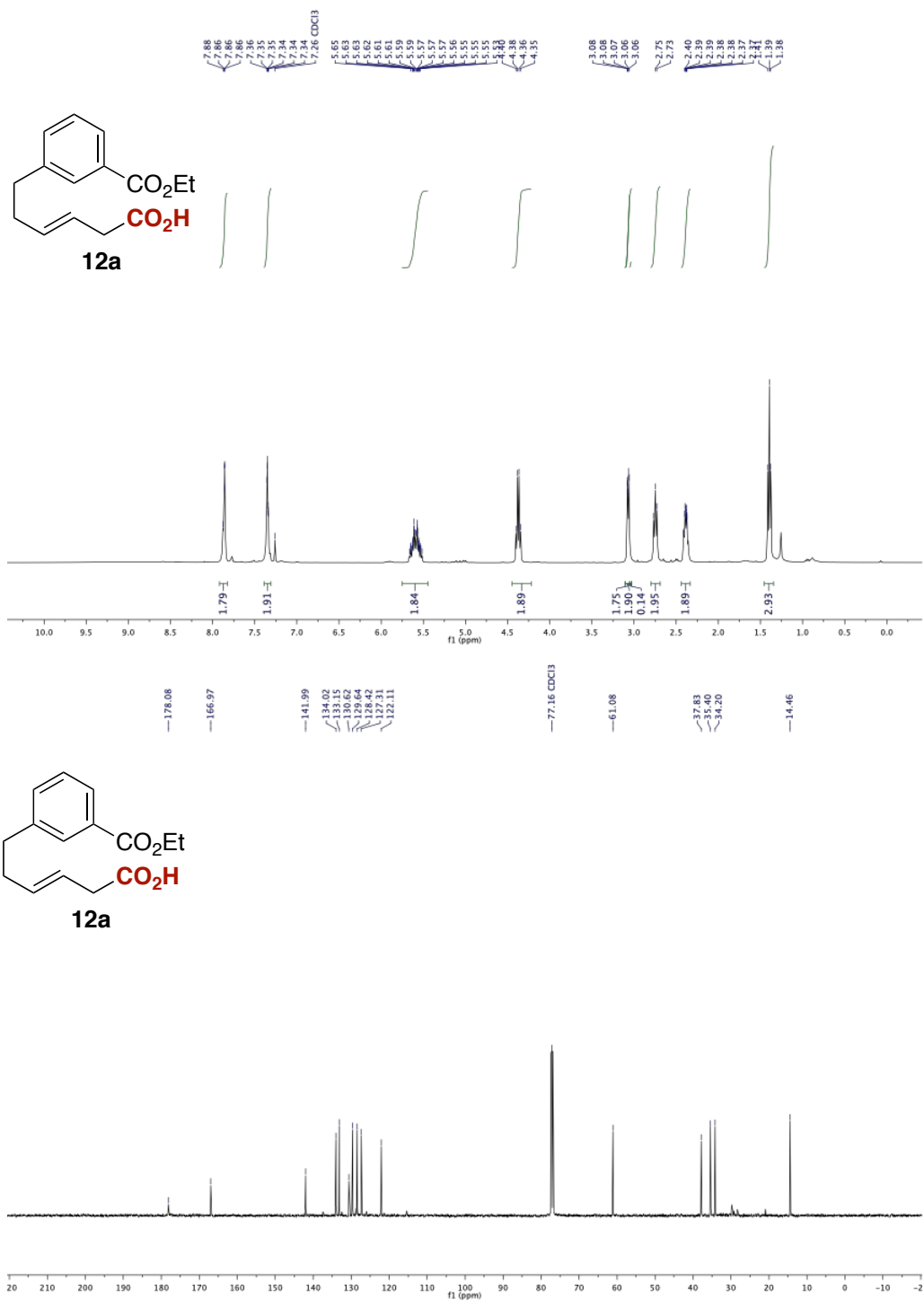


Figure 12. <sup>1</sup>H and <sup>13</sup>C NMR spectra of **12a**.

Chapter 2

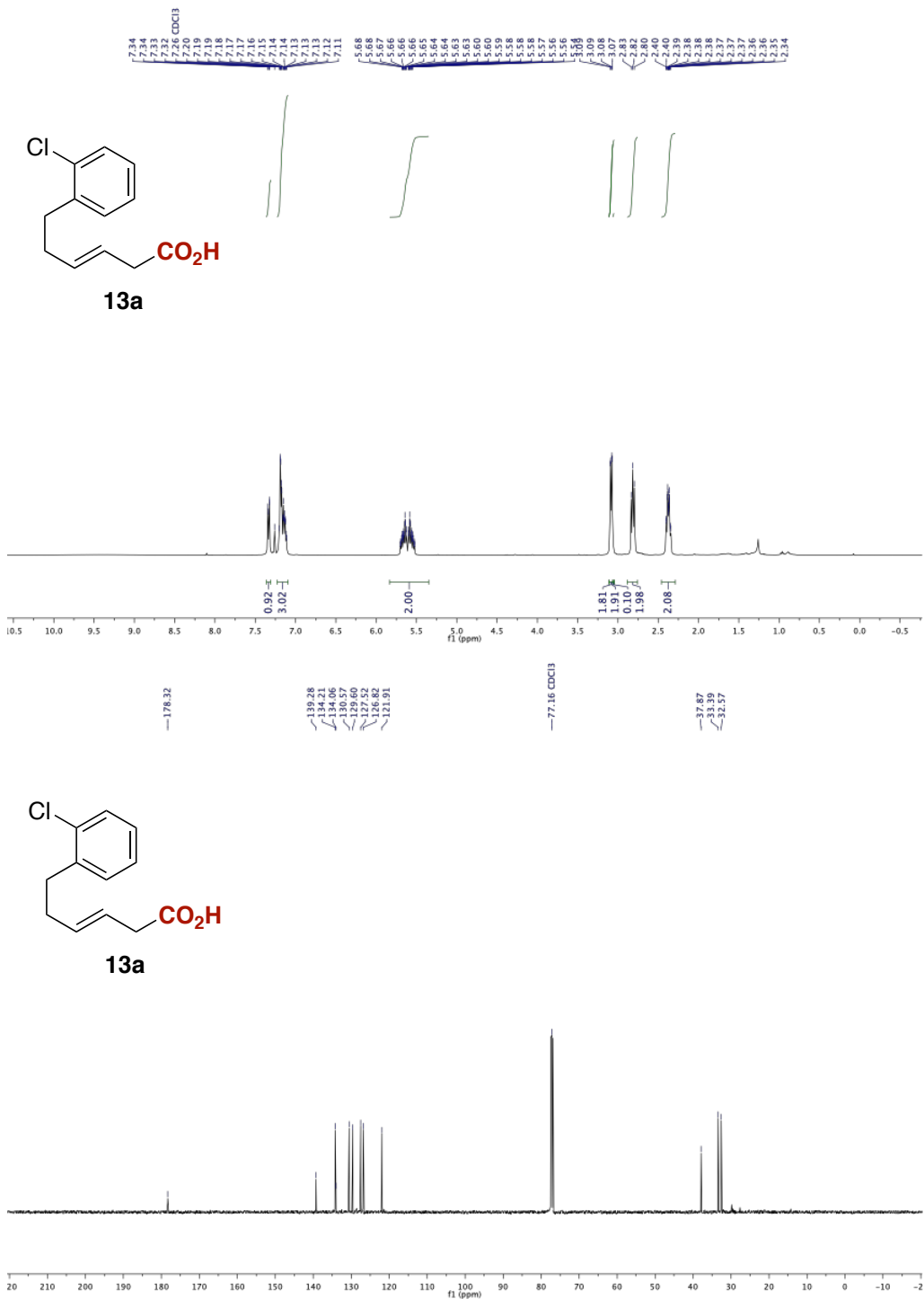


Figure 13. <sup>1</sup>H and <sup>13</sup>C NMR spectra of **13a**.



Site-Selective Catalytic Carboxylation of Allylic Alcohols with CO<sub>2</sub>

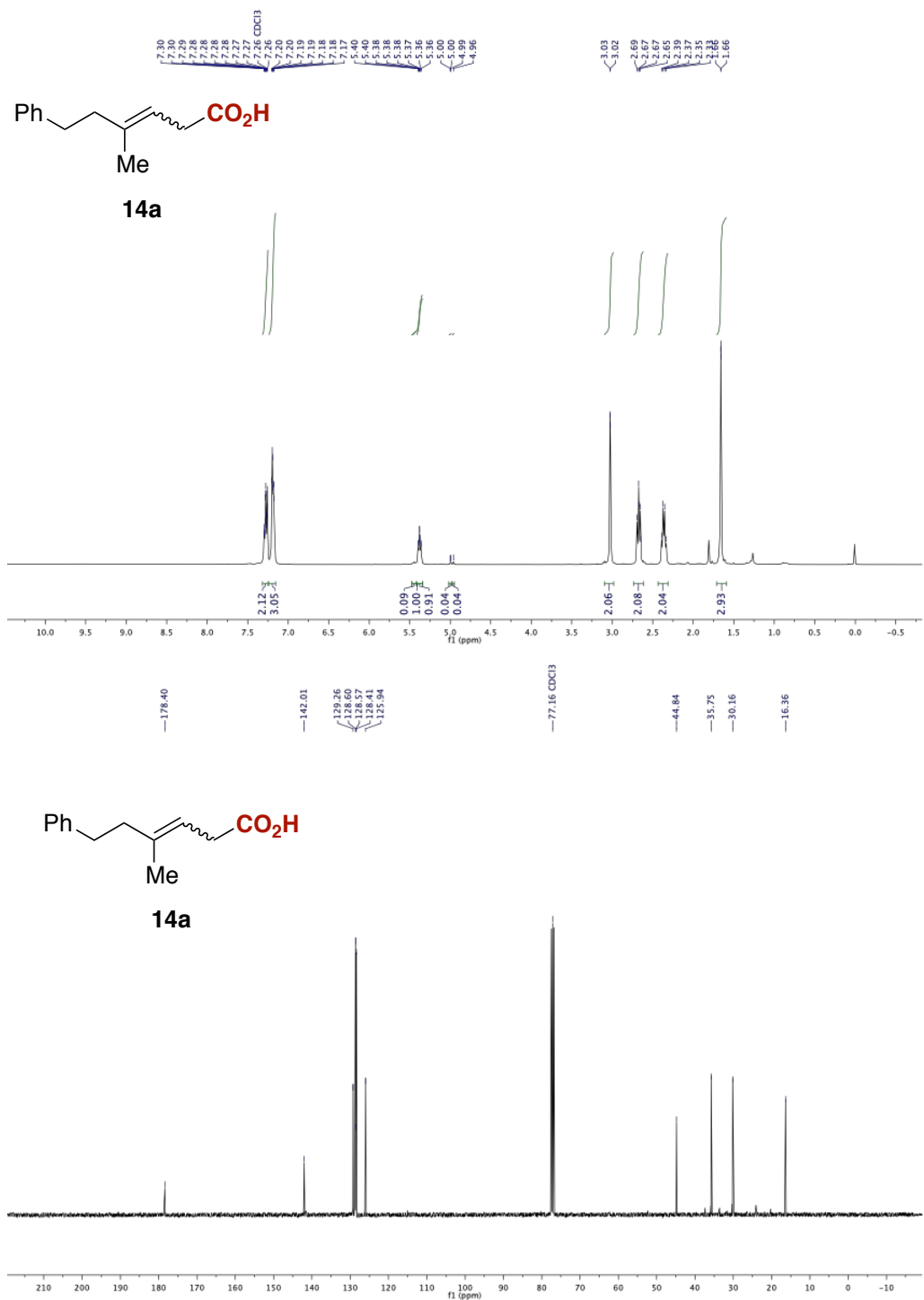


Figure 14. <sup>1</sup>H and <sup>13</sup>C NMR spectra of **14a**.



# Site-Selective Catalytic Carboxylation of Allylic Alcohols with CO<sub>2</sub>

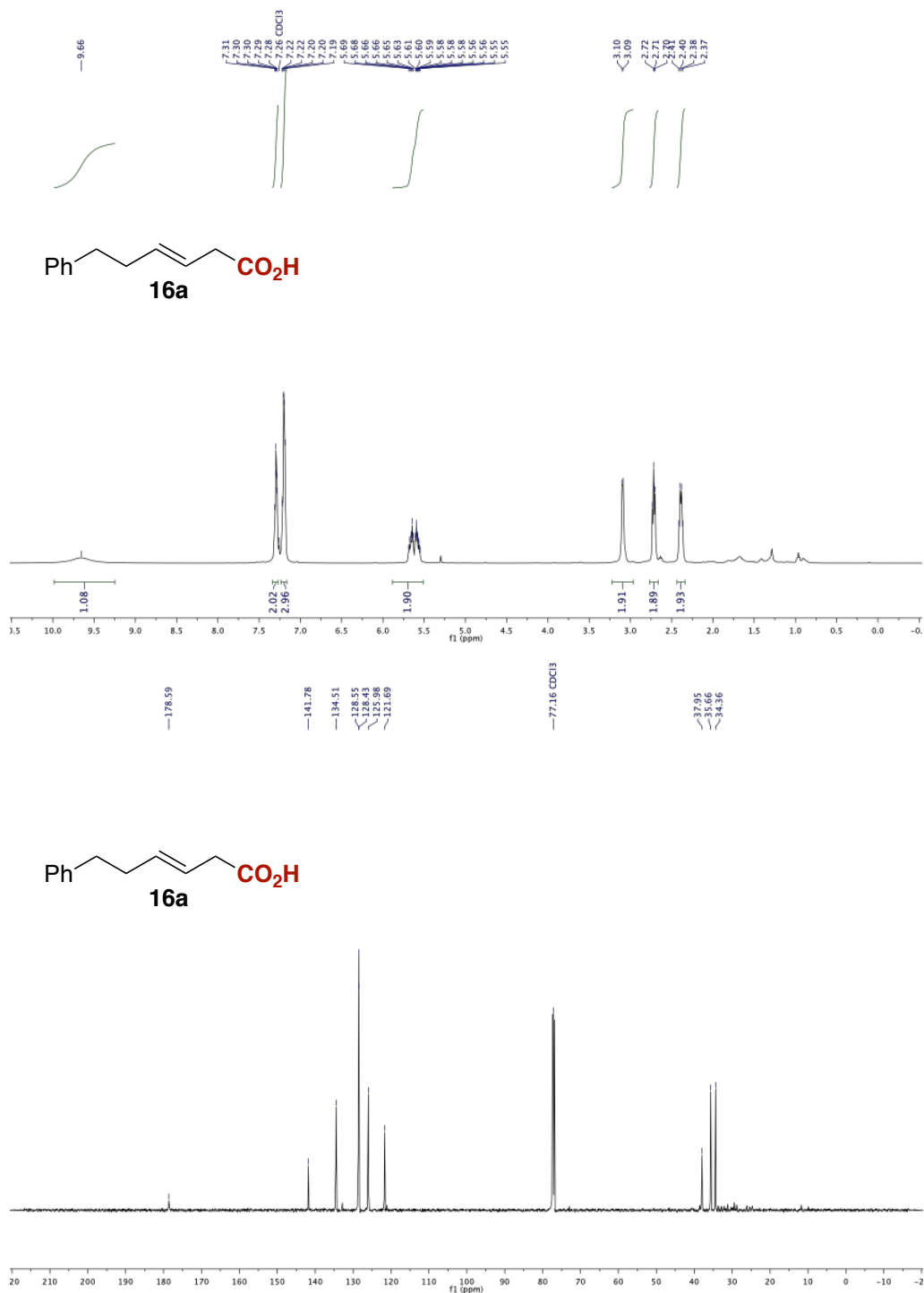


Figure 16. <sup>1</sup>H and <sup>13</sup>C NMR spectra of **16a**.



# Site-Selective Catalytic Carboxylation of Allylic Alcohols with CO<sub>2</sub>

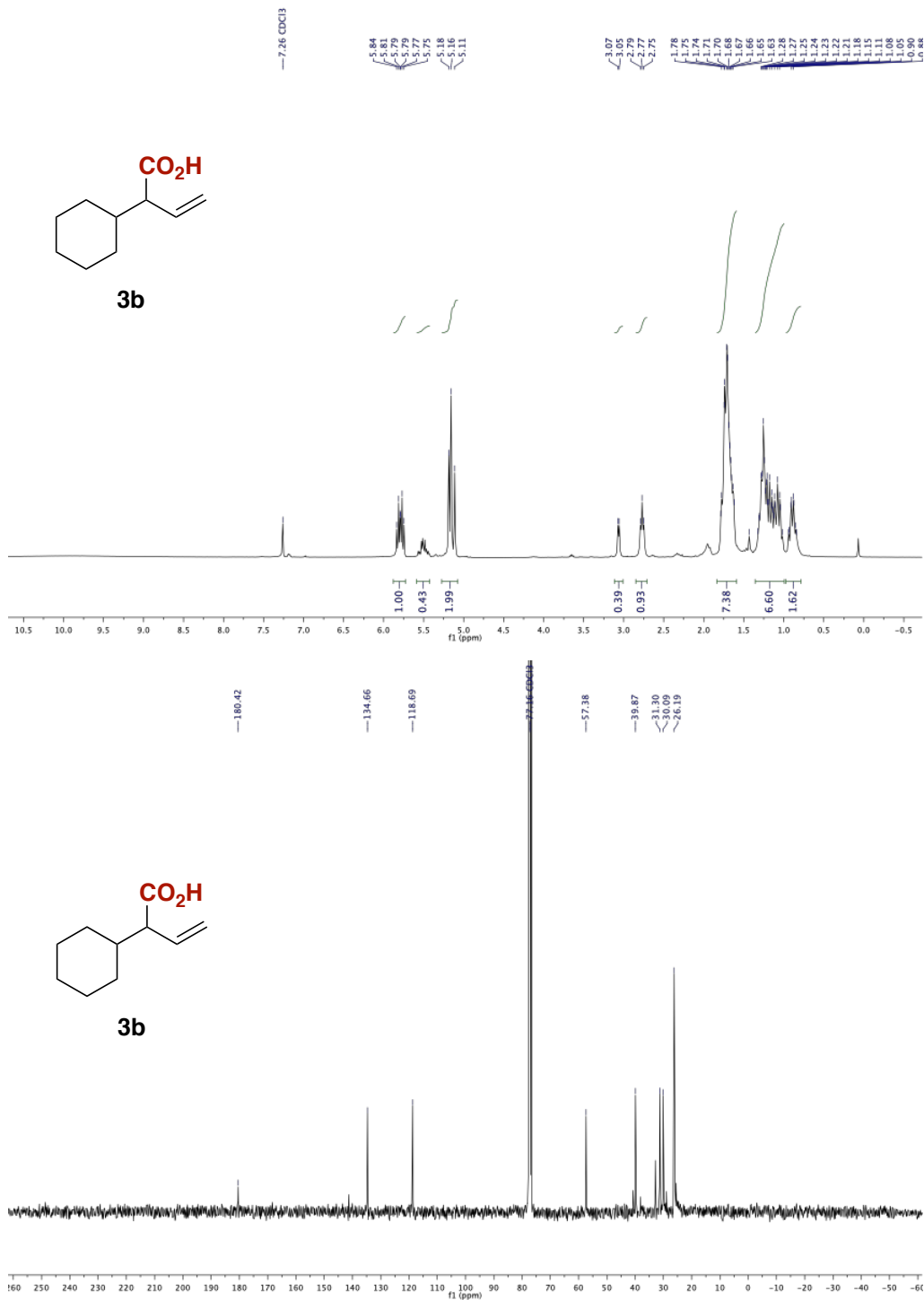


Figure 18. <sup>1</sup>H and <sup>13</sup>C NMR spectra of **3b**.

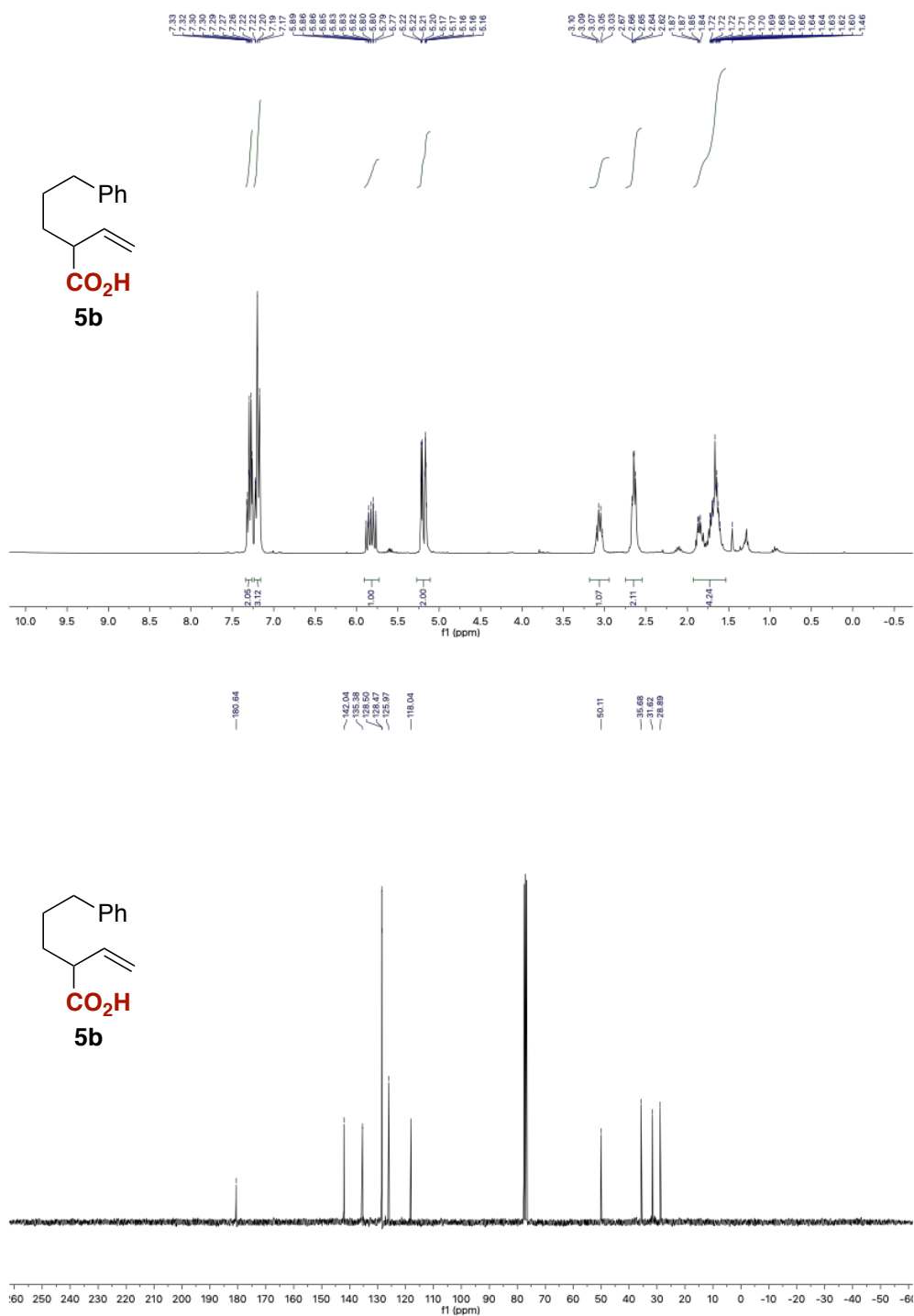


Figure 19.  $^1\text{H}$  and  $^{13}\text{C}$  NMR spectra of **5b**.







# Site-Selective Catalytic Carboxylation of Allylic Alcohols with CO<sub>2</sub>

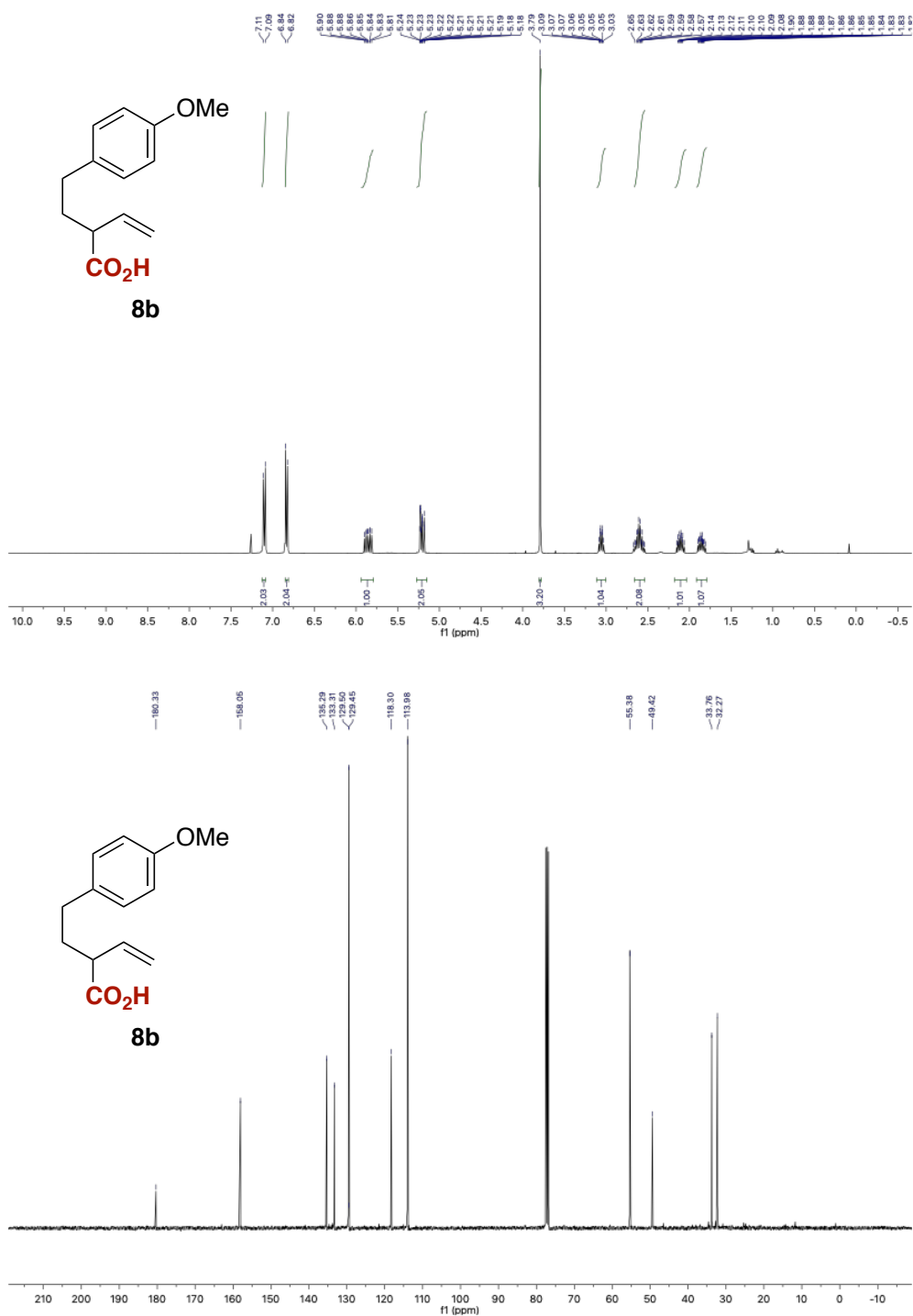


Figure 22. <sup>1</sup>H and <sup>13</sup>C NMR spectra of **8b**.

# Chapter 2

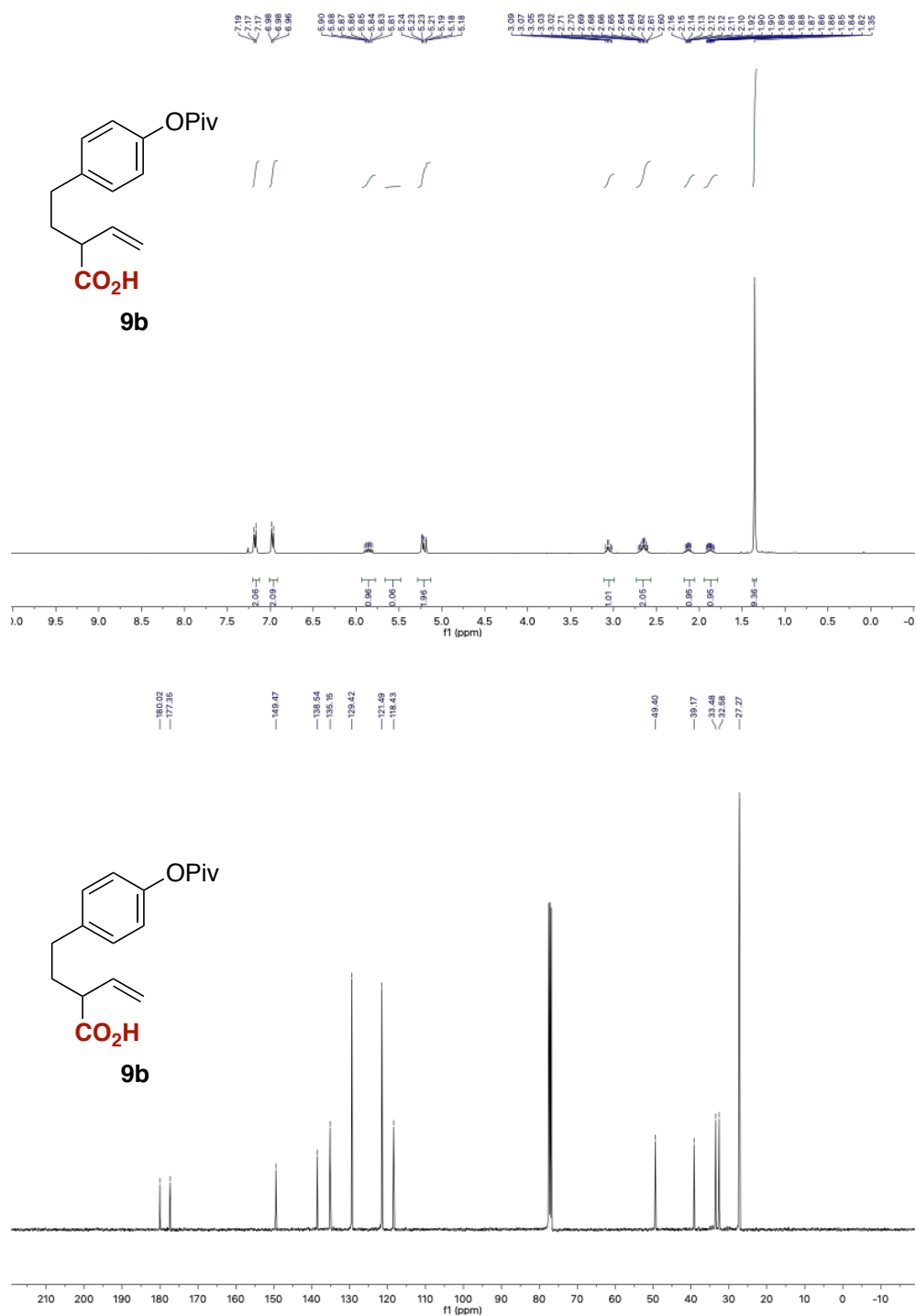


Figure 23. <sup>1</sup>H and <sup>13</sup>C NMR spectra of **9b**.

Site-Selective Catalytic Carboxylation of Allylic Alcohols with CO<sub>2</sub>

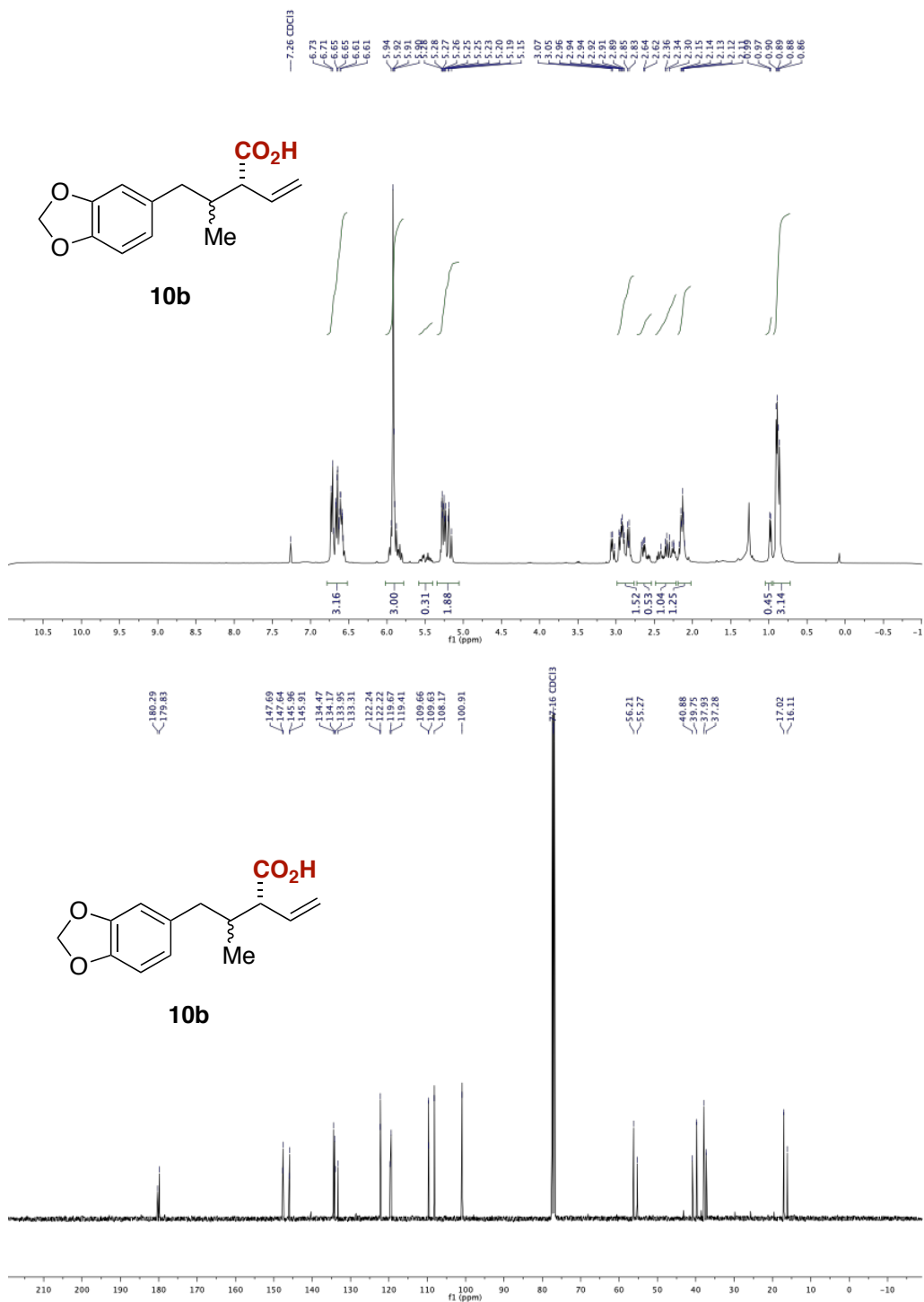


Figure 24. <sup>1</sup>H and <sup>13</sup>C NMR spectra of **10b**.



# Site-Selective Catalytic Carboxylation of Allylic Alcohols with CO<sub>2</sub>

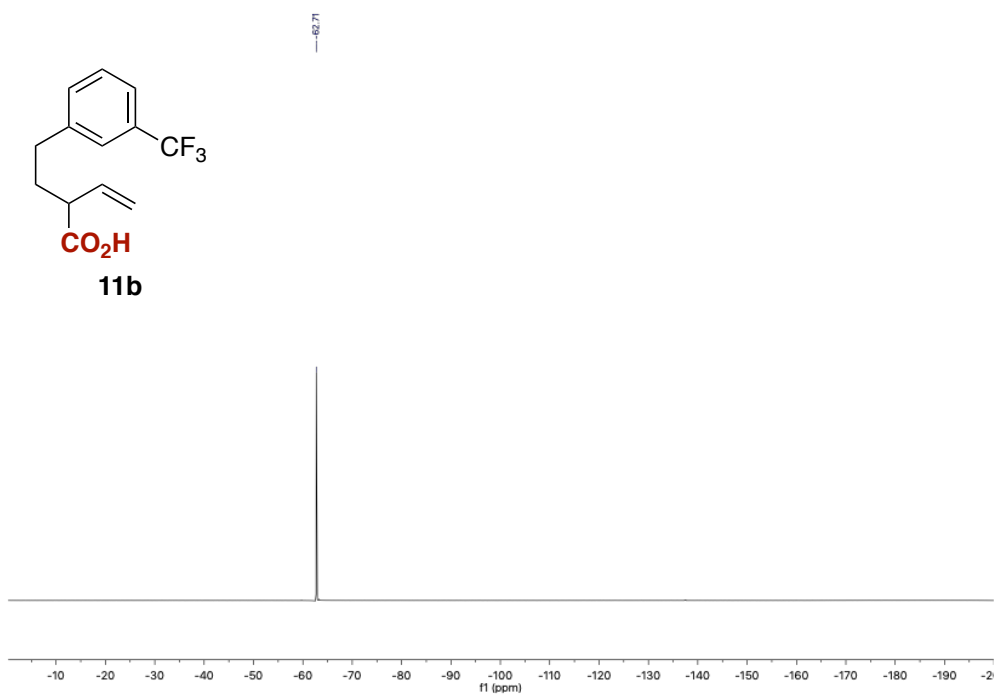


Figure 25. <sup>1</sup>H, <sup>13</sup>C and <sup>19</sup>F NMR spectra of **11b**.

# Chapter 2

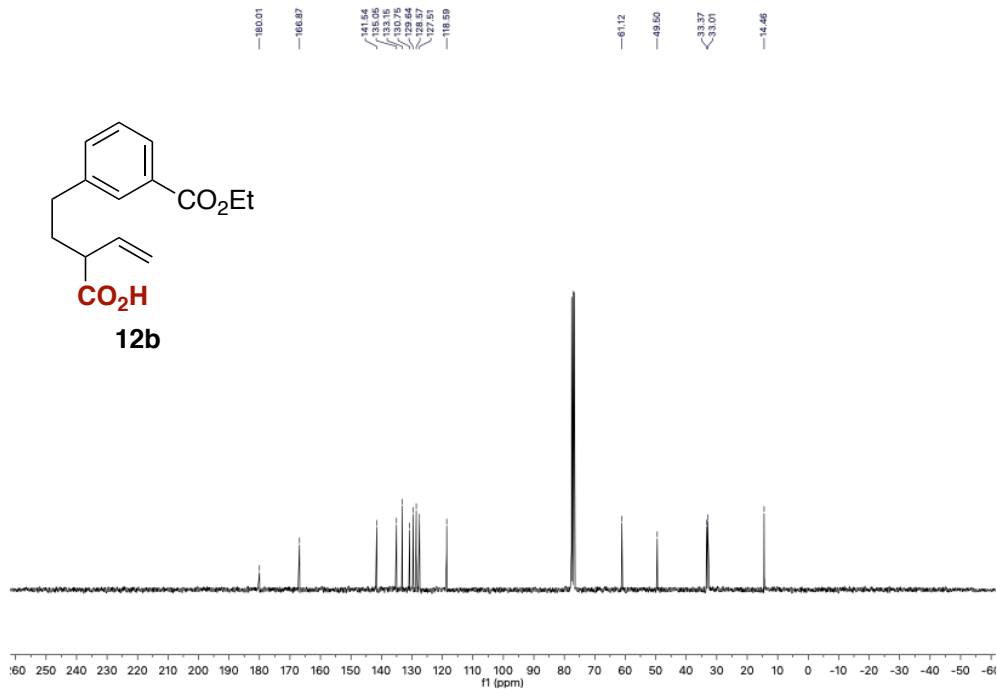
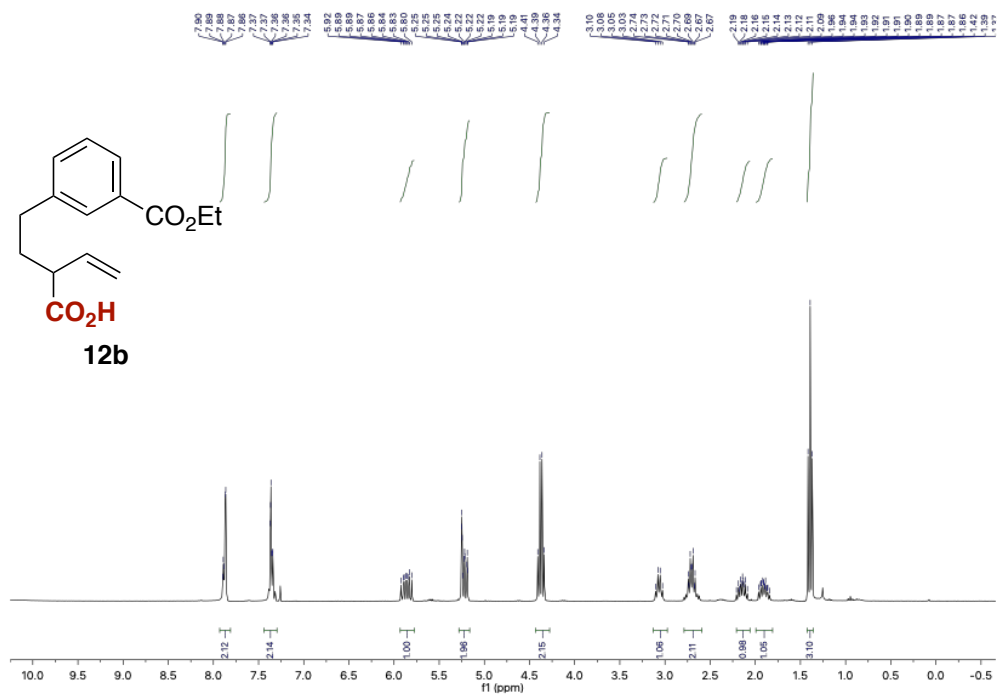


Figure 26.  $^1\text{H}$  and  $^{13}\text{C}$  NMR spectra of **12b**.

# Site-Selective Catalytic Carboxylation of Allylic Alcohols with CO<sub>2</sub>

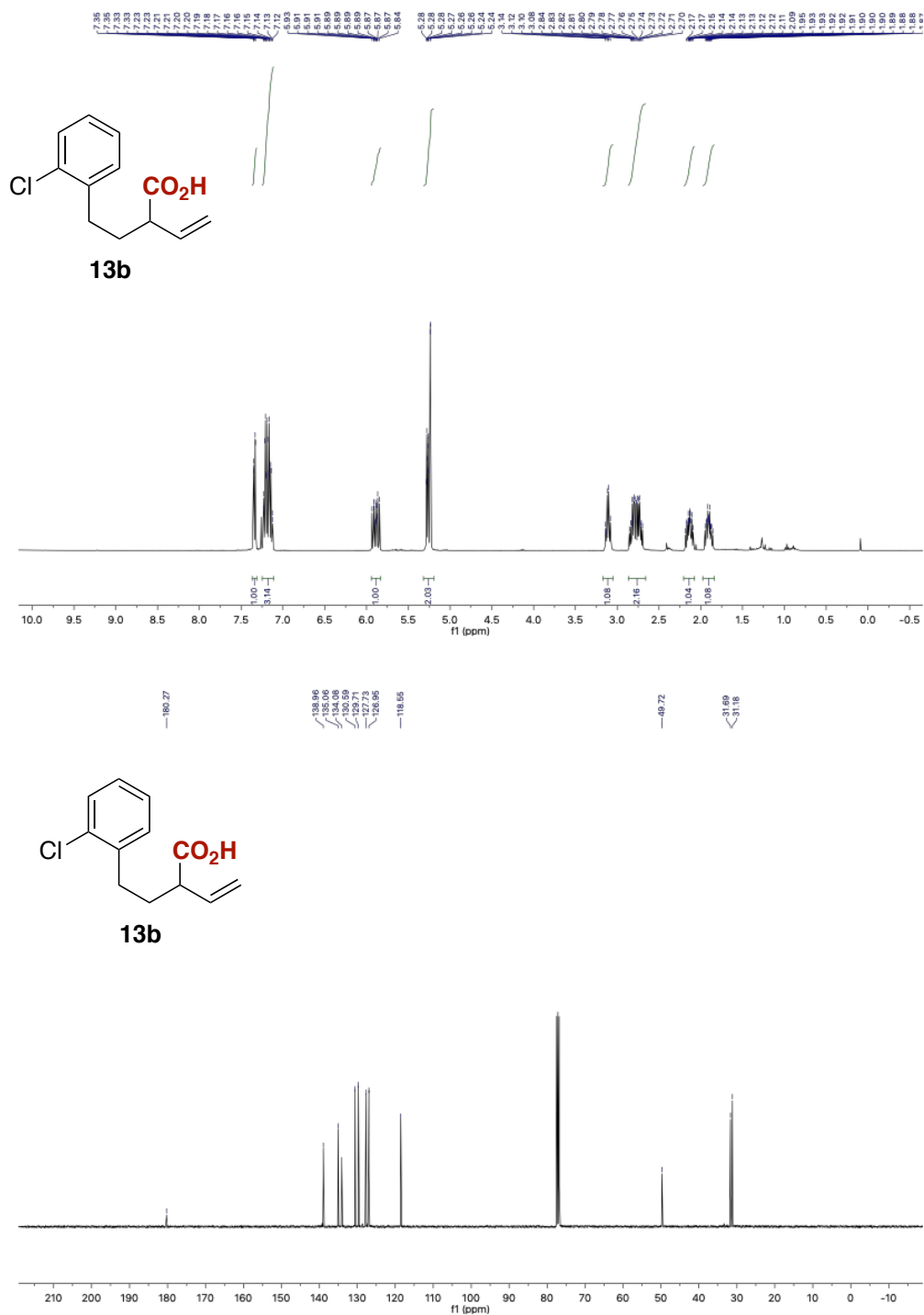


Figure 27. <sup>1</sup>H and <sup>13</sup>C NMR spectra of **13b**.

# Chapter 2

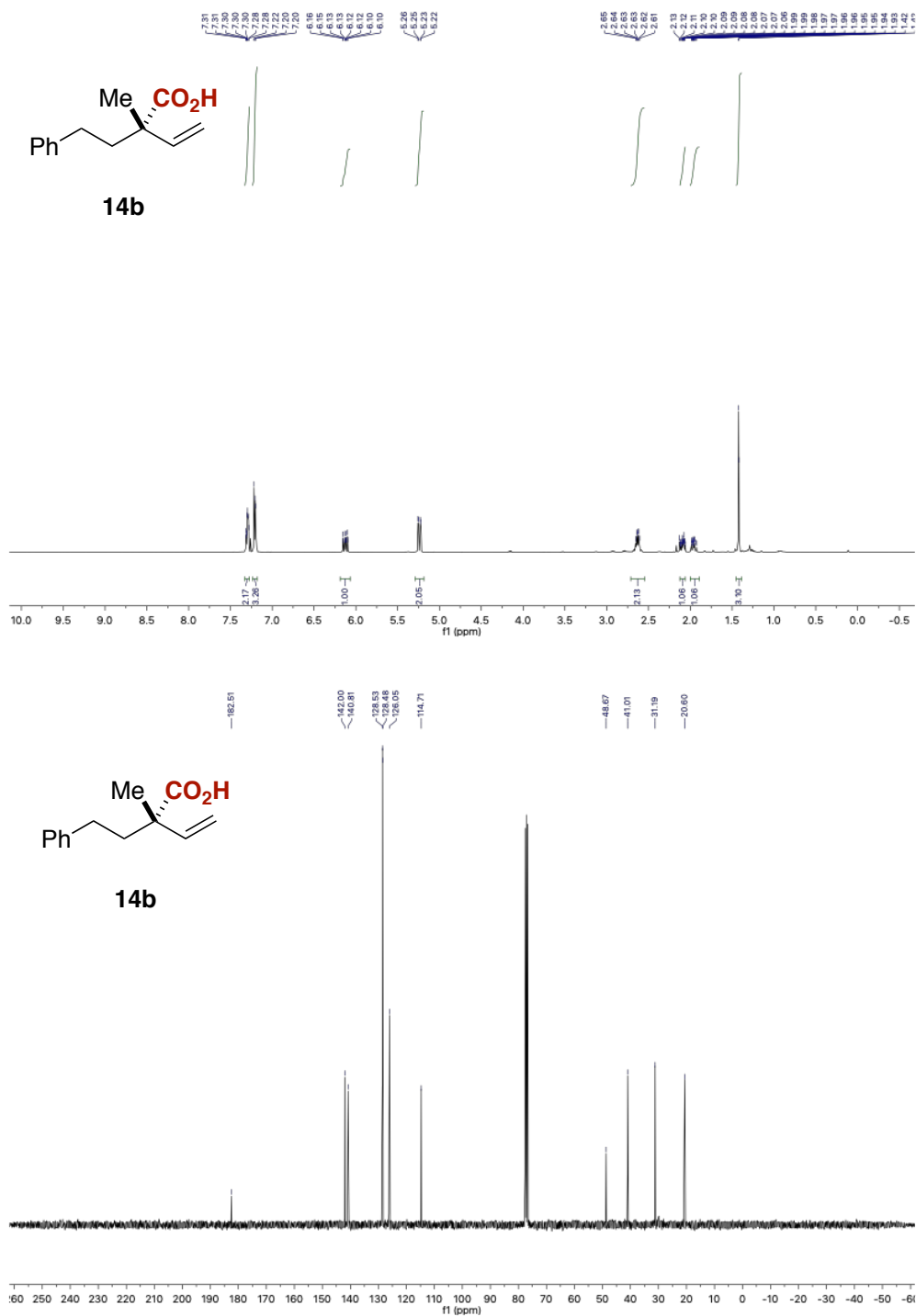


Figure 28. <sup>1</sup>H and <sup>13</sup>C NMR spectra of **14b**.



# Site-Selective Catalytic Carboxylation of Allylic Alcohols with CO<sub>2</sub>

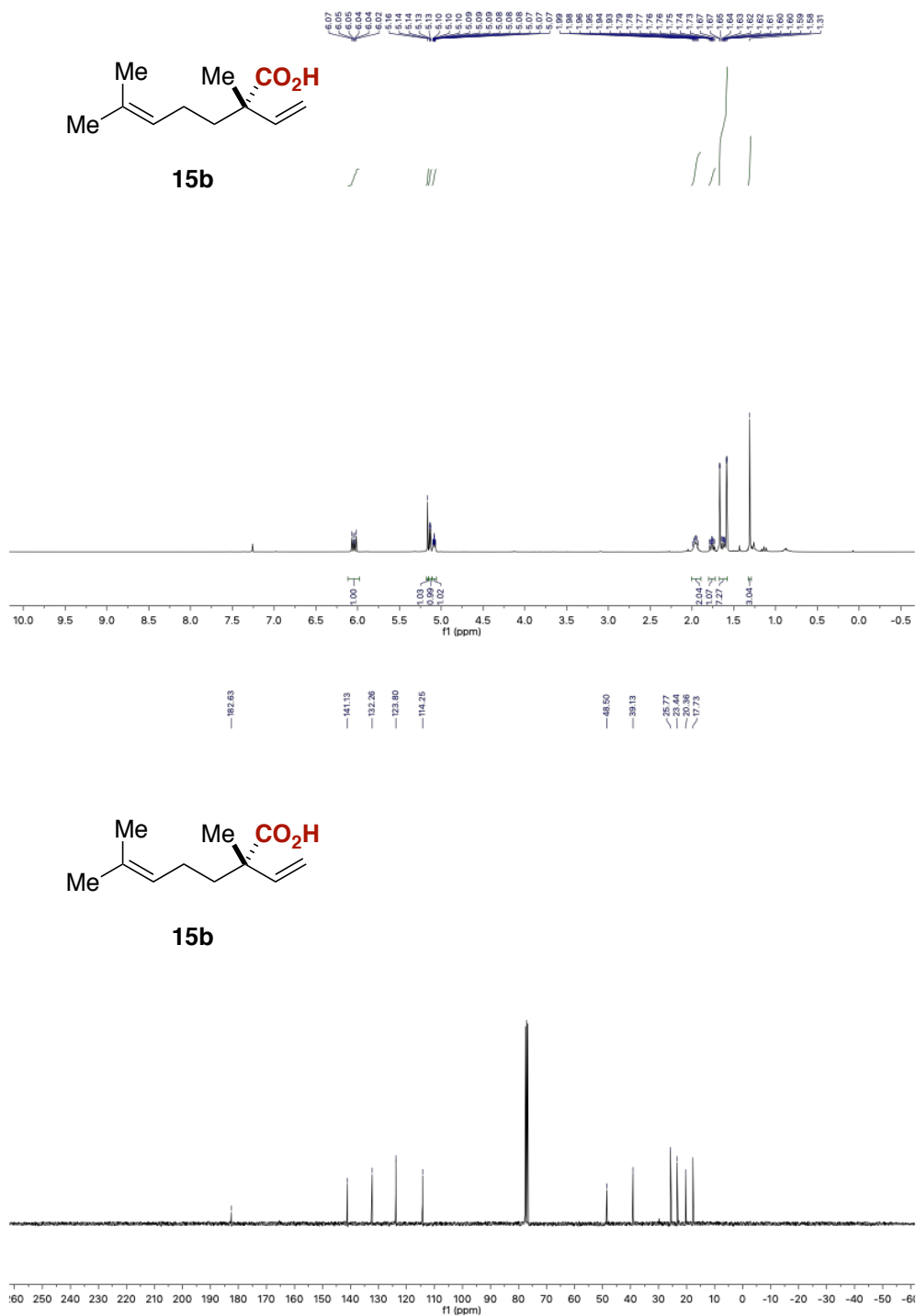


Figure 29. <sup>1</sup>H and <sup>13</sup>C NMR spectra of **15b**.

Chapter 2

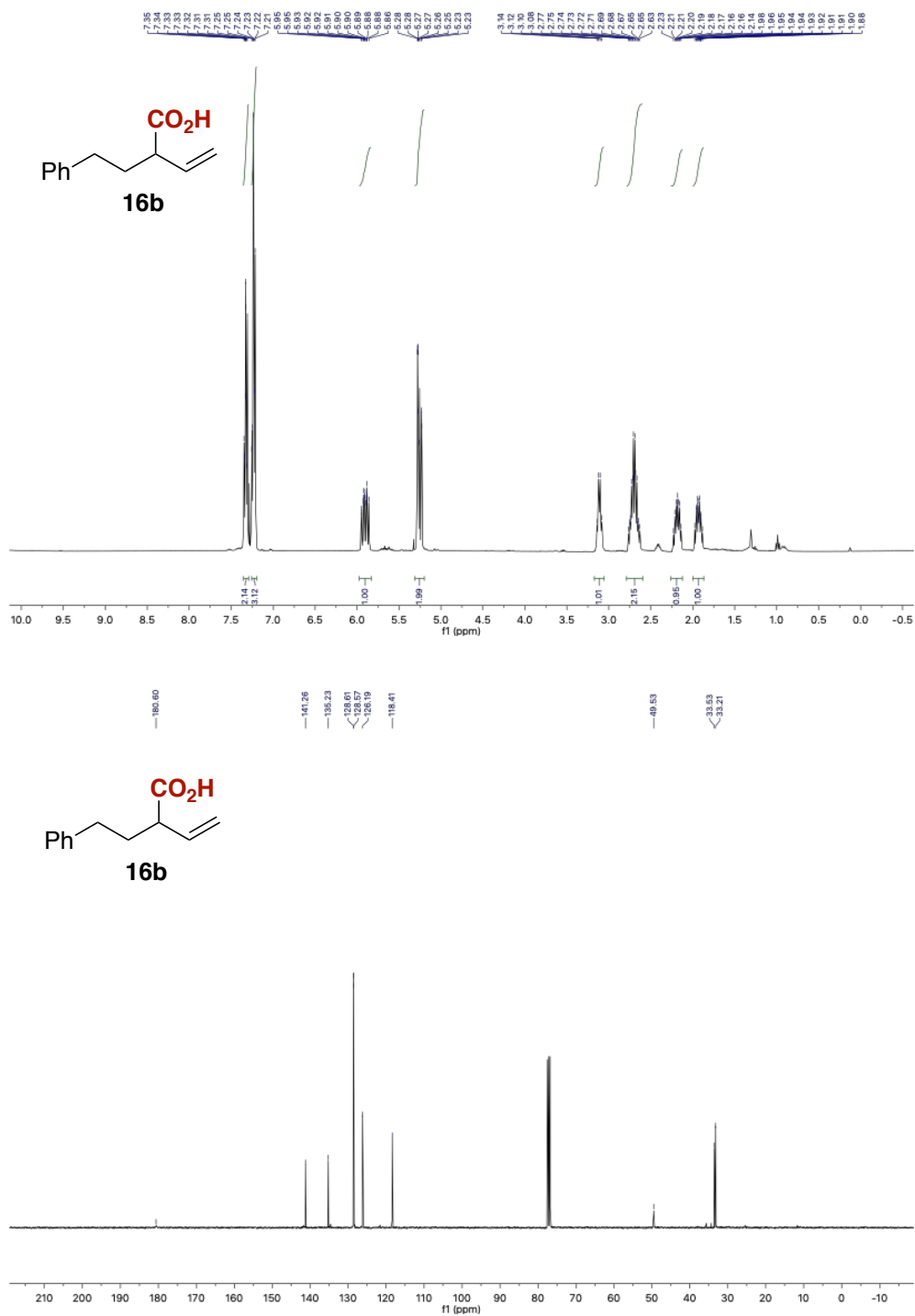


Figure 30. <sup>1</sup>H and <sup>13</sup>C NMR spectra of **16b**.

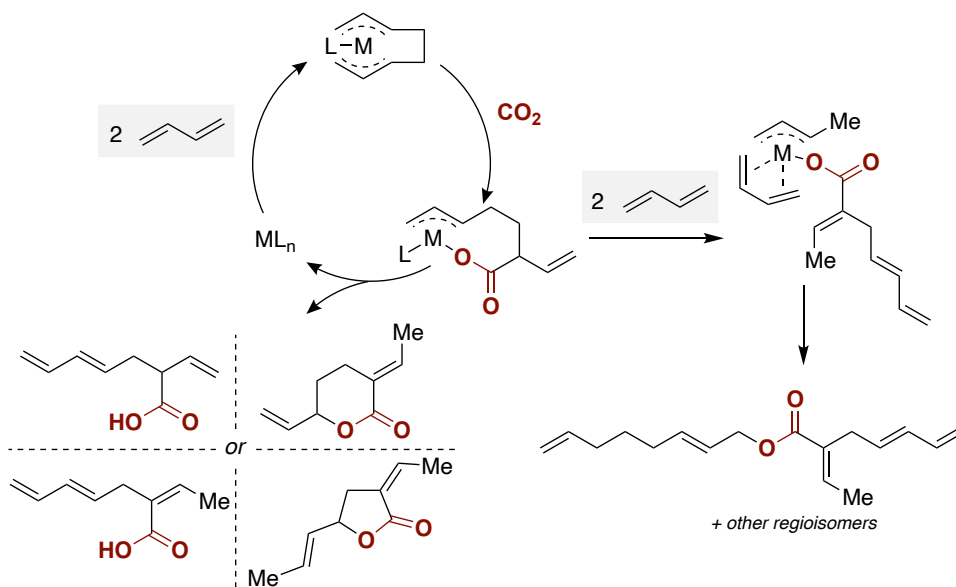
**Chapter 3:**  
***Ni-Catalyzed Site-Selective Dicarboxylation of***  
***1,3-Dienes with CO<sub>2</sub>***

*In collaboration with Ryo Ninokata*

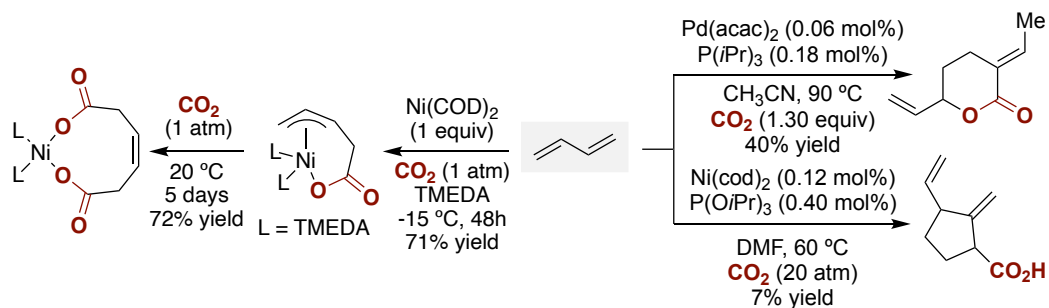


## 1. Introduction

Unlike simple alkenes or alkynes, dienes, enynes or diyne offer the advantage of possessing an additional unsaturated backbone that provides a different interaction with transition metals, most of the times resulting in an enhanced reactivity. Moreover, it adds to the product a  $\pi$ -system that could be used additionally for further functionalization. Such seemingly trivial observation can hardly be underestimated, as it could set the basis for promoting conceptually new carboxylation reactions that would be beyond reach otherwise. The first reports aimed at unravelling the potential of polyenes in carboxylation technologies appeared in the late 70's and 80's, when Inoue,<sup>1,2</sup> Behr,<sup>3</sup> Höberg,<sup>4</sup> Braustein<sup>5</sup> and others<sup>6,7</sup> reported the telomerization of butadiene in presence of CO<sub>2</sub> catalyzed by either palladium or nickel precatalysts (Scheme 1). As shown, a different range of products could be obtained from the incorporation of 2 or 4 molecules of butadiene per molecule of CO<sub>2</sub>, either forming esters or lactones via C–O reductive elimination or free carboxylic acids. In addition, the choice of ligand (mainly phosphines and phosphites were studied) and metal exerted a profound influence on both reactivity and selectivity, obtaining predominantly either a lactone or a carboxylic acid, albeit in low to moderate yields (Scheme 2, *right*).

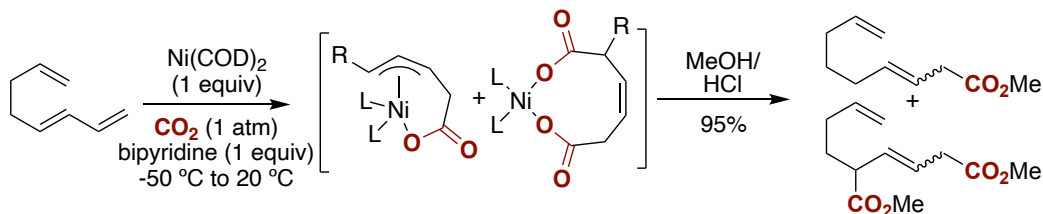


**Scheme 1.** Transition metal catalyzed butadiene telomerization with CO<sub>2</sub>.



**Scheme 2.** Transition metal mediated and catalyzed carboxylation of butadiene with CO<sub>2</sub>.

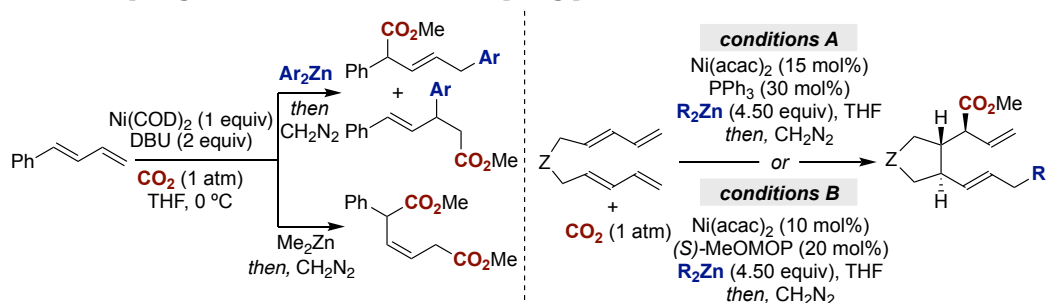
Hoberg<sup>8,9</sup> and Behr<sup>10</sup> independently studied also the combination of 1,3-dienes and Nickel (0) in a stoichiometric manner. Höberg found that TMEDA (*N,N,N',N'*-tetramethylethylenediamine), bipyridine or the chelating phosphine DCPE (1,2-bis(dicyclohexylphosphino)ethane) in combination with Nickel (0) gave the corresponding nickelalactones with a 1:1 ratio between butadiene and CO<sub>2</sub>. Moreover, they observed that in the case of the TMEDA complex it evolved after long reaction times at ambient temperature to the formation of a nickel complex that had incorporated a second molecule of CO<sub>2</sub> (Scheme 2, *left*).<sup>9</sup> It is worth mentioning that this finding represents the first example of multiple incorporation of CO<sub>2</sub> into a  $\pi$  system mediated by a transition metal. A couple of years later, they also reported the same transformation catalyzed by Fe(0),<sup>11</sup> albeit with an inferior selectivity towards the dicarboxylated product. At the same time, Behr showed the greater reactivity towards dienes in comparison to  $\alpha$ -olefins with a bipyridine/Ni(0) regime (Scheme 3),<sup>10</sup> proving that other nitrogen-based ligands could promote as well the multiple addition of CO<sub>2</sub> to dienes.<sup>10</sup>



**Scheme 3.** Nickel-mediated carboxylation of 1,3-dienes with CO<sub>2</sub>.

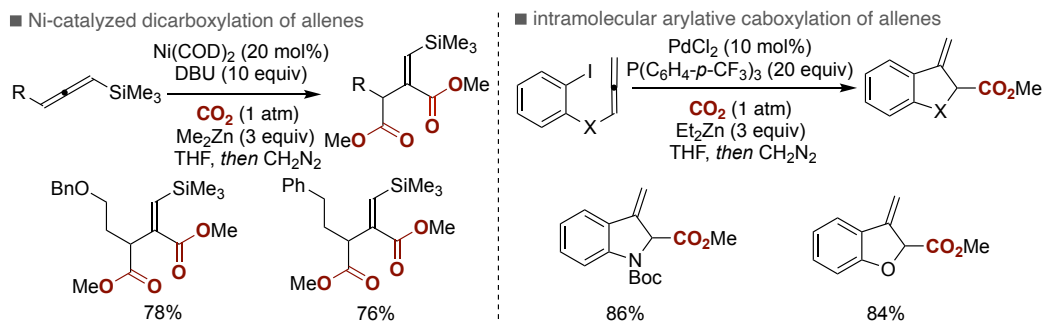
Despite the inherent potential of 1,3-dienes in carboxylation reactions, this field remained dormant until 2001, when Mori described the Ni-mediated carboxylation of bis-1,3-dienes with CO<sub>2</sub> and organozinc reagents (Scheme 4, *left*).<sup>12</sup> The authors proposed a similar  $\pi$ -allyl carboxylate nickelacycle intermediates to those suggested by Behr and Höberg that could be coupled with different organozinc reagents to yield the corresponding carboxylic acids. The utilization of diarylzinc resulted in a mixture of carboxylated products, whereas 1,6-dicarboxylation took place with

Me<sub>2</sub>Zn instead. This observation was rationalized by the reduction of the nickel(II) intermediate by Me<sub>2</sub>Zn, allowing for a second insertion of CO<sub>2</sub> in the presence of DBU as a supporting ligands. A year later, the same group described a catalytic process in which a bis-1,3-diene was coupled with an organozinc reagent and CO<sub>2</sub> (Scheme 4, right),<sup>13</sup> a reaction that is somewhat reminiscent of cycloaddition-type reactions. Shortly after, they also demonstrated the feasibility of promoting an enantioselective reaction with (*S*)-MeOMOP as chiral ligand. This result is particularly noteworthy, as it constituted the first metal-catalyzed enantioselective cross-coupling reaction with CO<sub>2</sub> as coupling partner.<sup>14</sup>



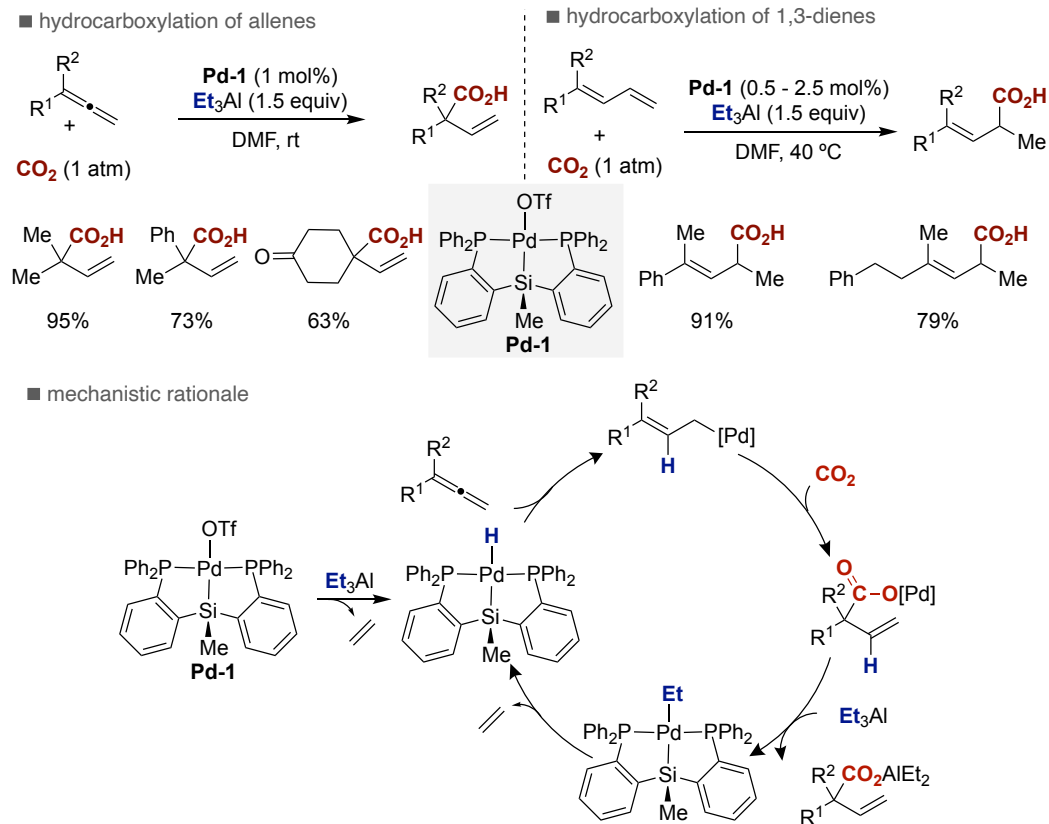
**Scheme 4.** Carboxylation of 1,3-dienes and Cycloisomerization of bis-1,3-dienes with CO<sub>2</sub>.

The first catalytic carboxylation of 1,2-dienes (allenes) was described in 2005 by Mori and co-workers using Ni(COD)<sub>2</sub> as catalyst and Me<sub>2</sub>Zn as reducing agent (Scheme 5, left).<sup>15</sup> Of particular importance was the requirement for a large excess of DBU and a silyl end-capped allene, the latter being attributed to a combination of stereoelectronic effects. More recently, an intramolecular reductive arylyative carboxylation of allenes with CO<sub>2</sub> was reported by Sato (Scheme 5, right).<sup>16</sup> Unlike Mori's protocol, the reaction was promoted by palladium catalysts supported by electron-poor phosphines with Et<sub>2</sub>Zn as a stoichiometric reducing agent.



**Scheme 5.** Catalytic carboxylation of allenes with CO<sub>2</sub>.

## Chapter 3



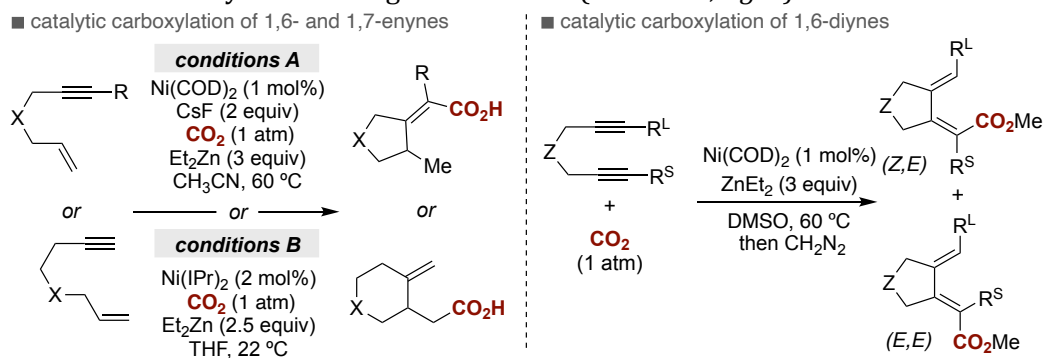
**Scheme 6.** Palladium catalyzed hydrocarboxylation of dienes with  $\text{CO}_2$  and mechanistic rationale.

In 2008, Iwasawa reported the hydrocarboxylation of allenes using **Pd-1** and  $\text{Et}_3\text{Al}$  as hydride source (Scheme 6, *left*).<sup>17</sup> The reaction was proposed to proceed via the formation of palladium hydrides, which was later confirmed by Hazari that isolated and characterized the putative reaction intermediates within the catalytic cycle.<sup>18</sup> The mechanism likely is initiated by the generation of a Pd(II) hydride followed by hydrometalation to yield an allylic Pd(II) intermediate (Scheme 6, *bottom*).  $\text{CO}_2$  insertion followed by transmetalation gives rise to an aluminium carboxylate while regenerating the Pd(II) hydride via  $\beta$ -hydride elimination. A few years later, the same group described an elegant and rather efficient hydrocarboxylation of 1,3-dienes (Scheme 6, *right*).<sup>19</sup> Critical for success was the employment of the same pincer-type Pd(II) precatalyst (**Pd-1**) and  $\text{Et}_3\text{Al}$  as the terminal reducing agent to form the corresponding  $\beta,\gamma$ -unsaturated carboxylic acids.

Prompted by Mori's cycloisomerization with  $\text{CO}_2$  and nickel catalysts,<sup>13</sup> Sato described the reductive carboxylation of 1,7-enynes as a means to access the core of (-)-Corynantheidine.<sup>20</sup> Subsequently, the groups of Ma<sup>21</sup> and Diao<sup>22</sup> independently

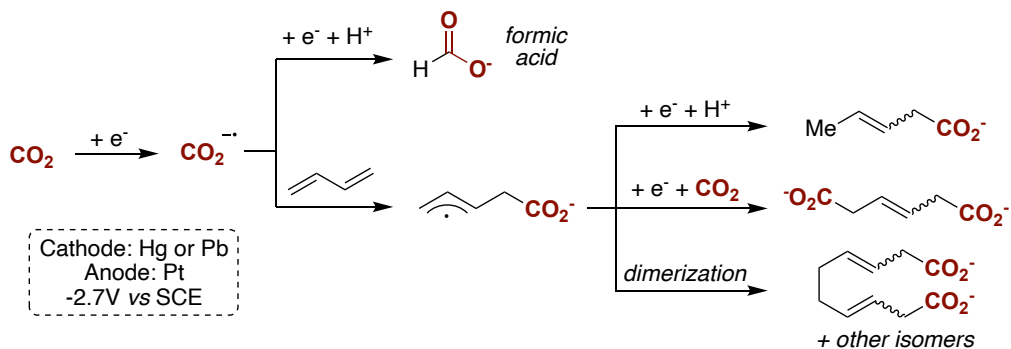


showed the ability of 1,6-enynes and 1,7-enynes to participate in related catalytic reductive carboxylations, furnishing the five- or six-membered ring, respectively (Scheme 7, *left*). These conceptions were complemented by Ma in a Ni-catalyzed hydrocarboxylation of 1,6-diynes to give access to  $\alpha,\beta,\gamma,\delta$ -unsaturated carboxylic acids in excellent yields and regioselectivities (Scheme 7, *right*).<sup>23</sup>

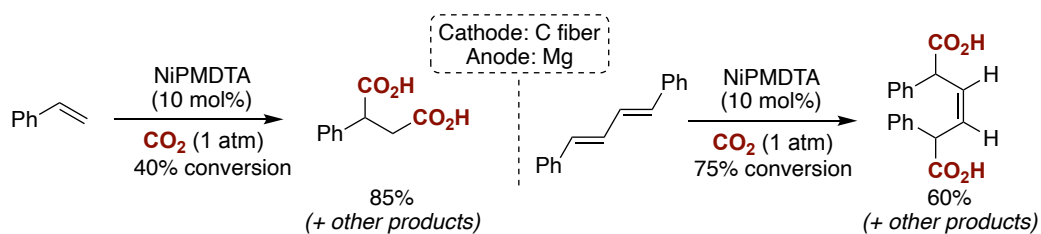


**Scheme 7.** Catalytic carboxylation of enynes and diynes with CO<sub>2</sub>.

In parallel to transition-metal promoted carboxylation of dienes, electrochemical settings have also been employed for similar purposes. In 1981, Tilborg and Smith reported the reduction of CO<sub>2</sub> in an electrochemical cell, which reacted with butadiene to give a mixture of different carboxylic acids, albeit with low selectivity (Scheme 8).<sup>24</sup> In this case, the authors suggest that the reaction pathway goes via the formation of CO<sub>2</sub> radical anions. A few years later, Duñach and Périchon reported the carboxylation of alkynes, alkenes and dienes by adding nickel(II) salts in the electrochemical cell (Scheme 9).<sup>25,26</sup> They propose the generation of Ni(0) species that promote the carboxylation of  $\pi$  systems in a similar pathway to that proposed by Hoberg and Behr. After these reports, the substitution of the cathode by metallic nickel and the addition of different nickel(II) salts have been shown to be beneficial for the dicarboxylation of dienes.<sup>27–30</sup> Nevertheless, the site-selectivity is still not a solved problem and as a result a mixture of products is generally observed. In addition, the mechanism by which these electrochemical carboxylation reactions operate is still unclear.



**Scheme 8.** Electrochemical carboxylation of butadiene.

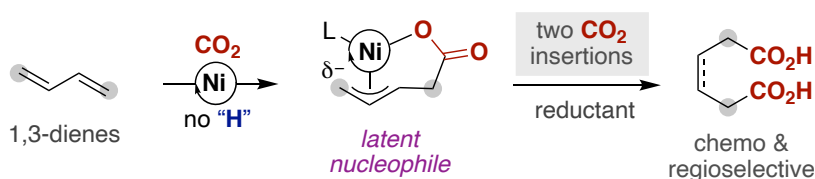


**Scheme 9.** Nickel catalyzed electrocarboxylation of alkenes and dienes. PMDTA: pentamethyldiethylenetriamine.

## 2. General aim of the project

In light of these results, the means to trigger a site-selective catalytic incorporation of CO<sub>2</sub> into unsaturated hydrocarbons continues to be of particular interest for accessing valuable carboxylic acids from simple and abundant precursors. Despite the knowledge acquired, a non-negligible number of methods still require the utilization of either stoichiometric metal complexes or air-sensitive metal reductants. In addition, the lack of mechanistic details in these processes limits the potential applicability of these endeavours.

At the outset of this Doctoral Thesis, the objective of this project was to investigate the carboxylation of dienes with CO<sub>2</sub> by means of nickel catalysis, widening the methods of obtaining carboxylic acids from abundant olefins (Scheme 10). If successful, this pathway might also offer an opportunity to complement recent catalytic difunctionalization of 1,3-dienes, as raw materials (CO<sub>2</sub>) would be used as electrophilic carbon synthons in lieu of nucleophilic reagents. However, such a scenario might bear considerable risk and could seem counterintuitive at first sight due to (a) the proclivity of 1,3-dienes to trigger telomerization reactions and (b) the fact that statistical mixtures of monocarboxylic acids were exclusively observed with hydrocarboxylation conditions previously employed for either alkynes<sup>31</sup> or alkenes,<sup>32</sup> reinforcing the notion that a multiple and controllable CO<sub>2</sub> insertion event would be particularly problematic.



**Scheme 10.** Dicarboxylation of 1,3-dienes.

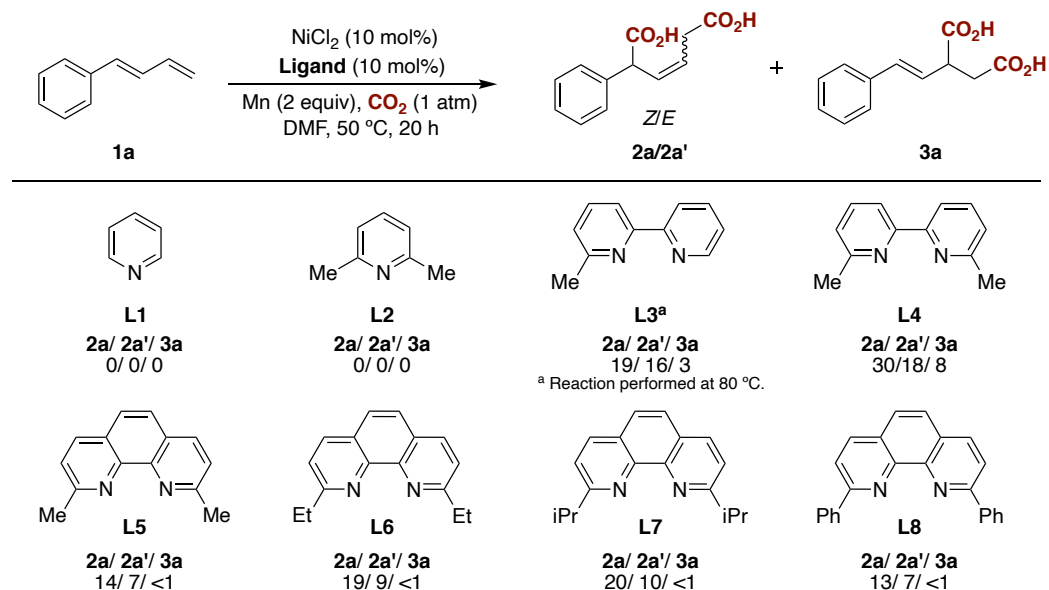
We envisioned that the catalytic formation of Ni(0) species by a reducing agent in the absence of a proton source could promote an oxidative cyclization to form  $\pi$ -allyl nickelalactones as described in the literature in a stoichiometric fashion. Under appropriate conditions, we anticipate that we could control the reactivity of the system, allowing to insert a second molecule of CO<sub>2</sub> into the  $\pi$ -allyl nickel complex to form a dicarboxylic acid. This transformation would represent the catalytic, site-selective incorporation of *multiple* CO<sub>2</sub> motifs into abundant 1,3-dienes en route to adipic acids, building blocks of particular relevance in the production of plastics and adhesives.<sup>33</sup>

### 3. Nickel catalyzed dicarboxylation of 1,3-dienes with CO<sub>2</sub>

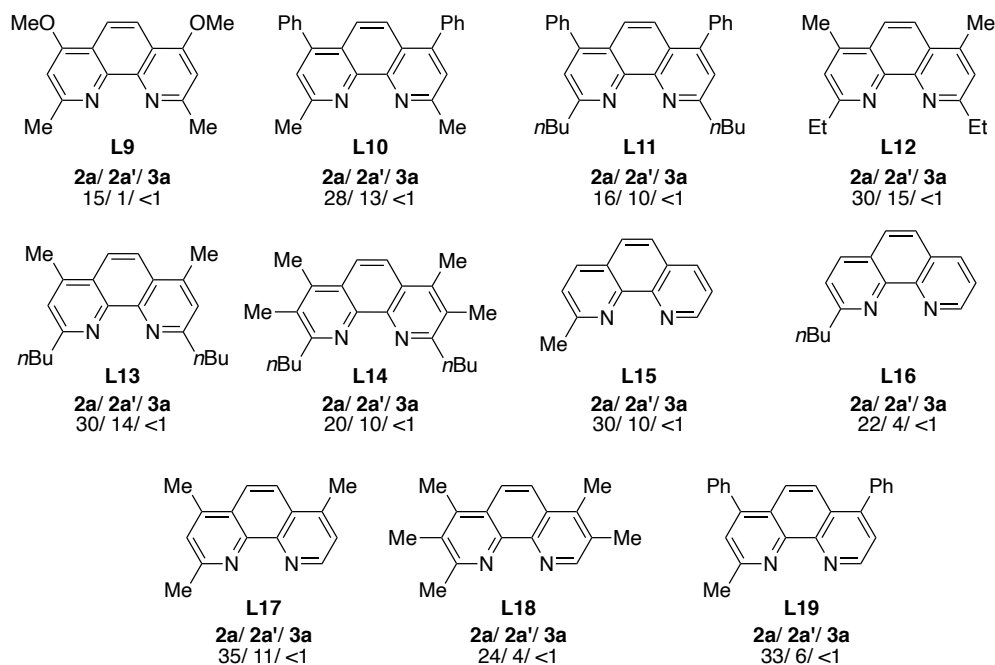
#### 3.1 Optimization of the reaction conditions:

The feasibility of the double carboxylation of 1,3-dienes with carbon dioxide was tested with 1-phenyl-1,3-butadiene (**1a**) as a model substrate, since it can be easily prepared, and it is a liquid with a relatively high boiling point. A first screening of different ligands, using nickel(II) chloride as a precatalyst and manganese as a reducing agent showed that only bidentate nitrogen-based ligands enabled the transformation (Table 1), not observing any carboxylation when phosphines, NHCs or pyridines were used as ligands. Interestingly, when bipyridine ligands were employed a mixture of 1,4-dicarboxylation and 1,2-dicarboxylation was observed. However, this selectivity problem was not observed when phenanthroline type ligands were employed, just observing in any case the formation of the 1,4-dicarboxylation product as an *E/Z*-mixture.

After an extensive examination of the ligand substitution, we observed the beneficial effect of a single substituent in the position next to the nitrogen atoms in opposition to a double substitutions in the abovementioned position (**L15/L5** or **L19/L10**) and the slight improvement in yield when phenyl groups were located in positions 4 and 7 of the ligand (**L5/L10** or **L15/L19**). The inclusion of longer alkyl chains in the ligands proved not to be beneficial to this transformation (**L11, L12, L13, L14, L16**).



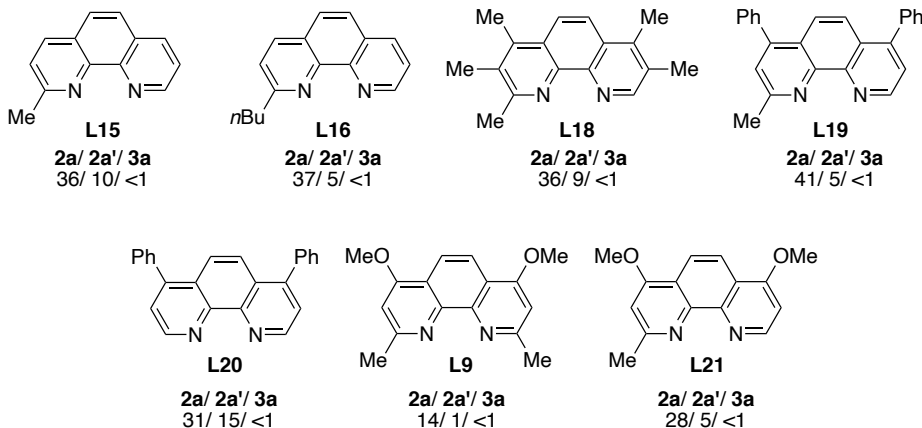
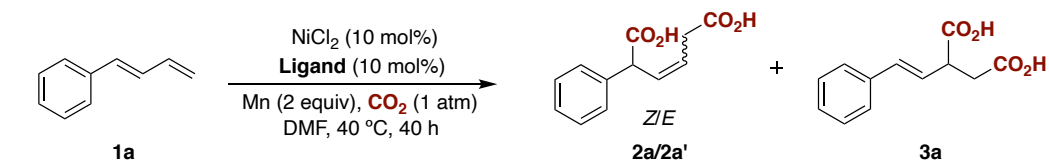
## Nickel-catalyzed double carboxylation of 1,3-dienes with CO<sub>2</sub>



Conditions: **1a** (0.20 mmol, 1 equiv), NiCl<sub>2</sub> (10 mol%), ligand (10 mol%), Mn (0.40 mmol), CO<sub>2</sub> (1 atm) in DMF (0.5 M) at 50 °C for 20 h. Yields determined by <sup>1</sup>H NMR spectroscopy of the crude mixture using fluorene as internal standard.

**Table 1.** Initial screening for the double carboxylation of 1,3-dienes.

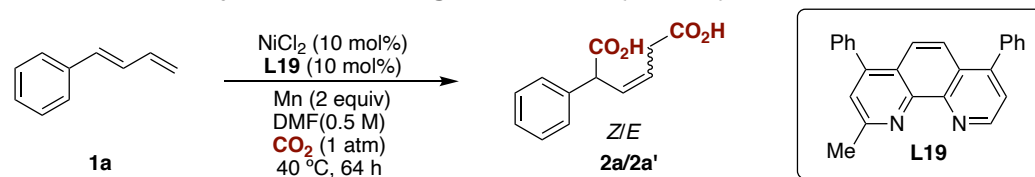
During this screening almost a full conversion of the 1,3-diene was observed in every case, so we decided to test again the best ligands at lower temperatures. When the reaction was performed at 40 °C (Table 2), the yield could be improved to a 46% when using **L15**, **L19** or **L20**, showing that the ligands without any substitutions in the positions next to the nitrogen atoms were efficient as well. As seen previously, the inclusion of electron-donating groups in the phenanthroline scaffold did not have a beneficial effect. (**L18/L15** or **L21/L15**)



Conditions: **1a** (0.20 mmol, 1 equiv),  $\text{NiCl}_2$  (10 mol%), ligand (10 mol%), Mn (0.40 mmol),  $\text{CO}_2$  (1 atm) in DMF (0.5 M) at 40 °C for 40 h. Yields determined by  $^1\text{H}$  NMR spectroscopy of the crude mixture using fluorene as internal standard.

**Table 2.** Phenanthroline type ligand screening.

After observing an improvement in the yield by lowering down the temperature and observing different *Z:E* ratios, we decided to test the effect of solvent and temperature. Choosing **L19** as the best ligand in terms of yield and selectivity, the use of polar non-protic amide solvents was tested. DMF and DMA gave similar results, whereas NMP resulted in a slightly better selectivity, albeit a reduced yield. Interestingly, performing the reaction at 30 °C increased the chemical yield to a 62% and the selectivity to a 9:1 favoring the *Z* isomer (Table 3).



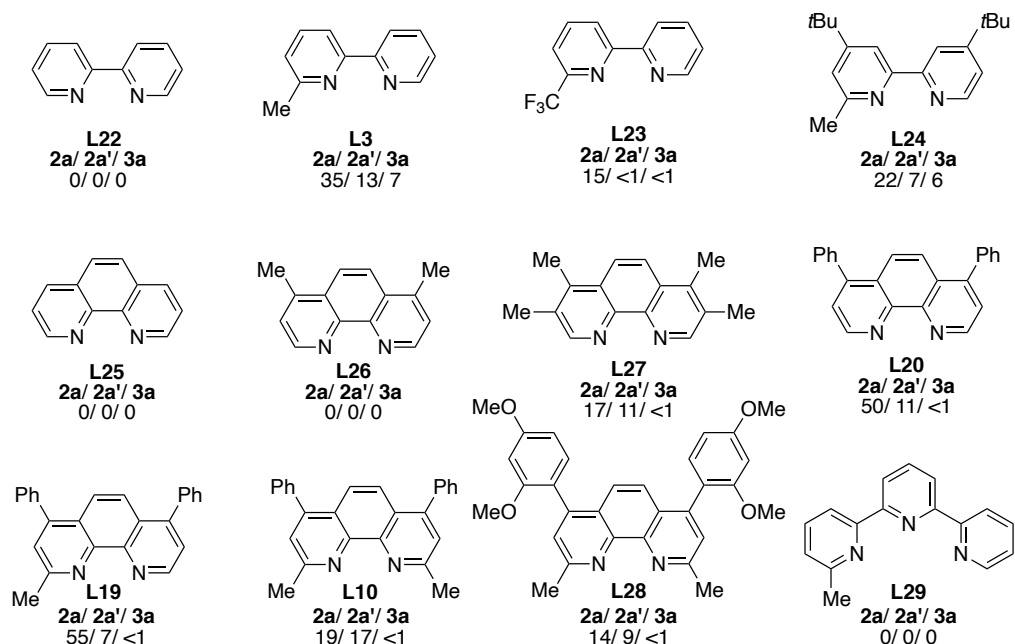
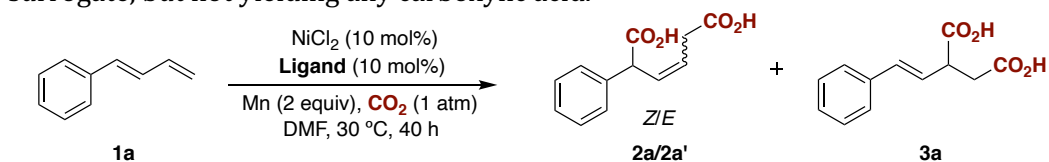
Deviation	Total Yield/ %	<i>Z:E</i> Selectivity
None	48	5:1
NMP	32	7:1
DMA	48	5:1
30 °C	62	9:1

## Nickel-catalyzed double carboxylation of 1,3-dienes with CO<sub>2</sub>

Conditions: **1a** (0.20 mmol, 1 equiv), NiCl<sub>2</sub> (10 mol%), **L19** (10 mol%), Mn (0.40 mmol), CO<sub>2</sub> (1 atm) in DMF (0.5 M) at 40 °C for 64 h. Yields and selectivity determined by <sup>1</sup>H NMR spectroscopy of the crude mixture using fluorene as internal standard.

**Table 3.** Screening of amide-based solvents.

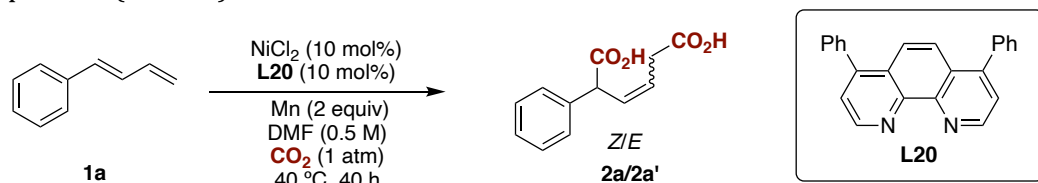
Before continuing the screening of other reaction parameters, we decided to test again bipyridine and phenanthroline ligands at lower temperatures (Table 4). Bipyridine ligands yielded a mixture of **2** and **3** as we observed in the first screening, whereas phenanthroline type ligands yielded product **2** exclusively. Unsubstituted phenanthroline did not yield the product efficiently (**L25**), unless phenyl groups were placed in the 4 and 7 position (**L20**). The inclusion of one methyl group (**L19**) resulted in a similar yield under these experimental conditions, whereas the inclusion of two methyl group proved to be again detrimental (**L10**). Lastly, methyl-substituted terpyridine ligand (**L29**) was tested as a disubstituted bipyridine surrogate, but not yielding any carboxylic acid.



Conditions: **1a** (0.20 mmol, 1 equiv), NiCl<sub>2</sub> (10 mol%), ligand (10 mol%), Mn (0.40 mmol), CO<sub>2</sub> (1 atm) in DMF (0.5 M) at 30 °C for 40 h. Yields determined by <sup>1</sup>H NMR spectroscopy of the crude mixture using fluorene as internal standard.

**Table 4.** Screening of ligands at 30 °C.

Seeing the similar results of **L19** and **L20**, we continued the screening with **L20**, since it is commercially available. As observed before, non-protic polar amide solvents were the best to achieve the carboxylation of 1,3-dienes. The use of manganese as a reducing agent was necessary, since other reducing agents as zinc, TDAE or MnCr alloys gave the product in low yields or did not give any carboxylation product (Table 5).



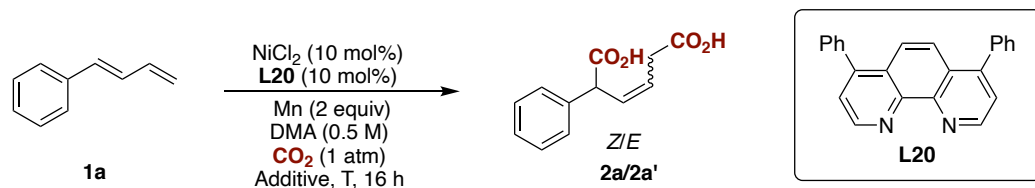
Entry	Deviation	Total Yield/ %	Z:E Selectivity
1	None	66	3:1
2	Zn instead of Mn	15	1.5:1
3	TDAE instead of Mn	0	-
4	MnCr alloy instead of Mn	0	-
5	DMA instead of DMF	70	6:1
6	THF instead of DMF	0	-
7	DMSO instead of DMF	31	2:1

Conditions: **1a** (0.20 mmol, 1 equiv),  $\text{NiCl}_2$  (10 mol%), **L20** (10 mol%), Mn (0.40 mmol),  $\text{CO}_2$  (1 atm) in DMF (0.5 M) at 40 °C for 40 h. Yields and selectivity determined by  $^1\text{H}$  NMR spectroscopy of the crude mixture using fluorene as internal standard.

**Table 5.** Reductants and solvent screening.

In all cases, the reactions were quite slow, requiring 40 h at least to achieve full conversion. In order to improve the catalytic system, different additives were tested to improve the reaction kinetics and see if the yields could be improved as well. First, different Lewis acids were tested, with the hypothesis that they could coordinate to a reaction intermediate (for example opening the nickelacycle and promoting the second  $\text{CO}_2$  incorporation). Many inorganic and organic Lewis acids were tested, obtaining in every case reaction inhibition or reduced yields (example of Lewis acid tested:  $\text{LiCl}$ ,  $\text{LiI}$ ,  $\text{MgCl}_2$ ,  $\text{MgBr}_2$ ,  $\text{CaCl}_2$ ,  $\text{AlCl}_3$ ,  $\text{Ti}(\text{O}i\text{Pr})_4$ ,  $\text{BF}_3(\text{OEt}_2)$ ). At the same time, it has been shown the beneficial effect of ammonium halide salts in carboxylation reactions in which an heterogeneous reducing agent is present,<sup>34</sup> so we decided to test them in our transformation. To evaluate the effect, we decided to screen them at low reaction times and temperatures ranging from 30 to 50 °C (Table 6). From the ammonium salts tested,  $n\text{Bu}_4\text{NBr}$  showed to be the best, improving the yield to 74% (even with just 20 mol%) or to 61% when the reaction was performed at 30 °C for 16 h.



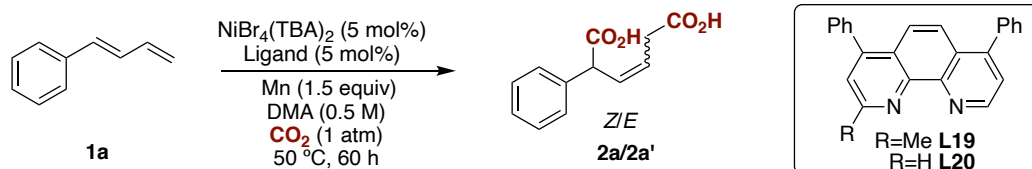
Nickel-catalyzed double carboxylation of 1,3-dienes with CO<sub>2</sub>


Entry	Temperature	Additive (1 equiv)	Total Yield/ %	Z:E Selectivity
1	30 °C	-	16	-
2	50 °C	-	70	3.7:1
3	50 °C	LiCl	68	2.4:1
4	50 °C	HexadecylMe <sub>3</sub> NBr	60	4.0:1
5	50 °C	<i>n</i> Bu <sub>4</sub> PBr	42	2.5:1
6	50 °C	<i>n</i> Pr <sub>4</sub> NBr	66	2.0:1
7	50 °C	<i>n</i> Et <sub>4</sub> NBr	62	2.9:1
8	50 °C	<i>n</i> Me <sub>4</sub> NBr	60	5.0:1
9	50 °C	<i>n</i> Bu <sub>4</sub> NBr	75	2.0:1
10	50 °C	<i>n</i> Bu <sub>4</sub> NBr (20 mol%)	74	2.0:1
11	30 °C	<i>n</i> Bu <sub>4</sub> NBr	61	5.0:1

Conditions: **1a** (0.20 mmol, 1 equiv), NiCl<sub>2</sub> (10 mol%), **L20** (10 mol%), Mn (0.40 mmol), CO<sub>2</sub> (1 atm) in DMA (0.5 M) for 14 h. Yields and selectivity determined by <sup>1</sup>H NMR spectroscopy of the crude mixture using fluorene as internal standard.

**Table 6.** Screening of halogen salts additives.

With the aim of lowering the catalyst loading to 5 mol%, we envisioned to prepare the nickel precatalyst NiBr<sub>4</sub>(TBA)<sub>2</sub>, which combined the nickel(II) salt and the ammonium salt that showed to increase the reactivity. This precatalyst resulted in a fine blue powder, with very low hygroscopic character which was ideal for its use on the bench. However, the use of lower catalyst loadings required raising the temperatures to 50 °C and extending the reaction times to 60 h. Under this conditions, ligand **L19** was tested again showing this time better yields than **L20**, reaching the 79% yield using only 5 mol% of nickel and ligand (Table 7).

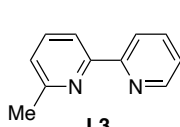
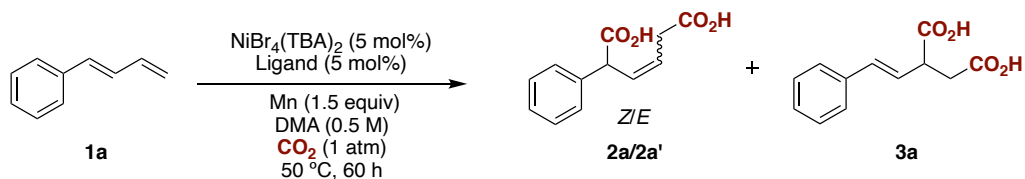


Entry	Deviation	Total yield /%	Z:E Selectivity
1	<b>L20</b>	56	6.0:1
2	<b>L19</b>	79	2.5:0
3	<b>L19, 30 °C</b>	<5	-
4	<b>L19, 40h</b>	47	2.0:1
5	<b>L19, 20h</b>	28	2.5:1

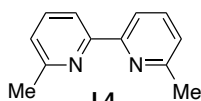
Conditions: **1a** (0.20 mmol, 1 equiv),  $\text{NiBr}_4(\text{TBA})_2$  (5 mol%), ligand (5 mol%), Mn (0.30 mmol),  $\text{CO}_2$  (1 atm) in DMA (0.5 M) at 50 °C for 60 h. Yields and selectivity determined by  $^1\text{H}$  NMR spectroscopy of the crude mixture using fluorene as internal standard.

**Table 7.** Comparison of temperature with **L19** and **L20**.

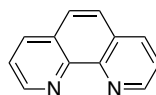
Once having the optimized conditions and before moving to test the substrate scope, ligands and reaction conditions were tested again (Table 8 and Table 9). Noteworthy is the need of halides in the nickel precatalyst or in the ammonium salt to observe the desired carboxylation, which might indicate an important role for the reaction success.

Nickel-catalyzed double carboxylation of 1,3-dienes with CO<sub>2</sub>


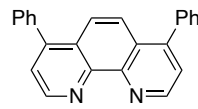
**2a/ 2a'/ 3a**  
33/ 13/ 6



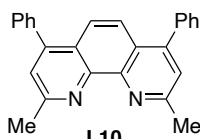
**2a/ 2a'/ 3a**  
20/ 10/ 6



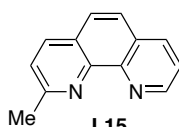
**2a/ 2a'/ 3a**  
3/ 1/ <1



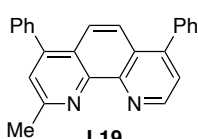
**2a/ 2a'/ 3a**  
42/ 14/ <1



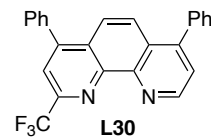
**2a/ 2a'/ 3a**  
22/ 11/ <1



**2a/ 2a'/ 3a**  
34/ 16/ <1



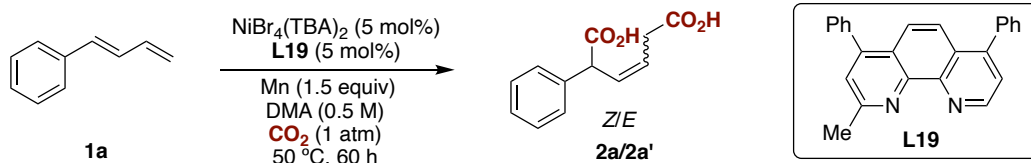
**2a/ 2a'/ 3a**  
56/ 23/ <1



**2a/ 2a'/ 3a**  
2/ 1/ <1

Conditions: **1a** (0.20 mmol, 1 equiv), NiBr<sub>4</sub>(TBA)<sub>2</sub> (5 mol%), ligand (5 mol%), Mn (0.3014 mmol), CO<sub>2</sub> (1 atm) in DMA (0.5 M) at 50 °C for 60 h. Yields and selectivity determined by <sup>1</sup>H NMR spectroscopy of the crude mixture using fluorene as internal standard.

**L20Table 8.** Re-screening of ligands with optimized reaction conditions.



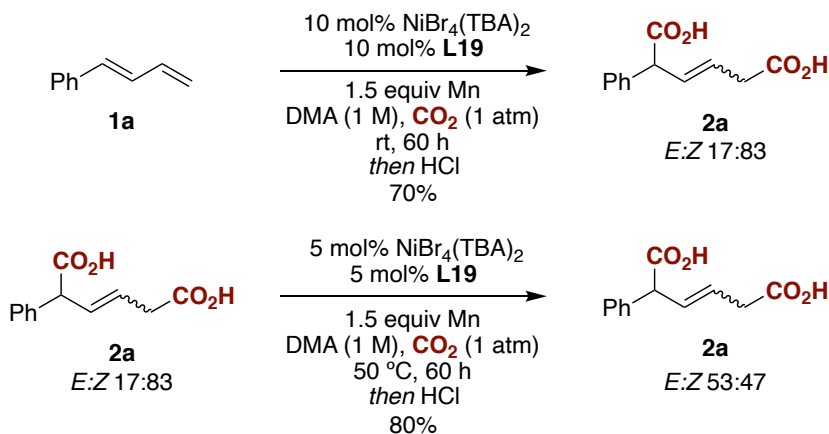
Entry	Deviation from standard conditions	Total yield	Z:E
		/%	Selectivity
1	None	79	2.4:1
2	5 mol% NiBr <sub>2</sub> ·dme	38	3.2:1
3	5 mol% NiBr <sub>2</sub> ·dme + 10 mol% TBABr	70	2.2:1
4	5 mol% Ni(COD) <sub>2</sub>	0	-
5	5 mol% Ni(COD) <sub>2</sub> + 10 mol% TBABr	60	1.4:1
6	30 °C	<5	-
7	10 mol% NiBr <sub>4</sub> (TBA) <sub>2</sub> at 30 °C	70	5.0:1
8	DMF as solvent	30	2.3:1
9	NMP as solvent	44	2.1:1
10	Zn instead of Mn	41	2.4:1

11	Me <sub>2</sub> Zn instead of Mn	0	-
12	No Ni, <b>L19</b> or Mn	0	-

Conditions: **1a** (0.20 mmol, 1 equiv), NiBr<sub>4</sub>(TBA)<sub>2</sub> (5.0 mol%), **L7** (5.0 mol%), Mn (0.30 mmol, 1.5 equiv), CO<sub>2</sub> (1 atm) in DMA (0.5 M) at 50 °C for 60 h. Determined by <sup>1</sup>H NMR of the crude mixture using fluorene as internal standard.

**Table 9.** Screening of precatalysts, solvents, reducing agents and blank experiments.

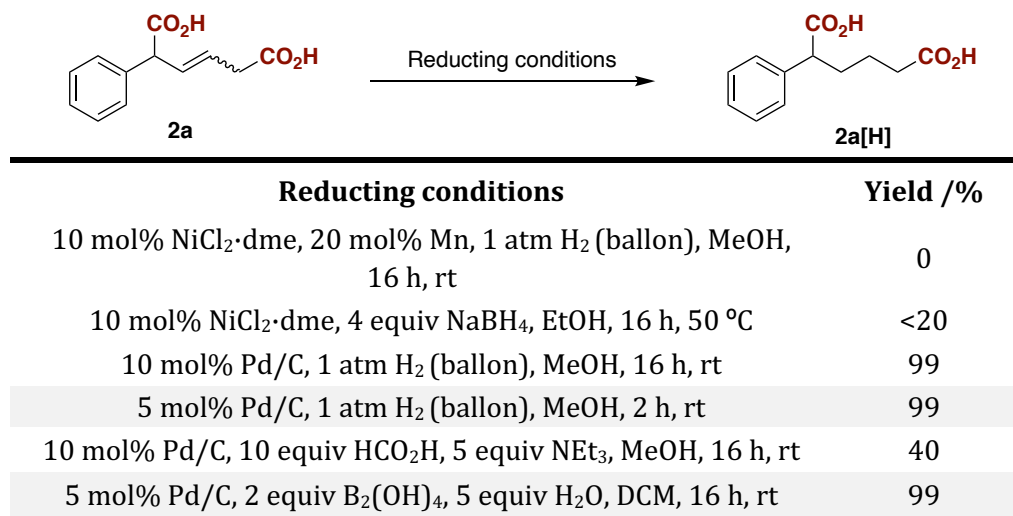
From the data shown in Table 9 it is worth to mention as well the different *Z:E* ratios observed in different reaction conditions. Whereas at 30 °C a ratio of 5:1 could be obtained, the maximum ratio obtained was 2.4:1 when NiBr<sub>4</sub>(TBA)<sub>2</sub> was used as a precatalyst at 50 °C. To have a better understanding of the reaction, we decided to study the isomerization of the obtained carboxylic acid under the reaction conditions (Scheme 11). When the product obtained with a 5:1 *Z:E* ratio was resubmitted to the reaction conditions at 50 °C, we could recover an 80% of the initial dicarboxylic acid as a nearly 1:1 *Z:E* mixture. It could suggest that the in-situ formed catalyst could promote the isomerization of the *Z* isomer into the *E* isomer, explaining that the longer reaction times, the higher temperatures or the higher catalyst loadings are used, the lower ratio of *Z:E* isomers is obtained.



**Scheme 11.** Isomerization of **2a** under the reaction condition.

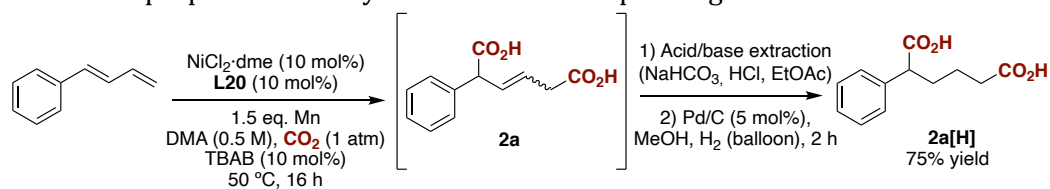
In parallel to these studies, we investigated the hydrogenation of the double bond to achieve the aliphatic 1,6-dicarboxylic acid, which can be seen as a substituted adipic acid (Table 10). These are building blocks used in industry and it could represent their obtention by combining 1,3-dienes and CO<sub>2</sub>, two abundant feedstocks. To do so first we tried different hydrogenations using nickel, with the aim of utilizing the metal already present in the catalytic dicarboxylation. The conditions either using H<sub>2</sub> or other reducing agents proved to be inefficient and we turned our attention to the use of Pd/C, a widely used heterogeneous catalyst for the hydrogenation of double bonds. The use of 5 mol% Pd/C in combination with H<sub>2</sub> or

B<sub>2</sub>(OH)<sub>4</sub>/H<sub>2</sub>O as a H<sub>2</sub> surrogate gave the desired substituted adipic acid **2a[H]** in a quantitative yield.



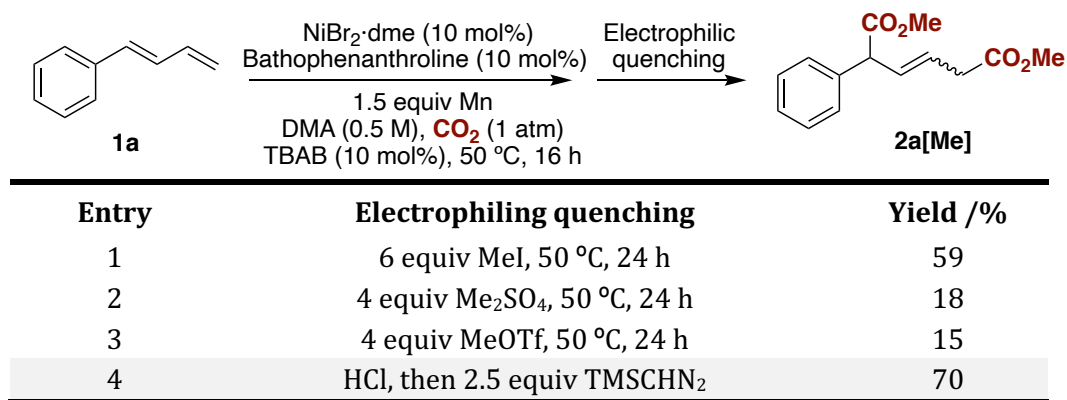
**Table 10.** Screening of reducing conditions.

With the optimized conditions, we proved that the carboxylation of 1,3-dienes could be coupled with the reduction of the double bond by simply acid/base extraction of the dicarboxylic acid followed by hydrogenation over Pd/C. However, the isolation and characterization of the free dicarboxylic acids turned out to be very difficult due to the high polarity of these molecules. To solve this problem, we decided to prepare the methyl ester of the corresponding acids.



**Scheme 12.** Carboxylation-reduction tandem reaction.

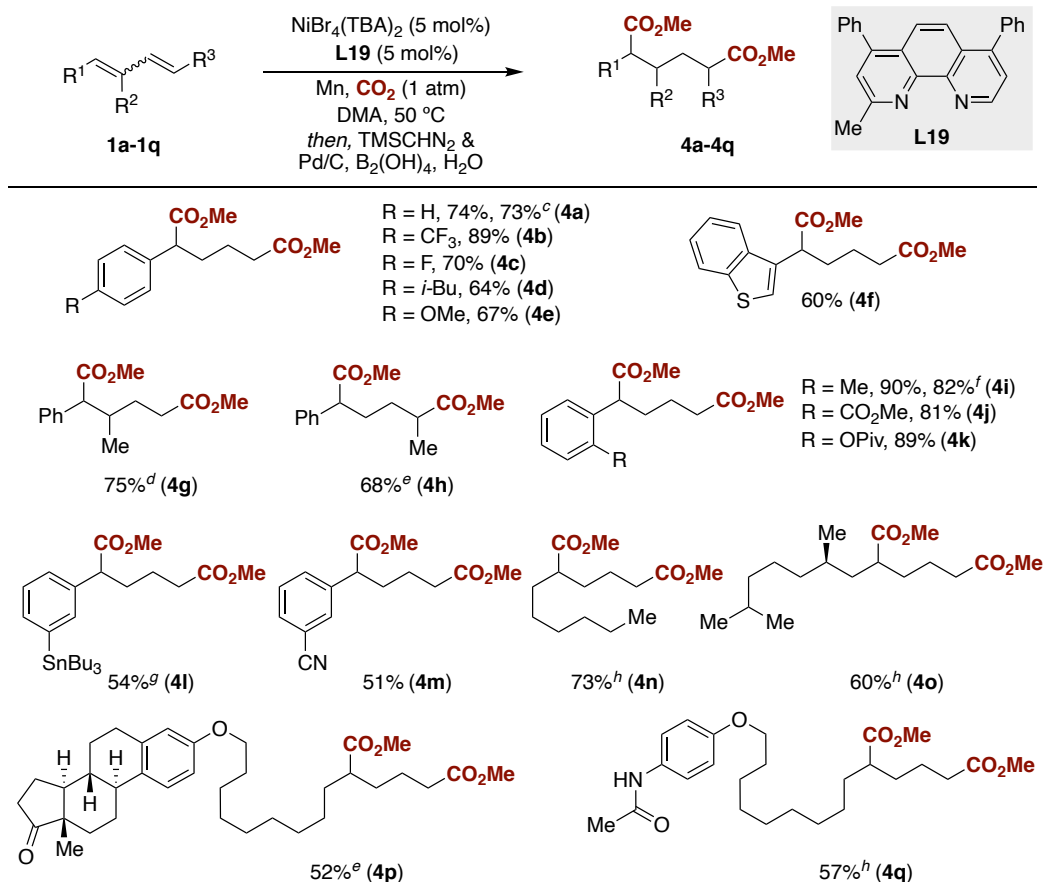
The esterification of the dicarboxylic acids was tested first by electrophilic quenching of the manganese carboxylates at the end of the reaction. Different alkylating reagents were used, obtaining the best yield when MeI was added and reacted for 24 h. However, full conversion was not achieved in any case and therefore we decided to do a standard quenching with HCl and then submit the crude samples to TMSCHN<sub>2</sub> esterification, to form the desired dimethyl ester nearly in quantitative yields.



**Table 11.** Screening of alkylating reagents.

### 3.2 Preparative substrate scope:

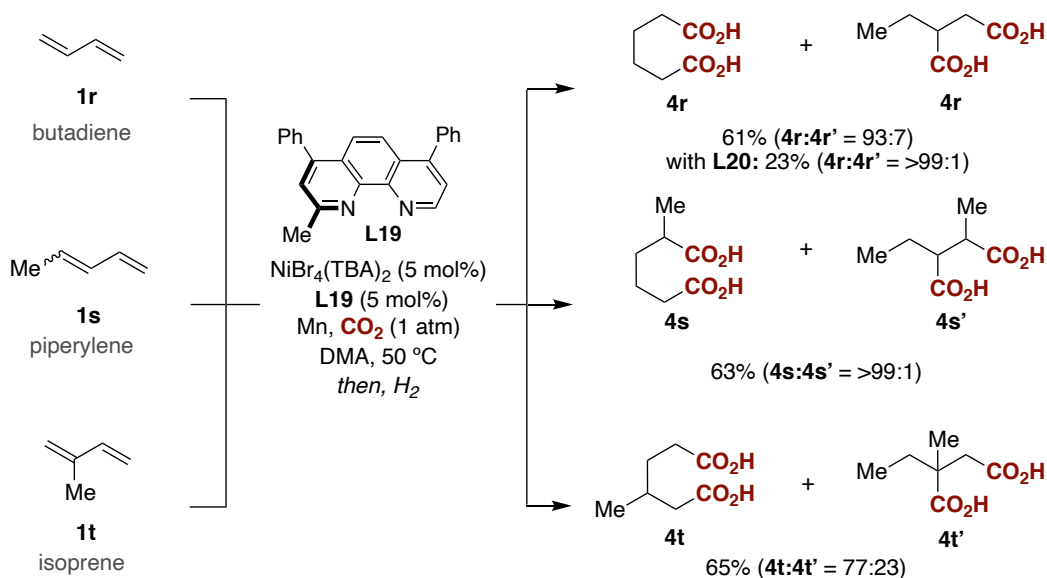
Once the reaction conditions for the carboxylation, the esterification and the hydrogenation reactions were optimized, we moved our attention into the substrate scope of the reaction. As expected, a host of 1,3-dienes substituted with either aliphatic (**1n-1q**) or aromatic backbones (**1a-1m**) reacted equally well. Changing the electronic properties of the aromatic diene by placing different substituents in the *para* position of the phenyl group had a small impact (**4a-4e**), obtaining better yields when electron withdrawing groups were present. The presence of *ortho*-substituents (**1i-1k**) did not have any deleterious effect, achieving the corresponding products in high yields. The site-selective incorporation of multiple CO<sub>2</sub> motifs into 1,3-dienes was accompanied by an excellent chemoselectivity, as esters (**4j**, **4k**), nitriles (**4m**), ketones (**4p**) or amides (**4q**) were well-tolerated. Interestingly, the presence of an organometallic reagent does not interfere with productive formation of **4l**, thus demonstrating the complementarity of our technique with classical nucleophilic/electrophilic regimes.<sup>35</sup> Likewise, the reaction could be applied in the presence of heterocyclic cores (**4f**). As illustrated by the successful preparation of **4g** and **4h**, the reaction could also be extended to disubstituted 1,3-dienes, albeit with lower diastereoselectivities. In the case of aliphatic 1,3-dienes (**4n-4q**), they showed to be slightly less reactive and a 10 mol% catalyst loading is needed to obtain full conversion of the starting materials.

Nickel-catalyzed double carboxylation of 1,3-dienes with CO<sub>2</sub>


<sup>a</sup> As Table 9 (entry 1), followed by exposure to TMSCHN<sub>2</sub> and Pd/C (5 mol%), B<sub>2</sub>(OH)<sub>4</sub> (2 equiv) and H<sub>2</sub>O (5 equiv) at rt. <sup>b</sup> Isolated yields, average of two independent runs, using 1,3-dienes as *E/Z* mixtures. <sup>c</sup> Using **E-1a**. <sup>d</sup> dr = 1.5:1. <sup>e</sup> dr = 1:1. <sup>f</sup> 1 mmol scale. <sup>g</sup> Using H<sub>2</sub> and Pd/C as reductant. <sup>h</sup> NiBr<sub>4</sub>(TBA)<sub>2</sub> (10 mol%) and **L19** (10 mol%).

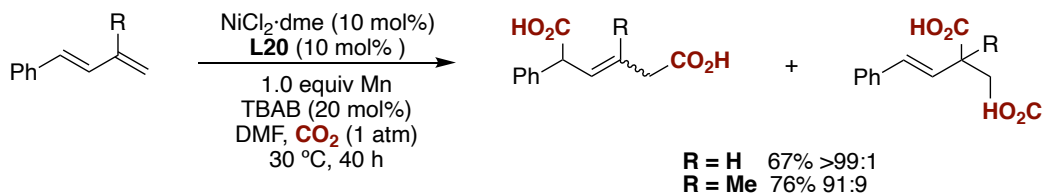
**Table 12.** 1,3-Diene substrate scope.

In light of these results, we wondered whether our protocol could be used for the valorization of butadiene, isoprene or piperylene, compounds that are obtained in bulk as byproducts of the steam cracking in the production of ethylene. As shown in Scheme 13, this turned out to be the case, and **4r-4t** were all obtained in good yields from the corresponding 1,3-diene feedstocks after a subsequent hydrogenolysis event. Strikingly, butadiene **1r** resulted in a 93:7 regioselectivity pattern whereas the presence of a methyl group in either **1s** or **1t** had a non-negligible effect on site-selectivity, with **1s** providing the best regiochemical discrimination (**4s**). Although the 1,4-ratio of **4r** and **4r'** could partially be improved by using **L20** in lieu of **L19**, significant lower yields were observed in this case.



**Scheme 13.** Carboxylation of butadiene, piperylene and isoprene.

Notably, the change of site-selectivity in isoprene (**1t**) is also observed in other 1,3-dienes in which a methyl group is placed in the 3-position of the diene (Scheme 14), obtaining in this case a 91:1 mixture of the 1,4 and 1,2-dicarboxylic acids with a global 76% yield. Taken all the data together, the results summarized in Table 12 and Scheme 13 stand as a prove to the potential of this catalytic technology for enabling a site-selective incorporation of multiple  $\text{CO}_2$  units into abundant 1,3-diene precursors.



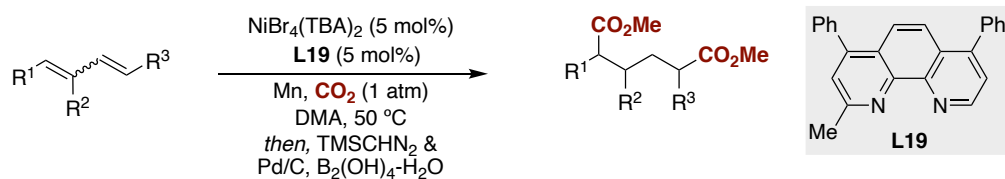
**Scheme 14.** 1,4 and 1,2 Site-selectivity.

It is worth noting that some 1,3-dienes did not react or gave the desired product in low yields. When dienes bearing coordinating groups such as thioethers, unprotected amines or pyridines were used, no carboxylic acid was detected, presumably by coordination of such groups to the nickel center. 1,3-Dienes with multiple substitution in C1 were unreactive, and more electron-rich methoxy-substituted 1,3-dienes, ethyl sorbate or 2,3-dibenzyl-1,3-butadiene did not give access to the targeted dicarboxylic acids. Finally, the presence of protected phenols, aromatic or aliphatic chlorides and *N*-tosyl amines delivered the dicarboxylic acids

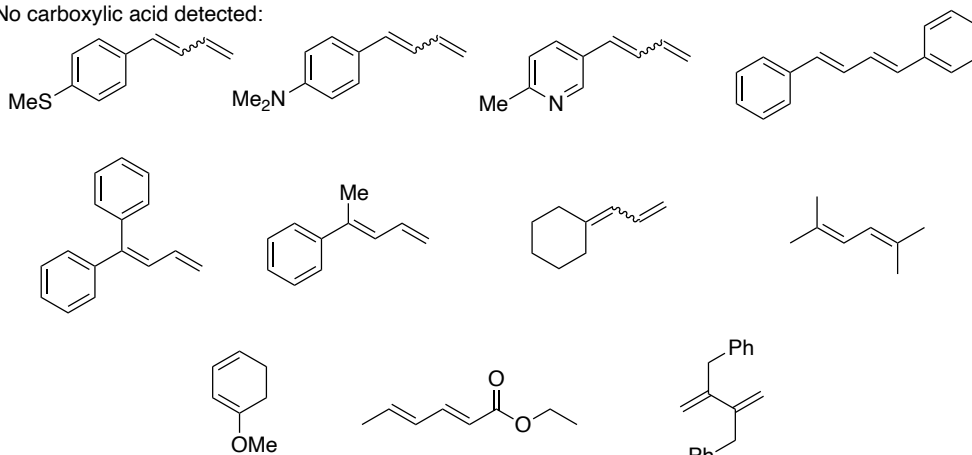


## Nickel-catalyzed double carboxylation of 1,3-dienes with CO<sub>2</sub>

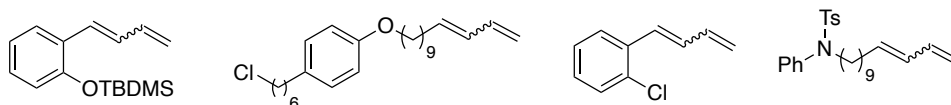
in low yields (< 30%), probably due to the deprotection of the silyl group, the oxidative addition of the organic chlorides to the nickel catalyst or the possible coordination of protected amines to the nickel center during catalysis.



No carboxylic acid detected:



Low yield of dicarboxylic acid detected:



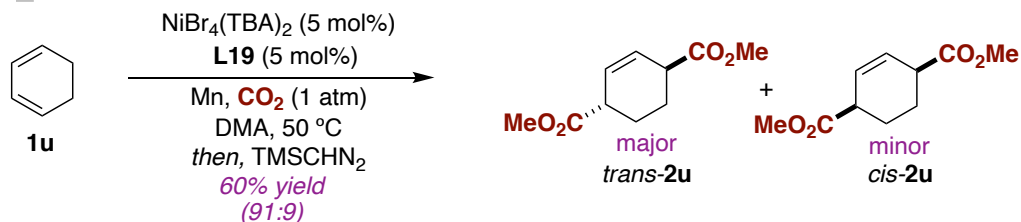
**Table 13.** Unsuccessful substrates.

#### 4. Mechanistic investigations.

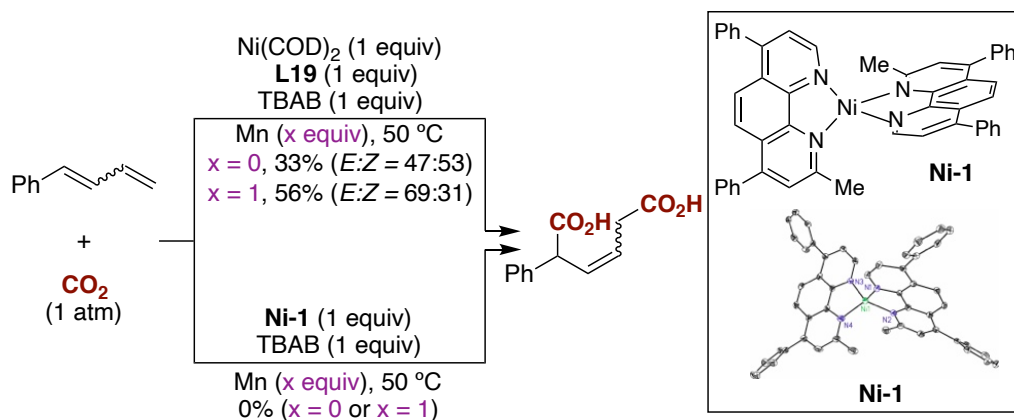
At this point, we decided to gather indirect evidence about the mechanism by studying the stereochemical course of **1u** with CO<sub>2</sub> (Scheme 15, *top*). Interestingly, *trans*-**2u** was preferentially formed over *cis*-**2u**, suggesting that the second CO<sub>2</sub> unit is inserted into the  $\pi$ -allyl complex **I** (Scheme 16) via formal backside attack. This seemingly trivial interpretation, however, does certainly not rule out a rapid interconversion of the putative  $\pi$ -allyl nickel complexes upon exposure to Ni(0)(**L19**) prior to CO<sub>2</sub> insertion.<sup>36</sup> To further explore the mechanistic details of the reaction, we turned our attention to study the reactivity of **Ni-1** (Scheme 15, *middle*). This complex was easily prepared by exposure of **L19** and Ni(COD)<sub>2</sub> in benzene at 40 °C, the structure of which was univocally determined by X-ray crystallography. Interestingly, the reactivity of **Ni-1** with **1a** was not comparable to that observed with Ni(COD)<sub>2</sub>/**L19**, with not even traces of **2a** being observed in the former. While one might attribute this finding to the non-innocent role of COD,<sup>37</sup> the reluctance of coordinatively saturated **Ni-1** to dissociate **L19** prior to 1,3-diene binding could be another possibility. Unfortunately, the preparation of  $\pi$ -allyl complex in pure analytical form bearing **L19** as ligand proved to be particularly elusive. Then we tried the synthesis of analogue  $\pi$ -allyl complexes with phosphine ligands, but the reaction of Ni(COD)<sub>2</sub> with either triphenylphosphine or tricyclohexylphosphine in a CO<sub>2</sub> atmosphere proved to be unsuccessful as well. Gratifyingly, we could prepare structurally related  $\pi$ -allyl complexes with tricyclohexylphosphine, **Ni-2** (Scheme 15, *bottom*), starting from 2,4-pentadienoic acid via a hydrogen migration,<sup>38</sup> and the  $\eta^3$ -hapticity of the allyl motif was revealed by X-ray structure analysis. Interestingly, we found that **Ni-2** only furnished **2a** in the presence of both **L19** and Mn. This result might point towards the formation of a Ni(I) intermediates via single electron transfer processes. To study this possibility, the reaction was performed with the addition of different radical scavengers (Table 14). The addition of TEMPO inhibited the reaction, whereas the addition of BHT and 1,1-diphenylethylene lowered the reaction yield and conversion. Analysis of the reaction crudes by GC-MS or <sup>1</sup>H NMR spectroscopy did not reveal the formation of any adduct with the radical scavengers, which does not allow us to confirm or rule out the intermediacy of radical species.

## Nickel-catalyzed double carboxylation of 1,3-dienes with CO<sub>2</sub>

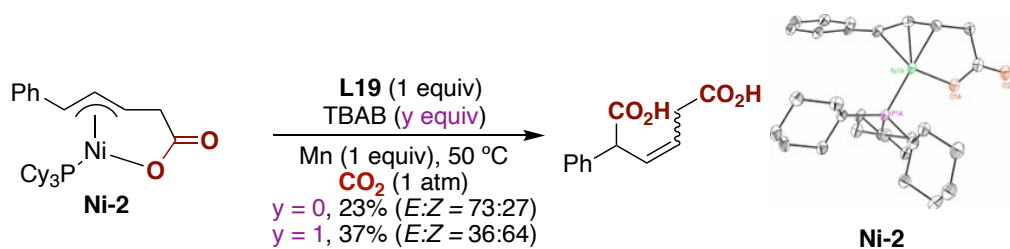
### stereochemical course of the dicarboxylation event



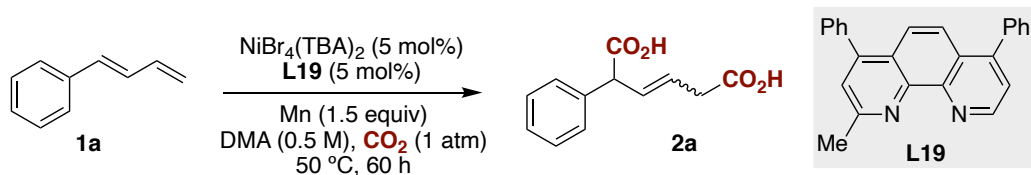
### stoichiometric studies with Ni(0)(L19)<sub>n</sub>



### stoichiometric studies with Ni-2



**Scheme 15.** Stoichiometric studies.

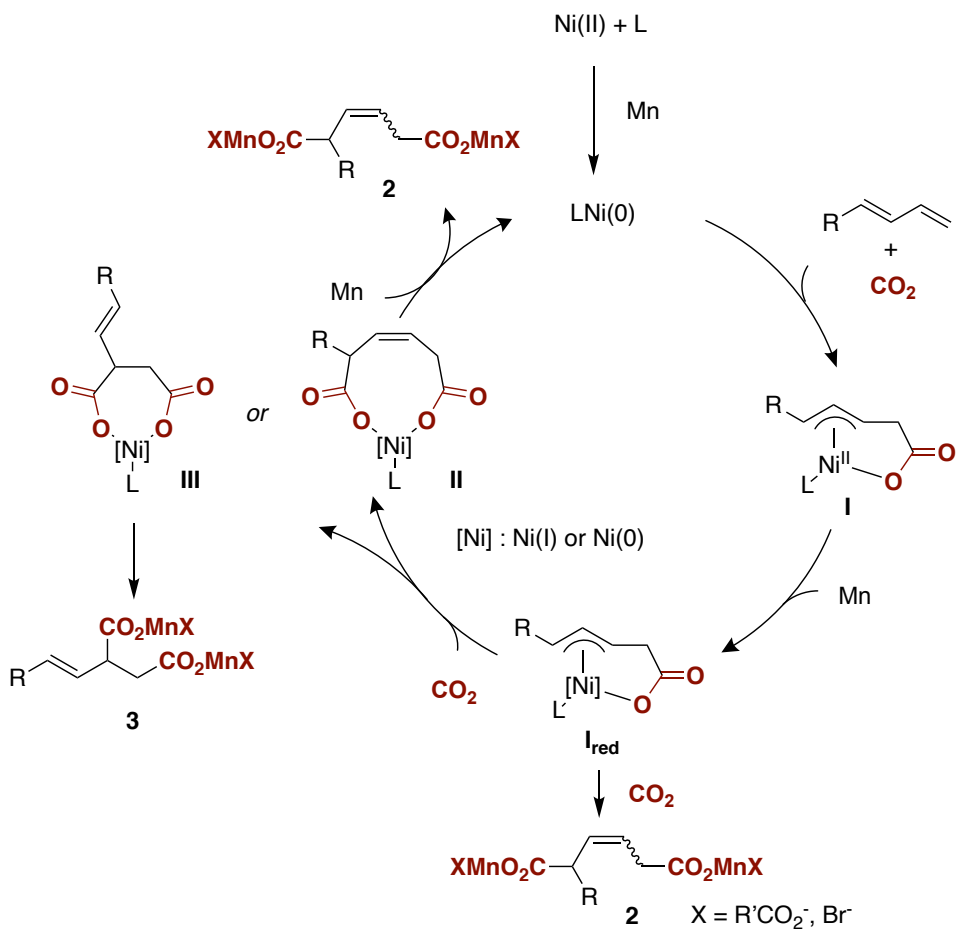


Entry	Additive (1 equiv)	Conv /%	Yield /%	Z:E ratio
1	None	100	59	2.4
2	TEMPO	5	18	-
3	BHT	81	15	3.0
4	1,1-Diphenylethylene	70	70	2.3

**Table 14.** Addition of different radical scavengers.

With all the gathered data, we propose a catalytic scenario based on an initial reduction of the nickel(II) salt to form the ligand ligated nickel(0) complex, which reacts with  $\text{CO}_2$  and the 1,3-diene in an oxidative cyclization to form the  $\pi$ -allyl carboxylate **I**. This intermediate might react with manganese by promoting a single-electron transfer, setting the stage for a subsequent insertion of a second molecule of  $\text{CO}_2$  to form **II**, **III** or a mixture of both depending on the supporting ligand. These intermediates might either trigger a subsequent single-electron transfer or a salt metathesis to form the manganese carboxylates and regenerate the propagating nickel(0) species. Alternatively, the experiments performed on cyclohexadiene (Scheme 15, *top*) might point towards the direct addition of  $\text{CO}_2$  into the  $\pi$ -allyl moiety instead of a second insertion of  $\text{CO}_2$  into the C–Ni bond. However, cyclic systems might have a different reactivity to linear substrates and therefore further experiments and/or in silico calculations might be necessary to shed light into the catalytic cycle.

Nickel-catalyzed double carboxylation of 1,3-dienes with CO<sub>2</sub>



**Scheme 16.** Mechanistic proposal for the dicarboxylation of 1,3-dienes.

## 5. Conclusions

A site-selective, catalytic incorporation of *multiple* CO<sub>2</sub> molecules into abundant 1,3-dienes have been described, thus giving access to adipic acids from simple and available precursors. Remarkably, simple butadiene, isoprene and piperylene were combined with CO<sub>2</sub> to form the corresponding dicarboxylic acids, which represent the combination of two feedstock materials to obtain products of industrial interest. The salient features of this method are its excellent regio- and chemoselectivity, mild conditions and ease of execution.

The mechanistic experiments suggest a Ni(0)/Ni(I)/Ni(II) catalytic cycle, in which a first oxidative cyclization form a Ni(II) allyl carboxylate that needs to be further reduced to Ni(I) or Ni(0) for the second addition of carbon dioxide to occur. Additional experiments, however, need to be conducted to confirm these observations, probably by DFT calculations.

Further extensions to other hydrocarbons, including asymmetric transformations, would represent the expansion of this methodology to more industrial relevant motifs, achieving carboxylic acids from 2 feedstock materials: CO<sub>2</sub> and olefins. The ability to control the regioselectivity of the transformation (1,4 or 1,2 dicarboxylation) by means of ligand modification would result in an attractive way to access dicarboxylic acids. Moreover, the use of different electrophiles other than CO<sub>2</sub> might allow to implement new pathways to valorize diene feedstocks and the conversion of these motifs into valuable chemicals.

## 6. Experimental section.

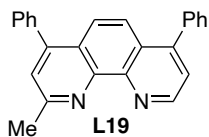
**Reagents.** All reactions were conducted in Schlenk tubes. Commercially available materials were used without further purification. Butadiene (**4**), piperylene (**5**) and isoprene (**7**) were purchased from commercial sources and used as received. Anhydrous *N,N*-dimethylacetamide (DMA), 1-methyl-2-pyrrolidinone (NMP), and *N,N*-dimethylformamide, (DMF) were purchased from Acros Organics (NOTE: *it is critical to have appropriately dried solvents to obtain reproducible results*, as old batches of these solvents provided variable results). Mn powder (99.99% trace metal basis), NiBr<sub>2</sub>·dme (97% purity) were purchased from Aldrich. Ni(COD)<sub>2</sub> was purchased from Strem. NiBr<sub>4</sub>(TBA)<sub>2</sub> was prepared according to a literature procedure.<sup>39</sup> All other reagents were purchased from commercial sources and used as received.

**Analytical methods.** <sup>1</sup>H NMR and <sup>13</sup>C NMR spectra are included for all compounds. <sup>1</sup>H and <sup>13</sup>C NMR spectra were recorded on a Bruker 300 MHz, a Bruker 400 MHz and a Bruker 500 MHz at 20 °C. All <sup>1</sup>H NMR spectra are reported in parts per million (ppm) downfield of TMS and were measured relative to the signals for CHCl<sub>3</sub> (7.26 ppm), acetone-*d*<sub>5</sub> (2.05 ppm) or benzene-*d*<sub>5</sub> (7.16 ppm). All <sup>13</sup>C NMR spectra were reported in ppm relative to CDCl<sub>3</sub> (77.2 ppm), acetone-*d*<sub>6</sub> (29.8 ppm) or benzene-*d*<sub>6</sub> (128.1 ppm) and were obtained with <sup>1</sup>H decoupling. Coupling constants, *J*, are reported in hertz. Melting points were measured using open glass capillaries in a Büchi B540 apparatus. Infrared spectra were recorded on a Bruker Tensor 27. Mass spectra were recorded on a Waters LCT Premier spectrometer. Flash chromatography was performed with EM Science silica gel 60 (230-400 mesh) and using bromocresol, potassium permanganate, or cerium molybdate as TLC stains.

### Optimization of the reaction conditions

**General procedure for the optimization of **1a** with CO<sub>2</sub>:** An oven-dried schlenk tube containing a stirring bar was charged with the corresponding reducing agent, ligand and nickel source. The schlenk tube was then evacuated and back-filled under a CO<sub>2</sub> flow (this sequence was repeated three times). Under atmospheric pressure of CO<sub>2</sub>, **1a** (0.20 mmol) and solvent were subsequently added by syringe and the solution was warmed up to 50 °C. The mixture was then carefully quenched with 2 M HCl, and 1 equivalent of fluorene was added. The crude was extracted with EtOAc, and a sample of such solution was analyzed by <sup>1</sup>H NMR. When required, **2a** was purified by conventional flash chromatography in silica gel using hexanes/EtOAc/HCO<sub>2</sub>H 70/30/0.5.

### Synthesis of the starting materials and L19



**2-methyl-4,7-diphenyl-1,10-phenanthroline (L19).** To a solution of **L20** (1.00 g, 3.0 mmol) in toluene (20 mL) at 0 °C under argon a few drops of MeLi were added until the reaction turned red. Then, 1 equiv of MeLi (1.88 mL, 1.6 M in Et<sub>2</sub>O) was added dropwise and the solution was stirred for 60 minutes at room temperature. The reaction was quenched with water and it was extracted with dichloromethane. The organic phases were collected, washed with brine and dried over magnesium sulfate. The solution was filtered and 3 equivalents of MnO<sub>2</sub> were added. The reaction was stirred for two hours at rt. Then, silica gel was directly added to the flask, the solvent was evaporated under reduced pressure and it was purified by column chromatography with silica gel (DCM:MeOH 99:1 to 98:2). 982 mg, 94% yield. Light orange solid.

**Mp:** 165-167 °C.

**<sup>1</sup>H NMR** (500 MHz, CDCl<sub>3</sub>) δ 9.25 (d, *J* = 4.5 Hz, 1H), 7.81 (d, *J* = 9.4 Hz, 1H), 7.78 (d, *J* = 9.4 Hz, 1H), 7.55 (d, *J* = 4.5 Hz, 1H), 7.54 – 7.44 (m, 11H), 3.01 (s, 3H) ppm.

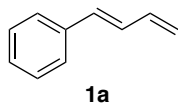
**<sup>13</sup>C NMR** (126 MHz, CDCl<sub>3</sub>) δ 159.1, 149.9, 148.7, 148.5, 138.3, 129.9, 129.8, 128.8, 128.7, 128.6, 128.5, 124.7, 124.3, 124.2, 123.4, 123.1, 26.1 ppm.

**IR** (neat, cm<sup>-1</sup>): 3056, 3028, 2939, 1561, 1547, 1487, 1436, 1378, 739, 701.

**HRMS** ESI, (C<sub>25</sub>H<sub>19</sub>N<sub>2</sub>) [M+H]<sup>+</sup> *calculated* 347.1543, *found* 347.1533

### Representative procedure for preparing 1,3-dienes via Wittig olefination:

**General procedure A:** A suspension of allyltriphenylphosphonium bromide (2.4 mmol) in 15 mL of THF under inert atmosphere was cooled at 0 °C with an ice bath. Then, *n*-BuLi (2.4 mmol, 0.96 mL, 2.5 M in hexanes) was added dropwise. The reaction was stirred for 40 minutes at 0 °C and then the corresponding aldehyde (2 mmol dissolved in 5 mL of THF) was added dropwise. The reaction was stirred for 12 hours at room temperature. After this time, it was quenched with a saturated aqueous solution of ammonium chloride and extracted with Et<sub>2</sub>O. The organic phases were collected, washed with brine and dried over magnesium sulfate. The solvent was removed under reduced pressure and the crude product was purified by flash column chromatography (hexanes:Et<sub>2</sub>O mixtures) on silica gel.



**(E)-buta-1,3-dien-1-ylbenzene (1a).** Following the general procedure A, but using methyltriphenylphosphonium bromide (6.86 g, 19.2 mmol), *E*-cinnamyl aldehyde (2.0 mL, 16 mmol) to give

**1a** (1.90 g, 90% yield). Colorless liquid.

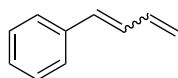
**<sup>1</sup>H NMR** (400 MHz, CDCl<sub>3</sub>) δ 7.45 – 7.41 (m, 2H), 7.37 – 7.31 (m, 2H), 7.28 – 7.22 (m, 1H), 6.82 (ddt, *J* = 15.5, 10.5, 0.8 Hz, 1H), 6.59 (d, *J* = 15.7 Hz, 1H), 6.54 (dt, *J* = 16.8,



10.4 Hz, 1H) 5.36 (ddd,  $J = 16.9, 1.6, 0.7$  Hz, 1H), 5.20 (ddd,  $J = 10.7, 1.5, 0.7$  Hz, 1H) ppm.

<sup>13</sup>C NMR (101 MHz, CDCl<sub>3</sub>)  $\delta$  137.4, 137.3, 133.0, 129.8, 128.7, 127.8, 126.6, 117.7 ppm.

Spectral data is in agreement with the literature.<sup>40</sup>

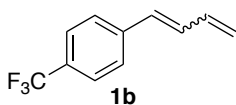


**(*E,Z*)-buta-1,3-dien-1-ylbenzene (1a')**. Following the general procedure A, benzaldehyde (0.10 mL, 1.4 mmol) was used, affording **1a'** (70 mg, 60% yield) as a mixture of isomers ( $E:Z = 1.2:1$ ).

Colorless liquid.

<sup>1</sup>H NMR (400 MHz, CDCl<sub>3</sub>)  $\delta$  7.46 – 7.19 (m, 5H), 6.89 (dddd,  $J = 16.9, 11.2, 10.1, 1.1$  Hz, 1H, *Z* isomer), 6.82 (ddt,  $J = 15.5, 10.5, 0.8$  Hz, 1H, *E* isomer), 6.59 (d,  $J = 15.7$  Hz, 1H, *E* isomer), 6.54 (dt,  $J = 16.8, 10.4$  Hz, 1H, *E* isomer), 6.47 (d,  $J = 10.0$ , 1H, *Z* isomer), 6.27 (t,  $J = 10.5$ , 1H, *Z* isomer), 5.38 (d,  $J = 16.9$ , 1H, *Z* isomer), 5.36 (ddd,  $J = 16.9, 1.6, 0.7$  Hz, 1H, *E* isomer), 5.23 (dt,  $J = 10.1, 1.1$  Hz, 1H, *Z* isomer), 5.20 (ddd,  $J = 10.7, 1.5, 0.7$  Hz, 1H, *E* isomer) ppm.

Spectral data is in agreement with the literature.<sup>40</sup>



**(*E,Z*)-1-(buta-1,3-dien-1-yl)-4-(trifluoromethyl)benzene (1b)**. Following the general procedure A using 4-trifluoromethylbenzaldehyde (348.2 mg, 2 mmol), affording

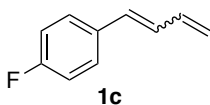
**1b** (237.7 mg, 60% yield) as a mixture of isomers ( $E:Z = 1:2$ ). Yellow liquid.

<sup>1</sup>H NMR (400 MHz, CDCl<sub>3</sub>)  $\delta$  7.59 (d,  $J = 8.2$  Hz, 2H, *Z* isomer), 7.57 (d,  $J = 8.8$  Hz, 2H, *E* isomer), 7.49 (d,  $J = 8.5$  Hz, 2H, *E* isomer), 7.41 (d,  $J = 8.5$  Hz, 2H, *Z* isomer), 6.89–6.76 (m, 1H), 6.58 (d,  $J = 15.7$  Hz, 1H, *E* isomer), 6.52 (dt,  $J = 16.9, 9.9$  Hz, 1H, *E* isomer), 6.47 (d,  $J = 11.6$  Hz, 1H, *Z* isomer), 6.35 (t,  $J = 11.4$  Hz, 1H, *Z* isomer), 5.44 (ddt,  $J = 16.8, 1.7, 0.8$  Hz, 1H, *Z* isomer), 5.41 (d,  $J = 16.9$  Hz, 1H, *E* isomer), 5.32 (dtd,  $J = 10.2, 1.6, 0.9$  Hz, 1H, *Z* isomer), 5.27 (m, 1H, *E* isomer) ppm.

<sup>13</sup>C NMR (101 MHz, CDCl<sub>3</sub>)  $\delta$  141.0 (*Z* isomer), 140.8 (*E* isomer), 136.8 (*E* isomer), 132.7 (*Z* isomer), 132.6 (*Z* isomer), 132.1 (*E* isomer), 131.4 (*E* isomer), 129.4 (*E* isomer), 129.3 (*Z* isomer), 128.9 (*E* isomer), 126.6 (*Z* isomer), 125.7 (q,  $J = 3.9$  Hz, *E* isomer), 125.3 (q,  $J = 3.9$  Hz, *Z* isomer), 124.3 (q,  $J = 272.9$  Hz, *Z* isomer), 123.0 (*E* isomer), 121.3 (*Z* isomer), 119.5 (*Z* isomer) ppm.

<sup>19</sup>F NMR (376 MHz, CDCl<sub>3</sub>)  $\delta$  -62.6 ppm.

Spectral data is in agreement with the literature.<sup>12</sup>



**(*E,Z*)-1-(buta-1,3-dien-1-yl)-4-fluorobenzene (1c)**.

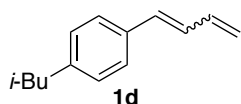
Following the general procedure A using 4-fluorobenzaldehyde (0.54 mL, 5 mmol), affording **1c** (585 mg, 79% yield) as a mixture of isomers ( $E:Z = 1:1.5$ ). Yellow liquid.

**<sup>1</sup>H NMR** (400 MHz, CDCl<sub>3</sub>) δ 7.44 – 7.36 (m, 2H, *E* isomer), 7.31 (dddd, *J* = 8.6, 5.4, 2.7, 1.6 Hz, 2H, *Z* isomer), 7.12 – 6.99 (m, 2H), 6.85 (dddd, *J* = 16.8, 11.2, 10.1, 1.1 Hz, 1H, *Z* isomer), 6.78 – 6.68 (m, 1H, *E* isomer), 6.55 (d, *J* = 15.6 Hz, 1H, *E* isomer), 6.52 (dt, *J* = 16.9, 10.3 Hz, 1H, *E* isomer), 6.44 (d, *J* = 11.5 Hz, 1H, *Z* isomer), 6.28 (t, *J* = 11.3 Hz, 1H, *Z* isomer), 5.41 (dd, *J* = 16.9, 1.8, 1H, *Z* isomer), 5.38 – 5.32 (m, 1H), 5.20 (dd, *J* = 9.6, 1.2 Hz, 1H, *E* isomer) ppm.

**<sup>13</sup>C NMR** (101 MHz, CDCl<sub>3</sub>) δ 162.3 (d, *J* = 248.2 Hz, *E* isomer), 162.0 (d, *J* = 247.6 Hz, *Z* isomer), 137.1 (*E* isomer), 133.6 (d, *J* = 3.5 Hz, *E* isomer), 133.5 (d, *J* = 3.5 Hz, *Z* isomer), 133.0 (*Z* isomer), 131.7 (*E* isomer), 130.9 (d, *J* = 1.3 Hz, *Z* isomer), 130.7 (d, *J* = 7.9 Hz, *Z* isomer), 129.5 (d, *J* = 2.5 Hz, *E* isomer), 129.3 (*Z* isomer), 128.1 (d, *J* = 8.0 Hz, *E* isomer), 120.0 (*Z* isomer), 117.8 (*E* isomer), 115.7 (d, *J* = 21.6 Hz, *E* isomer), 115.3 (d, *J* = 21.5 Hz, *Z* isomer) ppm.

**<sup>19</sup>F NMR** (376 MHz, CDCl<sub>3</sub>) δ -114.3 (*E* isomer), -115.0 (*Z* isomer) ppm.

Spectral data is in agreement with the literature.<sup>40</sup>



**(*E,Z*)-1-(buta-1,3-dien-1-yl)-4-isobutylbenzene (1d).**

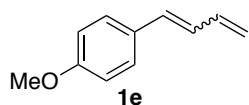
Following the general procedure A using 4-isobutylbenzaldehyde (1.7 mL, 2 mmol), affording **1d** (1.18 g, 63% yield) as a mixture of isomers (*E:Z* = 1:4). Colourless liquid.

**<sup>1</sup>H NMR** (400 MHz, CDCl<sub>3</sub>) δ 7.35 (d, *J* = 8.1 Hz, 2H, *E* isomer), 7.28 (d, *J* = 7.5 Hz, 1H, *Z* isomer), 7.15 (d, *J* = 8.2 Hz, 2H, *Z* isomer), 7.13 (d, *J* = 8.6 Hz, 2H, *E* isomer), 6.96 (dddd, *J* = 16.9, 11.2, 10.1, 1.1 Hz, 1H, *Z* isomer), 6.78 (ddt, *J* = 16.5, 10.5, 0.8 Hz, 1H, *E* isomer), 6.58 (d, *J* = 15.6 Hz, 1H, *E* isomer), 6.54 (dt, *J* = 16.8, 6.6 Hz, 1H, *E* isomer), 6.47 (d, *J* = 11.4 Hz, 1H, *Z* isomer), 6.26 (tt, *J* = 11.4, 0.9 Hz, 1H, *Z* isomer), 5.39 (ddt, *J* = 16.9, 1.9, 0.9 Hz, 1H, *Z* isomer), 5.34 (d, *J* = 16.0 Hz, 1H, *E* isomer), 5.24 (d, *J* = 10.1, 1H, *Z* isomer), 5.18 (ddd, *J* = 10.2, 1.7, 0.9 Hz, 1H, *E* isomer), 2.51 (d, *J* = 7.2 Hz, 2H, *Z* isomer), 2.49 (d, *J* = 7.2 Hz, 2H, *E* isomer), 1.96 – 1.86 (m, 1H), 0.95 (d, *J* = 6.6 Hz, 6H, *Z* isomer) 0.94 (d, *J* = 6.6 Hz, 6H, *E* isomer) ppm.

**<sup>13</sup>C NMR** (101 MHz, CDCl<sub>3</sub>) δ 141.6 (*E* isomer), 140.9 (*Z* isomer), 137.5 (*E* isomer), 134.9 (*Z* isomer), 134.8 (*E* isomer), 133.6 (*Z* isomer), 133.0 (*E* isomer), 130.6 (*Z* isomer), 130.3 (*Z* isomer), 129.5 (*Z* isomer), 129.1 (*E* isomer), 128.9 (*Z* isomer), 128.8 (*E* isomer), 126.4 (*E* isomer), 119.3 (*Z* isomer), 117.1 (*E* isomer), 45.3 (*E* isomer), 30.4 (*E* isomer), 30.3 (*Z* isomer), 22.5 (*Z* isomer), 22.4 (*E* isomer) ppm.

**IR** (neat, cm<sup>-1</sup>): 3084, 3020, 2954, 2922, 2868, 1509, 1465, 1002, 902, 854, 545, 497.

**HRMS** APCI, (C<sub>14</sub>H<sub>19</sub>) [M+H]<sup>+</sup> *calculated* 187.1481, *found* 187.1475.



**(*E,Z*)-1-(buta-1,3-dien-1-yl)-4-methoxybenzene (1e).**

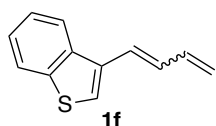
Following the general procedure A using 4-

methoxybenzaldehyde (0.43 mL, 2 mmol), affording **1e** (674 mg, 84% yield) as a mixture of isomers (*E:Z* = 1:1.7). Yellow liquid.

**<sup>1</sup>H NMR** (500 MHz, CDCl<sub>3</sub>) δ 7.35 (d, *J* = 8.7 Hz, 2H, *E* isomer), 7.27 (d, *J* = 8.5 Hz, 2H, *Z* isomer), 6.88 (d, *J* = 8.8 Hz, 2H, *Z* isomer), 6.86 (d, *J* = 8.7 Hz, 2H, *E* isomer), 6.52 (d, *J* = 15.7 Hz, 1H, *E* isomer), 6.49 (dt, *J* = 16.8, 10.3 Hz, 1H, *E* isomer), 6.40 (d, *J* = 11.5 Hz, 1H, *Z* isomer), 5.35 (ddt, *J* = 16.9, 1.8, 0.8 Hz, 1H, *Z* isomer), 5.28 (dd, *J* = 16.0, 0.8 Hz, 1H, *E* isomer), 5.20 (dddd, *J* = 10.2, 2.1, 1.4, 0.9 Hz, 1H, *Z* isomer), 5.12 (d, *J* = 9.3 Hz, 1H, *E* isomer), 3.82 (s, 3H, *E* isomer), 3.82 (s, 3H, *Z* isomer) ppm.

**<sup>13</sup>C NMR** (126 MHz, CDCl<sub>3</sub>) δ 159.4 (*E* isomer), 158.8 (*Z* isomer), 137.5 (*E* isomer), 133.5 (*Z* isomer), 132.5 (*E* isomer), 130.4 (*Z* isomer), 130.3 (*Z* isomer), 130.2 (*Z* isomer), 130.1 (*E* isomer), 129.5 (*Z* isomer), 119.1 (*Z* isomer), 127.9 (*E* isomer), 127.8 (*E* isomer), 116.6 (*E* isomer), 114.2 (*E* isomer), 113.8 (*Z* isomer), 55.4 (*Z* isomer), 55.3 (*E* isomer) ppm.

Spectral data is in agreement with the literature.<sup>41</sup>



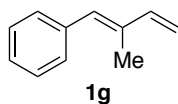
**3-(buta-1,3-dien-1-yl)benzo[*b*]thiophene (1f)**. Following the general procedure A using 1-benzothiophene-3-carbaldehyde (0.81 g, 5 mmol), affording **1f** (504 mg, 54% yield) as a mixture of isomers (*E:Z* = 1:1.5). Yellow liquid.

**<sup>1</sup>H NMR** (400 MHz, CDCl<sub>3</sub>) δ 7.95 – 7.86 (m, 2H), 7.77 (ddd, *J* = 7.1, 1.9, 0.8 Hz, 1H, *Z* isomer), 7.48 (m, 1H, *E* isomer), 7.45 – 7.34 (m, 2H), 6.93 – 6.83 (m, 2H), 6.64 – 6.54 (m, 1H, *E* isomer), 6.46 (td, *J* = 11.1, 0.9 Hz, 1H, *Z* isomer), 5.44 (ddd, *J* = 16.9, 1.8, 0.9 Hz, 1H, *Z* isomer), 5.38 (d, *J* = 16.8 Hz, 1H, *E* isomer), 5.26 – 5.21 (m, 1H) ppm.

**<sup>13</sup>C NMR** (101 MHz, CDCl<sub>3</sub>) δ 140.6, 139.9, 138.9, 137.8, 137.4, 134.0, 133.8, 132.7, 132.6, 131.2, 124.8, 124.7, 124.6, 124.5, 124.4, 124.3, 123.1, 122.8, 122.6, 122.4, 122.1, 122.0, 119.8, 117.9 ppm.

**IR** (neat, cm<sup>-1</sup>): 3085, 3067, 3029, 3008, 2961, 2926, 1628, 1507, 1459, 1424, 1000, 756, 731.

**HRMS** ESI, (C<sub>12</sub>H<sub>11</sub>S)[M+H]<sup>+</sup> *calculated* 187.0576, *found* 187.0575.

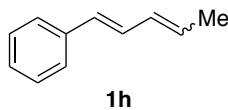


**(*E*)-(2-methylbuta-1,3-dien-1-yl)benzene (1g)**. Following the general procedure A but using methyltriphenylphosphonium bromide (2.14 g, 6 mmol) and α-methylcinnamylaldehyde (0.70 mL, 5 mmol), affording **1g** (520 mg, 72% yield). Yellow liquid.

**<sup>1</sup>H NMR** (400 MHz, CDCl<sub>3</sub>) δ 7.43 – 7.31 (m, 4H), 7.30 – 7.22 (m, 1H), 6.65 – 6.55 (m, 2H), 5.34 (dd, *J* = 17.3, 0.9 Hz, 1H), 5.17 (dd, *J* = 10.7, 0.9 Hz, 1H), 2.04 (t, *J* = 1.0 Hz, 3H) ppm.

**<sup>13</sup>C NMR** (101 MHz, CDCl<sub>3</sub>) δ 142.0, 137.9, 136.1, 131.8, 129.4, 128.3, 126.8, 113.1, 13.3 ppm.

Spectral data is in agreement with the literature.<sup>42</sup>



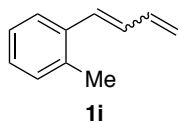
**Penta-1,3-dien-1-ylbenzene (1h).** Following the general procedure A but using ethyltriphenylphosphonium iodide (5.012 g, 12 mmol) and cinnamaldehyde (1.32 g, 10 mmol), affording **1h** (1.39 g, 96% yield) as a mixture of isomers (*E*:*Z* =

1.5:1). Colorless liquid.

**<sup>1</sup>H NMR** (500 MHz, CDCl<sub>3</sub>) δ 7.50 (d, *J* = 7.6 Hz, 2H, *Z* isomer), 7.45 (d, *J* = 7.5 Hz, 2H, *E* isomer), 7.41 – 7.35 (m, 2H), 7.31 – 7.25 (m, 1H), 7.17 (ddd, *J* = 15.6, 11.0, 1.1 Hz, 1H, *Z* isomer), 6.83 (dd, *J* = 15.7, 10.5 Hz, 1H, *E* isomer), 6.60 (d, *J* = 15.6 Hz, 1H, *Z* isomer), 6.50 (d, *J* = 15.7 Hz, 1H, *E* isomer), 6.34 – 6.23 (m, 1H), 5.91 (dq, *J* = 13.9, 6.8 Hz, 1H, *E* isomer), 5.68 (dq, *J* = 10.7, 7.2 Hz, 1H, *Z* isomer), 1.94 (dd, *J* = 7.2, 1.8 Hz, 3H, *Z* isomer), 1.90 (dd, *J* = 6.8, 1.6 Hz, 3H, *E* isomer) ppm.

**<sup>13</sup>C NMR** (126 MHz, CDCl<sub>3</sub>) δ 137.8, 132.1, 132.0, 130.4, 130.0, 129.8, 129.5, 128.7, 128.6, 127.5, 127.3, 127.2, 126.5, 126.3, 124.3, 18.5, 13.8.

Spectral data is in agreement with the literature.<sup>43</sup>

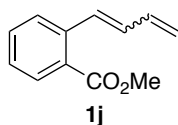


**(*E,Z*)-1-(buta-1,3-dien-1-yl)-2-methylbenzene (1i).** Following the general procedure A using 2-methylbenzaldehyde (0.23 mL, 2 mmol), affording **1i** (168mg, 58% yield) as a mixture of isomers (*E*:*Z* = 1:1.4). Colorless liquid.

**<sup>1</sup>H NMR** (400 MHz, CDCl<sub>3</sub>) δ 7.57 – 7.14 (m, 4H), 6.79 (t, *J* = 16.7 Hz, 1H, *Z* isomer), 6.70 (d, *J* = 15.3 Hz, 1H, *E* isomer), 6.69 – 6.54 (m, 2H, *E* isomer), 6.52 (d, *J* = 11.4 Hz, 1H, *Z* isomer), 6.39 – 6.28 (m, 1H, *Z* isomer), 5.36 (d, *J* = 16.9 Hz, 1H, *Z* isomer), 5.35 (d, *J* = 16.8 Hz, 1H, *E* isomer), 5.19 (d, *J* = 9.9 Hz, 1H, *E* isomer), 5.18 (d, *J* = 10.5 Hz, 1H, *Z* isomer) 2.38 (s, 3H, *E* isomer), 2.29 (s, 3H, *Z* isomer) ppm.

**<sup>13</sup>C NMR** (101 MHz, CDCl<sub>3</sub>) δ 137.6 (*E* isomer), 136.6 (*Z* isomer), 136.5 (*Z* isomer), 136.1 (*E* isomer), 135.8 (*E* isomer), 133.6 (*Z* isomer), 131.0 (*Z* isomer), 130.9 (*E* isomer), 130.6 (*E* isomer), 130.5 (*E* isomer), 130.1 (*Z* isomer), 130.0 (*Z* isomer), 129.7 (*Z* isomer), 127.7 (*E* isomer), 127.4 (*Z* isomer), 126.2 (*E* isomer), 125.5 (*Z* isomer), 125.3 (*E* isomer), 119.1 (*Z* isomer), 117.6 (*E* isomer), 20.1 (*Z* isomer), 20.0 (*E* isomer) ppm.

Spectral data is in agreement with the literature.<sup>41</sup>

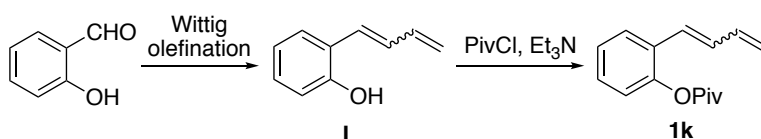


**Methyl 2-(buta-1,3-dien-1-yl)benzoate (1j).** Following the general procedure A using methyl 2-formylbenzoate (1.64 g, 10 mmol), affording **1j** (1.45 g, 77% yield) as a mixture of isomers (*E*:*Z* = 1:1). Yellowish liquid.

<sup>1</sup>H NMR (400 MHz, CDCl<sub>3</sub>) δ 8.00 (dd, *J* = 7.8, 1.2 Hz, 1H, *Z* isomer), 7.90 (dd, *J* = 7.9, 1.3 Hz, 1H, *E* isomer), 7.66 – 7.64 (m, 1H, *E* isomer), 7.53-7.47 (m, 1H), 7.42 (d, *J* = 15.5 Hz, 1H, *Z* isomer), 7.39-7.29 (m, 2H), 6.99 (d, *J* = 11.5 Hz, 1H, *Z* isomer), 6.74 (dd, *J* = 15.5, 10.5 Hz, 1H, *E* isomer), 6.65 – 6.54 (m, 1H), 6.36 (tt, *J* = 11.3, 0.8 Hz, 1H, *Z* isomer), 5.41-5.35 (m, 1H), 5.24 (ddt, *J* = 10.0, 1.6, 0.7 Hz, 1H, *Z* isomer), 5.18 (dt, *J* = 10.1, 2.0 Hz, 1H, *E* isomer), 3.93 (s, 3H, *Z* isomer), 3.90 (s, 3H, *E* isomer) ppm.

<sup>13</sup>C NMR (101 MHz, CDCl<sub>3</sub>) δ 168.0, 167.6, 138.8, 138.3, 137.5, 134.0, 133.8, 132.5, 132.1, 131.8, 131.6, 131.3, 130.7, 128.9, 128.7, 128.6, 127.3, 127.2, 126.9, 119.5, 118.5, 52.2, 52.1 ppm.

Spectral data is in agreement with the literature.<sup>41</sup>



**2-(buta-1,3-dien-1-yl)phenol (I).** Following the general procedure A using 2-hydroxybenzaldehyde (1.57 mL, 15 mmol) and 2.4 equivalents of allyltriphenylphosphonium bromide (13.8 g, 36 mmol), affording **I** (1535 mg, 70% yield) as a mixture of isomers (*E*:*Z* = 10:1). Yellow liquid.

<sup>1</sup>H NMR (400 MHz, CDCl<sub>3</sub>) δ 7.43 (dt, *J* = 7.9, 1.1 Hz, 1H), 7.12 (td, *J* = 7.7, 1.7 Hz, 1H), 6.92 (t, *J* = 7.7 Hz, 1H), 6.86 – 6.80 (m, 2H), 6.77 (dd, *J* = 8.0, 1.2 Hz, 1H), 6.63 – 6.48 (m, 1H), 5.34 (dd, *J* = 16.7, 1.5 Hz, 1H), 5.19 (dd, *J* = 9.9, 1.5 Hz, 1H), 5.04 (brs, 1H) ppm.

<sup>13</sup>C NMR (101 MHz, CDCl<sub>3</sub>) δ 153.0, 137.7, 131.3, 128.8, 127.6, 127.2, 124.5, 121.2, 117.7, 116.1 ppm.

Spectral data is in agreement with the literature.<sup>44</sup>

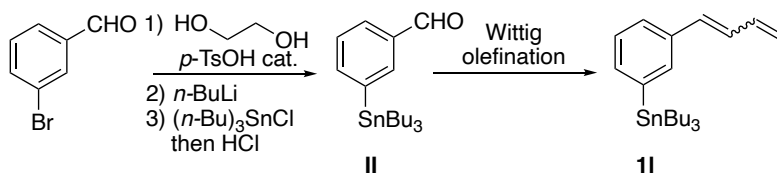
**2-(buta-1,3-dien-1-yl)phenyl pivalate (1k).** Trimethylacetyl chloride (0.34 mL, 2.75 mmol) was added to a solution of the 2-(buta-1,3-dien-1-yl)phenol (0.37 g, 2.50 mmol) and triethylamine (0.69 mL, 5.00 mmol) in THF (3.0 mL) at 0 °C. The mixture was then allowed to warm to room temperature, and stirred for 16 hours. The solvent was then removed in vacuo and the crude mixture was diluted with CH<sub>2</sub>Cl<sub>2</sub>, washed with 2 M HCl and brine, dried over MgSO<sub>4</sub> and concentrated in vacuo. The residual oil was subjected to column chromatography over silica gel (hexanes/Et<sub>2</sub>O 10/1) to give **1k** (507 mg, 88% yield) as a 10:1 *E*:*Z* mixture. Yellow liquid.

<sup>1</sup>H NMR (400 MHz, CDCl<sub>3</sub>) δ 7.58 (dd, *J* = 7.7, 1.8 Hz, 1H), 7.28 – 7.17 (m, 2H), 6.99 (dd, *J* = 8.0, 1.4 Hz, 1H), 6.77 (dd, *J* = 15.8, 10.4 Hz, 1H), 6.58 (d, *J* = 15.8 Hz, 1H), 6.47 (dt, *J* = 17.4, 10.3 Hz, 1H), 5.35 (d, *J* = 16.9 Hz, 1H), 5.20 (d, *J* = 10.0 Hz, 1H), 1.41 (s, 9H) ppm.

<sup>13</sup>C NMR (101 MHz, CDCl<sub>3</sub>) δ 176.7, 148.4, 137.2, 131.6, 129.8, 128.4, 126.3, 125.9, 125.8, 122.6, 118.4, 39.3, 27.2 ppm.

**IR** (neat,  $\text{cm}^{-1}$ ): 2973, 2935, 1750, 1479, 1455, 1108, 1001, 748.

**HRMS** ESI, ( $\text{C}_{15}\text{H}_{18}\text{NaO}_2$ )  $[\text{M}+\text{Na}]^+$  *calculated* 253.1199, *found* 253.1209.



**3-(tributylstannyl)benzaldehyde (II)**. To a solution of 3-bromobenzaldehyde (1.75 mL, 15 mmol) and ethylene glycol (3.76 mL, 67.5 mol) in toluene (10 mL) at room temperature was added *p*-TsOH (0.26 g, 1.5 mmol) and the reaction mixture was allowed to stirred at 140 °C for 16 hours. The mixture was allowed to warm to room temperature, diluted with water and extracted three times with EtOAc. The combined organic layers were washed with brine, dried over  $\text{MgSO}_4$ , and concentrated in vacuum. The residual oil was passed through a short pad of silica gel to give 2-(3-bromophenyl)-1,3-dioxolane. To a solution of 2-(3-bromophenyl)-1,3-dioxolane (3.43 g, 15 mmol) in THF (60 mL) at -78 °C was added *n*-BuLi (7.2 mL of 2.5 M in hexane, 18 mmol) under nitrogen atmosphere and stirred for 1 hour. After this time tributyltin chloride (4.5 mL, 16.5 mmol) was added dropwise and stirred for 15 min at -78 °C. The mixture was then allowed to warm to room temperature, and stirred for 1 hour. The reaction was next quenched by adding 20 mL of a 1 M HCl solution and stirred for 3 hours at room temperature. The reaction mixture was then extracted three times with EtOAc and the combined organic layers were washed with brine, dried over  $\text{MgSO}_4$  and concentrated in vacuum. The residual oil was purified by column chromatography over silica gel (pure hexanes to hexanes/EtOAc 9/1) to give **II** as a yellow liquid.

**<sup>1</sup>H NMR** (400 MHz,  $\text{CDCl}_3$ )  $\delta$  10.02 (s, 1H), 8.03 – 7.88 (m, 1H), 7.79 (dt,  $J = 7.7, 1.5$  Hz, 1H), 7.72 (dt,  $J = 7.2, 1.2$  Hz, 1H), 7.53 – 7.44 (m, 1H), 1.66 – 1.43 (m, 6H), 1.40 – 1.27 (m, 6H), 1.20 – 1.01 (m, 6H), 0.89 (t,  $J = 7.3$  Hz, 9H) ppm.

**<sup>13</sup>C NMR** (101 MHz,  $\text{CDCl}_3$ )  $\delta$  193.3, 143.7, 142.7, 137.8, 135.7, 129.6, 128.5, 29.2, 27.5, 13.8, 9.8 ppm.

Spectral data is in agreement with the literature.<sup>45</sup>

**3-(buta-1,3-dien-1-yl)phenyltributylstannane (11)**. Following the general procedure A using 3-(tributylstannyl)benzaldehyde (**II**) (0.99 g, 2.5 mmol), affording **11** (251.9 mg, 24% yield) as a mixture of isomers (*E*:*Z* = 1:2). Yellow oil.

**<sup>1</sup>H NMR** (500 MHz,  $\text{CDCl}_3$ )  $\delta$  7.50 – 7.23 (m, 4H), 6.90 (dddd,  $J = 16.9, 11.2, 10.1, 1.1$  Hz, 1H, *Z* isomer), 6.78 (ddt,  $J = 15.6, 10.5, 0.8$  Hz, 1H, *E* isomer), 6.59 – 6.50 (m, 2H, *E* isomer), 6.47 (d,  $J = 11.7$  Hz, 1H, *Z* isomer), 6.29 (tt,  $J = 11.4, 0.9$  Hz, 1H, *Z* isomer), 5.37 (ddt,  $J = 6.9, 1.8, 0.8$  Hz, 1H, *Z* isomer), 5.34 (ddt,  $J = 17.2, 1.6, 0.8$  Hz, 1H, *E* isomer), 5.23–5.20 (m, 1H, *Z* isomer), 5.17 (ddd,  $J = 10.1, 1.5, 0.7$  Hz, 1H, *E* isomer),

1.63 – 1.47 (m, 6H), 1.38 – 1.30 (m, 6H), 1.13 – 1.01 (m, 6H), 0.90 (t,  $J = 7.3$  Hz, 9H, *E* isomer), 0.89 (t,  $J = 7.3$  Hz, 9H, *Z* isomer) ppm.

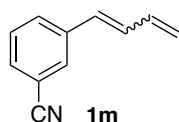
<sup>13</sup>C NMR (126 MHz, CDCl<sub>3</sub>) δ 142.3, 141.8, 137.3, 137.0, 136.7, 136.4, 135.9, 135.2, 134.7, 133.4, 130.9, 130.5, 129.3, 128.6, 128.0, 127.6, 125.9, 119.3, 117.3, 29.1, 29.0, 27.4, 27.3, 13.7, 9.6, 9.5 ppm.

<sup>119</sup>Sn NMR (149 MHz, CDCl<sub>3</sub>) δ -41.96 ppm.

IR (neat, cm<sup>-1</sup>): 2955, 2923, 2871, 2851, 1463, 1377, 1000, 902, 698, 653.

**HRMS** Obtaining a High Resolution Mass data of the molecular ion was proved to be difficult using ESI and APCI ionization modes. Using APCI we could just determine the exact mass of a fragment of the molecule: (C<sub>12</sub>H<sub>27</sub>Sn)<sup>+</sup> *calculated* 287.1136, *found* 287.1125.

We could obtain as well the nominal mass of [M-*n*Bu] = 363.2 m/z fragment by GC-MS analysis.



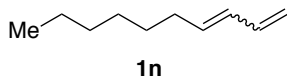
**(*E,Z*)- 3-(buta-1,3-dien-1-yl)benzonitrile (1m).** Following the general procedure A using 4-cyanobenzaldehyde (0.66 g, 5 mmol), affording **1m** (374 mg, 48% yield) as a mixture of isomers (*E:Z* = 1:1). Yellow liquid.

<sup>1</sup>H NMR (400 MHz, CDCl<sub>3</sub>) δ 7.66 – 7.39 (m, 4H), 6.82 (dd,  $J = 15.2, 10.9$  Hz, 1H, *E* isomer), 6.74 (dt,  $J = 16.7, 10.1$  Hz, 1H, *Z* isomer), 6.52 (d,  $J = 15.7$  Hz, 1H, *E* isomer), 6.50 (dt,  $J = 16.8, 10.1$  Hz, 1H, *E* isomer), 6.42 – 6.32 (m, 2H, *Z* isomer), 5.46 (dd,  $J = 16.3, 1.4$  Hz, 1H, *Z* isomer), 5.42 (dd,  $J = 16.2, 1.3$  Hz, 1H, *E* isomer), 5.33 (d,  $J = 10.1$  Hz, 1H, *Z* isomer), 5.28 (d,  $J = 9.7$  Hz, 1H, *E* isomer) ppm.

<sup>13</sup>C NMR (101 MHz, CDCl<sub>3</sub>) δ 138.6, 138.5, 136.5, 133.3, 133.0, 132.4, 132.2, 132.1, 130.8, 130.5, 130.3, 129.9, 129.5, 129.2, 127.8, 121.8, 119.9, 118.9, 118.8, 113.0, 112.7 ppm.

IR (neat, cm<sup>-1</sup>): 3088, 3015, 2963, 2230, 1601, 1575, 1478, 1432, 1002, 902, 811, 687, 664.

**HRMS** ESI, (C<sub>11</sub>H<sub>9</sub>N)[M<sup>+</sup>] *calculated* 155.0730, *found* 155.0723.



**Deca-1,3-diene (1n).** Following the general procedure A using acroleine (1.10 mL, 16.5 mmol), heptyltriphenylphosphonium bromide<sup>10</sup> (6.62 g, 15 mmol)

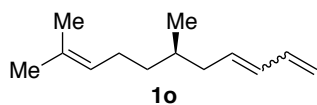
and diethyl ether (60 mL) as solvent, affording **1m** (865 mg, 42% yield) as a mixture of isomers (*E:Z* = 1:1). Colorless liquid (volatile).

<sup>1</sup>H NMR (500 MHz, CDCl<sub>3</sub>) δ 6.65 (dddd,  $J = 16.9, 11.2, 10.1, 1.1$  Hz, 1H, *Z* isomer), 6.32 (dt,  $J = 17.0, 10.1$  Hz, 1H, *E* isomer), 6.09 – 5.98 (m, 1H), 5.72 (dt,  $J = 14.6, 7.0$  Hz, 1H, *E* isomer), 5.50 – 5.43 (m, 1H, *Z* isomer), 5.18 (dd,  $J = 16.9, 2.1$  Hz, 1H, *Z*

isomer), 5.12 – 5.09 (m, 1H, *E* isomer), 5.09 – 5.06 (m, 1H, *Z* isomer), 4.97 – 4.93 (m, 1H, *E* isomer), 2.19 (qd,  $J = 7.5, 1.6$  Hz, 1H), 2.09 (q,  $J = 7.2$  Hz, 1H), 1.44 – 1.36 (m, 2H), 1.36 – 1.26 (m, 6H), 0.90 (t,  $J = 7.0$  Hz, 3H) ppm.

$^{13}\text{C}$  NMR (126 MHz,  $\text{CDCl}_3$ )  $\delta$  137.5, 135.7, 133.2, 132.5, 131.0, 129.3, 116.8, 114.7, 32.7, 31.9, 29.8, 29.3, 29.1, 29.0, 27.9, 22.8, 14.2 ppm.

Spectral data is in agreement with the literature.<sup>46</sup>



**(*R*)-6,10-dimethylundeca-1,3,9-triene (1o).**

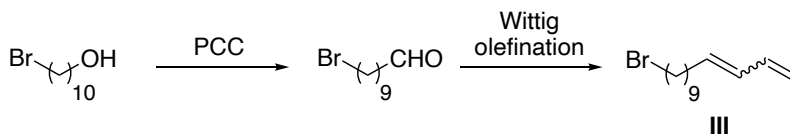
Following the general procedure A using citronelal (308.5 mg, 2 mmol), affording **1o** (269.2 mg, 75% yield)

as a mixture of isomers (*E:Z* = 1:1). Yellow liquid.

$^1\text{H}$  NMR (500 MHz,  $\text{CDCl}_3$ )  $\delta$  6.64 (dddd,  $J = 16.8, 11.1, 10.1, 1.1$  Hz, 1H, *Z* isomer), 6.32 (dtd,  $J = 17.0, 10.3, 0.7$  Hz, 1H, *E* isomer), 6.09 – 6.00 (m, 1H), 5.69 (dt,  $J = 14.6, 7.4$  Hz, 1H, *E* isomer), 5.52 – 5.42 (m, 1H, *Z* isomer), 5.18 (dd,  $J = 16.9, 2.0$  Hz, 1H, *Z* isomer), 5.13 – 5.05 (m, 2H), 4.95 (dd,  $J = 10.1, 1.8$  Hz, 1H, *E* isomer), 2.24 – 1.88 (m, 4H), 1.69 (d,  $J = 1.3$  Hz, 3H), 1.61 (d,  $J = 1.4$  Hz, 3H), 1.59 – 1.47 (m, 1H), 1.42 – 1.30 (m, 1H), 1.23 – 1.10 (m, 1H), 0.90 (d,  $J = 5.9$  Hz, 1.5H), 0.88 (d,  $J = 5.9$  Hz, 1.5H) ppm.

$^{13}\text{C}$  NMR (126 MHz,  $\text{CDCl}_3$ )  $\delta$  137.5, 134.2, 132.6, 132.3, 131.8, 131.3, 131.2, 130.1, 124.9, 124.8, 116.9, 114.7, 40.2, 36.9, 36.8, 35.0, 33.3, 32.9, 25.9, 25.8, 25.7, 19.6, 17.8 ppm.

Spectral data is in agreement with the literature.<sup>47</sup>



**13-Bromotrideca-1,3-diene (III).** 10-bromodecan-1-ol<sup>48</sup> (8.40 g, 35.0 mmol) was dissolved in 70 mL of dry dichloromethane. Pyridinium chlorochromate (8.30 g, 38.5 mmol) was added in portions, and stirred for 3 hours at room temperature. The crude mixture was filtered through a plug of celite and purified by column chromatography with silica gel (hexanes/EtOAc 3/1) to give 10-bromodecanal. Following the general procedure A, 10-bromodecanal was used without further purification, affording **III** (3.77 g, 41% yield) as a mixture of isomers (*E:Z* = 1:1). Colorless liquid (volatile).

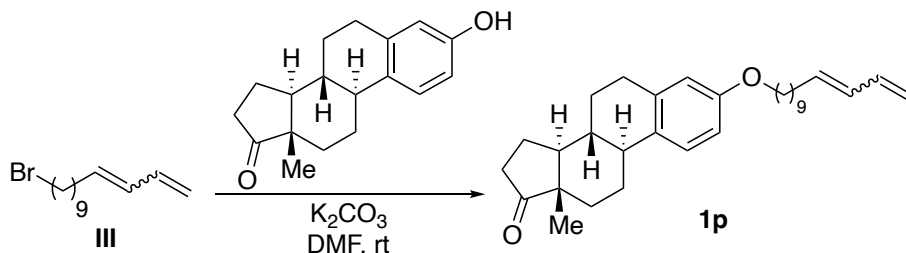
$^1\text{H}$  NMR (400 MHz,  $\text{CDCl}_3$ )  $\delta$  6.64 (dddd,  $J = 16.9, 11.2, 10.1, 1.1$  Hz, 1H, *Z* isomer), 6.31 (dt,  $J = 17.0, 10.3$  Hz, 1H, *E* isomer), 6.09 – 5.94 (m, 1H), 5.70 (dt,  $J = 14.6, 7.0$  Hz, 1H, *E* isomer), 5.50 – 5.40 (m, 1H, *Z* isomer), 5.18 (dd,  $J = 16.9, 2.1$  Hz, 1H, *Z* isomer), 5.12 – 5.08 (m, 1H, *E* isomer), 5.08 – 5.05 (m, 1H, *Z* isomer), 4.95 (dd,  $J = 10.2, 1.8$  Hz, 1H, *E* isomer), 3.40 (t,  $J = 6.9$  Hz, 2H), 2.18 (qd,  $J = 7.4, 1.6$  Hz, 1H), 2.08



(qd,  $J = 7.1, 1.4$  Hz, 1H), 1.91 – 1.79 (m, 2H), 1.46 – 1.34 (m, 4H), 1.32 – 1.27 (m, 8H) ppm.

<sup>13</sup>C NMR (101 MHz, CDCl<sub>3</sub>)  $\delta$  137.5, 135.6, 133.1, 132.5, 131.0, 129.3, 116.8, 114.7, 34.1, 33.0, 32.7, 29.7, 29.5, 29.3, 29.2, 28.9, 28.3, 27.8 ppm.

Spectral data is in agreement with the literature.<sup>49</sup>



**(8R,9R,13S,14R)-13-methyl-3-(((E)-trideca-10,12-dien-1-yl)oxy)-6,7,8,9,11,12,13,14,15,16-decahydro-17H-cyclopenta[*a*]phenanthren-17-one (1p).** 13-Bromotrideca-1,3-diene (**III**) (259.3 mg, 1.0 mmol), estrone (270.4 mg, 1.0 mmol) and potassium carbonate (208.0 mg, 1.5 mmol) were dissolved in DMF (1.5 mL) and stirred at room temperature for 3 days. The crude product was diluted with water, extracted with EtOAc and the combined organic phases were dried over MgSO<sub>4</sub>. After purification by column chromatography with silica gel (hexanes/EtOAc 9/1 to 8/2), **1p** was obtained as a 1:1 *E:Z* mixture (400.4 mg, 89 % yield). Colorless solid.

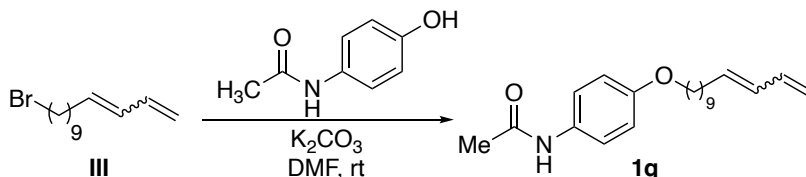
**Mp** 38-40 °C.

<sup>1</sup>H NMR (500 MHz, CDCl<sub>3</sub>)  $\delta$  7.19 (dd,  $J = 8.7, 1.0$  Hz, 1H), 6.71 (dd,  $J = 8.6, 2.8$  Hz, 1H), 6.69 – 6.60 (m, 1H, *Z* isomer), 6.64 (d,  $J = 2.7$  Hz, 1H), 6.31 (dt,  $J = 17.0, 10.3$  Hz, 1H, *E* isomer), 6.11 – 5.95 (m, 1H), 5.71 (dt,  $J = 14.6, 7.0$  Hz, 1H, *E* isomer), 5.46 (dtd,  $J = 10.1, 7.6, 1.2$  Hz, 1H, *Z* isomer), 5.18 (dd,  $J = 16.9, 2.0$  Hz, 1H, *Z* isomer), 5.12 – 5.07 (m, 1H, *E* isomer), 5.07 (d,  $J = 1.9$  Hz, 1H, *Z* isomer), 4.95 (d,  $J = 10.1$  Hz, 1H, *E* isomer), 3.92 (t,  $J = 6.6$  Hz, 2H), 2.94 – 2.85 (m, 2H), 2.55 – 2.45 (m, 1H), 2.42 – 2.37 (m, 1H), 2.29 – 2.22 (m, 1H), 2.21 – 1.93 (m, 6H), 1.79 – 1.71 (m, 2H), 1.67 – 1.36 (m, 10H), 1.36 – 1.26 (m, 8H), 0.91 (s, 3H) ppm.

<sup>13</sup>C NMR (126 MHz, CDCl<sub>3</sub>)  $\delta$  157.3, 137.8, 137.5, 135.7, 133.2, 132.5, 132.0, 131.0, 129.3, 126.4, 116.8, 114.7, 112.3, 68.1, 50.6, 48.2, 44.1, 38.6, 36.0, 32.7, 31.8, 29.8, 29.7, 29.6, 29.6, 29.5, 29.5, 29.3, 29.3, 27.9, 26.7, 26.2, 26.1, 21.7, 14.0 ppm.

**IR** (neat, cm<sup>-1</sup>): 2921, 2852, 1733, 1610, 1572, 1498, 1468, 1280, 1254, 1159, 1056, 1003, 898, 779.

**HRMS** ESI, (C<sub>31</sub>H<sub>44</sub>O<sub>2</sub>Na) [M+Na]<sup>+</sup> *calculated* 471.3234, *found* 471.3246.



***N*-(4-(trideca-10,12-dien-1-yloxy)phenyl)acetamide (1q).** 13-Bromotrideca-1,3-diene (**III**) (518.5 mg, 2.0 mmol), *p*-acetamidophenol (339 mg, 2.2 mmol) and potassium carbonate (415.0 mg, 3 mmol) were dissolved in DMF (3.3 mL) and stirred at room temperature for 3 days. The crude product was diluted with water, extracted with EtOAc and the combined organic phases were dried over MgSO<sub>4</sub>. After purification by column chromatography with silica gel (hexanes/EtOAc 9/1 to 8/2) gave **1p** as a 1:1 *E:Z* mixture (544.3 mg, 83 % yield). White solid.

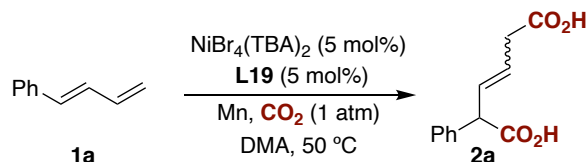
**Mp** 76-78 °C.

**<sup>1</sup>H NMR** (400 MHz, CDCl<sub>3</sub>) δ 7.36 (d, *J* = 9.0 Hz, 2H), 7.13 (s, 1H), 6.84 (d, *J* = 9.0 Hz, 2H), 6.64 (dddd, *J* = 16.9, 11.2, 10.2, 1.1 Hz, 1H, *Z* isomer), 6.31 (dt, *J* = 17.0, 10.3 Hz, 1H, *E* isomer), 6.10 – 5.95 (m, 1H), 5.70 (dt, *J* = 14.6, 6.9 Hz, 1H, *E* isomer), 5.45 (q, *J* = 7.8 Hz, 1H, *Z* isomer), 5.17 (dd, *J* = 16.9, 2.1 Hz, 1H, *Z* isomer), 5.13 – 5.07 (m, 1H, *E* isomer), 5.06 – 5.05 (m, 1H, *Z* isomer), 4.95 (dd, *J* = 10.2, 1.8 Hz, 1H, *E* isomer), 3.92 (t, *J* = 6.6 Hz, 2H), 2.21 – 2.14 (m, 1H), 2.14 (s, 3H), 2.07 (q, *J* = 6.9 Hz, 1H), 1.75 (p, *J* = 6.9 Hz, 2H), 1.48 – 1.32 (m, 6H), 1.31 – 1.24 (m, 6H) ppm.

**<sup>13</sup>C NMR** (101 MHz, CDCl<sub>3</sub>) δ 168.3, 156.2, 137.5, 135.7, 133.2, 132.5, 131.0, 130.9, 129.3, 122.0, 116.8, 114.9, 114.7, 68.4, 32.7, 29.7, 29.6, 29.6, 29.5, 29.4, 29.3, 29.3, 27.9, 26.2, 24.5 ppm.

**IR** (neat, cm<sup>-1</sup>): 3303, 2920, 2852, 1654, 1527, 1513, 1476, 1365, 1298, 1239, 1040, 1010, 1001, 821, 718.

**HRMS** ESI, (C<sub>21</sub>H<sub>31</sub>NO<sub>2</sub>Na) [M+Na]<sup>+</sup> calculated 352.2247, found 352.2250.

**Ni-catalyzed 1,4-dicarboxylation of 1,3-dienes with CO<sub>2</sub>**

**2-phenylhex-3-enedioic acid (2a).** An oven-dried Schlenk tube equipped with a magnetic stirring bar was charged with Mn dust (16.5 mg, 0.3 mmol, 1.5 equiv), 2-methyl-4,7-diphenyl-1,10-phenanthroline (**L19**) (3.5 mg, 0.01 mmol, 0.05 equiv) and NiBr<sub>4</sub>(TBA)<sub>2</sub> (8.7 mg, 0.01 mmol, 0.05 equiv). The schlenk tube was filled with carbon dioxide by applying three cycles of evacuation and filling with CO<sub>2</sub>. Subsequently, 1-phenyl-1,3-butadiene (**1a**, 0.20 mmol, 1 equiv) was added by syringe followed by DMA (0.40 mL) with a constant flow of CO<sub>2</sub>. The Schlenk flask was tightly sealed and stirred at 50 °C for 60 hours (otherwise stated) after which it was quenched by careful addition of 2 M aq. HCl sol. The reaction mixture was diluted with water and extracted 3 times with EtOAc. The combined organic phases were washed with brine, dried over MgSO<sub>4</sub> and filtered. The solvent was then removed under reduced pressure and it was purified by column chromatography (hexane/EtOAc/HCOOH 75/25/0 to 50/50/0.5) to obtain 32.2 mg (74% yield) of **2a** as a mixture of isomers (*E:Z* = 2.4:1). In a separate experiment, 32.8 mg (75%) were obtained, giving an average yield of 74%. White solid.

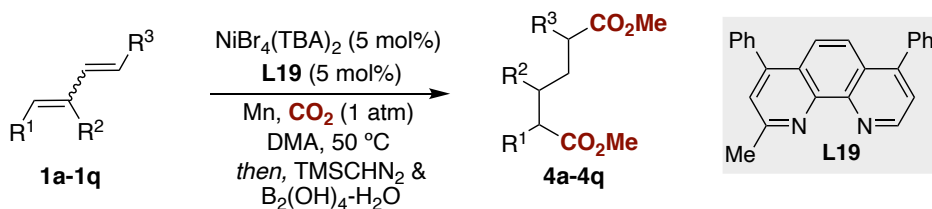
**Mp** 90-94 °C

**<sup>1</sup>H NMR** (400 MHz, Acetone-*d*<sub>6</sub>) δ 7.33 (tt, *J* = 31.9, 7.4 Hz, 5H), 6.13 – 6.00 (m, 1H), 5.86 – 5.73 (m, 1H), 4.68 (d, *J* = 9.7 Hz, 1H, *Z* isomer), 4.39 (d, *J* = 8.5 Hz, 1H, *E* isomer), 3.32 – 3.10 (m, 2H) ppm.

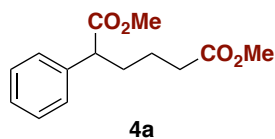
**<sup>13</sup>C NMR** (101 MHz, Acetone-*d*<sub>6</sub>) δ 173.7, 173.5, 172.7, 172.5, 140.1, 140.0, 132.3, 131.0, 129.5, 129.4, 128.8, 128.7, 127.9, 126.2, 124.8, 55.1, 50.2, 37.8, 33.0 ppm.

**IR** (neat, cm<sup>-1</sup>): 3028, 2909, 1692, 1598, 1408, 1271, 1207, 923, 695.

**HRMS** ESI, (C<sub>12</sub>H<sub>10</sub>O<sub>4</sub>) [M-H]<sup>-</sup> calculated 219.0663, found 219.0657.



**General procedure B:** An oven-dried Schlenk tube equipped with a magnetic stirring bar was charged with Mn dust (16.5 mg, 0.3 mmol, 1.5 equiv), **L19** (3.5 mg, 0.01 mmol, 0.05 equiv) and  $\text{NiBr}_4(\text{TBA})_2$  (8.7 mg, 0.01 mmol, 0.05 equiv). The Schlenk tube was filled with  $\text{CO}_2$  by applying three vacuum/ $\text{CO}_2$  cycles. Subsequently, the 1,3-diene (0.20 mmol, 1 equiv) was added by syringe followed by DMA (0.40 mL) with a constant flow of  $\text{CO}_2$ . The Schlenk flask was tightly sealed and stirred at 50 °C for 60 hours (unless stated otherwise) after which it was quenched by careful addition of HCl 2M (with the exception of **1g**, the starting material was totally consumed after the reaction). The reaction mixture was diluted with water and extracted 3 times with EtOAc. The combined organic phases were washed with brine, dried over  $\text{MgSO}_4$  and filtered. The solvent was then removed under vacuum and it was dissolved in a 1:1 MeOH:Et<sub>2</sub>O mixture and cooled down to 0 °C. TMSCHN<sub>2</sub> (0.4 mL of a 2 M solution in Et<sub>2</sub>O, 4 equiv) was added dropwise and after 30 minutes silica gel was added and solvent was removed under vacuum. The compound was purified by column chromatography (hexane/EtOAc mixtures), and the product was directly reduced by mixing it with 10% Pd/C (10.6 mg, 5 mol%),  $\text{B}_2(\text{OH})_4$  (35.8 mg, 0.4 mmol, 2 equiv) and H<sub>2</sub>O (18 μL, 1 mmol, 5 equiv) in dichloromethane (2 mL) and stirred at room temperature for 24 h. The solution was filtered through celite and the solvent was removed under reduced pressure to obtain the corresponding product.



#### Dimethyl 2-phenylhexanedioate (**4a**).

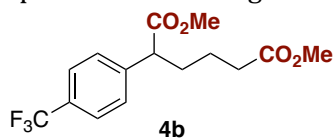
**From (*E,Z*)-buta-1,3-dien-1-ylbenzene:** General procedure B was followed using (*E,Z*)-buta-1,3-dien-1-ylbenzene (26.0 mg, 0.20 mmol), affording **4a** (36.0 mg, 72% yield). In a separate experiment, 37.7 mg (75%) were obtained, giving an average yield of 74%. Colorless oil.

**From (*E*)-buta-1,3-dien-1-ylbenzene:** General procedure B was followed using (*E*)-buta-1,3-dien-1-ylbenzene (26.0 mg, 0.20 mmol), affording **4a** (36.5 mg, 73% yield). Colorless oil.

**<sup>1</sup>H NMR** (500 MHz, CDCl<sub>3</sub>) δ 7.34 – 7.23 (m, 5H), 3.65 (s, 3H), 3.64 (s, 3H), 3.55 (t, *J* = 7.7 Hz, 1H), 2.37 – 2.26 (m, 2H), 2.14 – 2.05 (m, 1H), 1.86 – 1.77 (m, 1H), 1.66 – 1.50 (m, 2H) ppm.

<sup>13</sup>C NMR (126 MHz, CDCl<sub>3</sub>) δ 174.3, 173.7, 138.8, 128.8, 128.0, 127.5, 52.1, 51.6, 51.4, 33.8, 32.9, 23.0 ppm.

Spectral data is in agreement with the literature.<sup>50</sup>



**4b**

**Dimethyl 2-(4-(trifluoromethyl)phenyl)hexanedioate (4b).** General procedure B was followed using

1-(buta-1,3-dien-1-yl)-4-(trifluoromethyl)benzene (**1b**) (39.6 mg, 0.20 mmol), affording **4b** (59.2 mg, 93% yield). In a separate experiment, 53.8 mg (85%) were obtained, giving an average yield of 89%. Colorless oil.

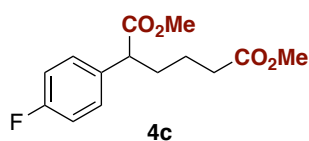
<sup>1</sup>H NMR (400 MHz, CDCl<sub>3</sub>) δ 7.62 – 7.55 (m, 2H), 7.42 (d, *J* = 8.1 Hz, 2H), 3.67 (s, 3H), 3.65 (s, 3H), 3.62 (t, *J* = 7.7 Hz, 1H), 2.40 – 2.24 (m, 2H), 2.11 (dddd, *J* = 13.2, 10.6, 7.7, 5.5 Hz, 1H), 1.82 (dddd, *J* = 13.4, 10.3, 7.6, 5.6 Hz, 1H), 1.69 – 1.46 (m, 2H) ppm.

<sup>13</sup>C NMR (101 MHz, CDCl<sub>3</sub>) δ 173.6, 173.5, 142.8 (d, *J* = 1.2 Hz), 129.9 (q, *J* = 32.5 Hz), 128.5, 125.8 (q, *J* = 3.8 Hz), 124.2 (q, *J* = 272.7 Hz), 52.4, 51.7, 51.3, 33.7, 32.9, 22.9 ppm.

<sup>19</sup>F NMR (376 MHz, CDCl<sub>3</sub>) δ -62.6 ppm.

IR (neat, cm<sup>-1</sup>): 2955, 1732, 1619, 1437, 1421, 1161, 1111, 1067, 1018, 839.

HRMS ESI, (C<sub>15</sub>H<sub>17</sub>F<sub>3</sub>NaO<sub>4</sub>) [M+Na]<sup>+</sup> *calculated* 341.0971, *found* 341.0972.



**4c**

**Dimethyl 2-(4-fluorophenyl)hexanedioate (4c).**

General procedure B was followed using 1-(buta-1,3-dien-1-yl)-4-fluorobenzene (**1c**) (29.6 mg, 0.20 mmol), affording **4c** (37.2 mg, 69% yield). In a separate experiment, 38.3 mg (71%) were obtained, giving an average yield of 70%. Colorless oil.

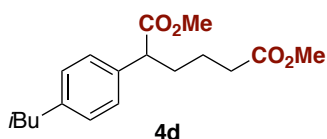
<sup>1</sup>H NMR (400 MHz, CDCl<sub>3</sub>) δ 7.29 – 7.22 (m, 2H), 7.04 – 6.97 (m, 2H), 3.65 (s, 3H), 3.65 (s, 3H), 3.53 (t, *J* = 7.7 Hz, 1H), 2.38 – 2.24 (m, 2H), 2.06 (dddd, *J* = 13.3, 10.4, 7.7, 5.7 Hz, 1H), 1.78 (dddd, *J* = 13.5, 10.0, 7.7, 5.9 Hz, 1H), 1.64 – 1.48 (m, 2H) ppm.

<sup>13</sup>C NMR (101 MHz, CDCl<sub>3</sub>) δ 174.2, 173.7, 162.2 (d, *J* = 245.8 Hz), 134.5 (d, *J* = 3.2 Hz), 129.6 (d, *J* = 7.9 Hz), 115.7 (d, *J* = 21.4 Hz), 52.2, 51.7, 50.7, 33.8, 33.0, 23.0 ppm.

<sup>19</sup>F NMR (376 MHz, CDCl<sub>3</sub>) δ -115.43 ppm.

IR (neat, cm<sup>-1</sup>): 2953, 1731, 1604, 1509, 1436, 1356, 1221, 1155, 1100, 836, 809.

HRMS ESI, (C<sub>14</sub>H<sub>17</sub>FNao<sub>4</sub>) [M+Na]<sup>+</sup> *calculated* 291.1003, *found* 291.1001.



**4d**

**Dimethyl 2-(4-isobutylphenyl)hexanedioate (4d).**

General procedure B was followed using (*E,Z*)-1-(buta-1,3-dien-1-yl)-4-isobutylbenzene (**1d**) (37.3 mg, 0.20 mmol), affording **4d** (40.0 mg, 65% yield). In a separate

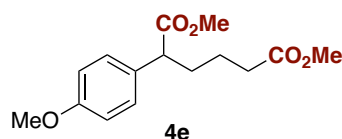
experiment, 38.2 mg (62%) were obtained, giving an average yield of 64%. Colorless oil.

**<sup>1</sup>H NMR** (500 MHz, CDCl<sub>3</sub>) δ 7.18 (d, *J* = 8.1 Hz, 2H), 7.08 (d, *J* = 8.1 Hz, 2H), 3.65 (s, 3H), 3.64 (s, 3H), 3.52 (t, *J* = 7.3 Hz, 1H), 2.44 (d, *J* = 7.2 Hz, 2H), 2.31 (ddd, *J* = 7.9, 7.0, 4.0 Hz, 2H), 2.13 – 2.01 (m, 1H), 1.90 – 1.73 (m, 2H), 1.64 – 1.51 (m, 2H), 0.89 (d, *J* = 6.6 Hz, 6H) ppm.

**<sup>13</sup>C NMR** (126 MHz, CDCl<sub>3</sub>) δ 174.5, 173.8, 140.9, 136.1, 129.5, 127.7, 52.1, 51.6, 51.1, 45.2, 33.9, 33.0, 30.3, 23.1, 22.5 ppm.

**IR** (neat, cm<sup>-1</sup>): 2952, 2926, 2868, 1734, 1512, 1435, 1365, 1259, 1200, 1163, 1021, 845, 798.

**HRMS** ESI, (C<sub>18</sub>H<sub>26</sub>NaO<sub>4</sub>) [M+Na]<sup>+</sup> *calculated* 329.1723, *found* 329.1721.



**Dimethyl 2-(4-methoxyphenyl)hexanedioate (4e).**

General procedure B was followed using 1-(buta-1,3-dien-1-yl)-4-methoxybenzene (**1e**) (32.0 mg, 0.20 mmol), affording **4e** (36.4 mg, 65% yield). In a separate experiment, 38.7 mg (69%) were obtained,

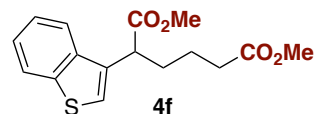
giving an average yield of 67%. Colorless oil.

**<sup>1</sup>H NMR** (500 MHz, CDCl<sub>3</sub>) δ 7.20 (d, *J* = 8.6 Hz, 2H), 6.85 (d, *J* = 8.7 Hz, 2H), 3.78 (s, 3H), 3.64 (s, 3H), 3.64 (s, 3H), 3.49 (t, *J* = 7.7 Hz, 1H), 2.38 – 2.23 (m, 2H), 2.05 (dddd, *J* = 13.4, 10.3, 7.7, 5.8 Hz, 1H), 1.78 (dddd, *J* = 13.6, 9.9, 7.8, 5.9 Hz, 1H), 1.64 – 1.49 (m, 2H) ppm.

**<sup>13</sup>C NMR** (126 MHz, CDCl<sub>3</sub>) δ 174.6, 173.8, 159.0, 130.9, 129.0, 114.2, 55.4, 52.1, 51.7, 50.6, 33.9, 33.0, 23.0 ppm.

**IR** (neat, cm<sup>-1</sup>): 2952, 1730, 1611, 1511, 1436, 1246, 1162, 1033, 832, 795.

**HRMS** ESI, (C<sub>15</sub>H<sub>20</sub>NaO<sub>5</sub>) [M+Na]<sup>+</sup> *calculated* 303.1203, *found* 303.1193.



**Dimethyl 2-(benzo[*b*]thiophen-3-yl)hexanedioate (4f).**

General procedure B was followed using 3-(buta-1,3-dien-1-yl)benzo[*b*]thiophene (**1f**) (37.3 mg, 0.20 mmol), affording **4f** (35.6 mg, 58% yield). In a separate

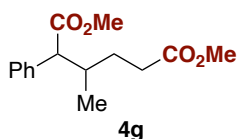
experiment, 38.2 mg (62%) were obtained, giving an average yield of 60%. Colorless oil.

**<sup>1</sup>H NMR** (400 MHz, CDCl<sub>3</sub>) δ 7.85 (ddt, *J* = 9.7, 8.0, 0.8 Hz, 2H), 7.45 – 7.32 (m, 2H), 7.37 (s, 1H), 4.03 (t, *J* = 7.6 Hz, 1H), 3.67 (s, 3H), 3.65 (s, 3H), 2.35 (td, *J* = 7.4, 1.5 Hz, 2H), 2.21 (dddd, *J* = 13.8, 10.1, 8.2, 6.1 Hz, 1H), 1.99 (ddt, *J* = 13.5, 9.3, 6.7 Hz, 1H), 1.78 – 1.63 (m, 2H) ppm.

**<sup>13</sup>C NMR** (101 MHz, CDCl<sub>3</sub>) δ 173.7, 173.6, 140.5, 138.2, 133.2, 124.6, 124.3, 123.4, 123.1, 121.8, 52.3, 51.7, 45.0, 33.8, 32.1, 23.2 ppm.

IR (neat, cm<sup>-1</sup>): 2950, 1730, 1432, 1195, 1153, 763, 732.

HRMS ESI, (C<sub>16</sub>H<sub>18</sub>NaO<sub>4</sub>S) [M+Na]<sup>+</sup> *calculated* 329.0817, *found* 329.0818.



**Dimethyl 3-methyl-2-phenylhexanedioate (4g).** General procedure B was followed using (*E*)-(2-Methylbuta-1,3-dien-1-yl)benzene (**1g**) (28.8 mg, 0.20 mmol), affording **4g** (40.9 mg, 77% yield) as a mixture of diastereoisomers (1.5:1). In a separate experiment, 38.3 mg (72%) were obtained, giving an average yield of 75%.

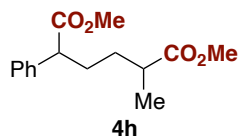
Colorless oil.

<sup>1</sup>H NMR (400 MHz, CDCl<sub>3</sub>) δ 7.34 – 7.22 (m, 10H), 3.68 (s, 3H), 3.65 (s, 3H), 3.64 (s, 3H), 3.59 (s, 3H), 3.27 (d, *J* = 10.5 Hz, 2H), 2.50 – 2.10 (m, 6H), 1.85 (dddd, *J* = 13.5, 9.9, 6.3, 3.4 Hz, 1H), 1.62 – 1.44 (m, 2H), 1.20 (dtd, *J* = 13.7, 9.5, 5.5 Hz, 1H), 1.01 (d, *J* = 6.5 Hz, 3H), 0.68 (d, *J* = 6.7 Hz, 3H) ppm.

<sup>13</sup>C NMR (126 MHz, CDCl<sub>3</sub>) δ 174.2 (M=major), 174.2 (m=minor), 174.0(m), 173.9(M), 137.9(m), 137.6(M), 128.8(M), 128.7(M), 128.7(m), 128.7(m), 127.6(M), 127.5(m), 58.7(M), 58.5(m), 52.0(m), 51.9(M), 51.7(m), 51.6(M), 36.1(m), 35.9(M), 31.9(m), 31.5(M), 30.5(m), 28.8(M), 17.8(M), 16.6(m) ppm.

IR (neat, cm<sup>-1</sup>): 2952, 1731, 1454, 1434, 1265, 1239, 1196, 1151, 1096, 1008, 732, 700.

HRMS ESI, (C<sub>15</sub>H<sub>20</sub>NaO<sub>4</sub>) [M+Na]<sup>+</sup> *calculated* 287.1254, *found* 287.1257.



**Dimethyl 2-methyl-5-phenylhexanedioate (4h).** General procedure B was followed using NiBr<sub>4</sub>(TBA)<sub>2</sub> (17.4 mg, 0.02 mmol, 10 mol%), **L19** (7.0 mg, 0.02 mmol, 10 mol%) and penta-1,3-dien-1-ylbenzene (**1h**) (28.8 mg, 0.20 mmol) at 60 °C,

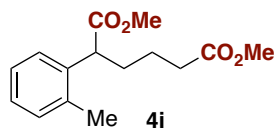
affording **4h** (34.2 mg, 65% yield) as a mixture of diastereoisomers (1:1). In a separate experiment, 37.1 mg (70%) were obtained, giving an average yield of 68%. Colorless oil.

<sup>1</sup>H NMR (500 MHz, CDCl<sub>3</sub>) δ 7.35 – 7.21 (m, 5H), 3.66 – 3.63 (m, 5H), 3.52 (t, *J* = 7.7 Hz, 1H), 2.48 – 2.39 (m, 1H), 2.12 – 2.00 (m, 1H), 1.84 – 1.71 (m, 1H), 1.68 – 1.54 (m, 1H), 1.44 – 1.28 (m, 1H), 1.13 (d, *J* = 7.1 Hz, 1H), 1.12 (d, *J* = 7.1 Hz, 2H) ppm.

<sup>13</sup>C NMR (126 MHz, CDCl<sub>3</sub>) δ 176.9, 174.3, 174.2, 138.9, 138.8, 128.8, 128.1, 128.0, 127.4, 52.1, 51.7, 51.6, 51.5, 39.4, 39.3, 31.7, 31.6, 31.2, 31.1, 17.3, 17.1 ppm.

IR (neat, cm<sup>-1</sup>): 2951, 1731, 1455, 1434, 1355, 1258, 1199, 1157, 734, 700.

HRMS ESI, (C<sub>15</sub>H<sub>20</sub>NaO<sub>4</sub>) [M+Na]<sup>+</sup> *calculated* 287.1254, *found* 287.1252.



**Dimethyl 2-(*o*-tolyl)hexanedioate (4i).** General procedure B was followed using (*E,Z*)-1-(buta-1,3-dien-1-yl)-2-methylbenzene (**1i**) (28.8 mg, 0.20 mmol), affording **4i** (46.5 mg, 88% yield). In a separate experiment, 48.2 mg

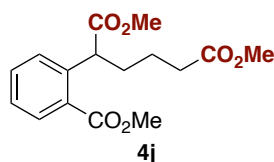
(91%) were obtained, giving an average yield of 90%. Colorless oil.

**<sup>1</sup>H NMR** (500 MHz, CDCl<sub>3</sub>) δ 7.27 (dt, *J* = 7.1, 1.3 Hz, 1H), 7.19 – 7.11 (m, 3H), 3.84 (t, *J* = 7.6 Hz, 1H), 3.65 (s, 3H), 3.64 (s, 3H), 2.38 (s, 3H), 2.35 – 2.29 (m, 2H), 2.16 – 2.07 (m, 1H), 1.83 – 1.72 (m, 1H), 1.70 – 1.51 (m, 2H) ppm.

**<sup>13</sup>C NMR** (126 MHz, CDCl<sub>3</sub>) δ 174.5, 173.8, 137.4, 136.2, 130.7, 127.2, 126.8, 126.6, 52.1, 51.6, 46.7, 34.0, 32.6, 23.1, 19.9 ppm.

**IR** (neat, cm<sup>-1</sup>): 3021, 2952, 2871, 1732, 1492, 1435, 1356, 1198, 1148, 1109, 736.

**HRMS** ESI, (C<sub>15</sub>H<sub>20</sub>NaO<sub>4</sub>) [M+Na]<sup>+</sup> *calculated* 287.1254, *found* 287.1253.



**Dimethyl 2-(2-(methoxycarbonyl)phenyl)hexanedioate (4j).** General procedure B was followed using methyl 2-(buta-1,3-dien-1-yl)benzoate (**1j**) (37.6 mg, 0.20 mmol), affording **4j** (49.6 mg, 80% yield). In a separate experiment, 50.5 mg (82%) were obtained, giving an

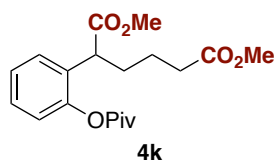
average yield of 81%. Colorless oil.

**<sup>1</sup>H NMR** (500 MHz, CDCl<sub>3</sub>) δ 7.89 (dd, *J* = 7.9, 1.4 Hz, 1H), 7.47 (td, *J* = 7.6, 1.5 Hz, 1H), 7.40 (dd, *J* = 7.9, 1.3 Hz, 1H), 7.34 – 7.28 (m, 1H), 4.63 (t, *J* = 7.3 Hz, 1H), 3.90 (d, *J* = 0.7 Hz, 3H), 3.63 (s, 3H), 3.63 (s, 3H), 2.38 – 2.26 (m, 2H), 2.13 (dddd, *J* = 13.0, 10.4, 7.5, 5.2 Hz, 1H), 1.81 (dddd, *J* = 13.0, 10.5, 7.1, 5.4 Hz, 1H), 1.73 – 1.49 (m, 2H) ppm.

**<sup>13</sup>C NMR** (101 MHz, CDCl<sub>3</sub>) δ 174.3, 173.8, 168.0, 140.3, 132.4, 130.9, 129.8, 128.7, 127.1, 52.3, 52.1, 51.6, 46.8, 33.9, 33.0, 23.1 ppm.

**IR** (neat, cm<sup>-1</sup>): 2952, 1719, 1577, 1434, 1255, 1193, 1166, 1130, 1085, 745, 712.

**HRMS** ESI, (C<sub>16</sub>H<sub>20</sub>NaO<sub>6</sub>) [M+Na]<sup>+</sup> *calculated* 331.1152, *found* 331.1154.



**Dimethyl 2-(2-(pivaloyloxy)phenyl)hexanedioate (4k)** General procedure B was followed using 2-(buta-1,3-dien-1-yl)phenyl pivalate (**1k**) (46.1 mg, 0.20 mmol), affording **4k** (60.8 mg, 87% yield). In a separate experiment, 62.9 mg (90%) were obtained, giving an average yield of 89%.

Colorless oil.

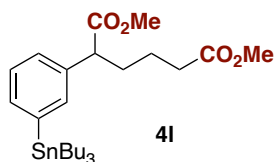
**<sup>1</sup>H NMR** (400 MHz, CDCl<sub>3</sub>) δ 7.38 (dd, *J* = 7.6, 1.8 Hz, 1H), 7.26 (td, *J* = 7.7, 1.8 Hz, 1H), 7.20 (td, *J* = 7.5, 1.5 Hz, 1H), 6.99 (dd, *J* = 8.0, 1.4 Hz, 1H), 3.75 (t, *J* = 7.6 Hz, 1H), 3.64 (s, 3H), 3.62 (s, 3H), 2.38 – 2.22 (m, 2H), 2.08 (dddd, *J* = 13.3, 10.6, 7.8, 5.5 Hz, 1H), 1.77 (dddd, *J* = 13.2, 10.2, 7.4, 5.6 Hz, 1H), 1.70 – 1.48 (m, 2H), 1.39 (s, 9H) ppm.



<sup>13</sup>C NMR (126 MHz, CDCl<sub>3</sub>) δ 176.8, 173.7, 149.0, 130.9, 128.6, 128.3, 126.2, 122.7, 100.1, 52.2, 51.6, 44.4, 39.4, 33.8, 31.8, 27.3, 23.1 ppm.

IR (neat, cm<sup>-1</sup>): 2954, 2032, 1734, 1435, 1206, 1107, 756.

HRMS ESI, (C<sub>19</sub>H<sub>26</sub>NaO<sub>6</sub>) [M+Na]<sup>+</sup> *calculated* 373.1622, *found* 373.1626.



4l

**Dimethyl 2-(3-(tributylstannyl)phenyl) hexanedioate**

**(4l).** General procedure B was followed, but the reduction step was performed with H<sub>2</sub> instead of B<sub>2</sub>(OH)<sub>4</sub> and H<sub>2</sub>O, using 3-(buta-1,3-dien-1-yl)phenyltributylstannane (**1l**) (83.8 mg, 0.20 mmol), affording **4l** (58.1 mg, 54% yield). In

a separate experiment, 57.4 mg (53%) were obtained, giving an average yield of 54%. Colorless oil.

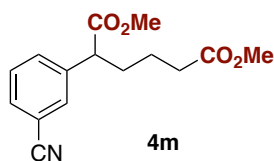
<sup>1</sup>H NMR (400 MHz, CDCl<sub>3</sub>) δ 7.35 – 7.23 (m, 4H), 3.65 (s, 3H), 3.65 (s, 3H), 3.55 (t, *J* = 7.7 Hz, 1H), 2.40 – 2.23 (m, 2H), 2.09 (dddd, *J* = 13.4, 10.4, 7.8, 5.7 Hz, 1H), 1.81 (dddd, *J* = 13.5, 10.0, 7.6, 5.8 Hz, 1H), 1.76 – 1.51 (m, 8H), 1.45 – 1.20 (m, 12H), 0.92 (t, *J* = 7.3 Hz, 9H) ppm.

<sup>13</sup>C NMR (101 MHz, CDCl<sub>3</sub>) δ 174.3, 173.8, 138.9, 128.8, 128.0, 127.5, 77.5, 77.2, 76.8, 52.2, 51.7, 51.5, 33.9, 33.0, 28.0, 27.0, 23.0, 17.7, 13.7 ppm.

<sup>119</sup>Sn NMR (149 MHz, CDCl<sub>3</sub>) δ 156.3 ppm.

IR (neat, cm<sup>-1</sup>): 2953, 2871, 1733, 1455, 1435, 1199, 1165, 700.

HRMS Obtaining a High Resolution Mass data of the molecular ion was proved to be difficult using ESI, APCI and MALDI ionization modes. However, using ESI we could determine the exact mass of two fragments of the molecule: (C<sub>8</sub>H<sub>19</sub>Sn)<sup>+</sup> *calculated* 231.0499, *found* 231.0506, (C<sub>14</sub>H<sub>18</sub>NaO<sub>4</sub>)<sup>+</sup> = [M-SnBu<sub>3</sub>+Na]<sup>+</sup> *calculated* 273.1097, *found* 273.1095.



4m

**Dimethyl 2-(3-cyanophenyl)hexanedioate**

**(4m).** General procedure B was followed using 3-(buta-1,3-dien-1-yl)benzotrinitrile (**1m**) (31.0 mg, 0.20 mmol), affording **4m** (29.3 mg, 53% yield). In a separate experiment, 58.5 mg (49%) were obtained, giving an average yield of 51%.

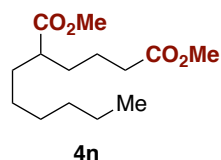
Colorless oil.

<sup>1</sup>H NMR (400 MHz, CDCl<sub>3</sub>) δ 7.60 (s, 1H), 7.57 – 7.53 (m, 2H), 7.43 (t, *J* = 7.7 Hz, 1H), 3.67 (s, 3H), 3.65 (s, 3H), 3.59 (t, *J* = 7.7 Hz, 1H), 2.32 (td, *J* = 7.4, 2.9 Hz, 2H), 2.10 (dddd, *J* = 13.2, 10.6, 7.8, 5.4 Hz, 1H), 1.80 (dddd, *J* = 13.3, 10.4, 7.6, 5.5 Hz, 1H), 1.57 (dtdd, *J* = 21.2, 10.7, 7.4, 5.5 Hz, 2H) ppm.

<sup>13</sup>C NMR (101 MHz, CDCl<sub>3</sub>) δ 173.5, 173.3, 140.3, 132.6, 131.8, 131.3, 129.6, 118.7, 113.0, 52.5, 51.7, 51.1, 33.6, 32.8, 22.9 ppm.

**IR** (neat,  $\text{cm}^{-1}$ ): 2953, 2927, 2853, 2230, 1730, 1435, 1195, 1165, 691.

**HRMS** ESI, ( $\text{C}_{15}\text{H}_{17}\text{NNaO}_4$ ) [ $\text{M}+\text{Na}$ ] $^+$  *calculated* 298.1050, *found* 298.1049.



**Dimethyl 2-hexylhexanedioate (4n).** General procedure B was followed using  $\text{NiBr}_4(\text{TBA})_2$  (17.4 mg, 0.02 mmol, 10 mol%), **L19** (7.0 mg, 0.02 mmol, 10 mol%) and (*E,Z*)-deca-1,3-diene (**1n**) (27.7 mg, 0.20 mmol), affording **4n** (36.9 mg, 71% yield). In a separate experiment, 38.8 mg (75%) were obtained, giving an

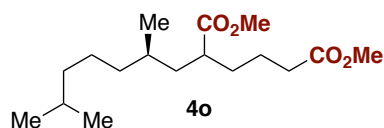
average yield of 73%. Colorless oil.

**$^1\text{H}$  NMR** (500 MHz,  $\text{CDCl}_3$ )  $\delta$  3.66 (s, 3H), 3.65 (s, 3H), 2.37 – 2.32 (m, 1H), 2.29 (t,  $J$  = 7.1 Hz, 2H), 1.60 (tdd,  $J$  = 14.7, 8.8, 6.1 Hz, 4H), 1.51 – 1.39 (m, 2H), 1.24 (q,  $J$  = 7.5, 5.4 Hz, 8H), 0.86 (t,  $J$  = 6.7 Hz, 3H) ppm.

**$^{13}\text{C}$  NMR** (126 MHz,  $\text{CDCl}_3$ )  $\delta$  176.7, 173.9, 51.6, 51.5, 45.5, 34.0, 32.5, 31.9, 31.8, 29.3, 27.4, 23.0, 22.7, 14.2 ppm.

**IR** (neat,  $\text{cm}^{-1}$ ): 2952, 2929, 2868, 1737, 1458, 1436, 1256, 1198, 1164.

**HRMS** ESI, ( $\text{C}_{14}\text{H}_{26}\text{NaO}_4$ ) [ $\text{M}+\text{Na}$ ] $^+$  *calculated* 281.1723, *found* 281.1722.



**Dimethyl 2-(2,6-dimethylheptyl) hexanedioate (4o).** General procedure B was followed using  $\text{NiBr}_4(\text{TBA})_2$  (17.4 mg, 0.02 mmol, 10 mol%), **L19** (7.0 mg, 0.02 mmol, 10 mol%) and **1o** (35.7 mg,

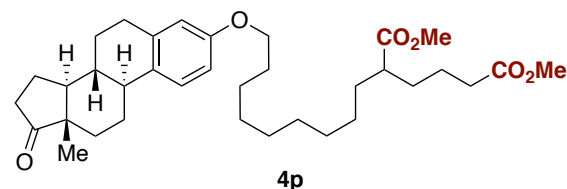
0.20 mmol), affording **4o** (34.9 mg, 58% yield) as a 1:1 mixture of diastereoisomers. In a separate experiment, 37.1 mg (62%) were obtained, giving an average yield of 60%. Colorless oil.

**$^1\text{H}$  NMR** (400 MHz,  $\text{CDCl}_3$ )  $\delta$  3.68 (s, 3H), 3.68 (s, 3H), 2.53 – 2.42 (m, 1H), 2.32 (t,  $J$  = 7.1 Hz, 2H), 1.76 – 1.57 (m, 4H), 1.57 – 1.45 (m, 2H), 1.44 – 1.05 (m, 8H), 0.92 – 0.82 (m, 9H) ppm.

**$^{13}\text{C}$  NMR** (75 MHz,  $\text{CDCl}_3$ )  $\delta$  176.9, 176.7, 173.7, 51.5, 51.4, 51.4, 43.2, 43.1, 40.0, 39.9, 39.2, 37.7, 36.7, 33.9, 32.6, 31.9, 31.0, 30.8, 27.9, 24.5, 24.5, 22.9, 22.8, 22.7, 22.6, 22.6, 19.7, 19.3 ppm.

**IR** (neat,  $\text{cm}^{-1}$ ): 2952, 2927, 2869, 1735, 1435, 1366, 1195, 1156.

**HRMS** ESI, ( $\text{C}_{17}\text{H}_{32}\text{NaO}_4$ ) [ $\text{M}+\text{Na}$ ] $^+$  *calculated* 325.2193, *found* 323.2185.



**Dimethyl 2-(9-(((8*R*,9*S*,13*S*,14*S*)-13-methyl-17-oxo-7,8,9,11,12,13,14,15,16,17-decahydro-6*H*-cyclopenta[*a*]phenanthren-3-yl)oxy)nonyl)hexanedioate (4p).**

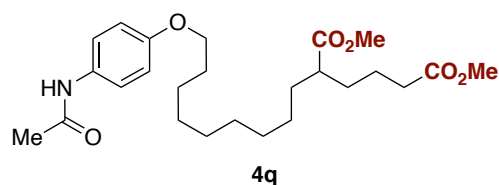
General procedure B was followed using NiBr<sub>4</sub>(TBA)<sub>2</sub> (17.4 mg, 0.02 mmol, 10 mol%), **L19** (7.0 mg, 0.02 mmol, 10 mol%) and **1p** (89.7 mg, 0.20 mmol) at 60 °C, affording **4p** (58.0 mg, 51% yield) as 1:1 mixture of diastereoisomers. In a separate experiment, 60.4 mg (53%) were obtained, giving an average yield of 52%. Light orange oil.

<sup>1</sup>H NMR (500 MHz, CDCl<sub>3</sub>) δ 7.18 (d, *J* = 8.6 Hz, 1H), 6.70 (dd, *J* = 8.6, 2.7 Hz, 1H), 6.63 (d, *J* = 2.7 Hz, 1H), 3.91 (t, *J* = 6.6 Hz, 2H), 3.67 (s, 3H), 3.66 (s, 3H), 2.93 – 2.85 (m, 2H), 2.49 (dd, *J* = 19.0, 8.7 Hz, 1H), 2.42 – 2.33 (m, 2H), 2.30 (t, *J* = 7.1 Hz, 2H), 2.27 – 2.21 (m, 1H), 2.17 – 1.91 (m, 4H), 1.74 (p, *J* = 6.7 Hz, 2H), 1.66 – 1.38 (m, 11H), 1.36 – 1.21 (m, 10H), 0.90 (s, 3H) ppm.

<sup>13</sup>C NMR (126 MHz, CDCl<sub>3</sub>) δ 176.7, 173.8, 157.3, 137.8, 131.9, 126.4, 114.7, 112.2, 68.0, 51.6, 51.5, 50.5, 48.1, 45.4, 44.1, 38.5, 36.0, 34.0, 32.5, 31.9, 31.7, 29.8, 29.6, 29.6, 29.5, 29.4, 27.5, 26.7, 26.2, 26.0, 22.9, 21.7, 14.0 ppm.

IR (neat, cm<sup>-1</sup>): 2925, 2855, 1734, 1609, 1499, 1455, 1435, 1281, 1253, 1195, 1157, 1055, 1007, 873, 819.

HRMS ESI, (C<sub>35</sub>H<sub>52</sub>NaO<sub>6</sub>) [M+Na]<sup>+</sup> calculated 591.3656, found 591.3683.



**Dimethyl 2-(9-(4-acetamidophenoxy)nonyl)hexanedioate (4q).** General procedure B was followed using NiBr<sub>4</sub>(TBA)<sub>2</sub> (17.4 mg, 0.02 mmol, 10 mol%), **L19** (7.0 mg, 0.02 mmol, 10 mol%) and **1q** (65.9 mg, 0.20 mmol), affording **4q** (50.7 mg, 56% yield) as a 1:1 mixture of diastereoisomers. In a separate experiment, 52.3 mg (58%) were obtained, giving an average yield of 57%. Light brown solid.

**Mp** 83-85 °C.

<sup>1</sup>H NMR (400 MHz, CDCl<sub>3</sub>) δ 7.36 (d, *J* = 8.9 Hz, 2H), 7.25 (s, 1H), 6.83 (d, *J* = 8.9 Hz, 2H), 3.91 (t, *J* = 6.6 Hz, 2H), 3.67 (s, 3H), 3.66 (s, 3H), 2.38 – 2.33 (m, 1H), 2.30 (t, *J* = 7.1 Hz, 2H), 2.14 (s, 3H), 1.80 – 1.67 (m, 4H), 1.66 – 1.54 (m, 4H), 1.51 – 1.38 (m, 4H), 1.35 – 1.20 (m, 8H) ppm.

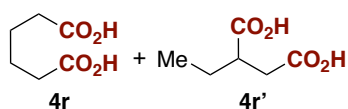
<sup>13</sup>C NMR (101 MHz, CDCl<sub>3</sub>) δ 176.7, 173.9, 168.3, 156.2, 130.9, 122.0, 114.9, 68.4, 51.7, 51.6, 45.5, 34.0, 32.5, 31.9, 29.6, 29.6, 29.5, 29.4, 29.4, 27.5, 26.1, 24.5, 23.0 ppm.

IR (neat, cm<sup>-1</sup>): 3341, 2924, 2893, 2850, 1730, 1708, 1678, 1599, 1547, 1510, 1434, 1367, 1301, 1232, 1210, 1173, 1034, 836.

HRMS ESI, (C<sub>25</sub>H<sub>39</sub>NNaO<sub>6</sub>) [M+Na]<sup>+</sup> calculated 472.2670, found 472.2677.

**Ni-catalysed carboxylation of Diene Feedstocks.**

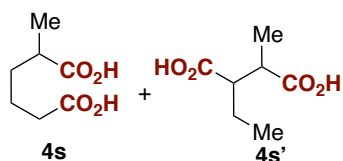
**General procedure C:** An oven-dried Schlenk tube equipped with a magnetic stirring bar was charged with Mn dust (11.0 mg, 0.2 mmol, 1.0 equiv), **L19** (7.0 mg, 0.02 mmol, 0.10 equiv) and NiBr<sub>4</sub>(TBA)<sub>2</sub> (17.4 mg, 0.02 mmol, 0.10 equiv). The Schlenk tube was filled with carbon dioxide by applying three cycles of vacuum/CO<sub>2</sub>. Subsequently, the 1,3-diene (0.40 mmol, 2 equiv) was added by syringe followed by DMA (0.40 mL) with a constant flow of CO<sub>2</sub>. The Schlenk flask was tightly sealed and stirred at 50 °C for 60 hours (unless stated otherwise) after which it was quenched by careful addition of HCl 2M. The reaction mixture was diluted with water and extracted 3 times with EtOAc. The combined organic phases were washed with brine, dried over MgSO<sub>4</sub> and filtered. The solvent was then removed under vacuum and it was purified by column chromatography (hexane/EtOAc/HCOOH 75/25/0 to 50/50/0.5), and the product was reduced by mixing it with 10% Pd/C (10.6 mg, 5 mol%) in MeOH (2 mL) under H<sub>2</sub> atmospheres at rt for 24 h. The solution was filtered through celite and the solvent was removed under reduced pressure to obtain the targeted product.



**Adipic acid (4r) [CAS: 124-04-9].** General procedure C was followed using 1,3-butadiene (0.2 mL of a 2.0M solution in THF, 0.40 mmol), affording **4r** (17.3 mg, 59% yield) as a 93:7 (**4r**:**4r'**) mixture. In a separate experiment, 18.3 mg (63%) were obtained, giving an average yield of 61%. White solid.

<sup>1</sup>H NMR (500 MHz, Acetone-*d*<sub>6</sub>) δ 2.31 (t, *J* = 5.9 Hz, 4H, **4r**), 1.64 (t, *J* = 5.8 Hz, 4H, **4r**), 0.94 (t, *J* = 7.4 Hz, 3H, **4r'**) ppm.

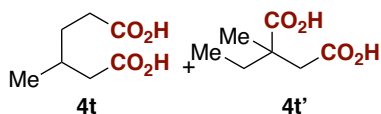
<sup>13</sup>C NMR (126 MHz, Acetone-*d*<sub>6</sub>) δ 174.8 (**4r**), 33.9 (**4r**), 25.1(**4r**), 11.6 (**4r'**) ppm.



**2-Methylhexanedioic acid (4s) [CAS: 626-70-0].** General procedure C was followed using 1,3-pentadiene (40 μL, 0.40 mmol), affording **4s** (19.9 mg, 62% yield) as a >99:1 (**4s**:**4s'**) mixture. In a separate experiment, 19.5 mg (61%) were obtained, giving an average yield of 61%. Colorless oil.

<sup>1</sup>H NMR (400 MHz, Acetone-*d*<sub>6</sub>) δ = 2.42 (q, *J* = 6.9 Hz, 1H), 2.29 (t, *J* = 7.1 Hz, 2H), 1.72 – 1.57 (m, 3H), 1.50 – 1.41 (m, 1H), 1.14 (d, *J* = 6.9 Hz, 3H) ppm.

<sup>13</sup>C NMR (101 MHz, Acetone-*d*<sub>6</sub>) δ 177.8, 174.7, 39.6, 34.1, 33.9, 23.4, 17.4 ppm.



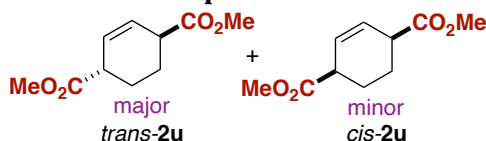
**3-Methylhexanedioic acid (4t) [CAS: 3058-01-3] / 2-ethyl-2-methylsuccinic acid (4t') [CAS: 631-31-2].** General procedure C was followed using

isoprene (40  $\mu$ L, 0.40 mmol), affording **4t** (20.8 mg, 65% yield) as a 77:23 (**4t**:**4t'**) mixture. In a separate experiment, 20.5 mg (64%) were obtained, giving an average yield of 61%. The major isomer was identified by its characteristic doublet that integrates 3 protons at  $\delta = 0.98$  in <sup>1</sup>H NMR. Colorless oil.

<sup>1</sup>H NMR (500 MHz, Acetone-*d*<sub>6</sub>)  $\delta$  2.71 (d, *J* = 16.1 Hz, 1H, **4t'**), 2.42 (d, *J* = 16.1 Hz, 1H, **4t'**), 2.37 – 2.31 (m, 2H, **4t**), 2.17 – 2.05 (m, 3H, **4t**), 2.02 – 1.93 (m, 2H, **4t'**), 1.75 – 1.62 (m, 1H, **4t'**), 1.58 – 1.48 (m, 1H, **4t'**), 1.24 (s, 3H, **4t'**), 0.98 (d, *J* = 6.7 Hz, 3H, **4t**), 0.88 (t, *J* = 7.5 Hz, 3H, **4t'**) ppm.

<sup>13</sup>C NMR (126 MHz, Acetone-*d*<sub>6</sub>)  $\delta$  174.1 (**4t'**), 174.0(**4t**), 173.3(**4t**), 172.5(**4t'**), 43.8(**4t'**), 41.8(**4t'**), 40.7(**4t**), 31.9(**4t'**), 31.4(**4t**), 31.1(**4t**), 29.6(**4t**), 21.1(**4t'**), 18.8(**4t**), 8.1(**4t'**) ppm.

### Mechanistic experiments



**Dimethyl cyclohex-2-ene-1,4-dicarboxylate (*trans*-**2u** and *cis*-**2u**).** An oven-dried Schlenk tube equipped with a magnetic stirring bar was charged with Mn dust (11.0 mg, 0.2 mmol, 1.0 equiv), **L19** (7.0 mg, 0.02 mmol, 0.10 equiv) and NiBr<sub>4</sub>(TBA)<sub>2</sub> (17.4 mg, 0.02 mmol, 0.10 equiv). The Schlenk tube was filled with CO<sub>2</sub> by applying three vacuum/CO<sub>2</sub> cycles. Subsequently, 1,3-cyclohexadiene (**1u**) (0.20 mmol, 1 equiv) was added followed by DMA (0.40 mL) with a constant flow of CO<sub>2</sub>. The Schlenk flask was sealed and stirred at 50 °C for 60 h after which it was quenched by careful addition of HCl 2M. The reaction mixture was diluted with water and extracted 3 times with EtOAc. The combined organic phases were washed with brine, dried over MgSO<sub>4</sub> and filtered. The solvent was then removed under vacuum and it was dissolved in a 1:1 MeOH:Et<sub>2</sub>O mixture and cooled down to 0 °C. TMSCHN<sub>2</sub> (0.4 mL of a 2 M solution in Et<sub>2</sub>O, 4 equiv) was added dropwise and after 30 minutes silica gel was added and solvent was removed under vacuum. The compound was purified by column chromatography (hexane/EtOAc mixtures) to give 24.1 mg (60% yield) of a mixture of isomers 91:9 *trans*-**2u**:*cis*-**2u**. Light orange oil.

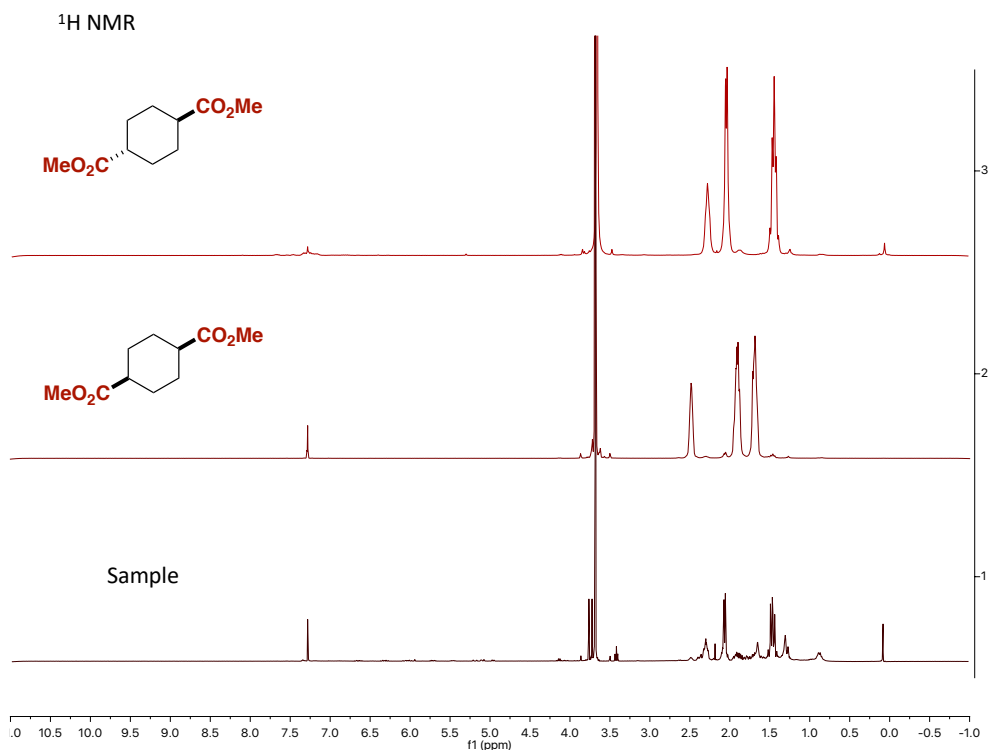
<sup>1</sup>H NMR (400 MHz, CDCl<sub>3</sub>)  $\delta$  5.94 – 5.93 (m, 2H, *cis*-**2u**), 5.92 – 5.91 (m, 2H, *trans*-**2u**), 3.73 (s, 6H, *cis*-**2u**), 3.69 (s, 6H, *trans*-**2u**), 3.16 – 3.08 (m, 1H), 2.11 – 2.02 (m, 1H), 1.86 – 1.77 (m, 1H) ppm.

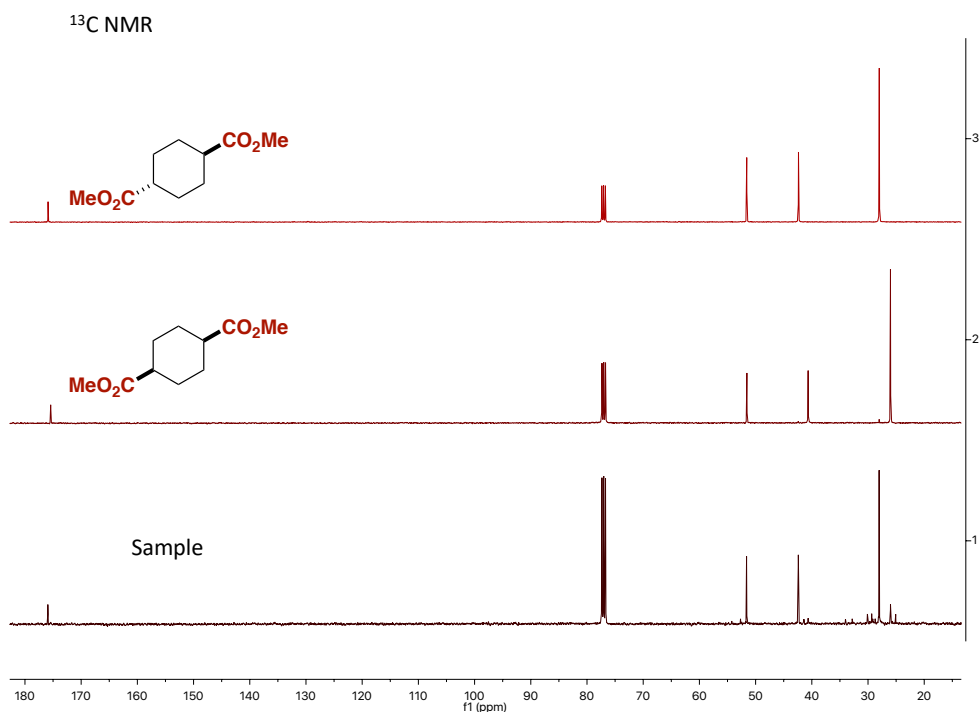
<sup>13</sup>C NMR (75 MHz, CDCl<sub>3</sub>)  $\delta$  174.3 (*trans*-**2u**), 173.4 (*cis*-**2u**), 126.8 (*trans*-**2u**), 126.1 (*cis*-**2u**), 52.1 (*trans*-**2u**), 51.7 (*cis*-**2u**), 40.9 (*trans*-**2u**), 40.5 (*cis*-**2u**), 24.0 (*trans*-**2u**), 23.6 (*cis*-**2u**) ppm.

Spectral data is in agreement with the literature.<sup>12</sup>

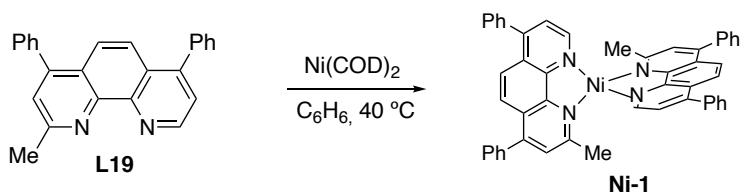
## Chapter 3

For the determination of the major isomer, the mixture of *trans*-**2u** and *cis*-**2u** were reduced using 10 mol% of 10% Pd/C under a H<sub>2</sub> atmosphere (balloon) in EtOAc. The solution was filtered through a pad of celite and the <sup>1</sup>H and <sup>13</sup>C NMR spectra was compared to the ones obtained from the commercially available *cis* and *trans* dimethyl cyclohexa-1,4-dicarboxylate, revealing that the major isomer was *trans*-configured:





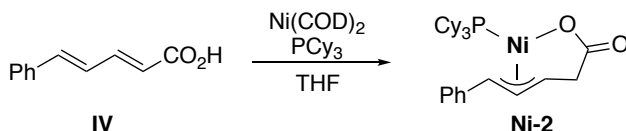
### Synthesis of Ni-1 and Ni-2.



**[Bis(2-methyl-4,7-diphenyl-1,10-phenanthroline)nickel(0)] (Ni-1).** In a glovebox, an oven-dried Schlenk tube containing a stirring bar was charged with Ni(COD)<sub>2</sub> (27.5 mg, 0.10 mmol, 1 equiv), **L19** (69.3 mg, 0.2 mmol, 2 equiv) and dissolved in anhydrous benzene (0.5 mL). The Schlenk tube was heated at 40 °C for 14 h. After the addition of 2 mL of cold pentane, a solid precipitated which was filtered and dried to provide 55.3 mg of **Ni-1** (74% yield) as a dark purple solid. X-Ray quality crystals were grown from slow evaporation of **Ni-1** in toluene at rt.

**<sup>1</sup>H NMR** (300 MHz, C<sub>6</sub>D<sub>6</sub>) δ 10.93 (bs, 1H), 8.05 – 7.71 (m, 4H), 7.82 – 7.52 (m, 6H), 7.50 – 7.29 (m, 4H), 2.71 (bs, 3H) ppm.

**<sup>13</sup>C NMR** (126 MHz, C<sub>6</sub>D<sub>6</sub>) δ 157.5, 148.0, 147.43, 146.7, 144.2, 143.4, 134.8, 134.2, 123.9, 123.3, 28.6 ppm (Some signals are overlapped with solvent peak).



**(2E,4E)-5-phenylpenta-2,4-dienoic acid (IV).** To a nitrogen-flushed 50 mL round bottom flask, *E*-cinnamyl aldehyde (1.0 mL, 8 mmol), malonic acid (1.66 g, 16 mmol), pyridine (5 mL) and piperidine (0.1 mL) were added sequentially. A condenser was placed on the flask and the mixture heated at 110 °C overnight (gas evolution was observed). After cooling to rt, 10 mL of water were added and the reaction was quenched with 2 M HCl until acidic pH (pH = 1-2). The aqueous solution was extracted with Et<sub>2</sub>O, the organic phases were combined, washed with brine then dried over MgSO<sub>4</sub>. The solvent was removed under reduced pressure and the residue was purified by silica gel flash chromatography (hexane:EtOAc 3:1 to 1:1). The compound was further purified by recrystallization in hot Et<sub>2</sub>O to give the compound **IV** (622.3 mg, 45% yield) as a mixture of stereoisomers (17:1 *E,E*: *E,Z*). Pale white solid.

<sup>1</sup>H NMR (400 MHz, CDCl<sub>3</sub>) δ 7.58 – 7.46 (m, 3H), 7.41 – 7.30 (m, 3H), 6.99 – 6.85 (m, 2H), 6.01 (d, *J* = 15.3 Hz, 1H) ppm.

<sup>13</sup>C NMR (101 MHz, CDCl<sub>3</sub>) δ 172.5, 147.1, 141.8, 136.0, 129.5, 129.0, 127.5, 126.1, 120.4 ppm.

Spectral data is in agreement with the literature.<sup>51</sup>

**[(3,4,5-η<sup>3</sup>-5-phenylpent-3-enylato)-(tricyclohexylphosphin)-nickel(II)] (Ni-2).** In a nitrogen-filled glovebox, a Schlenk flask was charged with **IV** (174.2 mg, 1 mmol), Ni(COD)<sub>2</sub> (275.0 mg, 1 mmol) and 5 mL degassed THF. Under magnetic stirring, PCy<sub>3</sub> (280.4 mg, 1 mmol) was added portion wise and the resulting orange solution was stirred overnight. The solvent was evaporated under reduced pressure and the resulting orange solid was washed with pentane and Et<sub>2</sub>O. The orange solid was then dried under high vacuum to obtain complex **5** (380 mg, 74% yield). X-Ray quality crystals were grown by slow evaporation of a benzene solution in the glovebox at rt.

<sup>1</sup>H NMR (400 MHz, C<sub>6</sub>D<sub>6</sub>) δ 7.18 (s, 2H), 7.05 (t, *J* = 6.5 Hz, 1H), 6.98 (d, *J* = 7.7 Hz, 2H), 5.59 (t, *J* = 11.9 Hz, 1H), 3.46 (s, 1H), 2.80 (s br, 1H), 2.72 (s, 1H), 2.69 (s, 1H), 2.04 – 0.83 (br, 33H) ppm.

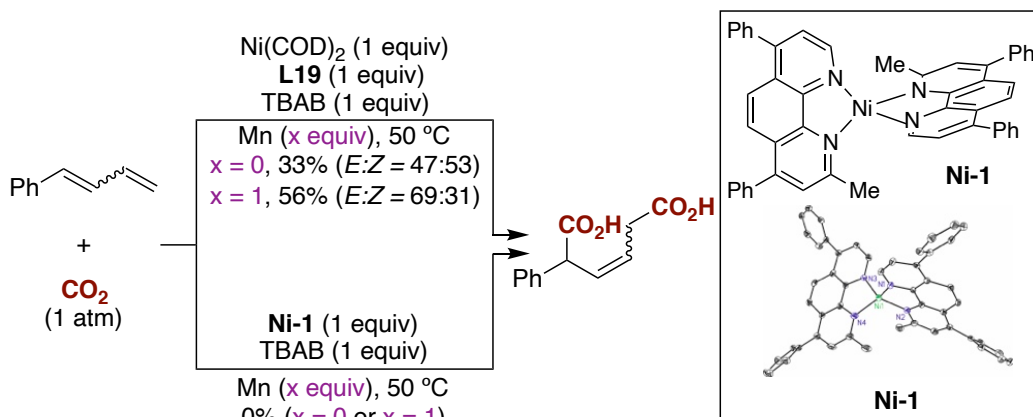
<sup>13</sup>C NMR (126 MHz, C<sub>6</sub>D<sub>6</sub>) δ 184.4, 141.8, 128.9, 128.2, 126.7, 125.3, 108.2, 79.5, 56.2, 32.3 (d, <sup>2</sup>*J*<sub>C-P</sub> = 18.2 Hz), 29.9 (d, <sup>2</sup>*J*<sub>C-P</sub> = 4.6 Hz), 27.4 (d, <sup>2</sup>*J*<sub>C-P</sub> = 10.5 Hz), 26.3 ppm.

<sup>31</sup>P NMR (202 MHz, C<sub>6</sub>D<sub>6</sub>) δ 31.2 ppm.

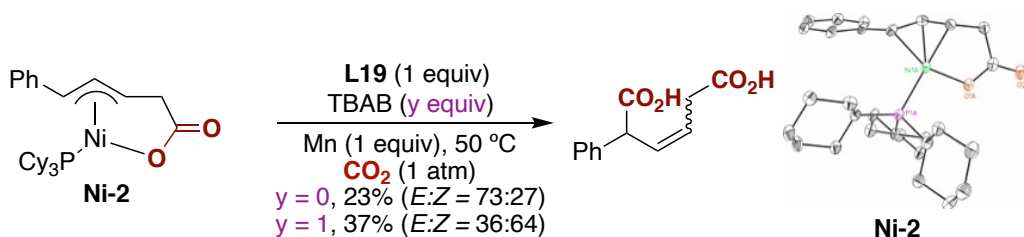


## Nickel-catalyzed double carboxylation of 1,3-dienes with CO<sub>2</sub>

### ■ stoichiometric studies with Ni(0)(L19)<sub>n</sub>

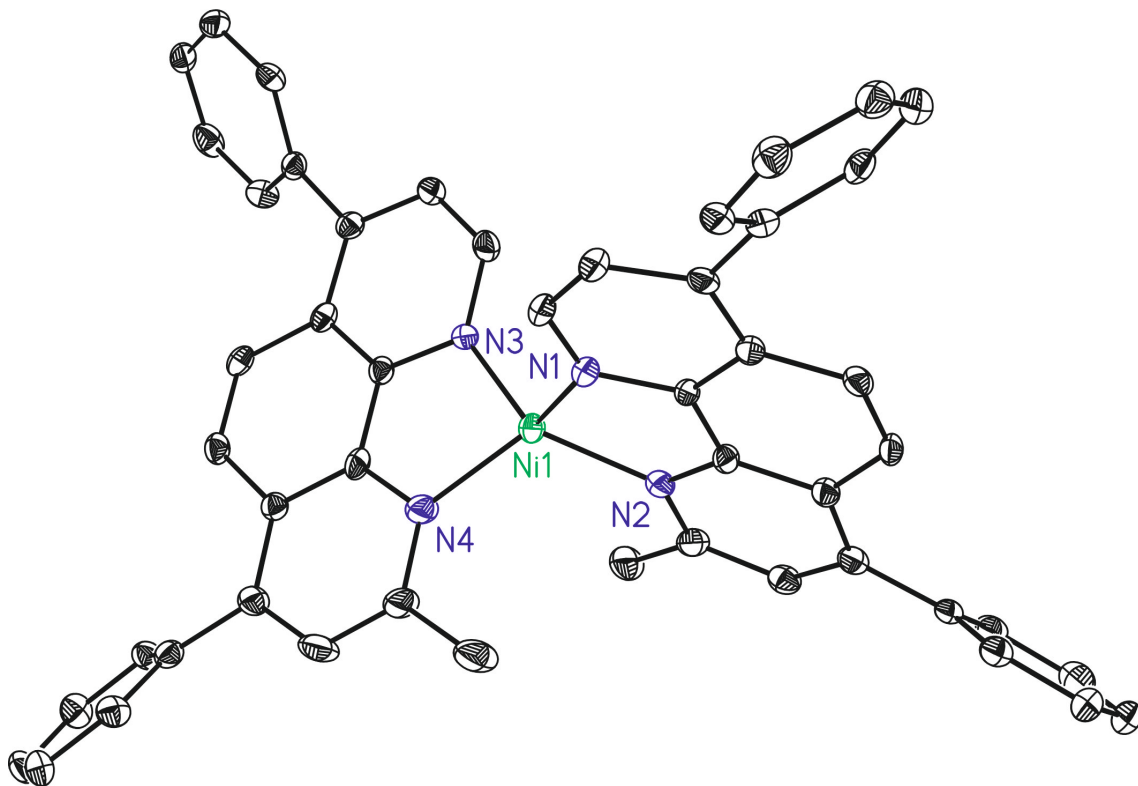


### ■ stoichiometric studies with Ni-2



An oven-dried Schlenk tube equipped with a magnetic stirring bar was charged with Mn dust (16.5 mg, 0.3 mmol, 1.5 equiv) and **L19**, and it was entered into a nitrogen-filled glovebox. Ni(COD)<sub>2</sub>, **Ni-1** or **Ni-2** were added and the Schlenk was closed and removed from the glovebox. Subsequently, it was filled with CO<sub>2</sub> by applying three vacuum/CO<sub>2</sub> cycles and the model substrate (0.20 mmol, 1 equiv) was added by syringe followed by the reaction solvent (0.40 mL) with a constant flow of CO<sub>2</sub>. The Schlenk flask was tightly sealed and stirred at 50 °C for 20 hours after which it was quenched by careful addition of HCl 2M and extracted 3 times with EtOAc. The combined organic phases were washed with brine and dried over MgSO<sub>4</sub> and concentrated under reduce pressure. Fluorene was added as a standard and an aliquot was taken, the solvent removed and redissolved in CDCl<sub>3</sub>. A <sup>1</sup>H NMR spectrum was recorded to calculate the yield of the reaction.

## X-Ray Crystallography of Ni-1 and Ni-2.

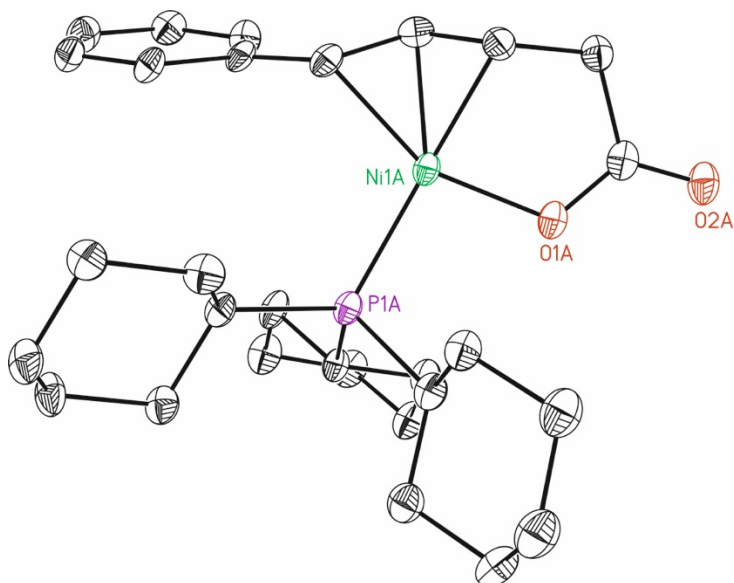


Crystal data and structure refinement for Ni-1.

Identification code	ATN1554	
Empirical formula	C <sub>214</sub> H <sub>160</sub> N <sub>16</sub> Ni <sub>4</sub>	
Formula weight	3190.41	
Temperature	100(2) K	
Wavelength	0.71073 Å	
Crystal system	Monoclinic	
Space group	P2(1)/c	
Unit cell dimensions	a = 25.681(2)Å	α = 90°.
	b = 14.1560(10)Å	β = 92.639(7)°.
	c = 10.7814(8)Å	γ = 90°.
Volume	3915.3(5) Å <sup>3</sup>	

Nickel-catalyzed double carboxylation of 1,3-dienes with CO<sub>2</sub>

Z	1
Density (calculated)	1.353 Mg/m <sup>3</sup>
Absorption coefficient	0.540 mm <sup>-1</sup>
F(000)	1668
Crystal size	0.03 x 0.05 x 0.15 mm <sup>3</sup>
Theta range for data collection	2.376 to 29.048°.
Index ranges	-34 ≤ h ≤ 33, -17 ≤ k ≤ 19, -14 ≤ l ≤ 13
Reflections collected	51376
Independent reflections	9117 [R(int) = 0.1407]
Completeness to theta = 29.048°	87.1%
Absorption correction	Multi-scan
Max. and min. transmission	0.984 and 0.757
Refinement method	Full-matrix least-squares on F <sup>2</sup>
Data / restraints / parameters	9117 / 106 / 550
Goodness-of-fit on F <sup>2</sup>	1.019
Final R indices [I > 2σ(I)]	R1 = 0.0686, wR2 = 0.1235
R indices (all data)	R1 = 0.1530, wR2 = 0.1507
Largest diff. peak and hole	0.563 and -0.600 e.Å <sup>-3</sup>

X Ray structure of compound **Ni-2**:Crystal data and structure refinement for **Ni-2**.

---

Identification code	mo_ATN737-05
Empirical formula	C <sub>35</sub> H <sub>49</sub> Ni O <sub>2</sub> P
Formula weight	591.42
Temperature	100(2) K
Wavelength	0.71073 Å
Crystal system	Triclinic
Space group	P-1
Unit cell dimensions	a = 11.7813(14) Å $\alpha$ = 89.326(3)° b = 13.5251(17) Å $\beta$ = 89.533(3)° c = 19.854(3) Å $\gamma$ = 79.092(3)°
Volume	3106.2(7) Å <sup>3</sup>

Nickel-catalyzed double carboxylation of 1,3-dienes with CO<sub>2</sub>

Z	4
Density (calculated)	1.265 Mg/m <sup>3</sup>
Absorption coefficient	0.705 mm <sup>-1</sup>
F(000)	1272
Crystal size	0.40 x 0.04 x 0.02 mm <sup>3</sup>
Theta range for data collection	1.026 to 28.786°.
Index ranges	-15 ≤ h ≤ 15, -18 ≤ k ≤ 18, 0 ≤ l ≤ 26
Reflections collected	47560
Independent reflections	15030 [R(int) = 0.0616]
Completeness to theta = 28.786°	94.3%
Absorption correction	Multi-scan
Max. and min. transmission	0.986 and 0.758
Refinement method	Full-matrix least-squares on F <sup>2</sup>
Data / restraints / parameters	15030 / 0 / 704
Goodness-of-fit on F <sup>2</sup>	1.012
Final R indices [I > 2σ(I)]	R1 = 0.0623, wR2 = 0.1515
R indices (all data)	R1 = 0.0956, wR2 = 0.1741
Largest diff. peak and hole	1.060 and -1.103 e.Å <sup>-3</sup>

## References:

- (1) Sasaki, Y.; Inoue, Y.; Hashimoto, H. Reaction of Carbon Dioxide with Butadiene Catalysed by Palladium Complexes. Synthesis of 2-Ethylidenehept-5-En-4-Olide. *J. Chem. Soc., Chem. Commun.* **1976**, No. 15, 605. <https://doi.org/10.1039/c39760000605>.
- (2) Inoue, Y.; Sasaki, Y.; Hashimoto, H. Incorporation of CO<sub>2</sub> in Butadiene Dimerization Catalyzed by Palladium Complexes. Formation of 2-Ethylidene-5-Hepten-4-Olide. *BCSJ* **1978**, *51* (8), 2375–2378. <https://doi.org/10.1246/bcsj.51.2375>.
- (3) Behr, A.; Juszak, K.-D. Palladium-Catalyzed Reaction of Butadiene and Carbon Dioxide. *Journal of Organometallic Chemistry* **1983**, *255* (2), 263–268. [https://doi.org/10.1016/0022-328X\(83\)87028-4](https://doi.org/10.1016/0022-328X(83)87028-4).
- (4) Hoberg, H.; Gross, S.; Milchereit, A. Nickel(0)-Catalyzed Production of a Functionalized Cyclopentanecarboxylic Acid from 1,3-Butadiene and CO<sub>2</sub>. *Angew. Chem. Int. Ed. Engl.* **1987**, *26* (6), 571–572. <https://doi.org/10.1002/anie.198705711>.
- (5) Braunstein, Pierre.; Matt, Dominique.; Nobel, Dominique. Carbon Dioxide Activation and Catalytic Lactone Synthesis by Telomerization of Butadiene and Carbon Dioxide. *J. Am. Chem. Soc.* **1988**, *110* (10), 3207–3212. <https://doi.org/10.1021/ja00218a033>.
- (6) Braunstein, P.; Matt, D.; Nobel, D. Reactions of Carbon Dioxide with Carbon-Carbon Bond Formation Catalyzed by Transition-Metal Complexes. *Chem. Rev.* **1988**, *88* (5), 747–764. <https://doi.org/10.1021/cr00087a003>.
- (7) Musco, A. Co-Oligomerization of Butadiene and Carbon Dioxide Catalysed by Tertiary Phosphine–Palladium Complexes. *J. Chem. Soc., Perkin Trans. 1* **1980**, No. 0, 693–698. <https://doi.org/10.1039/P19800000693>.
- (8) Hoberg, H.; Schaefer, D.; Oster, B. W. Diencarbonsäuren aus 1,3-dienen und CO<sub>2</sub> durch C-C-verknüpfung an nickel(0). *Journal of Organometallic Chemistry* **1984**, *266* (3), 313–320. [https://doi.org/10.1016/0022-328X\(84\)80144-8](https://doi.org/10.1016/0022-328X(84)80144-8).
- (9) Hoberg, H.; Apotecher, B.  $\alpha,\omega$ -Disäuren aus butadien und kohlendioxid an nickel(0). *Journal of Organometallic Chemistry* **1984**, *270* (1), c15–c17. [https://doi.org/10.1016/0022-328X\(84\)80346-0](https://doi.org/10.1016/0022-328X(84)80346-0).
- (10) Behr, A.; Kanne, U. Nickel Complex Induced C-C Linkage of Carbon Dioxide with Trienes. *Journal of Organometallic Chemistry* **1986**, *317* (3), C41–C44. [https://doi.org/10.1016/0022-328X\(86\)80550-2](https://doi.org/10.1016/0022-328X(86)80550-2).
- (11) Hoberg, H.; Jenni, K.; Krüger, C.; Raabe, E. CC-Kupplung von CO<sub>2</sub> und Butadien an Eisen(0)-Komplexen – ein neuer Weg zu  $\alpha,\omega$ -Dicarbonsäuren. *Angew. Chem.* **1986**, *98* (9), 819–820. <https://doi.org/10.1002/ange.19860980915>.
- (12) Takimoto, M.; Mori, M. Cross-Coupling Reaction of Oxo- $\pi$ -Allylnickel Complex Generated from 1,3-Diene under an Atmosphere of Carbon Dioxide. *J. Am. Chem. Soc.* **2001**, *123* (12), 2895–2896. <https://doi.org/10.1021/ja004004f>.
- (13) Takimoto, M.; Mori, M. Novel Catalytic CO<sub>2</sub> Incorporation Reaction: Nickel-Catalyzed Regio- and Stereoselective Ring-Closing Carboxylation of Bis-1,3-Dienes. *J. Am. Chem. Soc.* **2002**, *124* (34), 10008–10009. <https://doi.org/10.1021/ja026620c>.
- (14) Takimoto, M.; Nakamura, Y.; Kimura, K.; Mori, M. Highly Enantioselective Catalytic Carbon Dioxide Incorporation Reaction: Nickel-Catalyzed Asymmetric Carboxylative Cyclization of Bis-1,3-Dienes. *J. Am. Chem. Soc.* **2004**, *126* (19), 5956–5957. <https://doi.org/10.1021/ja049506y>.
- (15) Takimoto, M.; Kawamura, M.; Mori, M.; Sato, Y. Nickel-Catalyzed Regio- and Stereoselective Double Carboxylation of -Trimethylsilyllallene under an Atmosphere of Carbon Dioxide and Its -Application to the Synthesis of Chaetomelic Acid A Anhydride.

*Synlett* **2005**, No. 13, 2019–2022. <https://doi.org/10.1055/s-2005-872225>.

(16) Higuchi, Y.; Mita, T.; Sato, Y. Palladium-Catalyzed Intramolecular Arylative Carboxylation of Allenes with CO<sub>2</sub> for the Construction of 3-Substituted Indole-2-Carboxylic Acids. *Org. Lett.* **2017**, *19* (10), 2710–2713. <https://doi.org/10.1021/acs.orglett.7b01055>.

(17) Takaya, J.; Iwasawa, N. Hydrocarboxylation of Allenes with CO<sub>2</sub> Catalyzed by Silyl Pincer-Type Palladium Complex. *J. Am. Chem. Soc.* **2008**, *130* (46), 15254–15255. <https://doi.org/10.1021/ja806677w>.

(18) Suh, H.-W.; Guard, L. M.; Hazari, N. A Mechanistic Study of Allene Carboxylation with CO<sub>2</sub> Resulting in the Development of a Pd(II) Pincer Complex for the Catalytic Hydroboration of CO<sub>2</sub>. *Chem. Sci.* **2014**, *5* (10), 3859–3872. <https://doi.org/10.1039/C4SC01110D>.

(19) Takaya, J.; Sasano, K.; Iwasawa, N. Efficient One-to-One Coupling of Easily Available 1,3-Dienes with Carbon Dioxide. *Org. Lett.* **2011**, *13* (7), 1698–1701. <https://doi.org/10.1021/ol2002094>.

(20) Mizuno, T.; Oonishi, Y.; Takimoto, M.; Sato, Y. Total Synthesis of (-)-Corynantheidine by Nickel-Catalyzed Carboxylative Cyclization of Enynes. *Eur. J. Org. Chem.* **2011**, *2011* (14), 2606–2609. <https://doi.org/10.1002/ejoc.201100147>.

(21) Cao, T.; Yang, Z.; Ma, S. Selectivities in Nickel-Catalyzed Hydrocarboxylation of Enynes with Carbon Dioxide. *ACS Catal.* **2017**, *7* (7), 4504–4508. <https://doi.org/10.1021/acscatal.7b00556>.

(22) Diccianni, J. B.; Heitmann, T.; Diao, T. Nickel-Catalyzed Reductive Cycloisomerization of Enynes with CO<sub>2</sub>. *J. Org. Chem.* **2017**, *82* (13), 6895–6903. <https://doi.org/10.1021/acs.joc.7b01034>.

(23) Cao, T.; Ma, S. Highly Stereo- and Regioselective Hydrocarboxylation of Diynes with Carbon Dioxide. *Org. Lett.* **2016**, *18* (7), 1510–1513. <https://doi.org/10.1021/acs.orglett.6b00028>.

(24) van Tilborg, W. J. M.; Smit, C. J. The Electrosynthesis of Carboxylic Acids from Carbon Dioxide and Butadiene. *Recl. Trav. Chim. Pays-Bas* **1981**, *100* (11), 437–438. <https://doi.org/10.1002/recl.19811001113>.

(25) Dérien, S.; Clinet, J.-C.; Duñach, E.; Périchon, J. Coupling of Allenes and Carbon Dioxide Catalyzed by Electrogenerated Nickel Complexes. *Synlett* **1990**, *1990* (6), 361–364. <https://doi.org/10.1055/s-1990-21096>.

(26) Dérien, S.; Clinet, J.-C.; Duñach, E.; Périchon, J. Electrochemical Incorporation of Carbon Dioxide into Alkenes by Nickel Complexes. *Tetrahedron* **1992**, *48* (25), 5235–5248. [https://doi.org/10.1016/S0040-4020\(01\)89021-9](https://doi.org/10.1016/S0040-4020(01)89021-9).

(27) Bringmann, J.; Dinjus, E. Electrochemical Synthesis of Carboxylic Acids from Alkenes Using Various Nickel-Organic Mediators: CO<sub>2</sub> as C1-Synthon. *Applied Organometallic Chemistry* **2001**, *15* (2), 135–140. [https://doi.org/10.1002/1099-0739\(200102\)15:2<135::AID-AOC108>3.0.CO;2-L](https://doi.org/10.1002/1099-0739(200102)15:2<135::AID-AOC108>3.0.CO;2-L).

(28) Li, C.-H.; Yuan, G.-Q.; Ji, X.-C.; Wang, X.-J.; Ye, J.-S.; Jiang, H.-F. Highly Regioselective Electrochemical Synthesis of Dioic Acids from Dienes and Carbon Dioxide. *Electrochimica Acta* **2011**, *56* (3), 1529–1534. <https://doi.org/10.1016/j.electacta.2010.06.057>.

(29) Matthessen, R.; Fransaer, J.; Binnemans, K.; Vos, D. E. D. Electrochemical Dicarboxylation of Conjugated Fatty Acids as an Efficient Valorization of Carbon Dioxide. *RSC Adv.* **2013**, *3* (14), 4634. <https://doi.org/10.1039/c3ra00129f>.

(30) Steinmann, S. N.; Michel, C.; Schwiedernoch, R.; Wu, M.; Sautet, P. Electro-Carboxylation of Butadiene and Ethene over Pt and Ni Catalysts. *Journal of Catalysis* **2016**, *343*, 240–247. <https://doi.org/10.1016/j.jcat.2016.01.008>.

(31) Wang, X.; Nakajima, M.; Martin, R. Ni-Catalyzed Regioselective Hydrocarboxylation

of Alkynes with CO<sub>2</sub> by Using Simple Alcohols as Proton Sources. *J. Am. Chem. Soc.* **2015**, *137*, 8924–8927. <https://doi.org/10.1021/jacs.5b05513>.

(32) Gaydou, M.; Moragas, T.; Juliá-Hernández, F.; Martin, R. Site-Selective Catalytic Carboxylation of Unsaturated Hydrocarbons with CO<sub>2</sub> and Water. *J. Am. Chem. Soc.* **2017**, *139*, 12161–12164. <https://doi.org/10.1021/jacs.7b07637>.

(33) Musser, M. T. Adipic Acid. In *Ullmann's Encyclopedia of Industrial Chemistry*; Wiley-VCH Verlag GmbH & Co. KGaA, Ed.; Wiley-VCH Verlag GmbH & Co. KGaA: Weinheim, Germany, 2000. [https://doi.org/10.1002/14356007.a01\\_269](https://doi.org/10.1002/14356007.a01_269).

(34) Charboneau, D. J.; Brudvig, G. W.; Hazari, N.; Lant, H. M. C.; Saydjari, A. K. Development of an Improved System for the Carboxylation of Aryl Halides through Mechanistic Studies. *ACS Catal.* **2019**, *9* (4), 3228–3241. <https://doi.org/10.1021/acscatal.9b00566>.

(35) Correa, A.; Martín, R. Metal-Catalyzed Carboxylation of Organometallic Reagents with Carbon Dioxide. *Angew. Chem. Int. Ed.* **2009**, *48* (34), 6201–6204. <https://doi.org/10.1002/anie.200900667>.

(36) Yonova, I. M.; Johnson, A. G.; Osborne, C. A.; Moore, C. E.; Morrisette, N. S.; Jarvo, E. R. Stereospecific Nickel-Catalyzed Cross-Coupling Reactions of Alkyl Grignard Reagents and Identification of Selective Anti-Breast-Cancer Agents. *Angew. Chem. Int. Ed.* **2014**, *53* (9), 2422–2427. <https://doi.org/10.1002/anie.201308666>.

(37) Nett, A. J.; Zhao, W.; Zimmerman, P. M.; Montgomery, J. Highly Active Nickel Catalysts for C–H Functionalization Identified through Analysis of Off-Cycle Intermediates. *J. Am. Chem. Soc.* **2015**, *137* (24), 7636–7639. <https://doi.org/10.1021/jacs.5b04548>.

(38) Schulz, P. S.; Walter, O.; Dinjus, E. Facile Synthesis of a Tricyclohexylphosphine-Stabilized H<sub>3</sub>-Allyl-Carboxylato Ni(II) Complex and Its Relevance in Electrochemical Butadiene Carbon Dioxide Coupling. *App. Organomet. Chem.* **2005**, *19* (11), 1176–1179. <https://doi.org/10.1002/aoc.993>.

(39) Forníes, J.; Martín, A.; Martín, L. F.; Menjón, B.; Kalamarides, H. A.; Rhodes, L. F.; Day, C. S.; Day, V. W. Synthesis and Characterization of a New Family of Square-Planar Nickel(II) Carbonyl Derivatives. *Chem. Eur. J.* **2002**, *8* (21), 4925–4934. [https://doi.org/10.1002/1521-3765\(20021104\)8:21<4925::AID-CHEM4925>3.0.CO;2-4](https://doi.org/10.1002/1521-3765(20021104)8:21<4925::AID-CHEM4925>3.0.CO;2-4).

(40) Mundal, D. A.; Lutz, K. E.; Thomson, R. J. Stereoselective Synthesis of Dienes from *N*-Allylhydrazones. *Org. Lett.* **2009**, *11* (2), 465–468. <https://doi.org/10.1021/ol802585r>.

(41) Madden, K. S.; David, S.; Knowles, J. P.; Whiting, A. Heck–Mizoroki Coupling of Vinyl iodide and Applications in the Synthesis of Dienes and Trienes. *Chem. Commun.* **2015**, *51* (57), 11409–11412. <https://doi.org/10.1039/C5CC03273C>.

(42) Lee, R. J.; Lindley, M. R.; Pritchard, G. J.; Kimber, M. C. A Biosynthetically Inspired Route to Substituted Furans Using the Appel Reaction: Total Synthesis of the Furan Fatty Acid F5. *Chem. Commun.* **2017**, *53* (47), 6327–6330. <https://doi.org/10.1039/C7CC03229C>.

(43) Yamashita, M.; Hirano, K.; Satoh, T.; Miura, M. Synthesis of 1,4-Diarylbuta-1,3-Dienes through Palladium-Catalyzed Decarboxylative Coupling of Unsaturated Carboxylic Acids. *Adv. Synth. & Cat.* **2011**, *353* (4), 631–636. <https://doi.org/10.1002/adsc.201000897>.

(44) Pearson, E. L.; Kwan, L. C. H.; Turner, C. I.; Jones, G. A.; Willis, A. C.; Paddon-Row, M. N.; Sherburn, M. S. Intramolecular Diels–Alder Reactions of Ester Linked 1,3,9-Decatrienes: Cis/Trans Selectivity in Thermal and Lewis Acid Promoted Reactions of Ethylene-Tethered and Benzo-Tethered Systems. *J. Org. Chem.* **2006**, *71* (16), 6099–6109. <https://doi.org/10.1021/jo0607818>.

(45) Al-Deyab, S. S.; El-Newehy, M. H. Synthesis and Characterization of Novel Organotin-Phosphorous Compounds II. *Molecules* **2010**, *15* (3), 1425–1432.



<https://doi.org/10.3390/molecules15031425>.

(46) Meyers, A. I.; Ford, M. E. Oxazolines. XX. Synthesis of Achiral and Chiral Thiiranes and Olefins by Reaction of Carbonyl Compounds with 2-(Alkylthio)-2-Oxazolines. *J. Org. Chem.* **1976**, *41* (10), 1735–1742. <https://doi.org/10.1021/jo00872a015>.

(47) Campbell, N. E.; Sammis, G. M. Single-Electron/Pericyclic Cascade for the Synthesis of Dienes. *Angew. Chem. Int. Ed.* **2014**, *53* (24), 6228–6231. <https://doi.org/10.1002/anie.201403234>.

(48) Põhako-Esko, K.; Taaber, T.; Saal, K.; Lõhmus, R.; Kink, I.; Mäeorg, U. New Method for Synthesis of Methacrylate-Type Polymerizable Ionic Liquids. *Synth. Comm.* **2013**, *43* (21), 2846–2852. <https://doi.org/10.1080/00397911.2012.745159>.

(49) Keinan, E.; Sahai, M.; Poth, Z.; Nudelman, A.; Herzig, J. Organotin Nucleophiles. 6. Palladium-Catalyzed Allylic Etherification with Tin Alkoxides. *J. Org. Chem.* **1985**, *50* (19), 3558–3566. <https://doi.org/10.1021/jo00219a023>.

(50) Taylor, E. C.; Conley, R. A.; Katz, A. H.; McKillop, A. Thallium in Organic Synthesis. 62. A Convenient Synthesis of Alpha-Arylsuccinic Acids. *J. Org. Chem.* **1984**, *49* (20), 3840–3841. <https://doi.org/10.1021/jo00194a037>.

(51) Kokotos, G.; Hsu, Y.-H.; Burke, J. E.; Baskakis, C.; Kokotos, C. G.; Magrioti, V.; Dennis, E. A. Potent and Selective Fluoroketone Inhibitors of Group VIA Calcium-Independent Phospholipase A<sub>2</sub>. *J. Med. Chem.* **2010**, *53* (9), 3602–3610. <https://doi.org/10.1021/jm901872v>.



**<sup>1</sup>H NMR, <sup>13</sup>C NMR, <sup>19</sup>F NMR, <sup>31</sup>P NMR and <sup>119</sup>Sn NMR spectra**









# Chapter 3

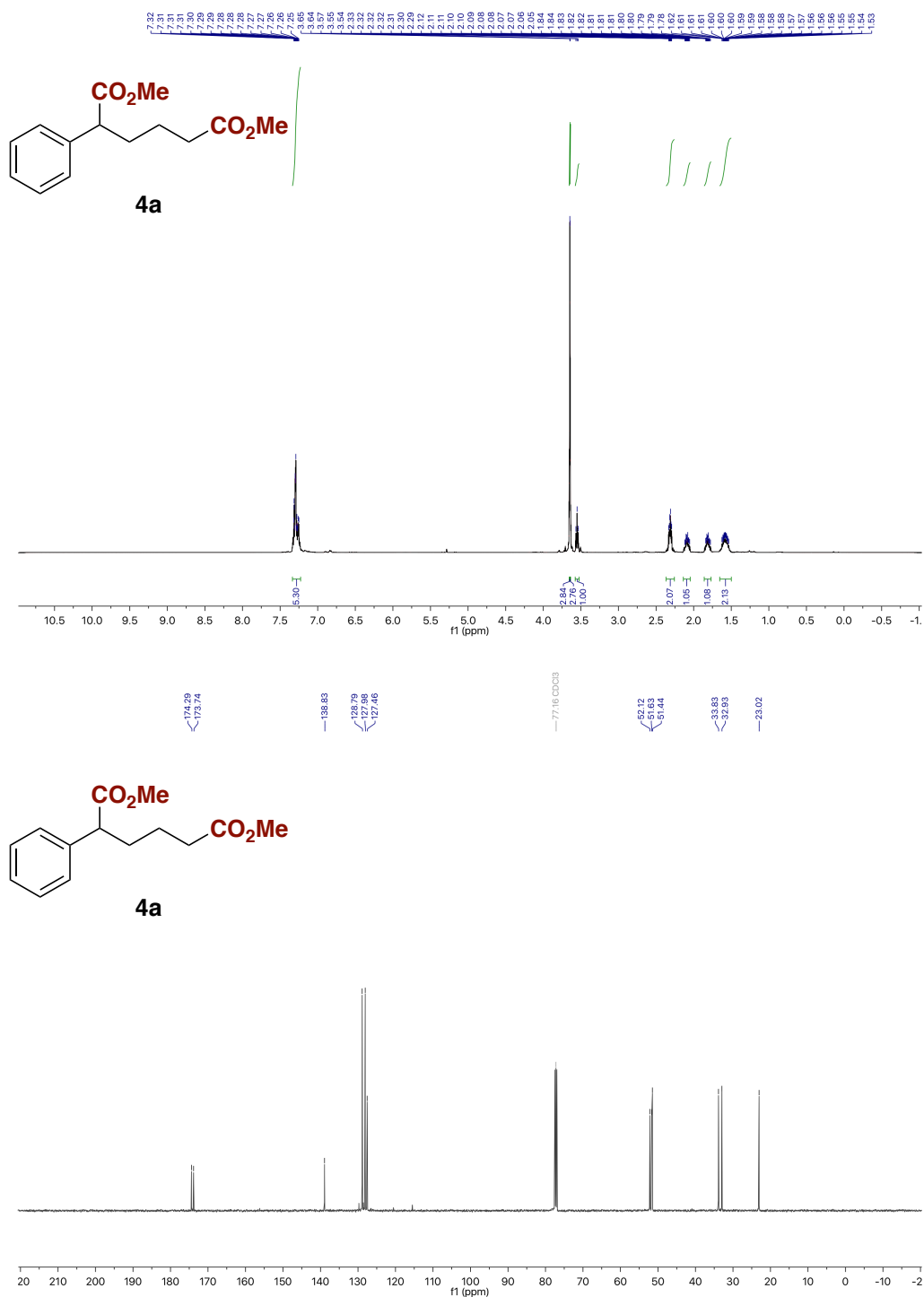


Figure 4. <sup>1</sup>H and <sup>13</sup>C NMR spectra of **4a**.





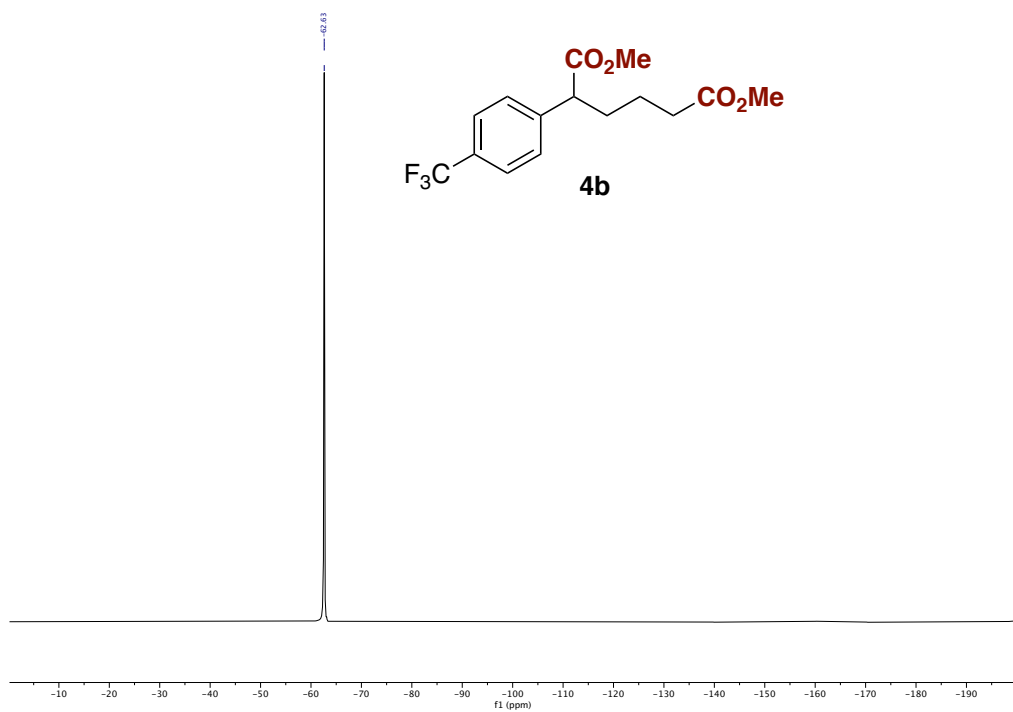
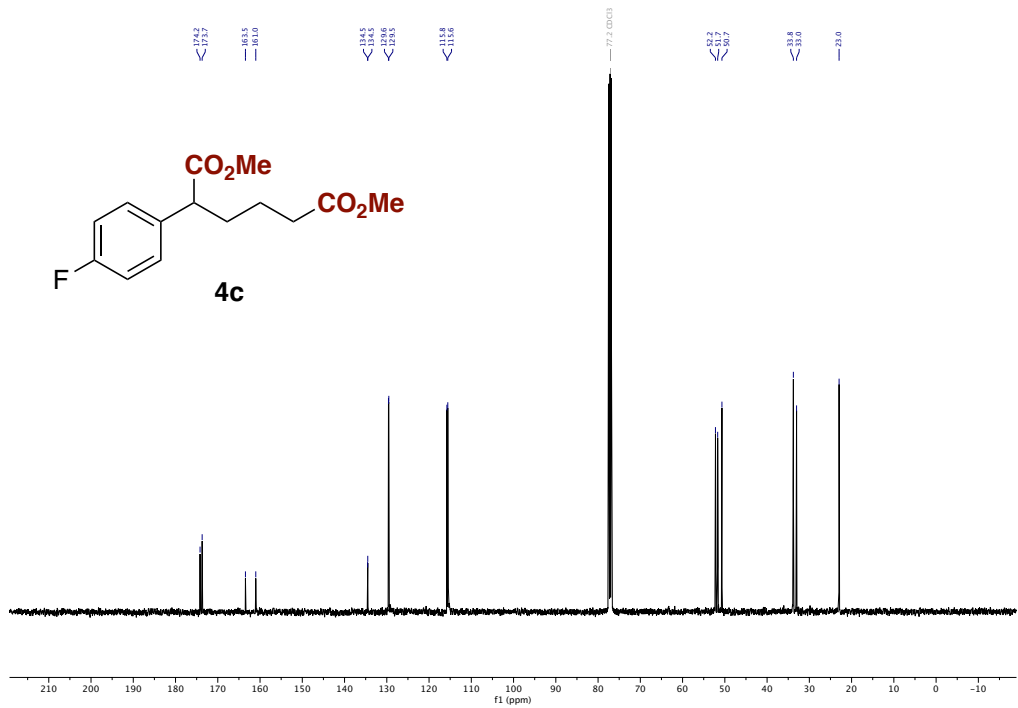
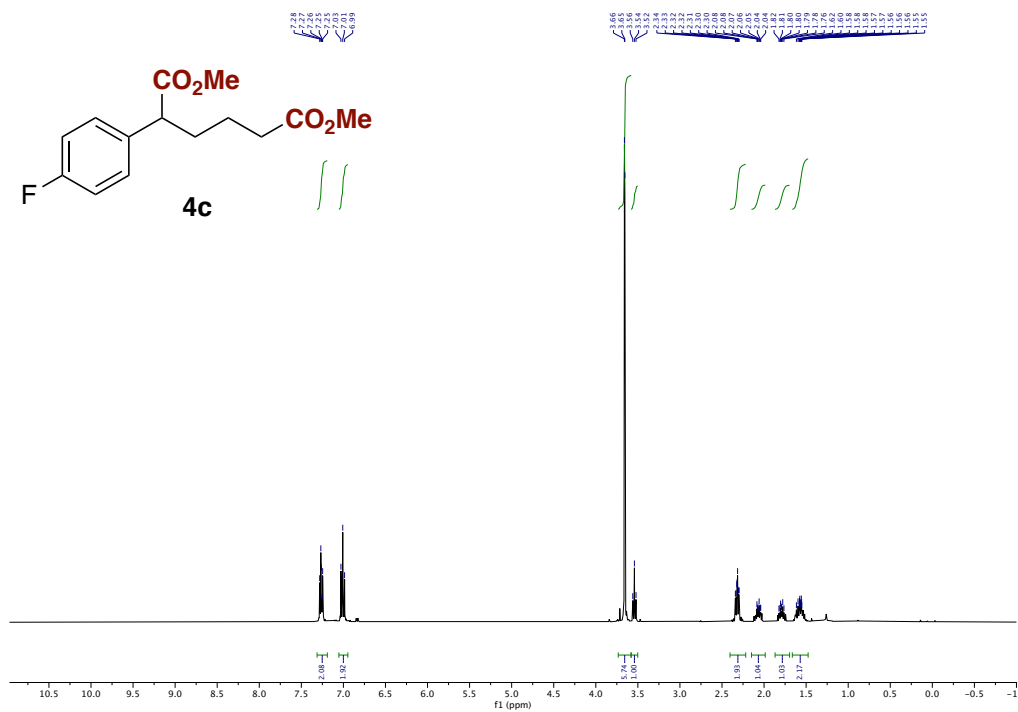


Figure 5.  $^1\text{H}$ ,  $^{13}\text{C}$  and  $^{19}\text{F}$  NMR spectra of **4b**.

# Nickel-catalyzed double carboxylation of 1,3-dienes with CO<sub>2</sub>



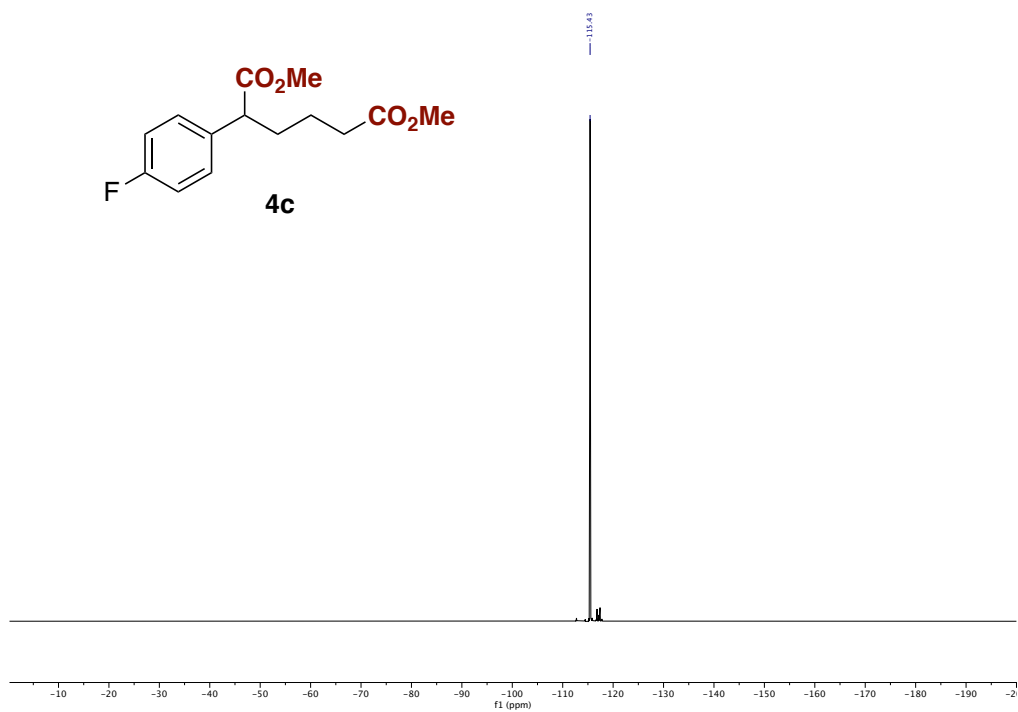


Figure 6.  $^1\text{H}$ ,  $^{13}\text{C}$  and  $^{19}\text{F}$  NMR spectra of **4c**.

Nickel-catalyzed double carboxylation of 1,3-dienes with CO<sub>2</sub>

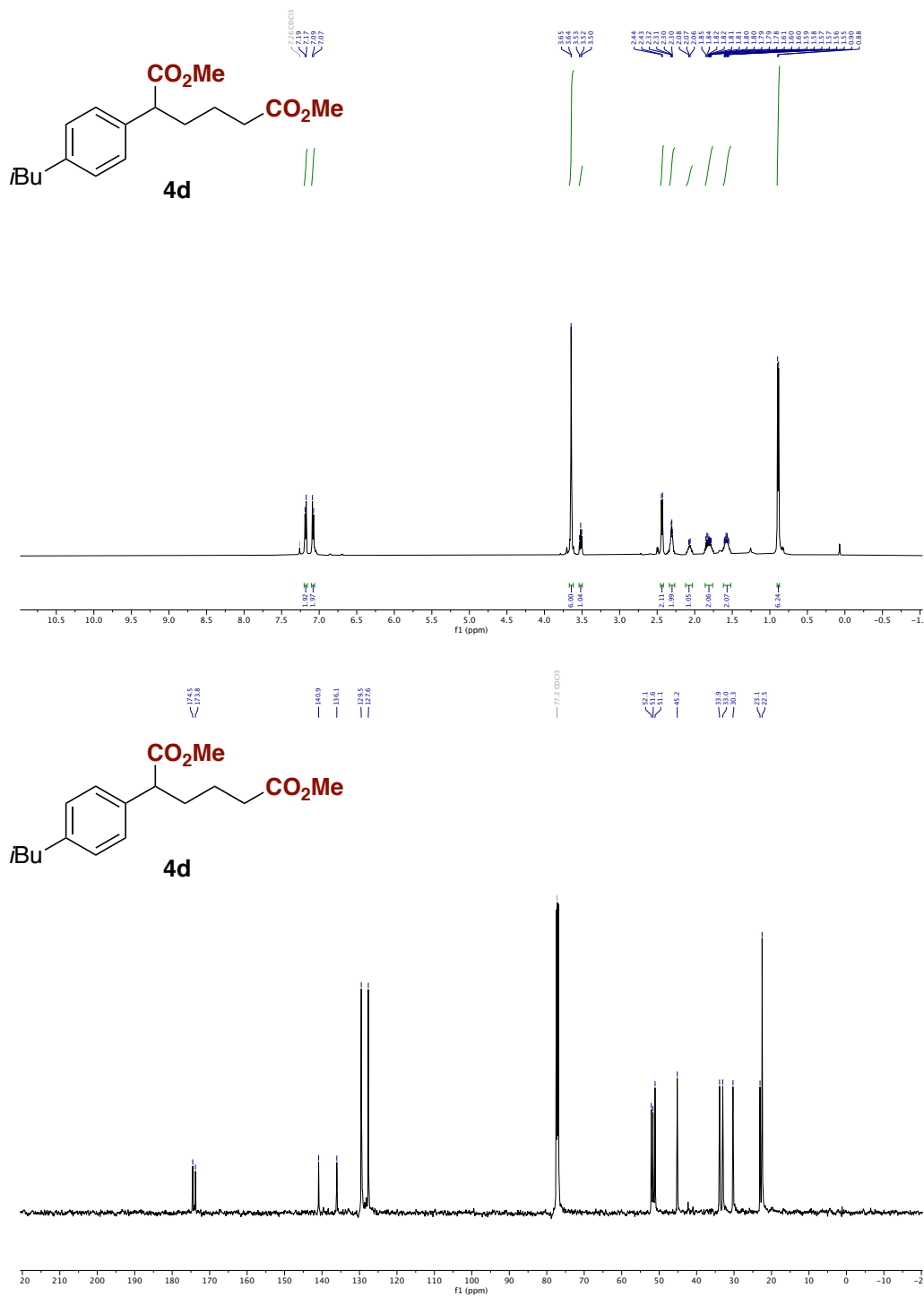


Figure 7. <sup>1</sup>H and <sup>13</sup>C NMR spectra of **4d**.

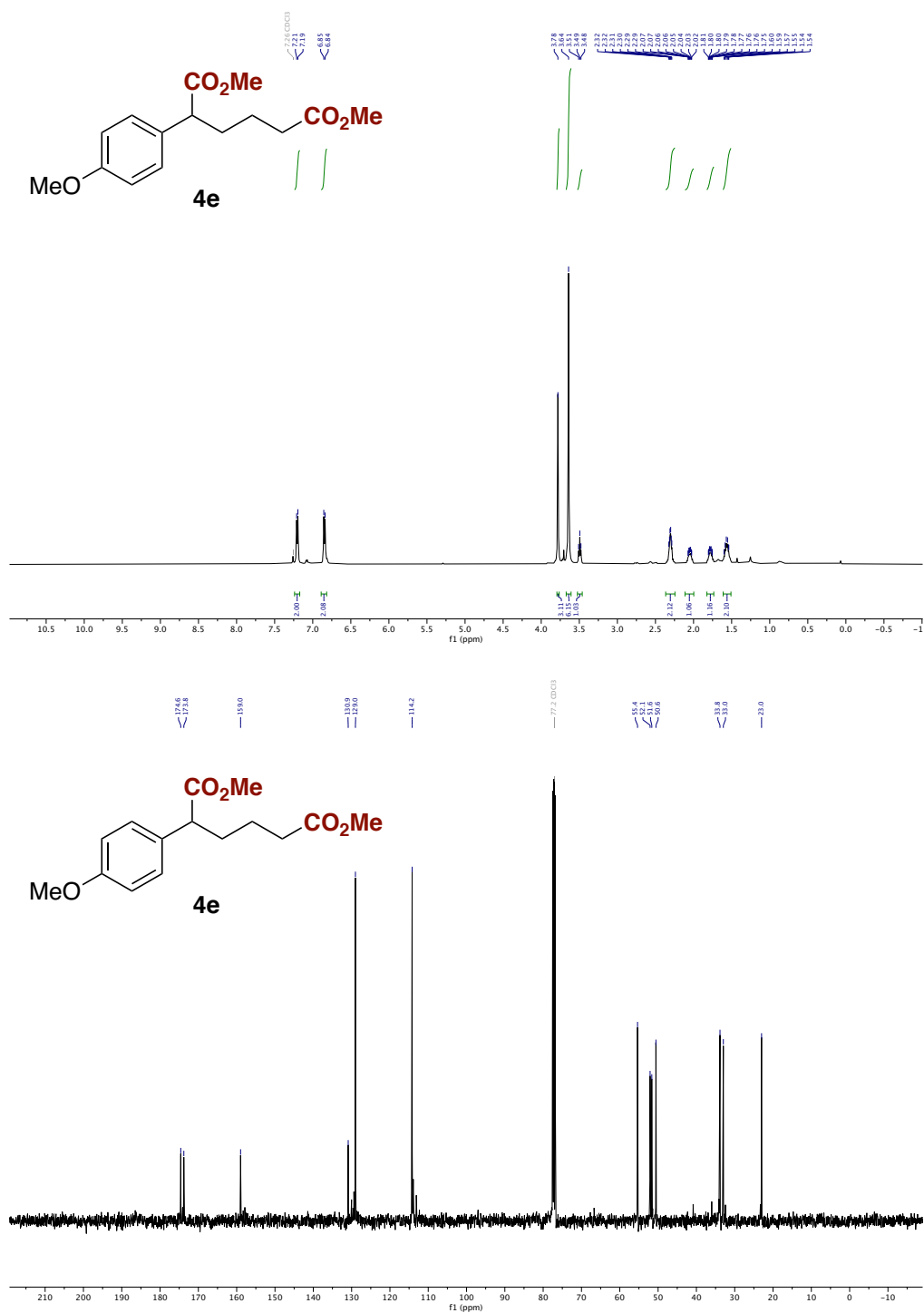


Figure 8. <sup>1</sup>H and <sup>13</sup>C NMR spectra of **4e**.

Nickel-catalyzed double carboxylation of 1,3-dienes with CO<sub>2</sub>

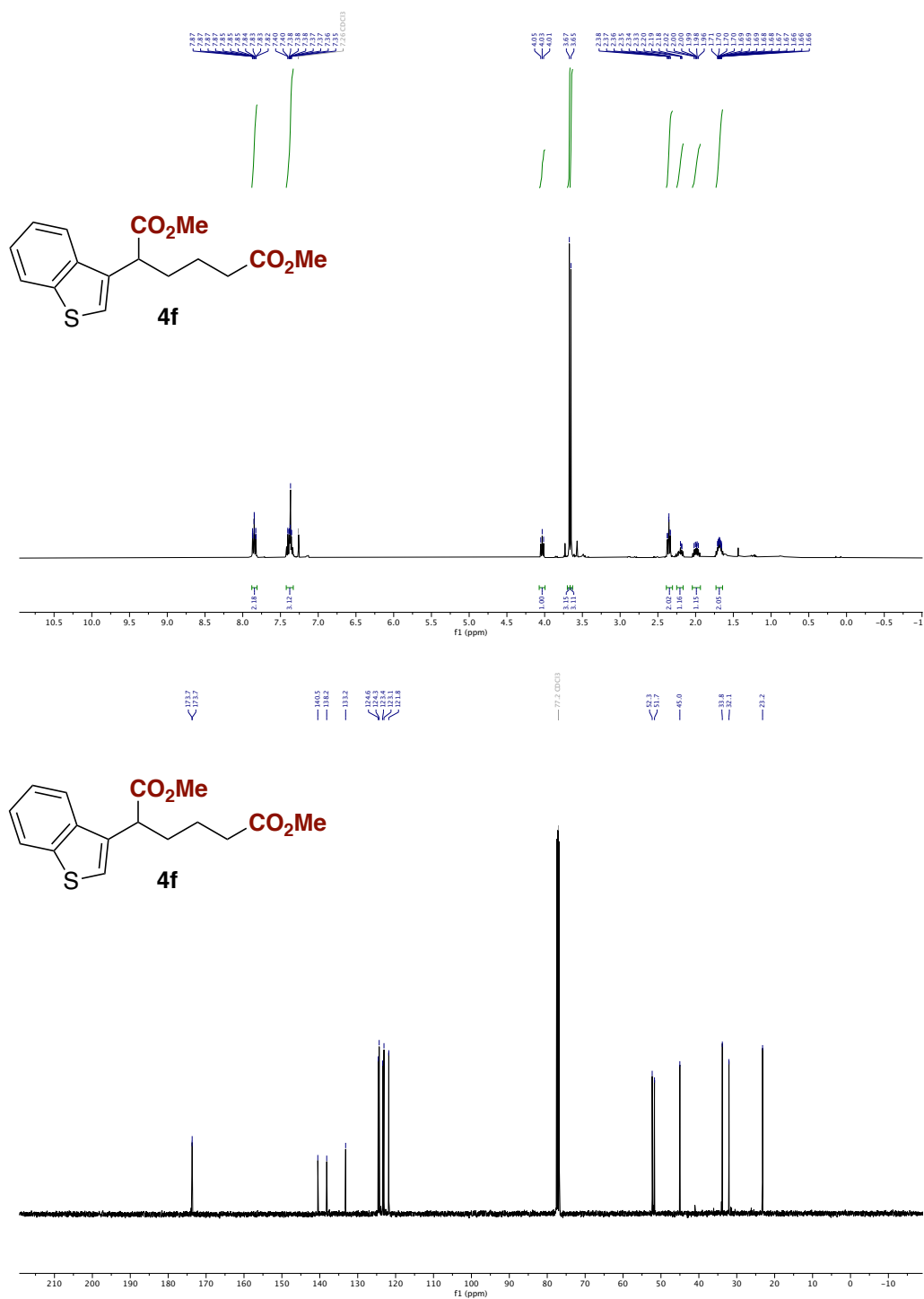


Figure 9. <sup>1</sup>H and <sup>13</sup>C NMR spectra of **4f**.





Nickel-catalyzed double carboxylation of 1,3-dienes with CO<sub>2</sub>

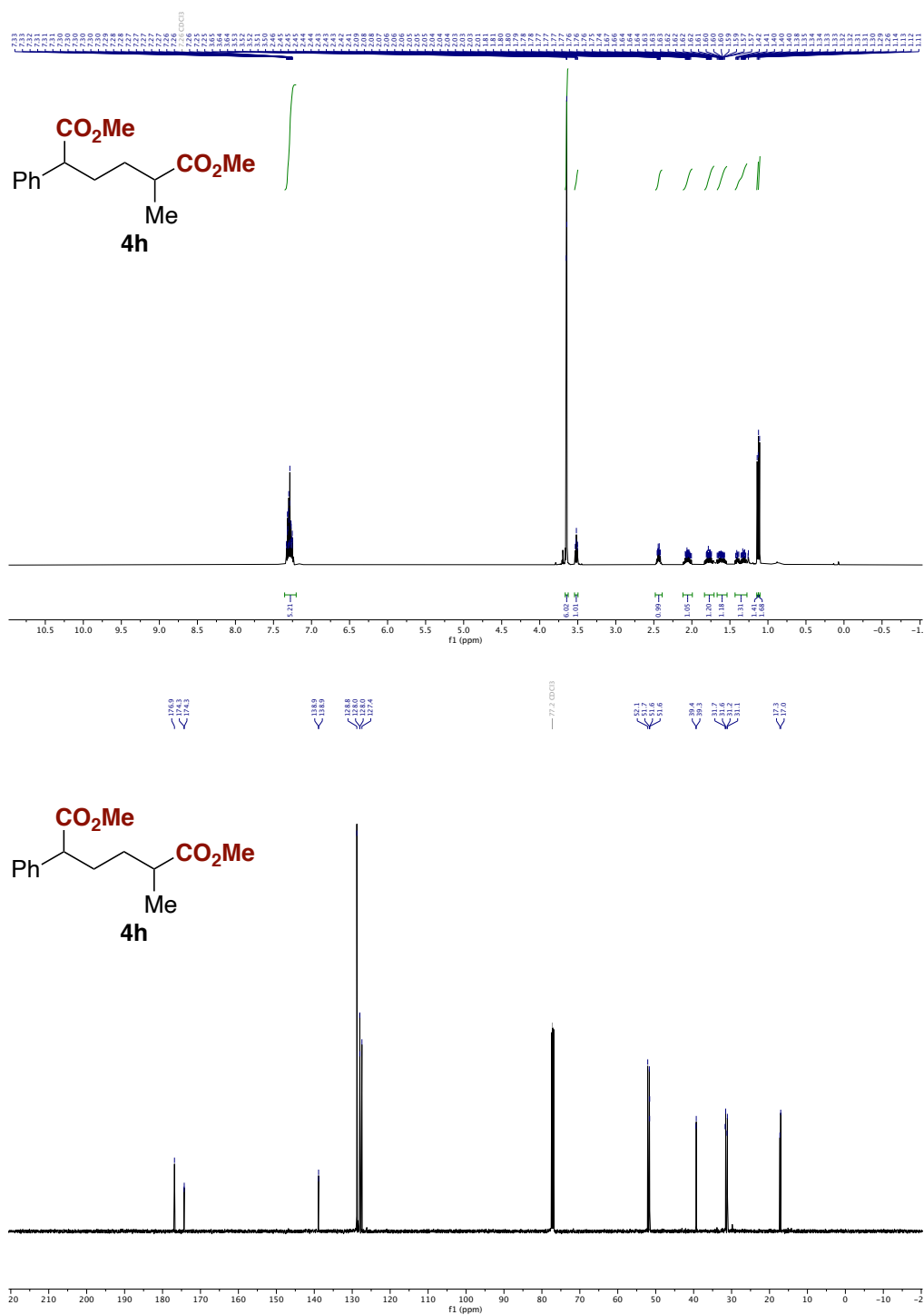


Figure 11. <sup>1</sup>H and <sup>13</sup>C NMR spectra of **4h**.

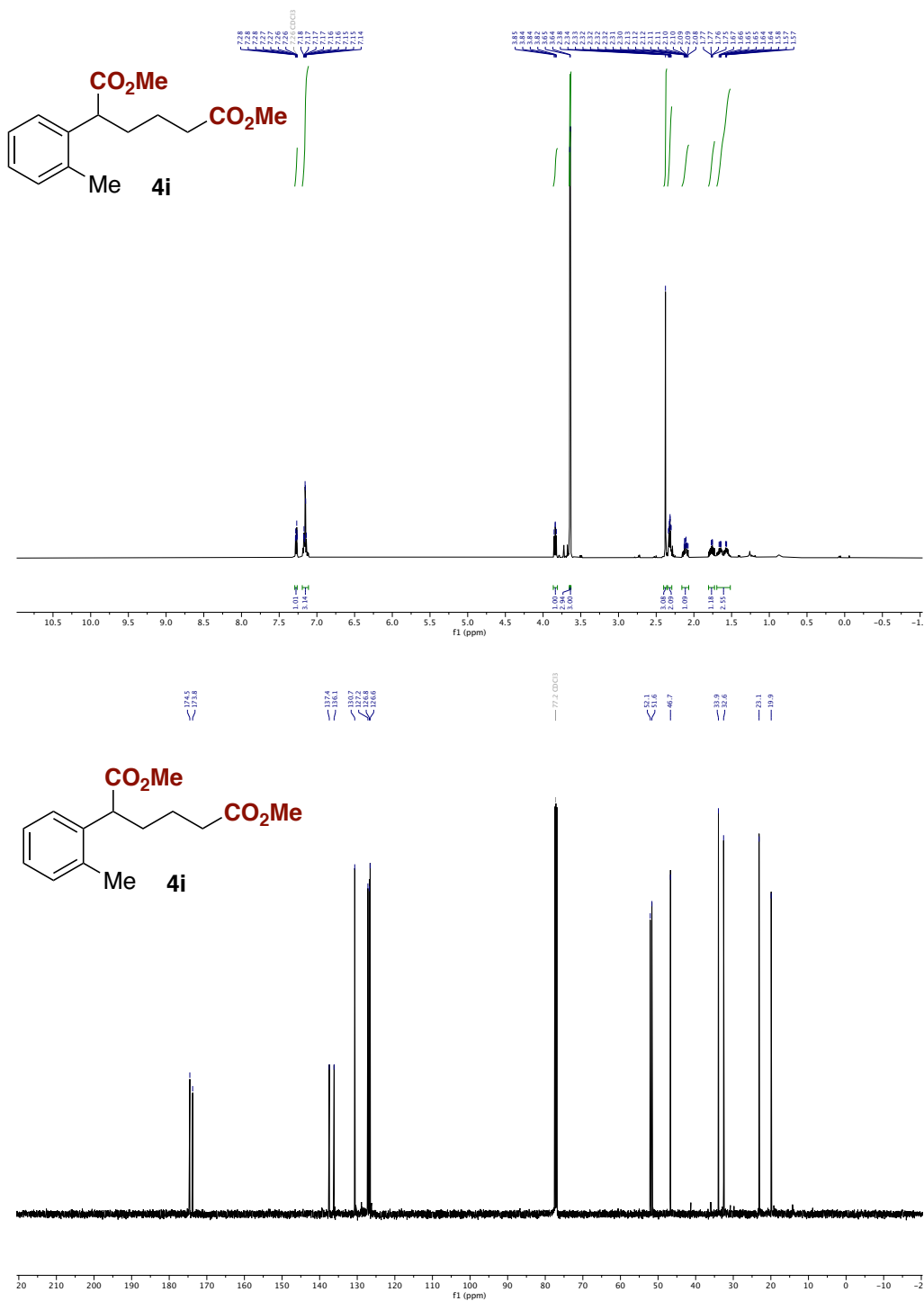


Figure 12. <sup>1</sup>H and <sup>13</sup>C NMR spectra of **4i**.



# Chapter 3

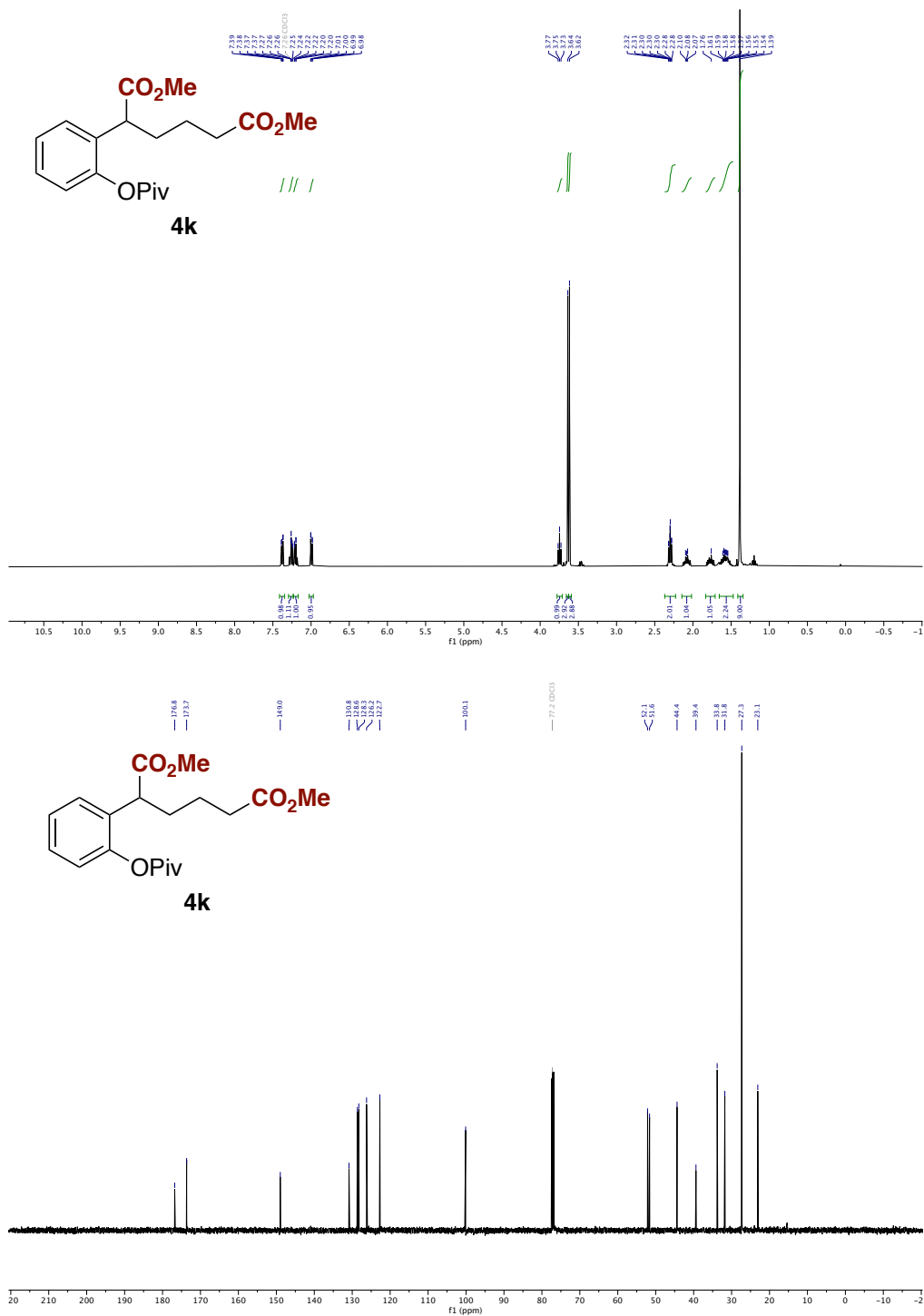
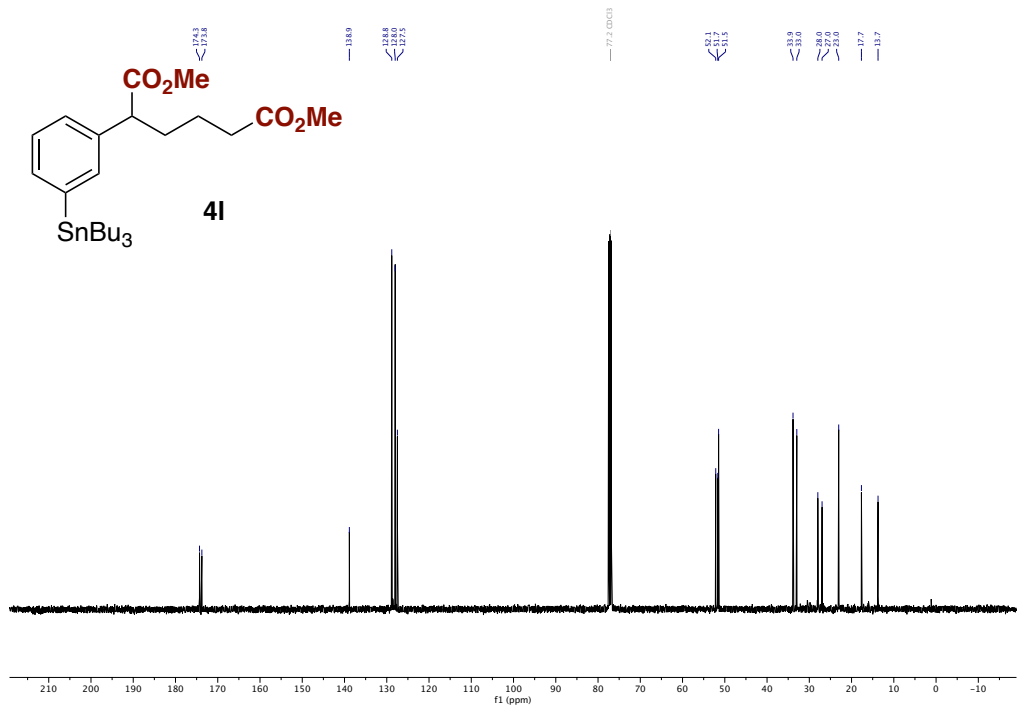
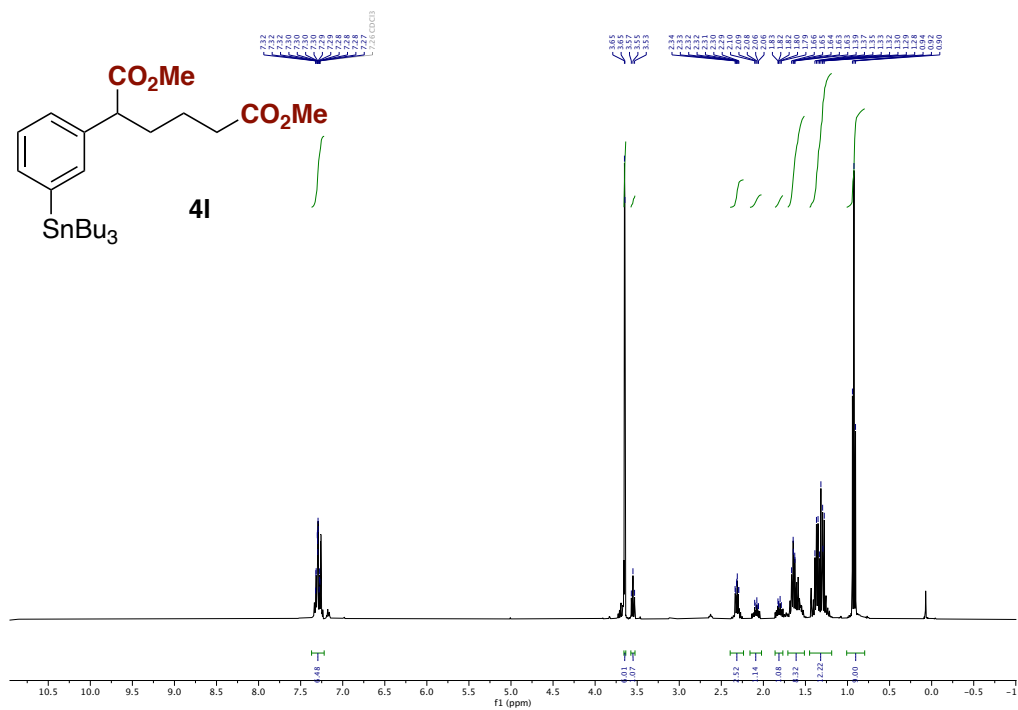


Figure 14. <sup>1</sup>H and <sup>13</sup>C NMR spectra of 4k.

# Nickel-catalyzed double carboxylation of 1,3-dienes with CO<sub>2</sub>



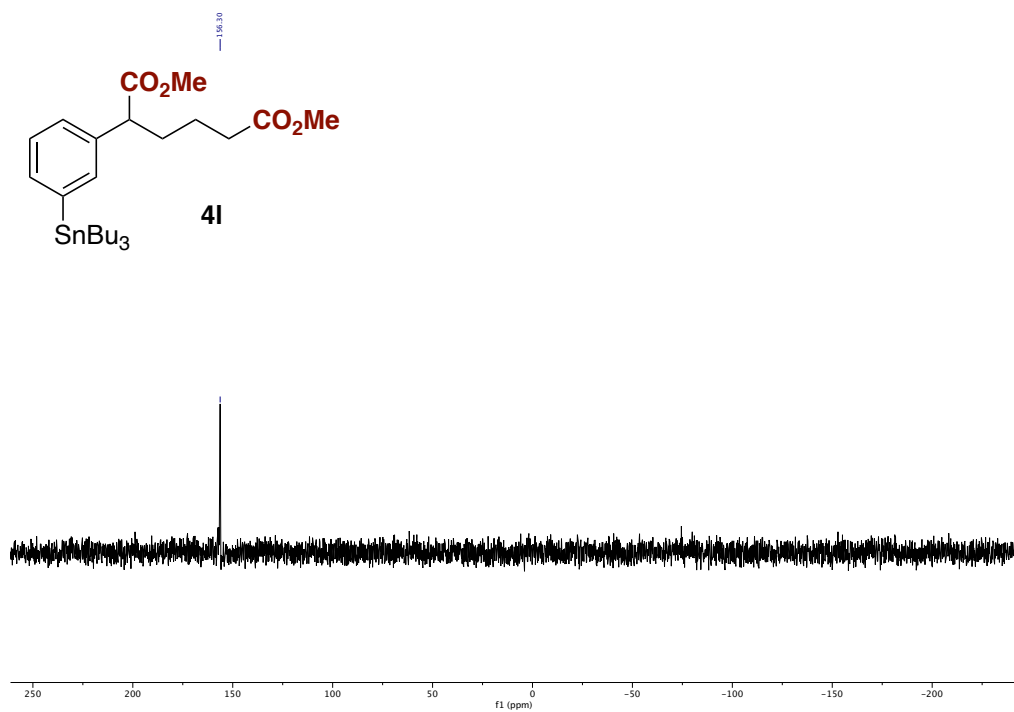


Figure 15.  $^1\text{H}$ ,  $^{13}\text{C}$  and  $^{119}\text{Sn}$  NMR spectra of **4I**.



# Chapter 3

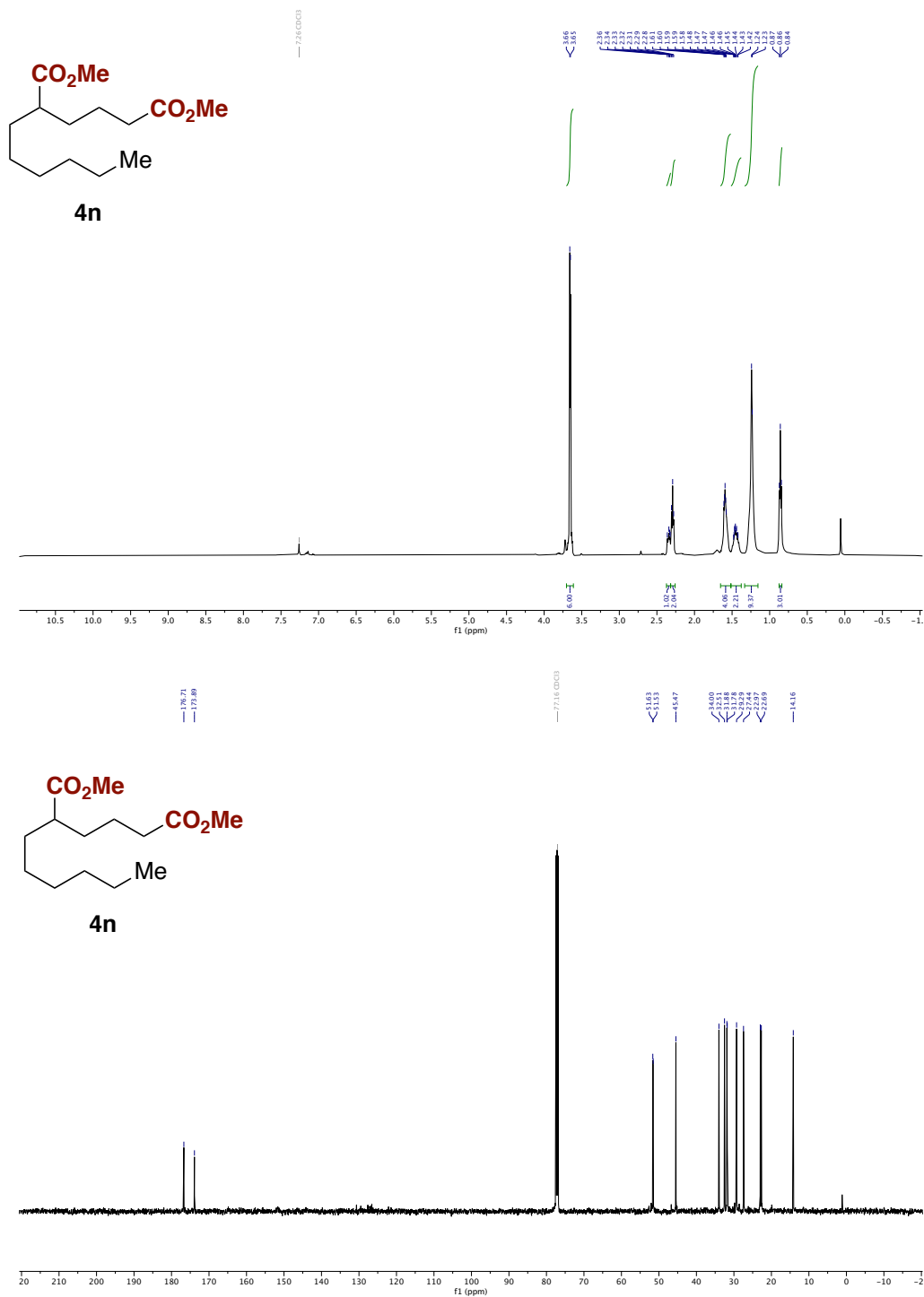


Figure 17. <sup>1</sup>H and <sup>13</sup>C NMR spectra of 4n.



Nickel-catalyzed double carboxylation of 1,3-dienes with CO<sub>2</sub>

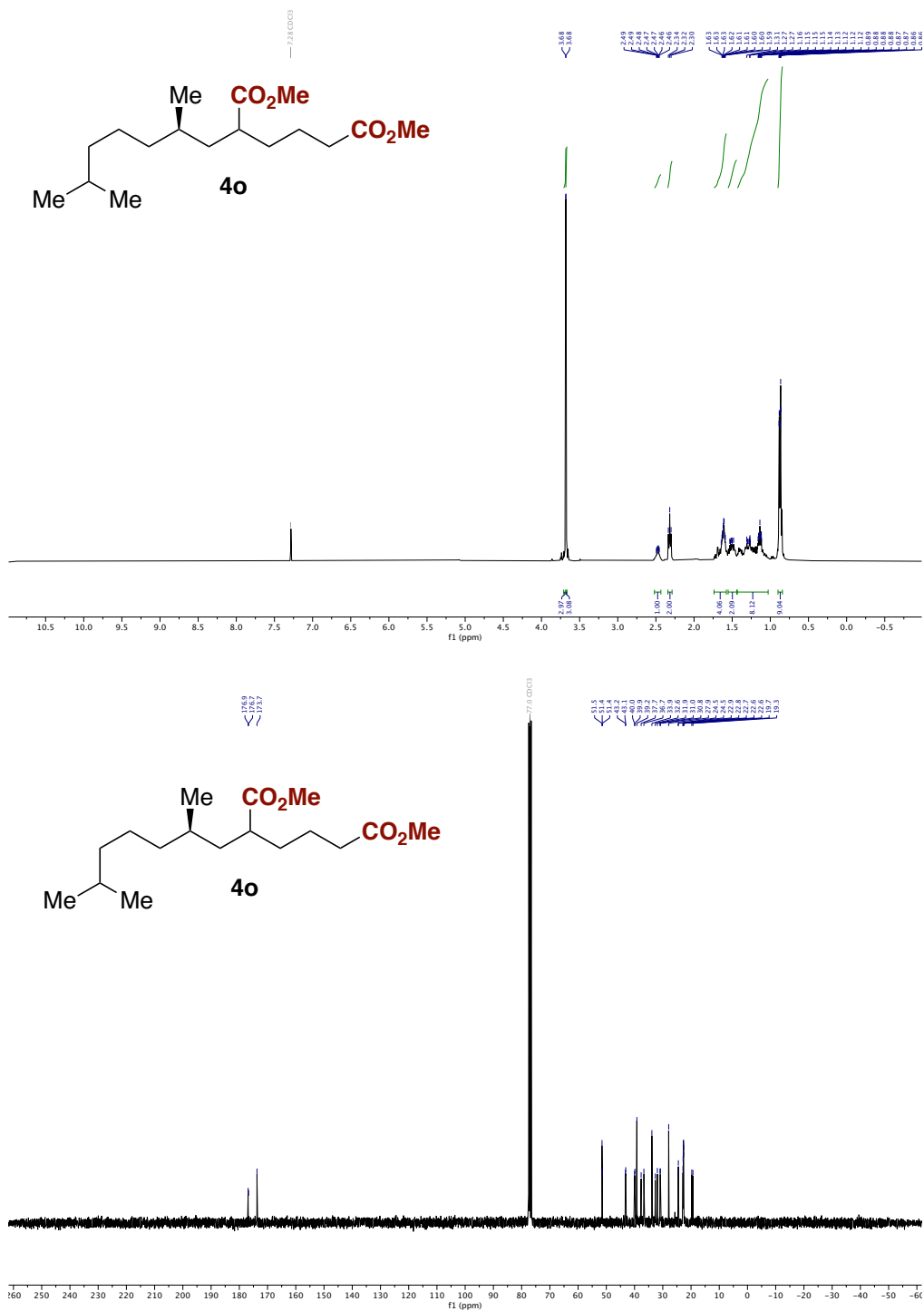


Figure 18. <sup>1</sup>H and <sup>13</sup>C NMR spectra of **4o**.



Nickel-catalyzed double carboxylation of 1,3-dienes with CO<sub>2</sub>

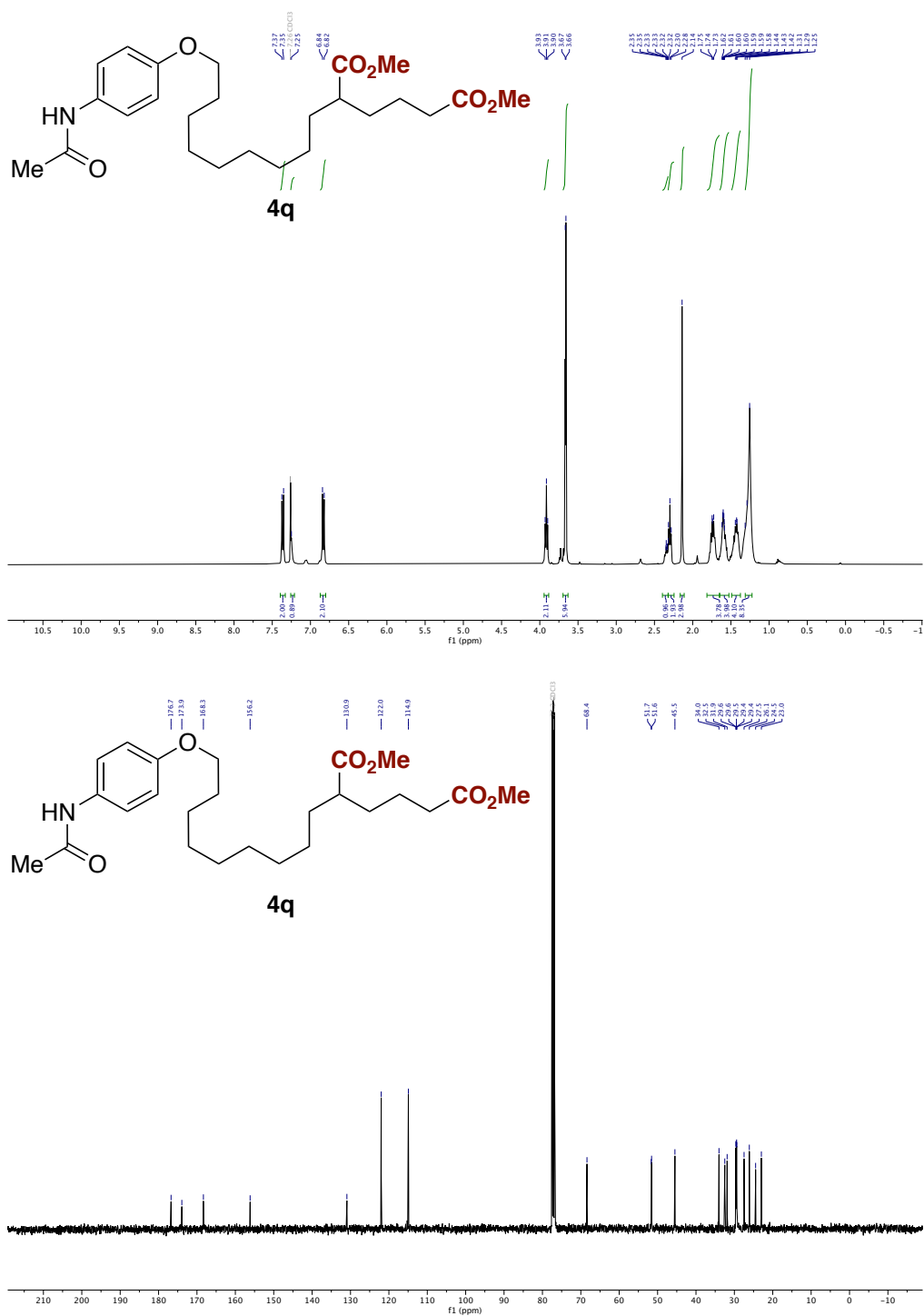


Figure 20. <sup>1</sup>H and <sup>13</sup>C NMR spectra of **4q**.

# Chapter 3

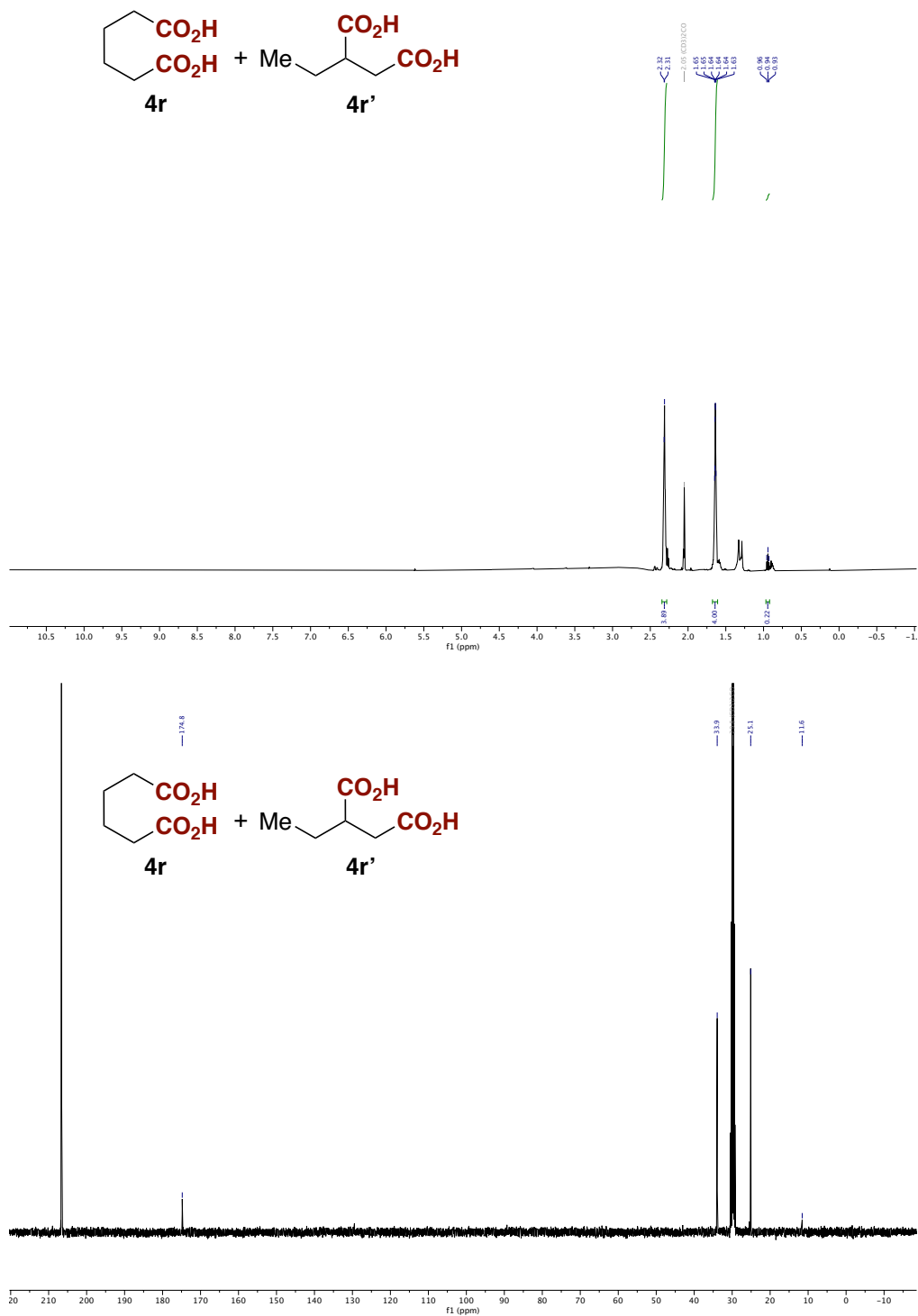


Figure 21. <sup>1</sup>H and <sup>13</sup>C NMR spectra of **4r/4r'**.

Nickel-catalyzed double carboxylation of 1,3-dienes with CO<sub>2</sub>

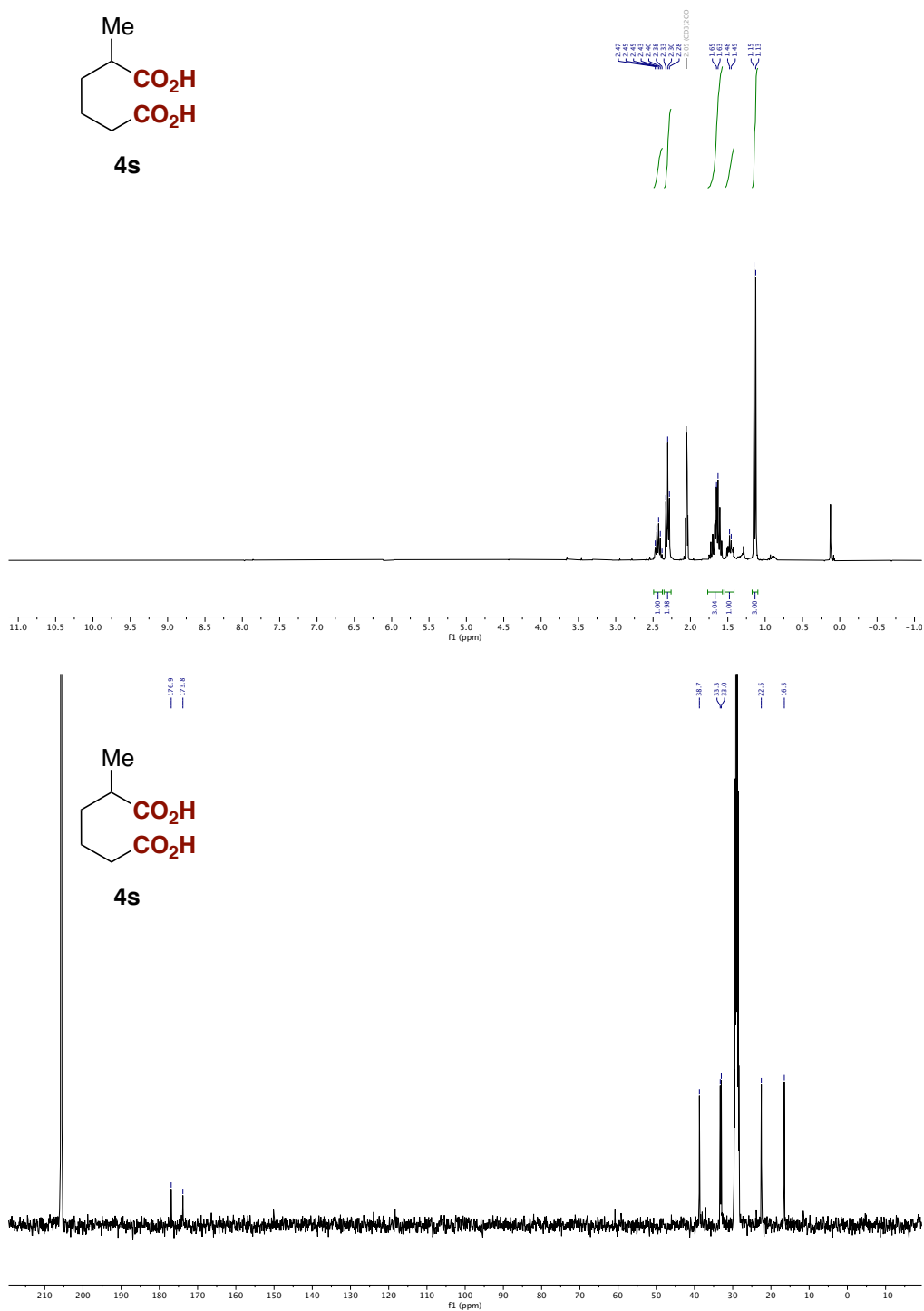


Figure 22. <sup>1</sup>H and <sup>13</sup>C NMR spectra of **4s**.

Chapter 3

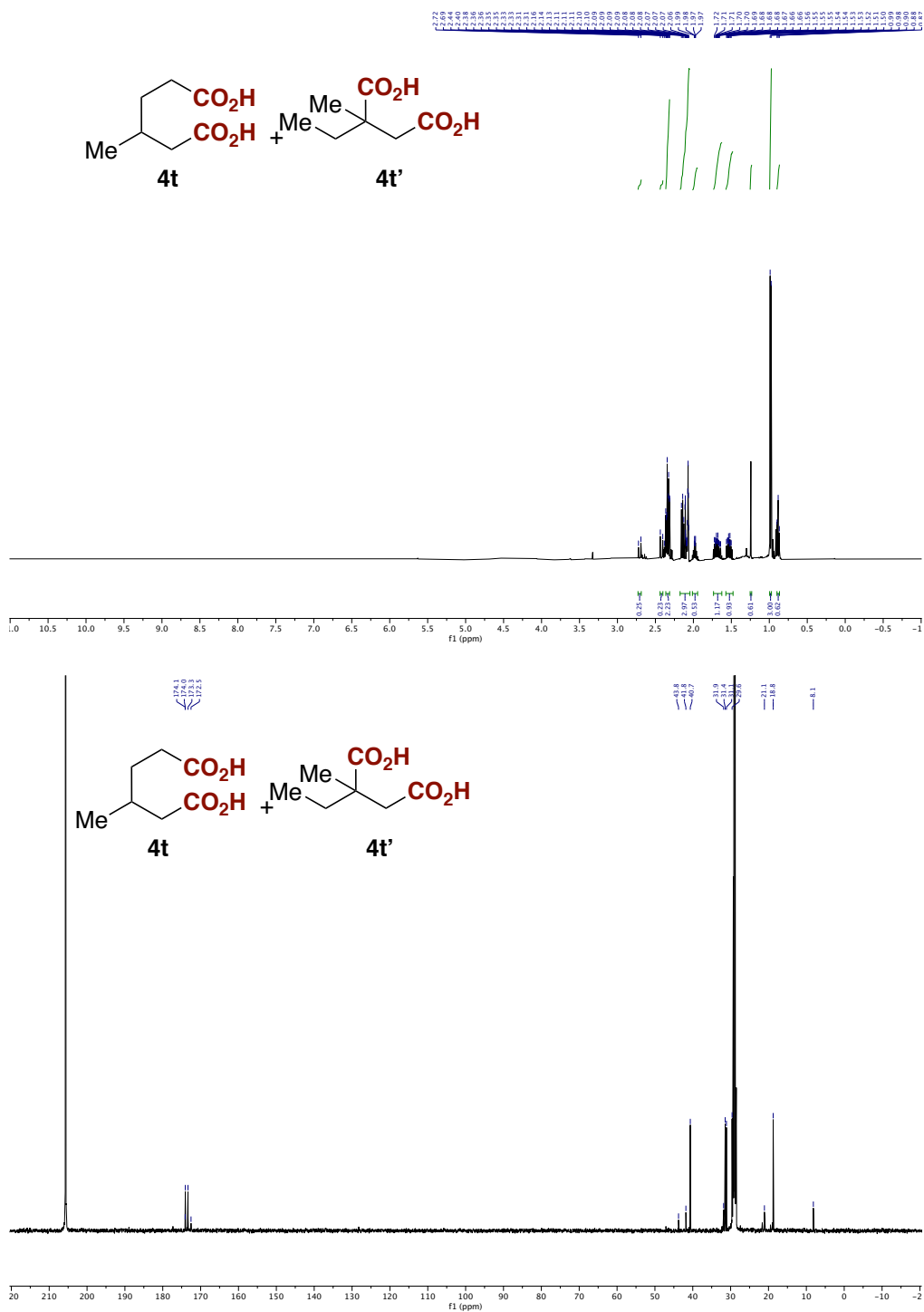


Figure 23. <sup>1</sup>H and <sup>13</sup>C NMR spectra of 4t/4t'.

Nickel-catalyzed double carboxylation of 1,3-dienes with CO<sub>2</sub>

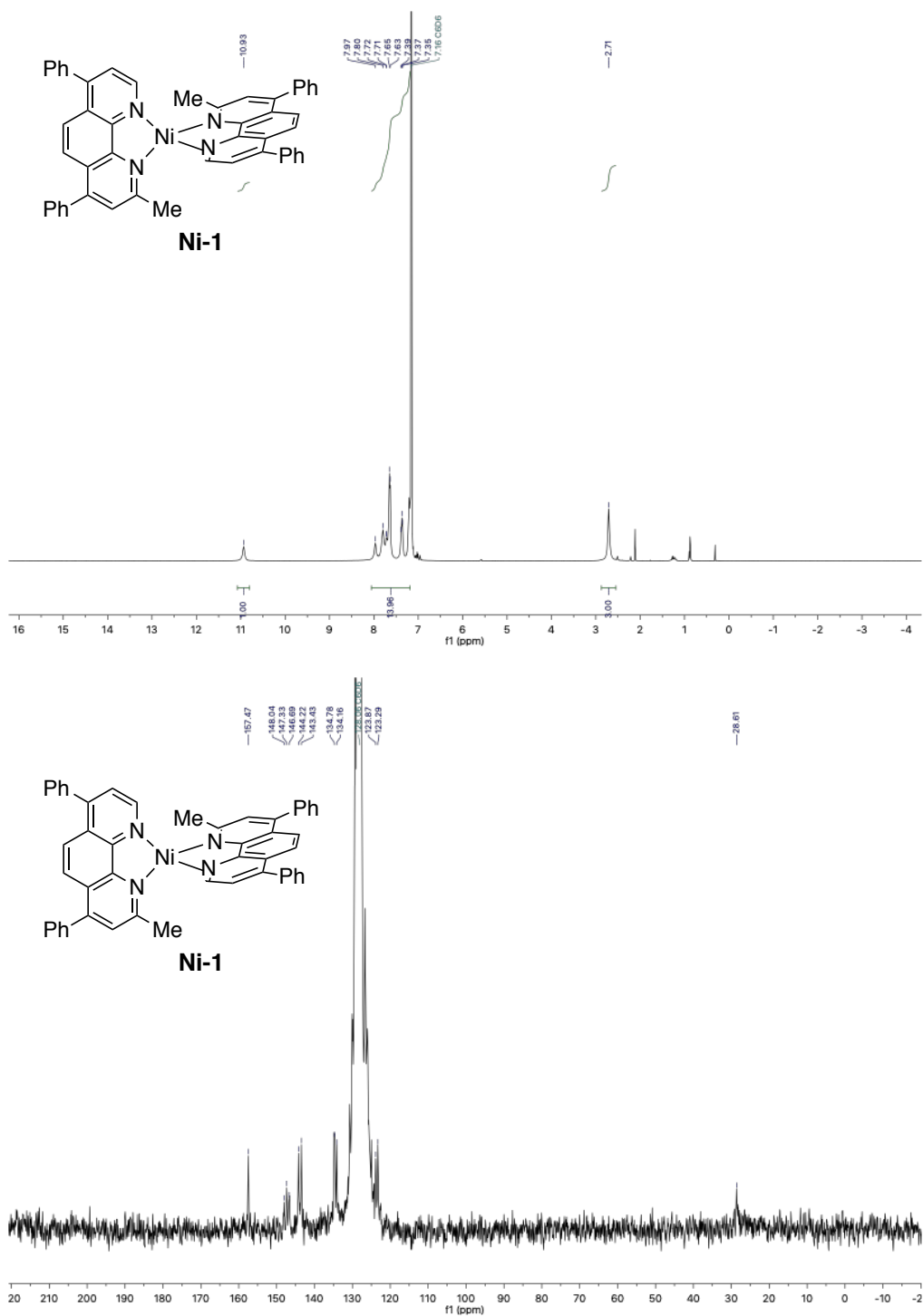
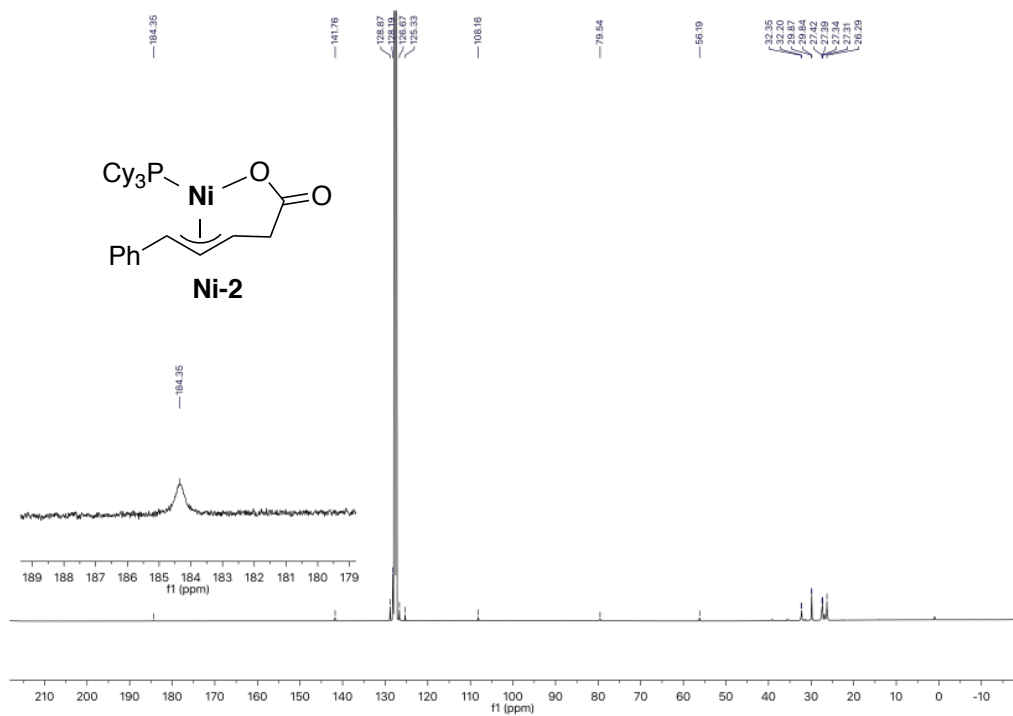
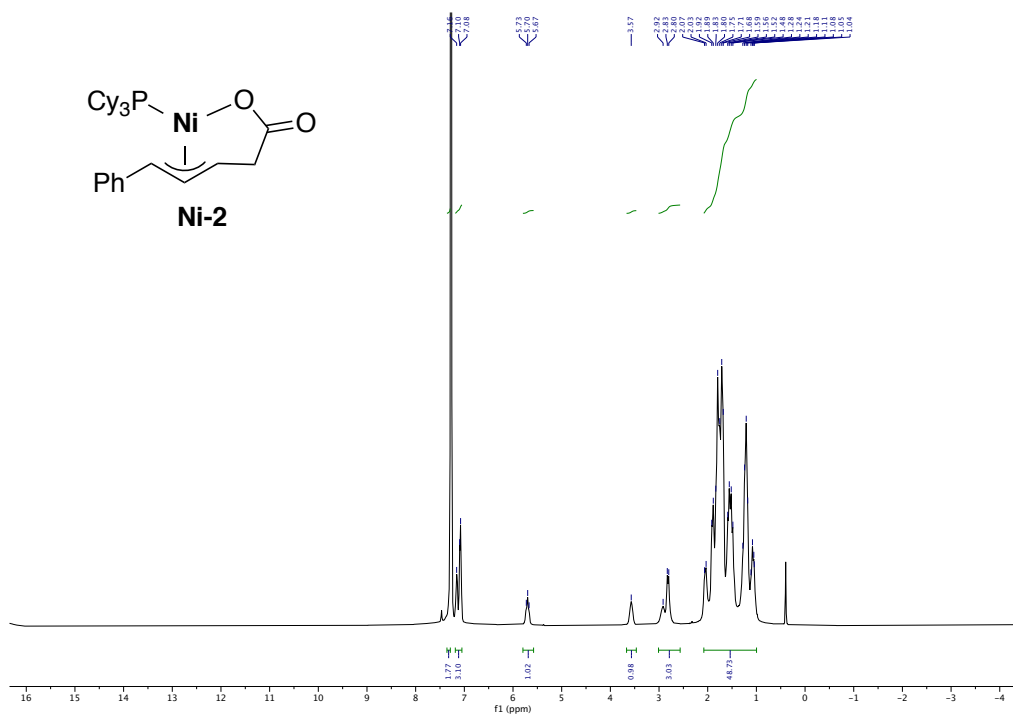


Figure 24. <sup>1</sup>H and <sup>13</sup>C NMR spectra of Ni-1.

# Chapter 3





# Nickel-catalyzed double carboxylation of 1,3-dienes with CO<sub>2</sub>

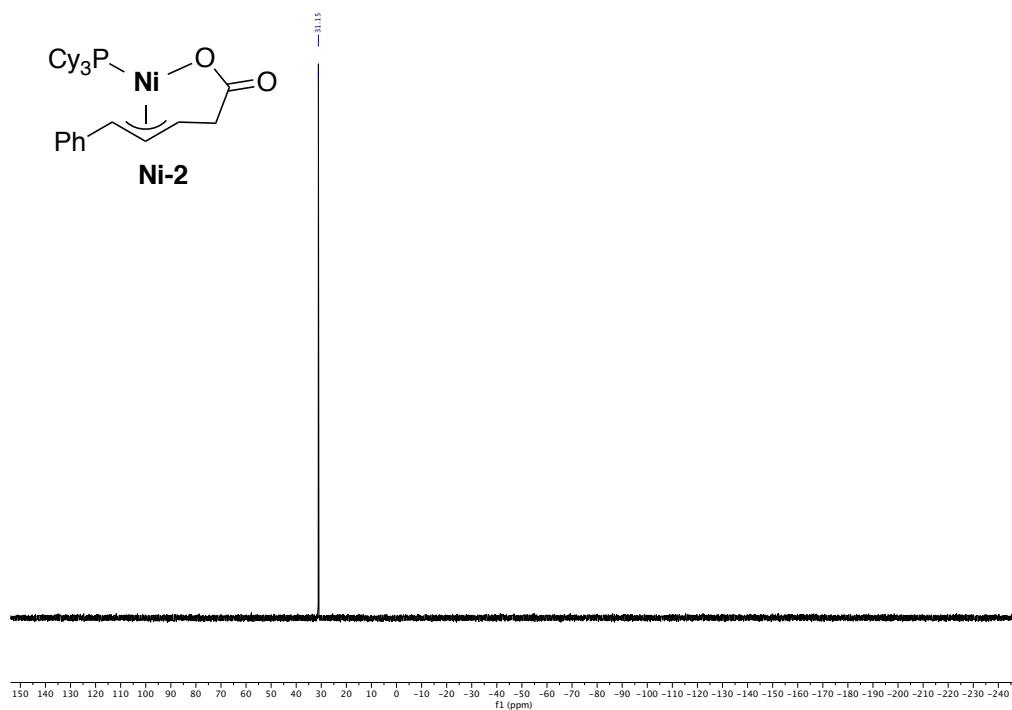


Figure 25. <sup>1</sup>H, <sup>13</sup>C NMR and <sup>31</sup>P spectra of **Ni-2**.



**Chapter 4:**  
***Catalytic Decarboxylation/Carboxylation Platform for  
Accessing Isotopically Labeled Carboxylic Acids***

*In collaboration with Georgios Toupalas, Dr. Yaya Duan, Dr. Basudev Sahoo,  
Fei Cong and the group of Prof. Davide Audisio*



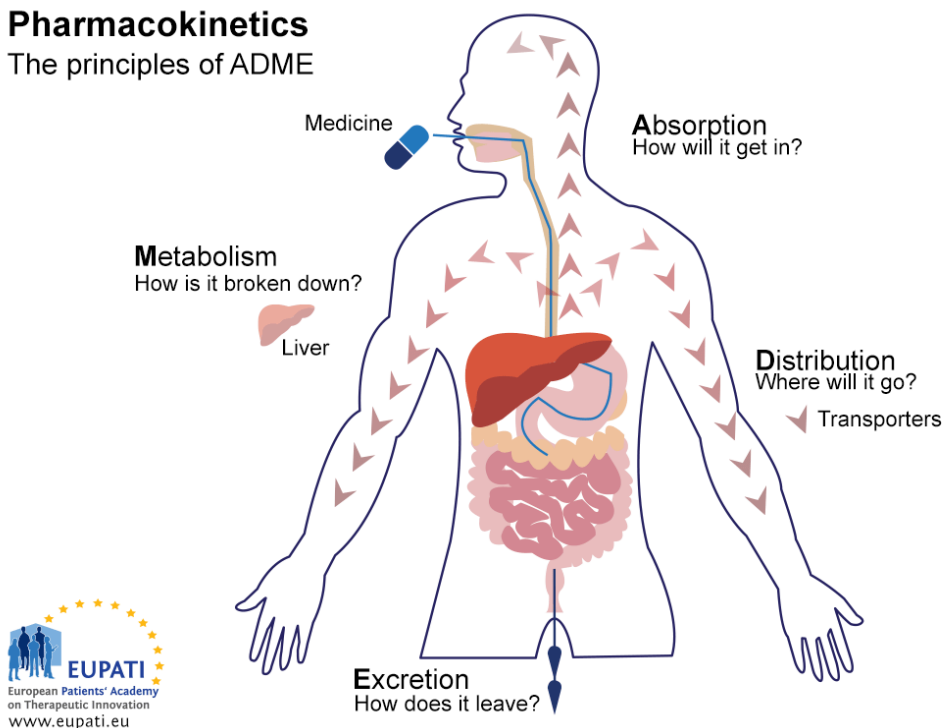
## 1. Introduction

### 1.1. Isotopic labeling and drug metabolism in drug discovery and development

The discovery and development of new drugs is a time-consuming and costly process, taking on average more than 10 years and over \$ 2600 million.<sup>1</sup> An essential step for the success of the drug development is the evaluation of the metabolic profile and the pharmacokinetics, which studies the fate of a drug molecule after administration. The disposition of a drug in the body involves absorption, distribution, metabolism and excretion (ADME, Figure 1). It is a complex process involving transporters and metabolizing enzymes with physiological consequences on pharmacological and toxicological effects. It can play a major role in drug design for identifying better drug molecules in a more efficient way.<sup>2,3</sup> To study the drug pharmacokinetics, the synthesis of isotopically labeled active pharmaceutical ingredients (APIs) is critical. Its synthesis is oftentimes more problematic than that of the parent compound, due to a limited number of methods for isotopic enrichment and incorporation, making necessary in most cases the design of a new synthetic route.

### Pharmacokinetics

The principles of ADME



**Figure 1.** The principles of ADME (<https://www.patientsacademy.eu/glossary/pharmacokinetics/>)

In the isotopic labeling field two different approaches can be considered:<sup>4</sup> a) the more widespread use of radioisotopes (<sup>3</sup>H, <sup>125</sup>I, <sup>35</sup>S, <sup>14</sup>C, <sup>11</sup>C, <sup>18</sup>F,...) which after radioactive decay emit a radiation that can be measured and are used to locate and quantify the API and its metabolites;<sup>5,6</sup> b) lately with the improvement of mass spectrometry analysis and NMR spectroscopy techniques the use of stable nonradioactive isotopes (<sup>13</sup>C, <sup>2</sup>H, <sup>15</sup>N...) has grown as internal standards for bioassays or for assessing the bioavailability of drugs.<sup>7</sup>

If we focus our attention in the traditional radioactive isotope incorporation for pharmacokinetics investigation, the introduction of carbon labels is often preferred to other atoms such as oxygen or hydrogen, due to the high sensitivity and lower risk of label metabolic cleavage of carbon, rendering the interpretation of preclinical data easier.<sup>8</sup>

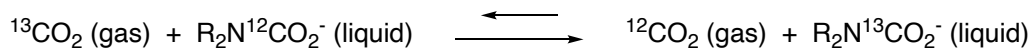
## 1.2. CO<sub>2</sub> as a source of isotopically labeled carbon.

Carbon has 15 known isotopes (<sup>8</sup>C to <sup>22</sup>C), of which <sup>12</sup>C and <sup>13</sup>C are stable. For isotopic labeling purposes <sup>11</sup>C, <sup>13</sup>C and <sup>14</sup>C have been utilized, since all other radioisotopes have half-lives < 20 seconds, too short for radiomedicine. Despite their different obtention methods, they all have in common that their main source is CO<sub>2</sub>:

Carbon-13 (<sup>13</sup>C). It is a natural, stable isotope with a 1.1% natural abundance on Earth. It has a spin quantum number of 1/2, and hence allows the structure of carbon-containing substances to be investigated using carbon-13 nuclear magnetic resonance. Recent advances during the last years in <sup>13</sup>C NMR spectroscopy have allowed the study of metabolic fluxes *in vivo* by this technique,<sup>8-11</sup> opening new paths for clinical applications. Moreover, molecules with multiple <sup>13</sup>C atoms incorporated into their structure have been used as well for bioavailability studies and bioassays with the support of mass spectrometry techniques.<sup>4,12,13</sup>

The first reports for the preparation of an isotopically enriched <sup>13</sup>C compound in an industrial scale was achieved by the low-temperature fractional distillation of carbon monoxide.<sup>14,15</sup> Its low separation factor, high energy demand, the complexity of the technological equipment, the rigorous requirements for pure CO and its toxicity have made necessary a change in strategy. Recently the industrial obtention of <sup>13</sup>C-enriched molecules has been achieved as well from chemical isotope exchange, a process in which a thermodynamically reversible separation in two-phase system is employed. The reversible formation of salt-like carbamates by reaction of secondary amines with CO<sub>2</sub> in anhydrous organic solvents has allowed the obtention of <sup>13</sup>CO<sub>2</sub> by multiple cycles of absorption and thermal release (Scheme 1). For this purpose, the system formed by piperazine as secondary amine and ethanolamine as solvent has shown good results in industrial settings.<sup>16,17</sup>

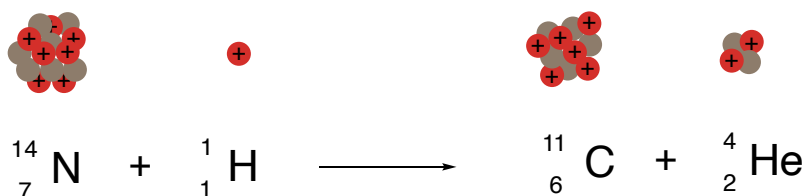
Catalytic Decarboxylation/Carboxylation Platform for Accessing Isotopically Labeled Carboxylic Acids



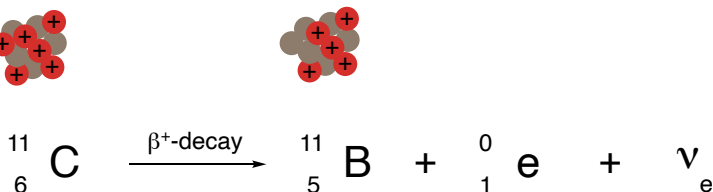
**Scheme 1.** Carbamate – CO<sub>2</sub> equilibrium

**Carbon-11 (<sup>11</sup>C).** It is a synthetic isotope usually produced by the irradiation of nitrogen gas with protons in a synchrotron using the <sup>14</sup>N(p,α)<sup>11</sup>C reaction (Scheme 2).<sup>18</sup> The <sup>11</sup>C formed reacts with traces of oxygen to give <sup>11</sup>CO<sub>2</sub>, which is obtained diluted generally with molecular nitrogen. It suffers a radioactive decay to <sup>11</sup>B with the liberation of a positron, with a half-life of 20.364 minutes. It is commonly used in medicine as a radioisotope in positron emission tomography (PET), an imaging technique to visualize and measure metabolic processes in the body.

□ Formation of <sup>11</sup>C in a cyclotron



□ Decay of <sup>11</sup>C to <sup>11</sup>B by positron emission

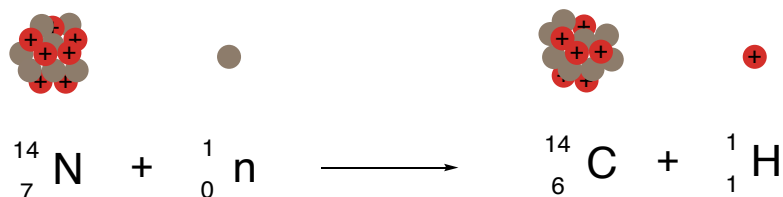


**Scheme 2.** Formation and β<sup>+</sup>-decay of <sup>11</sup>C.

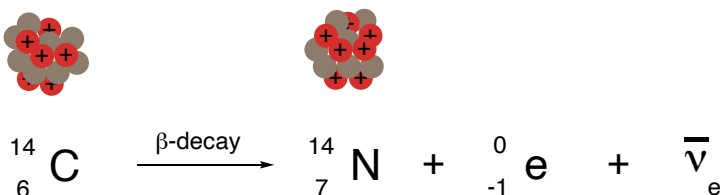
**Carbon-14 (<sup>14</sup>C).** It is a radioactive isotope of carbon containing six protons and eight neutrons in its nucleus. It was discovered in 1940 and was used in pioneering studies to date archaeological, geological and hydrogeological samples. This radioisotope is naturally produced in the upper layers of the troposphere and the stratosphere by thermal neutrons absorbed by nitrogen atoms (Scheme 3, *top*). When cosmic rays enter the atmosphere, they undergo various transformations, including the production of neutrons that participate in the n-p reaction to form <sup>14</sup>C. It can also be produced in the same way in a nuclear reactor, by exposing <sup>14</sup>N (typically, in the form of aluminium nitride) to thermal neutrons. <sup>14</sup>C suffers radioactive beta decay by emitting an electron and an electron antineutrino with a half-life of 5.700 ± 40 years,<sup>19</sup> and decays into the stable <sup>14</sup>N (Scheme 3, *bottom*). The beta particles emitted are estimated to have a maximum distance travel of 22 cm in air or 0.27 mm in body tissue. Although small amounts of <sup>14</sup>C are not easily detected by typical Geiger-Müller detectors, the liquid scintillation counting is the preferred

detection method, in which the sample is mixed with a liquid scintillator (e.g., zinc sulphide) that emits photons after absorbing the energy of the beta emission. Its use nowadays in medicine is mainly to study the ADME properties and pharmacokinetics profiles of drug candidates, since it allows tracing and quantifying the drugs and its metabolites in the body (Figure 1, *vide supra*).

□ Formation of  $^{14}\text{C}$  by thermal neutron irradiation



□  $\beta$ -Decay of  $^{14}\text{C}$  to  $^{14}\text{N}$

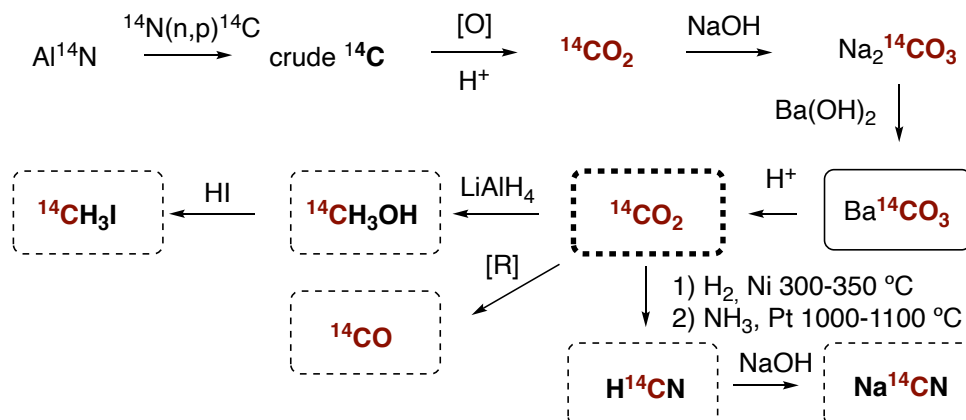


**Scheme 3.** Formation and  $\beta$ -decay of  $^{14}\text{C}$ .

Crude  $^{14}\text{C}$  generated in a nuclear plant is converted into  $^{14}\text{CO}_2$  and precipitated as  $\text{Ba}^{14}\text{CO}_3$ , which is considered the chemical primary source of  $^{14}\text{C}$ . Therefore, the vast majority of  $^{14}\text{C}$  syntheses utilize 1- and 2-carbon reagents prepared from  $\text{Ba}^{14}\text{CO}_3$  (Scheme 4).<sup>20</sup> The first step in every case is the protonation or decomposition of barium carbonate to form carbon dioxide, being  $^{14}\text{CO}_2$  considered the ideal synthon and the sole starting material. Direct fixation of carbon dioxide into an organic backbone is therefore of considerable advantage, but most of the established carboxylation techniques still rely on highly nucleophilic organometallic species (such as Grignard or organolithium reagents), hereby drastically limiting the synthetic value of this approach. Due to this,  $^{14}\text{CO}_2$  has been traditionally transformed into secondary synthons such as cyanides, methanol, carbon monoxide or methyl iodide, which facilitate the incorporation of the carbon label. The whole labeling procedures with  $^{14}\text{C}$  are multi-step, time-consuming and they have high costs associated ( $^{14}\text{CO}_2$ : 1600 €/mmol). In addition, the generation of long-lived radioactive waste (half-life 5700 years) affect even further the radiosynthesis. More advanced building blocks are commercially available, but they are often highly expensive and still a bottleneck when planning an actual synthesis.



## Catalytic Decarboxylation/Carboxylation Platform for Accessing Isotopically Labeled Carboxylic Acids



**Scheme 4.** Preparation of  $^{14}\text{C}$  synthons.

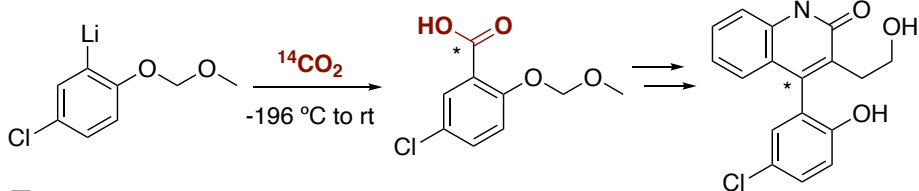
As described previously, carbon dioxide represents the main source of isotopically labeled carbon for either  $^{11}\text{C}$ ,  $^{13}\text{C}$  or  $^{14}\text{C}$ . Consequently, the rapid evolution of transition metal-catalyzed carboxylations over the past decade and the resulting availability of numerous protocols for C–C bond formation, arose interest for the application of the carboxylation reactions to the area of carbon labeling. The direct utilization of  $\text{CO}_2$  for the synthesis of APIs in a single or very few steps would represent a clear advantage for the study and development of drugs, providing a significant advance in the field.

### 1.3. Carboxylation reactions with isotopically labeled $\text{CO}_2$ .

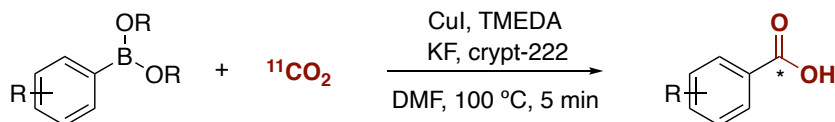
Traditional utilization of  $\text{CO}_2$  in isotopic labeling reactions involves the utilization of highly nucleophilic and reactive organometallic species, such as Grignard or organolithiums reagents. As an example, Almac Sciences reported the synthesis of a novel BK channel activator with a carbon-14 label for development studies by addition of an organolithium to  $^{14}\text{CO}_2$  (Scheme 5, *top*).<sup>21</sup> The poor functional group tolerance, their sometimes-difficult preparation and the requirement for special techniques for handling these compounds have limited their application. As described in chapter 1, the use of  $\text{CO}_2$  in combination with other electrophiles or olefins in the presence of a transition metal has recently become a viable alternative.

The first example of metal catalyzed isotopic labeling with carbon dioxide was reported by Pike and co-workers in 2012 (Scheme 5, *bottom*).<sup>22</sup> In this seminal work the authors used boronic esters,  $^{11}\text{CO}_2$  and a Cu-catalyst to form  $^{11}\text{C}$ -labeled benzoic acids. Furthermore, the addition of KF combined with a cryptand and elevated temperatures were shown to be essential for the reaction. This technique was later applied to the preparation of a labeled drug for PET studies.<sup>23</sup>

- Example of organolithium addition to  $^{14}\text{CO}_2$



- Cu-catalyzed carboxylation of boronic esters with  $^{11}\text{CO}_2$

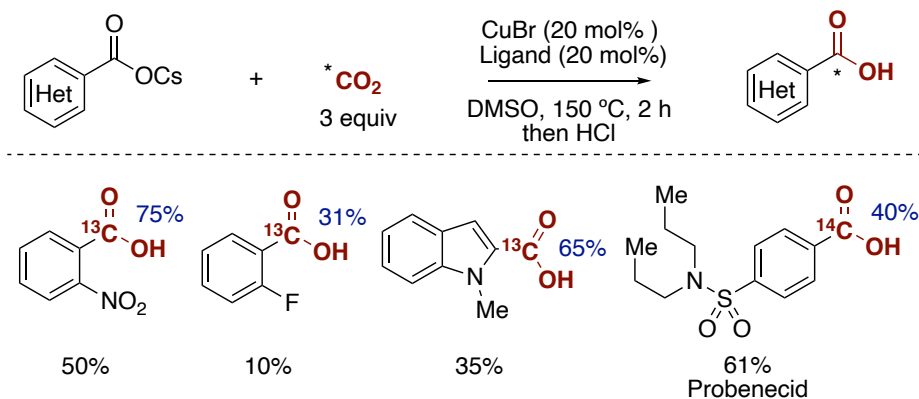


**Scheme 5.** Carboxylation reactions with labeled  $\text{CO}_2$ .

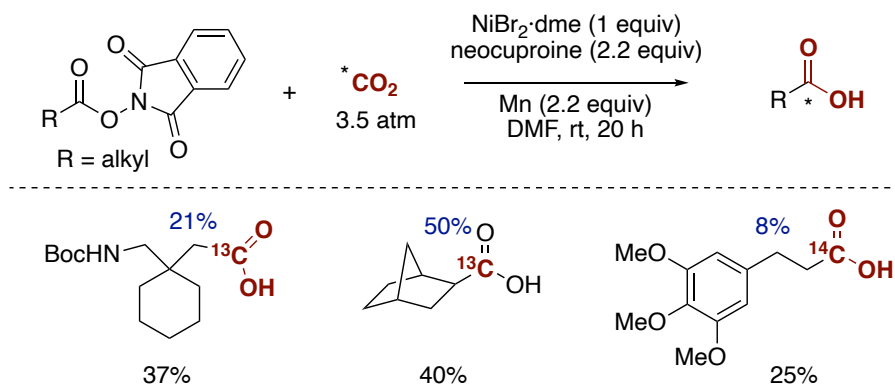
At the outset of the research project described in this chapter, no further examples of carboxylation with isotopically labeled  $\text{CO}_2$  in the absence of nucleophilic well-defined organometallic compounds were reported. This field has attracted the interest of different groups in the chemistry community in the past year and the different contributions that were developed in parallel or after the publication of our results will be discussed below. In 2019 Audisio and co-workers reported the dynamic carbon isotope exchange with labeled  $\text{CO}_2$ . They achieved the isotopic labeling of benzoic acids and other heteroaromatic carboxylic acids by means of copper catalysis at elevated temperatures with DMSO as solvent (Scheme 6, *top*).<sup>24</sup> By using only 3 equivalents of labeled  $\text{CO}_2$  up to 75% isotope incorporation was achieved with moderate to good yields, including different APIs. The same year, Baran and co-workers reported a nickel mediated isotope exchange of primary and secondary aliphatic carboxylic acid *N*-hydroxyphthalimide esters (Scheme 6, *bottom*).<sup>25</sup> This substrate could engage decarboxylation to generate the corresponding alkyl radical which is able to recombine with nickel and insert the labeled  $\text{CO}_2$ , although with moderate yields and isotopic incorporations. Notably, stoichiometric amount of nickel is necessary even though in the presence of an excess of a reducing agent.

## Catalytic Decarboxylation/Carboxylation Platform for Accessing Isotopically Labeled Carboxylic Acids

□ Copper catalyzed isotope exchange with labeled CO<sub>2</sub>



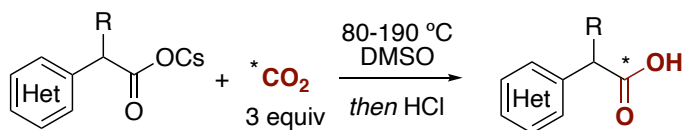
□ Nickel mediated isotope exchange with labeled CO<sub>2</sub>



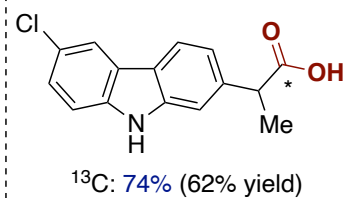
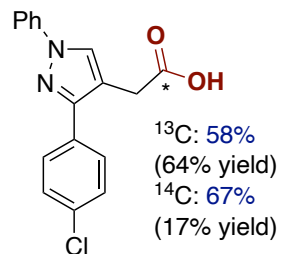
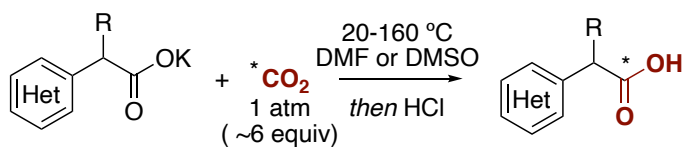
**Scheme 6.** Metal mediated isotope exchange with labeled CO<sub>2</sub>.

The direct isotope exchange with CO<sub>2</sub> has become a very attractive approach to prepare labeled compounds in a straightforward way. In 2020, two independent reports have been published regarding the transition-metal-free carbon isotope exchange of phenyl acetic acids with CO<sub>2</sub>. The Audisio group<sup>26</sup> and the Lundgren group<sup>27</sup> described a very similar approach in which the cesium or the potassium salts of the carboxylic acids are able to decarboxylate and carboxylate again in polar aprotic solvents to yield the isotopically labeled acids (Scheme 7). The advantage of this approach is the obtention of good yields and isotopic incorporations in the absence of transition metals in a single step from CO<sub>2</sub>, even with densely functionalized drugs and pharmaceuticals.

Audisio and coworkers:



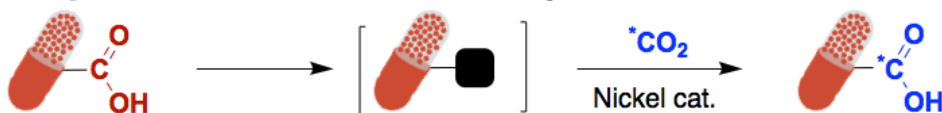
Lundgren and coworkers:

**Scheme 7.** Transition metal-free isotope exchange with  $\text{CO}_2$ .

## 2. General aim of the project

As seen in Chapter 1, the carboxylation of electrophiles and  $\pi$ -components with  $\text{CO}_2$  have received an increased attention in the last decades to provide different ways to use carbon dioxide as a C1 synthon in synthetic organic chemistry. However, at the outset of the present project, its use for isotopic labeling purposes was barely explored. Ideally, the carboxylation event should be conducted at late-stages, as the radioactive product would not have to be further transformed, thus increasing safety while decreasing the amount of radioactive waste generated by these transformations.

Bearing these premises in mind, we wondered whether it would be possible to develop a decarboxylation/carboxylation event, thus allowing to transform an advanced intermediate into the corresponding labeling analogue (Scheme 8). If successful, such transformation would be an ideal way of realizing a carbon isotope exchange in a single step from  $\text{CO}_2$ , thus avoiding the need for redesigning the synthesis route towards the labeled analogue. It is worth noting that this approach had no precedents at the outset of our investigations.



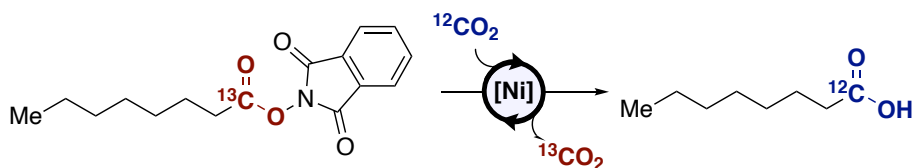
**Scheme 8.** Isotopic carbon labeling with  $\text{CO}_2$ .

The use of carboxylic acids in decarboxylative reductive couplings is well documented and has experienced a recent renaissance, resulting in various protocols for different transformations, yet usually requiring activation of the carboxylic acid.<sup>28-30</sup> Therefore, the use of redox-active esters has proved to be exceptionally useful especially *N*-hydroxyphthalimide esters.<sup>31</sup> Alternatively, the conversion of carboxylic acids into organic halides has been described as well,<sup>32-35</sup> providing a direct access to synthons from which its carboxylation has been studied in detail by our research group. Overall, we aimed at combining the advances made in transition metal catalyzed carboxylation reactions with the use of labeled  $\text{CO}_2$  to develop the envisaged late-stage carbon labeling method.

### 3. Catalytic decarboxylation/Carboxylation of carboxylic acids

#### 3.1. Isotope carbon exchange with *N*-hydroxyphthalimide esters

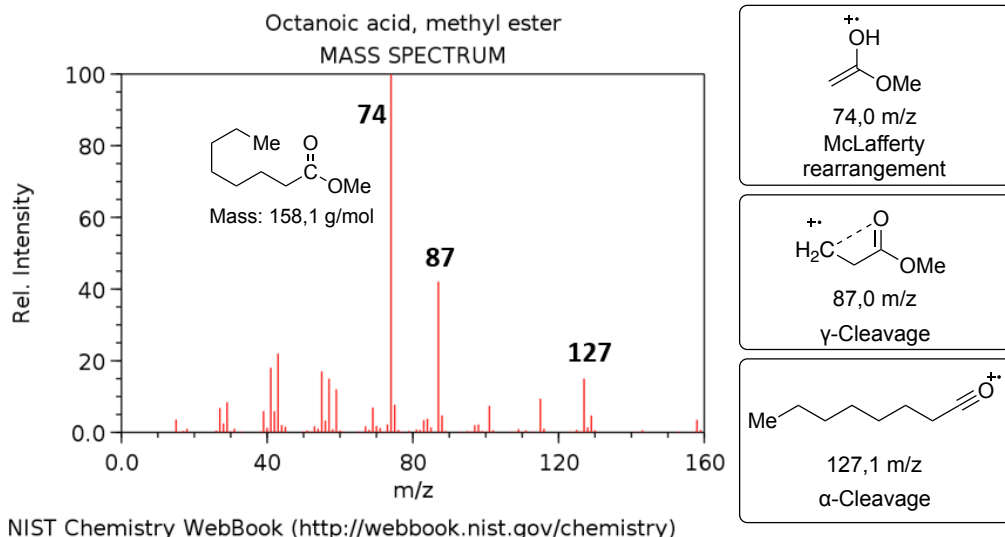
The project began with the search of a suitable model reaction which would allow the optimal reaction conditions to isotopically label organic molecules. The most straightforward approach would be to start with an *N*-hydroxyphthalimide (NHP) ester and employ labeled CO<sub>2</sub>. As a safe and an easy to handle source of labeled carbon dioxide for the development of this methodology, <sup>13</sup>CO<sub>2</sub> was chosen as the labeling material. Once a successful method was established, the protocol would prove the concept and be a labeling reaction itself but, moreover, it would allow the translation to other radioactive isotopes: <sup>11</sup>CO<sub>2</sub> and <sup>14</sup>CO<sub>2</sub>. However, the high price of <sup>13</sup>CO<sub>2</sub> and the fact that it is used typically in excess encouraged us to look for an alternative approach to study the feasibility of the project. To circumvent the above-mentioned problem, it was envisaged the use of a commercially available <sup>13</sup>C-labeled carboxylic acid (octanoic acid-1-<sup>13</sup>C, 150 €/g, Sigma Aldrich) and unlabeled carbon dioxide (Scheme 9). This reaction would essentially be the opposite reaction of the intended method, but once the optimal conditions would be found the reaction could readily be converted to the prior mentioned approach using <sup>13</sup>CO<sub>2</sub>.



**Scheme 9.** Model reaction using NHP ester.

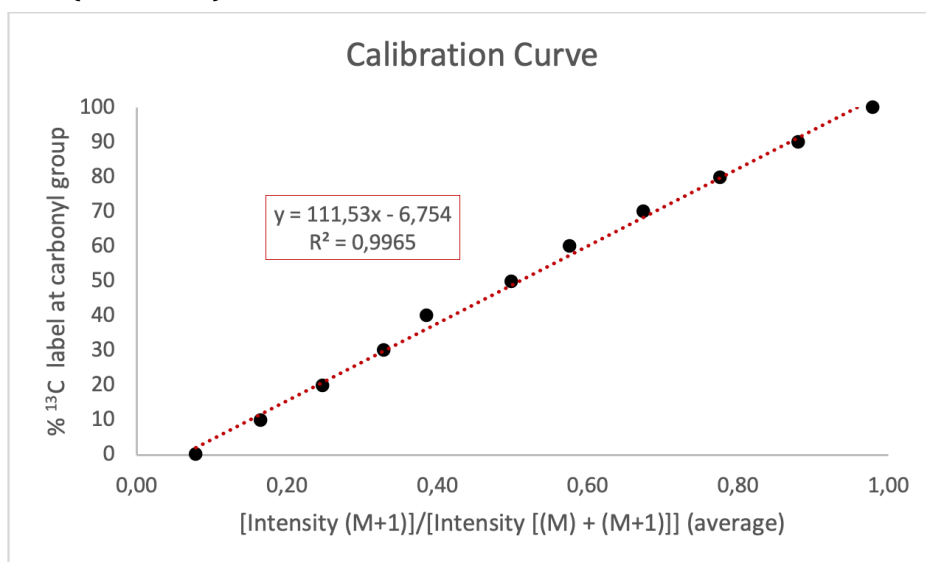
The next challenge that we encountered was to find a suitable analytical method to track and quantify the isotopic label. This analysis had to accomplish the following requirements: a) suitable for screening in terms of speed, practicality and low amounts of product to detect and b) high sensitivity to reliably quantify the label incorporation. Considering that the different isotopes can have a different atomic mass, mass spectrometry was envisioned as the optimal analysis technique. Taking into account the two above mentioned criteria, GC/MS was considered the ideal analytical method since it exhibits great sensitivity and can analyze multiple samples in a short period of time. Since the reaction affords a carboxylic acid, an appropriate and convenient method for its derivatization was needed. The methylation with TMS-diazomethane was chosen to prepare the corresponding methyl esters. They give 3 different signals that include the carbonyl carbon after fragmentation, allowing an easy quantification of the label incorporation (Figure 2).

## Catalytic Decarboxylation/Carboxylation Platform for Accessing Isotopically Labeled Carboxylic Acids



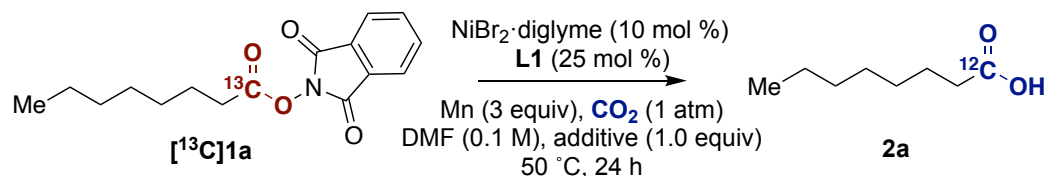
**Figure 2.** Mass fragmentation of methyl octanoate.

In order to take into account the natural abundance of  $^{13}\text{C}$  present in non-labeled  $\text{CO}_2$  and octanoic acid, a calibration curve was made by synthesizing labeled and non-labeled methyl octanoate from commercially available starting materials. Mixtures with different amounts of both labeled and unlabeled methyl octanoate were prepared and submitted to GC/MS analysis. Then, the average values obtained for the relative intensities of  $[M+1]$  for the most intense signals ( $M=75, 88$  and  $128$ , see Figure 2) were plotted against the  $^{13}\text{C}$ -incorporation in the carbonyl position of the different samples (Figure 3). A calibration curve with a good correlation was obtained ( $R^2=0.9965$ ).



**Figure 3.** Calibration curve.

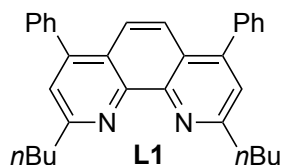
With a reliable way to quantify the labeling pattern into our target product, we started testing different reaction conditions. After esterification with TMS-CHN<sub>2</sub>, the samples were analyzed by GC-FID to obtain the yield and by GC/MS to obtain the change in the amount of <sup>13</sup>C. We started by applying previous developed conditions for the carboxylation of alkyl halides to our NHP ester. The use of phenanthroline **L1** in combination with halide salts gave promising results, observing a moderate carbon isotope exchange with bromide and chloride salts as additives (Table 1). In most cases, the conversion of the NHP ester was almost complete, being the main products the carboxylic acid **2a** and the corresponding 1-heptene, obtained from the β-hydride elimination of the Ni-alkyl intermediates. However, the carboxylic acid **2a** could be formed by CO<sub>2</sub> insertion at the Ni-alkyl intermediate (the desired reaction pathway), but it could also be formed by the hydrolysis or decomposition of **1a**, resulting in no isotopic exchange.



Entry	Additive (1 equiv)	Conversion /%	Yield <b>2a</b> /%	Δ <sup>13</sup> C /%
1	None	100	33	0
2	LiCl	100	12	1
3	LiBr	100	11	15
4	LiI	62	10	0
5	NaBr	100	30	14
6	KBr	99	12	6
7	MgBr <sub>2</sub>	100	14	24
8	MgCl <sub>2</sub>	100	24	28
9	AlBr <sub>3</sub>	100	15	17

Conditions: NHP-ester (0.1 mmol), NiBr<sub>2</sub>·diglyme (10 mol %), **L1** (25 mol %), Mn (0.3 mmol), CO<sub>2</sub> (1 atm) in DMF (0.1 M) at 50 °C.

**Table 1.** Screening halide salts for carbon isotope exchange.

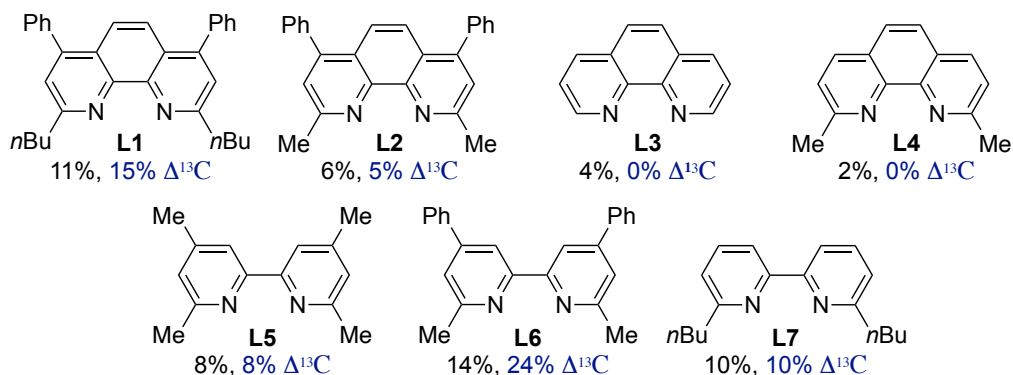
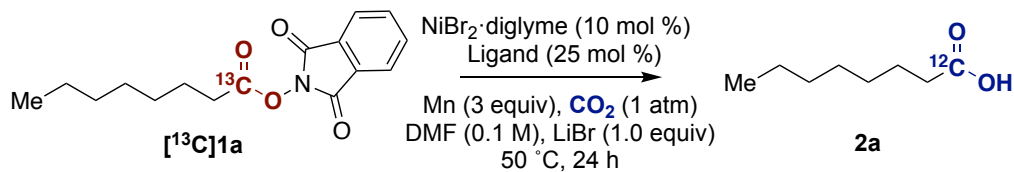


In parallel, LiBr was selected as an additive and we performed a ligand screening to explore the effect of the substituents and the ligand backbone (Table 2). Different phenanthroline and bipyridine ligands were tested, observing the need of



## Catalytic Decarboxylation/Carboxylation Platform for Accessing Isotopically Labeled Carboxylic Acids

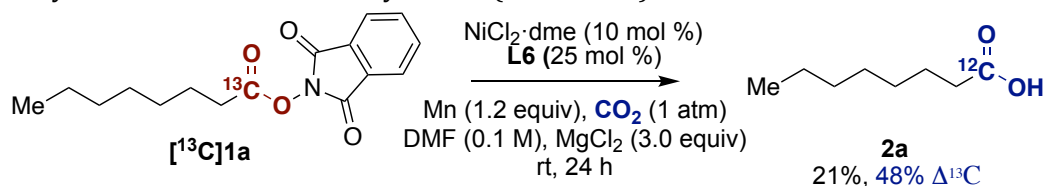
substituents in the position contiguous to the nitrogen atom and with better carbon isotope exchange when phenyl group were placed in C4 and C7 (**L1**, **L2** and **L6**), being notably better for the bipyridine ligand **L6**.



Conditions: NHP-ester (0.1 mmol),  $\text{NiBr}_2 \cdot \text{diglyme}$  (10 mol %), **L1** (25 mol %), Mn (0.3 mmol),  $\text{CO}_2$  (1 atm) in DMF (0.1 M) at  $50\text{ }^\circ\text{C}$ .

**Table 2.** Preliminary ligand screening.

Combining the use of  $\text{MgCl}_2$  and **L6** with modifications in the amount of additive, reductant and temperature, allowed to obtain 48% carbon isotope exchange with a 21% yield of the desired carboxylic acid (Scheme 10).



**Scheme 10.** Carbon isotope exchange with  $\text{MgCl}_2$  as additive.

Further improvement of the reaction by changing the reaction parameters could not be achieved and no significant advances could be made by using halide salts. Looking for alternative pathways, the addition of a protic solvent was envisioned. They have been reported to assist the photoreduction of NHP-esters by hydrogen-bonding to promote the corresponding radical generation.<sup>36</sup> As in the additive based strategy, where  $\text{Mg}^{2+}$  ions were hypothesized to coordinate to the NHP-ester for its activation, a similar scenario was foreseen for the reaction mechanism with alcohols.

With this precedent, we started by testing the reaction using a different set of alcohols in a 4 to 1 ratio with DMF (Table 3, entries 1-5). The addition of a protic cosolvent improved the carbon isotope exchange, being the best result obtained with MeOH. Further variation in the ratio and the reaction temperature could improve the system to obtain the desired carboxylic acid in a 68% yield with a 58% carbon isotope exchange (Table 3, entry 7). The use of other amide-based solvents did not yield better results (Table 3, entries 8-9).

Entry	Deviation	Conversion /%	Yield 2a /%	$\Delta^{13}\text{C}$ /%
1	DMF	100	40	15
2	DMF/MeOH, 4/1	100	50	60
3	DMF/ <i>i</i> PrOH, 4/1	100	29	28
4	DMF/ <i>t</i> BuOH, 4/1	100	27	21
5	DMF/HFIP, 4/1	100	9	24
6	DMF/MeOH, 4/1, 0 °C	97	63	54
7	DMF/MeOH, 3/1, 0 °C	100	68	58
8	NMP/MeOH, 3/1, 0 °C	100	61	58
9	DMA/MeOH, 3/1, 0 °C	100	57	47

Conditions: NHP-ester (0.1 mmol), NiCl<sub>2</sub>-dme (10 mol %), **L6** (25 mol %), Mn (0.12 mmol), CO<sub>2</sub> (1 atm) in DMF/ROH at rt.

**Table 3.** Alcohol screening for carbon isotope exchange.

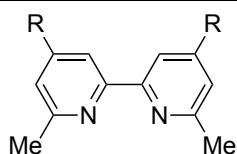
Final modification of the reductant equivalents and the reaction concentration could improve the yield obtained to 80%, maintaining the 60% carbon isotope exchange (Table 4, entry 1). Before proceeding to test the developed reaction conditions with <sup>13</sup>CO<sub>2</sub>, the different parameters of the reaction were tested again. A nickel(0) precatalyst, Ni(COD)<sub>2</sub>, showed no improvement for the reaction, probably due to the interference of the highly coordinating cyclooctadiene ligands (entry 2). The phenyl groups in the bipyridine ligands were found to be crucial for a good isotope exchange (entry 3) and the bipyridine scaffold was better than the analogous ligands with the phenanthroline backbone (entries 4-5). Zn proved to be worse than manganese as a reducing agent (entry 6), and the reaction proceeded with low isotope exchange in the absence of MeOH (entry 7) or at higher/lower temperatures (entries 8-9), showing the subtle balance between CO<sub>2</sub> insertion and the hydrolysis

Catalytic Decarboxylation/Carboxylation Platform for Accessing Isotopically Labeled Carboxylic Acids

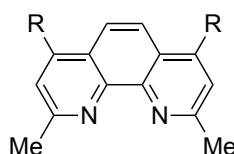
of the NHP ester. The omission of the nickel precatalyst, ligand, reducing agent or CO<sub>2</sub> yielded no carbon exchange, being the carboxylic acid observed most probably produced by degradation of the NHP ester (entries 10-13).



Entry	Deviation	Conversion /%	Yield 2a /%	$\Delta^{13}\text{C}$ /%
1	None	100	82	60
2	Ni(COD) <sub>2</sub>	100	30	24
3	<b>L8</b> instead of <b>L6</b>	100	48	28
4	<b>L4</b> instead of <b>L6</b>	100	43	14
5	<b>L2</b> instead of <b>L6</b>	100	47	30
6	Zn instead of Mn	100	42	10
7	Without MeOH	100	41	15
8	rt instead of 0 °C	100	70	25
9	-10 °C instead of 0 °C	100	80	37
10	Without Ni	100	33	0
11	Without <b>L6</b>	100	42	0
12	Without Mn	<5	0	-
13	Without CO <sub>2</sub>	100	15	0



R = Ph, **L6**  
R = H, **L8**

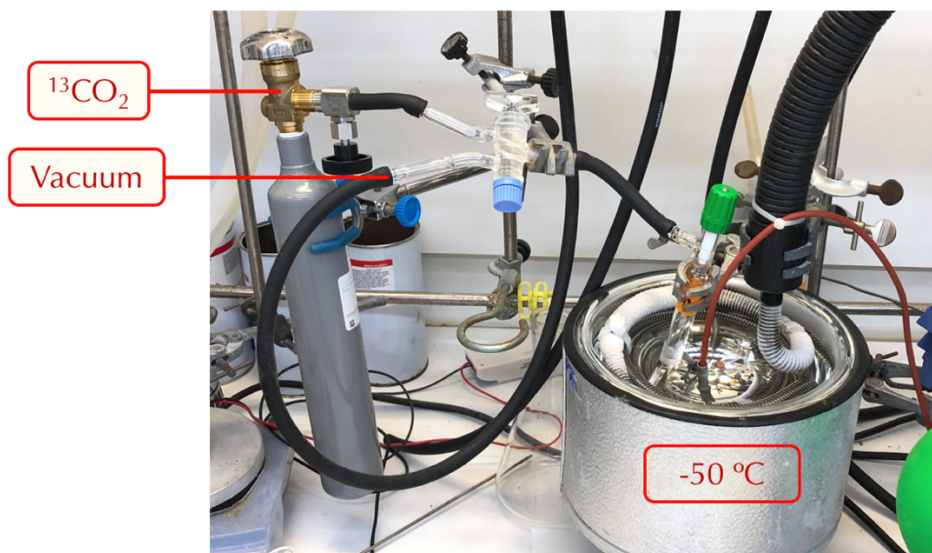


R = H, **L4**  
R = Ph, **L2**

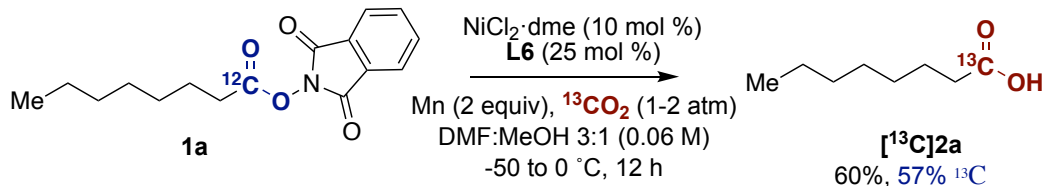
Conditions: NHP-ester (0.1 mmol), NiCl<sub>2</sub>-dme (10 mol %), **L6** (25 mol %), Mn (0.2 mmol), CO<sub>2</sub> (1 atm) in DMF/MeOH(0.06M) at 0 °C.

**Table 4.** Optimized reaction conditions for carbon isotope exchange.

With the optimized conditions in hand, we then conducted the reaction with <sup>13</sup>CO<sub>2</sub>. To such end, we built a system in which the reaction flask could be evacuated and backfilled with <sup>13</sup>CO<sub>2</sub> (Figure 4). The reaction flask was cooled down to -50 °C to ensure the transfer of most of the carbon dioxide. With this reaction set up a 60% yield and a 57% <sup>13</sup>C incorporation could be achieved (Scheme 11), showing the feasibility of the system for carbon isotope labeling with <sup>13</sup>CO<sub>2</sub>.



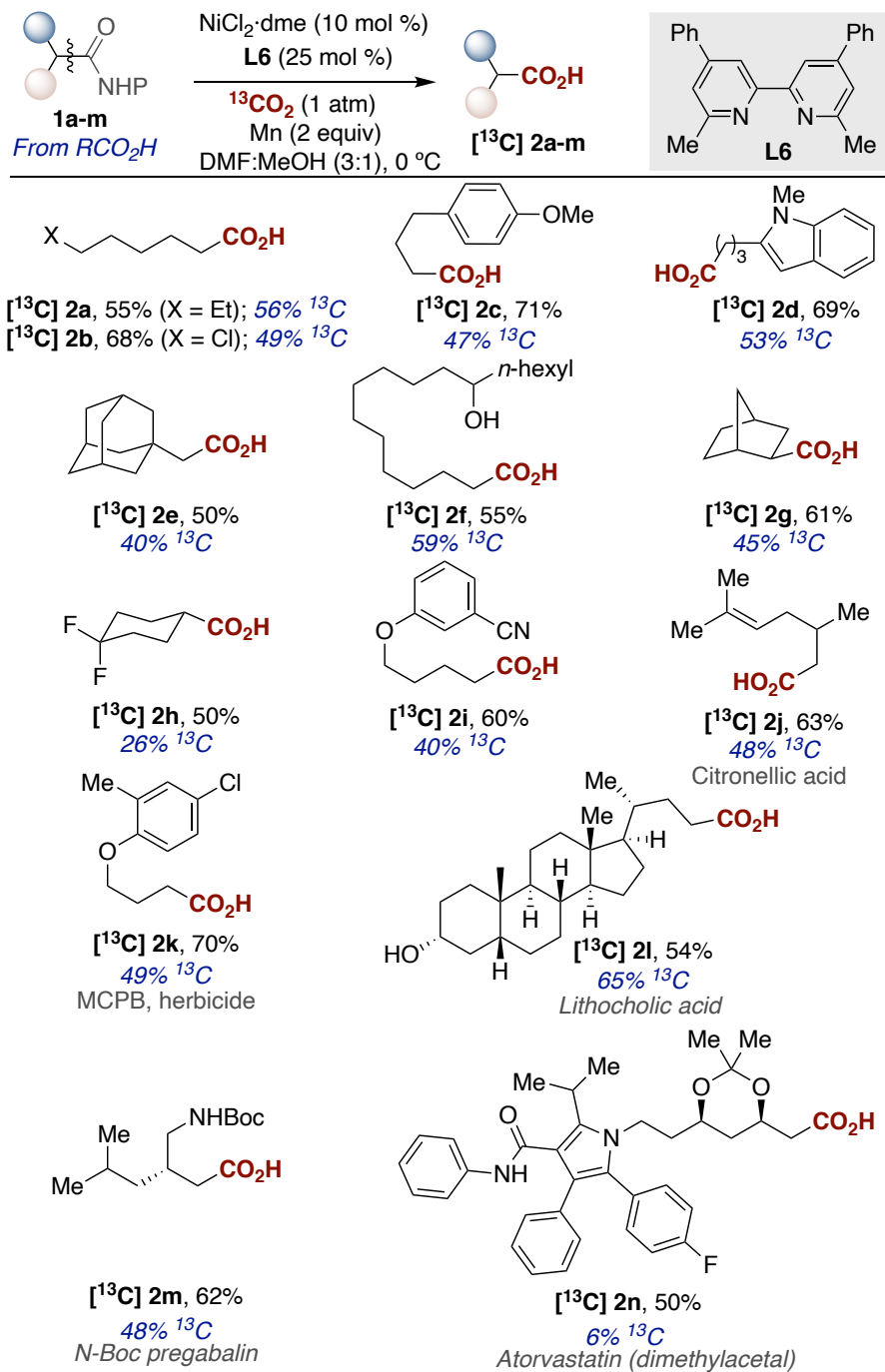
**Figure 4.** Experimental set-up for  $^{13}\text{CO}_2$  utilization.



**Scheme 11.** Carbon isotope exchange with  $^{13}\text{CO}_2$ .

Then we turned our attention to study the generality of the Ni-catalyzed decarboxylative/carboxylation of N-hydroxyphthalimido esters. As shown in Table 5, an array of linear (**2a-2f**, **2i-2n**) or  $\alpha$ -branched (**2g**, **2h**) labeled carboxylic acids could easily be within reach from their parent analogues. The chemoselectivity of our  $^{12}\text{C}/^{13}\text{C}$ -carbon labeling exchange posed no problems, as nitriles (**2i**), alkenes (**2j**), carbamates (**2m**) or nitrogen-containing heterocycles (**2d**) could all be well-accommodated. Interestingly, not even traces of competitive Ni-catalyzed carboxylation at the C-Cl terminus was observed in **2b** and **2k**, thus leaving ample room for further functionalization via conventional cross-coupling reactions. Particularly noteworthy was the ability to enable the targeted  $^{12}\text{C}/^{13}\text{C}$ -exchange at late-stages with more complex carboxylic acid intermediates such as citronellic acid (**2j**), MCPB (**2k**), lithocholic acid (**2l**), pregabalin (**2m**) or atorvastatin (**2n**). Even though the carbon exchange was low in some cases, it shows the potential that our catalytic protocol might have in preclinical studies for drug discovery.

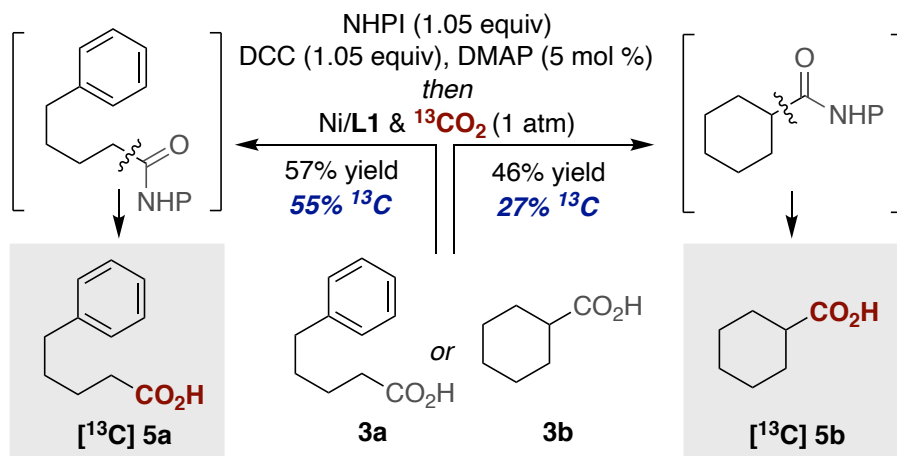
Catalytic Decarboxylation/Carboxylation Platform for Accessing Isotopically Labeled Carboxylic Acids



Conditions: NHP-ester (0.1 mmol),  $\text{NiCl}_2\cdot\text{dme}$  (10 mol %), **L1** (25 mol %), Mn (0.2 mmol),  $^{13}\text{CO}_2$  (1 atm) in DMF:MeOH (3:1, 0.06 M) at 0 °C.

**Table 5.** Substrate scope for the carbon isotope exchange with NHP-esters.

To further prove the simplicity of the procedure, the  $^{12}\text{C}/^{13}\text{C}$ -exchange from **3a** and **3b** into their  $[^{13}\text{C}]\mathbf{5a}$  and  $[^{13}\text{C}]\mathbf{5b}$  congeners was performed without chromatographic purification (Scheme 12). However, a number of daunting challenges remain. Among these, a seemingly trivial extension to  $^{13}\text{C}$ -labeled phenyl acetic acids or benzoic acids events was not known; substantial homodimerization is observed in the former whereas a difficult decarboxylation of aryl NHP-esters prevents a  $^{12}\text{C}/^{13}\text{C}$ -exchange in the latter. More importantly, modest isotope exchange was observed for all substrates shown in Table 5 due to unavoidable hydrolysis of the parent NHP-ester and competitive carboxylation with  $^{12}\text{CO}_2$ .

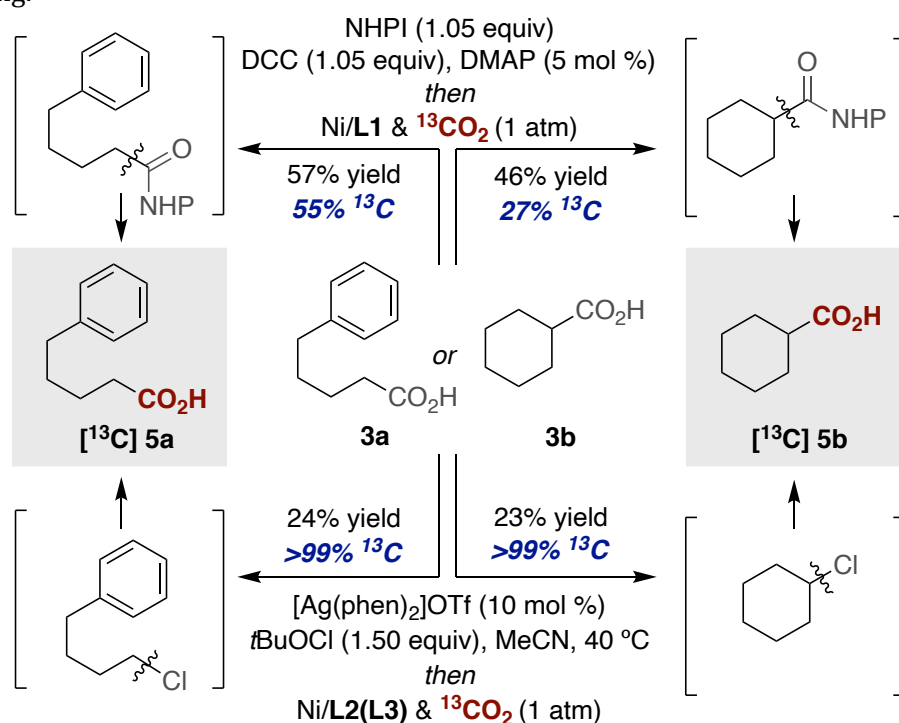


Conditions: NHP-ester (0.1 mmol),  $\text{NiCl}_2\cdot\text{dme}$  (10 mol %), **L1** (25 mol %), Mn (0.2 mmol),  $^{13}\text{CO}_2$  (1 atm) in DMF:MeOH (3:1, 0.06 M) at 0 °C.

**Scheme 12.** Carbon isotope exchange via NHP ester formation.

### 3.2. Isotope carbon exchange with alkyl halides.

With the aim of overcoming the limitations encountered in the previous approach of  $^{12}\text{C}/^{13}\text{C}$ -exchange via NHP esters, we anticipated that the merger of decarboxylative halogenation with the robustness of catalytic carboxylation of organic halides might offer a powerful platform for obtaining otherwise inaccessible carboxylic acids with  $>99\%$   $^{13}\text{C}$ -content. As shown in Scheme 13 (*bottom*), this turned out to be the case. Indeed, a Ag-catalyzed decarboxylative halogenation<sup>32</sup> followed by Ni/L2 or Ni/L3-catalyzed carboxylation afforded [ $^{13}\text{C}$ ]5a and [ $^{13}\text{C}$ ]5b in slightly lower overall yields to those shown for NHP esters, but with  $>99\%$   $^{13}\text{C}$ -labeling.

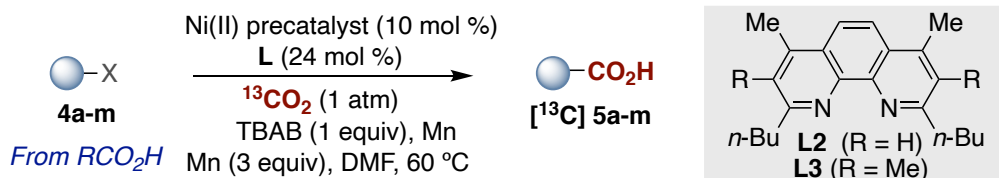


Conditions: **Ni/L1**: NHP-ester (0.1 mmol), NiCl<sub>2</sub>·dme (10 mol %), **L1** (25 mol %), Mn (0.2 mmol),  $^{13}\text{CO}_2$  (1 atm) in DMF:MeOH (3:1, 0.06 M) at 0 °C; **Ni/L2**: NiBr<sub>2</sub>·dme (10 mol %), **L2** (24 mol %), Mn (2 equiv), TBAB (1 equiv),  $^{13}\text{CO}_2$  (1 atm) in DMF (0.17 M), at 60 °C; **Ni/L3**: NiBr<sub>2</sub>·diglyme (10 mol %), **L3** (24 mol %), Mn (3 equiv), LiCl (1 equiv),  $^{13}\text{CO}_2$  (1 atm) in DMF (0.40 M), at 90 °C.

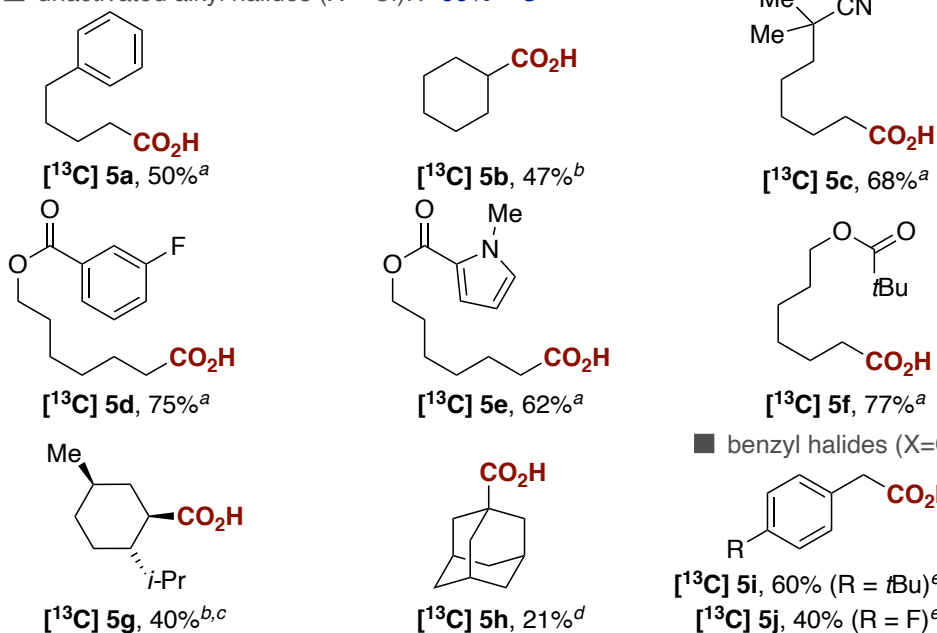
**Scheme 13.** Comparison of carbon isotope exchange via NHP ester or organic halide.

Encouraged by these results, we examined the  $^{13}\text{C}$ -carboxylation of a host of benzyl, aryl or unactivated alkyl chlorides obtained via decarboxylative halogenation of the parent carboxylic acids (Table 6). Notably, nitriles (**5c**), esters (**5d-5f**) or nitrogen-containing heterocycles (**5e**) do not interfere, obtaining in all cases  $>99\%$   $^{13}\text{C}$ -

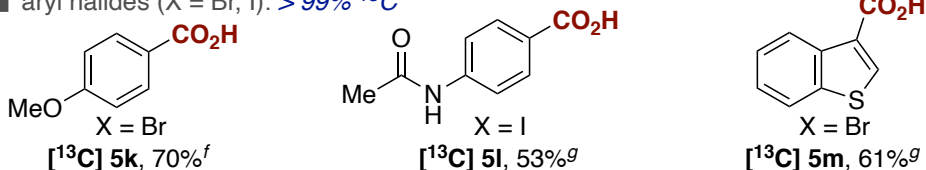
labeling. Albeit in lower yields, secondary and tertiary alkyl carboxylic acids such as **5b**, **5g** or **5h** were within reach, with **5g** being obtained as a single diastereoisomer. Importantly,  $^{13}\text{C}$ -labeled aryl acetic acids (**5i-j**) and (hetero)aryl carboxylic acids (**5k-m**), compounds that were beyond reach from NHP-esters, could also be coupled under Ni/neocuproine or Ni/ $\text{PPh}_3$  regimes, thus representing an opportunity to improve upon existing C-labeling techniques.



■ unactivated alkyl halides (X = Cl): > 99%  $^{13}\text{C}$



■ aryl halides (X = Br, I): > 99%  $^{13}\text{C}$



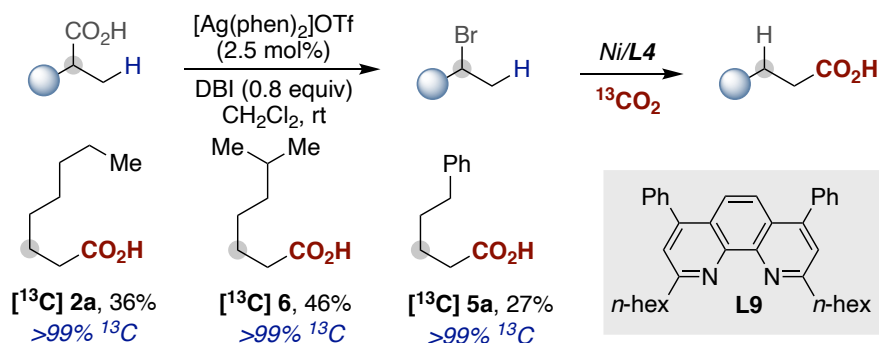
<sup>a</sup> As scheme 13, Ni/L2. <sup>b</sup> Ni/L3. <sup>c</sup> **4g** was obtained as a 1:1 mixture of diastereoisomers <sup>d</sup> As scheme 4, Ni/L3, TBAB (2 equiv), DMA (0.4 M) at 80 °C. <sup>e</sup>  $\text{NiCl}_2\cdot\text{dme}$  (10 mol %),  $\text{PCp}_3\cdot\text{HBF}_4$  (20 mol %),  $\text{MgCl}_2$  (2 equiv), Zn (5 equiv), DMF (0.5 M) at rt. <sup>f</sup>  $\text{NiBr}_2\cdot\text{dme}$  (10 mol %), neocuproine (20 mol %), Mn (2 equiv), DMA (0.2 M) at 50 °C. <sup>g</sup>  $\text{NiCl}_2(\text{PPh}_3)_2$  (5 mol %),  $\text{PPh}_3$  (10 mol %), TEAI (10 mol %), Mn (3 equiv), DMA (0.25 M) at rt.

**Table 6.** Substrate scope for carbon isotope exchange via organic halides.



## Catalytic Decarboxylation/Carboxylation Platform for Accessing Isotopically Labeled Carboxylic Acids

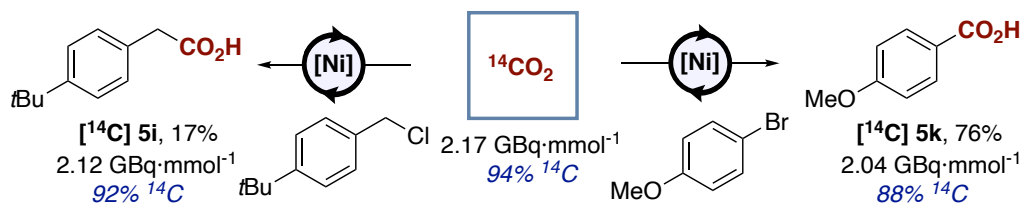
Aimed at extending the applicability of our carbon isotope exchange, we next focused our attention on converting  $\alpha$ -branched carboxylic acids into their labeled linear analogues via a chain-walking approach,<sup>37,38</sup> a transformation that has proven elusive in related labeling approaches.<sup>25</sup> Although in low yields, the preparation of [<sup>13</sup>C]2a,5a,6 with >99% <sup>13</sup>C-labeling does not only demonstrate the successful realization of this goal (Table 7), but also set the basis for designing site-selective radiolabeling techniques at remote  $sp^3$  C–H sites.



Conditions: NiI<sub>2</sub> (2.5 mol %), L4 (4.4 mol %), Mn (2 equiv), DMF (1.0 M), 25 °C, 20 h.

**Table 7.** Chain-walking carboxylation with <sup>13</sup>CO<sub>2</sub>.

Given the key role of <sup>14</sup>C-radiolabeling in pharmacokinetic and ADME studies, the ability to access <sup>14</sup>C-labeled molecules was then explored in collaboration with the Audisio group, since strict security measures are required for the manipulation of radioactive material. Preliminary results successfully highlighted the applicability of this method under similar conditions (Scheme 14). It is particularly noteworthy that [<sup>14</sup>C]5i and [<sup>14</sup>C]5k are obtained in high molar activities ( $\geq 2.04$  GBq mmol<sup>-1</sup>) with negligible isotope dilution, thus opening a gateway to study the metabolic activity of drugs containing carboxylic acid motifs or their derivatives.



**Scheme 14.** Carboxylation of organic halides with <sup>14</sup>CO<sub>2</sub>.

#### 4. Conclusions

We have developed a simple, efficient and highly versatile catalytic decarboxylation/carboxylation for carbon isotope exchange of carboxylic acids with  $^{13}\text{CO}_2$  or  $^{14}\text{CO}_2$ . This route enables the access to labeled aliphatic or aromatic carboxylic acids, even at late stages, without changing the already established sequence en route to the parent compound, thus offering a robust and economical gateway for rapidly and reliably obtaining preclinical data for lead generation in drug discovery.

The use of NHP-esters allows a direct and easy access of labeled aliphatic carboxylic acids in good yields, albeit in moderate or low isotopic incorporations, due to decomposition and carboxylation with the  $\text{CO}_2$  expelled. The conversion of carboxylic acids to organic halide solves in part this problem, decoupling the carboxylation event with the carboxylation, achieving in this way complete isotopic incorporation. Moreover, this strategy allows the expansion of the methodology to benzylic and aromatic substrates. However, the conditions for the decarboxylative halogenation are more drastic and certain functional groups are not tolerated. Overall, these two strategies are complementary and the election of one or the other will depend on the complexity of the molecule and the necessary levels of isotopic incorporation.

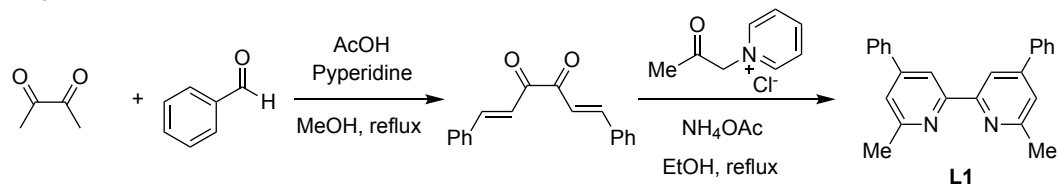
Further efforts will be necessary for the implementation of this synthetic route to the use of  $^{11}\text{CO}_2$  (reaction times shorter than 30 minutes are needed, which are not still feasible for nickel catalyzed carboxylations). Moreover, the direct use of barium carbonate as a  $\text{CO}_2$  source could improve drastically the efficiency of  $^{14}\text{C}$  isotope labeling, avoiding the previous generation and handling of  $^{14}\text{CO}_2$ . Investigations in these regards are currently being pursued in our group.

## 5. Experimental section

**Reagents.** All carboxylation reactions were conducted in Schlenk tubes unless otherwise stated. Commercially available materials were used without further purification.  $^{13}\text{C}$ CO<sub>2</sub> was purchased and used as received from SigmaAldrich. Anhydrous *N,N*-dimethylacetamide (DMA), 1-methyl-2-pyrrolidinone (NMP), *N,N*-dimethylformamide (DMF) and methanol (MeOH) were purchased from Acros Organics (NOTE: *it is critical to have appropriately dried solvents to obtain reproducible results*, as old batches of these solvents provided variable results). Mn powder (99.99% trace metal basis), Zn dust (<10  $\mu\text{m}$ , >99%), NiBr<sub>2</sub>·dme (>97%), MgCl<sub>2</sub> anhydrous (98%) were purchased from Aldrich. NiCl<sub>2</sub>·dme (>97%) was purchased from Strem.

**Analytical methods.**  $^1\text{H}$  NMR and  $^{13}\text{C}$  NMR spectra are included for all compounds.  $^1\text{H}$  and  $^{13}\text{C}$  NMR spectra were recorded on a Bruker 300 MHz, a Bruker 400 MHz and a Bruker 500 MHz at 20 °C. All  $^1\text{H}$  NMR spectra are reported in parts per million (ppm) downfield of TMS and were measured relative to the signals for CHCl<sub>3</sub> (7.26 ppm), acetone-*d*<sub>5</sub> (2.05 ppm) or DMSO-*d*<sub>5</sub> (2.50 ppm). All  $^{13}\text{C}$  NMR spectra were reported in ppm relative to CDCl<sub>3</sub> (77.2 ppm), acetone-*d*<sub>6</sub> (29.8 ppm) or DMSO-*d*<sub>6</sub> (39.5 ppm) and were obtained with  $^1\text{H}$  decoupling. Coupling constants, *J*, are reported in hertz (Hz). Melting points were measured using open glass capillaries in a Büchi B540 apparatus. Infrared spectra (FT-IR) measurements were carried out on a Bruker Optics FT-IR Alpha spectrometer equipped with a DTGS detector, KBr beamsplitter at 4 cm<sup>-1</sup> resolution using a one bounce ATR accessory with diamond windows. Mass spectra were recorded on a Waters LCT Premier spectrometer or in a MicroTOF Focus, Bruker Daltonics spectrometer. Specific optical rotation measurements were carried out on a Jasco P-1030 model polarimeter equipped with a PMT detector using the Sodium line at 589 nm. Flash chromatography was performed with EM Science silica gel 60 (230-400 mesh) using bromocresol, potassium permanganate, or cerium molybdate as TLC stains.

## Synthesis of L1



Bipyridine **L1** was prepared by adapting a literature procedure.<sup>39</sup>

Piperidine (5.69 g, 0.07 mol, 6.60 mL) and glacial AcOH (3.99 g, 0.07 mol, 3.80 mL) were added sequentially to a solution of benzaldehyde (142 g, 1.34 mol, 136 mL) and diacetyl (28.5 g, 0.33 mol, 29.0 mL) in MeOH (130 mL). The yellow mixture was refluxed for 2 h. Thereafter, MeOH (200 mL) was added and the mixture was cooled down to 0 °C. The resulting precipitate was collected via filtration and washed with MeOH (3 x 30 mL). The mother liquor was concentrated under reduced pressure and cooled to - 20 °C for 1 h. The resulting precipitate was collected via filtration and washed with MeOH (3 x 30 mL). Both fractions were combined and dried under high vacuum yielding 1,6-diphenylhexa-1,5-diene-3,4-dione as a brown solid (12.0 g) which was directly used for the next step without further purification.

1,6-Diphenylhexa-1,5-diene-3,4-dione, *N*-acetylpyridinium chloride (15.4 g, 90.0 mmol) and NH<sub>4</sub>OAc (27.8 g, 360 mmol) were suspended in abs. EtOH (150 mL). The brown mixture was refluxed for 6 h. After cooling to room temperature, the resulting precipitate was collected via filtration and washed with cold MeOH (3 x 30 mL). Thereafter, it was dissolved in CHCl<sub>3</sub> (200 mL) and washed with water (2 x 250 mL). The layers were separated and the aq. phase was extracted with CHCl<sub>3</sub> (200 mL). The combined org. phases were washed with brine (2 x 250 mL) and dried over Na<sub>2</sub>SO<sub>4</sub>. The solvent was removed under vacuum and the crude was recrystallized from CHCl<sub>3</sub>/pentane (1 / 1) yielding the title compound as light brown crystals (4.83 g, 14.4 mmol, 5 % over 2 steps).

**<sup>1</sup>H NMR (400 MHz, CDCl<sub>3</sub>):** δ = 8.55 – 8.49 (m, 2H), 7.82 – 7.74 (m, 4H), 7.56 – 7.39 (m, 8H), 2.73 (s, 6H) ppm.

**<sup>13</sup>C NMR (101 MHz, CDCl<sub>3</sub>):** δ = 158.5 (2C), 156.3 (2C), 150.0 (2C), 138.9 (2C), 129.1 (4C), 129.0 (2C), 127.40 (4C), 121.5 (2C), 117.1 (2C), 24.8 (2C) ppm.

**IR (neat):** ν = 2916, 1588, 1547, 1494, 1445, 1384, 1209, 1073, 1001, 900, 872, 768, 739, 699, 620 cm<sup>-1</sup>.

**Mp:** 234-236 °C

Spectroscopic data matches the literature.<sup>40</sup>

### Optimization of the reaction conditions

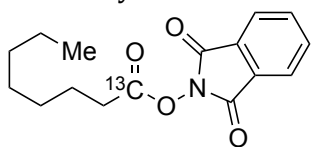
In order to optimize the reaction conditions, we decided to prepare the NHP-ester of the commercially available  $^{13}\text{C}$ -octanoic acid and use regular non-labeled  $^{12}\text{CO}_2$ .

**Procedure:** A Schlenk tube was charged with the  $^{13}\text{C}$ -NHP-ester (0.05 mmol, 1.0 equiv),  $\text{NiCl}_2\cdot\text{glyme}$  (0.005 mmol, 0.1 equiv), ligand (0.0125 mmol, 0.25 equiv) and manganese (0.1 mmol, 2.0 equiv). The tube was evacuated and backfilled with  $\text{CO}_2$  for three consecutive times before the solvent was added under  $\text{CO}_2$  flow. Thereafter, the tube was pressurized with  $\text{CO}_2$  until a constant atmospheric pressure of 1 bar was reached and sealed. The tube was brought to the corresponding temperature and stirred for the indicated time. Anisole was then added as an internal standard, and the reaction was quenched by the addition of aq. HCl (1 M). EtOAc was added and the tube was gently stirred. An aliquot was taken and filtered over a short plug of silica for GC/FID analysis. The remaining organic phase was separated by decantation with a pasteur pipette and filtered over the same plug of silica into a vial. The reaction mixture was extracted one more time with EtOAc. The solvent was removed under reduced pressure from the combined organic phases and the residue was dissolved in a mixture of  $\text{Et}_2\text{O}/\text{MeOH}$  (1/1). TMS-diazomethane (2 equivalents) was added and the mixture was stirred for 3 h at room temperature. Then, the reaction mixture was diluted with EtOAc and an aliquot was taken and filtered over a short plug of silica for GC/MS analysis.

The determination of the carbon exchange was done by GC/MS analysis of the reaction mixture after esterification with  $\text{TMSCHN}_2$  to obtain the corresponding methyl ester. In order to take the natural abundance of  $^{13}\text{C}$  into account, a calibration curve was made by synthesizing labeled and non-labeled methyl octanoate from commercially available starting materials and preparing different mixtures that were submitted to GC/MS analysis. Then, the C-incorporation of the different samples was obtained from the average values obtained of the relative intensities for  $M=74$ ,  $M=87$  and  $M=127$ .

**$^{12}\text{C}/^{13}\text{C}$  isotope exchange via *N*-hydroxyphthalimide esters****General procedure A (GP-A): preparation of NHP-esters**

NHP-esters were prepared adapting the procedure by Overman et al.<sup>41</sup>: A flask was charged with *N*-hydroxyphthalimide (1.66 equiv), DMAP (0.05 equiv) and, if solid, the corresponding acid (1.0 equiv). The flask was evacuated and backfilled with Ar three consecutive times before adding THF or  $\text{CH}_2\text{Cl}_2$  (0.25 M regarding the acid) and, if liquid, the corresponding acid (1.0 equiv). Thereafter, DIC (1.5 equiv) was added to the vigorously stirred suspension. The orange mixture was stirred overnight (ca. 16 h) at room temperature. The resulting pale-yellow suspension was filtered and the filtrate was concentrated under reduced pressure. Subsequent direct purification via flash column chromatography ( $\text{SiO}_2$ , hexanes / EtOAc) afforded the corresponding NHP-ester typically as a white solid. Further purification of the product was performed by recrystallization in DCM/hexanes or  $\text{Et}_2\text{O}$ /hexanes if necessary.

**1,3-Dioxoisindolin-2-yl octanoate-1- $^{13}\text{C}$  ([ $^{13}\text{C}$ ]1a).**

Following **GP-A** starting from  $^{13}\text{C}$  1-octanoic acid (1.00 g, 6.89 mmol) and using THF as solvent. Purification via flash column chromatography ( $\text{SiO}_2$ ,

hexanes/EtOAc, 95/5) afforded the title compound as a white solid (1.98 g, 6.83 mmol, 99 %).

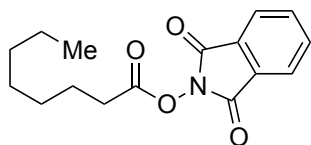
**$^1\text{H}$  NMR (400 MHz,  $\text{CDCl}_3$ ):**  $\delta$  = 7.89 (m, 2H), 7.79 (m, 2H), 2.66 (q,  $J$  = 7.5 Hz, 2H), 1.75 – 1.85 (m, 2H), 1.50 – 1.40 (m, 2H), 1.40 – 1.25 (m, 6H), 0.94 – 0.83 (m, 3H) ppm.

**$^{13}\text{C}$  NMR (101 MHz,  $\text{CDCl}_3$ ):**  $\delta$  = 169.8, 162.2 (2C), 134.9 (2C), 129.1 (2C), 124.1 (2C), 31.7, 31.1 (d,  $J$  = 56.7 Hz), 29.9, 28.9, 24.8 (d,  $J$  = 1.8 Hz), 22.7, 14.2 ppm.

**IR (neat):**  $\nu$  = 2955, 2929, 2857, 1802, 1742, 1467, 1414, 1363, 1325, 1186, 1133, 1081, 1053, 1032, 969, 878, 786, 697, 519  $\text{cm}^{-1}$ .

**Mp:** 45-46 °C.

**HRMS (ESI):**  $m/z$  calc. for ( $\text{C}_{15}^{13}\text{CH}_{19}\text{NNaO}_4^+$ ) [ $\text{M}+\text{Na}$ ] $^+$ : 313.1240; found: 313.1237.

**1,3-Dioxoisindolin-2-yl octanoate (1a).**

Following **GP-A** starting from octanoic acid (1.00 g, 6.89 mmol) and using THF as solvent. Purification via flash column chromatography ( $\text{SiO}_2$ , hexanes/EtOAc, 95 / 5) afforded

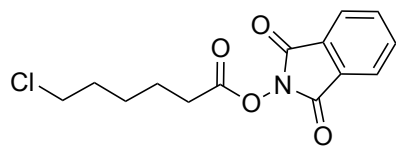
the title compound as a white solid (1.75 g, 6.05 mmol, 88 %).

**$^1\text{H}$  NMR (400 MHz,  $\text{CDCl}_3$ ):**  $\delta$  = 7.89 (m, 2H), 7.79 (m, 2H), 2.66 (q,  $J$  = 7.5 Hz, 2H), 1.75 – 1.85 (m, 2H), 1.50 – 1.40 (m, 2H), 1.40 – 1.25 (m, 6H), 0.94 – 0.83 (m, 3H) ppm.

**$^{13}\text{C}$  NMR (101 MHz,  $\text{CDCl}_3$ ):**  $\delta$  = 169.8, 162.2 (2C), 134.9 (2C), 129.1 (2C), 124.1 (2C), 31.7, 31.1, 29.9, 28.9, 24.8, 22.7, 14.2 ppm.

**Mp:** 43-44 °C

Spectral data was in agreement with the literature.<sup>42</sup>



**1,3-dioxoisindolin-2-yl 6-chlorohexanoate (1b).** Following GP-A starting from 6-chlorohexanoic acid (0.3012 g, 2.00 mmol) and using THF as solvent. Purification via flash column

chromatography (SiO<sub>2</sub>, hexanes/EtOAc, 80/20 to 75/25) afforded the title compound as a white solid (532 mg, 1.80 mmol, 90 %).

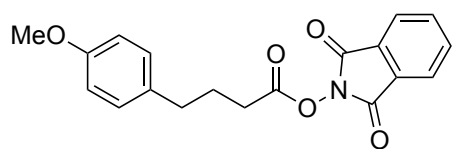
**<sup>1</sup>H NMR (400 MHz, CDCl<sub>3</sub>):**  $\delta$  = 7.92 – 7.87 (m, 2H), 7.82 – 7.77 (m, 2H), 3.57 (t,  $J$  = 6.6 Hz, 2H), 2.70 (t,  $J$  = 7.4 Hz, 2H), 1.89 – 1.77 (m, 4H), 1.66 – 1.57 (m, 2H) ppm.

**<sup>13</sup>C NMR (101 MHz, CDCl<sub>3</sub>):**  $\delta$  = 169.5, 162.1 (2C), 134.9 (2C), 129.1 (2C), 124.1 (2C), 44.7, 32.2, 31.0, 26.2, 24.1 ppm.

**Mp:** 64–65 °C.

**IR (neat):**  $\nu$  = cm<sup>-1</sup> 2942, 2880, 1812, 1787, 1737, 1607, 1464, 1408, 1356, 1185, 1139, 1081, 1063, 1043, 986, 962, 890, 872, 837, 786, 733, 694, 644, 517.

**HRMS (ESI):**  $m/z$  calc. for (C<sub>14</sub>H<sub>14</sub>ClNNaO<sub>4</sub><sup>+</sup>) [M+Na]<sup>+</sup>: 318.0504; found: 318.0498.



**1,3-dioxoisindolin-2-yl 4-(4-methoxyphenyl)butanoate (1c).** Following GP-A starting from 4-(4-methoxyphenyl)butanoic acid (388.5 mg,

2.00 mmol) and using THF as solvent. Purification via flash column chromatography (SiO<sub>2</sub>, hexanes/EtOAc, 80/20 to 75/25) afforded the title compound as a white solid (577.3 mg, 1.70 mmol, 85 %).

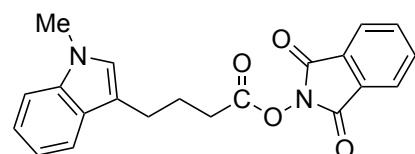
**<sup>1</sup>H NMR (400 MHz, CDCl<sub>3</sub>):**  $\delta$  = 7.94 – 7.86 (m, 2H), 7.83 – 7.72 (m, 2H), 7.14 (d,  $J$  = 8.7 Hz, 2H), 6.86 (d,  $J$  = 8.7 Hz, 1H), 3.80 (s, 3H), 2.72 (t,  $J$  = 7.5 Hz, 2H), 2.66 (t,  $J$  = 7.4 Hz, 2H), 2.08 (p,  $J$  = 7.5 Hz, 2H) ppm.

**<sup>13</sup>C NMR (101 MHz, CDCl<sub>3</sub>):**  $\delta$  = 169.6, 162.1(2C), 158.2, 134.9(2C), 132.9, 129.6(2C), 129.1 (2C), 124.1(2C), 114.1(2C), 55.4, 33.8, 30.3, 26.7 ppm.

**Mp:** 86–87 °C.

**IR (neat):**  $\nu$  = cm<sup>-1</sup> 2936, 1811, 1787, 1738, 1609, 1583, 1510, 1466, 1363, 1241, 1186, 1141, 1078, 1030, 963, 876, 807, 695, 521.

**HRMS (ESI):**  $m/z$  calc. for (C<sub>19</sub>H<sub>17</sub>NNaO<sub>5</sub><sup>+</sup>) [M+Na]<sup>+</sup>: 362.0999; found: 362.0995.



**1,3-dioxoisindolin-2-yl 4-(1-methyl-1H-indol-3-yl)butanoate (1d).** Following GP-A starting from 4-(1-methyl-1H-indol-3-yl)butanoic acid<sup>43</sup> (0.1738 g, 0.80 mmol), DCC (198.1 mg, 0.96 mmol, 1.2 equiv.), *N*-hydroxyphthalimide (156.7 mg, 0.96 mmol, 1.2 equiv) and using DCM as solvent.

Purification via flash column chromatography (SiO<sub>2</sub>, hexanes/EtOAc, 80/20 to 75/25) afforded the title compound as a yellow solid (0.2301 g, 0.63 mmol, 79 %).

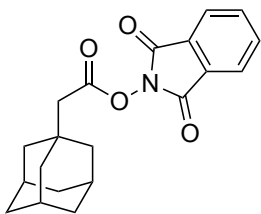
**<sup>1</sup>H NMR (400 MHz, CDCl<sub>3</sub>):**  $\delta$  = 7.92 – 7.86 (m, 2H), 7.82 – 7.77 (m, 2H), 7.62 (dt,  $J$  = 7.9, 1.0 Hz, 1H), 7.31 (dt,  $J$  = 8.2, 0.9 Hz, 1H), 7.26 – 7.20 (m, 1H), 7.12 (ddd,  $J$  = 7.9, 6.9, 1.1 Hz, 1H), 6.93 (s, 1H), 3.77 (s, 3H), 2.93 (td,  $J$  = 7.3, 0.8 Hz, 2H), 2.71 (t,  $J$  = 7.3 Hz, 2H), 2.18 (p,  $J$  = 7.3 Hz, 2H) ppm.

**<sup>13</sup>C NMR (101 MHz, CDCl<sub>3</sub>):**  $\delta$  = 169.8, 162.2 (2C), 137.3, 134.9 (2C), 129.1 (2C), 127.9, 127.0, 124.1 (2C), 121.7, 119.1, 118.9, 113.3, 109.4, 32.8, 30.4, 25.4, 24.0 ppm.

**Mp:** 105-107 °C.

**IR (neat):**  $\nu$  = cm<sup>-1</sup> 3051, 2930, 1808, 1782, 1745, 1610, 1555, 1483, 1466, 1435, 1373, 1356, 1328, 1248, 1184, 1134, 1081, 1047, 959, 879, 846, 822, 742, 518, 436.

**HRMS (ESI):**  $m/z$  calc. for (C<sub>21</sub>H<sub>19</sub>N<sub>2</sub>O<sub>4</sub>)<sup>+</sup> [M+H]<sup>+</sup>: 363.1339; found: 363.1335.



**1,3-dioxoisindolin-2-yl 2-((3r,5r,7r)-adamantan-1-yl)acetate (1e).** Following **GP-A** starting from 2-((3r,5r,7r)-adamantan-1-yl)acetic acid (583 mg, 3.00 mmol) and using THF as solvent. Purification via flash column chromatography (SiO<sub>2</sub>, hexanes/EtOAc, 90/10) afforded the title compound as a white solid (934 mg, 2.75 mmol, 92 %).

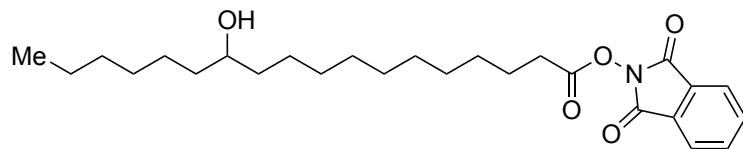
**<sup>1</sup>H NMR (300 MHz, CDCl<sub>3</sub>):**  $\delta$  = 7.88 – 7.84 (m, 2H), 7.79 – 7.76 (m, 2H), 2.38 (s, 2H), 2.02 (s, 3H), 1.74 (d,  $J$  = 3.0 Hz, 6H), 1.70 (d,  $J$  = 3.7 Hz, 6H) ppm.

**<sup>13</sup>C NMR (101 MHz, CDCl<sub>3</sub>):**  $\delta$  = 167.3, 162.2 (2C), 134.8 (2C), 129.1, 124.0 (2C), 45.5, 42.2 (3C), 36.6 (3C), 33.4, 28.7 (3C).

**Mp:** 136-138 °C.

**IR (neat):**  $\nu$  = 3202, 2901, 2847, 1681, 1467, 1363, 1308, 716 cm<sup>-1</sup>.

**HRMS (ESI):**  $m/z$  calc. for (C<sub>20</sub>H<sub>21</sub>NNaO<sub>4</sub>)<sup>+</sup> [M+Na]<sup>+</sup>: 362.1363; found: 362.1370.



**1,3-dioxoisindolin-2-yl 12-hydroxyoctadecanoate (1f).** Following **GP-A** starting from 12-hydroxyoctadecanoic acid (300.2 mg, 1.00 mmol) and using THF as solvent. Purification via flash column chromatography (SiO<sub>2</sub>, hexanes/EtOAc, 75/25) afforded the title compound as a white solid (378.8 mg, 0.85 mmol, 85 %).

**<sup>1</sup>H NMR (400 MHz, CDCl<sub>3</sub>):**  $\delta$  = 7.95 – 7.84 (m, 2H), 7.83 – 7.75 (m, 2H), 3.64 – 3.52 (m, 1H), 2.66 (t,  $J$  = 7.4 Hz, 2H), 1.78 (p,  $J$  = 7.2 Hz, 2H), 1.59 (s, 1H), 1.48 – 1.39 (m, 7H), 1.29 (s, 19H), 0.88 (t,  $J$  = 5.7 Hz, 3H) ppm.

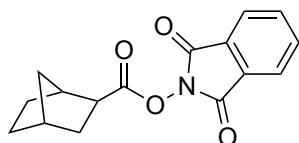
**<sup>13</sup>C NMR (101 MHz, CDCl<sub>3</sub>):**  $\delta$  = 169.8, 162.2 (2C), 134.9 (2C), 129.1 (2C), 124.1 (2C), 72.2, 37.6, 32.0, 31.1, 29.8, 29.7, 29.6, 29.5, 29.5, 29.2, 28.9, 25.8, 24.8, 22.8, 14.2 ppm.



**Mp:** 57-58 °C.

**IR (neat):**  $\nu = \text{cm}^{-1}$  3350, 2919, 2850, 1811, 1785, 1743, 1607, 1590, 1466, 1365, 1351, 1185, 1131, 1075, 960, 878, 862, 794, 695, 520.

**HRMS (ESI):**  $m/z$  calc. for  $(\text{C}_{26}\text{H}_{39}\text{NNaO}_5^+)$   $[\text{M}+\text{Na}]^+$ : 468.2720; found: 468.2720.



**1,3-dioxoisindolin-2-yl bicyclo[2.2.1]heptane-2-carboxylate (1g).** Following **GP-A** starting from bicyclo[2.2.1]heptane-2-carboxylic acid (421 mg, 3.0 mmol, >98% *endo* isomer) and using THF as solvent.

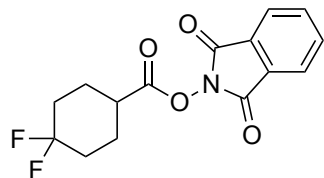
Purification via flash column chromatography ( $\text{SiO}_2$ , hexanes/EtOAc, 95/5) afforded the title compound as a white solid (741 mg, 2.60 mmol, 87 %).

**$^1\text{H}$  NMR (300 MHz,  $\text{CDCl}_3$ ):**  $\delta = 7.89 - 7.83$  (m, 2H), 7.79 - 7.74 (m, 2H), 3.15 - 3.08 (m, 1H), 2.81 - 2.78 (m, 1H), 2.34 - 2.31 (m, 1H), 1.87 - 1.77 (m, 1H), 1.73 - 1.41 (m, 6H), 1.35 - 1.24 (m, 1H) ppm.

**$^{13}\text{C}$  NMR (75 MHz,  $\text{CDCl}_3$ ):**  $\delta = 171.5, 162.3$  (2C), 134.8 (2C), 129.1 (2C), 124.0 (2C), 43.3, 41.0, 40.4, 36.9, 32.6, 29.0, 24.8 ppm.

**Mp:** 78-81 °C.

Spectral data was in agreement with the literature.<sup>44</sup>



**1,3-dioxoisindolin-2-yl 4,4-difluorocyclohexane-1-carboxylate (1h).** Following **GP-A** starting from 4,4-difluorocyclohexane-1-carboxylic acid (328.3 mg, 2.00 mmol) and using THF as solvent. Purification via flash column chromatography ( $\text{SiO}_2$ , hexanes/EtOAc, 80/20

to 75/25) afforded the title compound as a white solid (541.1 mg, 1.75 mmol, 87 %).

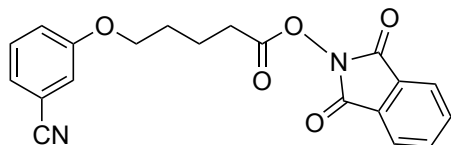
**$^1\text{H}$  NMR (400 MHz,  $\text{CDCl}_3$ ):**  $\delta = 7.93 - 7.86$  (m, 2H), 7.85 - 7.77 (m, 2H), 2.94 - 2.82 (m, 1H), 2.27 - 2.03 (m, 6H), 1.99 - 1.81 (m, 2H) ppm.

**$^{13}\text{C}$  NMR (126 MHz,  $\text{CDCl}_3$ ):**  $\delta = 170.6, 162.0$  (2C), 135.0 (2C), 129.1 (2C), 124.2 (2C), 122.3 (t,  $J = 241.4$  Hz), 38.0, 32.2 (t,  $J = 24.9$  Hz, 2C), 25.1 (t,  $J = 5.2$  Hz, 2C) ppm.

**IR (neat):**  $\nu = \text{cm}^{-1}$  3102, 2947, 1808, 1781, 1741, 1609, 1463, 1446, 1429, 1373, 1360, 1184, 1147, 1114, 1079, 980, 959, 947, 874, 837, 790, 697, 592, 517, 496.

**Mp:** 117-119 °C.

Spectral data was in agreement with the literature.<sup>45</sup>



**1,3-dioxoisindolin-2-yl 5-(3-cyanophenoxy)pentanoate (2i).** Following **GP-A** starting from 5-(3-cyanophenoxy)pentanoic acid (219.2 mg,

1.00 mmol) and using THF as solvent. Purification via flash column chromatography (SiO<sub>2</sub>, hexanes/EtOAc, 75/25 to 70/30) afforded the title compound as a white solid (0.2670 g, 0.73 mmol, 73 %).

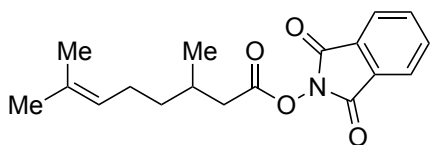
**<sup>1</sup>H NMR (400 MHz, CDCl<sub>3</sub>):**  $\delta$  = 7.94 – 7.85 (m, 2H), 7.84 – 7.75 (m, 2H), 7.37 (td,  $J$  = 7.7, 0.9 Hz, 1H), 7.26 – 7.21 (m, 1H), 7.17 – 7.11 (m, 2H), 4.04 (t,  $J$  = 5.6 Hz, 2H), 2.78 (t,  $J$  = 6.8 Hz, 2H), 2.03 – 1.95 (m, 4H) ppm.

**<sup>13</sup>C NMR (101 MHz, CDCl<sub>3</sub>):**  $\delta$  = 169.4, 162.1 (2C), 159.1, 135.0 (2C), 130.5, 129.1 (2C), 124.7, 124.2 (2C), 119.9, 118.9, 117.5, 113.4, 67.7, 30.8, 28.2, 21.6 ppm.

**Mp:** 84–86 °C.

**IR (neat):**  $\nu$  = cm<sup>-1</sup> 2956, 2876, 2231, 1815, 1785, 1739, 1607, 1576, 1470, 1413, 1375, 1293, 1257, 1185, 1145, 1123, 1061, 1037, 972, 877, 787, 695, 683, 518.

**HRMS (ESI):**  $m/z$  calc. for (C<sub>20</sub>H<sub>16</sub>N<sub>2</sub>NaO<sub>5</sub>)<sup>+</sup> [M+Na]<sup>+</sup>: 387.0951; found: 387.0952.



**1,3-dioxoisindolin-2-yl 3,7-dimethyloct-6-enoate (1j).** Following **GP-A** starting from citronellic acid (170 mg, 1 mmol) and using DCM as solvent. Purification via flash column

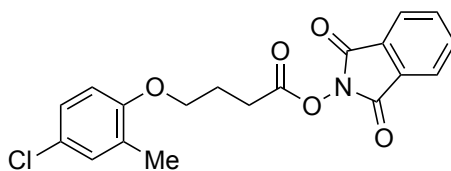
chromatography (SiO<sub>2</sub>, hexanes/EtOAc, 95/5 to 75/25) afforded the title compound as a white solid (220 mg, 0.70 mmol, 70 %).

**<sup>1</sup>H NMR (500 MHz, CDCl<sub>3</sub>):**  $\delta$  = 7.88 (dd,  $J$  = 5.5, 3.1 Hz, 2H), 7.78 (dd,  $J$  = 5.5, 3.1 Hz, 2H), 5.14 – 5.09 (m, 1H), 2.67 (dd,  $J$  = 15.0, 5.6 Hz, 1H), 2.46 (dd,  $J$  = 15.0, 8.3 Hz, 1H), 2.17 – 2.08 (m, 1H), 2.08 – 2.01 (m, 2H), 1.69 (s, 3H), 1.62 (s, 3H), 1.54 – 1.44 (m, 1H), 1.41 – 1.31 (m, 1H), 1.10 (d,  $J$  = 6.7 Hz, 3H) ppm.

**<sup>13</sup>C NMR (126 MHz, CDCl<sub>3</sub>):**  $\delta$  = 169.1, 162.2 (2C), 134.8 (2C), 132.1, 129.1 (2C), 124.1 (2C), 124.0, 38.4, 36.7, 30.4, 25.9, 25.5, 19.5, 17.8 ppm.

**Mp:** 46–48 °C.

Spectroscopic data in agreement with the literature.<sup>46</sup>



**1,3-dioxoisindolin-2-yl 4-(4-chloro-2-methylphenoxy)butanoate (1k).** Following **GP-A** starting from 4-(4-chloro-2-methylphenoxy)butanoic acid (457 mg, 2.0 mmol) and using THF as solvent. Purification

via flash column chromatography (SiO<sub>2</sub>, hexanes/EtOAc, 90/10 to 80 / 20) afforded the title compound as a white solid (398 mg, 1.07 mmol, 53 %).

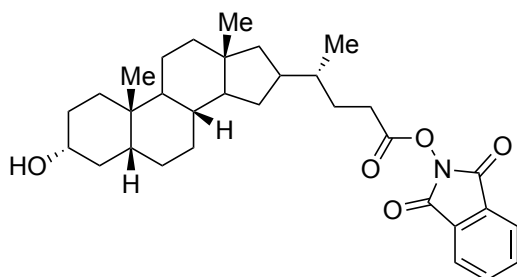
**<sup>1</sup>H NMR (300 MHz, CDCl<sub>3</sub>):** δ = 7.93 – 7.85 (m, 2H), 7.85 – 7.76 (m, 2H), 7.14 – 7.06 (m, 2H), 6.74 (d, *J* = 8.6 Hz, 1H), 4.07 (t, *J* = 5.9 Hz, 2H), 2.92 (t, *J* = 7.3 Hz, 2H), 2.33 – 2.23 (m, 2H), 2.21 (s, 3H) ppm.

**<sup>13</sup>C NMR (75 MHz, CDCl<sub>3</sub>):** δ = 169.4, 162.0 (2C), 155.4, 134.9 (2C), 130.6, 129.0 (2C), 128.9, 126.5, 125.4, 124.1 (2C), 112.2, 66.4, 27.9, 24.7, 16.3 ppm.

**Mp:** 102-105 °C.

**IR (neat):** ν = 2921, 1816, 1785, 1736, 1494, 1467, 1374, 1248, 1187, 1131, 1062, 972, 872, 812, 691 cm<sup>-1</sup>.

**HRMS (ESI):** *m/z* calc. for (C<sub>19</sub>H<sub>16</sub>ClNNaO<sub>5</sub><sup>+</sup>) [M+Na]<sup>+</sup>: 396.0609; found: 396.0612.



**1,3-dioxoisindolin-2-yl (4R)-4-((3R,5R,8S,10S,13R)-3-hydroxy-10,13-dimethylhexadecahydro-1H-cyclopenta[a]phenanthren-16-yl)pentanoate (11).**

Following **GP-A** starting from (4R)-4-((3R,5R,8S,10S,13R)-3-hydroxy-10,13-dimethylhexadecahydro-1H-cyclopenta[a]phenanthren-16-yl)pentanoic acid (1.00 g, 2.66 mmol) and using THF as solvent. Purification via flash column chromatography (SiO<sub>2</sub>, hexanes/EtOAc, 2/1) afforded the compound as a white solid (1.44 g, 83 %).

**<sup>1</sup>H NMR (400 MHz, CDCl<sub>3</sub>):** δ = 7.92 – 7.85 (m, 2H), 7.84 – 7.73 (m, 2H), 3.62 (tt, *J* = 11.0, 4.7 Hz, 1H), 2.75 – 2.66 (m, 1H), 2.65 – 2.52 (m, 1H), 2.00 – 1.07 (m, 27H), 0.98 (d, *J* = 6.3 Hz, 3H), 0.92 (s, 3H), 0.67 (s, 3H) ppm.

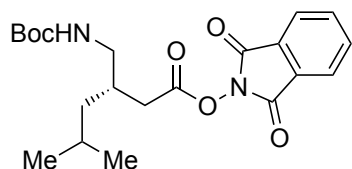
**<sup>13</sup>C NMR (101 MHz, CDCl<sub>3</sub>):** δ = 170.2, 162.2 (2C), 134.9 (2C), 129.1 (2C), 124.1 (2C), 72.0, 56.6, 56.0, 43.0, 42.2, 40.6, 40.3, 36.6, 36.0, 35.5, 35.4, 34.7, 30.9, 30.7, 28.3, 28.2, 27.3, 26.6, 24.3, 23.5, 21.0, 18.4, 12.2 ppm.

**Mp:** 160-161 °C.

**[α]<sub>D</sub><sup>20</sup>:** +15.8° (*c* = 0.1, CH<sub>2</sub>Cl<sub>2</sub>).

**IR (neat):** ν = 3427, 3373, 2928, 2863, 1808, 1784, 1742, 1468, 1446, 1359, 1185, 1133, 1068, 1015, 878, 696 cm<sup>-1</sup>.

**HRMS (ESI):** *m/z* calc. for (C<sub>32</sub>H<sub>43</sub>NNaO<sub>5</sub><sup>+</sup>) [M+Na]<sup>+</sup>: 544.3033; found: 544.3013.

**1,3-dioxoisindolin-2-yl****3-((*tert*-****butoxycarbonyl)amino)methyl)-5-****methylhexanoate (1m).**

To a solution of 477.6 mg Pregabalin in 3 mL THF, NaOH (6.15 mL, 1 M aq. ) was added. After stirring for 5 min, a solution of Boc

anhydride (3.5 mL THF) was added. The mixture was allowed to stir vigorously overnight. After the completion of the reaction, half volume of the solvent was removed and adjust the pH to about 2-3 carefully. The aqueous layer was extracted with Ethyl acetate 3 times, the combined organic layers were dried over anhydrous sodium sulfate and further concentrated to give 3-(((*tert*-butoxycarbonyl)amino)methyl)-5-methylhexanoic acid (White solid, used without further purification in the next step). Following **GP-A** starting from the crude acid (518.7 mg, 2.00 mmol) and using THF as solvent. Purification via flash column chromatography (SiO<sub>2</sub>, hexanes/EtOAc, 75/25) afforded the title compound as a white solid (728.1 mg, 1.80 mmol, 90 %).

**<sup>1</sup>H NMR (300 MHz, CDCl<sub>3</sub>):**  $\delta$  = 7.89 (dd,  $J$  = 5.5, 3.1 Hz, 2H), 7.79 (dd,  $J$  = 5.5, 3.1 Hz, 2H), 4.86 (s, 1H), 3.31 (dd,  $J$  = 12.8, 6.9 Hz, 1H), 3.10 (dt,  $J$  = 14.4, 7.4 Hz, 1H), 2.64 (d,  $J$  = 6.4 Hz, 2H), 2.28 (t,  $J$  = 6.7 Hz, 1H), 1.73 (dq,  $J$  = 13.3, 6.6 Hz, 1H), 1.44 (s, 9H), 1.29 (t,  $J$  = 7.1 Hz, 2H), 0.93 (t,  $J$  = 6.8 Hz, 6H) ppm.

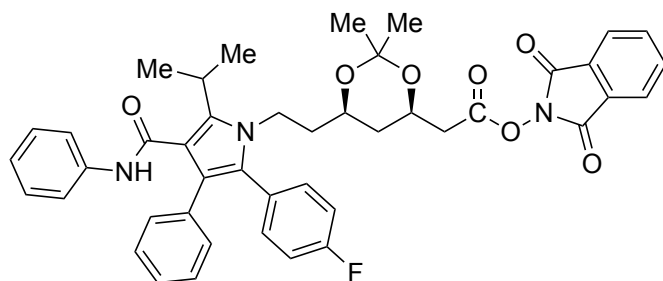
**<sup>13</sup>C NMR (101MHz, CDCl<sub>3</sub>):**  $\delta$  = 169.0, 162.1 (2C), 156.3, 134.9 (2C), 129.1 (2C), 124.1 (2C), 79.4, 43.9, 41.2, 34.4, 34.1, 28.5 (3C), 25.3, 22.9, 22.7 ppm.

**Mp:** 115-116 °C.

**[ $\alpha$ ]<sup>20</sup><sub>D</sub>:** -23° (c = 0.1, CH<sub>2</sub>Cl<sub>2</sub>)

**IR (neat):**  $\nu$  = cm<sup>-1</sup> 3373, 2966, 2930, 1808, 1782, 1743, 1681, 1520, 1467, 1365, 1249, 1184, 1159, 1130, 1087, 1052, 969, 877, 858, 789, 706, 695, 616, 588, 516.

**HRMS (ESI):**  $m/z$  calc. for (C<sub>21</sub>H<sub>28</sub>N<sub>2</sub>NaO<sub>6</sub>)<sup>+</sup> [M+Na]<sup>+</sup>: 427.1840; found: 427.1850.



**1,3-dioxoisindolin-2-yl 2-((4*R*,6*R*)-6-(2-(2-(4-fluorophenyl)-5-isopropyl-3-phenyl-4-(phenylcarbamoyl)-1*H*-pyrrol-1-yl)ethyl)-2,2-dimethyl-1,3-dioxan-4-yl)acetate (1n).** Atorvastatin<sub>2</sub>Ca·3 H<sub>2</sub>O (242 mg, 0.2 mmol) were suspended in a mixture of acetone (10 mL) and 2,2-dimethoxypropane (5 mL). Two drops of concentrated aqueous HCl were added and the clear solution was stirred overnight

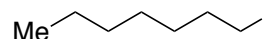
at room temperature. The solvent was then evaporated, and the crude mixture was used in the next step without further purification. Following **GP-A** with the oil obtained in the last step and using DCM as solvent, after purification via flash column chromatography (SiO<sub>2</sub>, hexanes/EtOAc, 75/25) afforded the title compound as a yellow oil (227.0 mg, 0.30 mmol, 76 %, 2 steps).

**<sup>1</sup>H NMR (500 MHz, CDCl<sub>3</sub>):**  $\delta$  = 7.91 – 7.86 (m, 2H), 7.82 – 7.77 (m, 2H), 7.22 – 7.12 (m, 10H), 7.11 – 6.95 (m, 4H), 6.88 (s, 1H), 4.35 – 4.26 (m, 1H), 4.13 – 4.04 (m, 1H), 3.90 – 3.81 (m, 1H), 3.77 – 3.70 (m, 1H), 3.58 (p,  $J$  = 7.1 Hz, 1H), 2.85 (dd,  $J$  = 15.3, 6.7 Hz, 1H), 2.69 (dd,  $J$  = 15.3, 6.6 Hz, 1H), 1.76 – 1.67 (m, 3H), 1.54 (d,  $J$  = 7.2 Hz, 6H), 1.53 – 1.51 (m, 1H), 1.40 (s, 3H), 1.35 (s, 3H) ppm.

**<sup>13</sup>C NMR (126 MHz, CDCl<sub>3</sub>):**  $\delta$  = 166.9, 165.0, 162.4 (d,  $J$  = 247.8 Hz), 161.9, 141.7, 138.5, 135.2, 135.0, 134.8, 134.3, 133.4, 133.3, 130.6, 129.0, 128.9, 128.8, 128.5, 128.4, 128.3, 126.7, 124.4, 124.2, 124.1, 123.8, 123.7, 123.5, 121.9, 119.7, 115.6, 115.4, 115.4, 99.3, 66.4, 65.6, 40.9, 38.4, 38.1, 35.8, 29.9, 26.2, 21.9, 21.7, 19.7 ppm. Spectral data was in agreement with the literature.<sup>47</sup>

**General procedure B (GP-B): decarboxylation/carboxylation of NHP-esters.**

A Schlenk tube was charged with the corresponding NHP-ester (0.1 mmol, 1.0 equiv), NiCl<sub>2</sub>·glyme (0.01 mmol, 0.1 equiv), **L1** (0.025 mmol, 0.25 equiv) and Mn (0.2 mmol, 2.0 equiv). The tube was evacuated and backfilled with argon for three consecutive times before the solvent (DMF:MeOH 3:1) was added under argon flow. Thereafter, the tube was cooled down to -50 °C, put under vacuum for 1 minute and then the <sup>13</sup>CO<sub>2</sub> was transferred to the schlenk flask, stirring the solution at this temperature for 30 minutes. After that, the schlenk was closed and stirred at 0 °C for 16 hours. The reaction was quenched by the addition of aq. HCl (1 M). The aqueous phase was extracted with EtOAc three times and the organic phases were combined. The desired carboxylic acid was isolated by an acid/base extraction using NaHCO<sub>3</sub> saturated solution/HCl 2 M and EtOAc as an organic solvent. The combined organic phases were dried over Na<sub>2</sub>SO<sub>4</sub> and the removal of the solvent under reduced pressure yielded the desired labeled carboxylic acid.

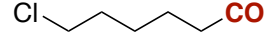
 **Octanoic-1-<sup>13</sup>C acid (2a)**. Following **GP-B** starting from **1a** (28.9 mg, 0.1 mmol) afforded the title compound as a colorless oil (8.0 mg, 0.055 mmol, 55 %). Its mass isotopic pattern analysis showed a 56% <sup>13</sup>C isotope incorporation.

**<sup>1</sup>H NMR (500 MHz, CDCl<sub>3</sub>):** δ = 2.38 – 2.32 (m, 2H), 1.67 – 1.59 (m, 2H), 1.38 – 1.22 (m, 10H), 0.88 (t, *J* = 6.8 Hz, 3H) ppm.

**<sup>13</sup>C NMR (126 MHz, CDCl<sub>3</sub>):** δ = 179.5, 34.1(d, *1J* = 55.3 Hz), 31.8, 29.2 (d, *2J* = 3.3 Hz), 29.0, 24.8, 22.7, 14.2 ppm.

**IR (neat):** ν = 2956, 2926, 2856, 1697, 1669, 1460, 1270 cm<sup>-1</sup>.

**HRMS (ESI):** *m/z* calc. for (C<sub>7</sub><sup>13</sup>CH<sub>15</sub>O<sub>2</sub>) [M-H]<sup>-</sup>: 144.1111; found: 144.1102.

 **6-chlorohexanoic-1-<sup>13</sup>C acid (2b)**. Following **GP-B** starting from **1b** (29,6 mg, 0.1 mmol) afforded the title compound as a colourless oil (10,3 mg, 0.068 mmol, 68%). Its mass isotopic pattern analysis showed a 47% <sup>13</sup>C isotope incorporation.

**<sup>1</sup>H NMR (400 MHz, CDCl<sub>3</sub>)** δ = 3.54 (t, *J* = 6.6 Hz, 2H), 2.38 (tt, *J* = 7.3, 3.5 Hz, 2H), 1.86 – 1.74 (m, 2H), 1.74 – 1.63 (m, 2H), 1.58 – 1.41 (m, 2H) ppm.

**<sup>13</sup>C NMR (101 MHz, CDCl<sub>3</sub>)** δ = 179.6, 44.9, 33.90 (d, *1J* = 55.3 Hz), 32.3, 26.4(d, *2J* = 3.6 Hz), 24.1 ppm.

**IR (neat):** ν = cm<sup>-1</sup> 2941, 2868, 1703, 1458, 1444, 1412, 1275, 1235, 1219, 1133, 931, 846, 735, 650.

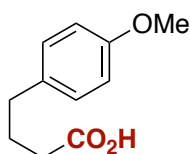
**HRMS (ESI):** We were not able to obtain a mass analysis due to its low molecular weight. For mass analysis it was derivatized into its *p*-nitrophenyl ester:

- Synthesis: To a mixture of the labeled acid (10.3 mg, 0.068 mmol), *p*-nitrophenol (15.3 mg, 0.11 mmol, 1.6 equiv) and DIC (25.2 mg, 0.2 mmol, 2.9 equiv.), 1 mL of ethyl acetate were added, and the mixture was stirred overnight at rt. After column purification, 31% derived product was obtained to measure the  $^{13}\text{C}$  content.  $m/z$  calc. for  $(\text{C}_{11}^{13}\text{CH}_{14}\text{ClNaNO}_4)$   $[\text{M}+\text{Na}]^+$ : 295.0537; found: 295.0532.

$^1\text{H NMR}$  (400 MHz,  $\text{CDCl}_3$ )  $\delta$  = 8.32 – 8.24 (m, 2H), 7.32 – 7.24 (m, 2H), 3.58 (t,  $J$  = 6.5 Hz, 2H), 2.63 (t,  $J$  = 7.4 Hz, 2H), 1.92 – 1.74 (m, 4H), 1.64 – 1.53 (m, 2H) ppm.

$^{13}\text{C NMR}$  (101 MHz,  $\text{CDCl}_3$ )  $\delta$  = 171.1, 155.6, 145.5, 125.4 (2C), 122.6 (2C), 44.8, 34.3 (d,  $^1J$  = 58.3 Hz), 32.3, 26.4, 24.1.

**IR (neat):**  $\nu$  =  $\text{cm}^{-1}$  2941, 2865, 1760, 1615, 1593, 1521, 1490, 1344, 1208, 1159, 1107, 1012, 918, 863, 747, 648.



**4-(4-methoxyphenyl)butanoic-1- $^{13}\text{C}$  acid (2c).** Following **GP-B** starting from **1c** (33,9 mg, 0.1 mmol) afforded the title compound as an off-white solid (13,9 mg, 0.071 mmol, 71%). Its mass isotopic pattern analysis showed a 49%  $^{13}\text{C}$  isotope incorporation.

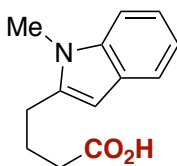
$^1\text{H NMR}$  (400 MHz,  $\text{CDCl}_3$ )  $\delta$  = 7.10 (d,  $J$  = 8.6 Hz, 1H), 6.83 (d,  $J$  = 8.6 Hz, 1H), 3.79 (s, 2H), 2.62 (t,  $J$  = 7.6 Hz, 1H), 2.46 – 2.28 (m, 1H), 1.99 – 1.88 (m, 1H) ppm.

$^{13}\text{C NMR}$  (101 MHz,  $\text{CDCl}_3$ )  $\delta$  = 178.7, 158.1, 133.4, 129.5 (2C), 114.0 (2C), 55.4, 34.2, 33.3, 26.7 ppm.

**IR (neat):**  $\nu$  =  $\text{cm}^{-1}$  3019, 2955, 2932, 2861, 1691, 1610, 1583, 1508, 1464, 1442, 1428, 1411, 1299, 1234, 1194, 1179, 1152, 1111, 1030, 923, 830, 812, 786, 700, 676, 558, 492.

**HRMS (ESI):**  $m/z$  calc. for  $(\text{C}_{10}^{13}\text{CH}_{13}\text{O}_3^-)$   $[\text{M}-\text{H}]^-$ : 194.0904; found: 194.0900.

**Mp:** 56-58 °C.



**4-(1-methyl-1H-indol-3-yl)butanoic-1- $^{13}\text{C}$  acid (2d).** Following **GP-B** starting from **1d** (36,2 mg, 0.1 mmol) afforded the title compound as a light yellow solid (15,0 mg, 0.069 mmol, 69%). Its mass isotopic pattern analysis showed a 53%  $^{13}\text{C}$  isotope incorporation.

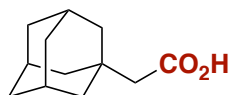
$^1\text{H NMR}$  (400 MHz,  $\text{CDCl}_3$ )  $\delta$  = 7.60 (dt,  $J$  = 7.9, 1.0 Hz, 1H), 7.33 – 7.26 (m, 1H), 7.27 – 7.19 (m, 1H), 7.11 (ddd,  $J$  = 8.0, 6.9, 1.1 Hz, 1H), 6.85 (s, 1H), 3.74 (s, 3H), 2.83 (t,  $J$  = 7.6 Hz, 2H), 2.43 (dq,  $J$  = 7.3, 3.9 Hz, 2H), 2.10 – 2.00 (m, 2H) ppm.

$^{13}\text{C NMR}$  (101 MHz,  $\text{CDCl}_3$ )  $\delta$  = 180.0, 137.2, 127.9, 126.5, 121.7, 119.1, 118.8, 114.0, 109.3, 33.7 (d,  $^1J$  = 55.2 Hz), 32.7, 25.4, 24.4 (d,  $^2J$  = 3.9 Hz) ppm.

**Mp:** 92-94 °C.

**IR (neat):**  $\nu = \text{cm}^{-1}$  3046, 2931, 2885, 2755, 2703, 1750, 1687, 1663, 1613, 1573, 1472, 1455, 1435, 1420, 1395, 1372, 1315, 1199, 1150, 1117, 1007, 921, 786, 740, 727, 686, 547, 427.

**HRMS (ESI):**  $m/z$  calc. for  $(\text{C}_{12}^{13}\text{CH}_{14}\text{NO}_2)^+$   $[\text{M}-\text{H}]^+$ : 217.1064; found: 217.1072.



**2-((3*r*,5*r*,7*r*)-adamantan-1-yl)acetic-1-<sup>13</sup>C acid (2e).**

Following **GP-B** starting from **1e** (34 mg, 0.1 mmol) afforded the title compound as a white solid (9.8 mg, 0.050 mmol, 50%).

Its mass isotopic pattern analysis showed a 40% <sup>13</sup>C isotope incorporation.

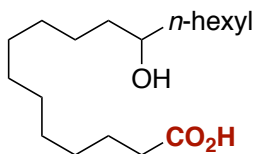
**<sup>1</sup>H NMR (400 MHz, CDCl<sub>3</sub>)**  $\delta = 2.10$  (t,  $J = 3.1$  Hz, 2H), 2.02 – 1.94 (m, 3H), 1.74 – 1.62 (m, 12H) ppm.

**<sup>13</sup>C NMR (101 MHz, CDCl<sub>3</sub>)**  $\delta = 177.9$ , 48.8 (d,  $^1J = 55.2$  Hz), 42.4 (3C), 36.8 (3C), 32.8, 28.8 (3C) ppm.

**Mp:** 128-132 °C.

**IR (neat):**  $\nu = \text{cm}^{-1}$  3202, 2901, 2847, 1681, 1467, 1448, 1363, 1308, 1265, 1140, 1090, 1048  $\text{cm}^{-1}$ .

**HRMS (ESI):**  $m/z$  calc. for  $(\text{C}_{11}^{13}\text{CH}_{17}\text{O}_2)^+$   $[\text{M}-\text{H}]^+$ : 194.1268; found: 194.1269.



**12-Hydroxyoctadecanoic-1-<sup>13</sup>C acid (2f).** Following **GP-B** starting from **1f** (44,6 mg, 0.1 mmol) afforded the title compound as a white solid (16,6 mg, 0.055 mmol, 55%). Its mass isotopic pattern analysis showed a 59% <sup>13</sup>C isotope incorporation.

**<sup>1</sup>H NMR (300 MHz, CDCl<sub>3</sub>)**  $\delta = 3.59$  (dd,  $J = 7.2$ , 4.2 Hz, 1H), 2.34 (t,  $J = 7.4$  Hz, 2H), 1.63 (t,  $J = 7.2$  Hz, 2H), 1.53 – 1.37 (m, 6H), 1.37 – 1.22 (m, 20H), 0.88 (t,  $J = 6.5$  Hz, 2H) ppm.

**<sup>13</sup>C NMR (75 MHz, CDCl<sub>3</sub>)**  $\delta = 178.7$ , 72.3, 37.6, 37.6, 34.0 (d,  $^1J = 55.2$  Hz), 32.0, 29.8, 29.6, 29.5, 29.5, 29.4, 29.3, 29.1, 25.8, 25.7, 24.8, 22.8, 14.2 ppm.

**Mp:** 79-80 °C.

**IR (neat):**  $\nu = \text{cm}^{-1}$  3297, 3192, 2913, 2848, 1693, 1469, 1439, 1413, 1294, 1276, 1223, 1194, 1130, 1076, 919, 862, 719, 682.

**HRMS (ESI):**  $m/z$  calc. for  $(\text{C}_{17}^{13}\text{CH}_{35}\text{O}_3)^+$   $[\text{M}-\text{H}]^+$ : 300.2625; found: 300.2630.



**bicyclo[2.2.1]heptane-2-carboxylic-<sup>13</sup>C acid (g).** Following **GP-B** starting from **1g** (57 mg, 0.2 mmol) afforded the title compound as a white solid (17 mg, 0.12 mmol, 61% as a 1:1 mixture of *endo* and *exo* isomers).

Its mass isotopic pattern analysis showed a 45% <sup>13</sup>C isotope incorporation.

**<sup>1</sup>H NMR (300 MHz, CDCl<sub>3</sub>)**  $\delta = \delta 2.81$  (dt,  $J = 10.4$ , 4.9 Hz, 0.5H), 2.62 – 2.52 (m, 1H), 2.40 – 2.24 (m, 1.5H), 1.92 – 1.78 (m, 0.5H), 1.74 – 1.13 (m, 5.5H) ppm.

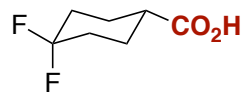


**$^{13}\text{C}$  NMR (75 MHz,  $\text{CDCl}_3$ )**  $\delta$  = 182.6, 181.6, 46.9, 46.1, 46.1, 41.1, 40.7, 40.4, 37.2, 36.7, 36.1, 34.2, 31.8, 29.6, 29.6, 29.2, 28.7, 25.0 ppm.

**IR (neat):**  $\nu$  = 3190, 3063, 2953, 2871, 1700, 1600, 1380, 1304, 1051, 710  $\text{cm}^{-1}$ .

**HRMS (ESI):**  $m/z$  calc. for  $(\text{C}_7^{13}\text{CH}_{11}\text{O}_2^-)$   $[\text{M}-\text{H}]^-$ : 140.0798; found: 140.0798.

Spectral data was in agreement with the literature.<sup>25</sup>



**4,4-difluorocyclohexane-1-carboxylic- $^{13}\text{C}$  acid (2h).**

Following **GP-B** starting from **1h** (30.9 mg, 0.1 mmol) afforded the title compound as a white solid (8.2 mg, 0.05 mmol, 50%).

Its mass isotopic pattern analysis showed a 26%  $^{13}\text{C}$  isotope incorporation.

**$^1\text{H}$  NMR (500 MHz,  $\text{CDCl}_3$ )**  $\delta$  = 2.51 – 2.43 (m, 2H), 2.16 – 2.06 (m, 2H), 2.06 – 1.99 (m, 2H), 1.94 – 1.83 (m, 2H), 1.83 – 1.73 (m, 2H) ppm.

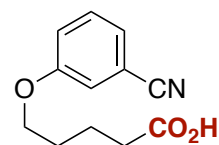
**$^{13}\text{C}$  NMR (126 MHz,  $\text{CDCl}_3$ )**  $\delta$  = 180.2, 122.7 (t,  $^1J_{\text{F-C}}$  = 241.1 Hz), 40.3 (d,  $^1J_{\text{C-C}}$  = 55.1 Hz), 32.7 (2C), 25.0 (2C) ppm.

**$^{19}\text{F}$  NMR (471 MHz,  $\text{CDCl}_3$ )**  $\delta$  = -94.83 (d,  $^2J$  = 238.3 Hz), -99.63 (d,  $^2J$  = 239.1 Hz) ppm.

**MP:** 94-96 °C.

**IR (neat):**  $\nu$  = 2949, 2922, 2853, 2636, 1690, 1668, 1432, 1376, 1359, 1321, 1264, 1215, 1096, 964, 929, 914, 591, 488  $\text{cm}^{-1}$ .

**HRMS (ESI):**  $m/z$  calc. for  $(\text{C}_6^{13}\text{CH}_9\text{F}_2\text{O}_2^-)$   $[\text{M}-\text{H}]^-$ : 164.0610; found: 164.0611.



**5-(3-cyanophenoxy)pentanoic-1- $^{13}\text{C}$  acid (2i).**

Following **GP-B** starting from **1i** (36.4 mg, 0.1 mmol) afforded the title compound as a colourless oil (12.9 mg, 0.059 mmol, 59%). Its mass isotopic pattern analysis showed a 40%  $^{13}\text{C}$  isotope

incorporation.

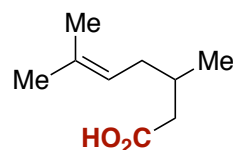
**$^1\text{H}$  NMR (300 MHz,  $\text{CDCl}_3$ )**  $\delta$  = 7.40 – 7.31 (m, 1H), 7.29 – 7.21 (m, 1H), 7.16 – 7.07 (m, 2H), 3.99 (t,  $J$  = 5.6 Hz, 2H), 2.46 (t,  $J$  = 6.8 Hz, 1H), 1.91 – 1.79 (m, 4H) ppm.

**$^{13}\text{C}$  NMR (75 MHz,  $\text{CDCl}_3$ )**  $\delta$  = 179.2, 159.1, 130.5, 124.6, 119.9, 118.9, 117.5, 113.3, 67.9, 33.6 (d,  $^1J$  = 55.4 Hz), 28.5, 21.4. ppm.

**Mp:** 78-79 °C.

**IR (neat):**  $\nu$  =  $\text{cm}^{-1}$  2948, 2875, 2229, 1705, 1603, 1577, 1479, 1442, 1399, 1333, 1297, 1258, 1207, 1185, 1148, 1051, 1031, 929, 879, 795, 683, 615, 477.

**HRMS (ESI):**  $m/z$  calc. for  $(\text{C}_{11}^{13}\text{CH}_{12}\text{O}_3^-)$   $[\text{M}-\text{H}]^-$ : 219.0856; found: 219.0866.



**3,7-dimethyloct-6-enoic-1- $^{13}\text{C}$  acid (2j).**

Following **GP-B** starting from **1j** (31.5 mg, 0.1 mmol) afforded the title compound as a colourless oil (10.7 mg, 0.063 mmol, 63%). Its mass isotopic pattern analysis showed a 48%  $^{13}\text{C}$  isotope

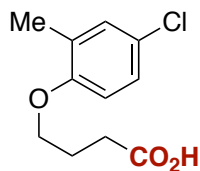
incorporation.

**$^1\text{H}$  NMR (400 MHz,  $\text{CDCl}_3$ )**  $\delta$  = 5.09 (t,  $J$  = 7.3 Hz, 1H), 2.42 – 2.30 (m, 1H), 2.21 – 2.10 (m, 1H), 2.04 – 1.94 (m, 4H), 1.68 (s, 3H), 1.60 (s, 3H), 1.44 – 1.34 (m, 1H), 1.30 – 1.21 (m, 2H), 0.98 (d,  $J$  = 6.7 Hz, 3H) ppm.

**$^{13}\text{C}$  NMR (101 MHz,  $\text{CDCl}_3$ )**  $\delta$  = 179.4, 131.8, 124.3, 41.6 (d,  $^1J$  = 55.0 Hz), 36.9 (d,  $^2J$  = 4.0 Hz), 30.0, 25.8, 25.5, 19.7, 17.8. ppm.

**IR (neat):**  $\nu$  = 2962, 2923, 2855, 1693, 1667, 1453, 1379, 1292, 1203, 1162, 1060, 939  $\text{cm}^{-1}$ .

**HRMS (ESI):**  $m/z$  calc. for ( $\text{C}_9^{13}\text{CH}_{17}\text{O}_2$ )  $[\text{M}-\text{H}]^-$ : 170.1268; found: 170.1270.



**4-(4-chloro-2-methylphenoxy)butanoic- $^{13}\text{C}$  acid (2k).**

Following **GP-B** starting from **1k** (37.4 mg, 0.1 mmol) afforded the title compound as a white solid (16 mg, 0.070 mmol, 70%). Its mass isotopic pattern analysis showed a 50%  $^{13}\text{C}$  isotope incorporation.

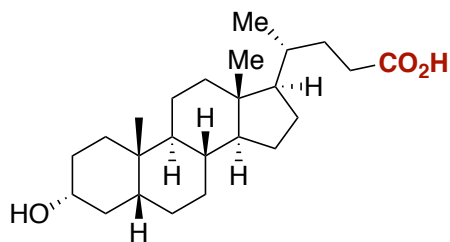
**$^1\text{H}$  NMR (500 MHz,  $\text{CDCl}_3$ )**  $\delta$  = 7.11 – 7.07 (m, 2H), 6.70 (d,  $J$  = 8.2 Hz, 1H), 3.99 (t,  $J$  = 5.9 Hz, 2H), 2.67 – 2.58 (m, 2H), 2.18 (s, 3H), 2.17 – 2.13 (m, 2H) ppm.

**$^{13}\text{C}$  NMR (101 MHz,  $\text{CDCl}_3$ )**  $\delta$  = 179.0, 155.6, 130.6, 128.8, 126.4, 125.2, 112.0, 66.9, 30.7, 24.6, 16.2 ppm.

**Mp:** 95–98  $^\circ\text{C}$ .

**IR (neat):**  $\nu$  = 2966, 2952, 2917, 2886, 1714, 1695, 1671, 1494, 1467, 1397, 1273, 1245, 1212, 1192, 1132, 1037, 920, 880, 813, 770, 660  $\text{cm}^{-1}$ .

**HRMS (ESI):** High Resolution Mass Spectrometry analysis proved to be difficult by ESI or MALDI ionization methods. Analysis of the C-exchange was performed with nominal mass data from GC-MS after in-situ derivatization to the corresponding methyl ester.



**(4R)-4-((3R,5R,8S,10S,13R)-3-hydroxy-10,13-dimethylhexadecahydro-1H-cyclopenta[*a*]phenanthren-16-yl)pentanoic- $^{13}\text{C}$  acid (2l).**

Following **GP-B** starting from **1l** (52.1 mg, 0.1 mmol), purification via flash column chromatography ( $\text{SiO}_2$ , hexanes/EtOAc/DCM, 10/1/1 to

6/2/1) afforded the title compound as a white solid (23.8 mg, 58 %). Its mass isotopic pattern analysis showed a 65%  $^{13}\text{C}$  isotope incorporation.

**$^1\text{H}$  NMR (400 MHz, Methanol- $d_4$ )**  $\delta$  = 3.54 (tt,  $J$  = 11.1, 4.6 Hz, 1H), 2.39 – 2.28 (m, 1H), 2.26 – 2.14 (m, 1H), 2.06 – 1.71 (m, 6H), 1.67 – 1.56 (m, 2H), 1.52 – 1.06 (m, 18H), 0.96 – 0.94 (m, 6H), 0.69 (s, 3H) ppm.

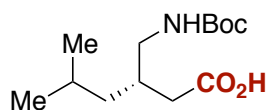
**$^{13}\text{C}$  NMR (101 MHz, Methanol- $d_4$ )**  $\delta$  = 178.1, 72.4, 57.9, 57.5, 43.9, 43.5, 41.9, 41.5, 37.2, 37.2, 36.7 (d,  $J$  = 3.7 Hz), 36.5, 35.7, 32.3, 32.0 (d,  $J$  = 55.2 Hz), 31.2, 29.2, 28.4, 27.7, 25.3, 24.0, 22.0, 18.8, 12.5 ppm.

**IR (neat):**  $\nu$  = 3283, 2854, 2539, 1700, 1659, 1448, 1366, 1329, 1200, 1040, 899, 739, 606, 499  $\text{cm}^{-1}$ .

**Mp:** 182-183  $^{\circ}\text{C}$

**$[\alpha]_{\text{D}}^{20}$ :** +10.5 $^{\circ}$  ( $c$  = 0.1,  $\text{CH}_2\text{Cl}_2$ ).

**HRMS (ESI):**  $m/z$  calc. for ( $\text{C}_{23}^{13}\text{CH}_{39}\text{O}_3$ )  $[\text{M}-\text{H}]^-$ : 376.2938; found: 376.2925.



**3-(((*tert*-butoxycarbonyl)amino)methyl)-5-methylhexanoic-1- $^{13}\text{C}$  acid (2m)** Following GP-B starting from **1m** (40.5 mg, 0.1 mmol) afforded the title compound as a white solid (16.1 mg, 0.062 mmol, 62%). Its mass isotopic pattern analysis showed a 49%  $^{13}\text{C}$  isotope incorporation.

**$^1\text{H}$  NMR (300 MHz,  $\text{CDCl}_3$ )**  $\delta$  = 6.24 (s, 0.3H, NH), 4.77 (s, 0.7H, NH), 3.30 – 3.16 (m, 1H), 3.13 – 2.75 (m, 1H), 2.40 – 2.01 (m, 3H), 1.76 – 1.57 (m, 1H), 1.45 (s, 9H), 1.16 (t,  $J$  = 7.6 Hz, 2H), 0.90 (d,  $J$  = 5.2 Hz, 3H), 0.88 (d,  $J$  = 5.2 Hz, 3H) ppm.

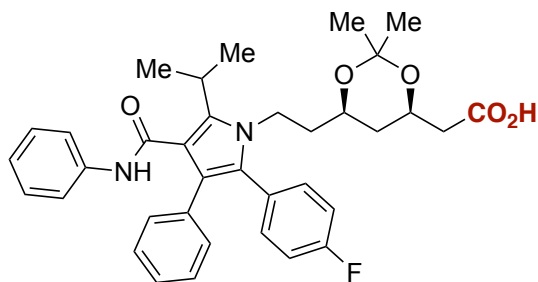
**$^{13}\text{C}$  NMR (101 MHz,  $\text{CDCl}_3$ )**  $\delta$  = 177.8, 156.7, 79.8, 44.0, 41.5, 37.3 (d,  $^1J$  = 56.4 Hz), 33.9, 28.5 (3C), 25.3, 22.8, 22.8 ppm.

**Mp:** 67-69  $^{\circ}\text{C}$ .

**IR (neat):**  $\nu$  =  $\text{cm}^{-1}$  3310, 3250, 3091, 2954, 2930, 2535, 1698, 1646, 1468, 1415, 1355, 1310, 1279, 1258, 1165, 1117, 1007, 978, 775.

**$[\alpha]_{\text{D}}^{20}$ :** -35.5 $^{\circ}$  ( $c$  = 0.1,  $\text{CH}_2\text{Cl}_2$ ).

**HRMS (ESI):**  $m/z$  calc. for ( $\text{C}_{12}^{13}\text{CH}_{24}\text{NO}_4$ )  $[\text{M}-\text{H}]^-$ : 589.1744; found: 259.1744.



**2-((4*R*,6*R*)-6-(2-(2-(4-fluorophenyl)-5-isopropyl-3-phenyl-4-(phenylcarbamoyl)-1*H*-pyrrol-1-yl)ethyl)-2,2-dimethyl-1,3-dioxan-4-yl)acetic-1- $^{13}\text{C}$  acid (2n)**. Following GP-B starting from **1n** (74.4 mg, 0.1 mmol), quenching the reaction with sat.  $\text{NH}_4\text{Cl}$  and performing the purification via flash column chromatography ( $\text{SiO}_2$ , hexanes/ $\text{EtOAc}/\text{HCO}_2\text{H}$ , 75/25/0 to 75/25/1) afforded the title compound as an orange solid (29.7 mg, 0.050 mmol, 50%). Its mass isotopic pattern analysis showed a 6%  $^{13}\text{C}$  isotope incorporation.

**$^1\text{H}$  NMR (400 MHz,  $\text{CDCl}_3$ )**  $\delta$  = 7.22 – 7.12 (m, 10H), 7.09 – 7.03 (m, 2H), 7.03 – 6.95 (m, 3H), 6.87 (s, 1H), 4.25 – 4.16 (m, 1H), 4.13 – 4.04 (m, 1H), 3.91 – 3.80 (m, 1H), 3.70 (td,  $J$  = 9.9, 9.4, 4.3 Hz, 1H), 3.57 (p,  $J$  = 7.1 Hz, 1H), 2.54 (dd,  $J$  = 15.9, 6.9 Hz, 1H),

2.39 (dd,  $J = 15.9, 5.9$  Hz, 1H), 1.75 – 1.49 (m, 4H), 1.53 (d,  $J = 7.1$  Hz, 6H), 1.37 (s, 3H), 1.32 (s, 3H) ppm.

**$^{13}\text{C}$  NMR (101 MHz,  $\text{CDCl}_3$ )**  $\delta = 174.9, 165.1, 162.4$  (d,  $^1J_{\text{F-C}} = 247.9$  Hz), 141.6, 138.4, 134.7, 133.3, 133.3, 130.6, 128.9, 128.8, 128.5, 128.4, 128.4, 126.7, 123.7, 122.0, 119.8, 115.6, 115.4, 99.1, 66.5, 65.6, 42.6, 41.1, 40.9, 38.0, 35.9, 30.0, 26.2, 23.4, 21.9, 21.7, 19.8 ppm.

**$^{19}\text{F}$  NMR (376 MHz,  $\text{CDCl}_3$ )**  $\delta = -113.7$  ppm.

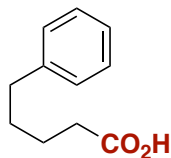
**IR (neat):**  $\nu = 3402, 3060, 2962, 1714, 1663, 1598, 1528, 1508, 1436, 1381, 1312, 1222, 1200, 1156, 909, 841, 729, 692$   $\text{cm}^{-1}$ .

**$[\alpha]^{20}_{\text{D}}$**  =  $-17.9^\circ$  ( $c = 0.1, \text{CH}_2\text{Cl}_2$ ).

**HRMS (ESI):**  $m/z$  calc. for  $(\text{C}_{35}^{13}\text{CH}_{40}\text{FN}_2\text{O}_5^+)$   $[\text{M}+\text{H}]^+$ : 600.2949; found: 600.2955.

<sup>12</sup>C/<sup>13</sup>C isotope exchange via NHP-esters and alkyl chlorides

▪ Via NHP-esters



**5-phenylpentanoic-1-<sup>13</sup>C acid (5a).** A flask was charged with *N*-hydroxyphthalimide (7.8 mg, 0.12 mmol, 1.2 equiv.), DMAP (1.2 mg, 0.1 eq.) and 5-phenylpentanoic acid (17.8 mg, 0.1 mmol). The flask was evacuated and backfilled with Ar three consecutive times before adding DCM (1 mL). Thereafter, DCC (10.0 mg, 0.12 mmol, 1.2 equiv.)

was added to the vigorously stirred suspension. The orange mixture was stirred overnight (ca. 16 h) at room temperature. The resulting pale-yellow suspension was filtered through a short pad of SiO<sub>2</sub> to remove the formed urea with DCM, the filtrate was concentrated under reduced pressure and it was used in the next step without further purification. Following **GP-B** afforded the title compound as a colorless oil (10.1 mg, 0.057 mmol, 57%). Its mass isotopic pattern analysis showed a 62% <sup>13</sup>C isotope incorporation.

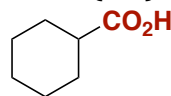
**<sup>1</sup>H NMR (400 MHz, CDCl<sub>3</sub>)** δ = 7.33 – 7.24 (m, 2H), 7.23 – 7.15 (m, 3H), 2.64 (t, *J* = 7.7, 6.7 Hz, 2H), 2.43 – 2.34 (m, 2H), 1.73 – 1.65 (m, 4H) ppm.

**<sup>13</sup>C NMR (101 MHz, CDCl<sub>3</sub>)** δ = 179.7, 142.1, 128.5 (2C), 128.5 (2C), 126.0, 35.7, 34.0 (d, <sup>1</sup>*J* = 55.3 Hz), 30.9 (d, <sup>2</sup>*J* = 3.8 Hz), 24.4. ppm.

**IR (neat):** ν = 2962, 2921, 2858, 1685, 1659, 1463, 1452, 1407, 1317, 1248, 1195, 927, 749, 698, 596, 492 cm<sup>-1</sup>.

**Mp:** 56-57 °C.

**HRMS (ESI):** *m/z* calc. for (C<sub>10</sub><sup>13</sup>CH<sub>13</sub>O<sub>2</sub>)<sup>-</sup> [M-H]<sup>-</sup>: 178.0955; found: 178.0957.



**Cyclohexanecarboxylic-<sup>13</sup>C acid (5b).** A flask was charged with *N*-hydroxyphthalimide (7.8 mg, 0.12 mmol, 1.2 equiv.), DMAP (1.2 mg, 0.1 eq.) and cyclohexanecarboxylic acid (12.8 mg, 0.1 mmol). The

flask was evacuated and backfilled with Ar three consecutive times before adding DCM (1 mL). Thereafter, DCC (10.0 mg, 0.12 mmol, 1.2 equiv.) was added to the vigorously stirred suspension. The orange mixture was stirred overnight (ca. 16 h) at room temperature. The resulting pale-yellow suspension was filtered through a short pad of SiO<sub>2</sub> to remove the formed urea, the filtrate was concentrated under reduced pressure and it was used in the next step without further purification. Following **GP-B** afforded the title compound as a colorless oil (5.9 mg, 0.046 mmol, 46%). Its mass isotopic pattern analysis showed a 27% <sup>13</sup>C isotope incorporation.

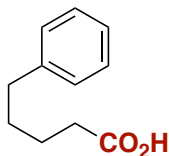
**<sup>1</sup>H NMR (400 MHz, CDCl<sub>3</sub>)** δ = 2.38 – 2.28 (m, 1H), 2.00 – 1.87 (m, 2H), 1.84 – 1.71 (m, 2H), 1.70 – 1.60 (m, 1H), 1.53 – 1.40 (m, 2H), 1.39 – 1.22 (m, 3H) ppm.

**<sup>13</sup>C NMR (101 MHz, CDCl<sub>3</sub>)** δ = 182.1, 43.0 (d, <sup>1</sup>*J* = 55.5 Hz), 28.9, 25.8 (2C), 25.5 (d, <sup>2</sup>*J* = 4.1 Hz, 2C) ppm.

**IR (neat):** ν = cm<sup>-1</sup> 2934, 2857, 2670, 1695, 1450, 1419, 1312, 1256, 1211, 1181, 947, 922, 893, 734, 685, 529, 506.

**HRMS (ESI):** *m/z* calc. for (C<sub>6</sub><sup>13</sup>CH<sub>11</sub>O<sub>2</sub>)<sup>-</sup> [M-H]<sup>-</sup>: 128.0798; found: 128.0796.

▪ **Via alkyl chlorides**



**5-phenylpentanoic-1-<sup>13</sup>C acid (5a).** To a solution of 5-phenylpentanoic acid (35.6 mg, 0.2 mmol) and Ag(Phen)<sub>2</sub>OTf (10 mol%) in anhydrous acetonitrile (2 mL, 0.1 M) was added *tert*-butyl hypochlorite (1.5 eq) at room temperature under nitrogen atmosphere. The reaction mixture was then stirred at 45 °C for 24 h, until the carboxylic acid was all consumed as monitored by TLC. 1 mL of water were then added, the resulting mixture was extracted with dichloromethane and the combined organic phases were dried over anhydrous Na<sub>2</sub>SO<sub>4</sub>. The solvent was removed under reduced pressure, diluted with hexanes/EtOAc (20/1) and filtered through a short pad of SiO<sub>2</sub> to afford the title compound as a colorless liquid, that was used in the next step without further purification. Following general procedure **GP-4-A** (page S34, assuming 50% yield in the chlorination step) and performing the purification by acid/base extraction (NaHCO<sub>3</sub>/EtOAc/HCl 2 M) afforded the title compound as a white solid (8.7 mg, 24 %). Its mass isotopic pattern analysis showed a >99% <sup>13</sup>C isotope incorporation.

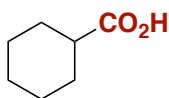
**<sup>1</sup>H NMR (400 MHz, CDCl<sub>3</sub>):** δ = 7.30 – 7.27 (m, 2H), 7.22 – 7.15 (m, 3H), 2.67 – 2.61 (m, 2H), 2.44 – 2.27 (m, 2H), 1.74 – 1.60 (m, 4H) ppm.

**<sup>13</sup>C NMR (126 MHz, CDCl<sub>3</sub>):** δ = 179.1, 142.1, 128.5 (2C), 128.5 (2C), 126.0, 35.7, 33.9 (d, <sup>1</sup>J = 55.3 Hz), 30.9 (d, <sup>2</sup>J = 3.4 Hz), 24.4 (d, <sup>3</sup>J = 1.8 Hz) ppm.

**IR (neat):** ν = 3027, 2921, 2853, 1656, 1494, 1452, 1413, 1315, 1244, 1189, 1073, 1047, 1029, 928, 749, 698, 676, 597, 492 cm<sup>-1</sup>.

**Mp:** 57-58 °C.

**HRMS (ESI):** *m/z* calc. for (C<sub>10</sub><sup>13</sup>CH<sub>13</sub>O<sub>2</sub>)<sup>-</sup> [M-H]<sup>-</sup>: 178.0955; found: 178.0949.



**Cyclohexanecarboxylic-1-<sup>13</sup>C acid (5b).** To a solution of cyclohexanecarboxylic acid (51.2 mg, 0.2 mmol) and Ag(Phen)<sub>2</sub>OTf (5 mol%) in anhydrous acetonitrile (4 mL, 0.1 M) was added *t*-butyl hypochlorite (1.5 equiv) at rt under nitrogen atmosphere. The reaction mixture was then stirred at rt for 24 h, until the carboxylic acid was all consumed as monitored by TLC. 2 mL of water were then added, the resulting mixture was extracted with diethyl ether and the combined organic phases were dried over anhydrous Na<sub>2</sub>SO<sub>4</sub>. The solvent was removed under reduced pressure, diluted with pentane and filtered through a short pad of SiO<sub>2</sub> to afford the title compound as a colorless liquid. Following general procedure **GP-4-B** (page S34, assuming 50% yield in the chlorination step) and performing the purification by acid/base extraction (NaHCO<sub>3</sub>/EtOAc/HCl 2 M) afforded the title compound as an oil (12.0 mg, 23 %). Its mass isotopic pattern analysis showed a >99% <sup>13</sup>C isotope incorporation.

**<sup>1</sup>H NMR (400 MHz, CDCl<sub>3</sub>):**  $\delta$  = 2.39 – 2.28 (m, 1H), 1.99 – 1.89 (m, 2H), 1.82 – 1.73 (m, 2H), 1.70 – 1.61 (m, 1H), 1.52 – 1.38 (m, 2H), 1.36 – 1.20 (m, 3H) ppm.

**<sup>13</sup>C NMR (101 MHz, CDCl<sub>3</sub>):**  $\delta$  = 182.6, 43.0 (d,  $^1J$  = 55.4 Hz), 28.9 (2C), 25.8, 25.5 (d,  $^2J$  = 4.1 Hz, 2C) ppm.

**IR (neat):**  $\nu$  = 3040, 2930, 2855, 1657, 1451, 1399, 1310, 1251, 1205, 1135, 920, 894, 724, 675, 528 cm<sup>-1</sup>.

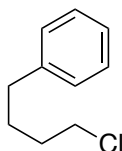
**HRMS (ESI):**  $m/z$  calc. for (C<sub>6</sub><sup>13</sup>CH<sub>11</sub>O<sub>2</sub>)<sup>-</sup> [M-H]<sup>-</sup>: 128.0798; found: 128.0768.

### <sup>12</sup>C/<sup>13</sup>C isotope exchange via aliphatic chlorides

#### General procedure (GP-3) for chlorination

Alkyl chlorides (**4a-4j**) were prepared adapting the procedure by Chaozhong Li et al.<sup>32</sup>

To a solution of carboxylic acid (1.0 equiv) and Ag(Phen)<sub>2</sub>OTf (5 mmol% - 10 mmol%) in anhydrous acetonitrile (0.1 M) was added *tert*-butyl hypochlorite (1.5 equiv) at room temperature under nitrogen atmosphere. The reaction mixture was then stirred at room temperature or 45 °C for 4-24 h, until the carboxylic acid was all consumed as monitored by TLC. 10 mL of water were then added, the resulting mixture was extracted with dichloromethane and the combined organic phases were dried over anhydrous Na<sub>2</sub>SO<sub>4</sub>. After the removal of solvent under reduced pressure, the crude product was purified by column chromatography on silica gel to give the pure product.



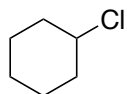
**(4-chlorobutyl)benzene (4a).** To a solution of 5-phenylpentanoic acid (178 mg, 1.0 mmol) and Ag(Phen)<sub>2</sub>OTf (10 mol%) in anhydrous acetonitrile (10 mL, 0.1 M) was added *tert*-butyl hypochlorite (1.5 equiv) at room temperature under nitrogen atmosphere. The reaction mixture was then stirred at 45 °C for 24 h, until the carboxylic acid was

all consumed as monitored by TLC. 10 mL of water were then added, the resulting mixture was extracted with dichloromethane and the combined organic phases were dried over anhydrous Na<sub>2</sub>SO<sub>4</sub>. The solvent was removed under reduced pressure, diluted with hexanes/EtOAc (20/1) and filtered through a short pad of SiO<sub>2</sub> to afford the title compound as a colorless liquid (88 mg, 52 %).

**<sup>1</sup>H NMR (500 MHz, CDCl<sub>3</sub>):**  $\delta$  = 7.31 – 7.27 (m, 2H), 7.22 – 7.17 (m, 3H), 3.55 (t,  $J$  = 6.4 Hz, 2H), 2.65 (t,  $J$  = 7.2 Hz, 2H), 1.85 – 1.75 (m, 4H) ppm.

**<sup>13</sup>C NMR (126 MHz, CDCl<sub>3</sub>):**  $\delta$  = 142.0, 128.5 (2C), 128.5 (2C), 126.0, 45.1, 35.2, 32.2, 28.7 ppm.

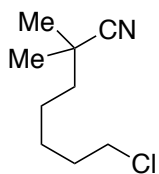
Spectral data was in agreement with the literature.<sup>48</sup>



**Chlorocyclohexane (4b)** CAS: 542-18-7. To a solution of cyclohexanecarboxylic acid (128 mg, 1.0 mmol) and Ag(Phen)<sub>2</sub>OTf (5 mol%) in anhydrous MeCN (10 mL, 0.1 M) was added *t*-butyl hypochlorite (1.5 equiv) at rt under nitrogen atmosphere. The reaction mixture was then stirred at rt for 24 h, until the carboxylic acid was all consumed as monitored by TLC. 10 mL of water was then added, the resulting mixture was extracted with diethyl ether and the combined organic phases were dried over anhydrous Na<sub>2</sub>SO<sub>4</sub>. The solvent was removed under reduced pressure, diluted with pentane and filtered through a short pad of SiO<sub>2</sub> to afford the title compound as a colorless liquid (63 mg, 53 %).

**<sup>1</sup>H NMR (400 MHz, CDCl<sub>3</sub>):** δ = 4.00 (tt, *J* = 9.4, 3.9 Hz, 1H), 2.11 – 2.01 (m, 2H), 1.85 – 1.76 (m, 2H), 1.73 – 1.60 (m, 2H), 1.54 – 1.47 (m, 1H), 1.42 – 1.26 (m, 3H) ppm.

**<sup>13</sup>C NMR (101 MHz, CDCl<sub>3</sub>):** δ = 60.5, 36.8 (2C), 25.3 (2C), 25.0 ppm.

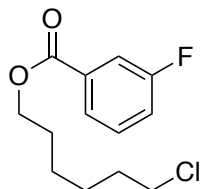


**8-chloro-2,2-dimethyloctanenitrile (4c)** Following GP-3 starting from 8-cyano-8-methylnonanoic acid (58.2 mg, 0.3 mmol) and Ag(Phen)<sub>2</sub>OTf (10 mmol%), the reaction mixture was stirred at 45 °C. Purification via flash column chromatography (SiO<sub>2</sub>, hexanes / EtOAc, 10/1) afforded the title compound as a colourless liquid (45 mg, 82 %).

**<sup>1</sup>H NMR (400 MHz, CDCl<sub>3</sub>):** δ = 3.53 (t, *J* = 6.6 Hz, 2H), 1.83 – 1.66 (m, 2H), 1.51 – 1.42 (m, 6H), 1.40 – 1.35 (m, 2H), 1.33 (s, 6H) ppm.

**<sup>13</sup>C NMR (101 MHz, CDCl<sub>3</sub>):** δ = 125.3, 45.1, 41.1, 32.6, 32.5, 28.9, 26.8 (2C), 26.7, 25.2 ppm.

Spectral data was in agreement with the literature.<sup>49</sup>



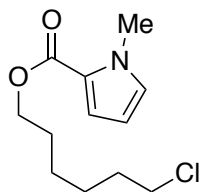
**6-chlorohexyl 3-fluorobenzoate (4d)** Following GP-3 starting from 7-((3-fluorobenzoyl)oxy)heptanoic acid (80 mg, 0.3 mmol) and Ag(Phen)<sub>2</sub>OTf (10 mmol%), the reaction mixture was stirred at 45 °C. Purification via flash column chromatography (SiO<sub>2</sub>, hexanes/EtOAc, 20/1) afforded the compound as a colorless liquid (48 mg, 62 %).

**<sup>1</sup>H NMR (400 MHz, CDCl<sub>3</sub>):** δ = 7.83 (ddd, *J* = 7.7, 1.5, 1.1 Hz, 1H), 7.71 (ddd, *J* = 9.3, 2.7, 1.5 Hz, 1H), 7.42 (td, *J* = 8.0, 5.5 Hz, 1H), 7.28 – 7.23 (m, 1H), 4.33 (t, *J* = 6.6 Hz, 2H), 3.55 (t, *J* = 6.6 Hz, 2H), 1.89 – 1.71 (m, 4H), 1.59 – 1.42 (m, 4H) ppm.

**<sup>13</sup>C NMR (101 MHz, CDCl<sub>3</sub>):** δ = 165.7 (d, *J* = 3.0 Hz), 162.7 (d, *J* = 246.8 Hz), 132.8 (d, *J* = 7.3 Hz), 130.1 (d, *J* = 7.7 Hz), 125.4 (d, *J* = 3.1 Hz), 120.1 (d, *J* = 21.3 Hz), 116.6 (d, *J* = 23.0 Hz), 65.4, 45.1, 32.6, 28.7, 26.7, 25.5 ppm.

Spectral data was in agreement with the literature.<sup>49</sup>



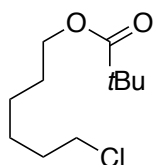


**6-chlorohexyl 1-methyl-1H-pyrrole-2-carboxylate (4e).** To an oven-dried screw-cap Schlenk tube equipped with a magnetic stir-bar was added 7-((1-methyl-1H-pyrrole-2-carbonyl)oxy)heptanoic acid (0.3 mmol, 1.0 equiv), cesium carbonate (0.3 mmol, 1.0 equiv.), *N*-chlorosuccinimide (0.6 mmol, 2.0 equiv) and [Ir(dF(CF<sub>3</sub>)ppy)<sub>2</sub>(dtbbpy)]PF<sub>6</sub> (0.006 mmol, 2 mol%). Chlorobenzene (6.0 mL, 0.05 M) was then, the reaction mixture was degassed using three freeze-pump-thaw cycles and the tube was finally back-filled with argon. The reaction mixture was allowed to stir at rt for 18 h under irradiation of visible light from 5 W blue LEDs ( $\lambda_{\text{max}} = 455 \text{ nm}$ ). The reaction mixture was filtered through a short (1 cm) pad of silica and the solvent was removed under reduced pressure. The crude reaction mixture was purified by flash column chromatography (SiO<sub>2</sub>, hexanes/EtOAc, 10/1) and afforded the title compound as a colorless liquid (28 mg, 36 %). We could recover 50% of the corresponding starting material.

**<sup>1</sup>H NMR (400 MHz, CDCl<sub>3</sub>):**  $\delta = 6.93$  (dd,  $J = 4.0, 1.8 \text{ Hz}$ , 1H), 6.78 (t,  $J = 2.3 \text{ Hz}$ , 1H), 6.11 (dd,  $J = 4.0, 2.5 \text{ Hz}$ , 1H), 4.22 (t,  $J = 6.6 \text{ Hz}$ , 2H), 3.92 (d,  $J = 0.4 \text{ Hz}$ , 3H), 3.54 (t,  $J = 6.7 \text{ Hz}$ , 2H), 1.89 – 1.67 (m, 4H), 1.55 – 1.40 (m, 4H) ppm.

**<sup>13</sup>C NMR (101 MHz, CDCl<sub>3</sub>):**  $\delta = 161.5, 129.5, 122.8, 117.8, 107.9, 63.8, 45.1, 36.9, 32.6, 28.8, 26.7, 25.6 \text{ ppm}$ .

Spectral data was in agreement with the literature.<sup>49</sup>

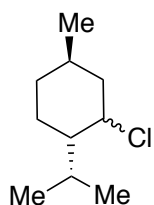


**6-chlorohexyl pivalate (4f).** Following GP-3 starting from 7-(pivaloyloxy)heptanoic acid (46 mg, 0.2 mmol) and Ag(Phen)<sub>2</sub>OTf (10 mmol%), the reaction mixture was stirred at 45 °C. Purification via flash column chromatography (SiO<sub>2</sub>, hexanes/EtOAc, 10/1) afforded the compound as a white liquid (36 mg, 83 %).

**<sup>1</sup>H NMR (400 MHz, CDCl<sub>3</sub>):**  $\delta = 4.05$  (t,  $J = 6.6 \text{ Hz}$ , 2H), 3.53 (t,  $J = 6.7 \text{ Hz}$ , 2H), 1.83 – 1.74 (m, 2H), 1.69 – 1.60 (m, 2H), 1.52 – 1.43 (m, 2H), 1.43 – 1.34 (m, 2H), 1.19 (s, 9H) ppm.

**<sup>13</sup>C NMR (101 MHz, CDCl<sub>3</sub>):**  $\delta = 178.8, 64.3, 45.1, 38.9, 32.6, 28.6, 27.4$  (3C), 26.7, 25.4 ppm.

Spectral data was in agreement with the literature.<sup>49</sup>



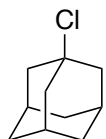
**Menthyl chloride (4g)** Following GP-3 starting from (-)-menthyl carboxylic acid (18.4 mg, 0.2 mmol) and Ag(Phen)<sub>2</sub>OTf (5 mmol%), the reaction mixture was stirred at rt. Purification via flash column chromatography (SiO<sub>2</sub>, hexanes) afforded the compound as colorless liquid (21.6 mg, 62 %) as a 1:1 mixture of diastereoisomers.

**<sup>1</sup>H NMR (500 MHz, CDCl<sub>3</sub>):**  $\delta = 4.51$  (dd,  $J = 2.9, 1.5 \text{ Hz}$ , 0.5H), 3.78

(td,  $J = 11.1, 4.2$  Hz, 0.5H), 2.41 – 2.26 (m, 0.5H), 2.28 – 2.16 (m, 0.5H), 2.06 (dtd,  $J = 14.0, 3.4, 2.3$  Hz, 0.5H), 1.98 – 1.83 (m, 0.5H), 1.77 – 1.67 (m, 2H), 1.62 – 1.49 (m, 0.5H), 1.47 – 1.24 (m, 3H), 1.08 – 0.97 (m, 1H), 0.96 – 0.90 (m, 6.5H), 0.88 (d,  $J = 6.6$  Hz, 1.5H), 0.77 (d,  $J = 6.9$  Hz, 1.5H) ppm.

$^{13}\text{C}$  NMR (126 MHz,  $\text{CDCl}_3$ ):  $\delta = 64.0, 63.5, 50.6, 49.1, 46.9, 43.5, 35.0, 34.4, 33.5, 30.2, 27.3, 26.0, 24.4, 22.1, 22.0, 21.1, 20.9, 20.3, 15.3$  ppm.

Spectral data was in agreement with the literature.<sup>49</sup>

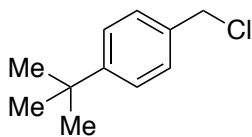


**1-chloroadamantane (4h)** Following **GP-3** starting from adamantane-1-carboxylic acid (180 mg, 1.0 mmol) and  $\text{Ag}(\text{Phen})_2\text{OTf}$  (5 mmol%), the reaction mixture was stirred at rt. Purification via flash column chromatography ( $\text{SiO}_2$ , hexanes) afforded the compound as a white solid (159 mg, 94 %).

$^1\text{H}$  NMR (500 MHz,  $\text{CDCl}_3$ ):  $\delta = 2.14$  (s, 9H), 1.68 (s, 6H) ppm.

$^{13}\text{C}$  NMR (126 MHz,  $\text{CDCl}_3$ ):  $\delta = 69.0, 47.9$  (3C), 35.7 (3C), 31.9 (3C) ppm.

Spectral data was in agreement with the literature.<sup>32</sup>

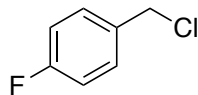


**1-(tert-butyl)-4-(chloromethyl)benzene (4i)** Following **GP-3** starting from 2-(4-(tert-butyl)phenyl)acetic acid (192 mg, 1.0 mmol) and  $\text{Ag}(\text{Phen})_2\text{OTf}$  (5 mmol%), the reaction mixture was stirred at rt. Purification via flash column chromatography ( $\text{SiO}_2$ , hexanes) afforded the title compound as colorless liquid (141 mg, 77 %).

$^1\text{H}$  NMR (500 MHz,  $\text{CDCl}_3$ ):  $\delta = 7.36$  (d,  $J = 7.6$  Hz, 2H), 7.30 (d,  $J = 7.6$  Hz, 2H), 4.55 (s, 2H), 1.29 (s, 9H) ppm.

$^{13}\text{C}$  NMR (101 MHz,  $\text{CDCl}_3$ ):  $\delta = 151.7, 134.7, 128.5$  (2C), 125.9 (2C), 46.3, 34.8, 31.4 (3C) ppm.

Spectral data was in agreement with the literature.<sup>32</sup>



**1-(chloromethyl)-4-fluorobenzene (4j)** Following **GP-3** starting from 2-(4-fluorophenyl)acetic acid (77 mg, 0.5 mmol) and  $\text{Ag}(\text{Phen})_2\text{OTf}$  (5 mmol%), the reaction mixture was stirred at rt. Purification via flash column chromatography ( $\text{SiO}_2$ , hexanes) afforded the compound as colorless liquid (54 mg, 75 %).

$^1\text{H}$  NMR (400 MHz,  $\text{CDCl}_3$ ):  $\delta = 7.43 - 7.29$  (m, 2H), 7.13 – 6.97 (m, 2H), 4.57 (s, 2H) ppm.

$^{13}\text{C}$  NMR (101 MHz,  $\text{CDCl}_3$ ):  $\delta = 162.8$  (d,  $^1J = 247.6$  Hz), 133.5 (d,  $^4J = 3.3$  Hz), 130.6 (d,  $^3J = 8.4$  Hz, 2C), 115.8 (d,  $2J = 21.8$  Hz, 2C), 45.6 ppm.

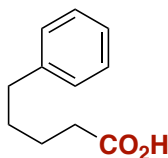
$^{19}\text{F}$  NMR (376 MHz,  $\text{CDCl}_3$ )  $\delta = -115.5$  ppm.

Spectral data was in agreement with the literature.<sup>50</sup>

**General procedure (GP-4-A) for the carboxylation of alkyl chlorides.** The alkyl carboxylic acids were prepared adapting the procedure by Martin et al.<sup>49</sup> An oven-dried Schlenk tube containing a stirring bar was charged with Mn powder (3.0 equiv), TBAB (1.0 equiv) and **L2** (24 mol%). The Schlenk tube was then introduced in a glovebox where it was charged with NiBr<sub>2</sub>·glyme (10 mol%). The tube was taken out of the glovebox, evacuated and backfilled with argon for three consecutive times. Then, the corresponding alkyl chloride (0.1-0.2 mmol) and the solvent DMF (0.167 M) were added under argon flow. The tube was cold down to -50 °C, put under vacuum for 20 seconds and then the <sup>13</sup>CO<sub>2</sub> was transferred to the Schlenk flask. It was closed and stirred at 60 °C for 20 hours unless otherwise stated. The mixture was quenched with 2 M HCl to hydrolyze the resulting carboxylate and extracted 3 times with EtOAc. The combined organic layers were dried over Na<sub>2</sub>SO<sub>4</sub> and concentrated under reduced pressure. The crude obtained was purified by flash chromatography on silica gel (hexanes/EtOAc).

**General procedure GP-4-B:** An oven-dried Schlenk tube containing a stirring bar was charged with Mn powder (3.0 equiv), LiCl (1.0 equiv), **L3** (24 mol%), The Schlenk tube was then introduced in a glovebox where it was charged with NiBr<sub>2</sub>·diglyme (10 mol%). The tube was taken out of the glovebox and evacuate and backfill with argon for three consecutive times. Then, the corresponding alkyl chloride (0.1-0.2 mmol) and the solvent DMF (0.4 M) were added under argon flow. The reaction tube was cold down to -50 °C, put under vacuum for 20 seconds and then the <sup>13</sup>CO<sub>2</sub> was transferred to the Schlenk flask. was closed and stirred at 90 °C for 20 hours unless otherwise stated. The mixture was quenched with 2 M HCl to hydrolyze the resulting carboxylate and extracted 3 times with EtOAc. The combined organic layers were dried over Na<sub>2</sub>SO<sub>4</sub> and concentrated under reduced pressure. The products were purified by flash chromatography on silica gel (hexanes/EtOAc).

**General procedure GP-4-C:** An oven-dried Schlenk tube containing a stirring bar was charged with PCp<sub>3</sub>·HBF<sub>4</sub> (20 mol%), MgCl<sub>2</sub> (2.0 eq) and Zn (dust, 5.0 equiv). The Schlenk tube was then introduced in a glovebox where it was charged with NiCl<sub>2</sub>·glyme (10 mol%). The tube was taken out of the glovebox and evacuate and backfill with argon for three consecutive times. Then, the corresponding alkyl chloride (0.1-0.2 mmol) and the solvent DMF (0.5 M) were added under argon flow. The tube was cold down to -50 °C, put under vacuum for 20 seconds and then the <sup>13</sup>CO<sub>2</sub> was transferred to the Schlenk flask. It was closed and stirred at RT overnight. The mixture was quenched with 2 M HCl to hydrolyze the resulting carboxylate and extracted 3 times with EtOAc. The combined organic layers were dried over Na<sub>2</sub>SO<sub>4</sub> and concentrated under reduced pressure. The product was purified by flash chromatography on silica gel (hexanes/EtOAc).



**5-phenylpentanoic-1-<sup>13</sup>C acid (5a)** Following general procedure **GP-4-A**, using (4-chlorobutyl)benzene **4a** (16.8 mg, 0.1 mmol) and performing the purification by acid/base extraction (NaHCO<sub>3</sub>/EtOAc/HCl 2 M) afforded the title compound as a white solid (8.8 mg, 50 %). Its mass isotopic pattern analysis showed a

>99% <sup>13</sup>C isotope incorporation.

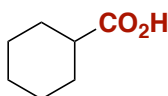
**<sup>1</sup>H NMR (400 MHz, CDCl<sub>3</sub>):** δ = 7.30 – 7.27 (m, 2H), 7.22 – 7.15 (m, 3H), 2.67 – 2.61 (m, 2H), 2.44 – 2.27 (m, 2H), 1.74 – 1.60 (m, 4H) ppm.

**<sup>13</sup>C NMR (126 MHz, CDCl<sub>3</sub>):** δ = 179.1, 142.1, 128.5 (2C), 128.5 (2C), 126.0, 35.7, 33.9 (d, <sup>1</sup>J = 55.3 Hz), 30.9 (d, <sup>2</sup>J = 3.4 Hz), 24.4 (d, <sup>3</sup>J = 1.8 Hz) ppm.

**IR (neat):** ν = 3027, 2921, 2853, 1656, 1494, 1452, 1413, 1315, 1244, 1189, 1073, 1047, 1029, 928, 749, 698, 676, 597, 492 cm<sup>-1</sup>.

**Mp:** 57-58 °C.

**HRMS (ESI):** *m/z* calc. for (C<sub>10</sub><sup>13</sup>CH<sub>13</sub>O<sub>2</sub>)<sup>-</sup> [M-H]<sup>-</sup>: 178.0955; found: 178.0949.



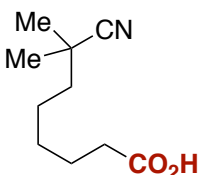
**Cyclohexanecarboxylic-1-<sup>13</sup>C acid (5b)** Following general procedure **GP-4-B**, using chlorocyclohexane **4b** (23.7 mg, 0.2 mmol) and performing the purification by acid/base extraction (NaHCO<sub>3</sub>/EtOAc/HCl 2 M) afforded the title compound as an oil (12.0 mg, 47 %). Its mass isotopic pattern analysis showed a >99% <sup>13</sup>C isotope incorporation.

**<sup>1</sup>H NMR (400 MHz, CDCl<sub>3</sub>):** δ = 2.39 – 2.28 (m, 1H), 1.99 – 1.89 (m, 2H), 1.82 – 1.73 (m, 2H), 1.70 – 1.61 (m, 1H), 1.52 – 1.38 (m, 2H), 1.36 – 1.20 (m, 3H) ppm.

**<sup>13</sup>C NMR (101 MHz, CDCl<sub>3</sub>):** δ = 182.6, 43.0 (d, <sup>1</sup>J = 55.4 Hz), 28.9 (2C), 25.8, 25.5 (d, <sup>2</sup>J = 4.1 Hz, 2C) ppm.

**IR (neat):** ν = 3040, 2930, 2855, 1657, 1451, 1399, 1310, 1251, 1205, 1135, 920, 894, 724, 675, 528 cm<sup>-1</sup>.

**HRMS (ESI):** *m/z* calc. for (C<sub>6</sub><sup>13</sup>CH<sub>11</sub>O<sub>2</sub>)<sup>-</sup> [M-H]<sup>-</sup>: 128.0798; found: 128.0768.



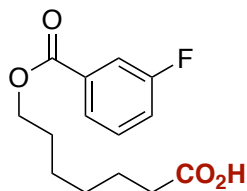
**8-cyano-8-methylnonanoic-1-<sup>13</sup>C acid (5c).** Following general procedure **GP-4-A**, using 8-chloro-2,2-dimethyloctanenitrile **4c** (18.7 mg, 0.1 mmol) and purification by column chromatography on silica gel (hexanes/EtOAc 10/1 followed by hexanes/EtOAc 1/1) afforded the title compound as an oil (13.3 mg, 68 %). Its mass isotopic pattern analysis showed a >99% <sup>13</sup>C isotope incorporation.

**<sup>1</sup>H NMR (400 MHz, CDCl<sub>3</sub>):** 2.36 (q, *J* = 7.3 Hz, 2H), 1.70 – 1.58 (m, 2H), 1.54 – 1.45 (m, 4H), 1.44 – 1.34 (m, 4H), 1.33 (s, 6H) ppm.

**<sup>13</sup>C NMR (126 MHz, CDCl<sub>3</sub>):** δ = 179.2, 125.3, 41.2, 33.9 (d, <sup>1</sup>J = 55.4 Hz), 32.5, 29.4, 29.0 (d, <sup>2</sup>J = 3.4 Hz), 26.8 (2C), 25.2, 24.7 (d, <sup>3</sup>J = 1.8 Hz) ppm.

**IR (neat):** ν = 2976, 2936, 2861, 2235, 1666, 1470, 1393, 1370, 1271, 1228, 1206, 1120, 1076, 939 cm<sup>-1</sup>.

**HRMS (ESI):**  $m/z$  calc. for  $(C_{10}^{13}CH_{18}NO_2)^-$   $[M-H]^-$ : 197.1377; found:197.1375.



**7-((3-fluorobenzoyl)oxy)heptanoic-1-<sup>13</sup>C acid (5d)**

Following general procedure **GP-4-A**, using 6-chlorohexyl 3-fluorobenzoate **4d** (25.8 mg, 0.1 mmol). Purification by column chromatography on silica gel (hexanes/EtOAc 10/1 followed by hexanes/ EtOAc 1/1) afforded the title compound as a white solid (20 mg, 75 %). Its mass isotopic pattern

analysis showed a >99% <sup>13</sup>C isotope incorporation.

**<sup>1</sup>H NMR (500 MHz, CDCl<sub>3</sub>):**  $\delta$  = 7.83 (dt,  $J$  = 7.7, 1.0 Hz, 1H), 7.71 (ddd,  $J$  = 9.3, 2.7, 1.5 Hz, 1H), 7.41 (td,  $J$  = 8.0, 5.5 Hz, 1H), 7.28 – 7.20 (m, 1H), 4.32 (t,  $J$  = 6.6 Hz, 2H), 2.37 (q,  $J$  = 7.3 Hz, 2H), 1.78 (p,  $J$  = 6.6 Hz, 2H), 1.73 – 1.63 (m, 2H), 1.51 – 1.39 (m, 4H) ppm.

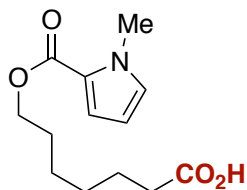
**<sup>13</sup>C NMR (126 MHz, CDCl<sub>3</sub>):**  $\delta$  = 179.9, 165.7 (d,  $^4J_{F-C}$  = 3.0 Hz), 162.7 (d,  $^1J_{F-C}$  = 246.9 Hz), 132.7 (d,  $^3J_{F-C}$  = 7.4 Hz), 130.1 (d,  $^3J_{F-C}$  = 7.8 Hz), 125.4 (d,  $^4J_{F-C}$  = 2.9 Hz), 120.1 (d,  $^2J_{F-C}$  = 21.3 Hz), 116.6 (d,  $^2J_{F-C}$  = 23.0 Hz), 65.4, 34.0 (d,  $^1J_{C-C}$  = 55.2 Hz), 28.8 (d,  $^2J_{C-C}$  = 3.5 Hz), 28.6, 25.8, 24.6 ppm.

**<sup>19</sup>F NMR (376 MHz, CDCl<sub>3</sub>):**  $\delta$  = -112.5 ppm.

**IR (neat):**  $\nu$  = 3054, 2941, 2859, 1712, 1657, 1589, 1475, 1445, 1415, 1269, 1201, 1091, 1071, 963, 896, 803, 753, 726, 674, 530 cm<sup>-1</sup>.

**Mp:** 34-35 °C.

**HRMS (ESI):**  $m/z$  calc. for  $(C_{13}^{13}CH_{16}FO_4)^-$   $[M-H]^-$ : 268.1072; found:268.1070.



**7-((1-methyl-1H-pyrrole-2-carbonyl)oxy)heptanoic-1-<sup>13</sup>C acid (5e)**

Following general procedure **GP-4-A**, using 6-chlorohexyl 1-methyl-1H-pyrrole-2-carboxylate **4e** (24.3 mg, 0.1 mmol). Purification by column chromatography on silica gel (hexanes/EtOAc t 10/1 followed by hexanes/EtOAc 1/1) afforded the title compound as a solid (15.6 mg, 62 %). Its

mass isotopic pattern analysis showed a >99% <sup>13</sup>C isotope incorporation.

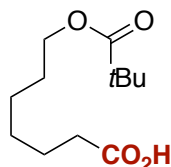
**<sup>1</sup>H NMR (400 MHz, CDCl<sub>3</sub>):**  $\delta$  = 6.93 (dd,  $J$  = 4.0, 1.8 Hz, 1H), 6.77 (t,  $J$  = 2.2 Hz, 1H), 6.10 (dd,  $J$  = 4.0, 2.5 Hz, 1H), 4.21 (t,  $J$  = 6.6 Hz, 2H), 3.92 (s, 3H), 2.36 (q,  $J$  = 7.3 Hz, 2H), 1.75 – 1.58 (m, 4H), 1.52 – 1.39 (m, 4H) ppm.

**<sup>13</sup>C NMR (101 MHz, CDCl<sub>3</sub>):**  $\delta$  = 179.3, 161.6, 129.5, 122.8, 117.8, 107.9, 63.9, 36.9, 33.9 (d,  $^1J$  = 55.0 Hz), 28.9, 28.8 (d,  $^2J$  = 3.6 Hz), 25.9, 24.7 (d,  $^3J$  = 1.7 Hz) ppm.

**IR (neat):**  $\nu$  = 2946, 2853, 1693, 1657, 1523, 1467, 1415, 1380, 1320, 1245, 1194, 1105, 1054, 944, 745, 733, 675, 609, 524, 450 cm<sup>-1</sup>.

**Mp:** 55-56 °C.

**HRMS (ESI):**  $m/z$  calc. for  $(C_{12}^{13}CH_{18}NO_4)^-$   $[M-H]^-$ : 253.1275; found:253.1277.



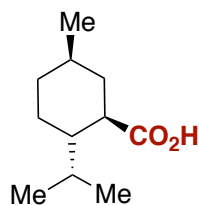
**7-(pivaloyloxy)heptanoic-1-<sup>13</sup>C acid (5f)** Following general procedure **GP-4-A**, using 6-chlorohexyl pivalate **4f** (22.0 mg, 0.1 mmol). Purification by column chromatography on silica gel (hexanes/ EtOAc 10/1 followed by hexanes/EtOAc 1/1) afforded the title compound as an oil (17.7 mg, 77 %). Its mass isotopic pattern analysis showed a >99% <sup>13</sup>C isotope incorporation.

**<sup>1</sup>H NMR (400 MHz, CDCl<sub>3</sub>):** δ = 4.04 (t, *J* = 6.6 Hz, 2H), 2.35 (q, *J* = 7.3 Hz, 2H), 1.67 – 1.54 (m, 4H), 1.43 – 1.34 (m, 4H), 1.19 (s, 9H) ppm.

**<sup>13</sup>C NMR (101 MHz, CDCl<sub>3</sub>):** δ = 179.8, 64.4, 38.9, 34.0 (d, <sup>1</sup>*J* = 55.2 Hz), 28.8 (d, <sup>2</sup>*J* = 3.6 Hz), 28.6, 27.3 (3C), 25.7, 24.7 (d, *J* = 1.7 Hz) ppm.

**IR (neat):** ν = 2935, 2866, 1727, 1707, 1666, 1481, 1461, 1398, 1366, 1284, 1152, 1034, 940, 891, 772 cm<sup>-1</sup>.

**HRMS (ESI):** *m/z* calc. for (C<sub>11</sub><sup>13</sup>CH<sub>21</sub>O<sub>4</sub>) [M-H]<sup>-</sup>: 230.1479; found: 230.1475.



**(-)-Menthyl carboxylic-1-<sup>13</sup>C acid (5g)** Following general procedure **GP-4-B**, using 1-Menthyl chloride **4g** (17.4 mg, 0.2 mmol), stirred at 50 °C. Purification by column chromatography on silica gel (hexanes/EtOAc 20/1 followed by hexanes/EtOAc 3/1) afforded the title compound as a solid (7.4 mg, 40 %). Its mass isotopic pattern analysis showed a >99% <sup>13</sup>C isotope incorporation.

**<sup>1</sup>H NMR (400 MHz, CDCl<sub>3</sub>):** δ = 2.31 (tdd, *J* = 11.7, 6.3, 3.4 Hz, 1H), 1.97 – 1.88 (m, 1H), 1.80 – 1.64 (m, 3H), 1.55 – 1.45 (m, 1H), 1.44 – 1.32 (m, 1H), 1.27 – 1.14 (m, 1H), 1.09 – 0.95 (m, 2H), 0.92 (d, *J* = 6.8 Hz, 3H), 0.90 (d, *J* = 6.4 Hz, 3H), 0.81 (d, *J* = 6.9 Hz, 3H) ppm

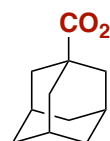
**<sup>13</sup>C NMR (101 MHz, CDCl<sub>3</sub>):** δ = 182.6, 47.7 (d, <sup>1</sup>*J* = 55.3 Hz), 44.4 (d, <sup>3</sup>*J* = 1.4 Hz), 38.9 (d, <sup>3</sup>*J* = 1.8 Hz), 34.7, 32.2 (d, <sup>2</sup>*J* = 4.4 Hz), 29.4, 23.9 (d, <sup>2</sup>*J* = 4.5 Hz), 22.4, 21.4, 16.1 ppm.

**IR (neat):** ν = 2953, 2925, 2861, 1656, 1454, 1371, 1262, 1197, 1139, 1086, 949, 879, 696, 556 cm<sup>-1</sup>.

**Mp:** 58-59 °C.

**[α]<sub>D</sub><sup>20</sup>:** -49.5° (*c* = 0.1, CH<sub>2</sub>Cl<sub>2</sub>).

**HRMS (ESI):** *m/z* calc. for (C<sub>10</sub><sup>13</sup>CH<sub>19</sub>O<sub>2</sub>) [M-H]<sup>-</sup>: 184.1424; found: 184.1425.



**Adamantane-1-carboxylic-<sup>13</sup>C acid (5h)** Following general procedure **GP-4-B**, using 1-chloroadamantane **4h** (34.0 mg, 0.2 mmol), TBAB (2.0 equiv) instead of LiCl, Zn dust (3.0 equiv) instead of the Mn powder and DMA (0.4 M). The reaction was stirred at 80 °C for 20 hours. Purification by column chromatography on silica gel (hexanes/EtOAc 20/1 followed by

hexanes/EtOAc 3/1) afforded the title compound as a solid (7.7 mg, 21 %). Its mass isotopic pattern analysis showed a >99%  $^{13}\text{C}$  isotope incorporation.

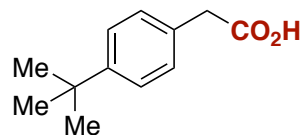
$^1\text{H}$  NMR (400 MHz,  $\text{CDCl}_3$ ):  $\delta$  = 2.03 (s, 3H), 1.91 (s, 6H), 1.78 – 1.65 (m, 6H) ppm.

$^{13}\text{C}$  NMR (101 MHz,  $\text{CDCl}_3$ ):  $\delta$  = 183.7, 40.6 (d,  $^1J$  = 56.6 Hz), 38.7 (3C), 36.6 (3C), 28.0 (d,  $^2J$  = 3.2 Hz, 3C) ppm.

**Mp:** 167-168 °C.

**IR (neat):**  $\nu$  = 3020, 2904, 2850, 2615, 1646, 1451, 1389, 1344, 1275, 1245, 1102, 1083, 937, 817, 740, 668, 526  $\text{cm}^{-1}$ .

**HRMS (ESI):**  $m/z$  calc. for ( $\text{C}_{10}^{13}\text{CH}_{15}\text{O}_2$ )  $[\text{M}-\text{H}]^-$ : 180.1111; found: 180.1115.



**2-(4-(*tert*-butyl)phenyl)acetic- $^{1-13}\text{C}$  acid (5i)**

Following general procedure **GP-4-C** using 1-(*tert*-butyl)-4-(chloromethyl)benzene **4i** (18.2 mg, 0.1 mmol).

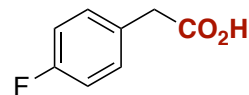
Purification by column chromatography on silica gel (hexanes/ EtOAc 10/1 followed by hexanes/EtOAc 1/1) afforded the compound as a pale-yellow oil (11.4 mg, 59 %). Its mass isotopic pattern analysis showed a >99%  $^{13}\text{C}$  isotope incorporation.

$^1\text{H}$  NMR (300 MHz,  $\text{CDCl}_3$ ):  $\delta$  7.36 (d,  $J$  = 8.4 Hz, 2H), 7.22 (d,  $J$  = 8.2 Hz, 2H), 3.62 (d,  $J$  = 7.8 Hz, 2H), 1.31 (s, 9H) ppm.

$^{13}\text{C}$  NMR (126 MHz,  $\text{CDCl}_3$ ):  $\delta$  = 177.3, 150.4, 130.4 (d,  $^2J$  = 2.8 Hz), 129.2 (d,  $^3J$  = 1.9 Hz, 2C), 125.8 (2C), 40.5 (d,  $^1J$  = 55.5 Hz), 34.6, 31.5 (3C) ppm.

**IR (neat):**  $\nu$  = 3032, 2953, 2906, 2868, 2709, 1670, 1519, 1478, 1403, 1390, 1366, 1329, 1270, 1225, 1192, 1111, 1021, 918, 811, 745, 695, 658, 558, 424  $\text{cm}^{-1}$ .

**HRMS (ESI):**  $m/z$  calc. for ( $\text{C}_{11}^{13}\text{CH}_{15}\text{O}_2$ )  $[\text{M}-\text{H}]^-$ : 192.1111; found: 192.1108.



**2-(4-fluorophenyl)acetic- $^{1-13}\text{C}$  acid (5j)**

Following general procedure **GP-4-C**, using 1-(chloromethyl)-4-fluorobenzene **4j** (28.9 mg, 0.2 mmol). Purification by column chromatography on silica gel (hexanes/EtOAc 10/1 followed by hexanes/EtOAc 1/1) afforded the compound as a solid (12.2 mg, 40 %). Its mass isotopic pattern analysis showed a %  $^{13}\text{C}$  isotope incorporation. **Mp:** 77-78 °C.

$^1\text{H}$  NMR (400 MHz,  $\text{CDCl}_3$ ):  $\delta$  = 7.31 – 7.19 (m, 2H), 7.10 – 6.96 (m, 2H), 3.63 (d,  $J$  = 7.8 Hz, 2H) ppm.

$^{13}\text{C}$  NMR (101 MHz,  $\text{CDCl}_3$ ):  $\delta$  = 177.3, 162.3 (d,  $^1J_{\text{F-C}}$  = 245.9 Hz), 131.1 (dd,  $^3J_{\text{F-C}}$  = 8.1,  $^3J_{\text{C-C}}$  = 1.9 Hz), 129.3 – 128.7 (m), 115.7 (d,  $^2J_{\text{F-C}}$  = 21.6 Hz), 40.2 (d,  $^1J_{\text{C-C}}$  = 55.6 Hz) ppm.

$^{19}\text{F}$  NMR (376 MHz,  $\text{CDCl}_3$ )  $\delta$  = -113.4 ppm.

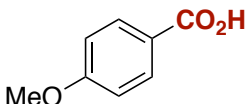
**IR (neat):**  $\nu$  = 3047, 2921, 2716, 1651, 1611, 1510, 1409, 1339, 1223, 1186, 1156, 1098, 904, 862, 823, 784, 714, 666, 546, 508, 418  $\text{cm}^{-1}$ .

**HRMS (ESI):**  $m/z$  calc. for ( $\text{C}_7^{13}\text{H}_6\text{FO}_2$ )  $[\text{M}-\text{H}]^-$ : 154.0391; found: 154.0397

**$^{12}\text{C}/^{13}\text{C}$  isotope exchange via aromatic halides**

**Bromination/iodination of benzoic acids.** Compounds **4k-m** were prepared following the procedure of decarboxylation /halogenation described by Larrosa et al.<sup>34,35</sup>

**Carboxylation of aryl bromides/iodides**

 **4-Methoxybenzoic-1- $^{13}\text{C}$  acid (5k).** An oven-dried screw-capped Schlenk tube equipped with a magnetic stir bar was charged with  $\text{NiBr}_2\cdot\text{DME}$  (6.2 mg, 0.1 equiv), neocuproine (8.3 mg, 0.2 equiv) and manganese (22 mg, 2.0 equiv). Then 4-bromoanisole (37.4 mg, 0.2 mmol) followed by DMA (1.0 mL) was added to the tube under argon. After keeping for 1 min the mixture under vacuum at  $-20\text{ }^\circ\text{C}$ , the Schlenk tube was refilled with  $^{13}\text{CO}_2$  (two cycles) and kept for 15 min. The reaction mixture was allowed to stir at  $50\text{ }^\circ\text{C}$  for 24 h. The reaction mixture was quenched with 2 M HCl (aq) and extracted with EtOAc (3 times). The organic phase was washed with brine and dried over  $\text{MgSO}_4$ . The crude mixture was purified by flash column chromatography through silica (eluent: Hex/EA = 19/1 – 4/1) to afford a white solid (21 mg, 0.14 mmol, 70% isolated yield).

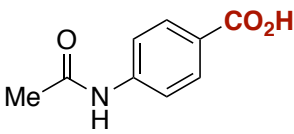
**$^1\text{H}$  NMR (500 MHz,  $\text{DMSO}-d_6$ ):**  $\delta$  = 7.89 (dd,  $J$  = 8.8, 3.8 Hz, 1H), 7.01 (d,  $J$  = 8.4 Hz, 1H), 3.82 (s, 2H) ppm.

**$^{13}\text{C}$  NMR (126 MHz,  $\text{DMSO}-d_6$ ):**  $\delta$  = 167.0, 162.8, 131.4 (d,  $^3J$  = 3.0 Hz, 2C), 123.0 (d,  $^1J$  = 73.6 Hz), 113.8 (d,  $^2J$  = 4.6 Hz, 2C), 55.4 ppm.

**Mp:** 185-188  $^\circ\text{C}$ .

**IR (neat):**  $\nu$  = 2980, 2938, 2847, 2783, 1634, 1599, 1572, 1513, 1448, 1422, 1288, 1256, 1163, 1023, 923, 839, 759, 689, 614  $\text{cm}^{-1}$ .

**HRMS (ESI):**  $m/z$  calc. for  $(\text{C}_7^{13}\text{CH}_7\text{O}_3)^-$   $[\text{M}-\text{H}]^-$ : 152.0434; found: 152.0433.

 **4-Acetamidobenzoic- $^{13}\text{C}$  acid (5l).** *N*-(4-iodophenyl) acetamide (52.6 mg, 0.2 mmol, 1.0 equiv),  $\text{NiCl}_2(\text{PPh}_3)_2$  (6.5 mg, 0.01 mmol, 5 mol%),  $\text{Ph}_3\text{P}$  (5.3 mg, 0.02 mmol, 10 mol %), TEAI (5.1 mg, 0.02 mmol, 10 mol %), Mn (33.0 mg, 0.6 mmol, 3.0 equiv) were mixed in an oven-dried Schlenk tube and was evacuated-back refill with argon 3 times. 0.4 mL DMAc was added under argon and the mixture was evacuated for about 1 minute. After  $^{13}\text{CO}_2$  was introduced at rt, the tube was sealed and stirred at rt for 24 hours. The reaction was quenched with 1 M HCl and extracted with EtOAc, further purification through flash column chromatography (DCM to DCM/Methanol = 20/1 to 15/1) to give white solid (19.1 mg, 0.106 mmol, 53% isolated yield).



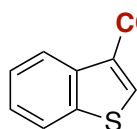
**$^1\text{H}$  NMR (300 MHz, Methanol- $d_4$ ):**  $\delta$  = 7.96 (d,  $J$  = 9.2 Hz, 2H), 7.66 (d,  $J$  = 8.3 Hz, 2H), 2.15 (s, 3H) ppm.

**$^{13}\text{C}$  NMR (75 MHz, Methanol- $d_4$ ):**  $\delta$  = 171.9, 169.5, 144.4, 131.8 (2C), 126.9 (d,  $^1J$  = 73.2 Hz), 120.0 (2C), 24.0 ppm.

**Mp:** 239-240 °C.

**IR (neat):**  $\nu$  = 3290, 2929, 2413, 2215, 2052, 1633, 1603, 1576, 1515, 1435, 1387, 1323, 1182, 1117, 1043, 983, 863, 752, 707, 489  $\text{cm}^{-1}$ .

**HRMS (ESI):**  $m/z$  calc. for ( $\text{C}_8^{13}\text{CH}_3\text{NO}_3$ ) $^-$  [M-H] $^-$ : 179.0543; found: 179.0543.



**$\text{CO}_2\text{H}$  Benzo[*b*]thiophene-3-carboxylic-1- $^{13}\text{C}$  acid (5m).** 3-

bromobenzo[*b*]thiophene (42.6 mg, 0.2 mmol, 1.0 equiv),  $\text{NiCl}_2(\text{PPh}_3)_2$  (6.5 mg, 0.01 mmol, 5 mol%),  $\text{Ph}_3\text{P}$  (5.3 mg, 0.02 mmol, 10 mol%), TEAI (5.1 mg, 0.02 mmol, 10 mol%), Mn (33.0 mg, 0.6 mmol, 3.0 equiv) were mixed in an oven-dried Schlenk tube and was evacuated-back refill with argon 3 times. 0.4 mL DMA was added under argon and the mixture was evacuated for about 1 minute. After  $^{13}\text{CO}_2$  was introduced at rt, the tube was sealed and stirred at rt for 24 hours. The reaction was quenched with 1 M HCl and extracted with EtOAc, further purification through flash column chromatography (Hexane/EtOAc = 3/1 to 1/1) to give a white solid (21.7 mg, 0.122 mmol, 61% isolated yield).

**$^1\text{H}$  NMR (400 MHz, DMSO- $d_6$ ):**  $\delta$  = 8.63 (s, 1H), 8.50 (d,  $J$  = 7.5 Hz, 1H), 8.07 (d,  $J$  = 7.9 Hz, 1H), 7.50 (ddd,  $J$  = 8.2, 7.1, 1.3 Hz, 1H), 7.44 (ddd,  $J$  = 8.3, 7.0, 1.4 Hz, 1H) ppm.

**$^{13}\text{C}$  NMR (126 MHz DMSO- $d_6$ ):**  $\delta$  = 163.8, 139.8 (d,  $^3J$  = 5.5 Hz), 137.9 (d,  $^2J$  = 4.5 Hz), 136.6 (d,  $^2J$  = 5.1 Hz), 127.3 (d,  $^1J$  = 76.6 Hz), 125.3, 124.9, 124.2, 123.0 ppm.

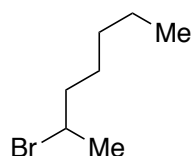
**Mp:** 175-176 °C.

**IR (neat):**  $\nu$  = 3107, 2837, 2765, 2583, 1666, 1502, 1465, 1416, 1363, 1271, 1249, 1150, 1068, 1007, 917, 858, 772, 752, 722, 704, 602, 416  $\text{cm}^{-1}$ .

**HRMS (ESI):**  $m/z$  calc. for ( $\text{C}_8^{13}\text{CH}_5\text{SO}_2$ ) $^-$  [M-H] $^-$ : 178.0049; found: 178.0047.

**<sup>12</sup>C/<sup>13</sup>C isotope exchange via chain walking strategies****General procedure (GP-5) for Bromination**

Secondary alkyl bromides were prepared following the procedure reported by Chaozhong Li et al.<sup>33</sup> To a solution of carboxylic acid (1.0 equiv) and [Ag(Phen)<sub>2</sub>]OTf (2.5 mol%) in anhydrous dichloromethane (0.025 M) was added dibromoisocyanuric acid (DBI, 0.8 equiv) at room temperature under nitrogen atmosphere. The reaction mixture was then stirred at room temperature 24-36 h. The reaction mixture was filtered through the celite and washed with dichloromethane. After the removal of solvent under reduced pressure, the crude product was purified by flash column chromatography through silica gel (eluent: hexane) to afford the pure product.



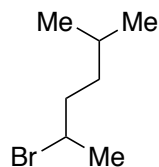
**2-Bromoheptane (2a-Br):** Following GP-5 starting from 2-methylheptanoic acid (144.2 mg, 1.0 mmol) afforded the title compound as a colorless oil (108.0 mg, 0.61 mmol, 61 %).

**<sup>1</sup>H NMR (300 MHz, CDCl<sub>3</sub>):**  $\delta$  = 4.19 – 4.08 (m, 1H), 1.90 – 1.71 (m, 2H), 1.70 (d,  $J$  = 6.6 Hz, 3H), 1.54 – 1.39 (m, 2H), 1.36 – 1.21 (m, 4H),

0.89 (t,  $J$  = 6.9 Hz, 3H) ppm.

**<sup>13</sup>C NMR (75 MHz, CDCl<sub>3</sub>):**  $\delta$  = 52.2, 41.3, 31.3, 27.6, 26.6, 22.7, 14.1 ppm.

Spectral data was in agreement with the literature.<sup>51</sup>



**2-Bromo-5-methylhexane (6-Br):** Following GP-5 starting from 2-methylheptanoic acid (72.1 mg, 0.50 mmol) afforded the title compound as a colorless oil (36.0 mg, 0.20 mmol, 40 %).

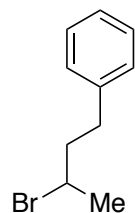
**<sup>1</sup>H NMR (300 MHz, CDCl<sub>3</sub>):**  $\delta$  = 4.16 – 4.05 (m, 1H), 1.90 – 1.75 (m, 2H), 1.71 (d,  $J$  = 6.7 Hz, 3H), 1.62 – 1.49 (m, 1H), 1.45 – 1.22 (m, 2H),

0.91 (d,  $J$  = 3.0 Hz, 3H), 0.88 (d,  $J$  = 3.0 Hz, 3H) ppm.

**<sup>13</sup>C NMR (75 MHz, CDCl<sub>3</sub>):**  $\delta$  = 52.4, 39.3, 37.0, 27.8, 26.6, 22.8, 22.6 ppm.

**IR (neat):**  $\nu$  = 2956, 2928, 2870, 1467, 1379, 1368, 1240, 1191, 1150, 994, 901, 760, 612 cm<sup>-1</sup>.

**HRMS (ESI):** The exact mass of this compound was difficult to analyze by ESI analysis.



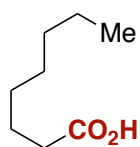
**(3-bromobutyl)benzene (5a-Br):** Following GP-5 starting from 2-methyl-4-phenylbutanoic acid (178.2 mg, 1.0 mmol) afforded the title compound as a colorless oil (75.1 mg, 0.35 mmol, 35 %).

**<sup>1</sup>H NMR (300 MHz, CDCl<sub>3</sub>):**  $\delta$  = 7.39 – 7.15 (m, 5H), 4.18 – 4.00 (m, 1H), 2.92 – 2.65 (m, 2H), 2.20 – 1.97 (m, 2H), 1.74 (d,  $J$  = 6.6 Hz, 3H) ppm.

$^{13}\text{C}$  NMR (75 MHz,  $\text{CDCl}_3$ ):  $\delta$  = 141.1, 128.7 (2C), 128.6 (2C), 126.2, 51.0, 42.8, 34.1, 26.7 ppm.

Spectral data was in agreement with the literature.<sup>52</sup>

**General procedure for Chain-Walking Carboxylation (GP-6):** An oven-dried Schlenk tube containing a stirring bar was charged with  $\text{NiI}_2$  (3.9 mg, 0.0125 mmol, 2.5 mol%), **L4** (11.0 mg, 0.022 mmol, 4.4 mol%), and Mn powder (82.4 mg, 1.50 mmol, 3 equiv). The corresponding alkyl bromide (0.5 mmol) and DMF (0.5 mL, 1 M) were added under an argon flow. The tube was cold down to  $-50^\circ\text{C}$ , put under vacuum for 20 seconds and then the  $^{13}\text{CO}_2$  was transferred to the Schlenk flask. It was closed and stirred at  $60^\circ\text{C}$  for 20 hours. The mixture was then carefully quenched with 2 M HCl to hydrolyze the resulting carboxylate and extracted with EtOAc. The combined organic layer was washed with brine, dried over anhydrous  $\text{MgSO}_4$  filtrated and evaporated under reduced pressure. The resulting crude carboxylic acid was purified by conventional flash chromatography in silica gel using hexanes/EtOAc 3:1 with 1% formic acid.

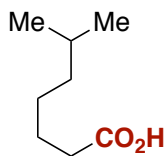


**Octanoic-1- $^{13}\text{C}$  acid (2a).** Following **GP-6** starting from 2-Bromoheptane (**2a-Br**) (89.6 mg, 0.5 mmol) afforded the title compound as a colorless oil (26.0 mg, 0.18 mmol, 36%). Its mass isotopic pattern analysis showed a  $>99\%$   $^{13}\text{C}$  isotope incorporation.

$^1\text{H}$  NMR (300 MHz,  $\text{CDCl}_3$ ):  $\delta$  = 2.38 – 2.31 (m, 2H), 1.69 – 1.58 (m, 2H), 1.35 – 1.28 (m, 8H), 0.88 (t,  $J$  = 6.8 Hz, 3H) ppm.

$^{13}\text{C}$  NMR (75 MHz,  $\text{CDCl}_3$ ):  $\delta$  = 180.3, 34.2 (d,  $^1J$  = 54.9 Hz), 31.8, 29.2 (d,  $^2J$  = 3.7 Hz), 29.1, 24.8, 22.7, 14.2 ppm.

**HRMS (ESI):**  $m/z$  calc. for ( $\text{C}_7^{13}\text{CH}_{15}\text{O}_2$ )  $[\text{M}-\text{H}]^-$ : 144.1111; found: 144.1116.



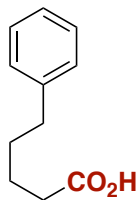
**6-Methylheptanoic-1- $^{13}\text{C}$  acid (6).** Following **GP-6** starting from 2-bromo-5-methylhexane (**6-Br**) (89.5 mg, 0.5 mmol) afforded the title compound as a colorless oil (33.0 mg, 0.23 mmol, 46 %). Its mass isotopic pattern analysis showed a  $>99\%$   $^{13}\text{C}$  isotope incorporation.

$^1\text{H}$  NMR (300 MHz,  $\text{CDCl}_3$ ):  $\delta$  = 2.39 – 2.32 (m, 2H), 1.67 – 1.47 (m, 3H), 1.39 – 1.28 (m, 2H), 1.23 – 1.15 (m, 2H), 0.87 (d,  $J$  = 6.6 Hz, 6H) ppm.

$^{13}\text{C}$  NMR (75 MHz,  $\text{CDCl}_3$ ):  $\delta$  = 180.3, 38.7, 34.2 (d,  $^1J$  = 55.3 Hz), 28.0, 27.0 (d,  $^2J$  = 3.5 Hz), 25.1, 22.7 (2C) ppm.

**IR (neat):**  $\nu$  = 2954, 2927, 2869, 1464, 1398, 1276, 1243, 1226, 1198, 1109, 935, 738  $\text{cm}^{-1}$ .

**HRMS (ESI):**  $m/z$  calc. for ( $\text{C}_7^{13}\text{CH}_{15}\text{O}_2$ )  $[\text{M}-\text{H}]^-$ : 144.1111; found: 144.1104.



**5-phenylpentanoic-1-<sup>13</sup>C acid (5a).** Following **GP-6** starting from (3-bromobutyl)benzene (**5a-Br**) (106.6 mg, 0.5 mmol) afforded the title compound as a colorless oil (24.0 mg, 0.14 mmol, 27 %). Its mass isotopic pattern analysis showed a >99% <sup>13</sup>C isotope incorporation.

**<sup>1</sup>H NMR (500 MHz, CDCl<sub>3</sub>):** δ = 7.31 – 7.28 (m, 2H), 7.21 – 7.18 (m, 3H), 2.68 – 2.64 (m, 2H), 2.42 – 2.37 (m, 2H), 1.71 – 1.68 (m, 4H) ppm.

**<sup>13</sup>C NMR (126 MHz, CDCl<sub>3</sub>):** δ = 180.2, 142.1, 128.5 (2C), 128.5 (2C), 126.0, 35.7, 34.1 (d, <sup>1</sup>J = 55.2 Hz), 30.9 (d, <sup>2</sup>J = 3.6 Hz), 24.4 ppm.

**HRMS (ESI):** *m/z* calc. for (C<sub>7</sub><sup>13</sup>CH<sub>15</sub>O<sub>2</sub>)<sup>-</sup> [M-H]<sup>-</sup>: 178.0955; found: 178.0954.

## $^{12}\text{C}/^{14}\text{C}$ isotope exchange

### General information for the $^{14}\text{C}$ -labeling

All reactions and manipulations were performed in a recirculating mBraun LabMaster DP inert atmosphere (Ar) drybox.  $^{14}\text{CO}_2$  cartridges were purchased from RC TRITEC. Controlled addition of  $^{13}\text{C}$  or  $^{14}\text{C}$ - $\text{CO}_2$  into Wilmad NMR tubes was performed using a carbon Tritec manifold (figure 5). Radioactive TLC were performed using a Rita Star  $\beta$  radioactivity thin-layer-chromatography detector.

See: <http://www.rctritec.com/en/tritium-handling-technology/c-14-manifold-system.html>

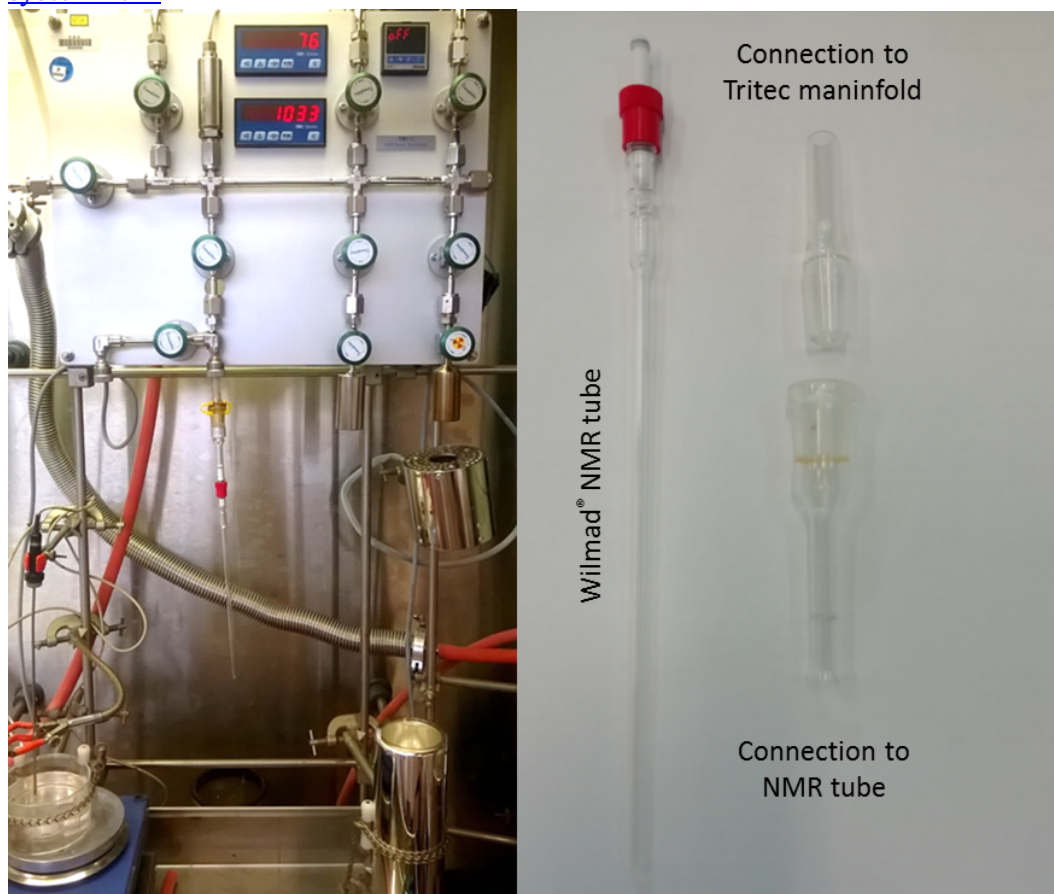
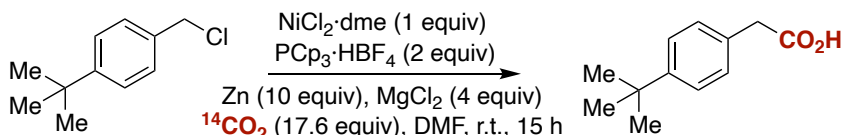


Figure 5. Tritec manifold

**[1-<sup>14</sup>C]-2-(4-*tert*-butylphenyl)acetic acid, [<sup>14</sup>C]-5i**

An oven-dried Wilmad NMR tube with a *J*-Young valve equipped with a magnetic stir bar was introduced into a glove box. It was charged with PCp<sub>3</sub>·HBF<sub>4</sub> (16.25 mg, 0.05 mmol, 2 equiv), MgCl<sub>2</sub> (10.0 mg, 0.1 mmol, 4 equiv), NiCl<sub>2</sub>·dme (5.5 mg, 0.025 mmol, 1 equiv), and Zn (dust, 16.25 mg, 0.25 mmol, 10 equiv) were added into the tube followed by the benzyl chloride (4.6 mg, 0.025 mmol, 1 equiv) and anhydrous DMF (100 μL). The NMR tube was sealed and took out of the glove box. It was then attached to a <sup>14</sup>C manifold system and the reaction mixture was frozen with a liquid nitrogen bath. The NMR tube was evacuated and <sup>14</sup>CO<sub>2</sub> (2.17 GBq·mmol<sup>-1</sup>, 957 MBq, 0.441 mmol, 17.6 equiv) was condensed using the freezing bath. The NMR tube was closed, detached from the manifold system and kept at room temperature for 15 hours. After concentration, purification using Flash Chromatography on SiO<sub>2</sub> (DCM/MeOH (96/4)) gave [1-<sup>14</sup>C]-*tert*-butylphenylacetic acid [<sup>14</sup>C]-5i (2.12 GBq·mmol<sup>-1</sup>, 8.95 MBq, 0.0042 mmol, yield: 17%).

**Specific activity (MS (ESI)):** 2.12 GBq·mmol<sup>-1</sup>.

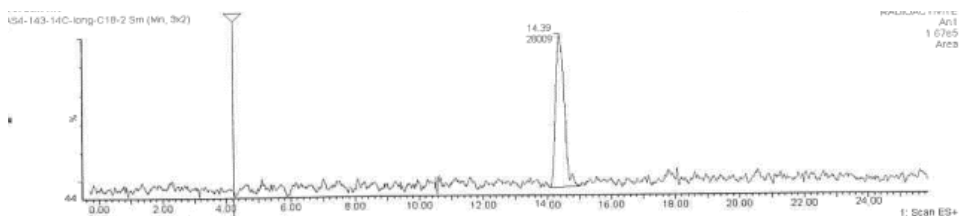
**TLC (silicagel 60F254, hexane/AcOEt/AcOH (70/30/0.1))** R<sub>f</sub> = 0.3.

Radiochemical purity > 99%.

Radiochemical purity

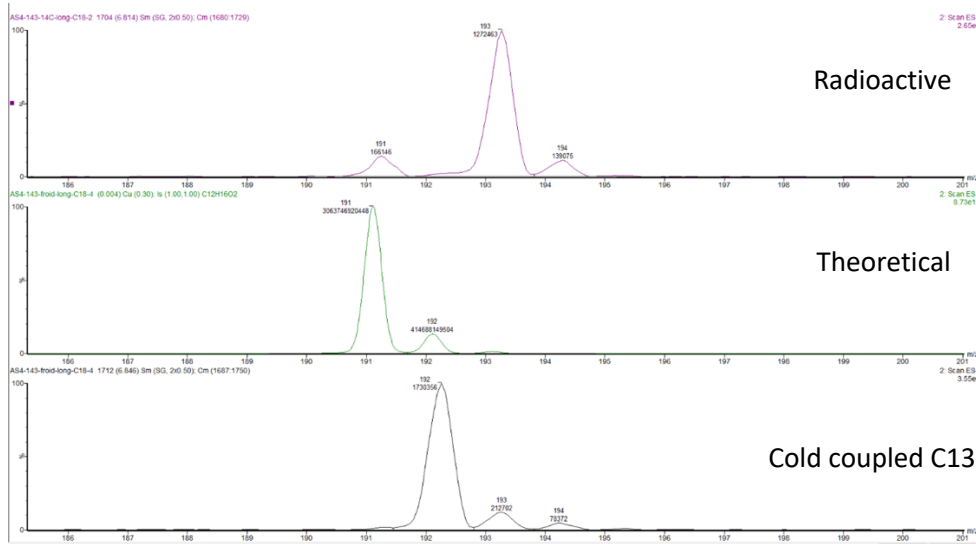
Column	Xbridge C18 3,5μm 4,6x100mm Column	
Flow	1 ml/min	
Detection	mass and UV	
Temperature	TA	
Solvent		
A	H <sub>2</sub> O + 0,1% HCOOH	
B	ACN + 0,1% HCOOH	
Gradient		
	% A	% B
t initial	95	5
t= 8 min	0	100
t= 13 min	0	100
t= 13,50 min	95	5
t= 17 min	95	5

# Catalytic Decarboxylation/Carboxylation Platform for Accessing Isotopically Labeled Carboxylic Acids



Specific activity:

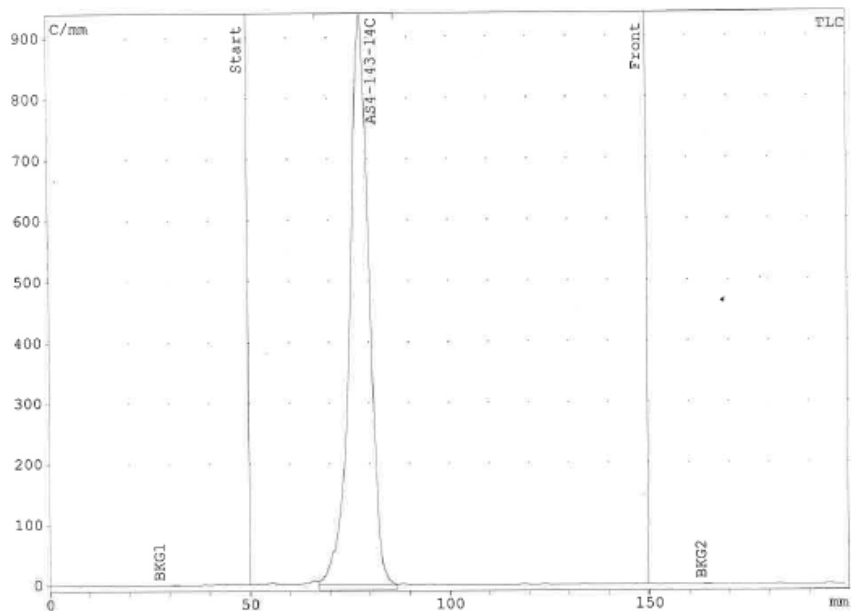
Radioactive	M+1	M+2 (1D)	M+3 (2D)	M+4 (3D)	M+5 (4D)	M+6 (5D)
	191	192	193	194		
aire tot	166146	0	1272463	139075		
S contrib	0	22488	-3044	172644	-4544	615
aire D	0	-22488	1275507	-33569	4544	-615
% D	0	-1,6%	91,8%	-2,4%	0,3%	0,0%
Specific activity			91,8%			



## Chapter 4

### Radioactive TLC

Mesure AS4-143-14C-Pur\_02.rta raytest GmbH Page 1/1  
 C:\PROGRA-1\raytest\Rita Control\list\ANTOINE\C14\AS4-143-14C-PUR\_02.RTADate d'impression : 16/01/2019 17:47



#### Description de l'échantillon

Etude: ANTOINE  
 Mesure: AS4-143-14C-Pur\_02.rta, commencé: 16/01/2019 17:47  
 Méthode: C14  
 Origine: 50 mm Front 150 mm  
 Meas. time: 0,1 min Résolution: 0,4 mm  
 Tray number: 1,0 Position de scan: 215,0 mm  
 Haute tension: 1620,0 V

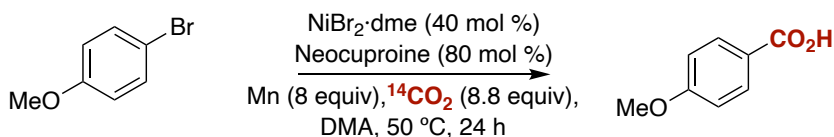
AS4-143-14C-Pur  
 Silicagel Merck 60F254 - CH2Cl2 96 MeOH 4  
 Détecteur de radioactivité: raytest RITA  
 Autre Square flow cell #0  
 Cell volume 0 ul

#### Intégration TLC

Substance	R/F	Type	Aire	%Aire
			Counts	%
AS4-143-14C	0,282	DD	5274,555	100,00
Sum in ROI			5274,555	
Aire totale			5344,264	
Aire RF			5328,921	
BKG1			0,0737	
BKG2			0,0718	
Remainder RF			54,37	1,02
Remainder (Tot)			69,71	1,30



#### 4-methoxybenzoic acid-[carboxyl-<sup>14</sup>C], [<sup>14</sup>C]-5k



An oven-dried NMR tube with a *J*-Young valve equipped with a magnetic stir bar was introduced into a glove box. It was charged with NiBr<sub>2</sub>·DME (6.2 mg, 0.02 mmol, 0.4 equiv), neocuproine (8.3 mg, 0.04 mmol, 0.8 equiv) and manganese (22 mg, 0.4 mmol, 8.0 equiv). Then 4-bromoanisole (6.3 μL, 0.05 mmol, 1 equiv) followed by DMA (100 μL) was added to the tube. The NMR tube was sealed and took out of the glove box. It was then attached to a <sup>14</sup>C manifold system and the reaction mixture was frozen with a liquid nitrogen bath. The NMR tube was evacuated and <sup>14</sup>CO<sub>2</sub> (2.17 GBq·mmol<sup>-1</sup>, 957 MBq, 0.441 mmol, 8.8 equiv) was condensed using the freezing bath. The NMR tube was closed, detached from the manifold system and kept at 50 °C for 24 hours. After concentration, purification using Flash Chromatography on SiO<sub>2</sub> (hexane/AcOEt/AcOH (70/30/0.1)) gave methoxybenzoic acid-[carboxyl-<sup>14</sup>C] [<sup>14</sup>C]-5k (2.04 GBq mmol<sup>-1</sup>, 76.849 MBq, 0.038 mmol, yield: 76%).

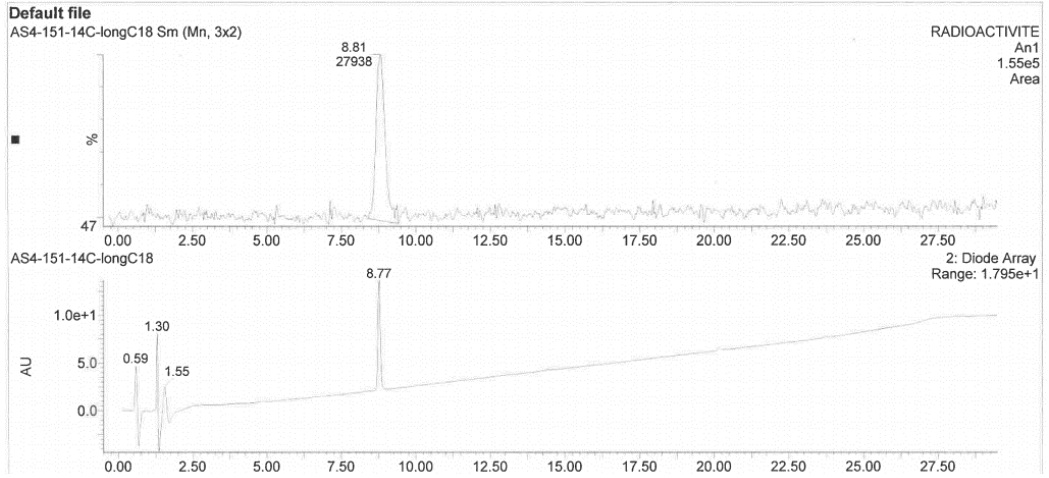
**Specific activity (MS (ESI)):** 2.04 GBq·mmol<sup>-1</sup>.

**TLC (silicagel 60F254, hexane /AcOEt / AcOH (70/30/0.1))** R<sub>f</sub> = 0.25. Radiochemical purity > 99%.

Radiochemical purity:

Column	Xbridge C18 3,5μm 4,6x100mm Column	
Flow	1 ml/min	
Detection	mass and UV	
Temperature	TA	
Solvent		
A	H <sub>2</sub> O + 0,1% HCOOH	
B	ACN + 0,1% HCOOH	
Gradient		
	% A	% B
t initial	95	5
t= 8 min	0	100
t= 13 min	0	100
t= 13,50 min	95	5
t= 17 min	95	5

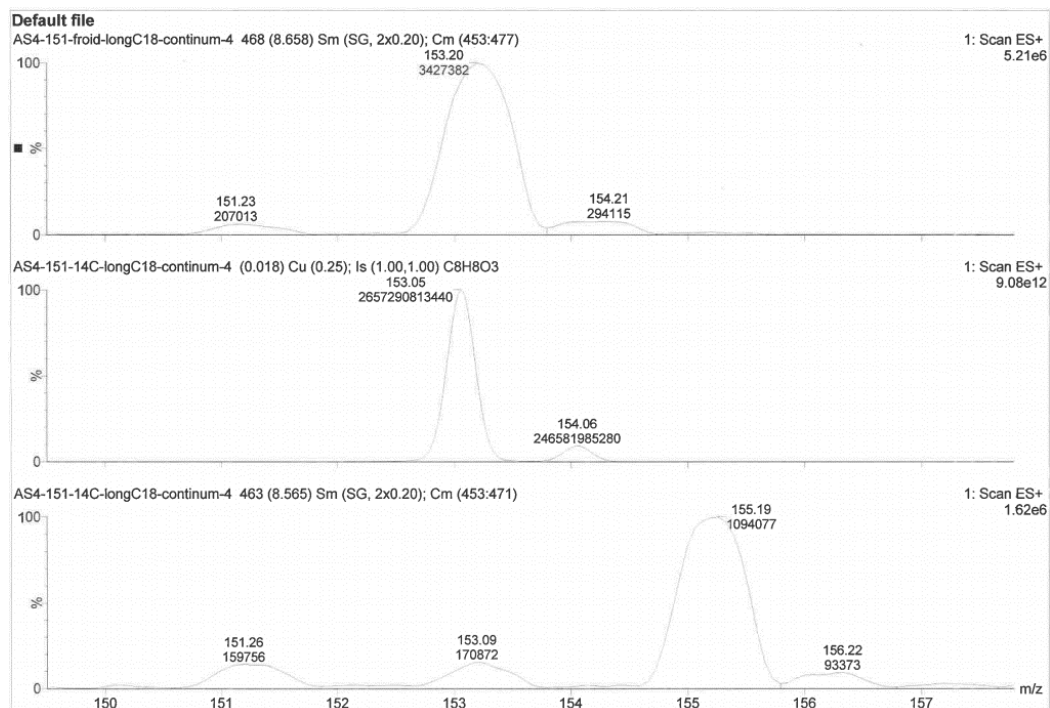
# Chapter 4



## Specific activity

Radioactive	M+1	M+2 (1D)	M+3 (2D)	M+4 (3D)	M+5 (4D)	M+6 (5D)
	153	154	155	156		
aire tot	170872	0	1094077	93373		
S contrib	0	15856	-1471	101661	-4544	615
aire D	0	-15856	1095548	-8288	4544	-615
% D	0	-1,3%	88,1%	-0,7%	0,3%	0,0%
Specific activity			88,1%			

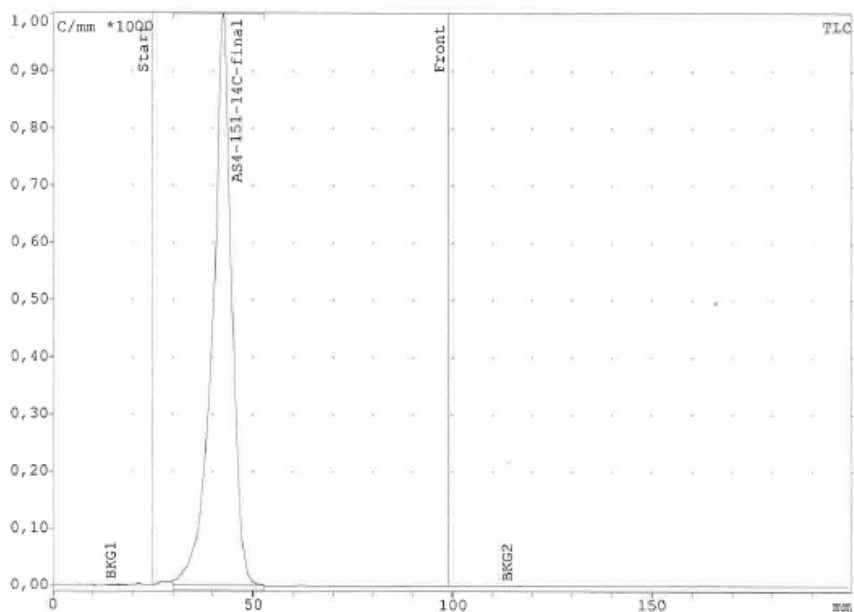
# Catalytic Decarboxylation/Carboxylation Platform for Accessing Isotopically Labeled Carboxylic Acids



## Chapter 4

### Radioactive TLC

Mesure AS4-151-14C-final\_03.rta raytest GmbH Page 1/1  
 C:\PROGRA-1\raytest\Rita Control\list\ANTOINE\C14\AS4-151-14C-FINAL\_03.RTADate d'impression :



#### Description de l'échantillon

Etude: ANTOINE  
 Mesure: AS4-151-14C-final\_03.rta, commencé: 07/02/2019 16:29  
 Méthode: C14  
 Origine: 25 mm Front 99 mm  
 Meas. time: 0,1 min Résolution: 0,4 mm  
 Tray number: 2,0 Position de scan: 230,0 mm  
 Haute tension: 1620,0 V

AS4-151-14C-final silica gel 7/3/0.1 Hex/AE/AcCOOH  
 Détecteur de radioactivité: raytest RITA  
 Autre Square flow cell #0  
 Cell volume 0 ul

#### Intégration TLC

Substance	R/F	Type	Aire	%Aire
			Counts	%
AS4-151-14C-fin	0,238	DD	5521,855	100,00
Sum in ROI			5521,855	
Aire totale			5592,917	
Aire RF			5569,000	
BKG1			0,7955	
2 ROIs BKG			0,4339	
Remainder RF			47,15	0,85
Remainder (Tot)			71,06	1,27



**References:**

- (1) DiMasi, J. A.; Grabowski, H. G.; Hansen, R. W. Innovation in the Pharmaceutical Industry: New Estimates of R&D Costs. *Journal of Health Economics* **2016**, *47*, 20–33. <https://doi.org/10.1016/j.jhealeco.2016.01.012>.
- (2) Zhang, Z.; Tang, W. Drug Metabolism in Drug Discovery and Development. *Acta Pharmaceutica Sinica B* **2018**, *8* (5), 721–732. <https://doi.org/10.1016/j.apsb.2018.04.003>.
- (3) Ruiz-Garcia, A.; Bermejo, M.; Moss, A.; Casabo, V. G. Pharmacokinetics in Drug Discovery. *Journal of Pharmaceutical Sciences* **2008**, *97* (2), 654–690. <https://doi.org/10.1002/jps.21009>.
- (4) Elmore, C. S.; Bragg, R. A. Isotope Chemistry; a Useful Tool in the Drug Discovery Arsenal. *Bioorganic & Medicinal Chemistry Letters* **2015**, *25* (2), 167–171. <https://doi.org/10.1016/j.bmcl.2014.11.051>.
- (5) Marathe, P. H.; Shyu, W. C.; Humphreys, W. G. The Use of Radiolabeled Compounds for ADME Studies in Discovery and Exploratory Development. *Current Pharmaceutical Design* **2004**, *10* (24), 2991–3008. <https://doi.org/10.2174/1381612043383494>.
- (6) Elmore, C. S. Chapter 25 The Use of Isotopically Labeled Compounds in Drug Discovery. In *Annual Reports in Medicinal Chemistry*; Macor, J. E., Ed.; Academic Press, 2009; Vol. 44, pp 515–534. [https://doi.org/10.1016/S0065-7743\(09\)04425-X](https://doi.org/10.1016/S0065-7743(09)04425-X).
- (7) Jiang, H.; Zeng, J.; Li, W.; Bifano, M.; Gu, H.; Titsch, C.; Easter, J.; Burrell, R.; Kandoussi, H.; Aubry, A.-F.; Arnold, M. E. Practical and Efficient Strategy for Evaluating Oral Absolute Bioavailability with an Intravenous Microdose of a Stable Isotopically-Labeled Drug Using a Selected Reaction Monitoring Mass Spectrometry Assay. *Anal. Chem.* **2012**, *84* (22), 10031–10037. <https://doi.org/10.1021/ac3024558>.
- (8) Rizi, R. R. A New Direction for Polarized Carbon-13 MRI. *Proceedings of the National Academy of Sciences* **2009**, *106* (14), 5453–5454. <https://doi.org/10.1073/pnas.0901843106>.
- (9) Brindle, K. M. Imaging Metabolism with Hyperpolarized <sup>13</sup>C-Labeled Cell Substrates. *J. Am. Chem. Soc.* **2015**, *137* (20), 6418–6427. <https://doi.org/10.1021/jacs.5b03300>.
- (10) Capozzi, A.; Patel, S.; Gunnarsson, C. P.; Marco-Rius, I.; Comment, A.; Karlsson, M.; Lerche, M. H.; Ouari, O.; Ardenkjær-Larsen, J. H. Efficient Hyperpolarization of U-<sup>13</sup>C-Glucose Using Narrow-Line UV-Generated Labile Free Radicals. *Angew. Chem. Int. Ed.* **2019**, *58* (5), 1334–1339. <https://doi.org/10.1002/anie.201810522>.
- (11) Orlando, T.; Dervişoğlu, R.; Levien, M.; Tkach, I.; Prisner, T. F.; Andreas, L. B.; Denysenkov, V. P.; Bennati, M. Dynamic Nuclear Polarization of <sup>13</sup>C Nuclei in the Liquid State over a 10 Tesla Field Range. *Angew. Chem. Int. Ed.* **2019**, *58* (5), 1402–1406. <https://doi.org/10.1002/anie.201811892>.
- (12) Ma, S.; Chowdhury, S. K. The Use of Stable Isotope-Labeled Drug as Microtracers with Conventional LC–MS/MS to Support Human Absolute Bioavailability Studies: Are We There Yet? *Bioanalysis* **2016**, *8* (8), 731–733. <https://doi.org/10.4155/bio.16.25>.
- (13) Kim, I.-Y.; Suh, S.-H.; Lee, I.-K.; Wolfe, R. R. Applications of Stable, Nonradioactive Isotope Tracers in in Vivo Human Metabolic Research. *Experimental & Molecular Medicine* **2016**, *48* (1), e203–e203. <https://doi.org/10.1038/emm.2015.97>.
- (14) McInteer, B. B. Isotope Separation by Distillation: Design of a Carbon-13 Plant. *Separation Science and Technology* **1980**, *15* (3), 491–508. <https://doi.org/10.1080/01496398008068494>.
- (15) Oziashvili, E. D.; Egiazarov, A. S. The Separation of Stable Isotopes of Carbon. *Russ. Chem. Rev.* **1989**, *58* (4), 325. <https://doi.org/10.1070/RC1989v058n04ABEH003443>.
- (16) Dugas, R. E.; Rochelle, G. T. CO<sub>2</sub> Absorption Rate into Concentrated Aqueous

Monoethanolamine and Piperazine. *J. Chem. Eng. Data* **2011**, *56* (5), 2187–2195. <https://doi.org/10.1021/je101234t>.

(17) Muresan, V.; Abrudean, M.; Valean, H.; Colosi, T.; Unguresan, M.-L.; Sita, V.; Clitan, I.; Moga, D. Neural Modeling and Control of a  $^{13}\text{C}$  Isotope Separation Process. In *2015 12th International Conference on Informatics in Control, Automation and Robotics (ICINCO)*; 2015; Vol. 01, pp 254–263.

(18) Vandewalle, T.; Vandecasteele, C. Optimisation of the Production of  $^{11}\text{C}$  by Proton Irradiation of Nitrogen Gas. *The International Journal of Applied Radiation and Isotopes* **1983**, *34* (10), 1459–1464. [https://doi.org/10.1016/0020-708X\(83\)90047-9](https://doi.org/10.1016/0020-708X(83)90047-9).

(19) Bé, M. M.; Chechev, V. P.  $^{14}\text{C}$  - Comments on Evaluation of Decay Data. [http://www.nucleide.org/DDEP\\_WG/Nuclides/C-14\\_com.pdf](http://www.nucleide.org/DDEP_WG/Nuclides/C-14_com.pdf)

(20) McCarthy, K. E. Recent Advances in the Design and Synthesis of Carbon-14 Labeled Pharmaceuticals from Small Molecule Precursors. *Current Pharmaceutical Design* **2000**, *6*(10), 1057–1083. <https://doi.org/10.2174/1381612003400029>.

(21) Kitson, S. L.; Jones, S.; Watters, W.; Chan, F.; Madge, D. Carbon-14 Radiosynthesis of 4-(5-Chloro-2-Hydroxyphenyl)-3-(2-Hydroxyethyl)-6-(Trifluoromethyl)-[4- $^{14}\text{C}$ ]Quinolin-2(1H)-One (XEN-D0401), A Novel BK Channel Activator. *J. Label. Compd. Radiopharm.* **2010**, *53* (3), 140–146. <https://doi.org/10.1002/jlcr.1740>.

(22) Riss, P. J.; Lu, S.; Telu, S.; Aigbirhio, F. I.; Pike, V. W. CuI-Catalyzed  $^{11}\text{C}$  Carboxylation of Boronic Acid Esters: A Rapid and Convenient Entry to  $^{11}\text{C}$ -Labeled Carboxylic Acids, Esters, and Amides. *Angew. Chem. Int. Ed.* **2012**, *51* (11), 2698–2702. <https://doi.org/10.1002/anie.201107263>.

(23) Rotstein, B. H.; Hooker, J. M.; Woo, J.; Collier, T. L.; Brady, T. J.; Liang, S. H.; Vasdev, N. Synthesis of [ $^{11}\text{C}$ ]Bexarotene by Cu-Mediated [ $^{11}\text{C}$ ]Carbon Dioxide Fixation and Preliminary PET Imaging. *ACS Med. Chem. Lett.* **2014**, *5* (6), 668–672. <https://doi.org/10.1021/ml500065q>.

(24) Destro, G.; Loreau, O.; Marcon, E.; Taran, F.; Cantat, T.; Audisio, D. Dynamic Carbon Isotope Exchange of Pharmaceuticals with Labeled  $\text{CO}_2$ . *J. Am. Chem. Soc.* **2019**, *141* (2), 780–784. <https://doi.org/10.1021/jacs.8b12140>.

(25) Kingston, C.; Wallace, M. A.; Allentoff, A. J.; deGruyter, J. N.; Chen, J. S.; Gong, S. X.; Bonacorsi, S.; Baran, P. S. Direct Carbon Isotope Exchange through Decarboxylative Carboxylation. *J. Am. Chem. Soc.* **2019**, *141* (2), 774–779. <https://doi.org/10.1021/jacs.8b12035>.

(26) Destro, G.; Horkka, K.; Loreau, O.; Buisson, D.-A.; Kingston, L.; Vecchio, A. D.; Schou, M.; Elmore, C. S.; Taran, F.; Cantat, T.; Audisio, D. Transition-Metal-Free Carbon Isotope Exchange of Phenyl Acetic Acids. *Angew. Chem. Int. Ed. ASAP*. <https://doi.org/10.1002/anie.202002341>.

(27) Kong, D.; Moon, P. J.; Lui, E. K. J.; Bsharat, O.; Lundgren, R. J. Direct Reversible Decarboxylation from Stable Organic Acids in Dimethylformamide Solution. *Science* **2020**, eabb4129. <https://doi.org/10.1126/science.abb4129>.

(28) Yan, M.; Lo, J. C.; Edwards, J. T.; Baran, P. S. Radicals: Reactive Intermediates with Translational Potential. *J. Am. Chem. Soc.* **2016**, *138* (39), 12692–12714. <https://doi.org/10.1021/jacs.6b08856>.

(29) Kaga, A.; Chiba, S. Engaging Radicals in Transition Metal-Catalyzed Cross-Coupling with Alkyl Electrophiles: Recent Advances. *ACS Catal.* **2017**, *7* (7), 4697–4706. <https://doi.org/10.1021/acscatal.7b01405>.

(30) Sandfort, F.; O'Neill, M. J.; Cornella, J.; Wimmer, L.; Baran, P. S. Alkyl-(Hetero)Aryl Bond Formation via Decarboxylative Cross-Coupling: A Systematic Analysis. *Angew. Chem.*

*Int. Ed.* **2017**, *56* (12), 3319–3323. <https://doi.org/10.1002/anie.201612314>.

(31) Murarka, S. N-(Acyloxy)Phthalimides as Redox-Active Esters in Cross-Coupling Reactions. *Adv. Synth. Cat.* **2018**, *360* (9), 1735–1753. <https://doi.org/10.1002/adsc.201701615>.

(32) Wang, Z.; Zhu, L.; Yin, F.; Su, Z.; Li, Z.; Li, C. Silver-Catalyzed Decarboxylative Chlorination of Aliphatic Carboxylic Acids. *J. Am. Chem. Soc.* **2012**, *134* (9), 4258–4263. <https://doi.org/10.1021/ja210361z>.

(33) Tan, X.; Song, T.; Wang, Z.; Chen, H.; Cui, L.; Li, C. Silver-Catalyzed Decarboxylative Bromination of Aliphatic Carboxylic Acids. *Org. Lett.* **2017**, *19* (7), 1634–1637. <https://doi.org/10.1021/acs.orglett.7b00439>.

(34) Perry, G. J. P.; Quibell, J. M.; Panigrahi, A.; Larrosa, I. Transition-Metal-Free Decarboxylative Iodination: New Routes for Decarboxylative Oxidative Cross-Couplings. *J. Am. Chem. Soc.* **2017**, *139* (33), 11527–11536. <https://doi.org/10.1021/jacs.7b05155>.

(35) Quibell, J. M.; Perry, G. J. P.; Cannas, D. M.; Larrosa, I. Transition-Metal-Free Decarboxylative Bromination of Aromatic Carboxylic Acids. *Chem. Sci.* **2018**, *9* (15), 3860–3865. <https://doi.org/10.1039/C8SC01016A>.

(36) Tlahuext-Aca, A.; Garza-Sanchez, R. A.; Glorius, F. Multicomponent Oxyalkylation of Styrenes Enabled by Hydrogen-Bond-Assisted Photoinduced Electron Transfer. *Angew. Chem. Int. Ed.* **2017**, *56* (13), 3708–3711. <https://doi.org/10.1002/anie.201700049>.

(37) Juliá-Hernández, F.; Moragas, T.; Cornella, J.; Martin, R. Remote Carboxylation of Halogenated Aliphatic Hydrocarbons with Carbon Dioxide. *Nature* **2017**, *545* (7652), 84–88. <https://doi.org/10.1038/nature22316>.

(38) Sahoo, B.; Bellotti, P.; Juliá-Hernández, F.; Meng, Q.-Y.; Crespi, S.; König, B.; Martin, R. Site-Selective, Remote Sp<sup>3</sup> C–H Carboxylation Enabled by the Merger of Photoredox and Nickel Catalysis. *Chem. Eur. J.* **2019**, *25* (38), 9001–9005. <https://doi.org/10.1002/chem.201902095>.

(39) KRÖHNKE, F. The Specific Synthesis of Pyridines and Oligopyridines. *Synthesis* **1976**, *1976* (1), 1–24. <https://doi.org/10.1055/s-1976-23941>.

(40) Mukkala, V.-M.; Kankare, J. J. New 2,2'-Bipyridine Derivatives and Their Luminescence Properties with Europium(III) and Terbium(III) Ions. *Helvetica Chimica Acta* **1992**, *75* (5), 1578–1592. <https://doi.org/10.1002/hlca.19920750512>.

(41) Pratsch, G.; Lackner, G. L.; Overman, L. E. Constructing Quaternary Carbons from N-(Acyloxy)Phthalimide Precursors of Tertiary Radicals Using Visible-Light Photocatalysis. *J. Org. Chem.* **2015**, *80* (12), 6025–6036. <https://doi.org/10.1021/acs.joc.5b00795>.

(42) Xu, X.; Sun, J.; Lin, Y.; Cheng, J.; Li, P.; Yan, Y.; Shuai, Q.; Xie, Y. Copper Nitrate-Catalyzed Oxidative Coupling of Unactivated C(Sp<sup>3</sup>)-H Bonds of Ethers and Alkanes with N-Hydroxyphthalimide: Synthesis of N-Hydroxyimide Esters. *Org. Biomol. Chem.* **2017**, *15* (46), 9875–9879. <https://doi.org/10.1039/C7OB02249B>.

(43) Judd, K. E.; Mahon, M. F.; Caggiano, L. Efficient Synthesis of Tetrahydro-β-Carbolin-1-One and Dihydroisoquinolin-1-One Derivatives as Versatile Intermediates. *Synthesis* **2009**, *2009* (16), 2809–2817. <https://doi.org/10.1055/s-0029-1216904>.

(44) Hu, D.; Wang, L.; Li, P. Decarboxylative Borylation of Aliphatic Esters under Visible-Light Photoredox Conditions. *Org. Lett.* **2017**, *19* (10), 2770–2773. <https://doi.org/10.1021/acs.orglett.7b01181>.

(45) Zhao, W.; Wurz, R. P.; Peters, J. C.; Fu, G. C. Photoinduced, Copper-Catalyzed Decarboxylative C–N Coupling to Generate Protected Amines: An Alternative to the Curtius Rearrangement. *J. Am. Chem. Soc.* **2017**, *139* (35), 12153–12156. <https://doi.org/10.1021/jacs.7b07546>.



- (46) Yu, L.; Tang, M.-L.; Si, C.-M.; Meng, Z.; Liang, Y.; Han, J.; Sun, X. Zinc-Mediated Decarboxylative Alkylation of Gem-Difluoroalkenes. *Org. Lett.* **2018**, *20* (15), 4579–4583. <https://doi.org/10.1021/acs.orglett.8b01866>.
- (47) Baran, P.; Li, C.; Wang, J.; Chatterjee, A. K.; Kumar, M.; Yu, S.; Johnson, K. A.; Qin, T.; Shang, M. Cu- and Ni-Catalyzed Decarboxylative Borylation Reactions. WO2018175173A1, September 27, 2018.
- (48) Candish, L.; Standley, E. A.; Gómez-Suárez, A.; Mukherjee, S.; Glorius, F. Catalytic Access to Alkyl Bromides, Chlorides and Iodides via Visible Light-Promoted Decarboxylative Halogenation. *Chem. Eur. J.* **2016**, *22* (29), 9971–9974. <https://doi.org/10.1002/chem.201602251>.
- (49) Börjesson, M.; Moragas, T.; Martin, R. Ni-Catalyzed Carboxylation of Unactivated Alkyl Chlorides with CO<sub>2</sub>. *J. Am. Chem. Soc.* **2016**, *138* (24), 7504–7507. <https://doi.org/10.1021/jacs.6b04088>.
- (50) León, T.; Correa, A.; Martin, R. Ni-Catalyzed Direct Carboxylation of Benzyl Halides with CO<sub>2</sub>. *J. Am. Chem. Soc.* **2013**, *135* (4), 1221–1224. <https://doi.org/10.1021/ja311045f>.
- (51) Montoro, R.; Wirth, T. Direct Bromination and Iodination of Non-Activated Alkanes by Hypohalite Reagents. *Synthesis* **2005**, *2005* (9), 1473–1478. <https://doi.org/10.1055/s-2005-865322>.
- (52) Dai, C.; Narayanam, J. M. R.; Stephenson, C. R. J. Visible-Light-Mediated Conversion of Alcohols to Halides. *Nature Chemistry* **2011**, *3* (2), 140–145. <https://doi.org/10.1038/nchem.949>.



**$^1\text{H}$  NMR,  $^{13}\text{C}$  NMR and  $^{19}\text{F}$  NMR spectra**



# Catalytic Decarboxylation/Carboxylation Platform for Accessing Isotopically Labeled Carboxylic Acids

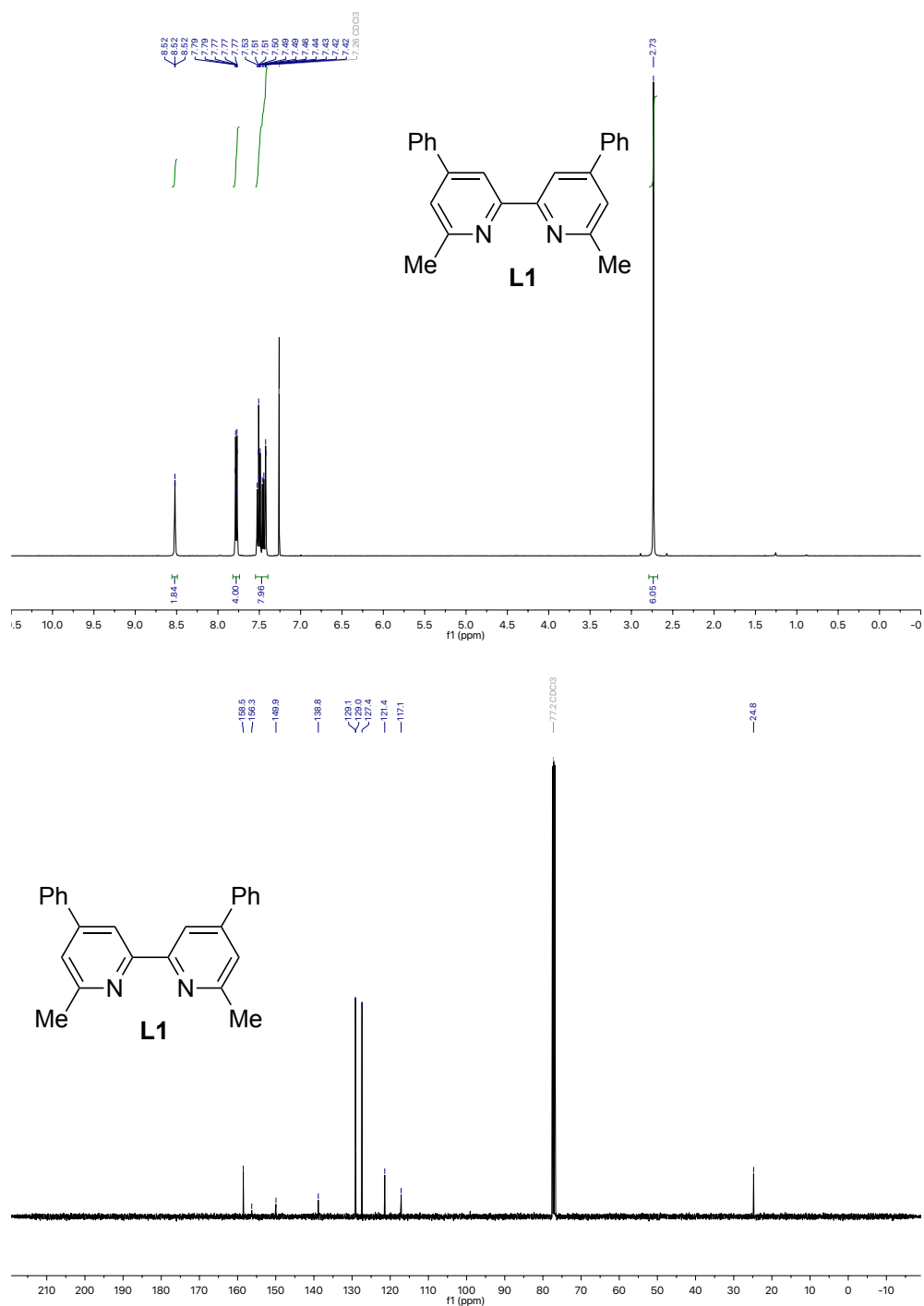


Figure 6.  $^1\text{H}$  and  $^{13}\text{C}$  NMR spectra of **L1**.

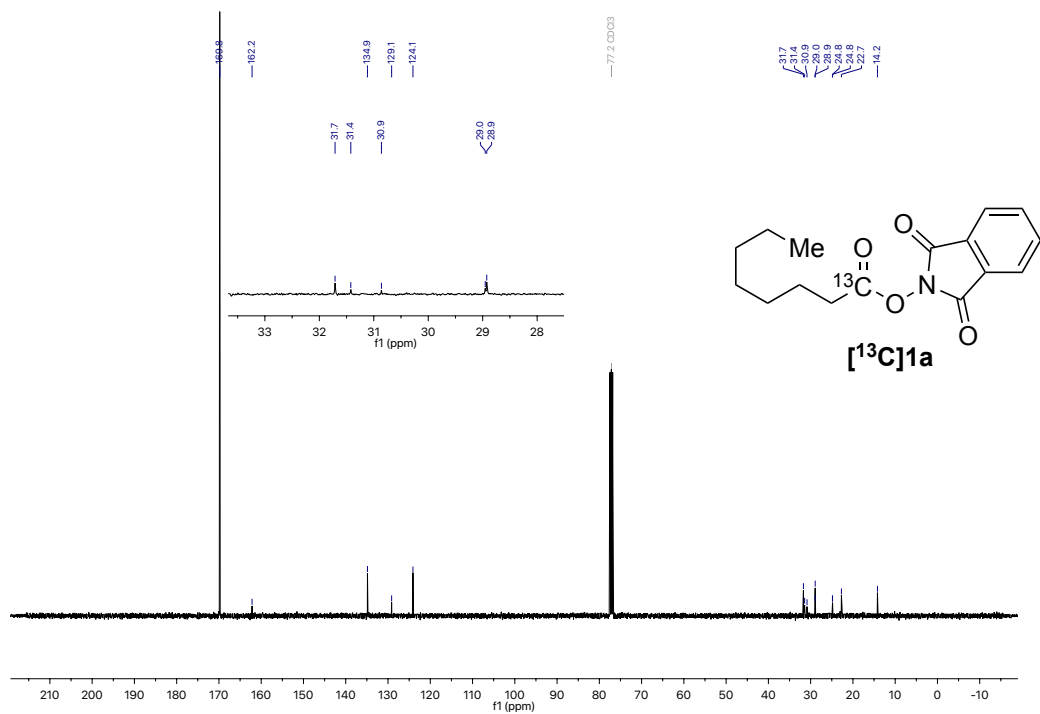
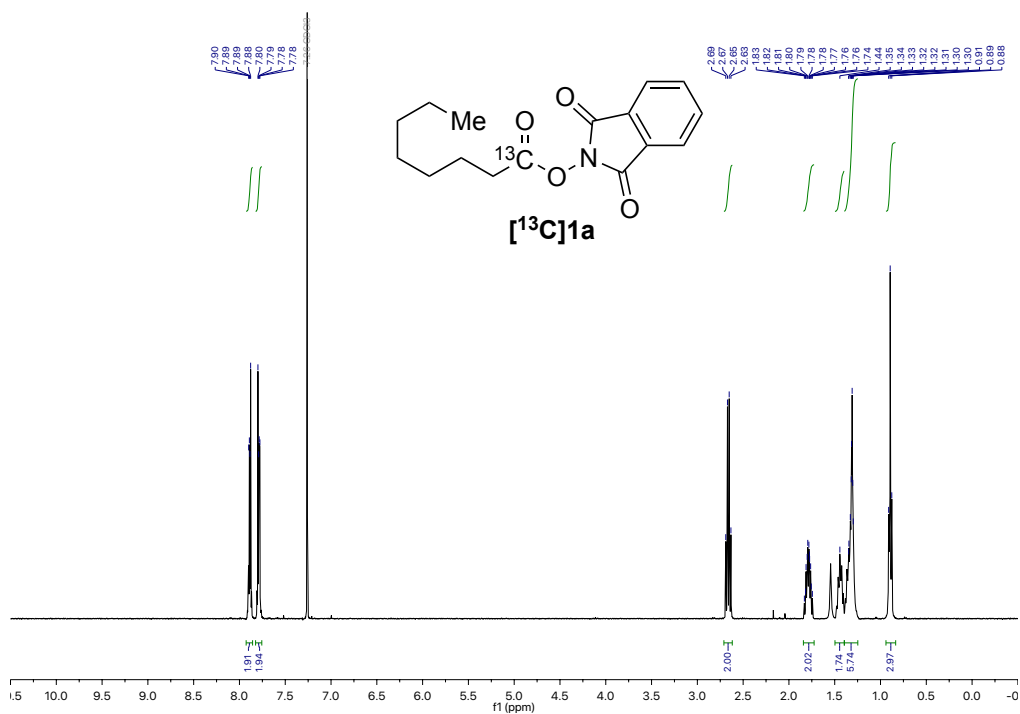


Figure 7. <sup>1</sup>H and <sup>13</sup>C NMR spectra of [13C]1a.

# Catalytic Decarboxylation/Carboxylation Platform for Accessing Isotopically Labeled Carboxylic Acids

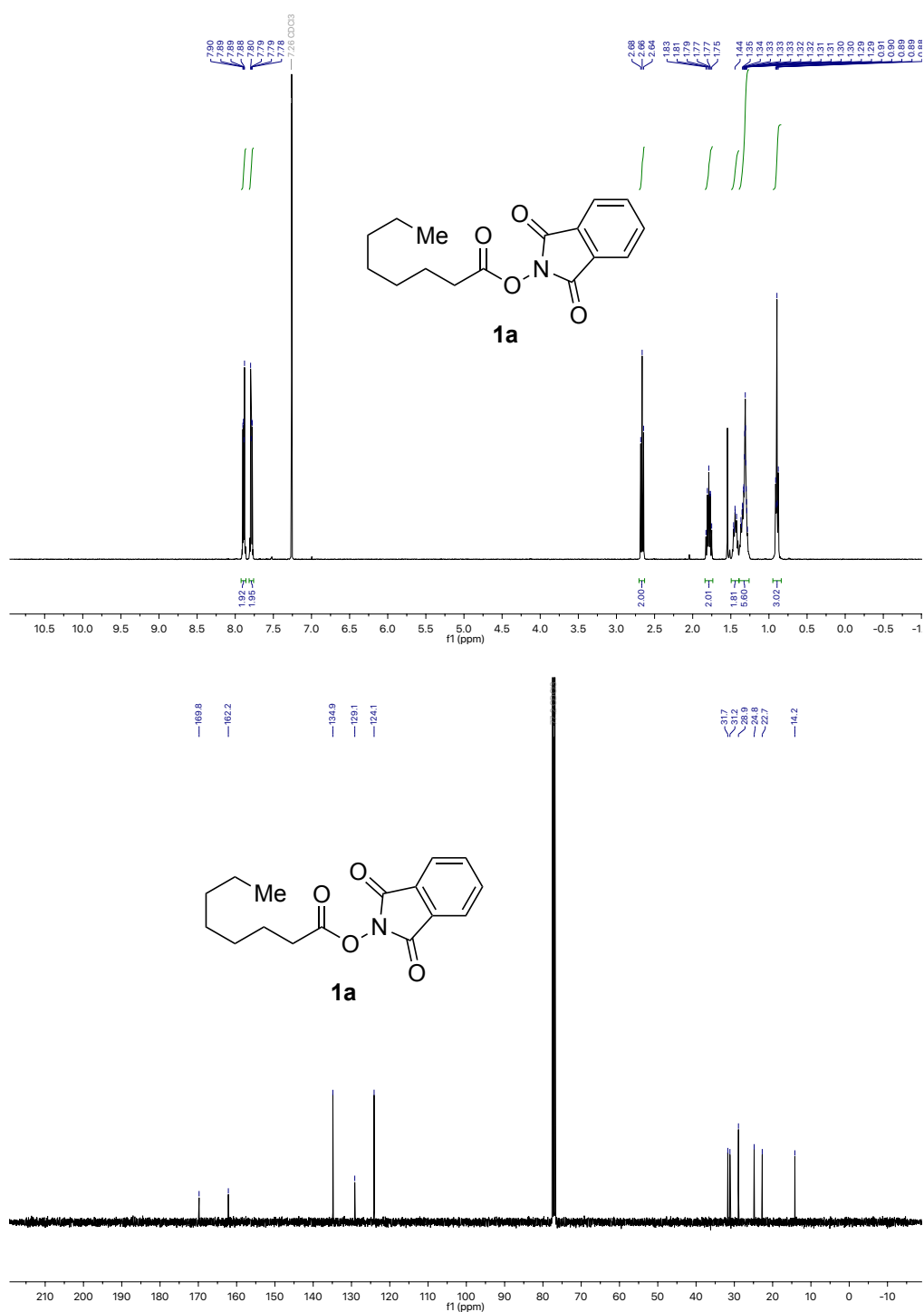
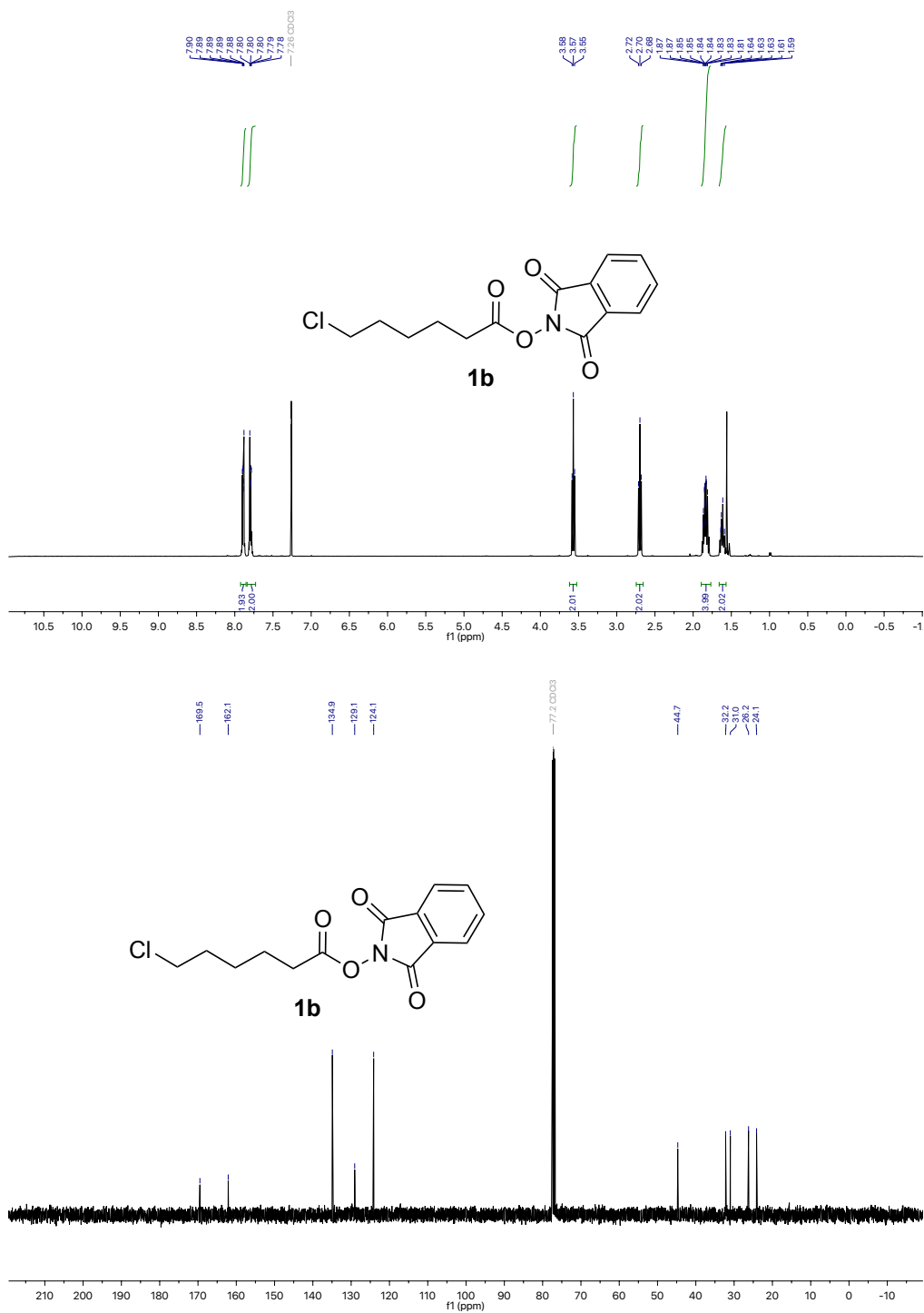


Figure 8.  $^1\text{H}$  and  $^{13}\text{C}$  NMR spectra of **1a**.

Figure 9. <sup>1</sup>H and <sup>13</sup>C NMR spectra of **1b**.



# Catalytic Decarboxylation/Carboxylation Platform for Accessing Isotopically Labeled Carboxylic Acids

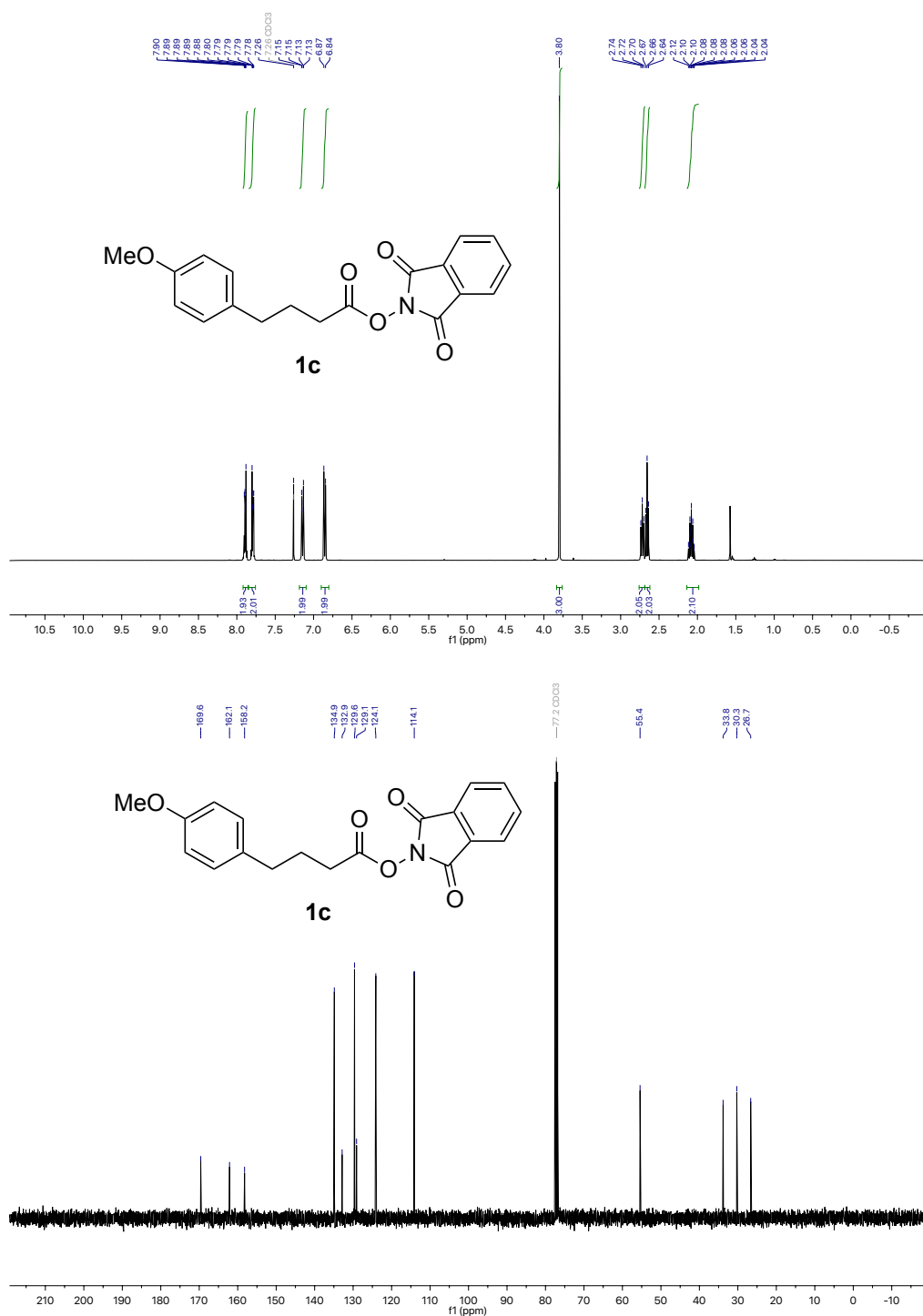


Figure 10. <sup>1</sup>H and <sup>13</sup>C NMR spectra of **1c**.

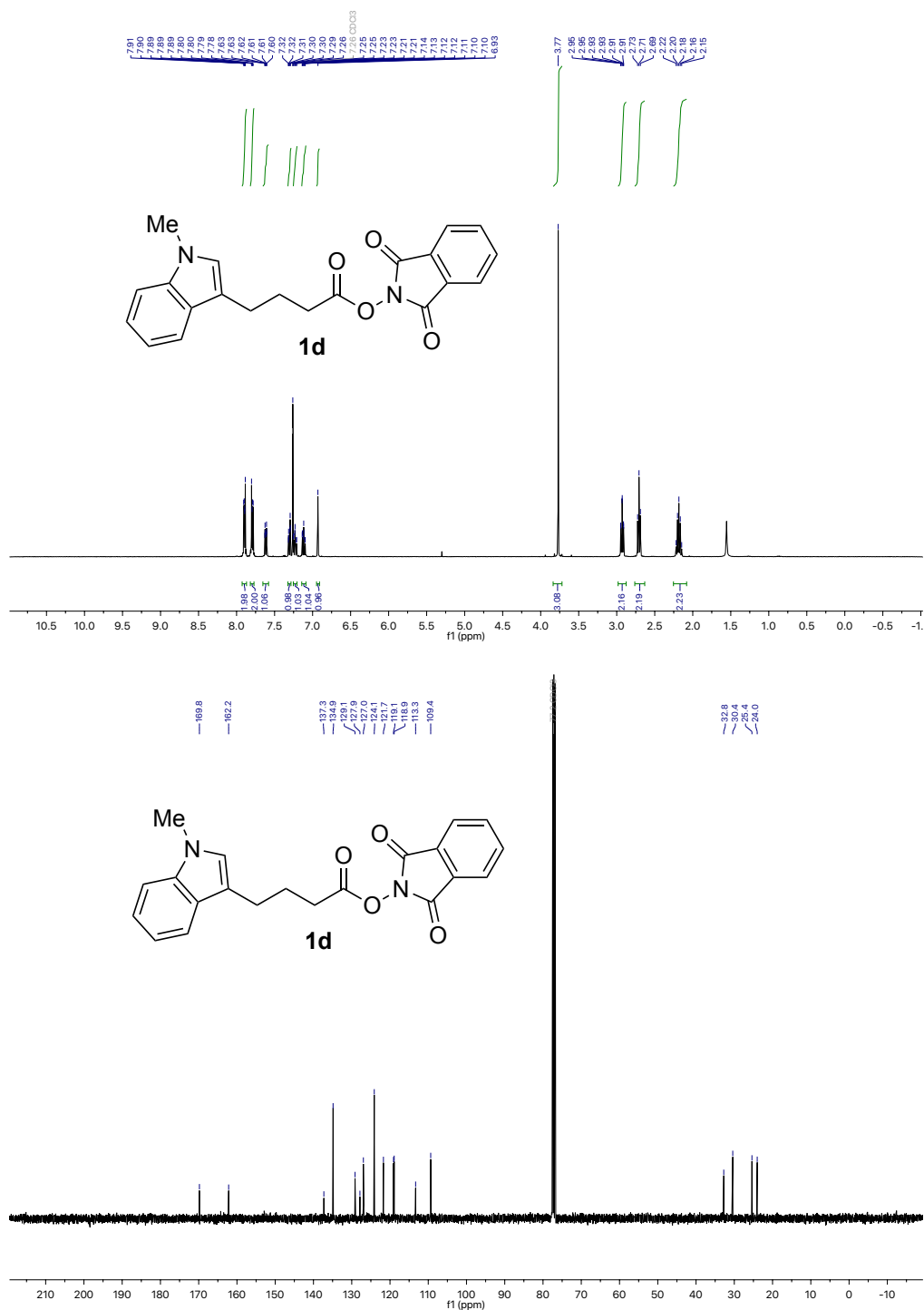


Figure 11.  $^1\text{H}$  and  $^{13}\text{C}$  NMR spectra of **1d**.

# Catalytic Decarboxylation/Carboxylation Platform for Accessing Isotopically Labeled Carboxylic Acids

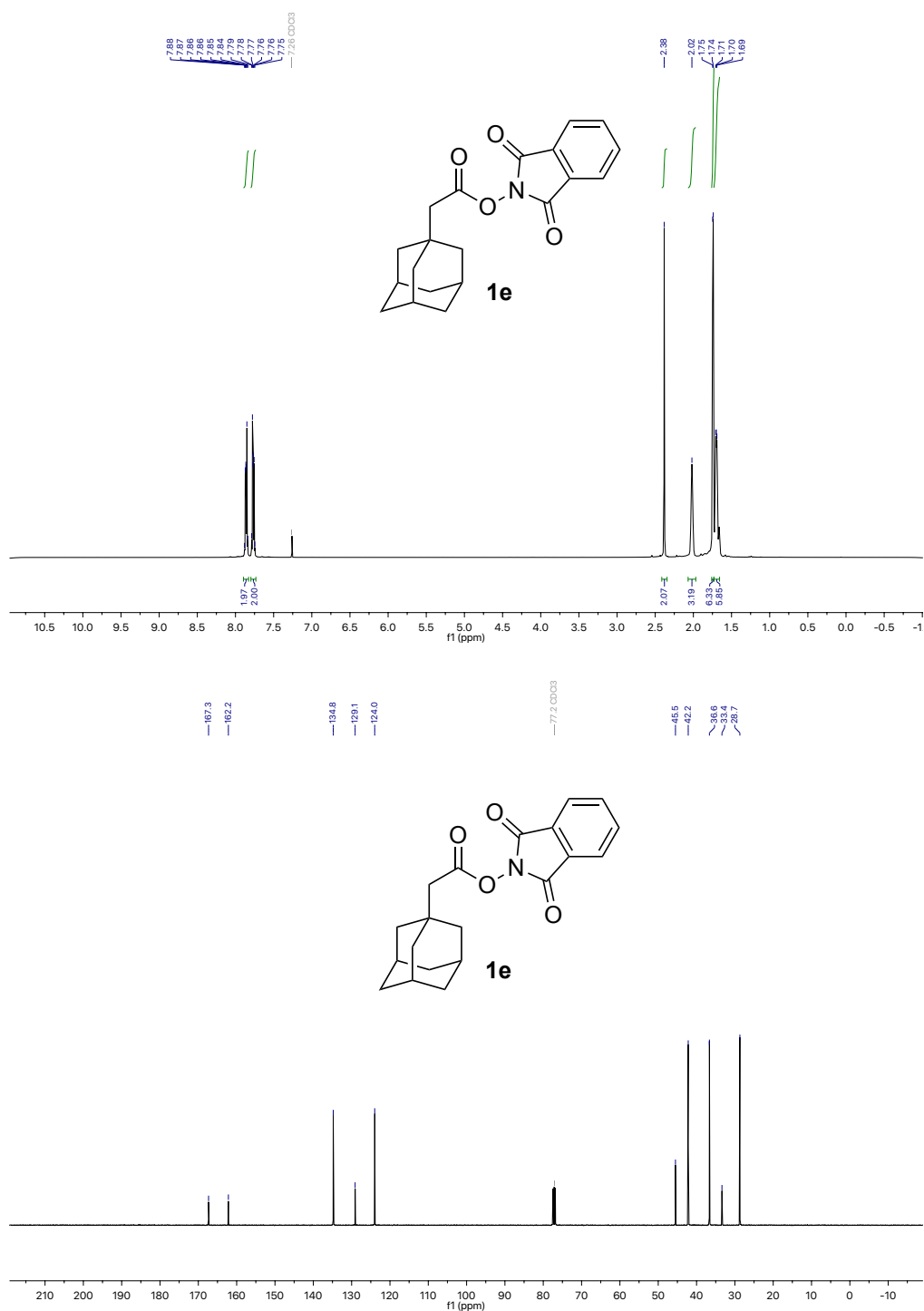


Figure 12. <sup>1</sup>H and <sup>13</sup>C NMR spectra of **1e**.

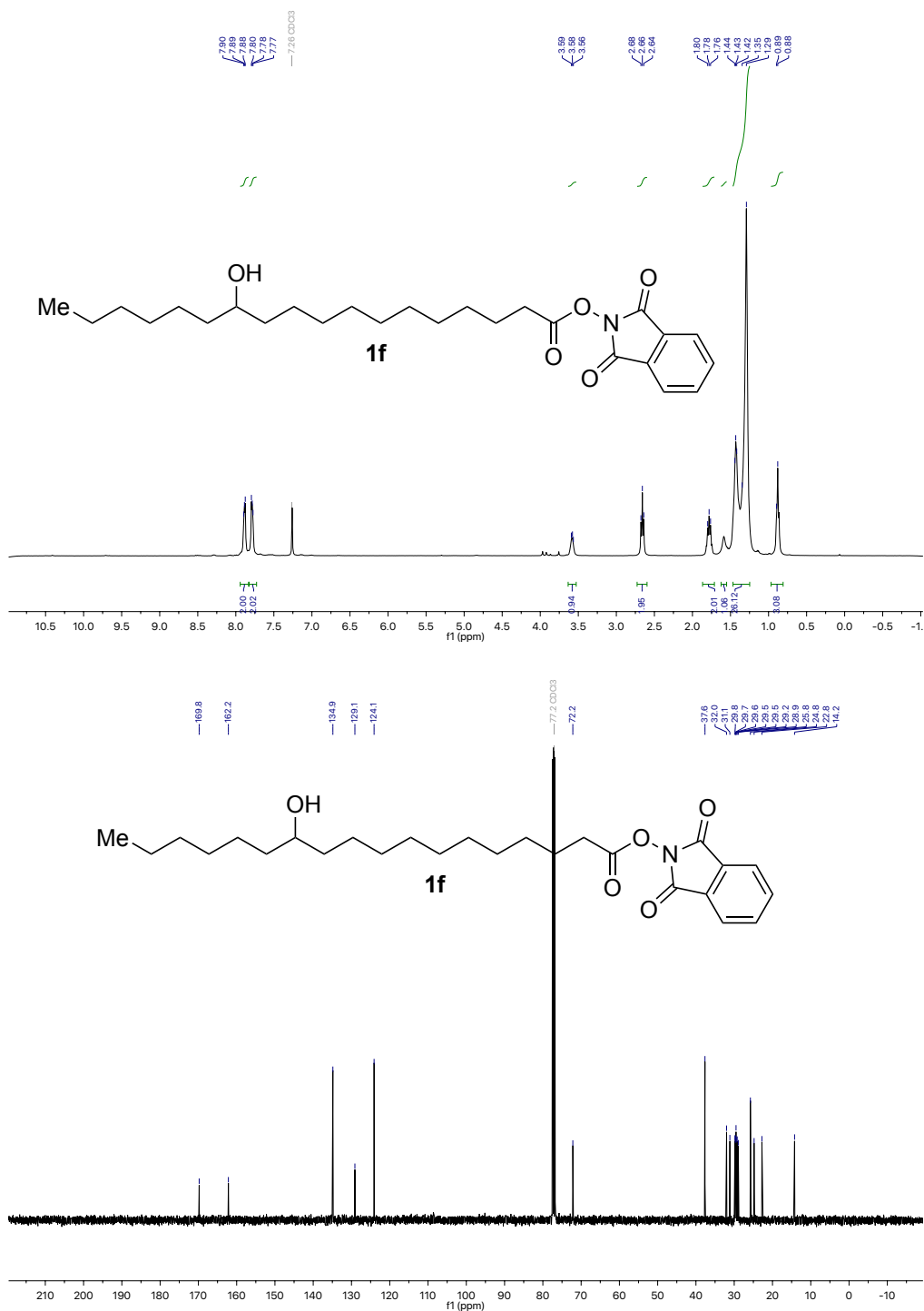


Figure 13. <sup>1</sup>H and <sup>13</sup>C NMR spectra of **1f**.

# Catalytic Decarboxylation/Carboxylation Platform for Accessing Isotopically Labeled Carboxylic Acids

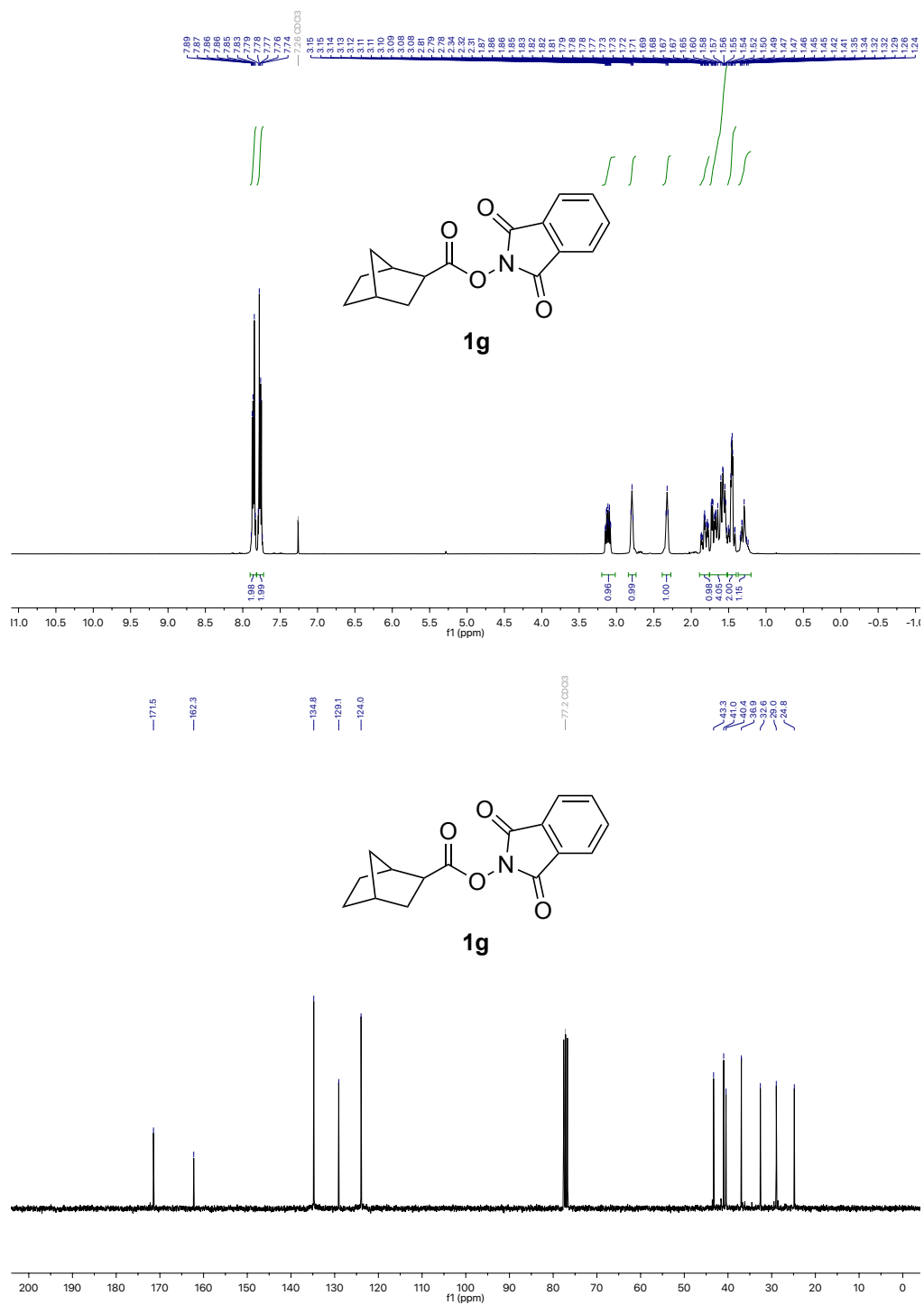
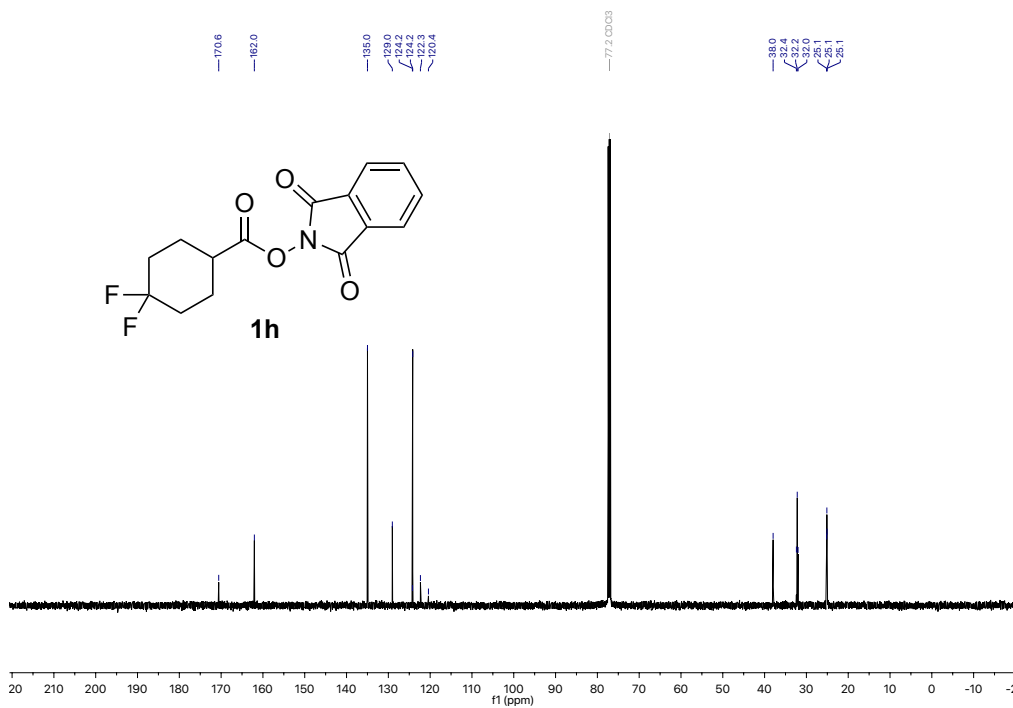
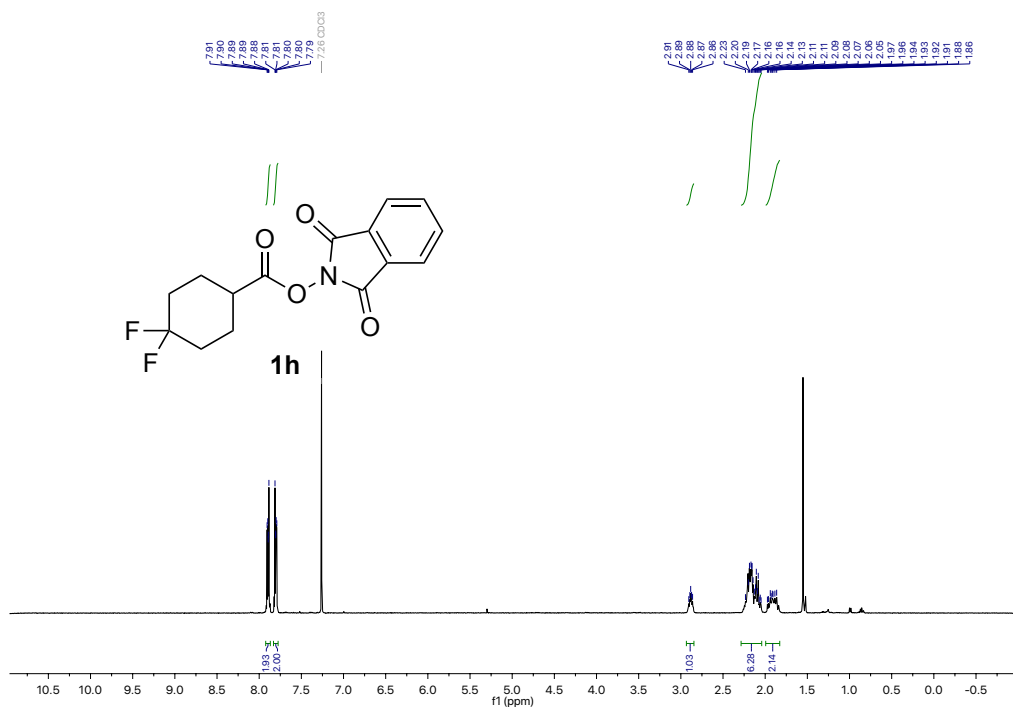


Figure 14.  $^1\text{H}$  and  $^{13}\text{C}$  NMR spectra of **1g**.

Chapter 4



Catalytic Decarboxylation/Carboxylation Platform for Accessing Isotopically Labeled Carboxylic Acids

85.14  
85.77  
87.89  
88.54

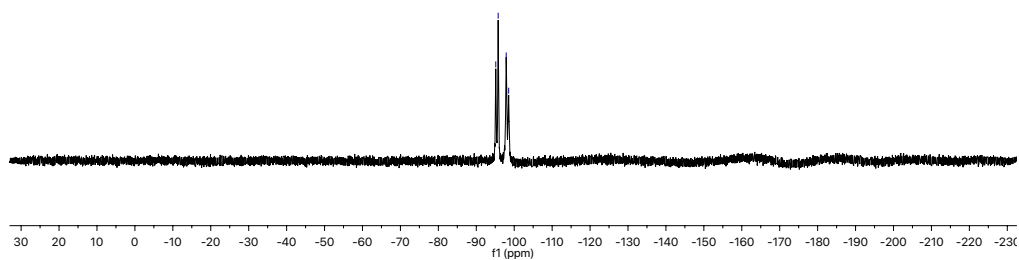
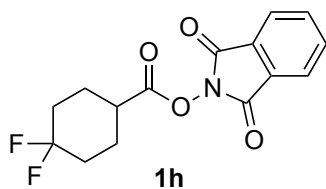
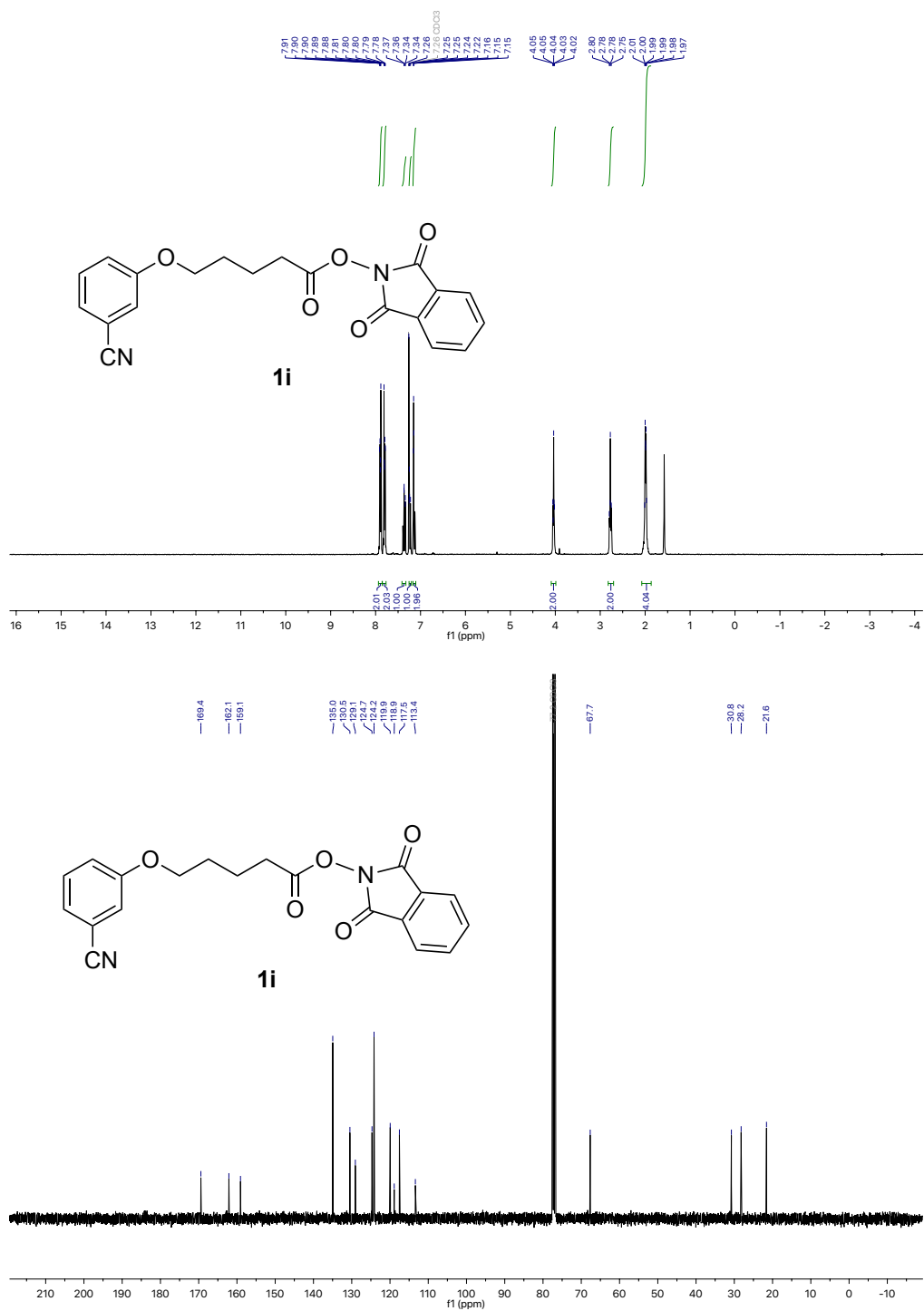


Figure 15.  $^1\text{H}$ ,  $^{13}\text{C}$  and  $^{19}\text{F}$  NMR spectra of **1h**.

Figure 16. <sup>1</sup>H and <sup>13</sup>C NMR spectra of **1i**.





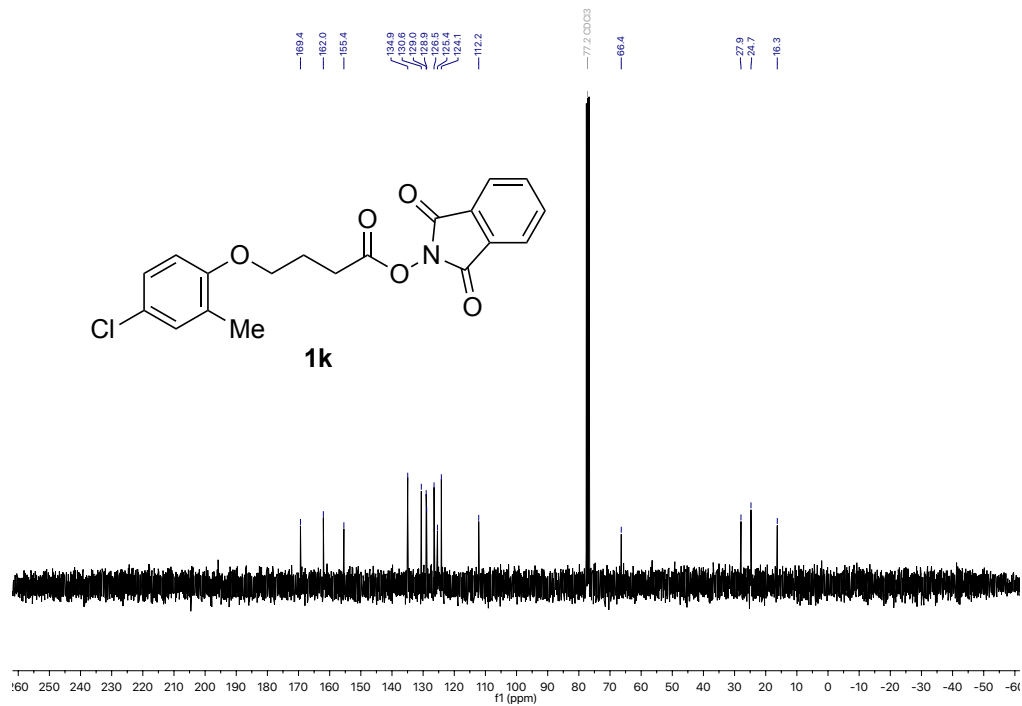
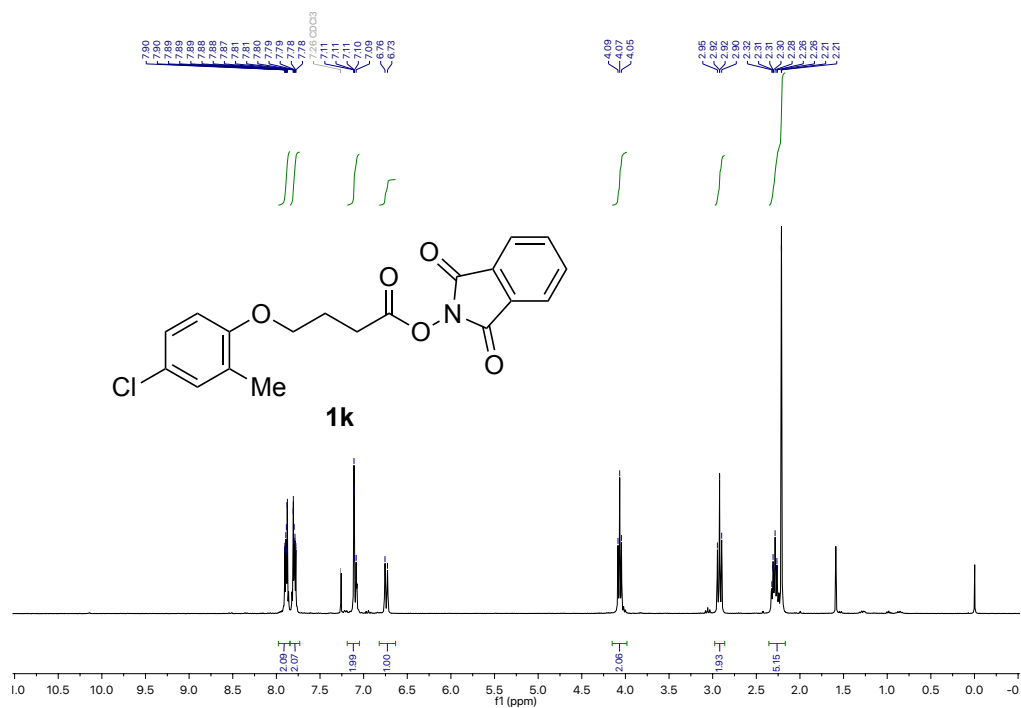


Figure 18. <sup>1</sup>H and <sup>13</sup>C NMR spectra of **1k**.

# Catalytic Decarboxylation/Carboxylation Platform for Accessing Isotopically Labeled Carboxylic Acids

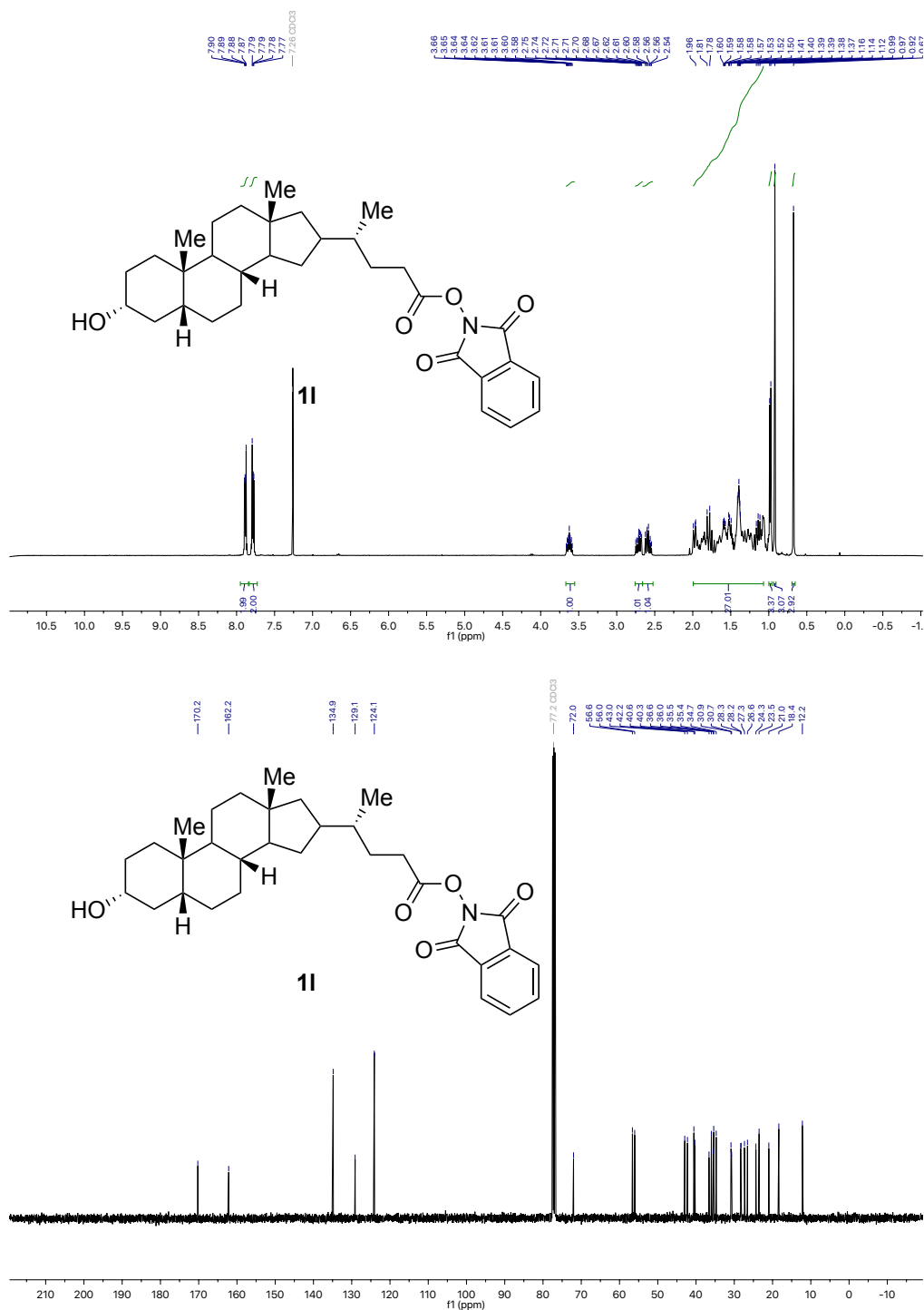


Figure 19. <sup>1</sup>H and <sup>13</sup>C NMR spectra of **11**.





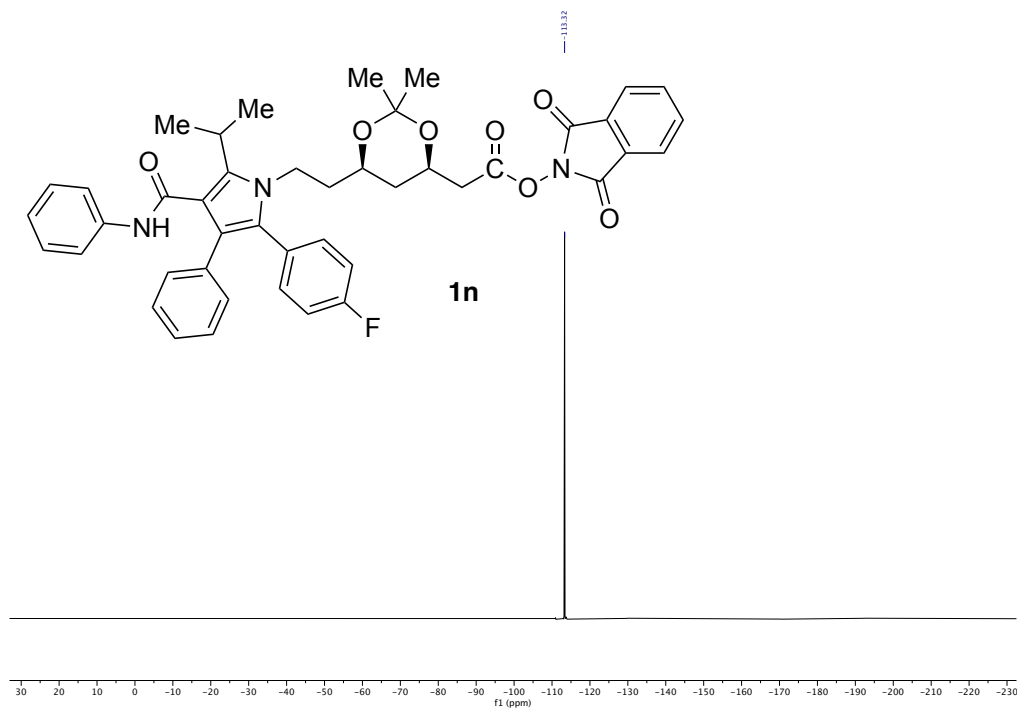


Figure 21.  $^1\text{H}$ ,  $^{13}\text{C}$  and  $^{19}\text{F}$  NMR spectra of **1n**.

# Catalytic Decarboxylation/Carboxylation Platform for Accessing Isotopically Labeled Carboxylic Acids

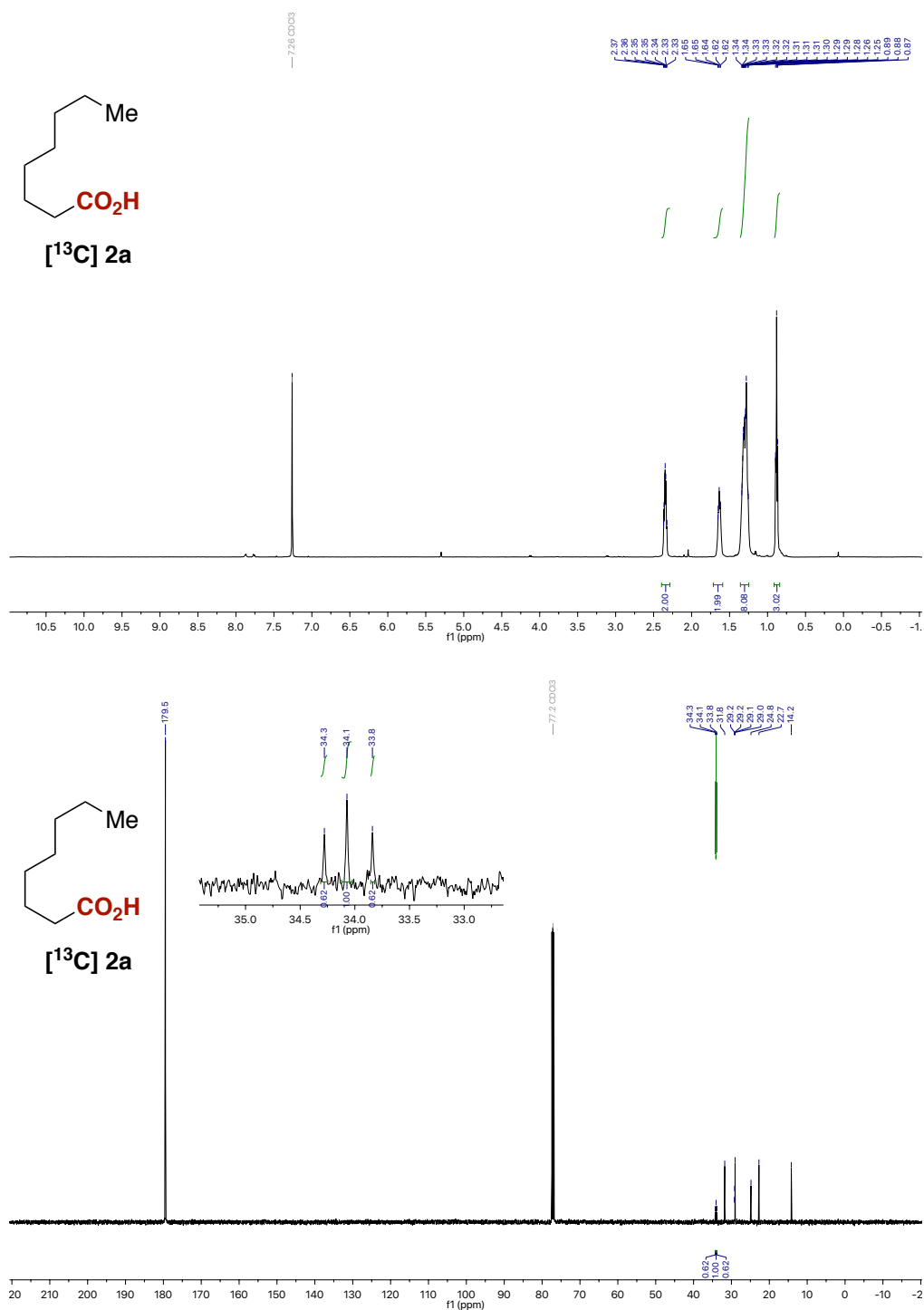


Figure 22. <sup>1</sup>H and <sup>13</sup>C NMR spectra of [<sup>13</sup>C]2a.

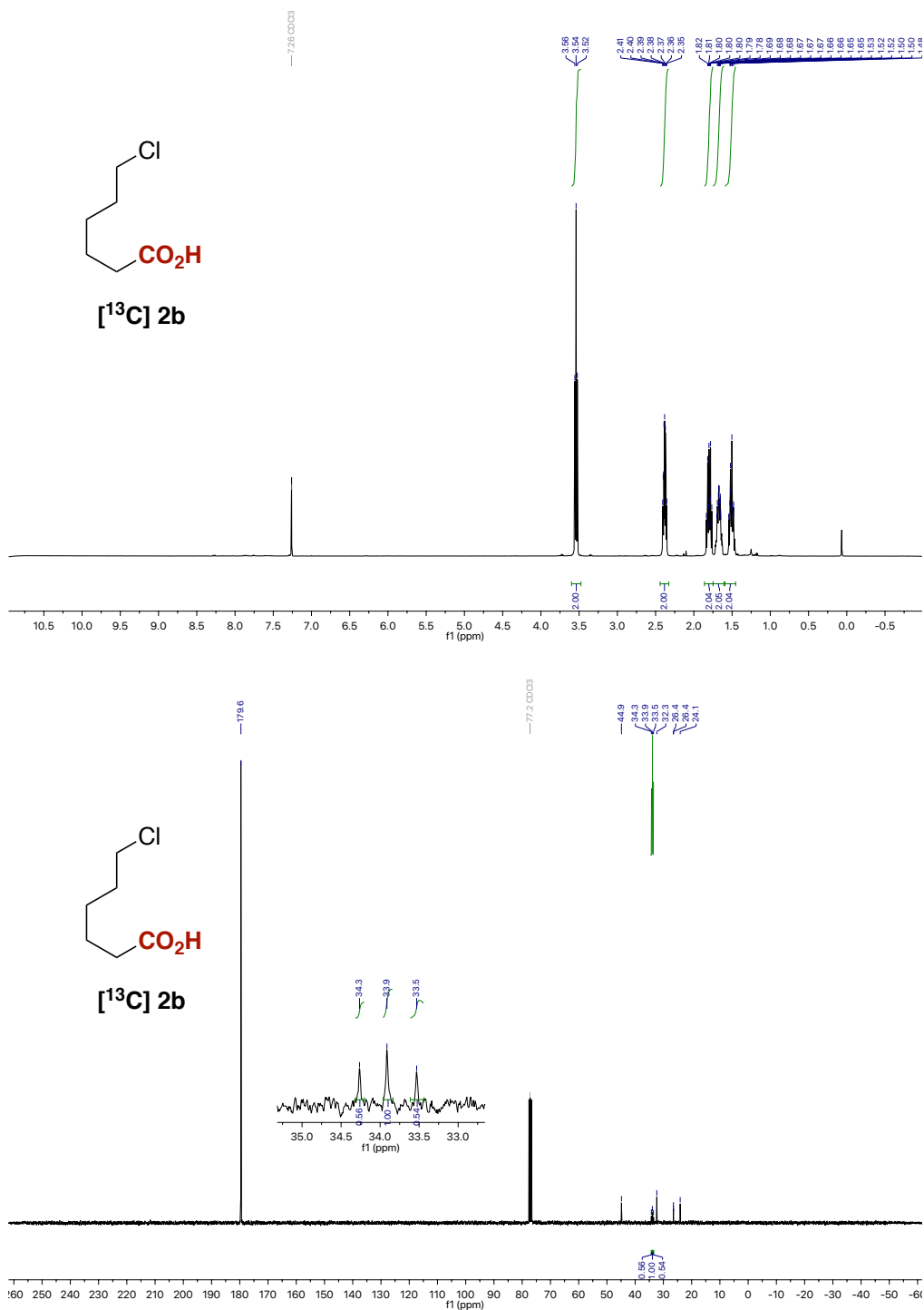


Figure 23. <sup>1</sup>H and <sup>13</sup>C NMR spectra of [<sup>13</sup>C]2b.



# Catalytic Decarboxylation/Carboxylation Platform for Accessing Isotopically Labeled Carboxylic Acids

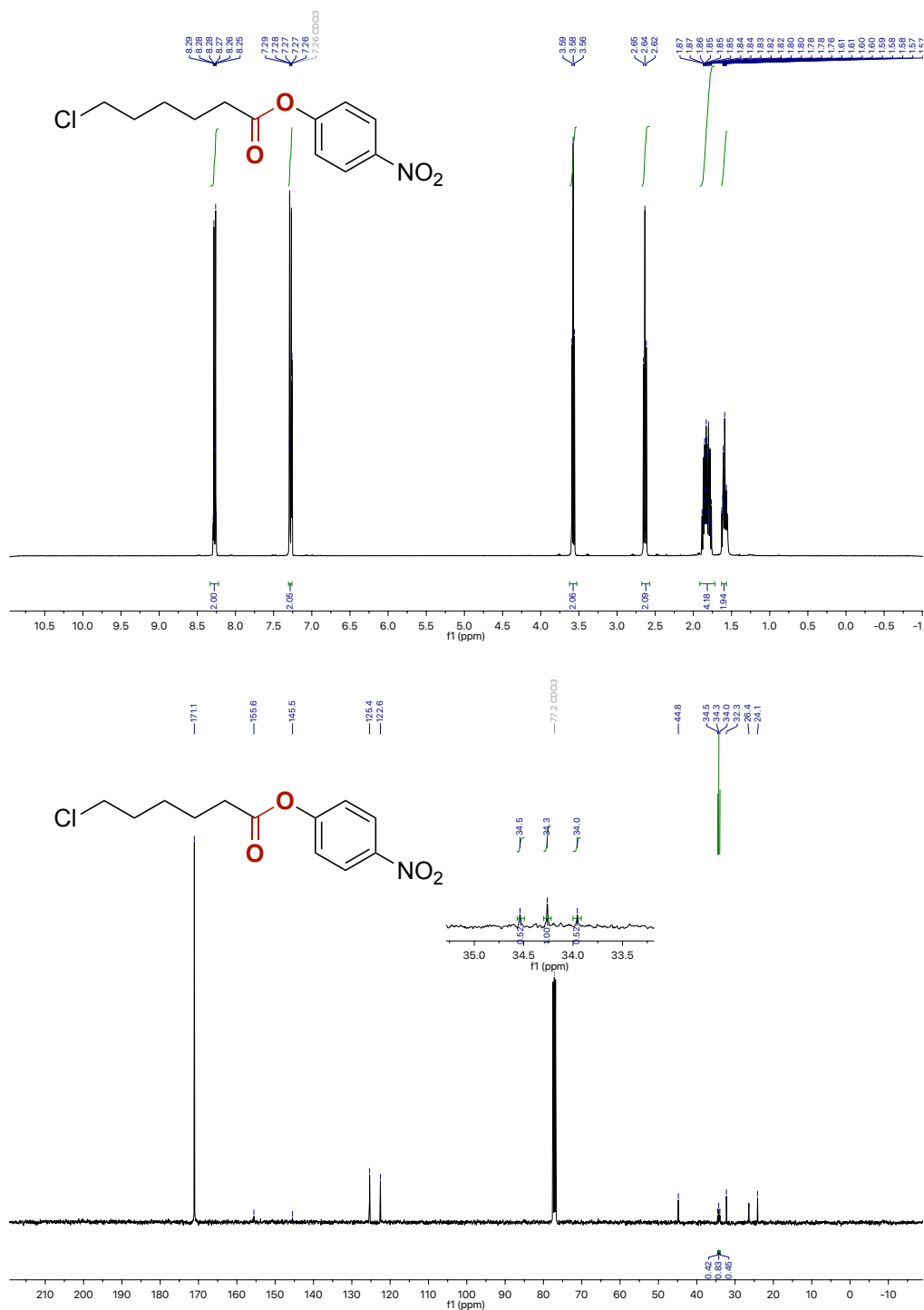
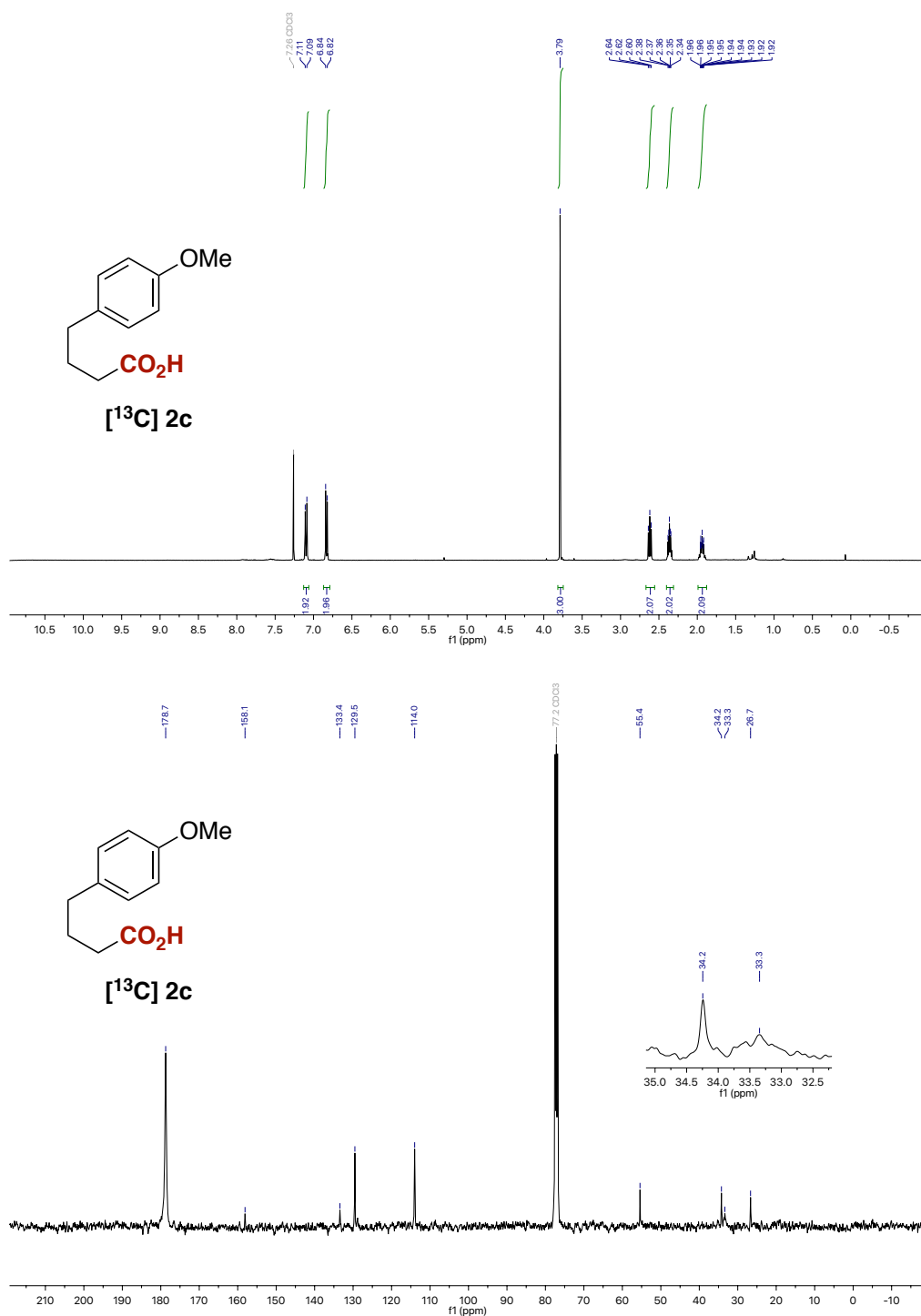


Figure 24.  $^1\text{H}$  and  $^{13}\text{C}$  NMR spectra of  $[^{13}\text{C}]2\text{b-ester}$ .

Figure 25. <sup>1</sup>H and <sup>13</sup>C NMR spectra of [<sup>13</sup>C]2c.

# Catalytic Decarboxylation/Carboxylation Platform for Accessing Isotopically Labeled Carboxylic Acids

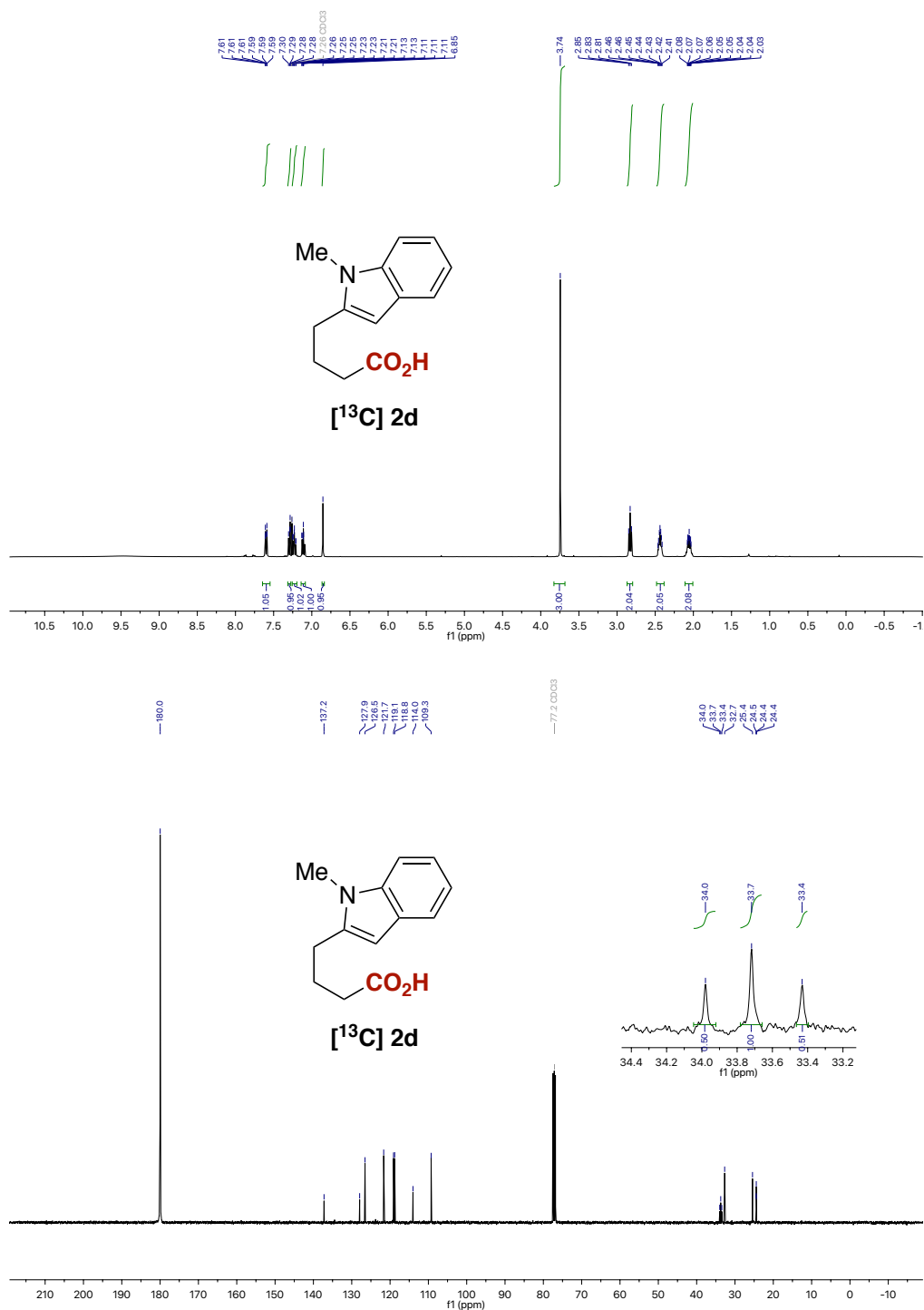


Figure 26.  $^1\text{H}$  and  $^{13}\text{C}$  NMR spectra of  $[^{13}\text{C}]$  2d.

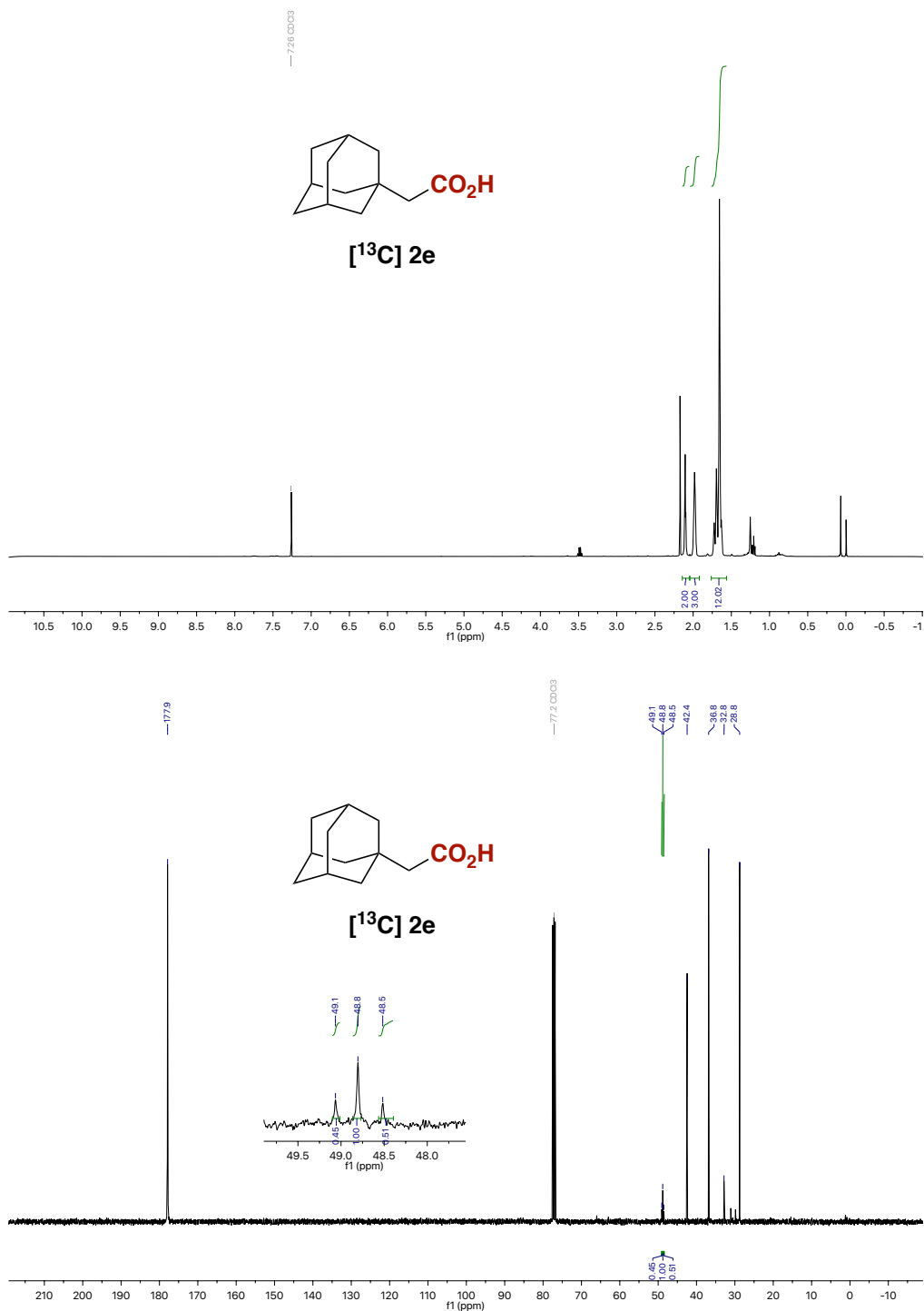


Figure 27. <sup>1</sup>H and <sup>13</sup>C NMR spectra of [13C] 2e.

Catalytic Decarboxylation/Carboxylation Platform for Accessing Isotopically Labeled Carboxylic Acids

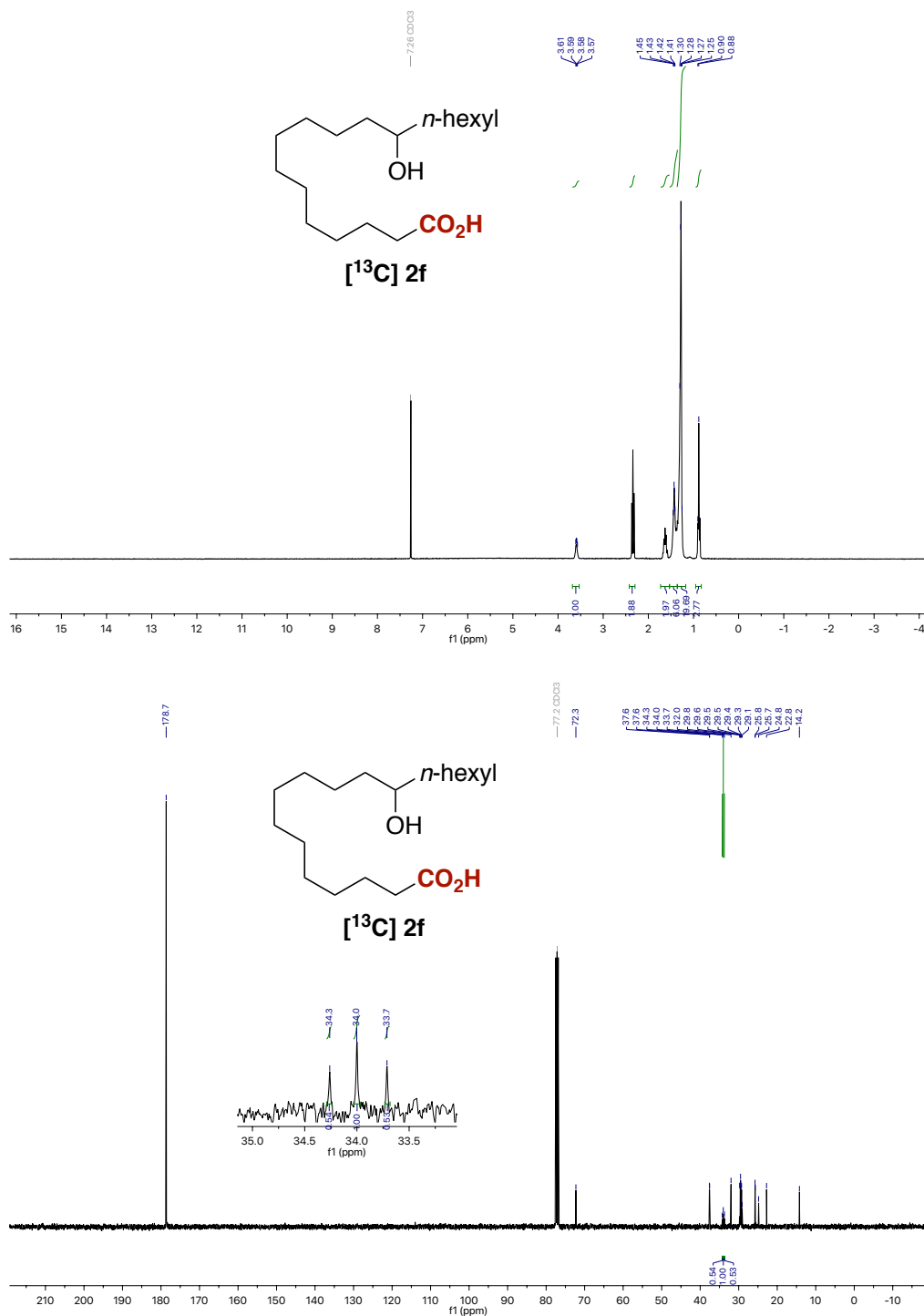


Figure 28.  $^1\text{H}$  and  $^{13}\text{C}$  NMR spectra of  $^{13}\text{C}$  2f.

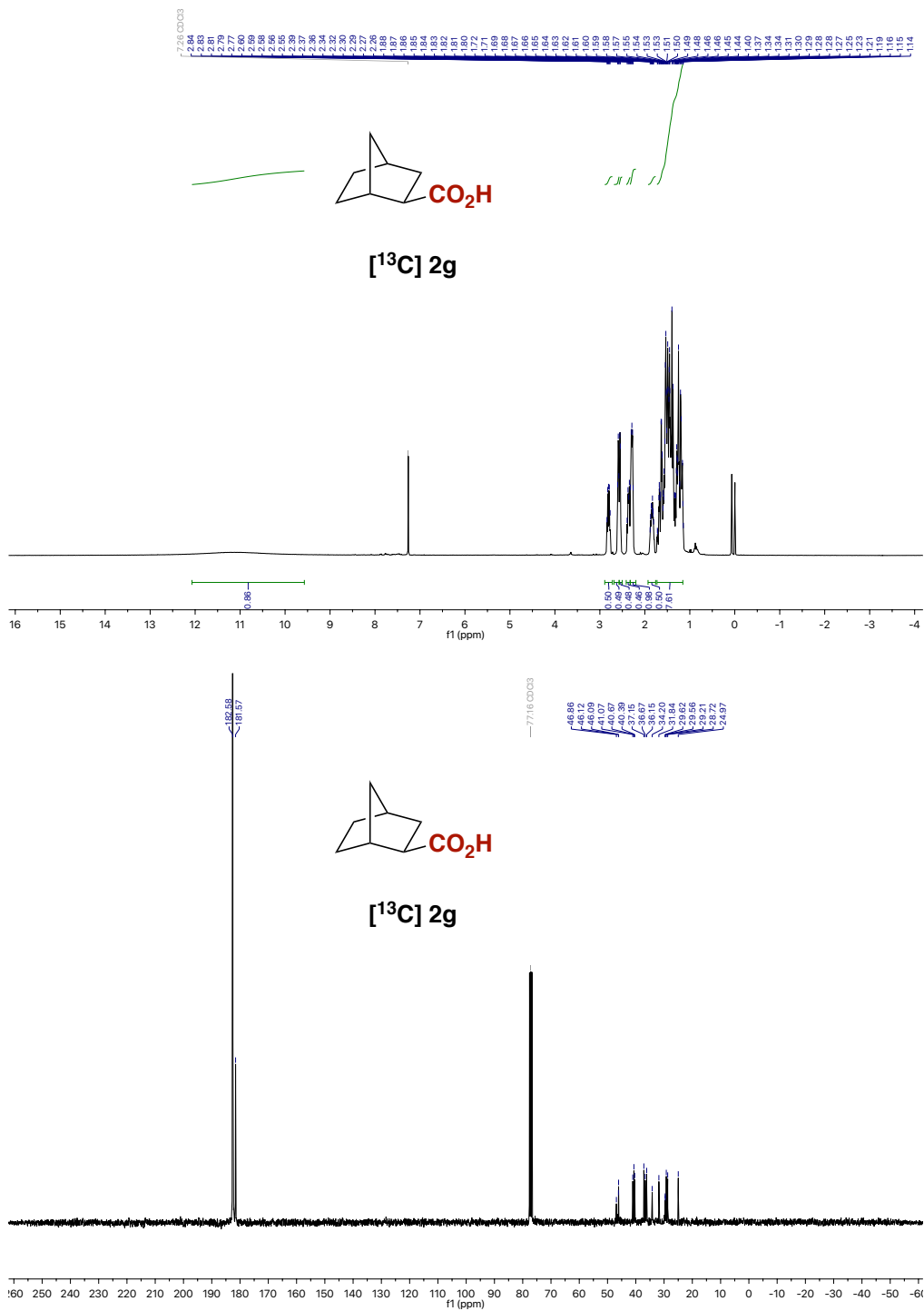
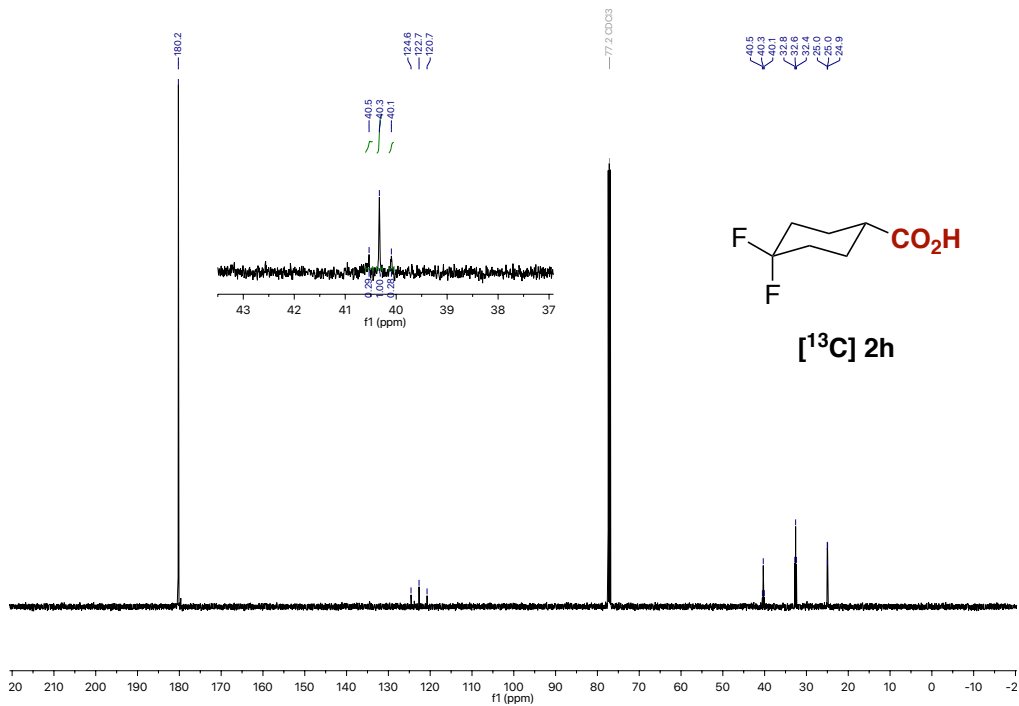
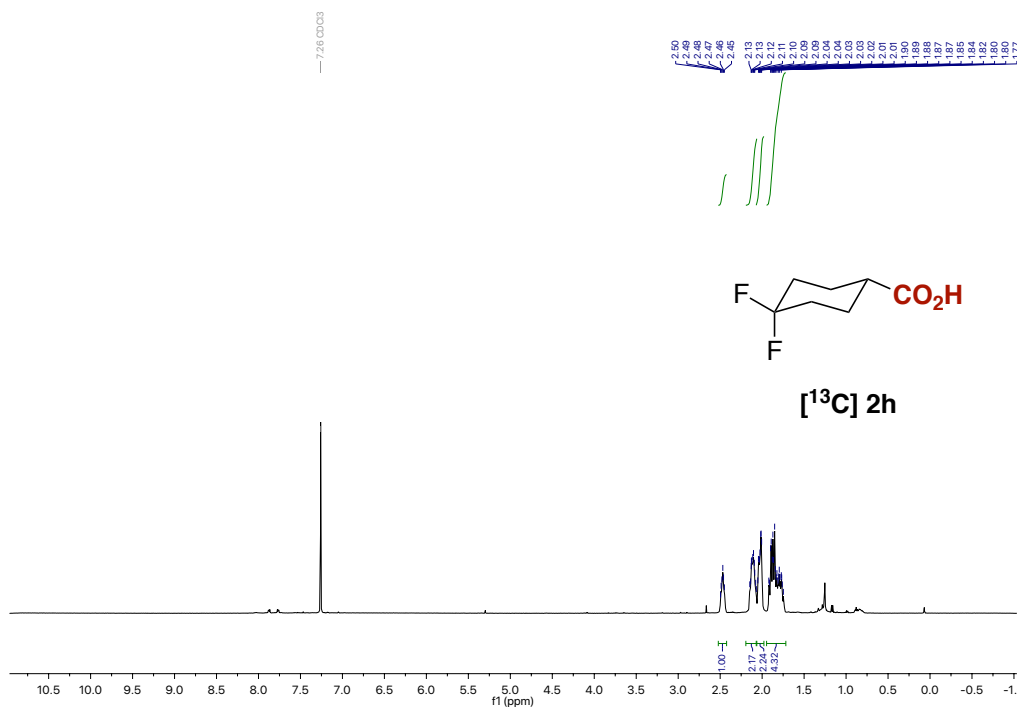


Figure 29. <sup>1</sup>H and <sup>13</sup>C NMR spectra of [<sup>13</sup>C]2g.

# Catalytic Decarboxylation/Carboxylation Platform for Accessing Isotopically Labeled Carboxylic Acids



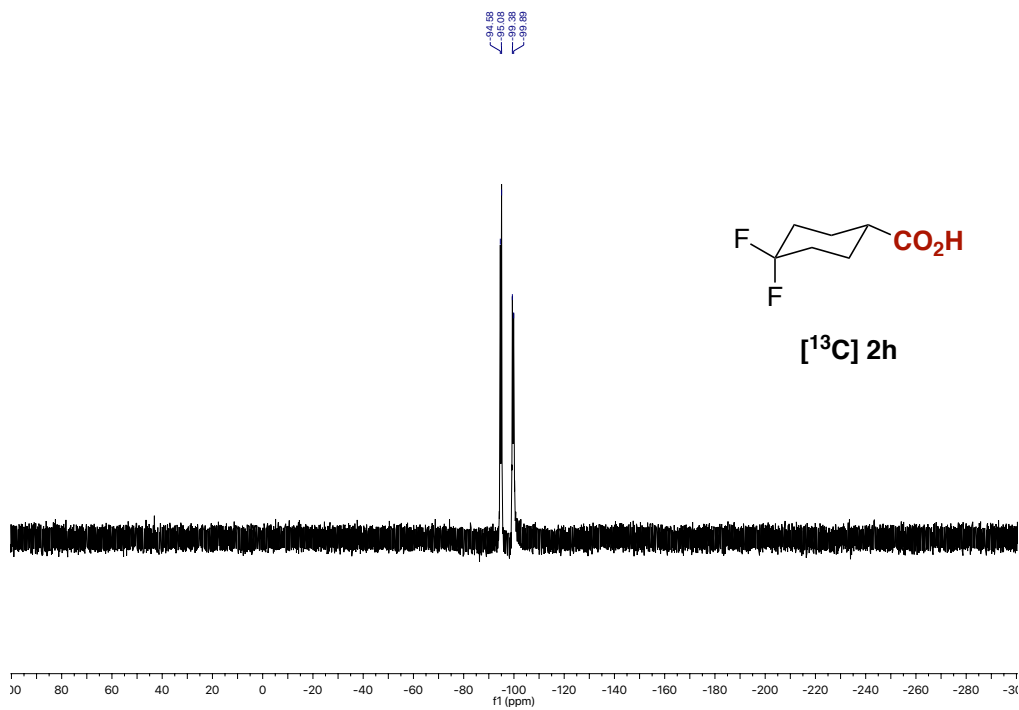


Figure 30.  $^1\text{H}$ ,  $^{13}\text{C}$  and  $^{19}\text{F}$  NMR spectra of  $[\text{C}^{13}]2\text{h}$ .



Catalytic Decarboxylation/Carboxylation Platform for Accessing Isotopically Labeled Carboxylic Acids

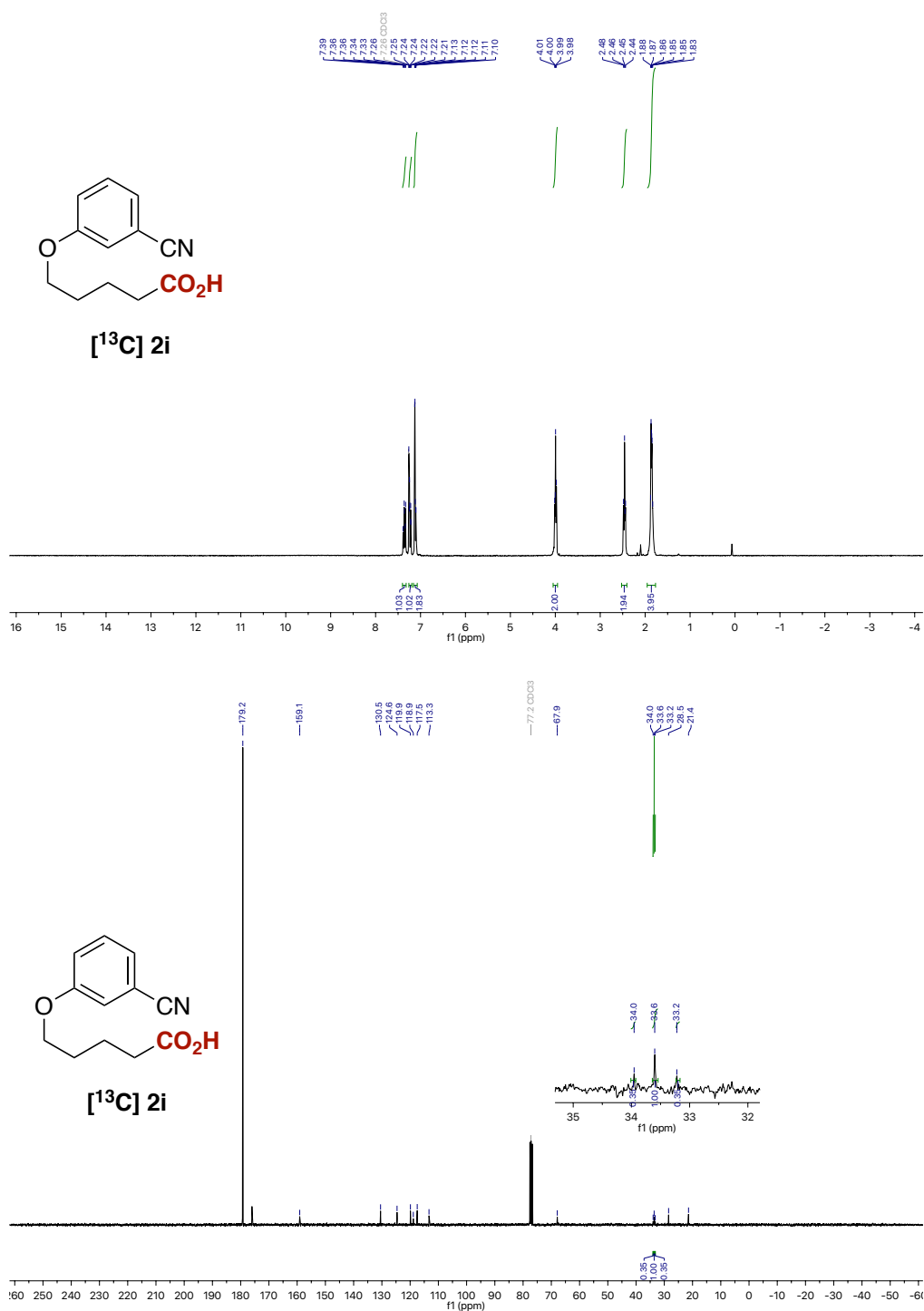


Figure 31. <sup>1</sup>H and <sup>13</sup>C NMR spectra of [<sup>13</sup>C]2i.

Chapter 4

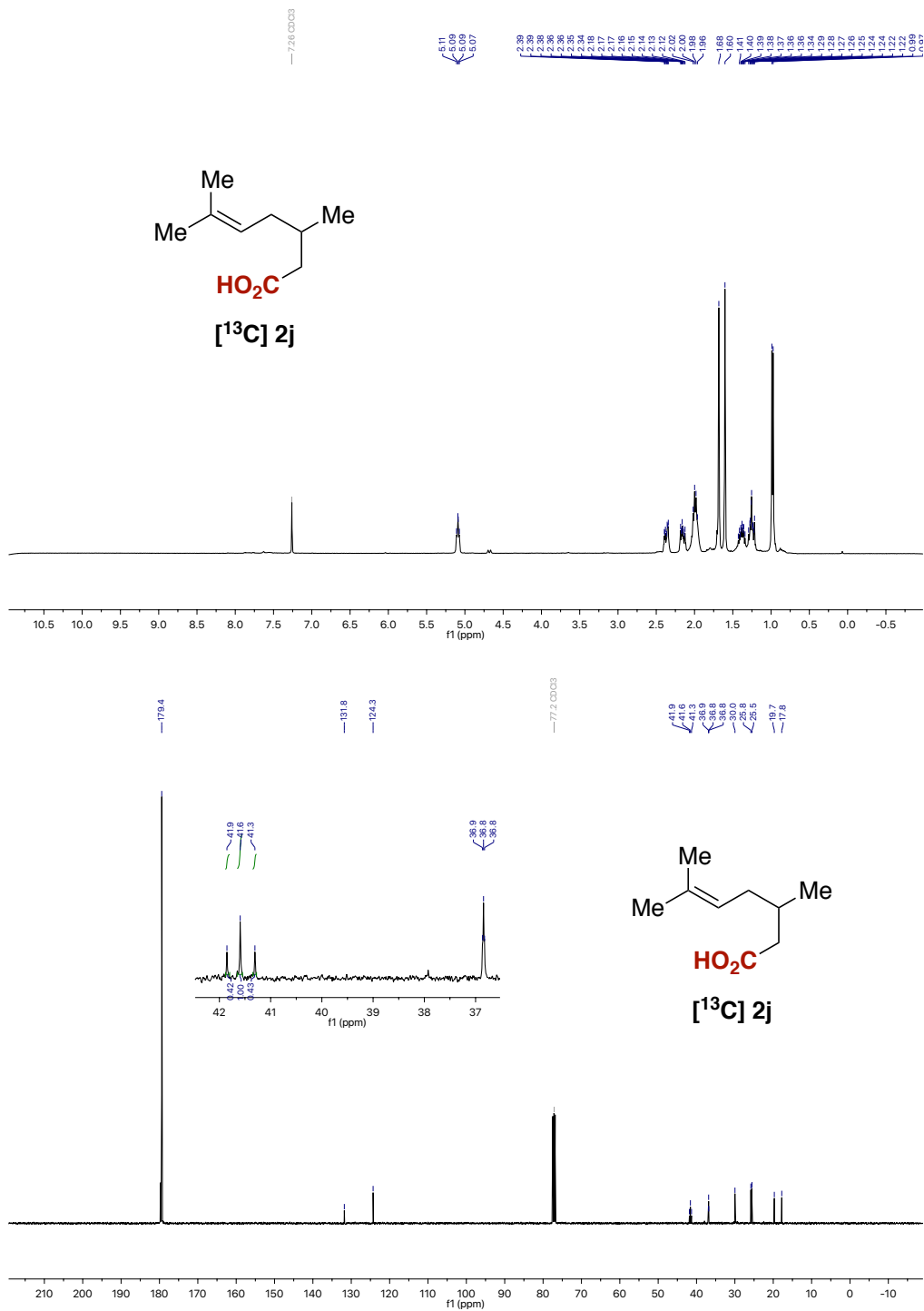


Figure 32.  $^1\text{H}$  and  $^{13}\text{C}$  NMR spectra of **[ $^{13}\text{C}$ ]2j**.

Catalytic Decarboxylation/Carboxylation Platform for Accessing Isotopically Labeled Carboxylic Acids

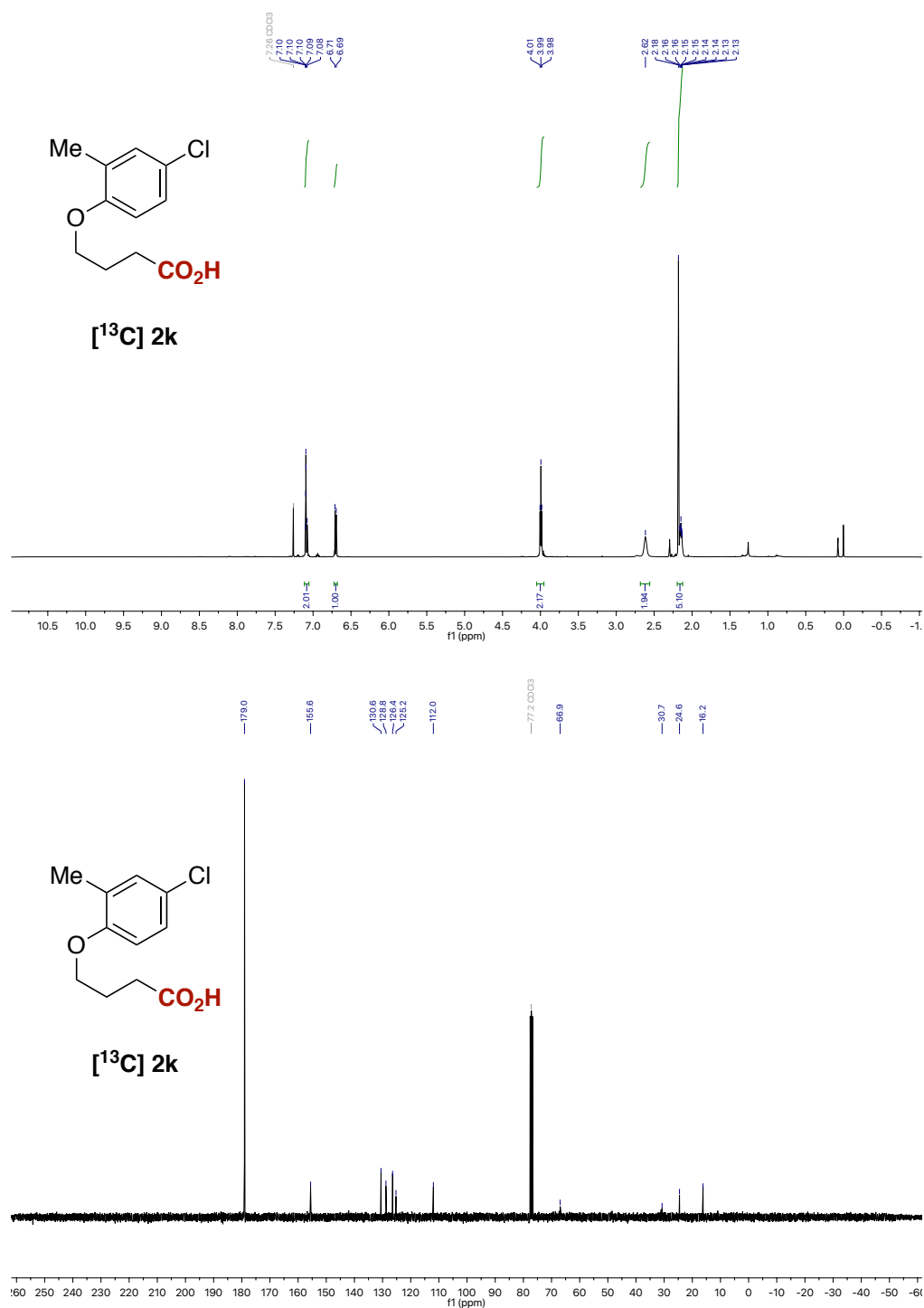


Figure 33. <sup>1</sup>H and <sup>13</sup>C NMR spectra of [<sup>13</sup>C]2k.

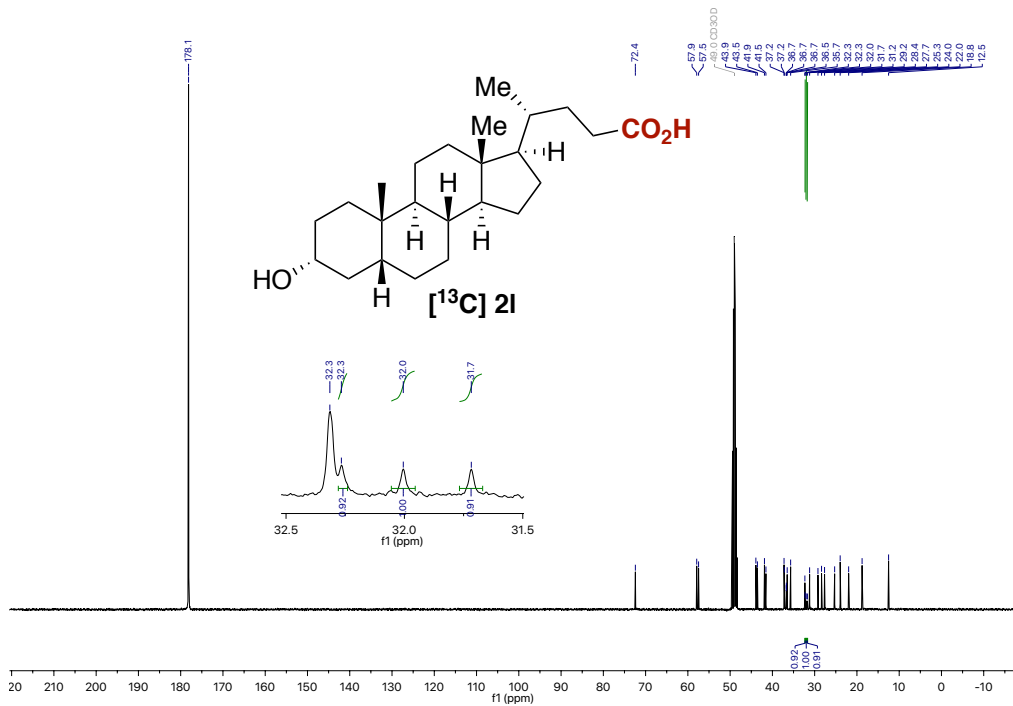
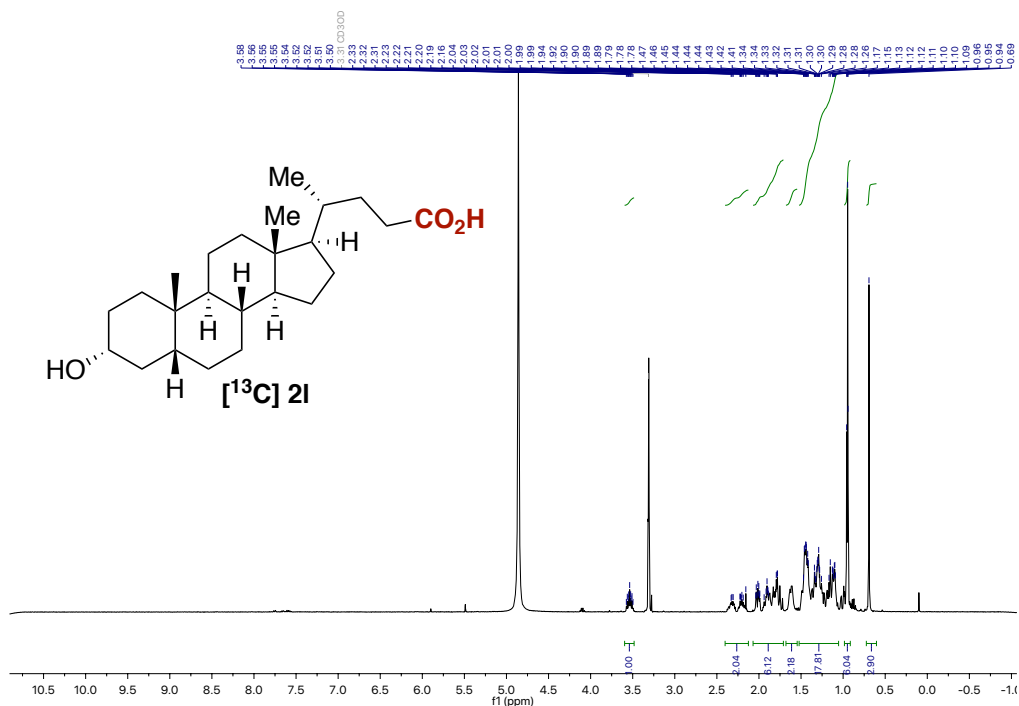


Figure 34. <sup>1</sup>H and <sup>13</sup>C NMR spectra of [13C]2I.

# Catalytic Decarboxylation/Carboxylation Platform for Accessing Isotopically Labeled Carboxylic Acids

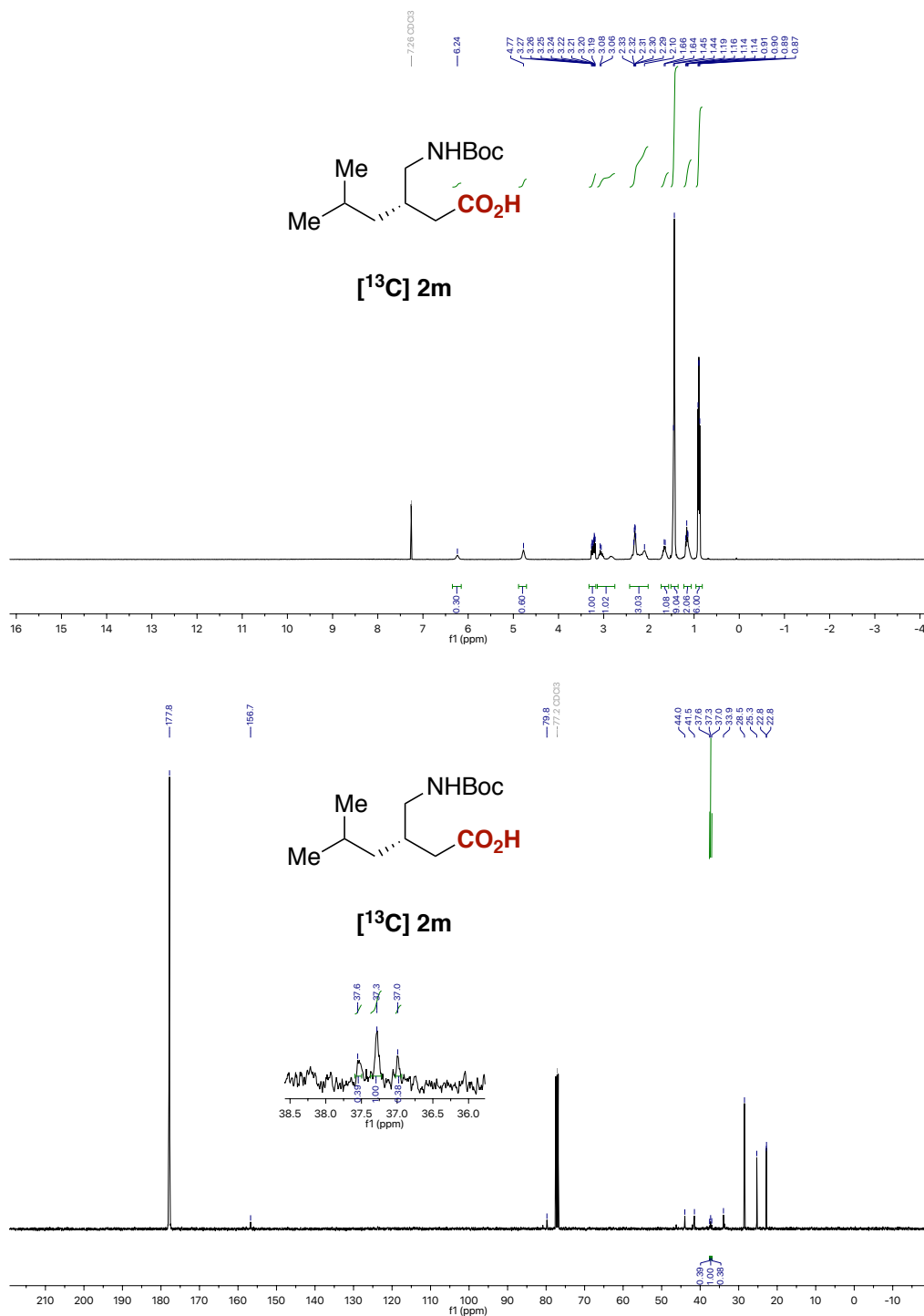


Figure 35. <sup>1</sup>H and <sup>13</sup>C NMR spectra of [13C]2m.



Catalytic Decarboxylation/Carboxylation Platform for Accessing Isotopically Labeled Carboxylic Acids

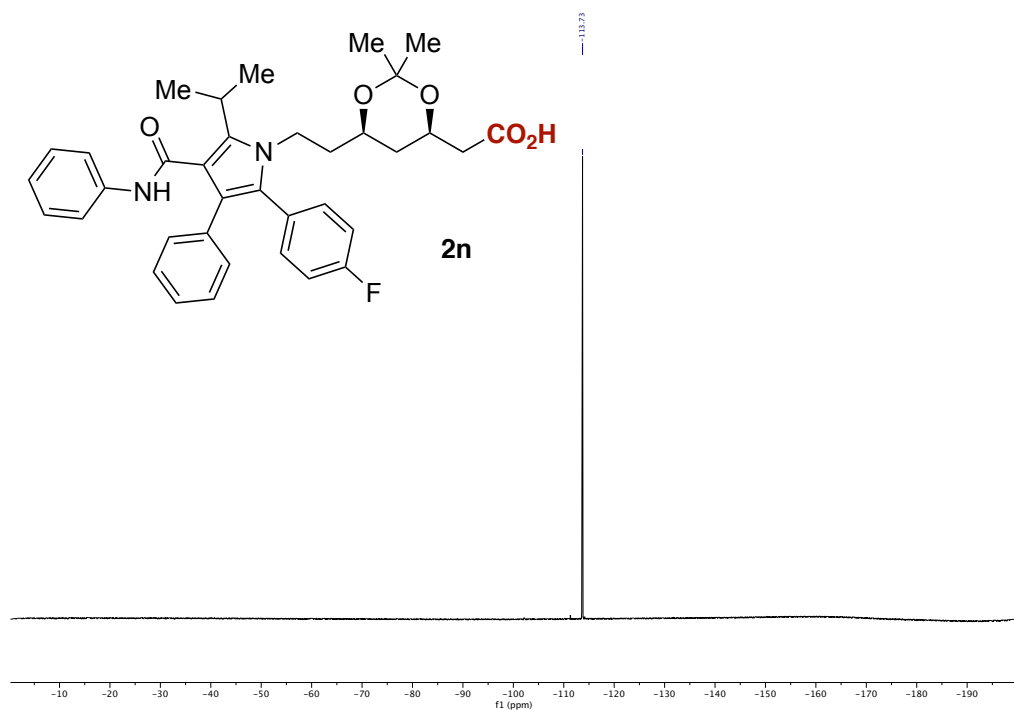


Figure 36.  $^1\text{H}$ ,  $^{13}\text{C}$  and  $^{19}\text{F}$  NMR spectra of  $[^{13}\text{C}]\mathbf{2n}$ .

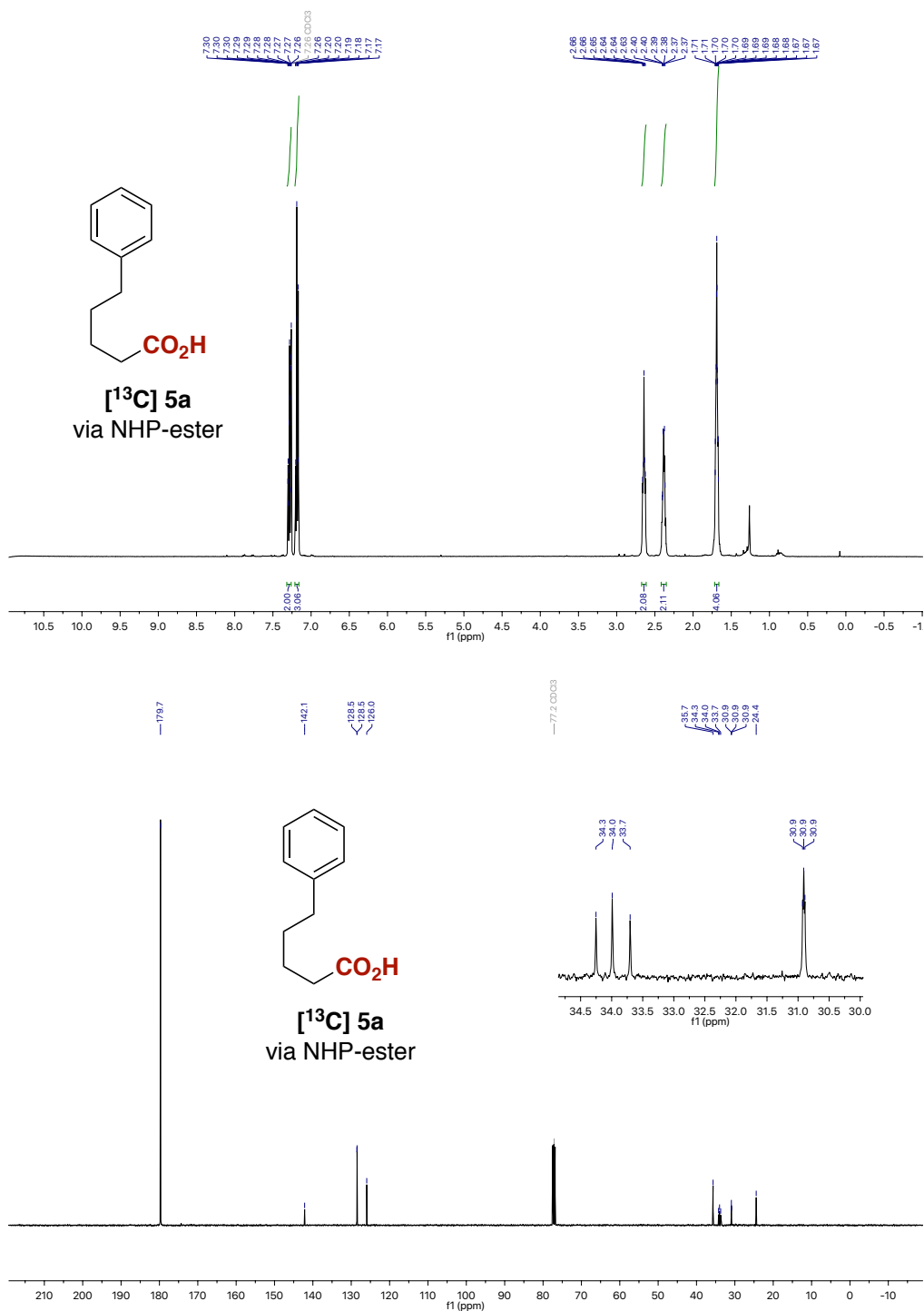


Figure 37. <sup>1</sup>H and <sup>13</sup>C NMR spectra of [<sup>13</sup>C]5a via NHP-ester.



Catalytic Decarboxylation/Carboxylation Platform for Accessing Isotopically Labeled Carboxylic Acids

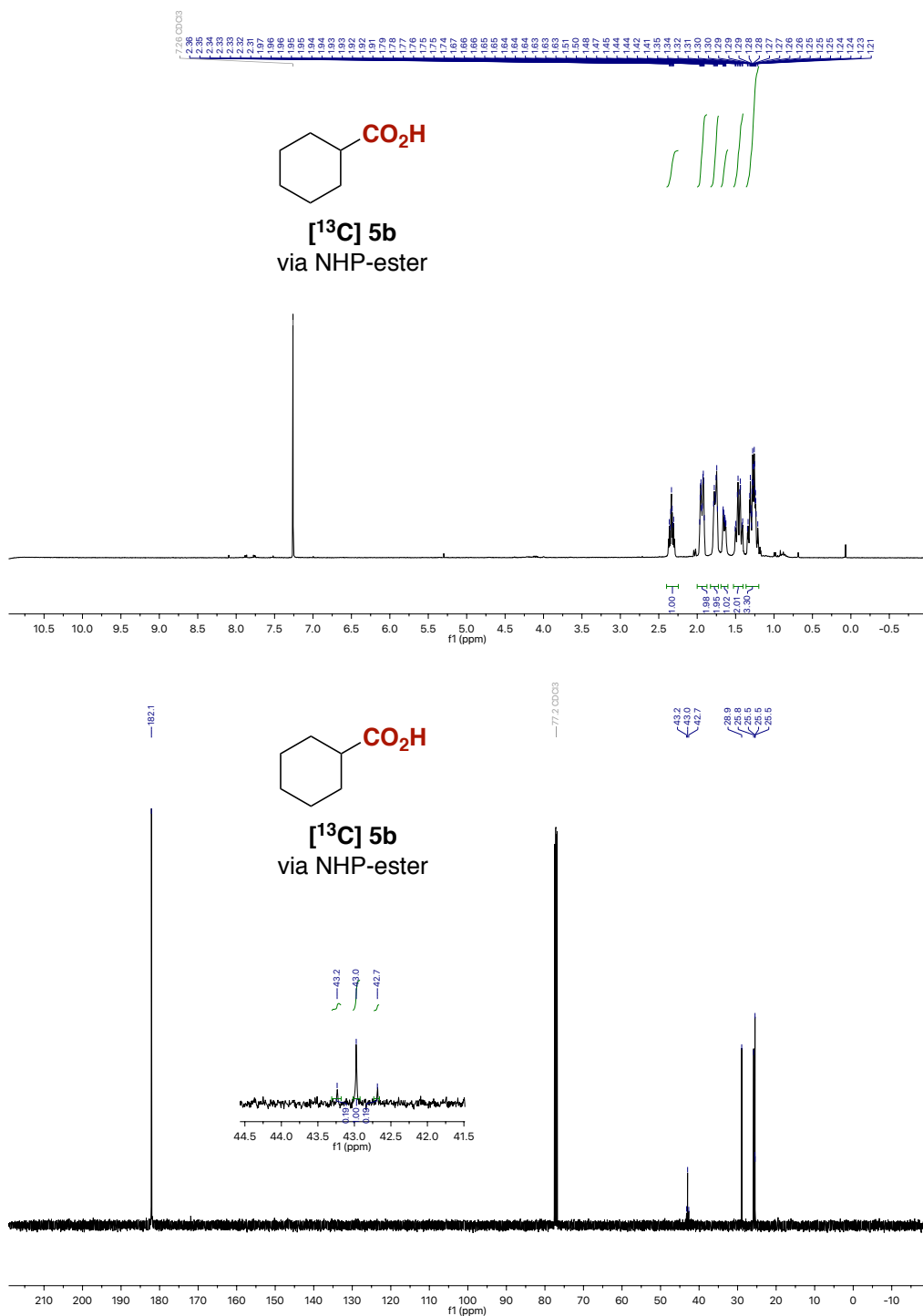


Figure 38.  $^1\text{H}$  and  $^{13}\text{C}$  NMR spectra of  $^{13}\text{C}$  5b via NHP-ester.

Chapter 4

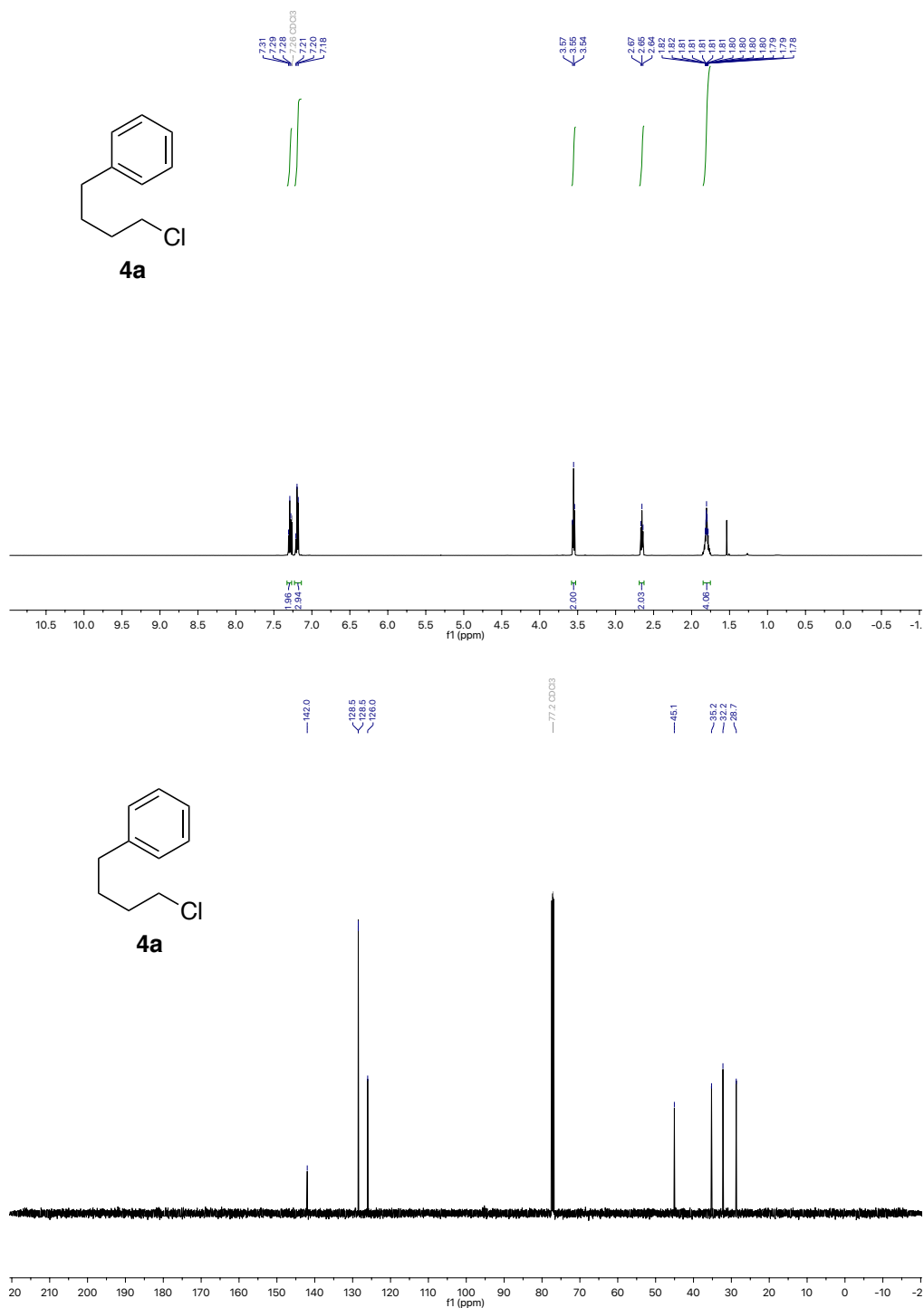


Figure 39. <sup>1</sup>H and <sup>13</sup>C NMR spectra of **4a**.

# Catalytic Decarboxylation/Carboxylation Platform for Accessing Isotopically Labeled Carboxylic Acids

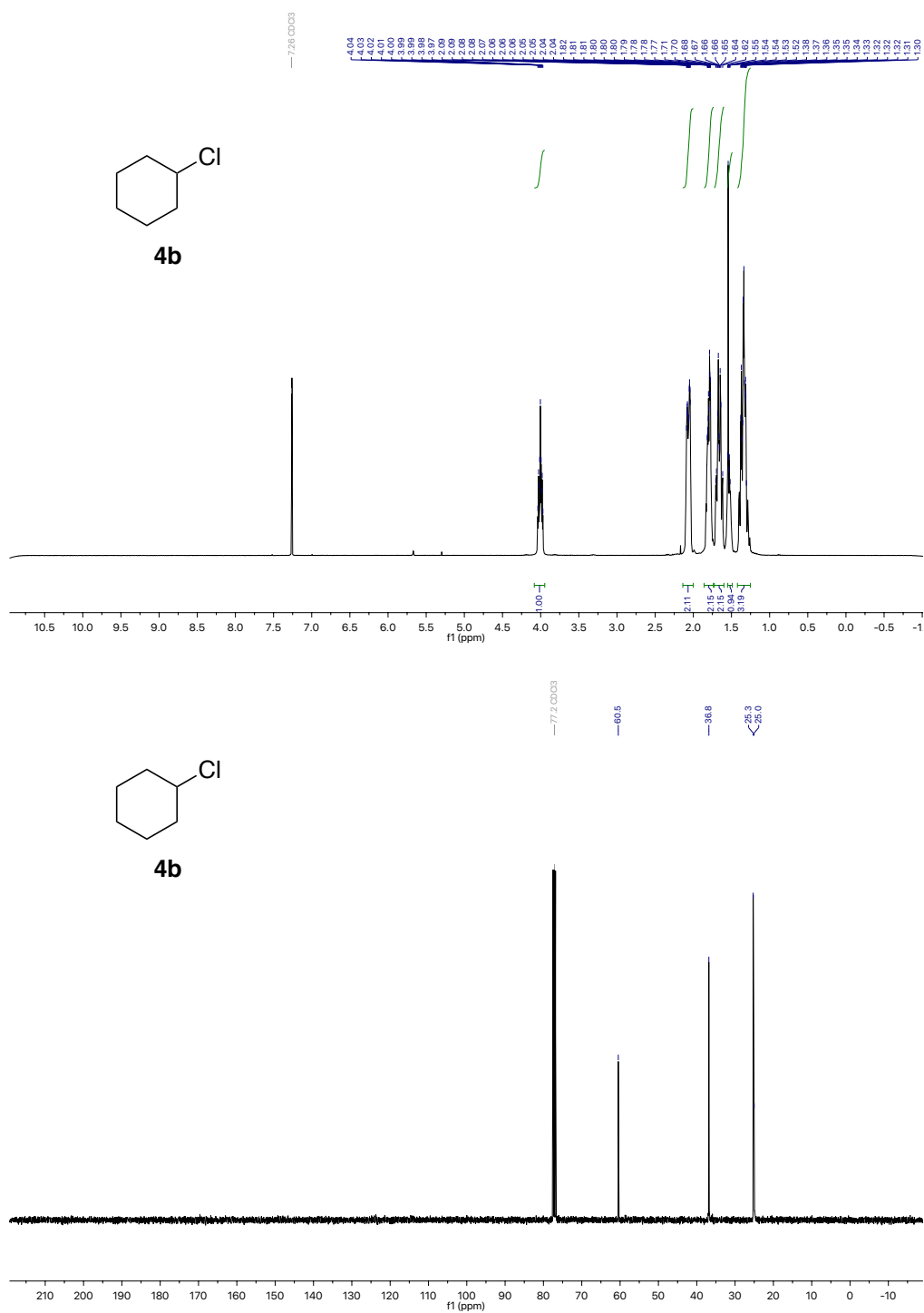
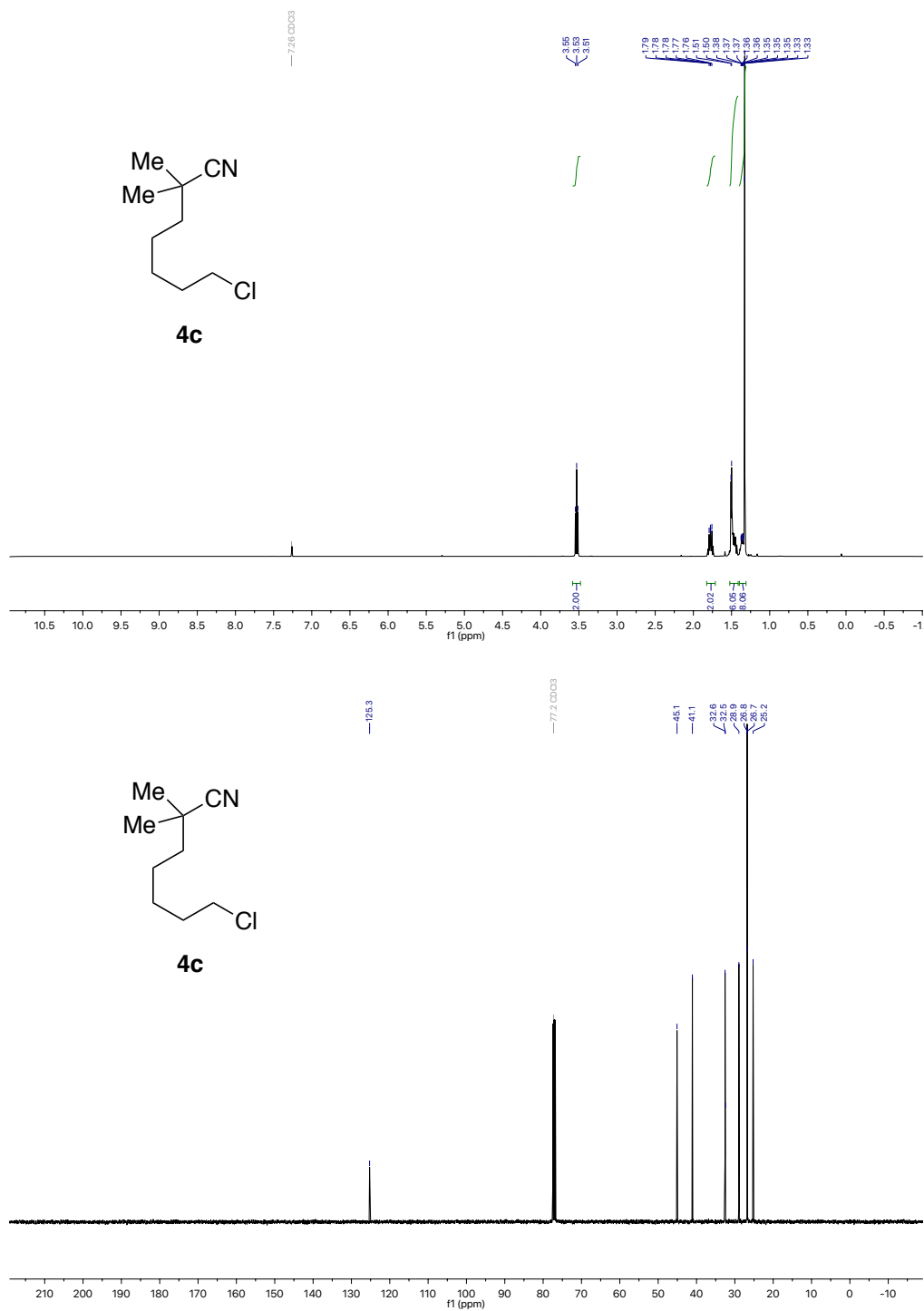


Figure 40. <sup>1</sup>H and <sup>13</sup>C NMR spectra of **4b**.

Figure 41.  $^1\text{H}$  and  $^{13}\text{C}$  NMR spectra of **4c**.

# Catalytic Decarboxylation/Carboxylation Platform for Accessing Isotopically Labeled Carboxylic Acids

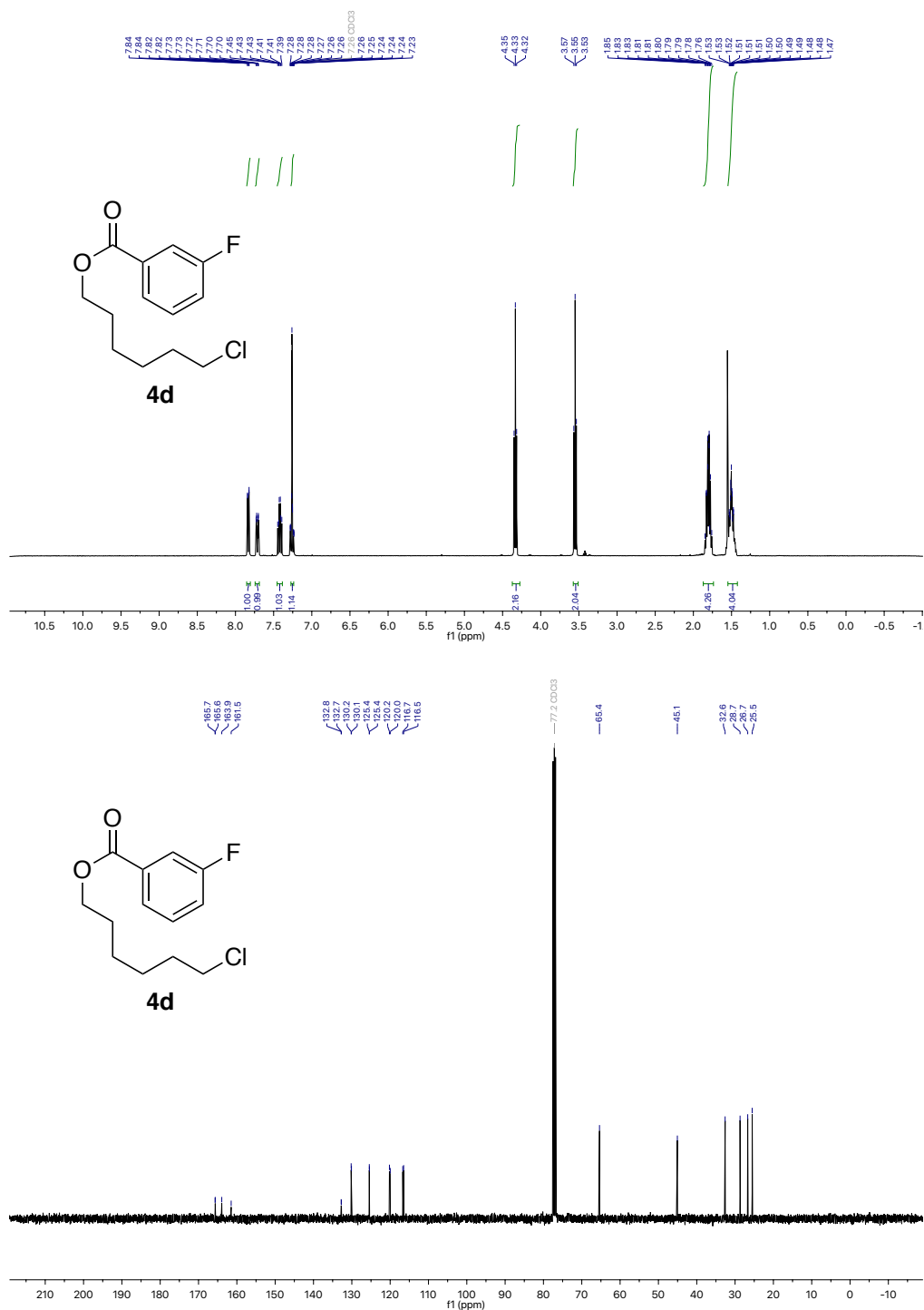


Figure 42. <sup>1</sup>H and <sup>13</sup>C NMR spectra of **4d**.

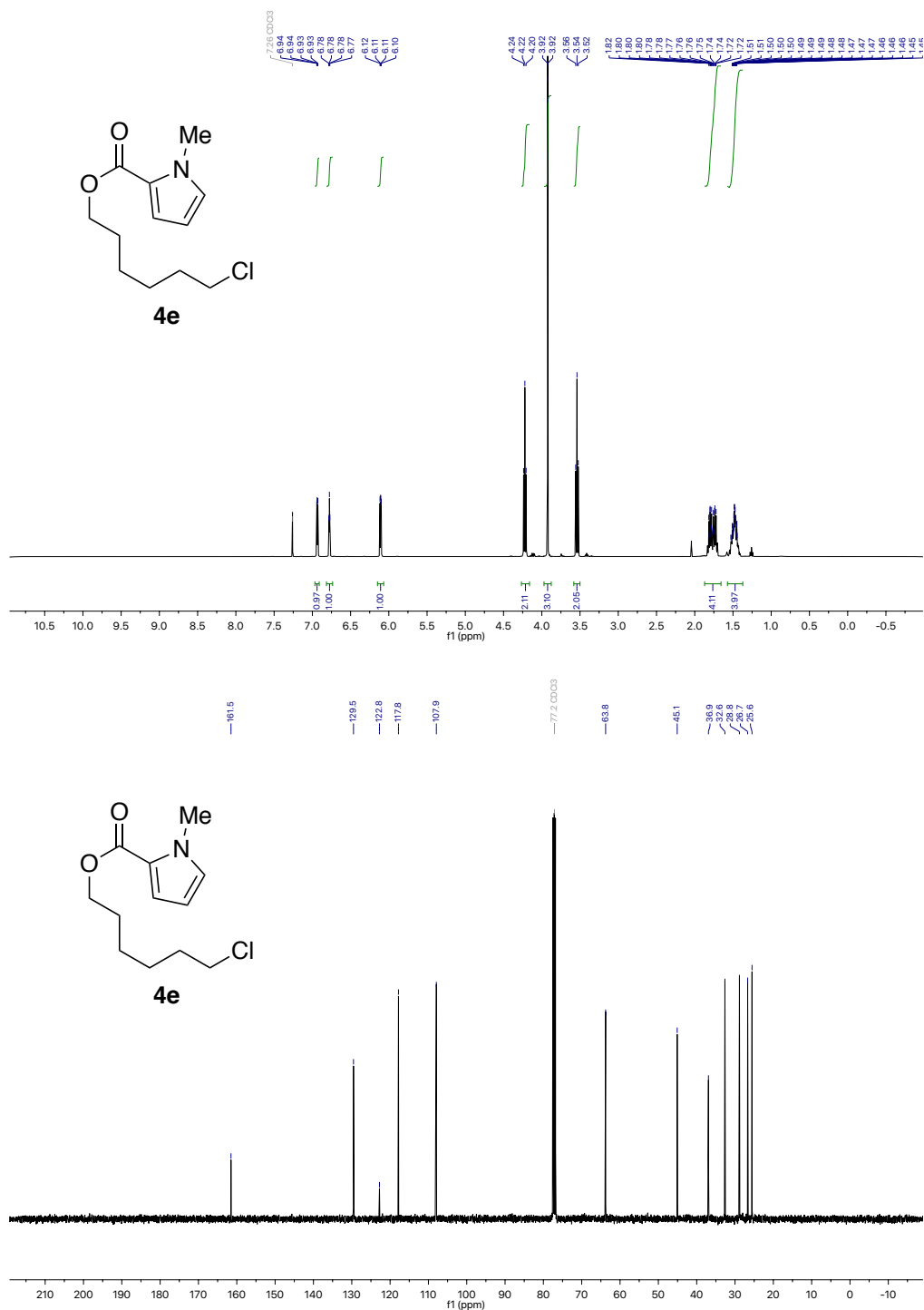


Figure 43. <sup>1</sup>H and <sup>13</sup>C NMR spectra of **4e**.

# Catalytic Decarboxylation/Carboxylation Platform for Accessing Isotopically Labeled Carboxylic Acids

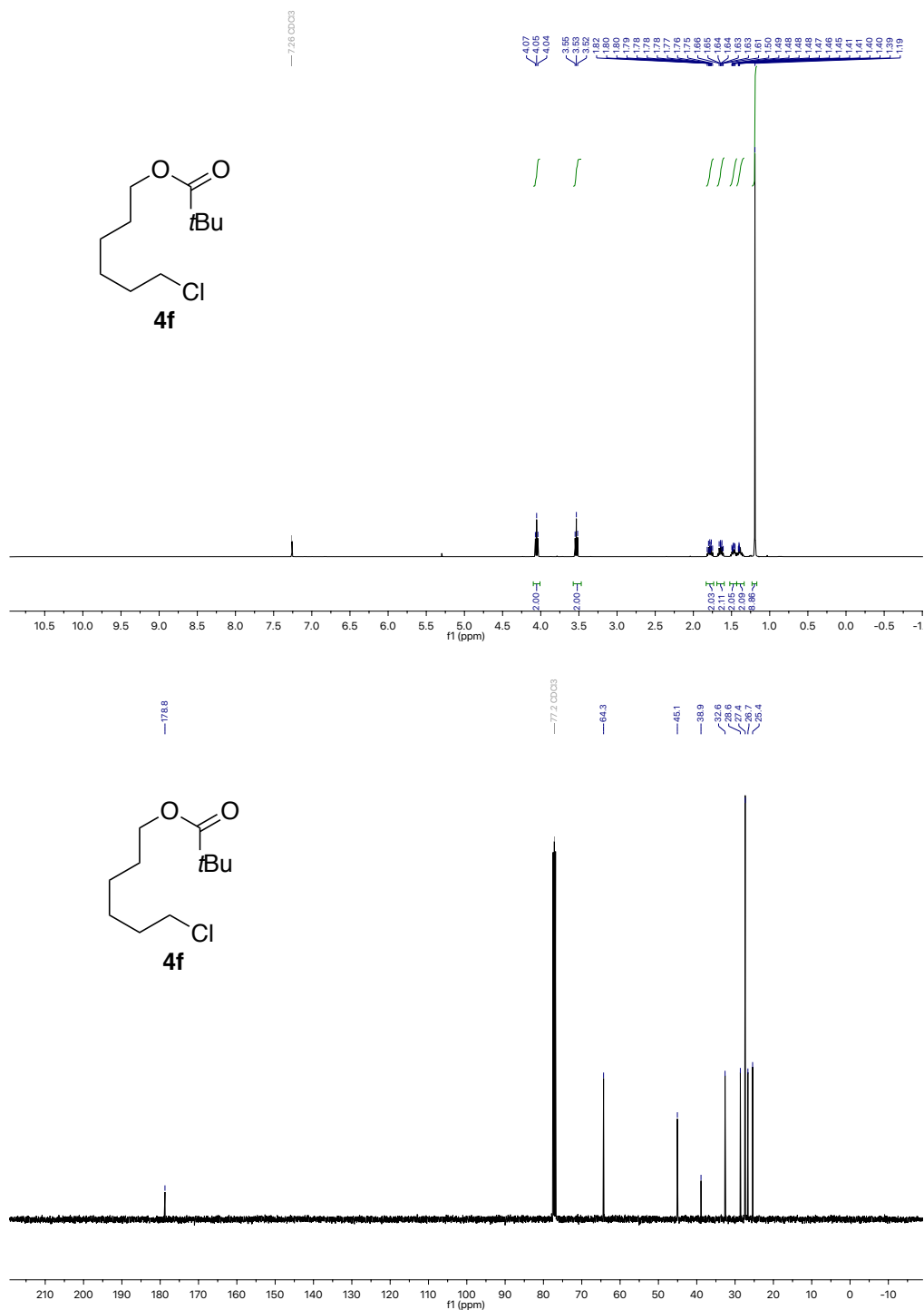


Figure 44. <sup>1</sup>H and <sup>13</sup>C NMR spectra of **4f**.

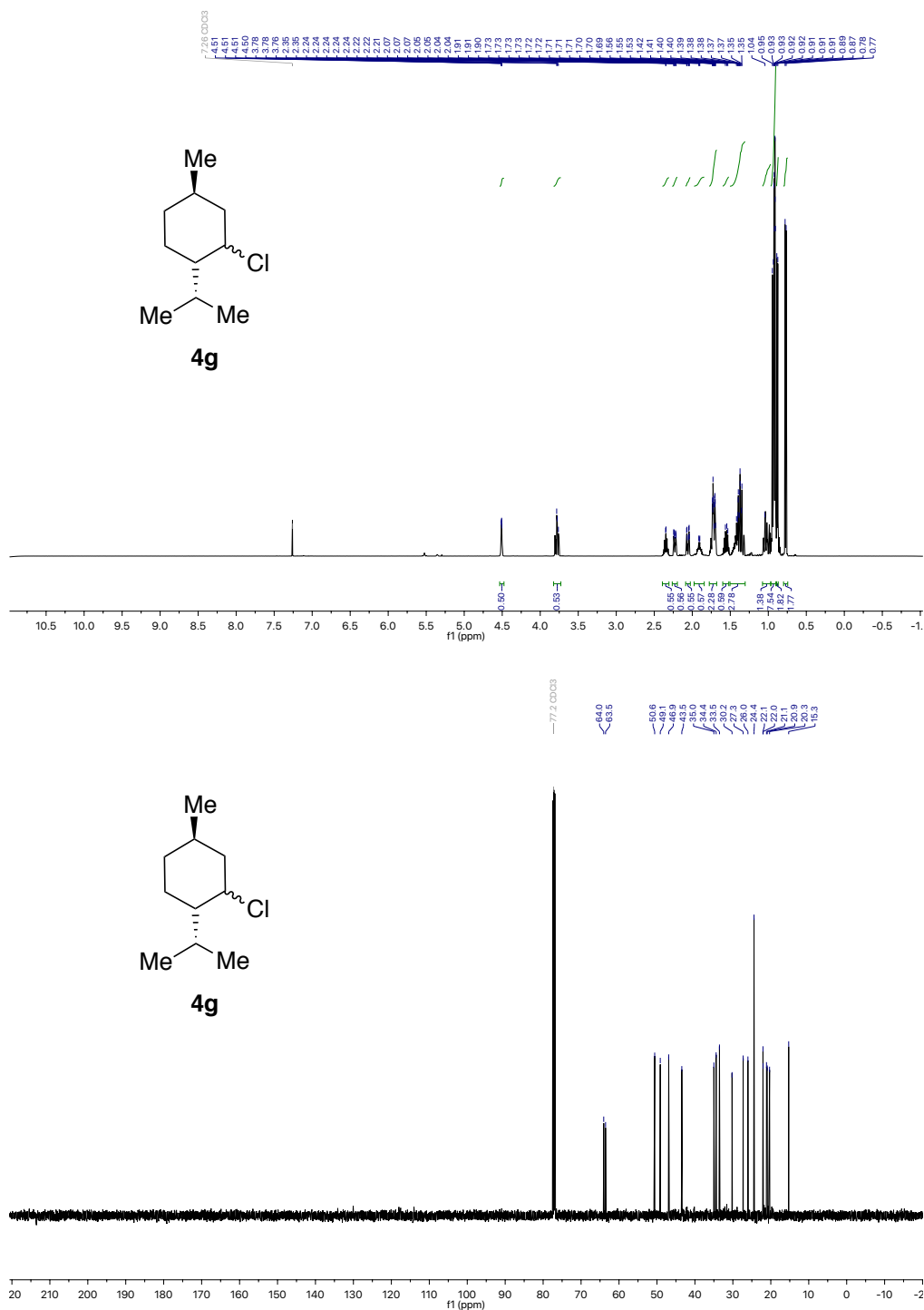


Figure 45. <sup>1</sup>H and <sup>13</sup>C NMR spectra of **4g**.



Catalytic Decarboxylation/Carboxylation Platform for Accessing Isotopically Labeled Carboxylic Acids

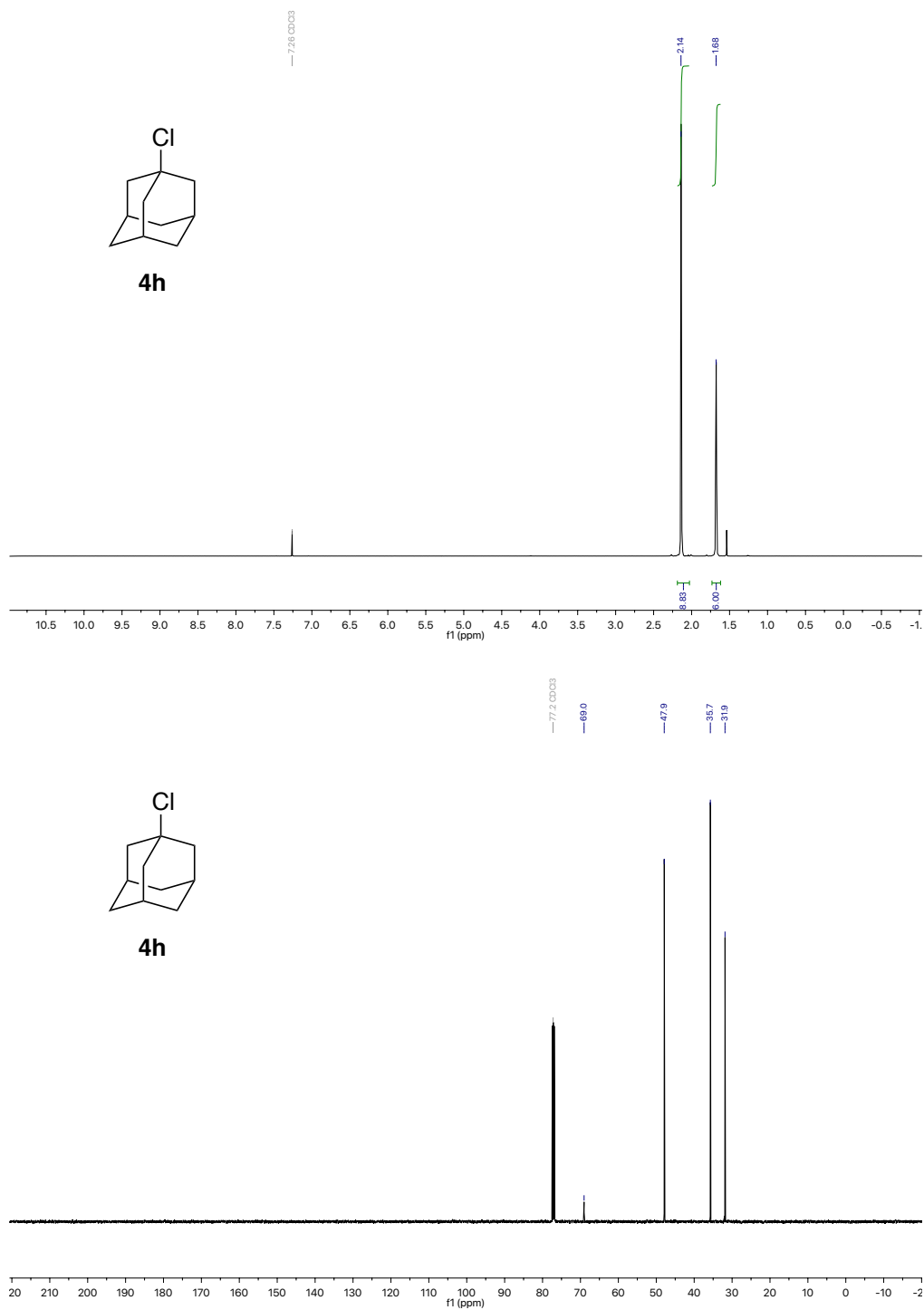


Figure 46.  $^1\text{H}$  and  $^{13}\text{C}$  NMR spectra of **4h**.

Chapter 4

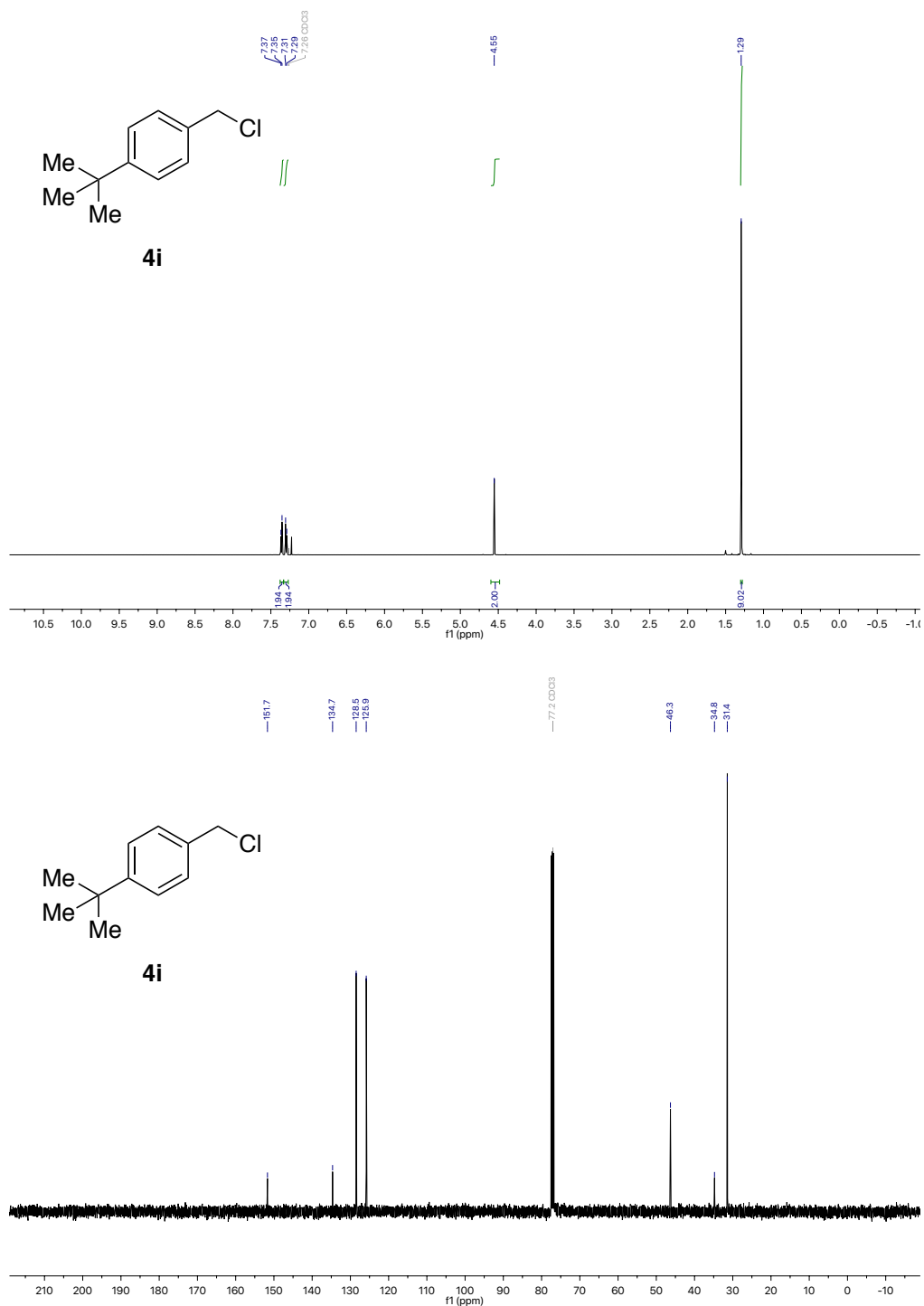
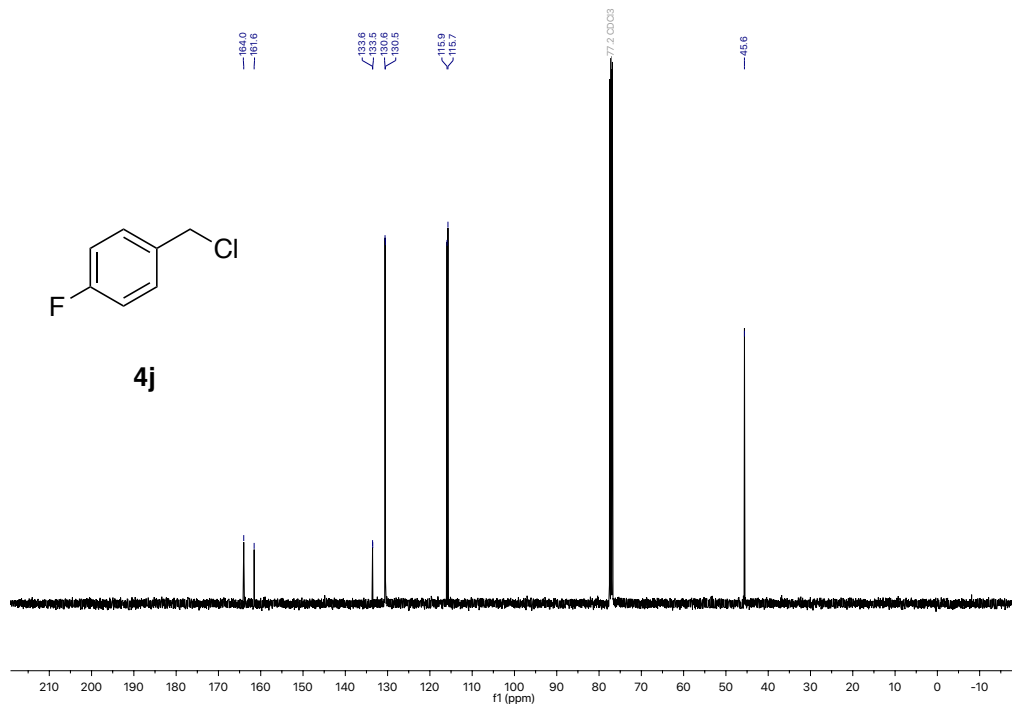
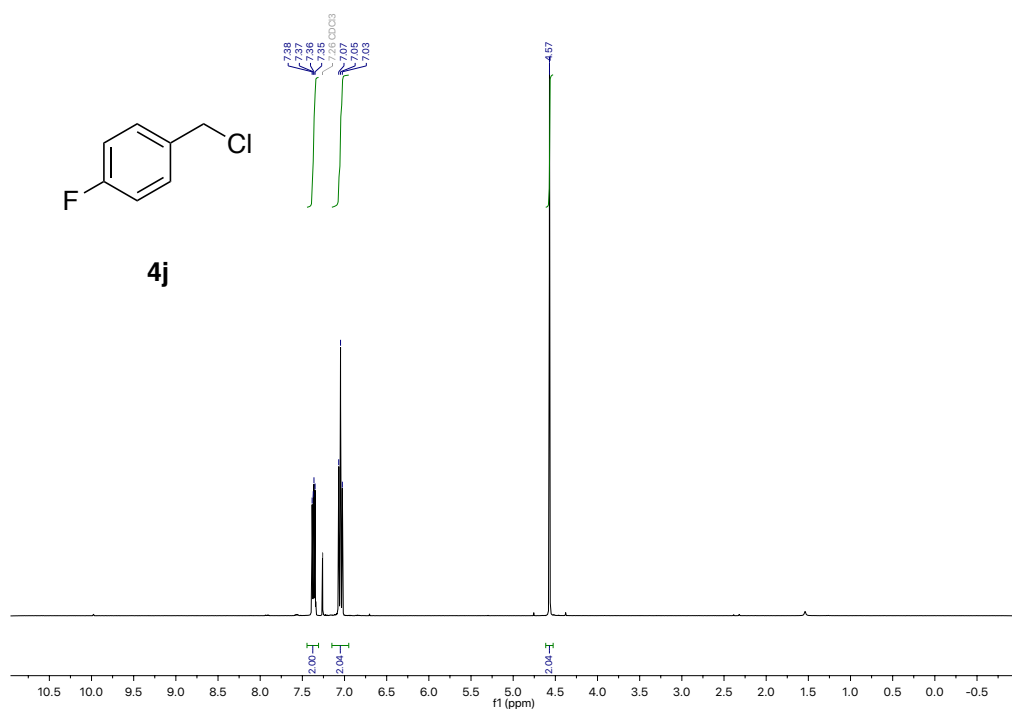


Figure 47. <sup>1</sup>H and <sup>13</sup>C NMR spectra of **4i**.

# Catalytic Decarboxylation/Carboxylation Platform for Accessing Isotopically Labeled Carboxylic Acids



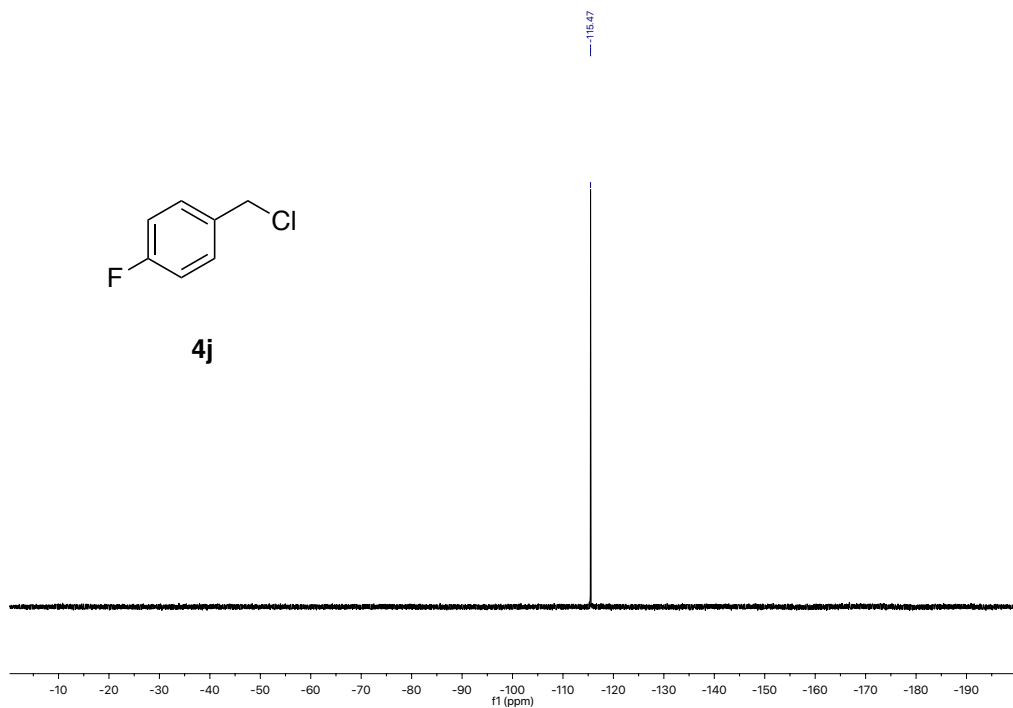


Figure 48.  $^1\text{H}$ ,  $^{13}\text{C}$  and  $^{19}\text{F}$  NMR spectra of **4j**.

# Catalytic Decarboxylation/Carboxylation Platform for Accessing Isotopically Labeled Carboxylic Acids

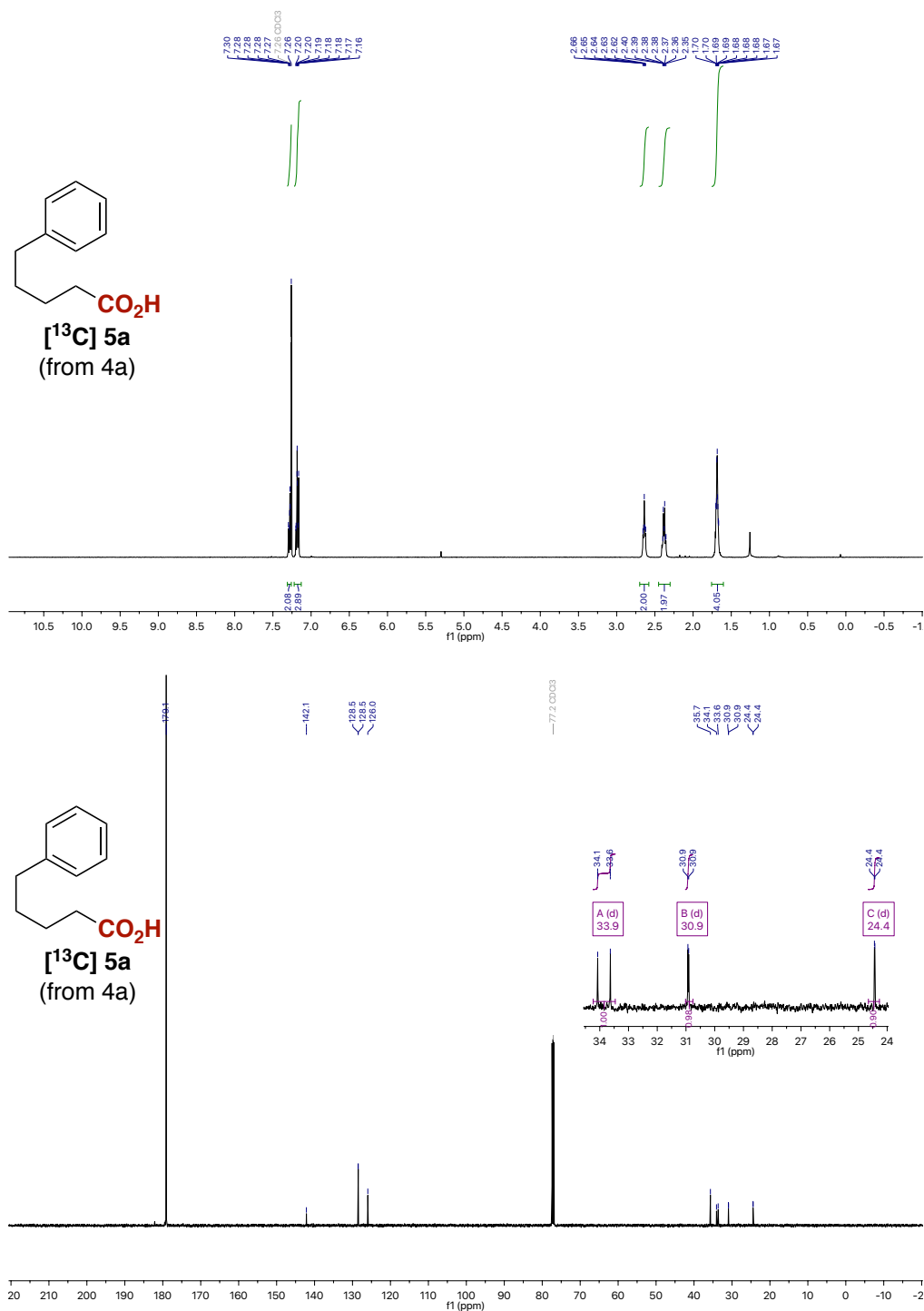


Figure 49. <sup>1</sup>H and <sup>13</sup>C NMR spectra of [<sup>13</sup>C]5a from 4a.

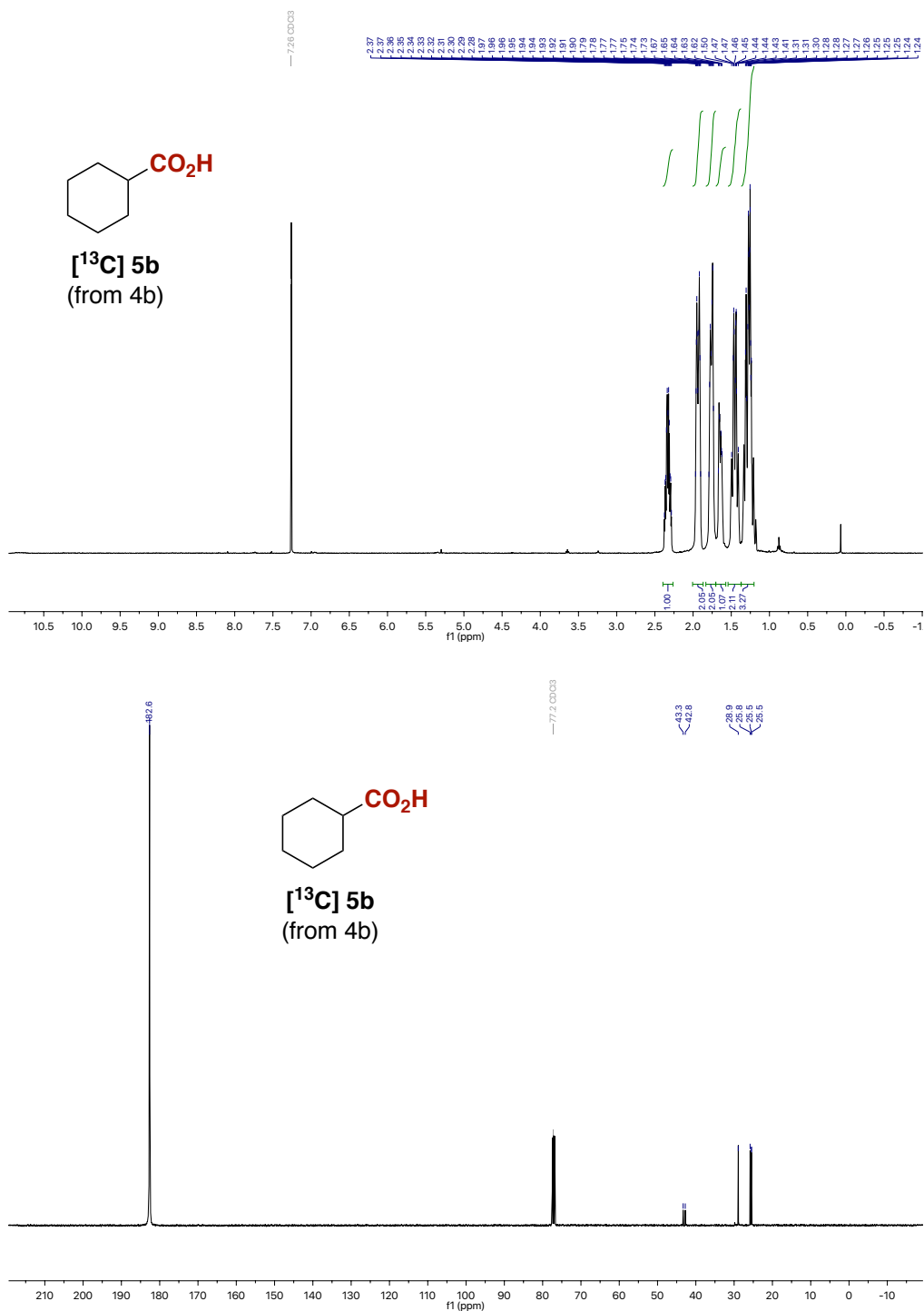


Figure 50. <sup>1</sup>H and <sup>13</sup>C NMR spectra of [13C]5b from 4.

# Catalytic Decarboxylation/Carboxylation Platform for Accessing Isotopically Labeled Carboxylic Acids

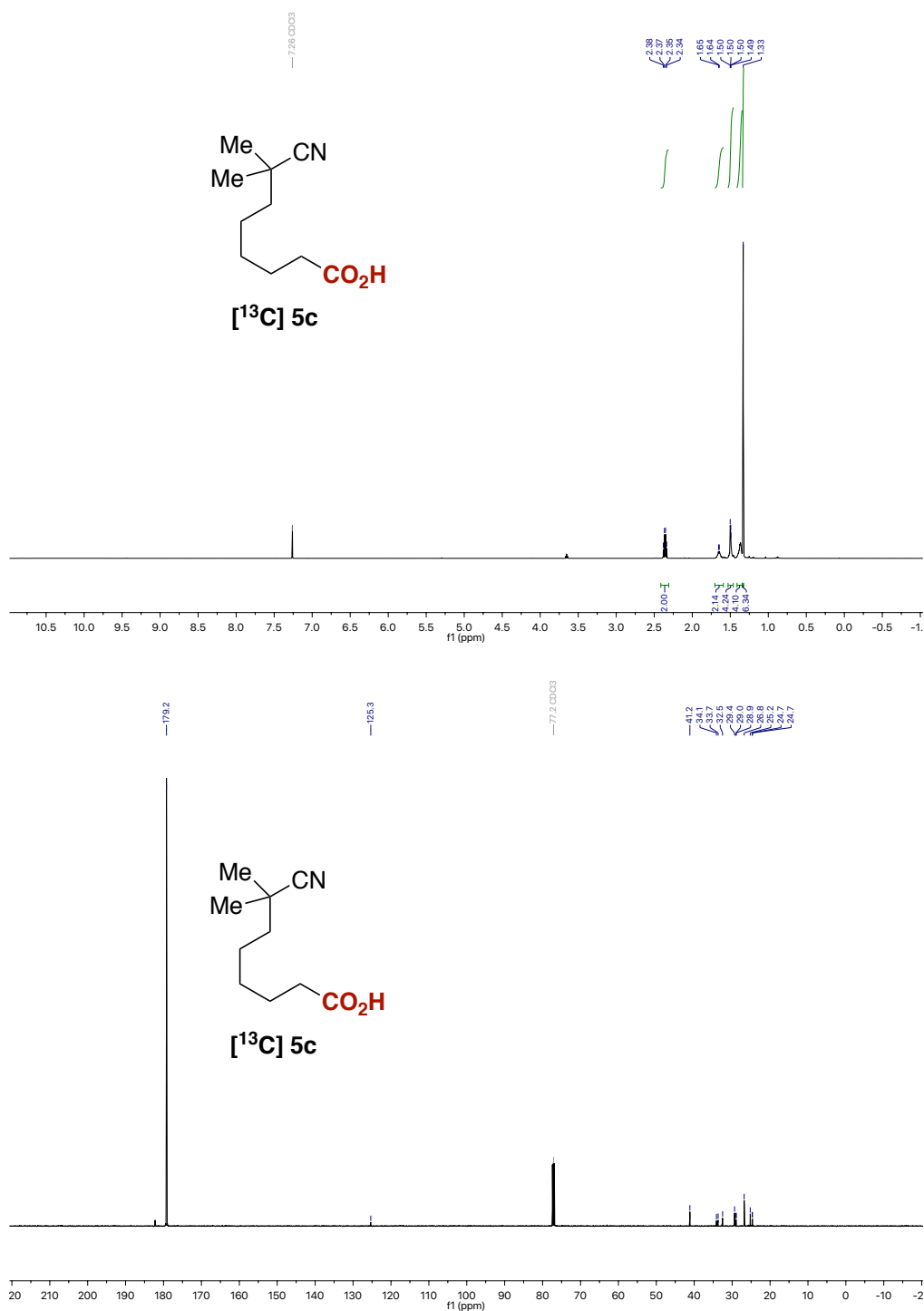
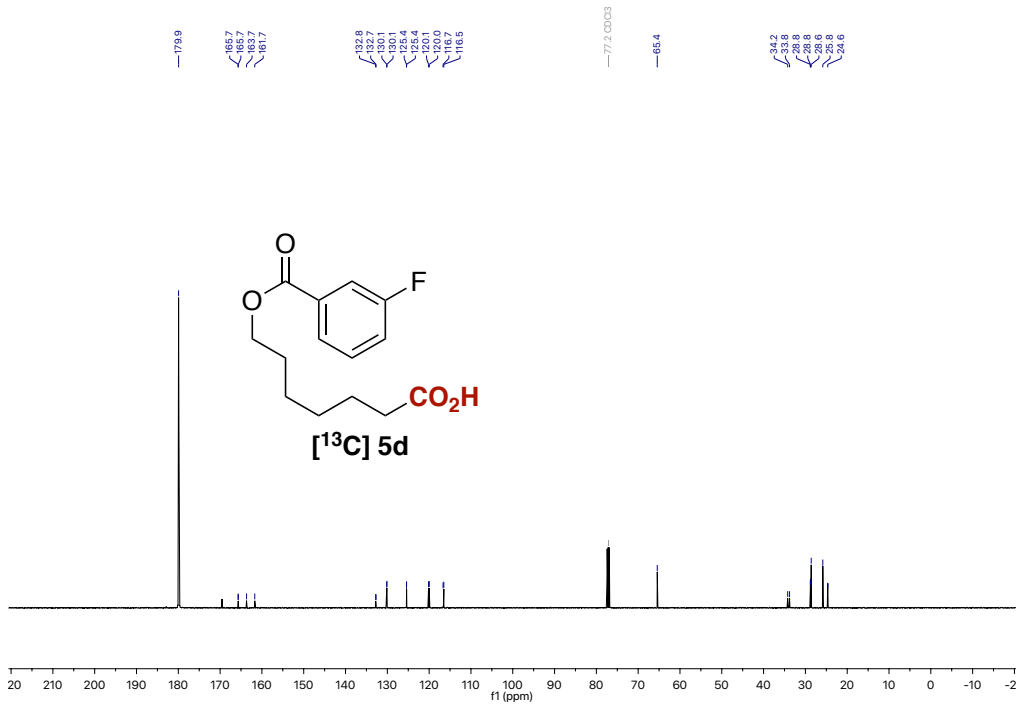
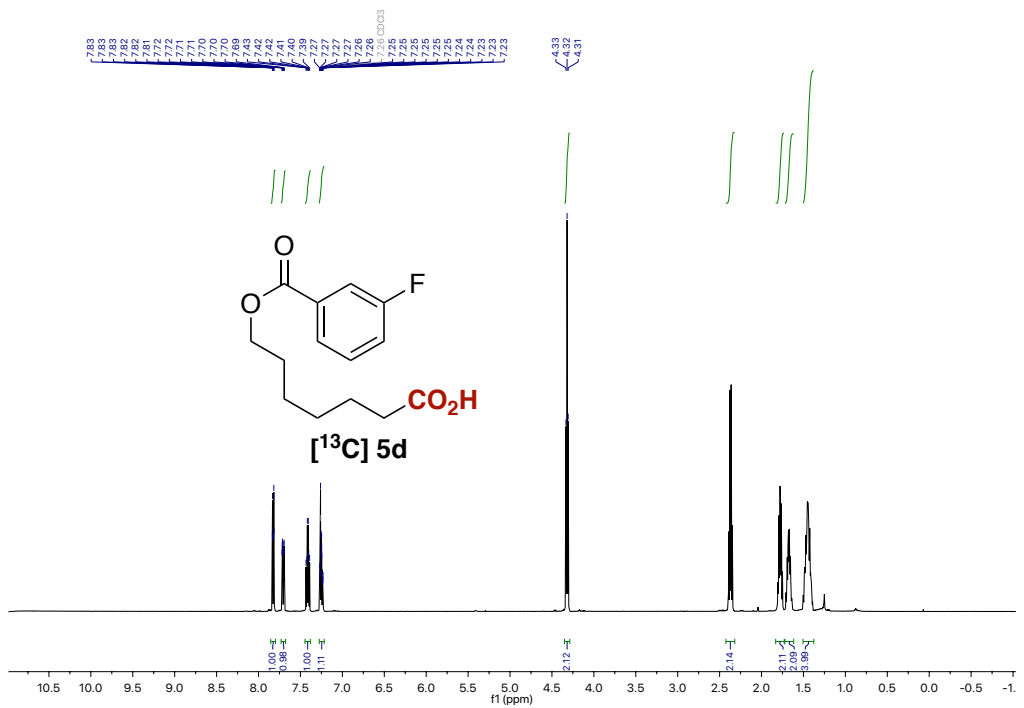


Figure S1. <sup>1</sup>H and <sup>13</sup>C NMR spectra of [<sup>13</sup>C]5c.

Chapter 4





Catalytic Decarboxylation/Carboxylation Platform for Accessing Isotopically Labeled Carboxylic Acids

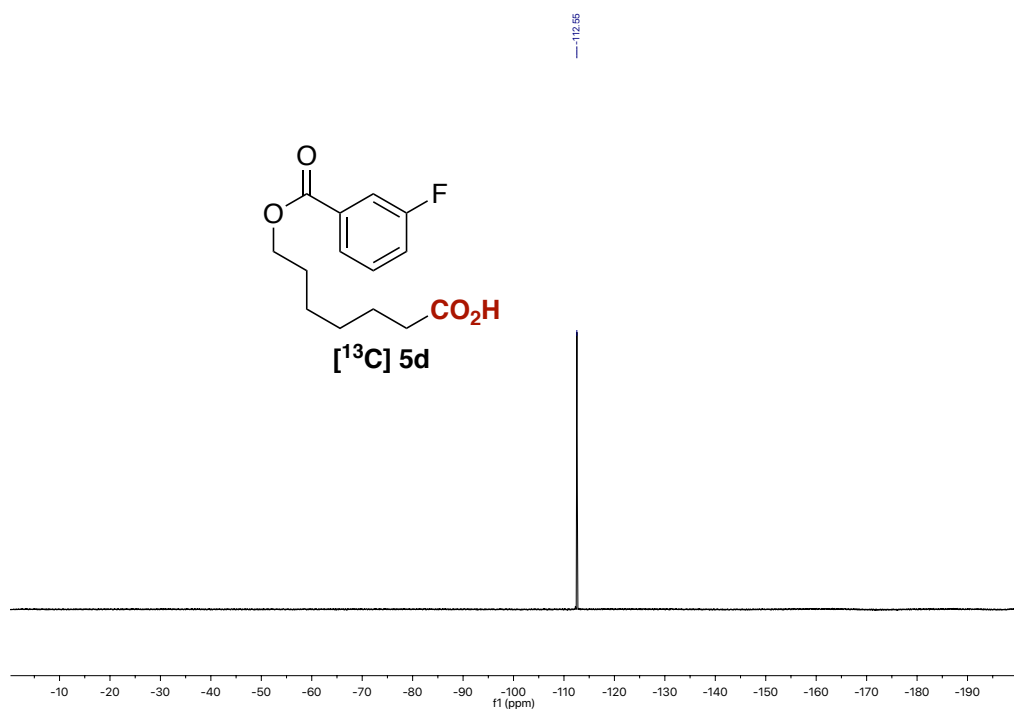
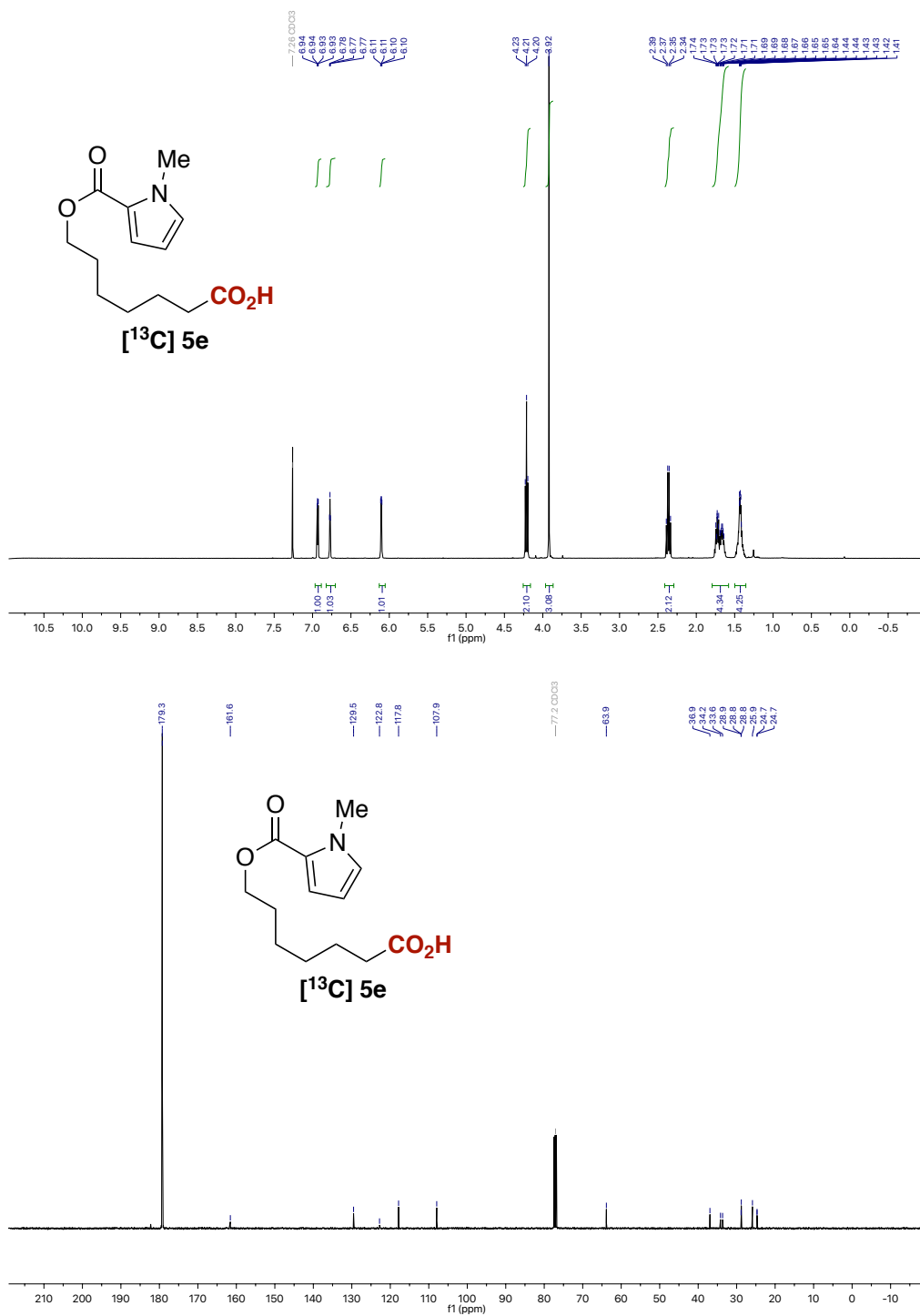


Figure 52.  $^1\text{H}$ ,  $^{13}\text{C}$  and  $^{19}\text{F}$  NMR spectra of  $[^{13}\text{C}]$ 5d.

Figure 53. <sup>1</sup>H and <sup>13</sup>C NMR spectra of [<sup>13</sup>C]5e.

Catalytic Decarboxylation/Carboxylation Platform for Accessing Isotopically Labeled Carboxylic Acids

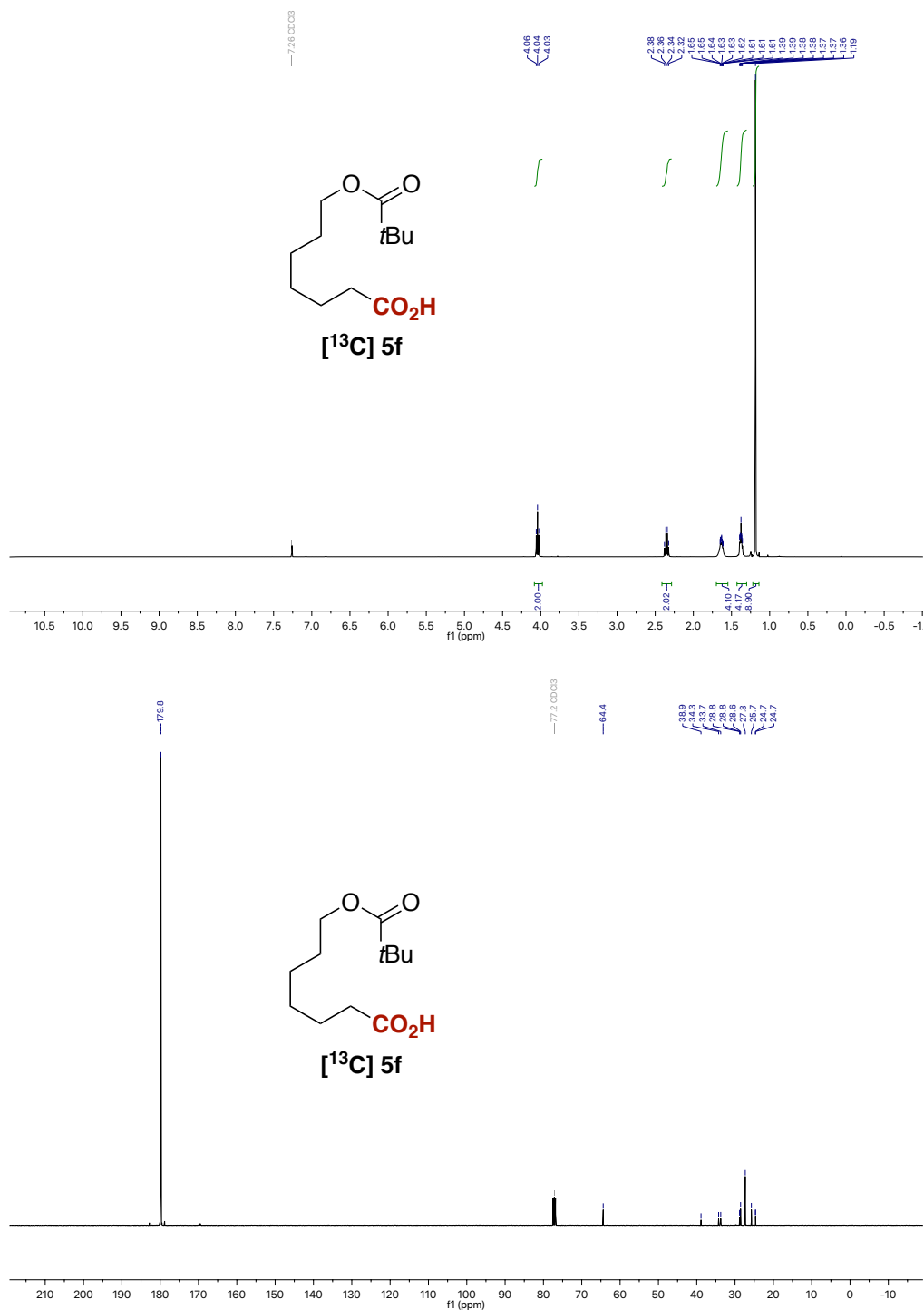


Figure 54.  $^1\text{H}$  and  $^{13}\text{C}$  NMR spectra of  $[^{13}\text{C}]5\text{f}$ .

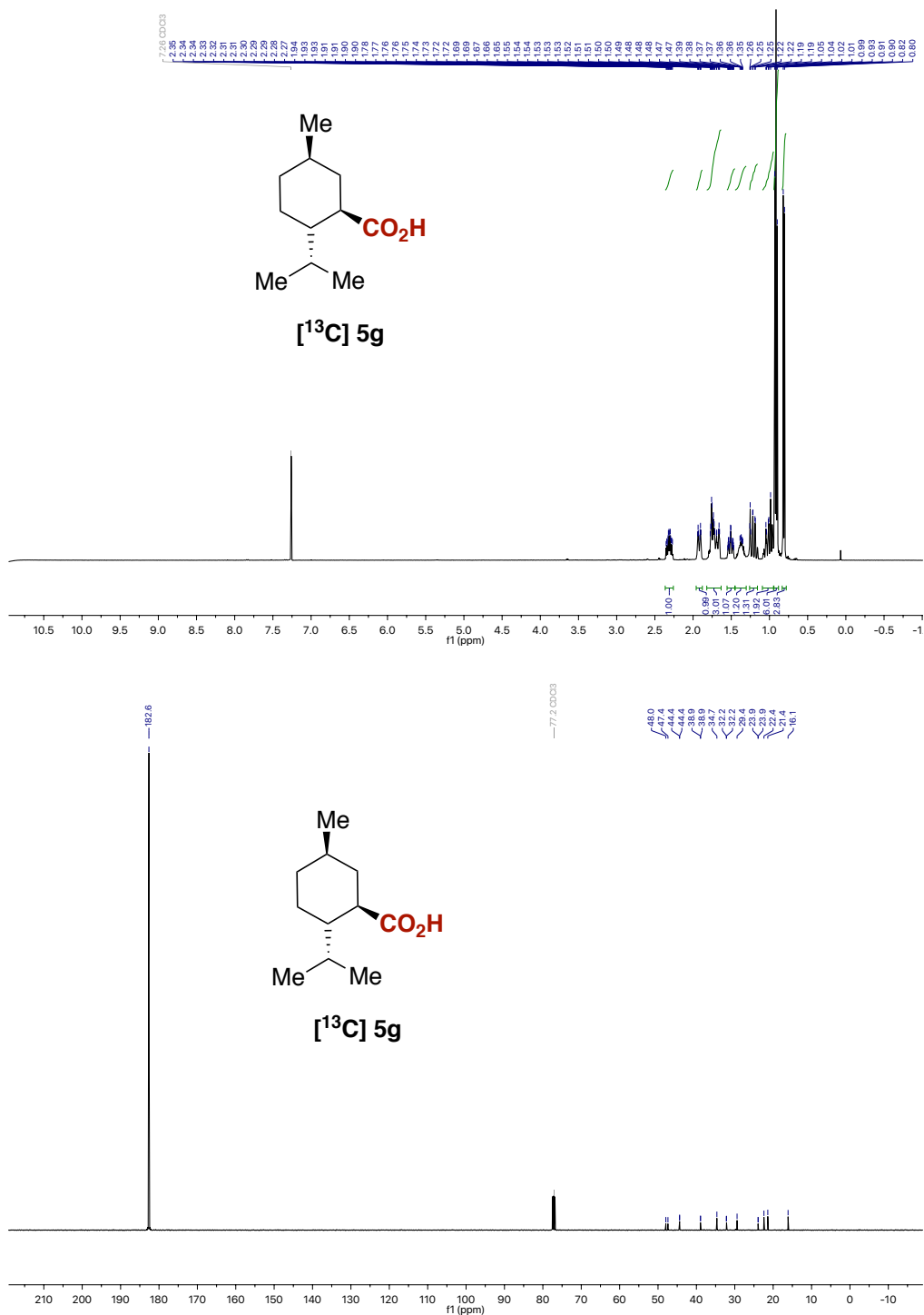


Figure 55. <sup>1</sup>H and <sup>13</sup>C NMR spectra of [13C]5g.

# Catalytic Decarboxylation/Carboxylation Platform for Accessing Isotopically Labeled Carboxylic Acids

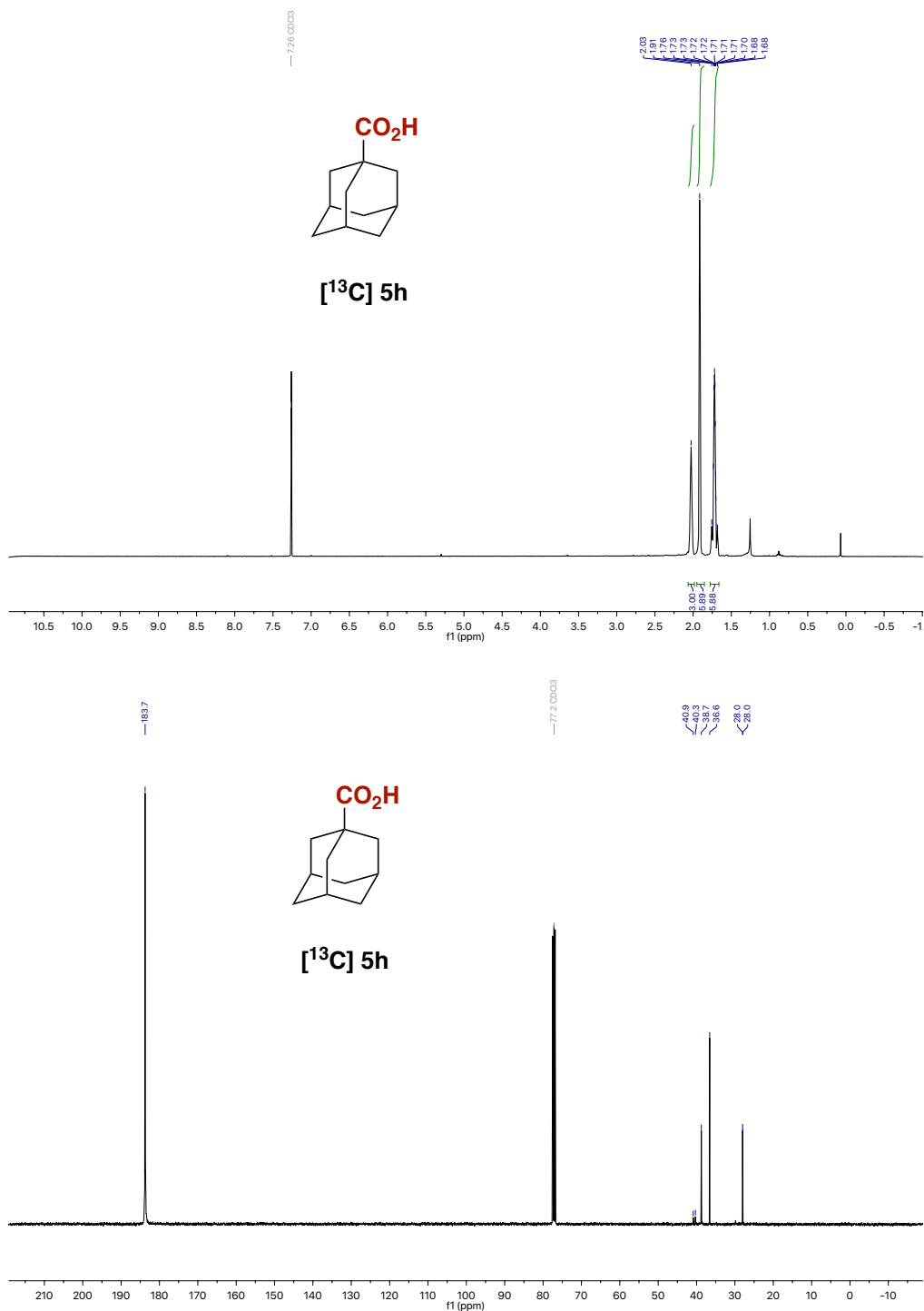


Figure 56. <sup>1</sup>H and <sup>13</sup>C NMR spectra of [<sup>13</sup>C]5h.

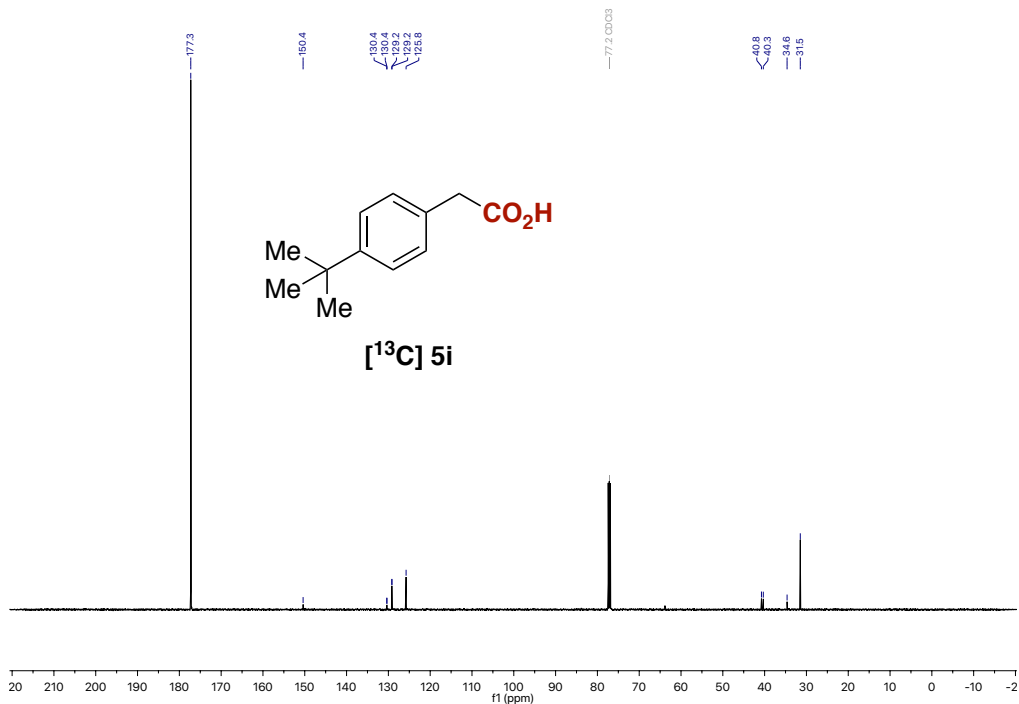
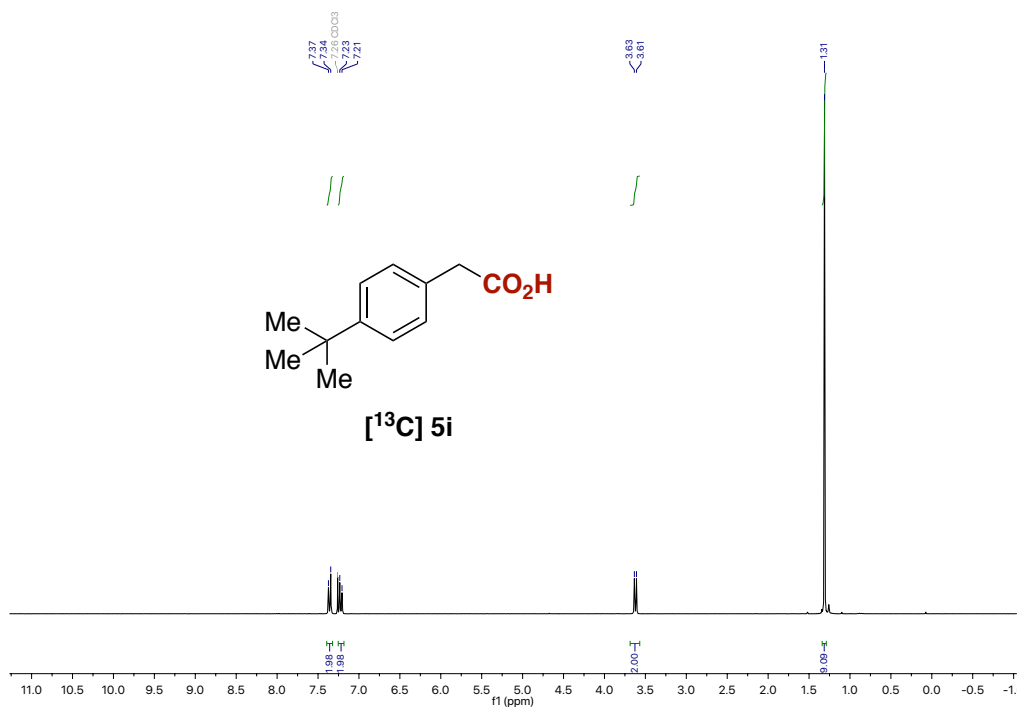
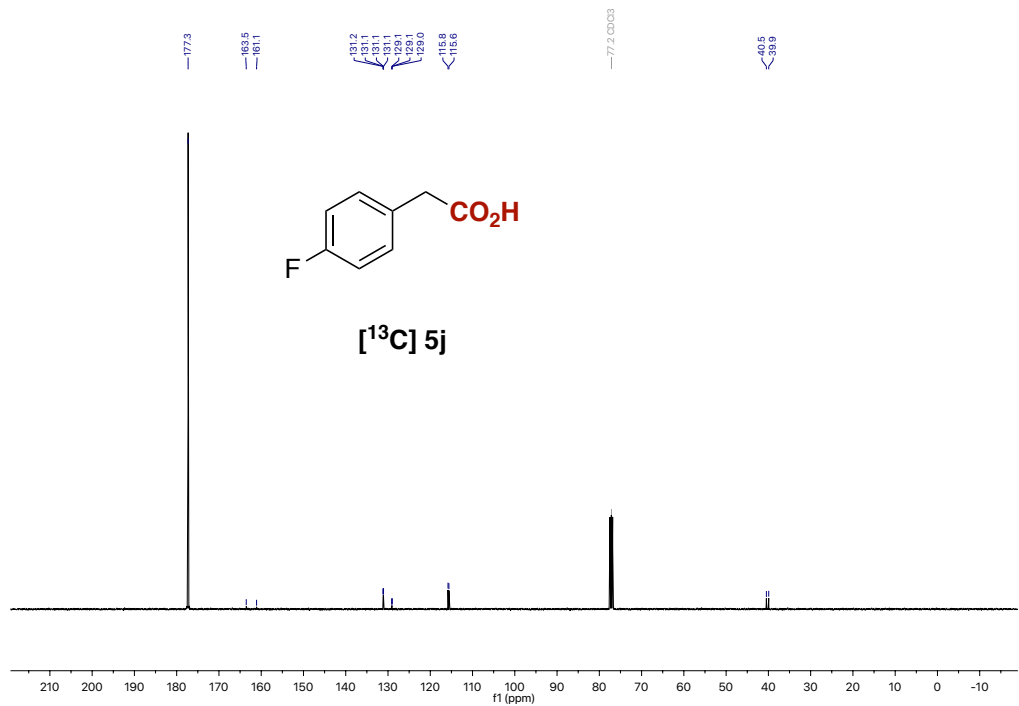
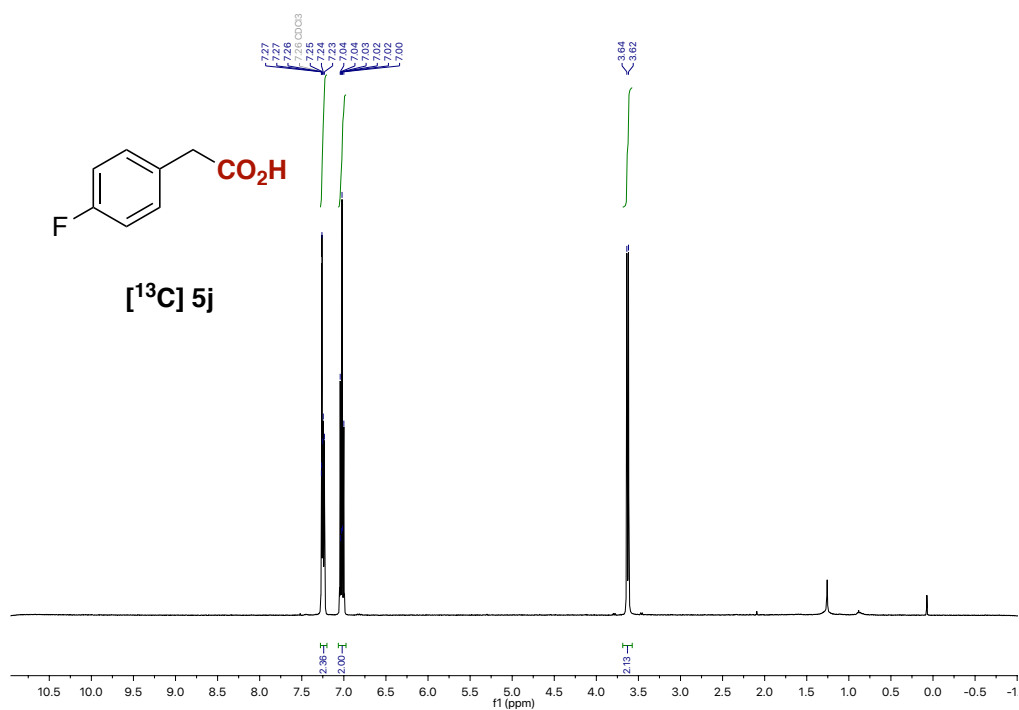


Figure 57. <sup>1</sup>H and <sup>13</sup>C NMR spectra of [13C]5i.

# Catalytic Decarboxylation/Carboxylation Platform for Accessing Isotopically Labeled Carboxylic Acids



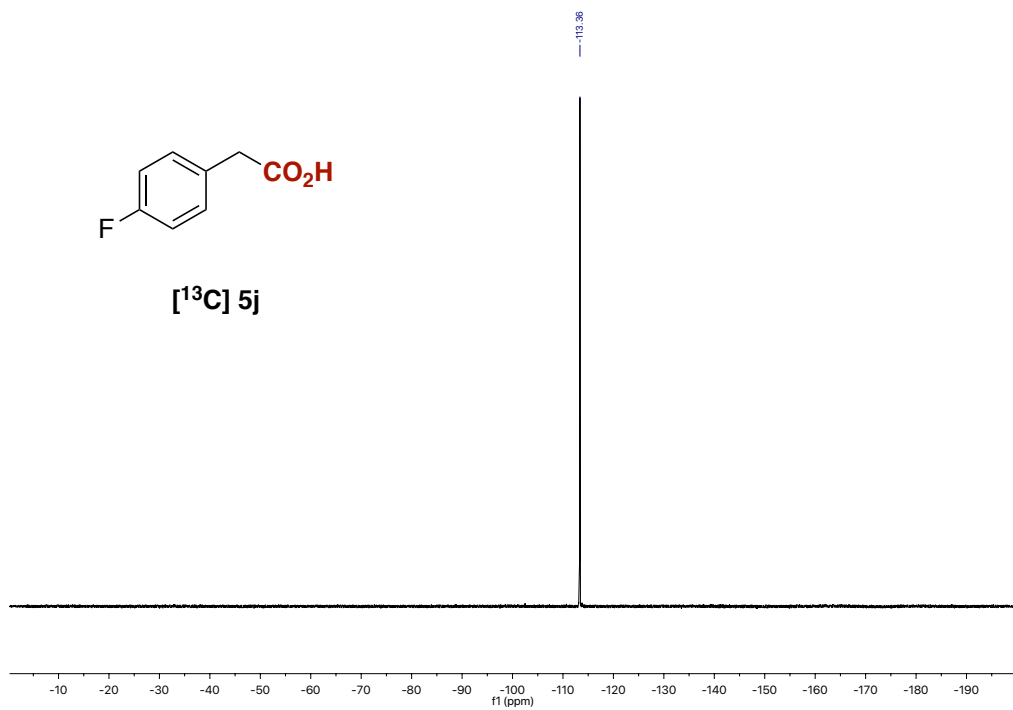


Figure 58.  $^1\text{H}$ ,  $^{13}\text{C}$  and  $^{19}\text{F}$  NMR spectra of  $[^{13}\text{C}] \mathbf{5j}$ .



# Catalytic Decarboxylation/Carboxylation Platform for Accessing Isotopically Labeled Carboxylic Acids

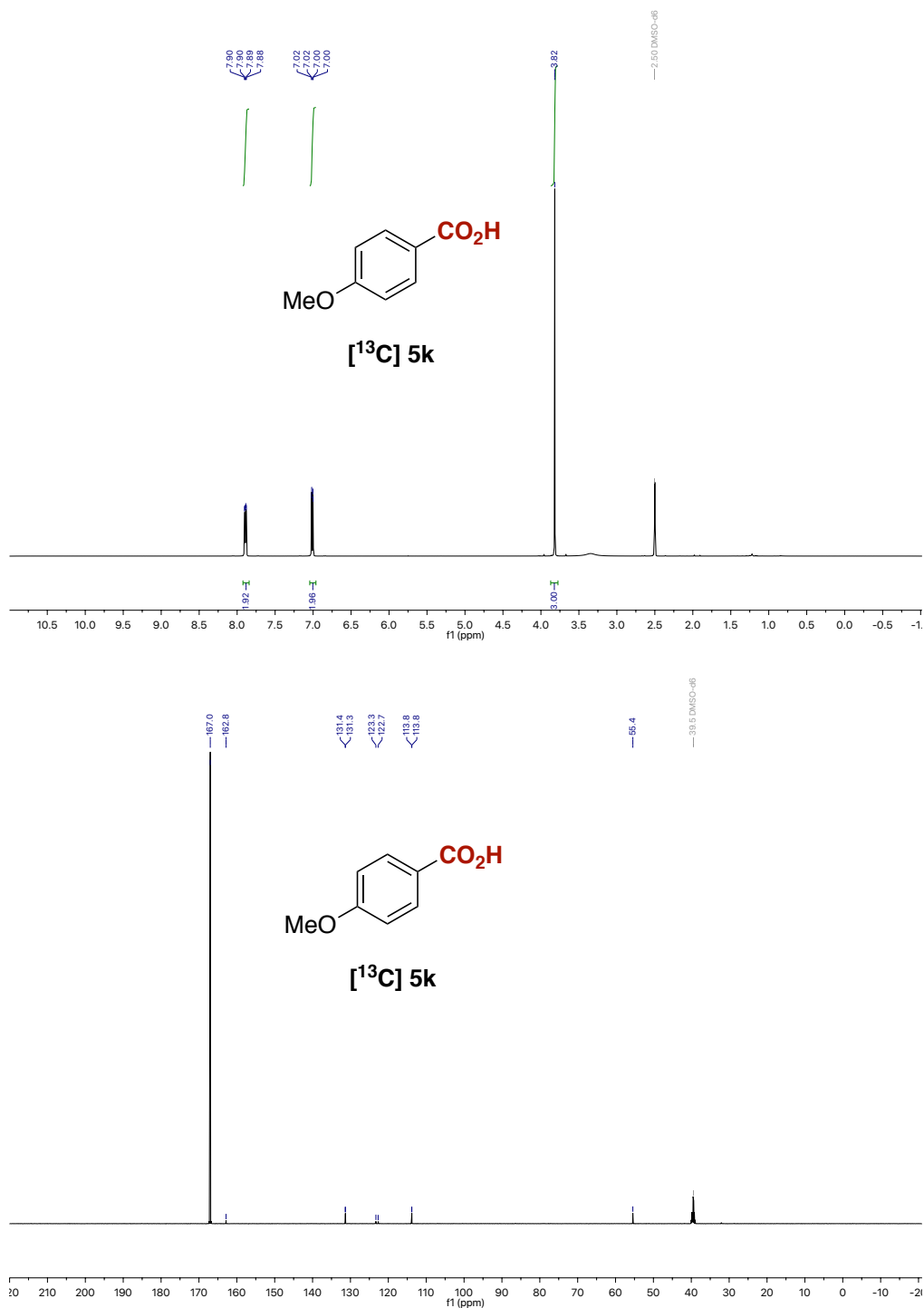


Figure 59. <sup>1</sup>H and <sup>13</sup>C NMR spectra of [<sup>13</sup>C]5k.

Chapter 4

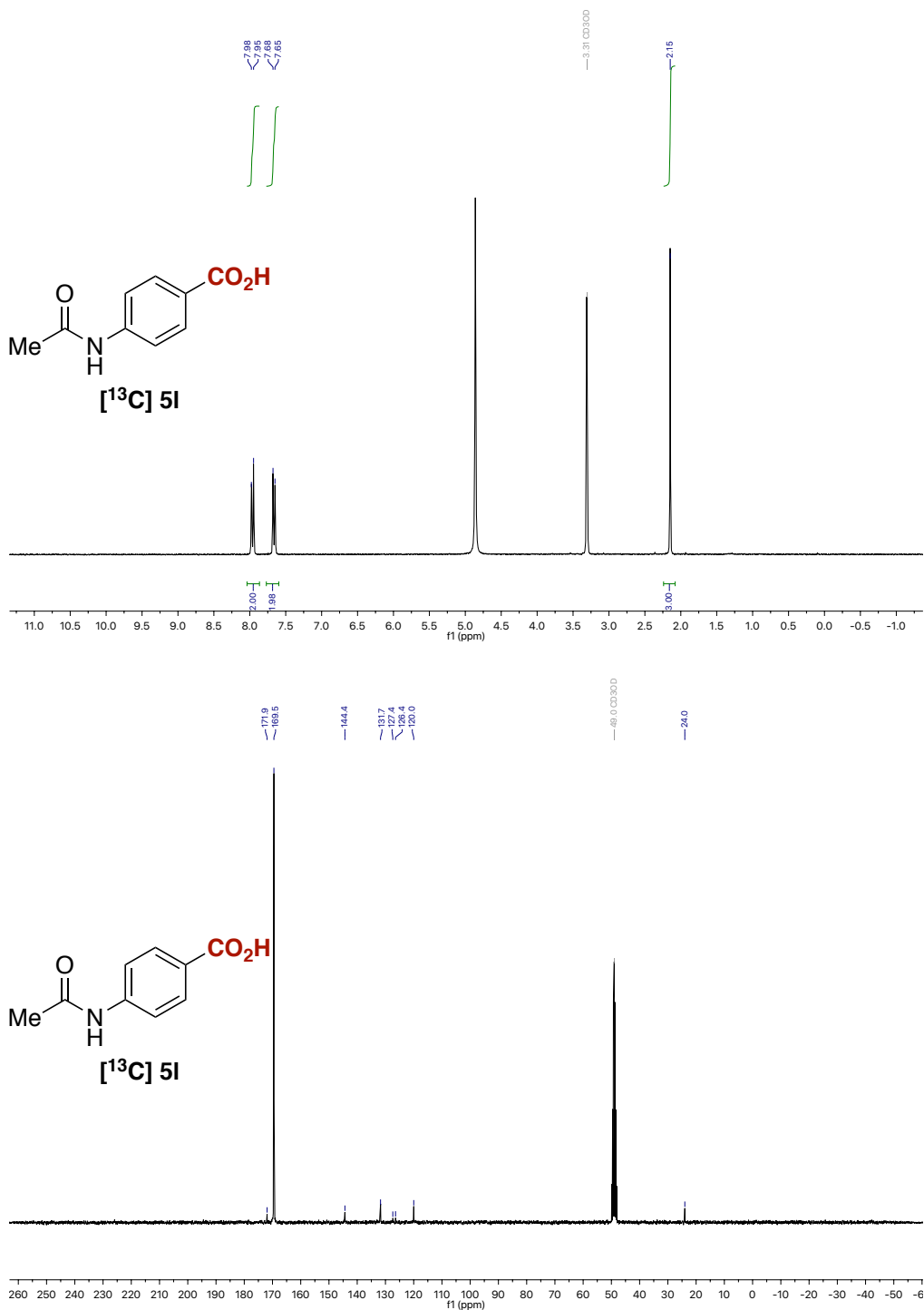


Figure 60. <sup>1</sup>H and <sup>13</sup>C NMR spectra of [13C]5I.

# Catalytic Decarboxylation/Carboxylation Platform for Accessing Isotopically Labeled Carboxylic Acids

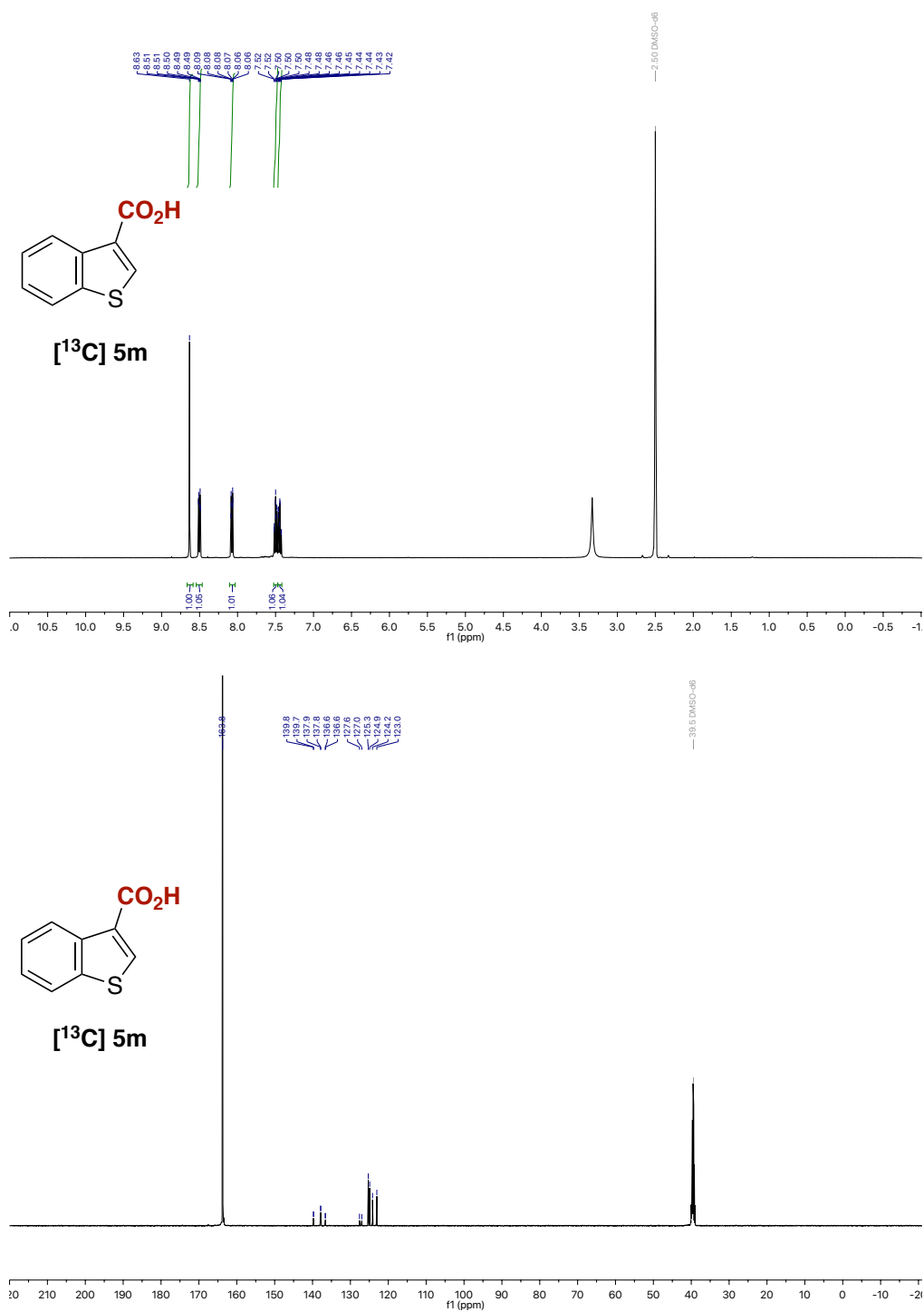


Figure 61. <sup>1</sup>H and <sup>13</sup>C NMR spectra of [13C]5m.

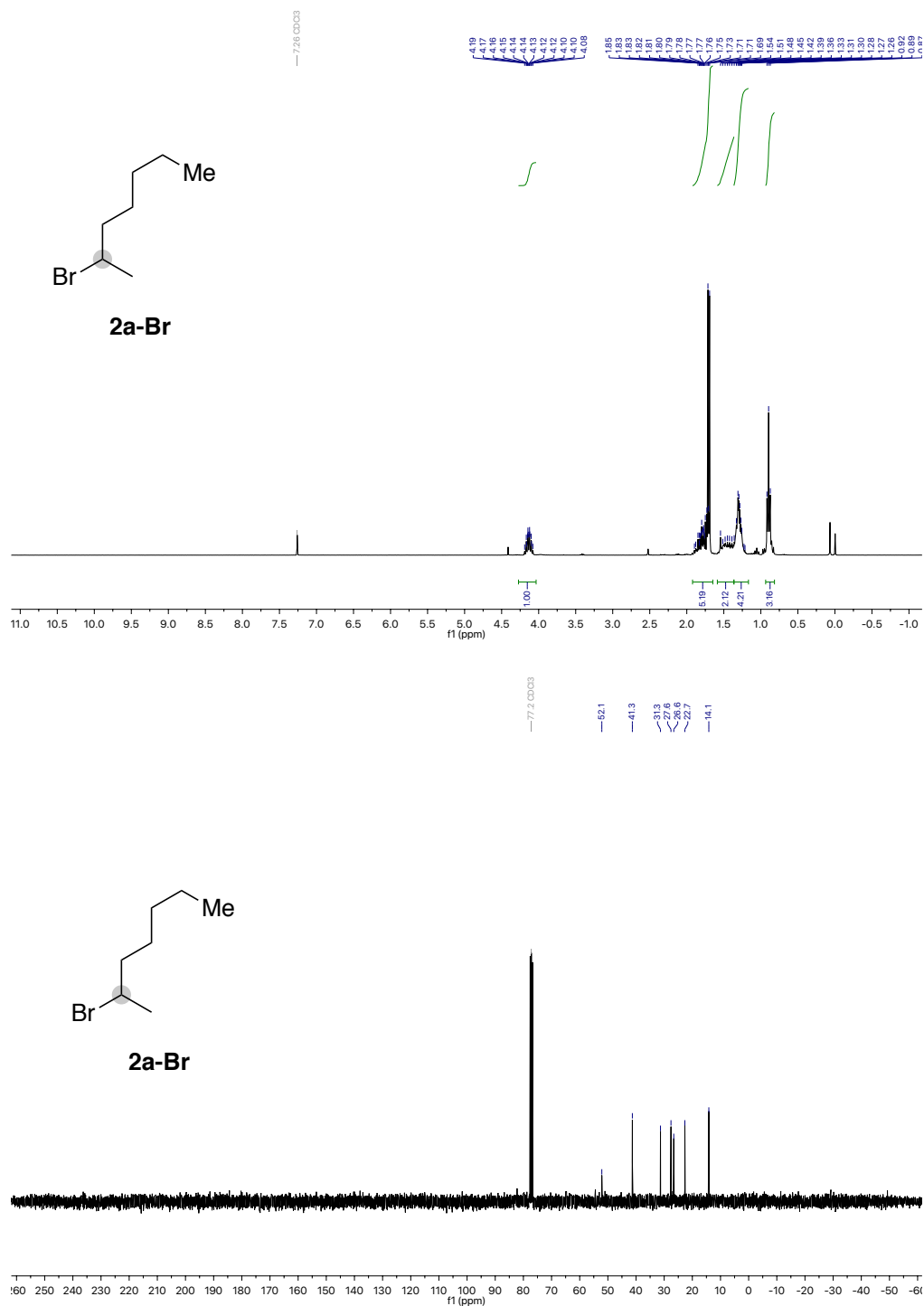


Figure 62.  $^1\text{H}$  and  $^{13}\text{C}$  NMR spectra of **2a-Br**.

Catalytic Decarboxylation/Carboxylation Platform for Accessing Isotopically Labeled Carboxylic Acids

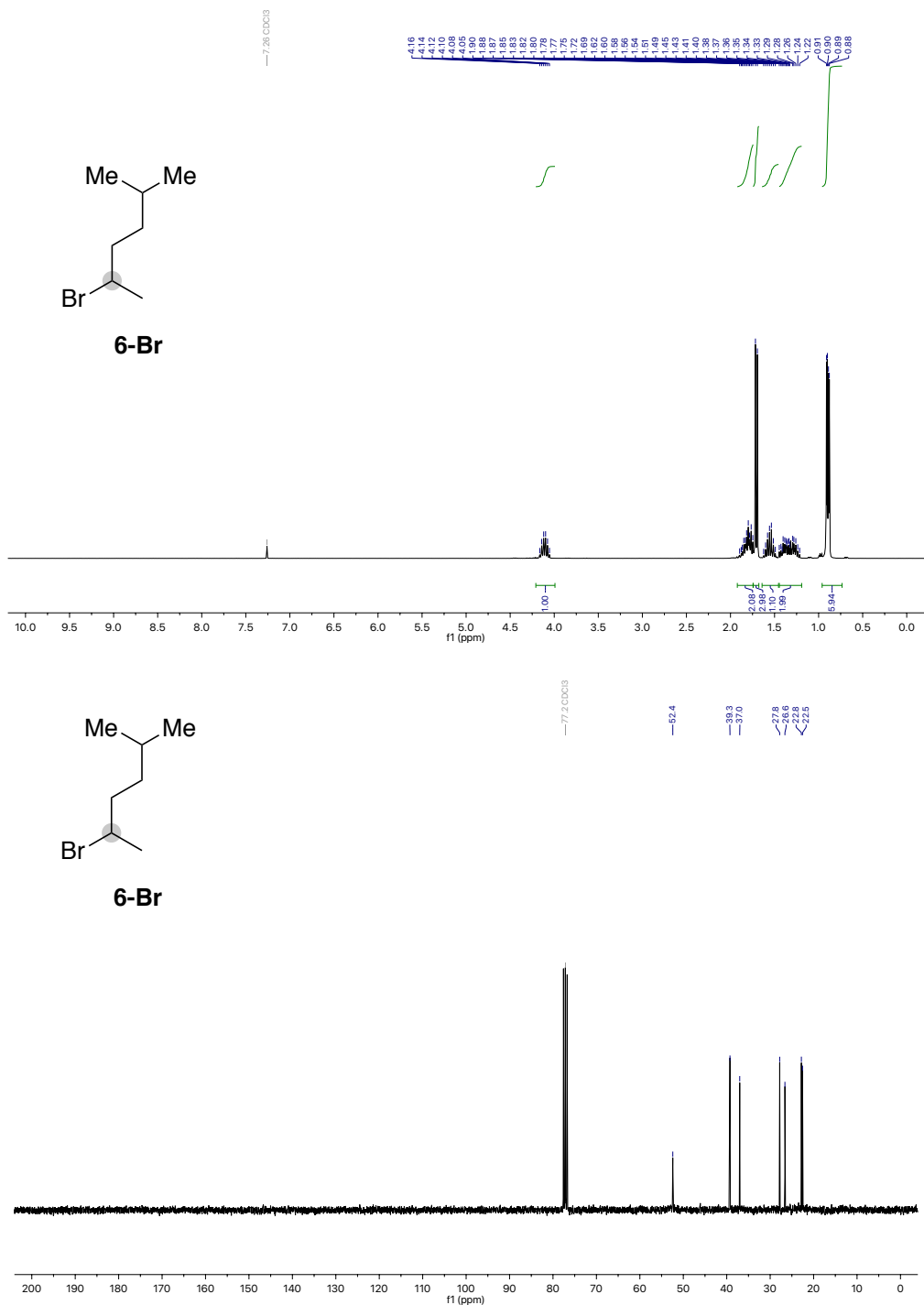


Figure 63. <sup>1</sup>H and <sup>13</sup>C NMR spectra of **6-Br**.

Chapter 4

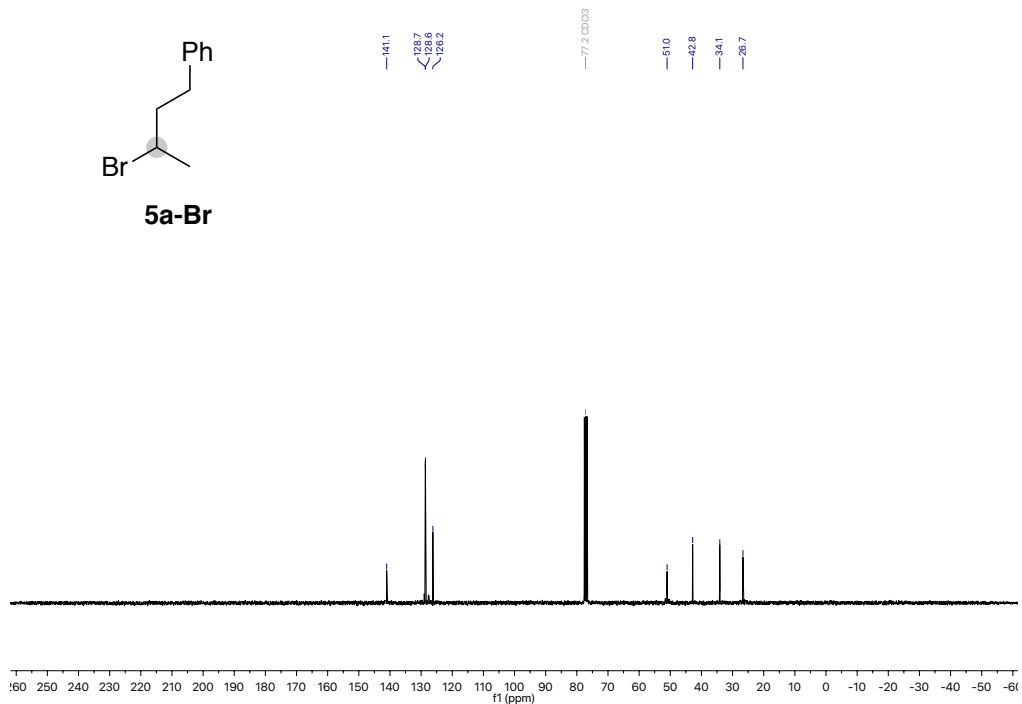
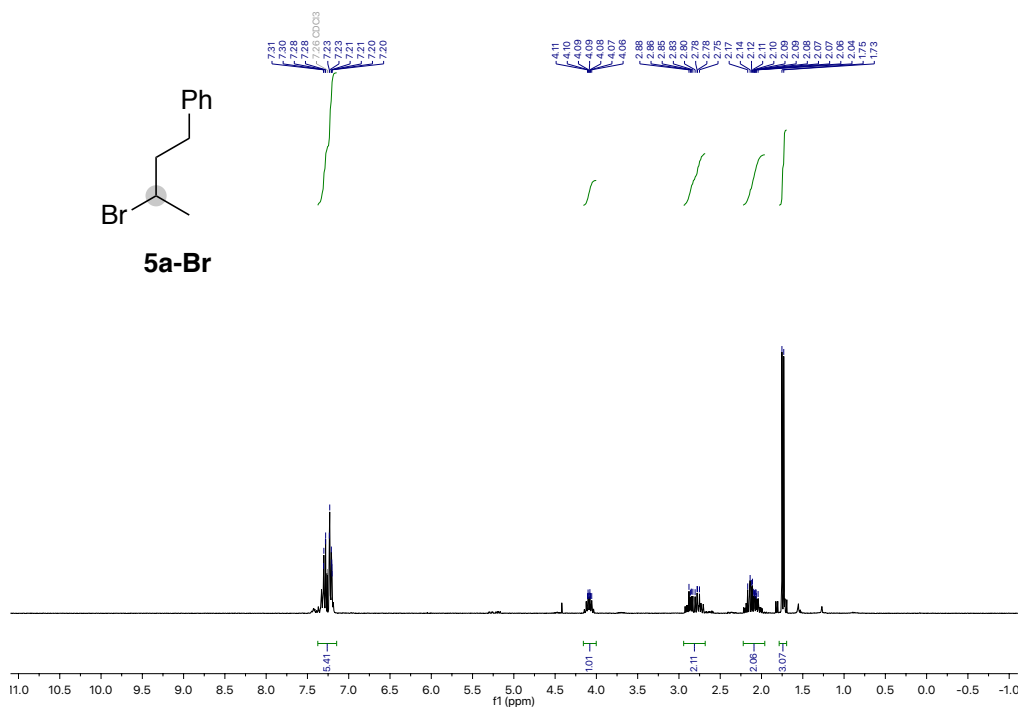


Figure 64. <sup>1</sup>H and <sup>13</sup>C NMR spectra of **5a-Br**.

Catalytic Decarboxylation/Carboxylation Platform for Accessing Isotopically Labeled Carboxylic Acids

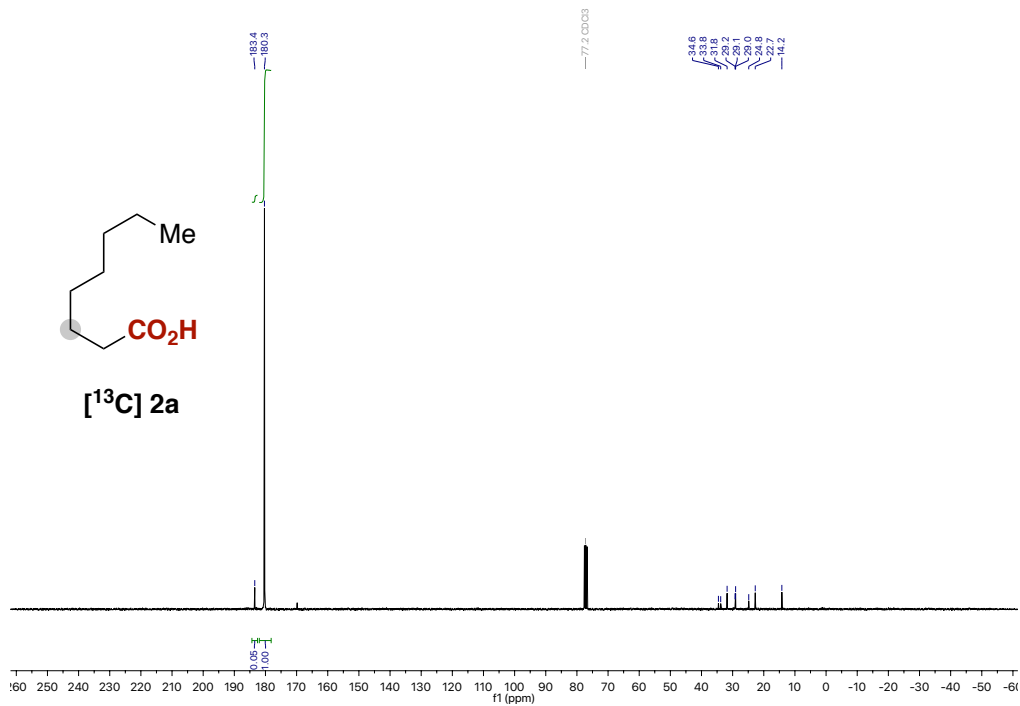
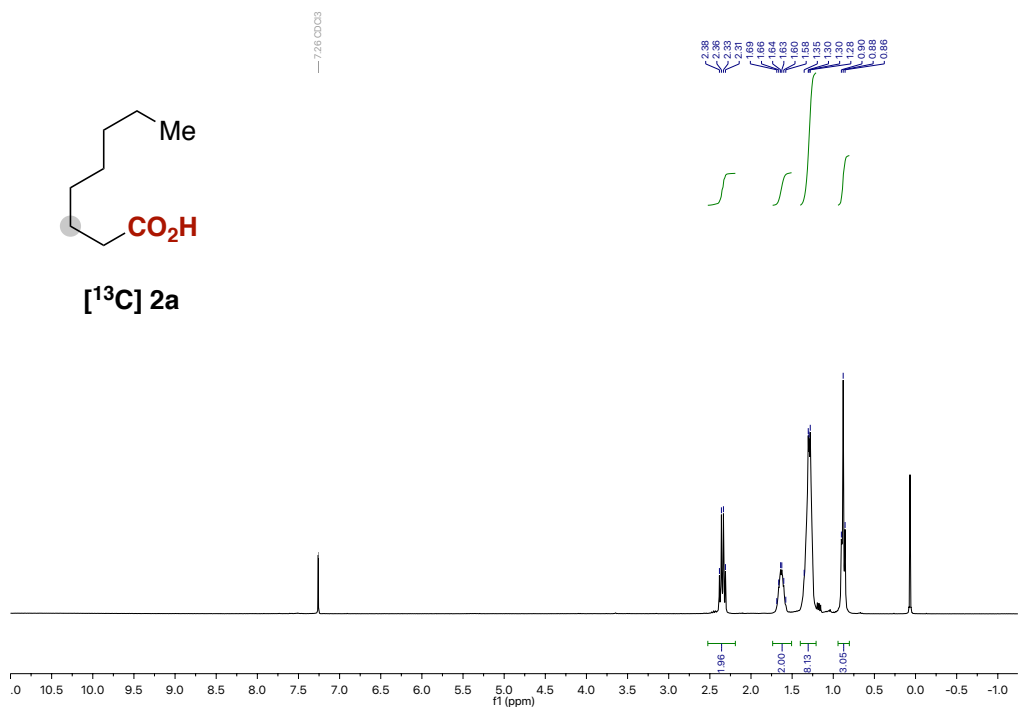


Figure 65. <sup>1</sup>H and <sup>13</sup>C NMR spectra of [<sup>13</sup>C]2a.

Chapter 4

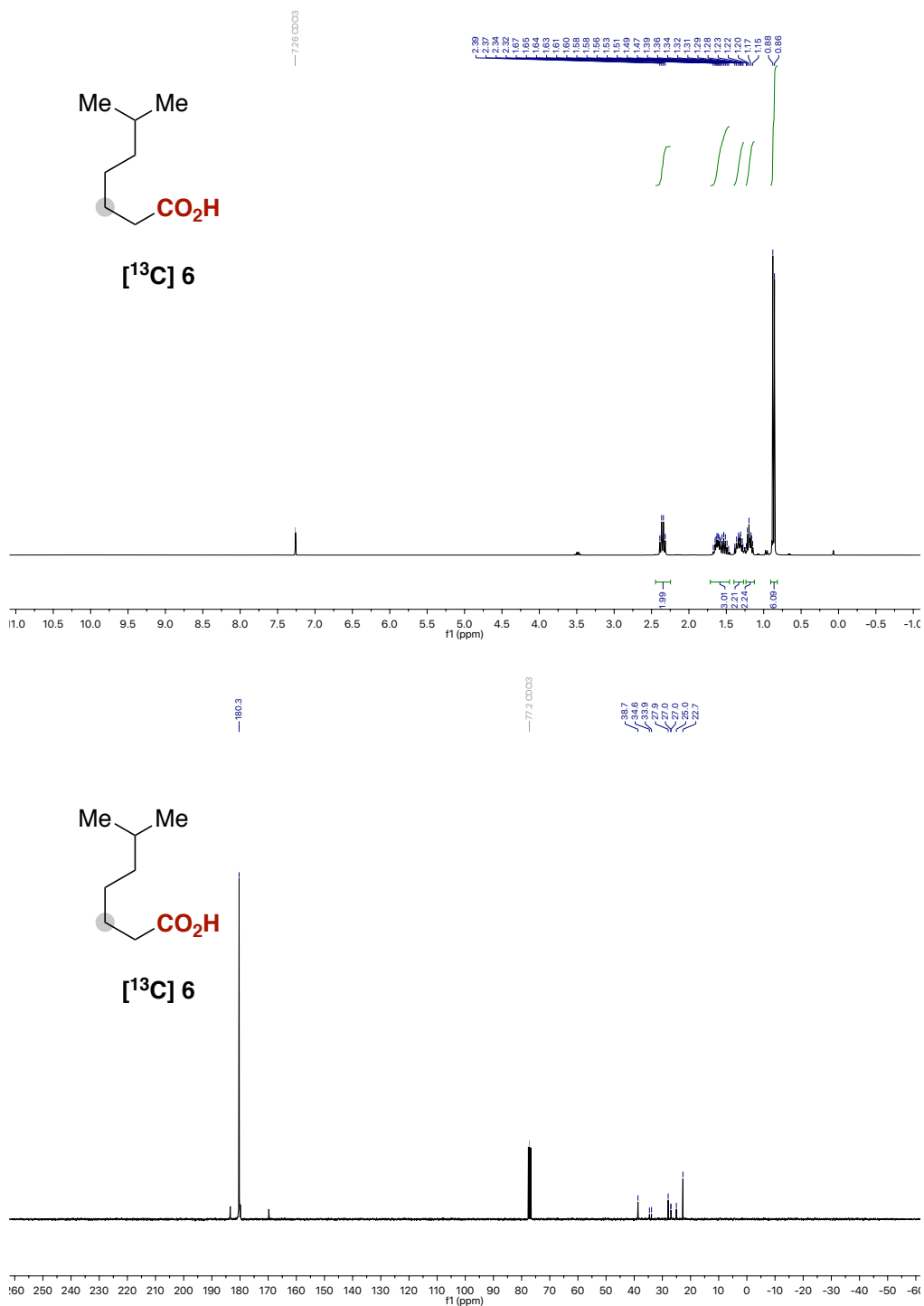


Figure 66. <sup>1</sup>H and <sup>13</sup>C NMR spectra of [<sup>13</sup>C]6.



# Catalytic Decarboxylation/Carboxylation Platform for Accessing Isotopically Labeled Carboxylic Acids

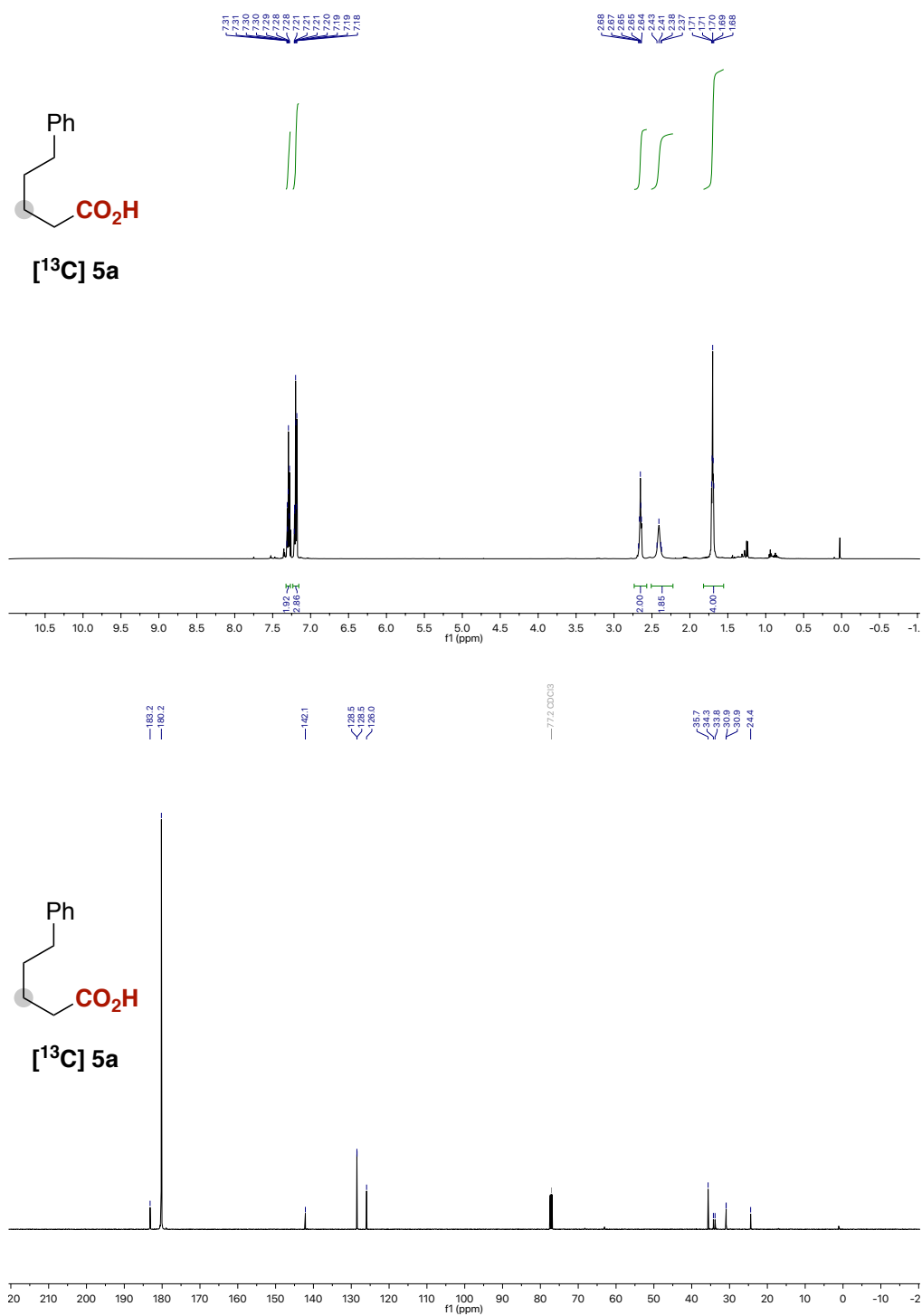


Figure 67. <sup>1</sup>H and <sup>13</sup>C NMR spectra of [<sup>13</sup>C] 5a.



**Chapter 5:**  
***Regiodivergent Ligand-Controlled Ni-Catalyzed Reductive  
Amidation of Unactivated Secondary Alkyl Bromides***

*In collaboration with Dr. Eloisa Serrano, Dr. Alicia Monleón, Dr. Tiago Menezes,  
Alberto Tampieri, Craig Day and Dr. Francisco Juliá-Hernández*

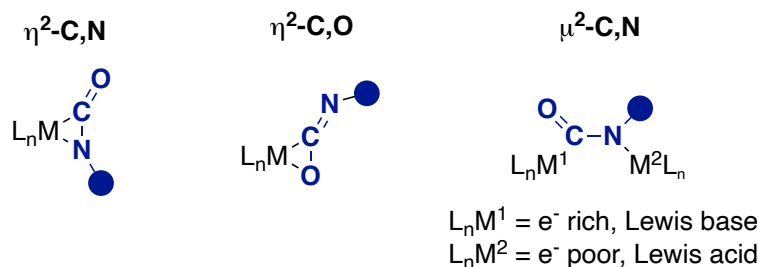


## 1. Introduction

### 1.1 Isocyanates as Amide Synthons

Isocyanates are isoelectronic with carbon dioxide, but the polarization generated by the amido group in the former results in a much higher reactivity when compared with the latter. Even though the nitrogen and oxygen atoms present in the molecule are nucleophilic, the strong electrophilic character of the central carbon dictates the reactivity of isocyanates. This is also modulated by the nitrogen substituent, with aromatic isocyanates being more reactive than alkyl substituted isocyanates for electronic reasons.<sup>1</sup>

Isocyanates can coordinate to transition metals in side-on  $\eta^2$ -C,N or  $\eta^2$ -C,O fashion, where the first mode is more common due to the lower electronegativity of the nitrogen atom.<sup>2,3</sup> Other coordination modes involve  $\mu^2$ - or even  $\mu^3$ - in which the isocyanates act as a bridging ligand between different metallic centers. Coordination of an isocyanate to a metal bends the molecule with the loss of its linearity (in a similar way to CO<sub>2</sub>). This effect significantly lowers its activation energy, hence favoring reactions with less-reactive nucleophilic partners (Figure 1).

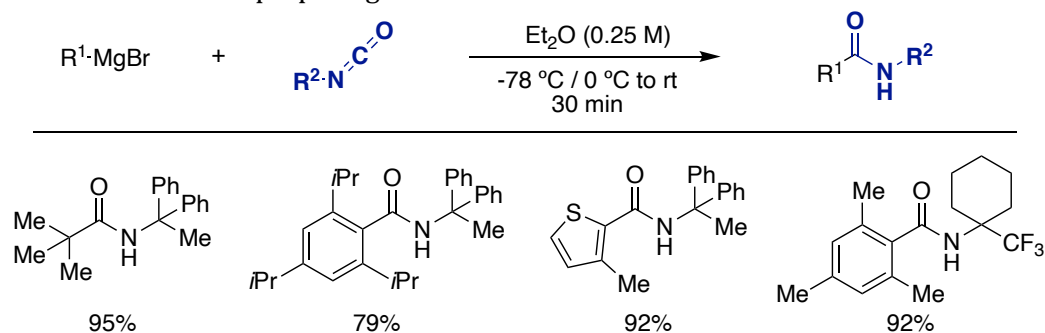


**Figure 1.** Common coordination modes of isocyanates.

The activation of isocyanates by transition metals has been exploited for the synthesis of industrially relevant compounds. One example are polyurethanes, which are formed by condensation reactions with nucleophiles and diisocyanates. Other examples are isocyanurates, and related compounds, which are produced by metal-mediated or metal-catalyzed dimerization and (cyclo)trimerization reactions as well as carbamates or ureas, which are generated by reaction of isocyanates with nucleophiles.<sup>1,4</sup> However, this reactivity hampers the use of isocyanates as amide synthons in metal-catalyzed transformations, as it leads to the generation of undesired products, and often increases the amount of isocyanate required for the reaction. Metal catalysts relevant to this chapter, such as nickel(II) halide salts<sup>5</sup> and zero-valent metal complexes,<sup>6,7</sup> have been reported to trimerize aryl and alkyl isocyanates.

The first use of isocyanates as amide synthons was within the context of coupling reactions with organometallic reagents. These methods have mostly been developed

using well-defined Grignard reagents, organolithium, and organozinc derivatives. Although these species can be accessed via classical metallation techniques, their air sensitivity, high reactivity, and low functional group tolerance are the major drawbacks that have restricted their wide application for the synthesis of amides. The first reports on the addition of organolithium or Grignard reagents to isocyanates date back to the early 19th century by Blaise<sup>8</sup> and Gilman<sup>9-11</sup> groups. This seminal work inspired the development of various methods for the addition of these reagents to isocyanates and isothiocyanates, including the stereospecific addition of chiral alkyl lithium reagents.<sup>12</sup> In 2012 the group of Bode reported a general method for the addition of organomagnesium bromides to isocyanates to access sterically hindered and electron-deficient secondary amides (Scheme 1),<sup>13</sup> which are difficult to access via traditional C–N bond-forming methods. This protocol tolerated sensitive functional groups by employing low reaction temperatures. Moreover, a variety of organozinc reagents have been added as well to isocyanates to afford aliphatic and aromatic amides. Although these organometallic species have a good functional group tolerance, their use still remains limited for preparing amides.



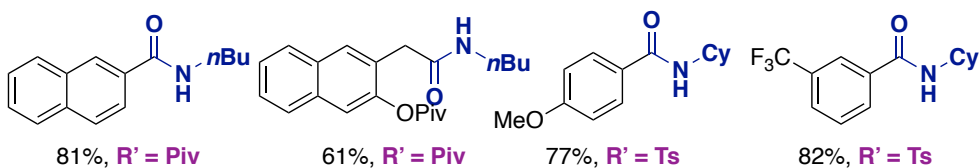
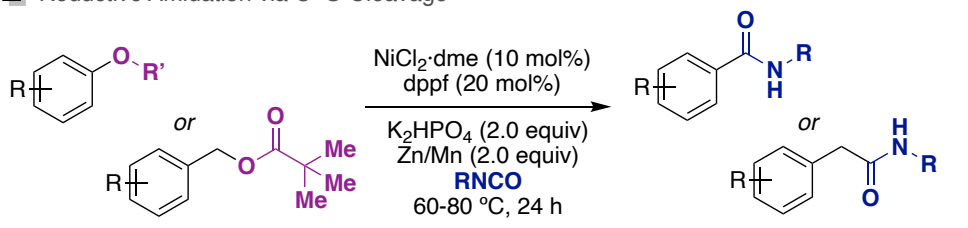
**Scheme 1.** Direct addition of Grignard to isocyanates.

An alternative approach to the direct addition of carbogenic nucleophiles to isocyanates for the formation of amides is the transition metal-catalyzed C–C coupling. Ni, Pd, Ti and Rh have been the most used transition metals in combination with nucleophiles (i.e. organostannanes, Grignard reagents or boronic acids) or electrophiles (alkyl silicates,  $\pi$ -component or alkyl halides).<sup>14</sup> The combination of isocyanates with electrophiles constitutes formal cross-reductive coupling (see Chapter 1) and therefore a reducing agent is necessary. Our group has reported in the last years the nickel-catalyzed amidation of different electrophiles with isocyanates. In 2014, the amidation of aryl/benzyl pivalates and tosylates was reported by means of C–O cleavage using phosphines as supporting ligands for the nickel center (Scheme 2, *top*).<sup>15</sup> Two years later, the amidation of unactivated alkyl bromides was described, using this time bipyridine ligands for the formation of aliphatic hindered amides (Scheme 2, *middle*).<sup>16</sup> On the same year, and by exploiting

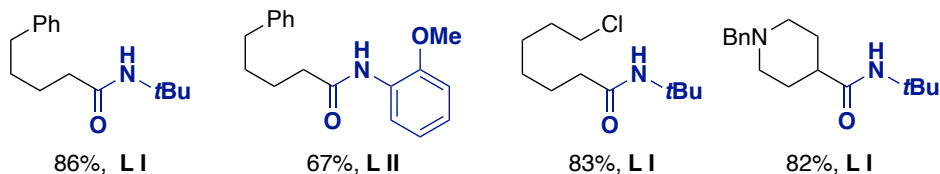
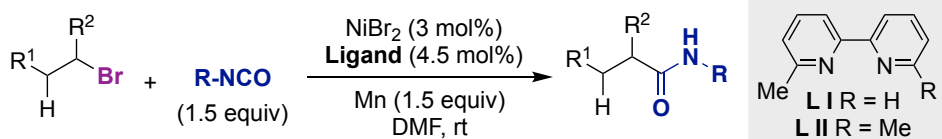
## Regiodivergent Ligand-Controlled Ni-Catalyzed Reductive Amidation of Unactivated Secondary Alkyl Bromides

the easy decomposition of alkyl nickel species to form nickel hydrides, we developed a hydroamidation of alkynes en route to acrylamides (Scheme 2, *bottom*).<sup>17</sup>

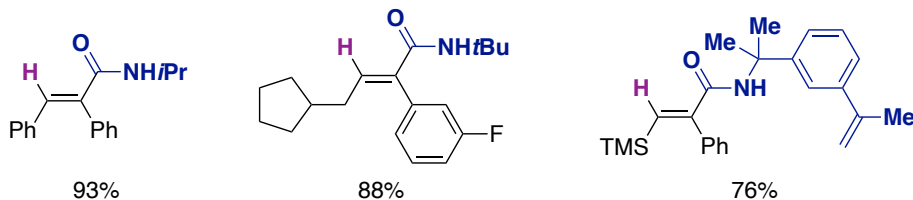
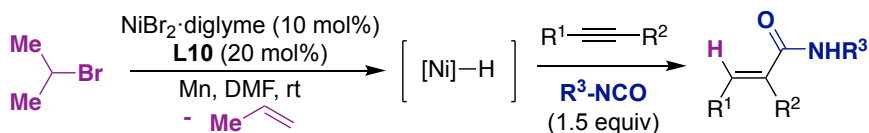
### □ Reductive Amidation via C–O Cleavage



### □ Ni-catalyzed Amidation of Unactivated Alkyl Bromides



### □ Alkyl Bromides as Mild Hydride Source for Hydroamidations of Alkynes with Isocyanates

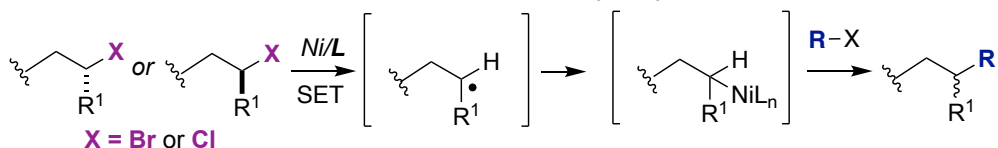


**Scheme 2.** Ni-catalyzed amidation with isocyanates.

## 1.2 Metal-Catalyzed Functionalization of Unactivated Secondary Alkyl Halides

The cross-coupling of unactivated alkyl halides is typically hampered by a more difficult oxidative addition compared to aromatic electrophiles, a slower reductive elimination for  $C(sp^3)-M-C(sp^2)/C(sp^3)$  than for  $C(sp^2)-M-C(sp^2)$  species, and a propensity to undergo undesired pathways. The typical undesired side reactions are protodemetalation,  $\beta$ -hydride elimination and dimerization reactions, which arise from the lower stability of alkyl-metal species. Specifically, for secondary and tertiary alkyl halides the added steric hindrance in comparison with primary alkyl halides hampers oxidative addition, and the presence of additional neighboring  $\beta$ -hydrogens in the alkyl-metal intermediates increases the probability of  $\beta$ -hydride elimination.<sup>18,19</sup>

The pioneering work of Fu and Zhou on the Ni-catalyzed Negishi cross-coupling of secondary alkyl bromides and iodides represented a significant step forward on the use of unactivated alkyl halides in cross-coupling methodologies,<sup>20</sup> unlocking new disconnection that are not available via traditional approaches. These methods have been developed with Ni, Co, Fe and Pd catalysis.<sup>21</sup> Due to the lower propensity of nickel to undergo  $\beta$ -hydride elimination, in comparison to more electronegative metals such as Pd, Ni based catalysts have proven to be particularly suitable for the formation of  $C(sp^3)-C(sp^2)$  and  $C(sp^3)-C(sp^3)$  bonds from unactivated alkyl halides via traditional cross-coupling reactions with organometallic reagents,<sup>22</sup> reductive cross-electrophile couplings<sup>23,24</sup> or metallaphotoredox reactions.<sup>25-27</sup> The mechanism of such transformations generally includes the intermediacy of radical species (Scheme 3), which inspired the development of enantioconvergent transformations that start from racemic secondary alkyl halides.<sup>28,29</sup>



**Scheme 3.** SET-type oxidative addition.

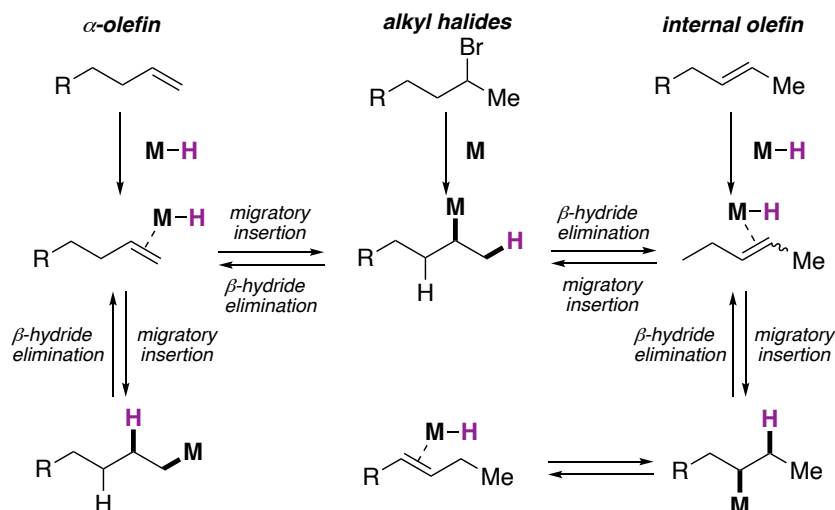
## 1.3 Metal Chain-Walking, a Strategy for Remote $sp^3$ C-H Functionalization

The selective functionalization of  $C(sp^3)-H$  bonds is a non-trivial task due to its high bond energy, the lack of  $\pi$ -bonds that readily interact with transition metals, and the difficult-to-control site-selectivity, which arises from the presence of multiple similar  $C(sp^3)-H$  bonds within a hydrocarbon scaffold.<sup>30</sup> Different approaches have been followed towards overcoming these challenges: the use of pre-installed directing groups,<sup>31</sup> more challenging undirected approaches based on the intermediacy of radical species<sup>32</sup> and non-covalent interactions between an enzyme



and a substrate.<sup>33</sup> Despite these efforts, the site site-selective C–C bond formation at stronger, primary C(*sp*<sup>3</sup>)–H bonds remains a challenging task.

An alternative approach towards remote C(*sp*<sup>3</sup>)–H functionalization that has been studied is the use of transition metals capable of migrating the reactive site of a molecule along a hydrocarbon skeleton to reach a terminal primary position where a terminating reaction takes place.<sup>34</sup> In this strategy, a suitable transition metal reacts with the substrate's most reactive site to form an alkyl metal intermediate. From this species, the metal is able to migrate via iterative  $\beta$ -hydride elimination/migratory insertion reactions along the hydrocarbon chain, in a process called "chain walking" or "chain running".<sup>35</sup> The formation of the active migrating species can be triggered by either reaction between the transition metal and a C–C double bond present in the substrate, or by oxidative addition to alkyl electrophiles (Figure 2). Different transition metals such as Zr, Rh, Ru, Ir and Pd have been used to achieve chain-walking hydroboration, hydrosilylation, hydroformylation and hydroarylation reactions, among others.<sup>36</sup> More recently, methods that use more sustainable systems based on base-metal catalysts such as Co, Fe and Ni have received increased attention.<sup>34</sup>



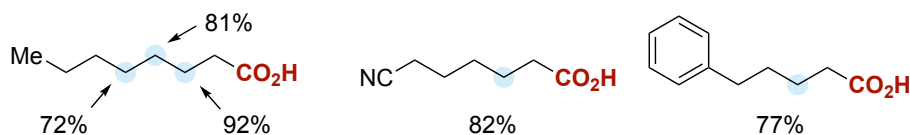
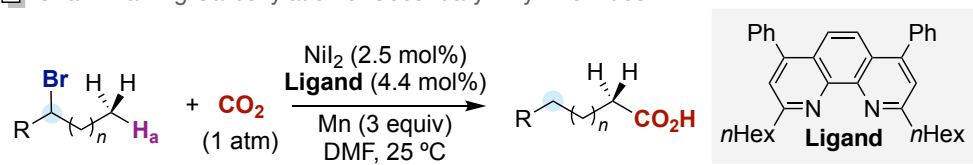
**Figure 2.** Chain-walking by migratory insertion and  $\beta$ -hydride elimination.

#### 1.4 Ni-Catalyzed Chain-Walking Functionalization

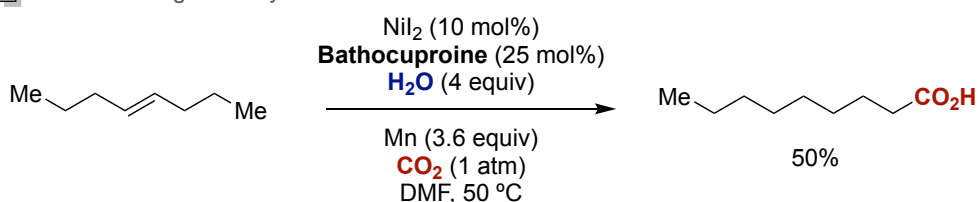
The utilization of Ni-catalysts capable of olefin isomerization has been of high importance in multi-ton industrial processes such as the Shell higher olefin process (SHOP) for ethylene oligomerization to  $\alpha$ -olefins and DuPont's hydrocyanation of 1,3-butadiene for adiponitrile production.<sup>37,38</sup> Moreover, in the 1990's, Brookhart

and co-workers reported cationic Ni- $\alpha$ -diimine complexes that were highly active in the polymerization of  $\alpha$ -olefins. These catalysts were able to generate polymers with linear segments via chain-walking olefin isomerization.<sup>35,39</sup> These discoveries set the stage for designing new Ni-catalyzed chain-walking transformations that enable the formal C( $sp^3$ )-H functionalization at remote positions within a saturated hydrocarbon chain.<sup>40</sup> Our research group has reported several contribution to this field of expertise in the past years. As described in Chapter 1, in 2017 the chain-walking carboxylation of secondary unactivated alkyl bromides was reported to form the corresponding carboxylic acids (Scheme 4, *top*).<sup>41</sup> In 2019, this reaction was also performed by photometalloreduct catalysis, avoiding the use of a metallic reductant.<sup>42</sup> The hydrocarboxylation of unactivated internal olefins was achieved by using water as hydride source (Scheme 4, *middle*)<sup>43</sup> and the hydrofunctionalization of unactivated alkenes was further developed with the chain-walking alkylation using this time silanes as hydride source (Scheme 4, *bottom*),<sup>44,45</sup> forming a diverse set of densely functionalized compounds with an excellent chemoselectivity.

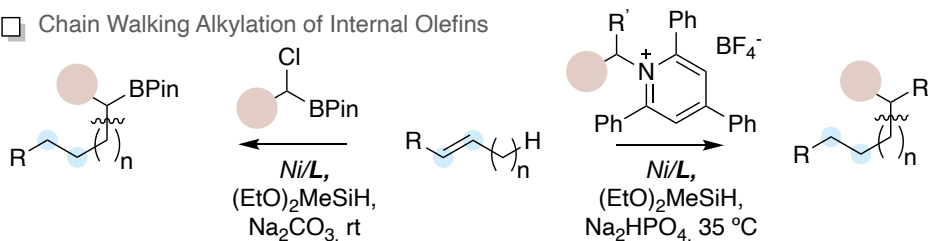
□ Chain Walking Carboxylation of Secondary Alkyl Bromides



□ Chain Walking Carboxylation of Internal Olefins to Linear Acids



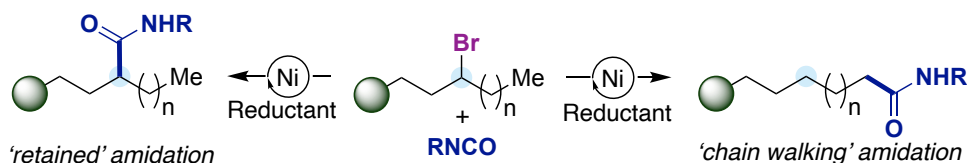
□ Chain Walking Alkylation of Internal Olefins



**Scheme 4.** Chain walking functionalizations reported by our group.

## 2. General aim of the project

The capability to control the outcome of catalytic reactions by fine-tuning modulation of the catalyst is of utmost synthetic relevance within the cross-coupling arena.<sup>46</sup> Indeed, the development of catalytic regiodivergent protocols from common precursors with precise control of the selectivity pattern is still an important challenge, thus providing an opportunity to improve our chemical portfolio. Notably, while unactivated secondary alkyl halides are electrophiles that have been used extensively in classical metal-catalyzed cross-coupling reactions, the vast majority of these processes trigger the functionalization event at the initial site of the carbon-halide bond. It was not until recently that the functionalization of remote positions via ‘chain walking’ strategies using these electrophiles has been investigated, providing a new approach for selective functionalization of C(*sp*<sup>3</sup>)-H bonds. It is considered a non-trivial task due to its high bond energy, the lack of  $\pi$ -bonds that readily interact with transition metals and the difficult-to-control site-selectivity. However, the development of catalytic regiodivergent strategies to functionalize a secondary alkyl bromide at will and with high selectivity remains unexplored and represents the main goal of this chapter. Achieving this goal would require the design of two different catalytic systems that either suppress or facilitate  $\beta$ -hydride elimination from the alkyl-metal intermediates generated upon oxidative addition into the C-Br bond (Scheme 5).



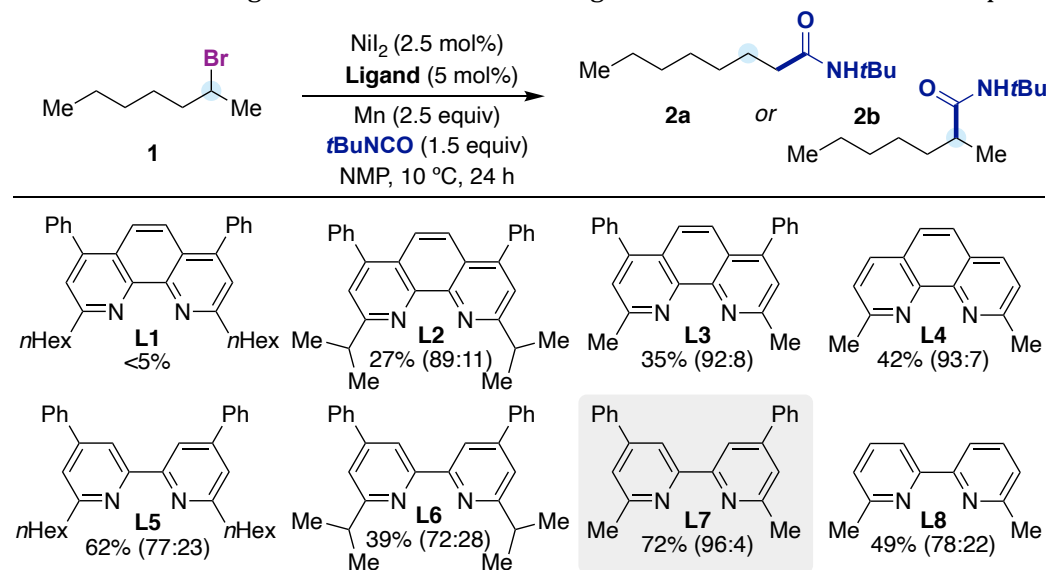
**Scheme 5.** Ni-catalyzed regiodivergent amidation of alkyl bromides.

The main challenges associated with the development of an amidation procedure for secondary alkyl halides are the high propensity of branched alkyl-Ni species to suffer decomposition by  $\beta$ -hydride elimination or other undesired pathways, and the increased steric hindrance of the substrate that could slow the oxidative additions and difficult isocyanate insertion. Furthermore, the development of a remote amidation protocol of primary *sp*<sup>3</sup> C-H bonds has an increased complexity because of the strong binding properties of isocyanates to transition metals (unlike CO<sub>2</sub> or other electrophiles) and the higher solubility and reactivity of isocyanates compared to CO<sub>2</sub>, which facilitates the amidation at the initial reactive site.

### 3. Regiodivergent Reductive Amidation of Unactivated Secondary Alkyl Bromides with Isocyanates.

#### 3.1. Optimization of the reaction conditions

The first efforts towards the Ni-catalyzed amidation of secondary alkyl bromides in the remote primary position were made with similar conditions to the chain-walking carboxylation with CO<sub>2</sub>. 2-Bromoheptane (**1**) was chosen as a model substrate and different bipyridine and phenanthroline ligands were tested, using NiI<sub>2</sub> as a nickel source and *t*BuNCO as the model isocyanate (Table 1). When the ligand previously used for the carboxylation project was used (**L1**), very low yield of amidation product was observed. The change of the hexyl group by an isopropyl group (**L2**) improved the yield observed up to 27%, while its substitution by a methyl group (**L3**) results in 35% yield with a similar selectivity. The removal of the phenyl groups in the backbone of the phenanthroline ligand (**L4**) had a small impact. If the same substitutions are tested with the bipyridine scaffold (**L5-L8**) better amidation yields are observed. Larger hexyl and isopropyl groups in the positions next to the nitrogen atoms (**L5** and **L6**) showed worse yields and selectivity than placing a methyl group (**L7**). In this occasion the phenyl groups in the bipyridine were crucial to obtain good amidation selectivity and yield. As it can be seen, small differences in the ligand backbone exerted a big influence in the amidation output.

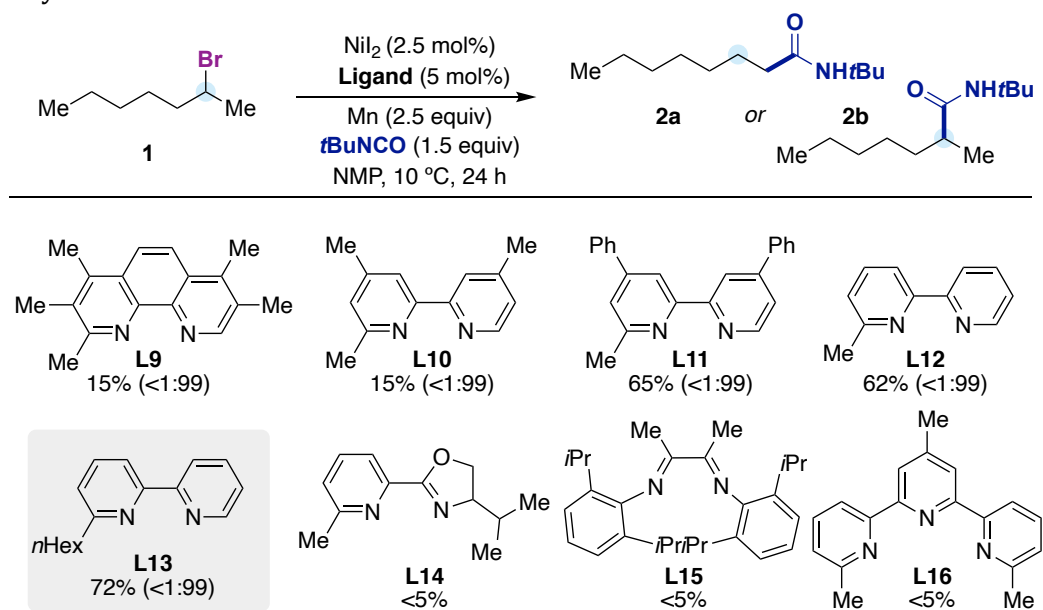


Conditions: **1** (0.50 mmol), *t*BuNCO (0.75 mmol), NiI<sub>2</sub> (2.5 mol%), ligand (5 mol%), Mn (1.25 mmol), NMP (1 mL) at 10 °C, 24 h.

**Table 1.** Ligand screening for the amidation of 2-bromoheptane with isocyanates.

## Regiodivergent Ligand-Controlled Ni-Catalyzed Reductive Amidation of Unactivated Secondary Alkyl Bromides

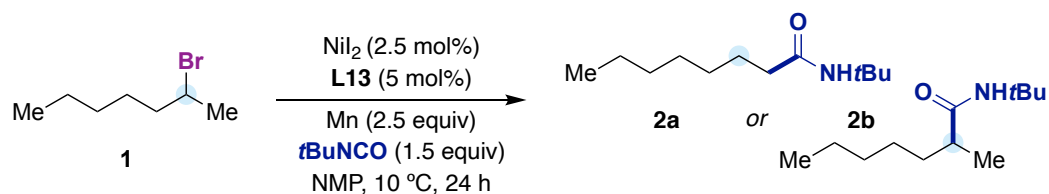
At this point we decided to investigate monosubstituted ligands and related ligand scaffolds (Table 2). As observed previously in our group, monosubstituted phenanthrolines and bipyridines gave a complete change in selectivity, favoring in every case the retained amidation. The introduction of additional methyl groups resulted in a lower yield (**L9** and **L10**). While the inclusion of phenyl groups did not have a big influence on reactivity, (**L11** vs **L12**) the presence a longer alkyl chain adjacent to the nitrogen atom gave the best yield (**L13**). Related pyridine amines (**L14**), diimines or terpyridines were not competent in the amidation of secondary alkyl bromides.



Conditions: **1** (0.50 mmol), *t*BuNCO (0.75 mmol), NiI<sub>2</sub> (2.5 mol%), ligand (5 mol%), Mn (1.25 mmol), NMP (1 mL) at 10 °C, 24h.

**Table 2.** Monosubstituted polypyridyl ligand screening.

If we apply the reported condition for the amidation of unactivated primary alkyl bromides (Table 3, entry 2), variable yields with a maximum of a 30% yield were obtained. Controlling the reaction temperature (entries 1, 3 and 4) afforded good yields of the corresponding retained amide, presumably by avoiding the β-hydride elimination of the intermediate alkyl-nickel and other undesired side reactions. By testing different solvents and temperatures, the best amidation conditions could be obtained with DMF at 3 °C, giving rise to **2b** in 93% yield.



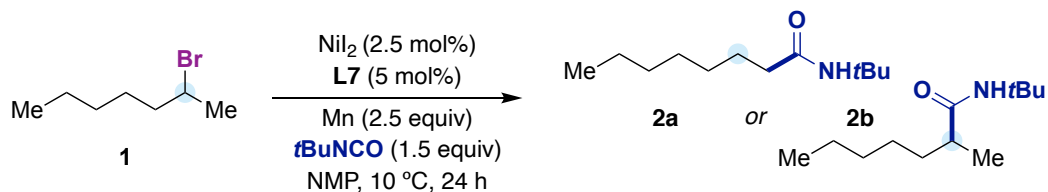
Entry	Deviation	Conversion /%	Yield (2a+2b) /%	2a:2b
1	None	100	72	<1:99
2	NiBr <sub>2</sub> (3 mol%), <b>L12</b> (4.5 mol%), DMF, rt <sup>a</sup>	100	25-30 <sup>a</sup>	<1:99
3	<b>L12</b> instead of <b>L13</b>	100	62	<1:99
4	NiBr <sub>2</sub> and DMF at 3 °C	100	93	<1:99

Conditions: **1** (0.50 mmol), *t*BuNCO (0.75 mmol), NiI<sub>2</sub> (2.5 mol%), **L13** (5 mol%), Mn (1.25 mmol), NMP (1 mL) at 10 °C, 24 h. <sup>a</sup> Conditions reported for the amidation of unactivated alkyl bromides by our group. Variable yields with a maximum of 30% were obtained.

**Table 3.** Retained amidation of secondary alkyl bromides.

With a good system for the retained amidation in hand, we decided to test the other reaction parameters using **L7** with the aim of improving the chain walking amidation outcome. First of all, a set of different nickel precatalyst was tested (Table 4). Only the halide salts were competent precatalyst (entries 1-3), being the best of them NiI<sub>2</sub>. Other nickel sources (entries 4 and 5) could not promote the desired transformation. Polar non-protic solvent such as DMF or DMA gave lower results and the use of Zn as a reducing agent afforded the desired product in moderate yield and a slightly worse selectivity. The reduction of the reaction temperature to 3 °C (entry 9) gave a similar yield but favored the formation of the amidation at the initial site.

Regiodivergent Ligand-Controlled Ni-Catalyzed Reductive Amidation of Unactivated Secondary Alkyl Bromides

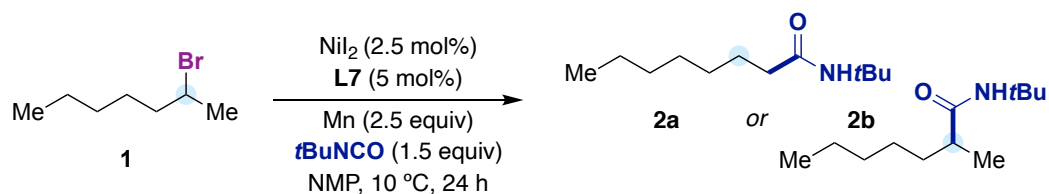


Entry	Deviation	Conversion /%	Yield (2a+2b) /%	2a:2b
1	None	100	72	96:4
2	NiBr <sub>2</sub> ·dme	100	48	94:6
3	NiCl <sub>2</sub> ·dme	100	19	84:16
4	Ni(acac) <sub>2</sub>	4	1	–
5	Ni(COD) <sub>2</sub>	24	4	–
6	DMF instead of NMP	100	66	96:4
7	DMA instead of NMP	100	45	80:20
8	Zn instead of Mn	100	42	93:7
9	3 °C	92	68	91:9

Conditions: **1** (0.50 mmol), *t*BuNCO (0.75 mmol),  $\text{NiI}_2$  (2.5 mol%), **L7** (5 mol%), Mn (1.25 mmol), NMP (1 mL) at 10 °C, 24 h.

**Table 4.** Reaction parameter screening.

Having optimized all the reaction parameters, we then tested the effect of different additives (Table 5). The addition of ammonium salts, that has been beneficial for different reductive couplings and carboxylations (see chapter 1), in our case did not have a positive effect. A similar trend to the case of nickel precatalyst was observed: chloride gave a lower yield and selectivity than bromide (entries 2 and 3), and worse than iodide (entry 4). This observation could be rationalized if we assume that the formation of a cationic alkyl nickel intermediate is needed for an effective chain-walking. Other less soluble iodide salts gave low yields (entry 5). The addition of a larger amount of isocyanate gave a similar result (entry 6). The main byproduct observed in every case was the corresponding heptane mixture, produced by  $\beta$ -hydride elimination and subsequent discoordination. With the aim of reentering the heptene formed into the catalytic cycle, different additives known to produce nickel hydrides were added (entries 7-11). However, the addition of either simple alkyl bromides or silanes did not improve the yield or the selectivity. Finally, the use of alkyl iodide instead of an alkyl bromide resulted in lower yields of the primary amide, along with large amount of heptene isomers (entry 12).



Entry	Deviation	Conversion /%	Yield (2a+2b) /%	2a:2b
1	None	100	72	96:4
2	+TBACl (1 equiv)	96	11	73:27
3	+TBABr (1 equiv)	86	36	94:6
4	+TBAI (1 equiv)	82	49	96:4
5	+NaI (1 equiv)	94	15	80:20
6	2 equiv <i>t</i> BuNCO	100	68	96:4
7	+ <i>i</i> PrBr (0.5 equiv)	100	67	96:4
8	+ <i>n</i> PrBr (0.5 equiv)	100	60	96:4
9	+ <i>t</i> BuBr (0.5 equiv)	91	49	88:12
10	+ $(\text{EtO})_2\text{MeSiH}$ (0.5 equiv)	100	69	91:9
11	+ $\text{Et}_3\text{SiH}$ (0.5 equiv)	100	48	85:15
12	2-iodoheptane instead of <b>1</b>	100	18	83:17

Conditions: **1** (0.50 mmol), *t*BuNCO (0.75 mmol),  $\text{NiI}_2$  (2.5 mol%), **L7** (5 mol%), Mn (1.25 mmol), NMP (1 mL) at 10 °C, 24 h.

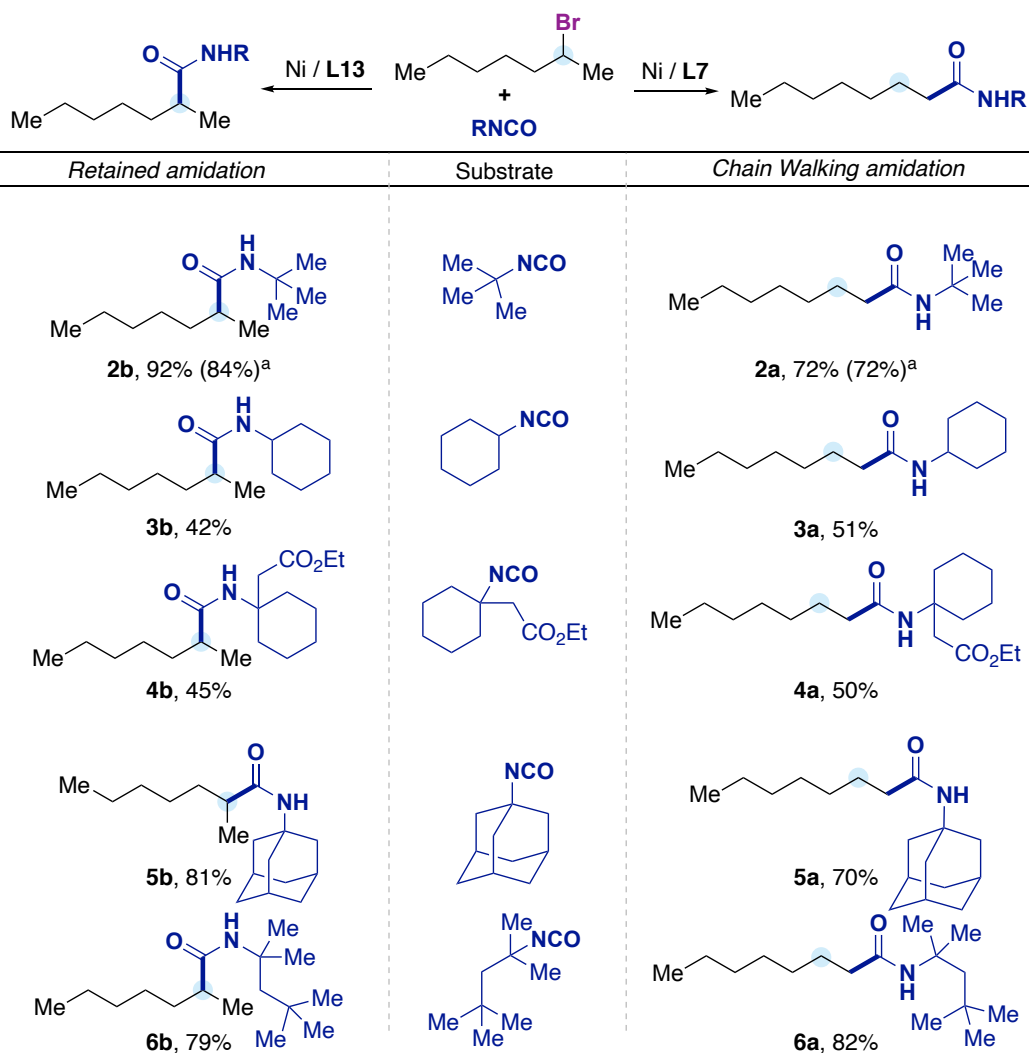
**Table 5.** Screening of additives.

### 3.2. Preparative substrate scope

After the optimization of all the parameters, we decided to move forward and test the scope of the transformation. To this end, we started testing different isocyanates with 2-bromoheptane using the developed conditions with **L7** or **L13**. Bulky tertiary and secondary isocyanates gave the corresponding branched or terminal amides (Table 6, **2a/b-6a/b**) with moderate to good yields. These results show the ability of this methodology to form bulky amides with ease in contrast with other amidation protocols where these compounds are typically beyond reach. However, the use of primary alkyl isocyanates or aromatic isocyanates did not yield the desired amides with full conversion of both the alkyl bromide and the isocyanate.



Regiodivergent Ligand-Controlled Ni-Catalyzed Reductive Amidation of Unactivated Secondary Alkyl Bromides

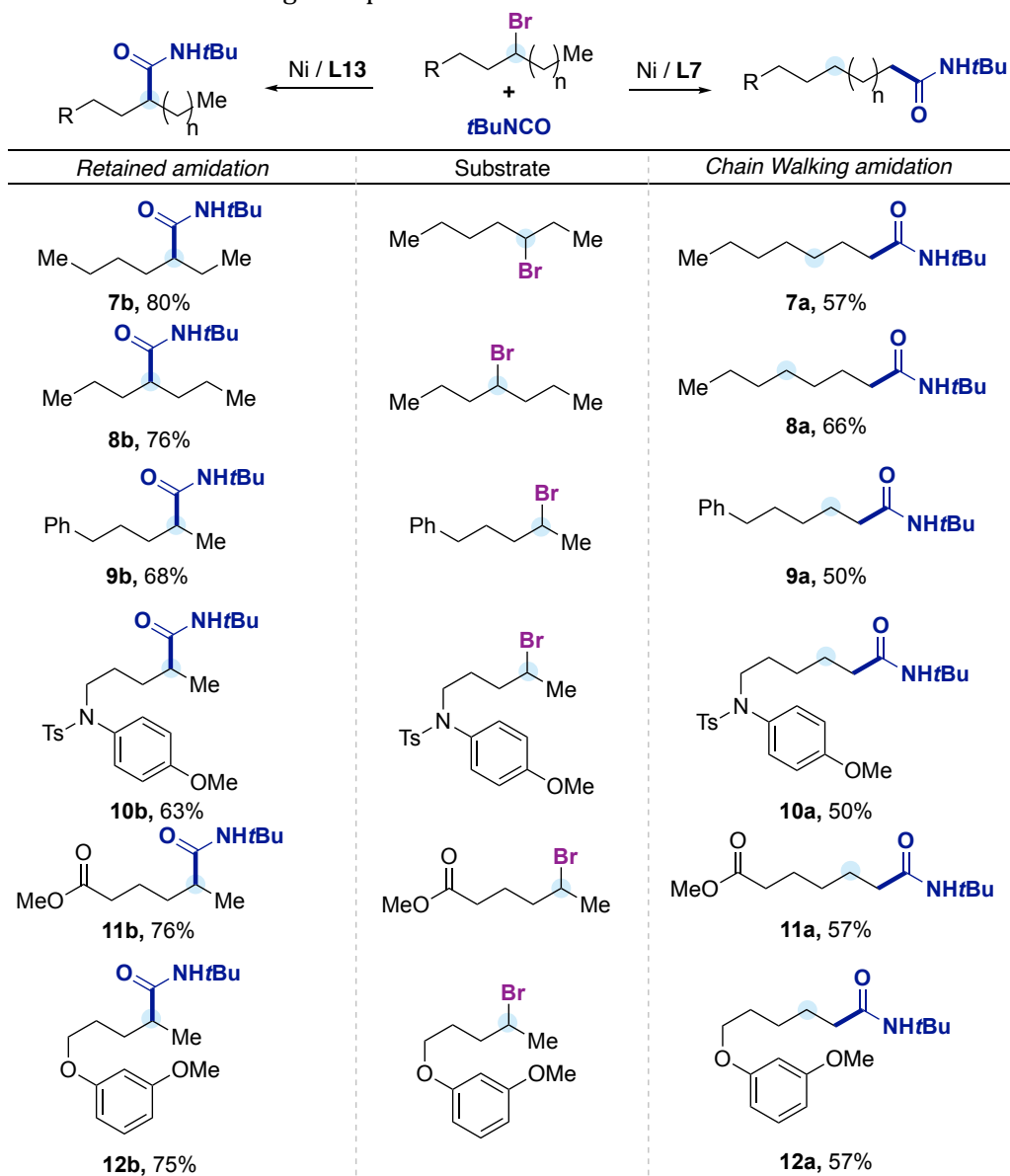


Conditions Ni/L7: **1** (0.50 mmol), RNCO (0.75 mmol), NiI<sub>2</sub> (2.5 mol%), L7 (5 mol%), Mn (1.25 mmol), NMP (1 mL) at 10 °C, 24 h. Conditions Ni/L13: **1** (0.50mmol), RNCO (0.75mmol), NiBr<sub>2</sub> (2.5mol%), L13 (5 mol%), Mn (0.75 mmol), DMF (0.5 mL) at 3 °C, 24 h. <sup>a</sup> 1 mmol scale.

**Table 6.** Isocyanate scope of the reductive amidation.

Next we moved our attention to test different secondary alkyl bromides (Table 7). The use of 3-bromoheptane and 4-bromoheptane delivered the corresponding amidation product in the terminal or the original position (**7a/b** and **8a/b**) in good yields. The presence of amines (**10a/b**), esters (**11a/b**), nitriles (**13a/b**) or heterocycles (**15a/b** and **16a/b**) show the good chemoselectivity profile of the procedure. Boronic esters (**17a/b**) were tolerated as well, leaving an additional handle for further functionalization. Particularly illustrative was the excellent selectivity observed in the remote amidation using Ni/L7, since in the presence of

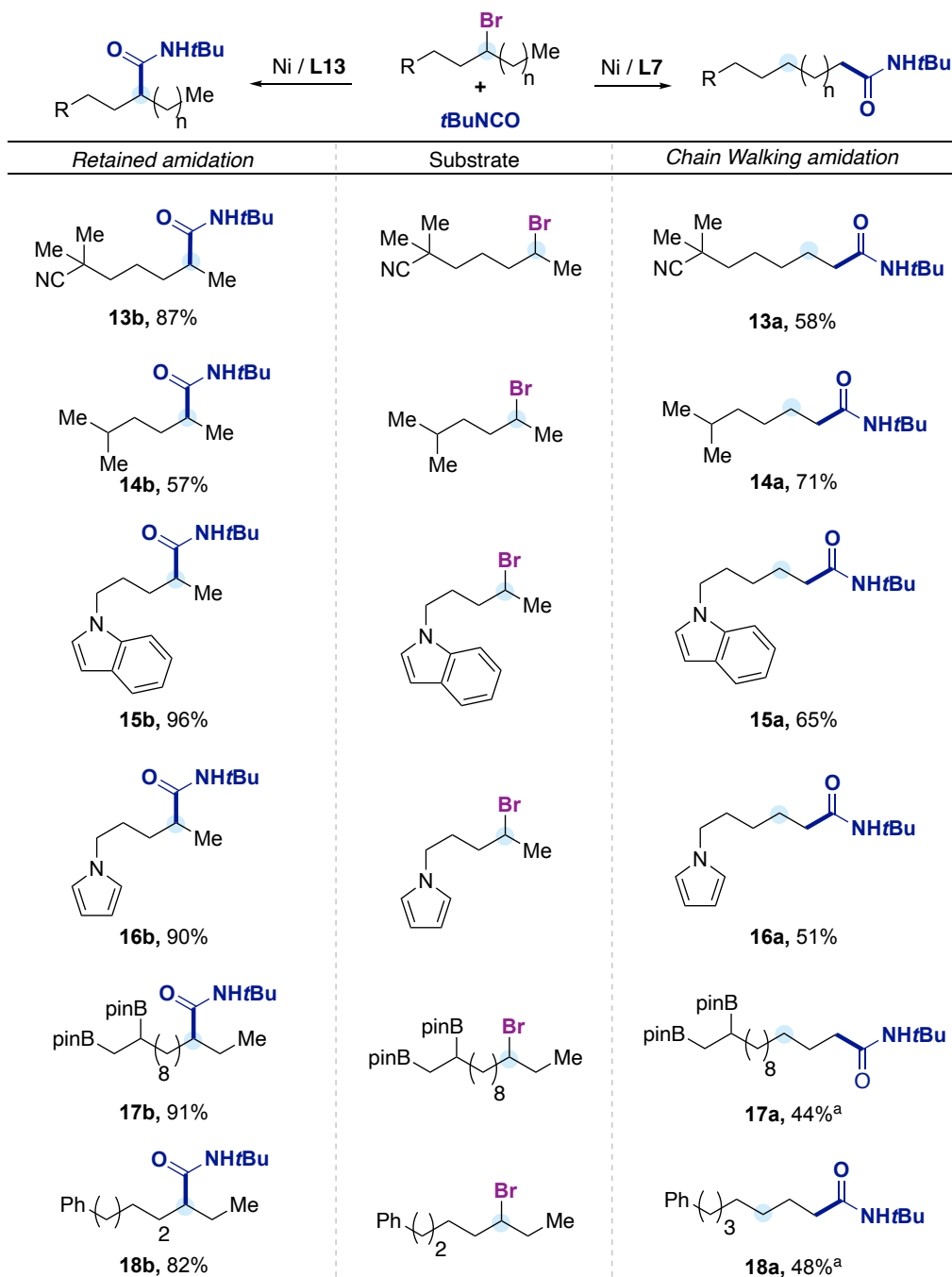
an ester (**11a**), an aryl group (**8a** and **18a**) or different terminal methyl groups (**14a**) the amidation event might be problematic.<sup>15</sup>



Conditions Ni/L7: alkyl bromide (0.50 mmol), *t*BuNCO (0.75 mmol), Ni<sub>2</sub> (2.5 mol%), L7 (5 mol%), Mn (1.25 mmol), NMP (1 mL) at 10 °C, 24h. Conditions Ni/L13: alkyl bromide (0.50 mmol), *t*BuNCO (0.75 mmol), NiBr<sub>2</sub> (2.5mol%), L13 (5 mol%), Mn (0.75 mmol), DMF (0.5 mL) at 3 °C, 24 h.

**Table 7.** Alkyl bromides scope

Regiodivergent Ligand-Controlled Ni-Catalyzed Reductive Amidation of Unactivated Secondary Alkyl Bromides

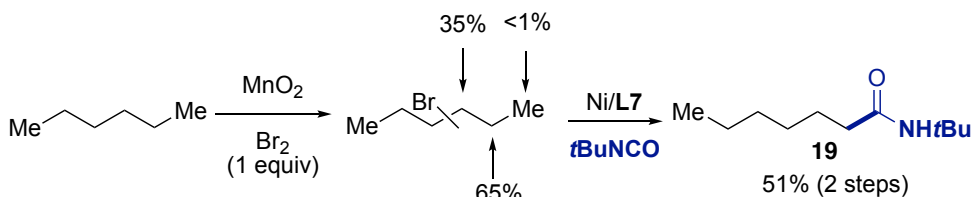


Conditions Ni/L7: alkyl bromide (0.50 mmol), *t*BuNCO (0.75 mmol), NiI<sub>2</sub> (2.5 mol%), L7 (5 mol%), Mn (1.25 mmol), NMP (1 mL) at 10 °C, 24h. Conditions Ni/L13: alkyl bromide (0.50 mmol), *t*BuNCO (0.75 mmol), NiBr<sub>2</sub> (2.5 mol%), L13 (5 mol%), Mn (0.75 mmol), DMF (0.5 mL) at 3 °C, 24 h. <sup>a</sup> NiI<sub>2</sub> (5 mol%), L7 (10 mol%).

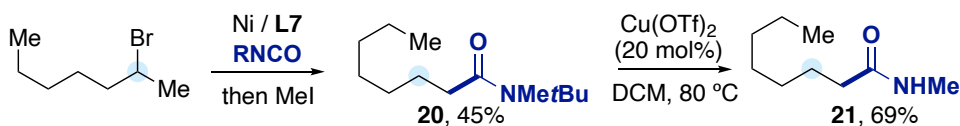
Table 7 (cont.). Alkyl bromides scope.

To further explore the synthetic applicability of our methodology, we performed an unselective bromination of *n*-hexane, which was then submitted to the amidation reaction conditions using Ni/**L7**. This 2-step sequence gave the terminal amide with excellent selectivity and good yield (Scheme 6, *top*). Moreover, an electrophilic quenching of the obtained amidate was performed to give the disubstituted amide with moderate yield, which could then be deprotected to obtain the amide that would formally arise from the use of methyl isocyanate, a very toxic reagent (Scheme 6, *bottom*).

□ Unselective bromination followed by remote amidation:



□ Electrophilic quenching and *tert*-butyl group deprotection:



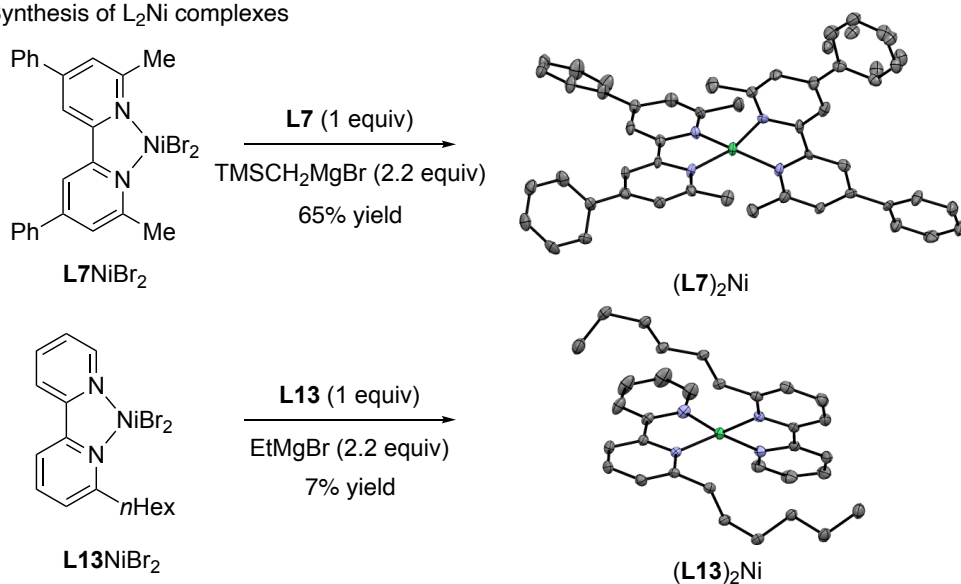
Scheme 6. Synthetic applications.

#### 4. Mechanistic investigations

To gain further information about the mechanistic subtleties of the reaction, we decided to study the reactivity of the low valent  $\text{NiL}_2$  complexes that are a priori generated within the catalytic cycle. Initial attempts to synthesize  $(\text{L7})_2\text{Ni}$  and  $(\text{L13})_2\text{Ni}$  from  $\text{Ni}(\text{COD})_2$  were unsuccessful due to the low solubility of the ligands and their inability to fully displace COD. However, an alternative route via reduction of  $\text{LNiX}_2$  with  $\text{TMSCH}_2\text{MgBr}$  or  $\text{EtMgBr}$  afforded  $(\text{L7})_2\text{Ni}$  and  $(\text{L13})_2\text{Ni}$  which were characterized by X-ray crystallography (Scheme 7). Closer inspection of the crystal structures reveals a significant difference in their geometry, with  $(\text{L7})_2\text{Ni}$  showing a more traditional tetrahedral geometry while  $(\text{L13})_2\text{Ni}$  is distorted between square planar and tetrahedral geometries ( $81^\circ$  vs  $65^\circ$ ).

## Regiodivergent Ligand-Controlled Ni-Catalyzed Reductive Amidation of Unactivated Secondary Alkyl Bromides

### □ Synthesis of L<sub>2</sub>Ni complexes

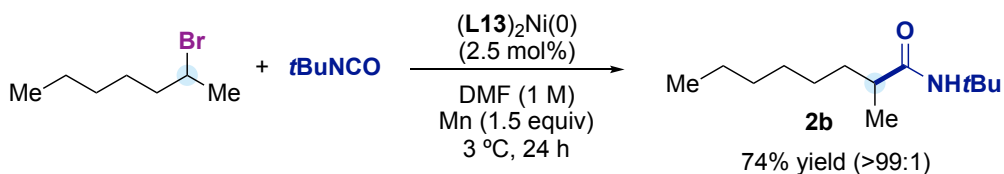
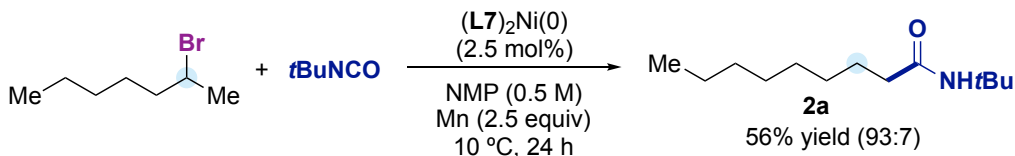


**Scheme 8.** Synthesis of NiL<sub>2</sub>.

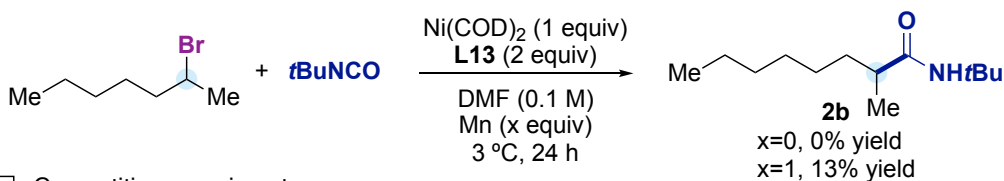
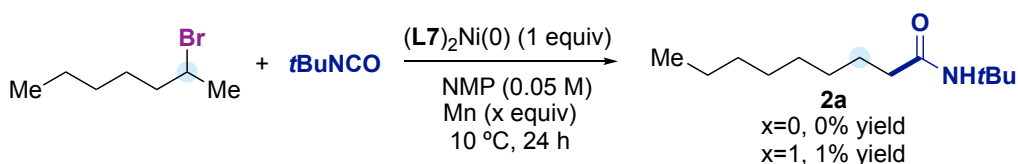
As expected, (L7)<sub>2</sub>Ni and (L13)<sub>2</sub>Ni were found to be competent precatalysts, delivering **2a** in 56% yield and **2b** in 74% yield respectively (Scheme 9, *top*). Due to the low yields obtained for the synthesis of (L13)<sub>2</sub>Ni, we decided to continue testing with a mixture of Ni(COD)<sub>2</sub>/L13, since Ni(COD)<sub>2</sub> is a competent precatalyst in catalytic conditions for the retained amidation. Performing stoichiometric experiments with (L7)<sub>2</sub>Ni or Ni(COD)<sub>2</sub>/L13 and **1a** without reductant afforded full conversion of alkyl halide to the corresponding alkenes as the major products (Scheme 10, *middle*). These results support the notion that isocyanate insertion to the *in situ* generated (L)Ni(II)(Br)(Alk) is slow or does not occur while β-hydride elimination to form an heptene is significantly faster. Unfortunately, under stoichiometric conditions with Mn, we were unable to efficiently promote the isocyanate insertion and alkene was observed as the major product. Moreover, a competitive experiment in which both ligands were added in the standard reaction conditions formed exclusively the ‘retained’ amidation **2b** (Scheme 11, *bottom*), which might indicate a stronger binding of L13 than L7 to the nickel center. Closer inspection of the crystal structures reveals a significant difference in the C<sub>py</sub>-C<sub>py</sub> bond. As these bond’s lengths constitute an indirect evidence on the degree of backdonation from the metal, we can further evaluate how ligand effects and geometry stabilize our proposed catalytic intermediate. Comparing the C<sub>py</sub>-C<sub>py</sub> bonds between (L7)<sub>2</sub>Ni(0) and (L13)<sub>2</sub>Ni(0) we observe longer C<sub>py</sub>-C<sub>py</sub> bonds for (L7)<sub>2</sub>Ni(0), suggesting less backdonation of the tetrahedral (L7)<sub>2</sub>Ni(0) (1.453(8) vs 1.437(2) Å). Noteworthy, when we compare (L7)<sub>2</sub>Ni(0) to the free ligand, we

observe that the  $C_{py}-C_{py}$  bond is still significantly contracted suggesting significant backdonation from Ni(0) (1.453(8) vs 1.497(6)).

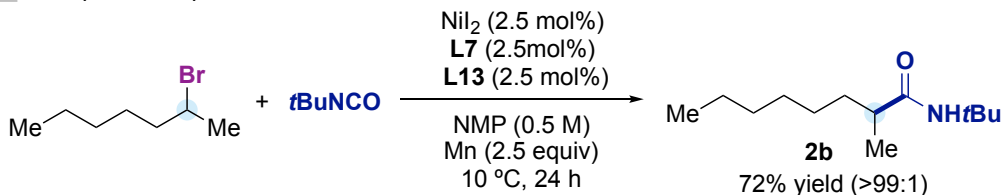
□ Activity of  $L_2Ni$  as catalyst



□ Stoichiometric experiments



□ Competitive experiment

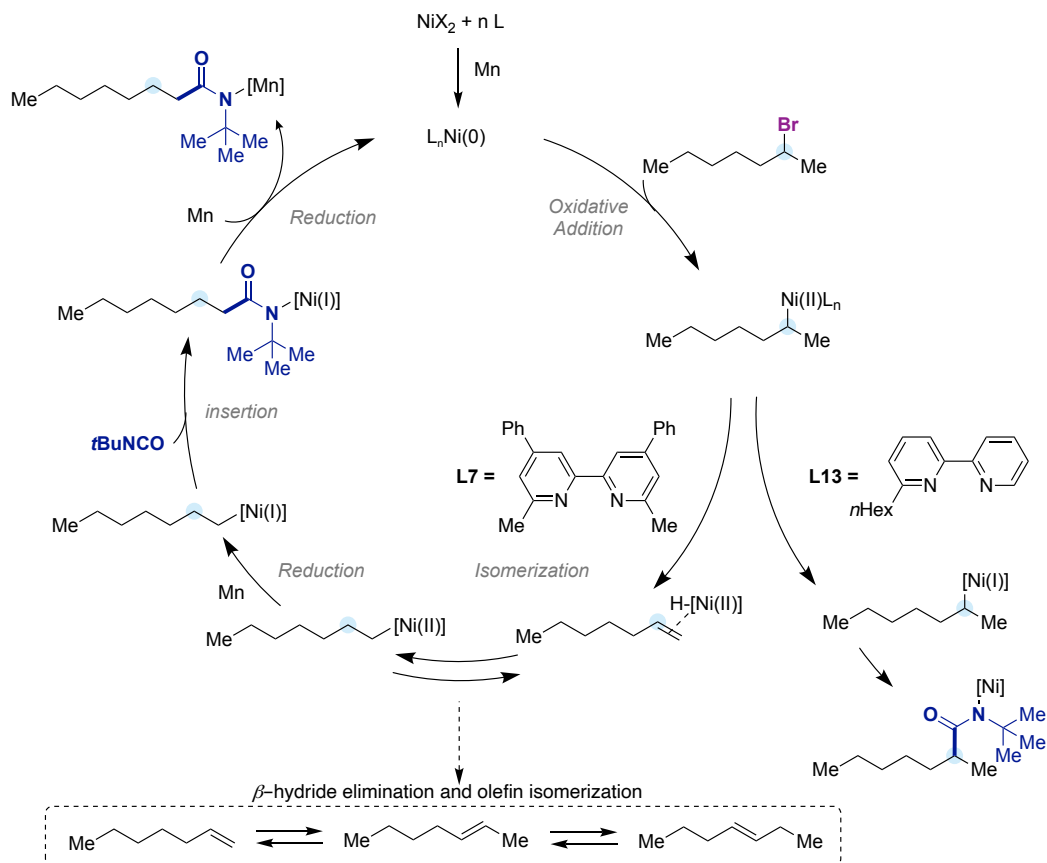


**Scheme 9.** Mechanistic investigations.

With all this information in hand, we propose a mechanistic scenario based on Ni(II)-alkyl species generated after stepwise oxidative addition of the alkyl halide to Ni(0) (Scheme 10). These species might be incapable to undergo insertion of isocyanate in an efficient way and require the reduction to Ni(I)-alkyl species, since the stoichiometric experiments need the addition of manganese to observe amidation product. The secondary Ni(II)-alkyl is also believed to be unstable and we infer that **L13** slows  $\beta$ -hydride elimination compared to **L7** to allow the access of the different amidation products with high selectivity. After isocyanate insertion into

## Regiodivergent Ligand-Controlled Ni-Catalyzed Reductive Amidation of Unactivated Secondary Alkyl Bromides

the C-Ni(I) bond, a reductive transmetalation with Mn recovers the propagating Ni(0) and generates the Mn-amidate, which renders the desired amide after acidic work-up.



**Scheme 10.** Proposed reaction mechanism.

## 5. Conclusions

A nickel-catalyzed regiodivergent amidation of secondary alkyl bromides has been described, showing the influence of the ligand backbone into the outcome of the reaction. The reaction proceeds under mild conditions, thus minimizing unproductive dimerization/trimerization events of the isocyanate, accommodating a wide range of substrates with an excellent chemoselectivity profile and controlling the  $\beta$ -hydride elimination processes at will by ligand modulation to obtain branched or terminal amides. One of the major limitations of this chapter is the narrow scope of isocyanates. Specifically, only bulky and electron-rich isocyanates can be used as other isocyanates afford only traces of the desired product. One alternative option towards overcoming this limitation could be the use of isocyanate surrogates, that would allow the slow release of these species in situ. Moreover, the need for superstoichiometric quantities of metals as reductants, which need to be quenched at the end of the reaction and generate metal waste, can be considered as a drawback for the wide application of reductive cross-electrophile reactions. Alternatives using photocatalysis with terminal organic electron donors would be a good alternative for this problem. Undoubtedly, future developments with chiral ligands would a priori allow to access chiral aliphatic amides via enantioconvergent events, which are important molecules in pharmaceuticals and agrochemicals.



## 6. Experimental section

### General considerations:

**Reagents and Reaction Set-up.** NiBr<sub>2</sub> (anhydrous, 98% purity), NiI<sub>2</sub> (anhydrous, 99% purity), manganese powder (99.9% trace metal basis), *tert*-butyl isocyanate (97% purity), cyclohexyl isocyanate (98% purity), adamantyl isocyanate (97% purity) and 1,1,3,3-tetramethylbutyl isocyanate (98% purity) were purchased from Aldrich. Ethyl 2-(1-isocyanatocyclohexyl) acetate was purchased from Fluorochem. (NOTE: *the purity of the isocyanates was found crucial for the reaction*; higher yields and better reproducibility were achieved by purifying the isocyanates through a short plug of dried neutral alumina inside a nitrogen-filled glovebox. Old batches of isocyanates provide consistently lower yields and variable results). 2-Bromoheptane (technical grade) was purchased from Aldrich, 3-bromoheptane (97% purity) and 4-bromoheptane (97% purity) were purchased from Alfa Aesar and used as received. Anhydrous *N,N*-dimethylformamide (DMF, 99.8% purity), anhydrous *N,N*-dimethylacetamide (DMA, 99.5% purity) and anhydrous 1-methyl-2-pyrrolidinone (NMP, 99.5% purity) were purchased from Acros Organics (NOTE: *it is critical to have appropriately dried DMF, DMA and NMP to obtain reproducible results*, since old batches of these solvents provided variable results). The temperature of the reactions was controlled by using a chiller (Huber Minichiller 300) connected to an aluminum block with an internal recirculation circuit.

**Analytical methods.** <sup>1</sup>H NMR and <sup>13</sup>C NMR spectra are included for all compounds. <sup>1</sup>H and <sup>13</sup>C NMR spectra were recorded on a Bruker 300 MHz, a Bruker 400 MHz or a Bruker 500 MHz at 20 °C. All <sup>1</sup>H NMR spectra are reported in parts per million (ppm) downfield of TMS and were measured relative to the signals for CHCl<sub>3</sub> (7.26 ppm). All <sup>13</sup>C NMR spectra were reported in ppm relative to residual CHCl<sub>3</sub> (77.2 ppm) and were obtained with <sup>1</sup>H decoupling. Coupling constants, *J*, are reported in hertz (Hz). Melting points were measured using open glass capillaries in a Büchi B540 apparatus. Infrared spectra (FT-IR) measurements were carried out on a Bruker Optics FT-IR Alpha spectrometer equipped with a DTGS detector, KBr beamsplitter at 4 cm<sup>-1</sup> resolution using a one bounce ATR accessory with diamond windows. Mass spectra were recorded on a Waters LCT Premier spectrometer or in a MicroTOF Focus, Bruker Daltonics spectrometer. Flash chromatography was performed with EM Science silica gel 60 (230-400 mesh) using potassium permanganate, vanillin or cerium molybdate as TLC stains.

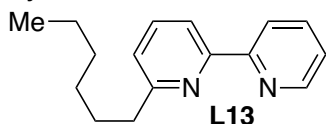
### Optimization of the reaction conditions

In a nitrogen-filled glovebox, an oven-dried screw-capped test tube containing a stirring bar was charged with the nickel source, ligand and Mn. The obtained mixture was stirred at rt, until a colored complex was obtained (*ca.* 5 to 10 min), after which *tert*-butyl isocyanate (0.75 mmol; 1.5 equiv) was added. Subsequently, the reaction mixture was cooled down to 10 °C outside the glovebox, and 2-bromoheptane was added (0.5 mmol; 1 equiv). The resulting mixture was stirred for 24 h, at 10 °C using a chiller. The crude reaction mixture was carefully quenched with 5% aq. HCl (1 mL) and extracted with ethyl acetate. A sample of the obtained solution was filtered through a silica-celite plug, eluted with ethyl acetate and analyzed by GC-FID using anisole as internal standard.

### Ligand synthesis:

-L7 was prepared in chapter 4.

-Synthesis of L13:



**6-hexyl-2,2'-bipyridine (L13).** Hexyl lithium (13.9 mL of a 2.3 M in hexane, 32 mmol; 1 equiv), was added slowly to a solution of bipyridine (5.0 g, 32 mmol; 1 equiv) in dry diethyl ether (150 mL, 0.2 M), at -40 °C.

The resulting red solution was stirred for 1 h under vigorous agitation. Then, the reaction mixture was quenched with brine (200 mL). The resulting biphasic yellow mixture was separated and the organic phase was extracted with diethyl ether (3 × 50 mL), dried over MgSO<sub>4</sub> and evaporated under reduced pressure. The obtained dark orange crude product was dissolved in dichlorometane (50 mL) and MnO<sub>2</sub> (11.1 g, 128 mmol; 4 equiv) were added under vigorous agitation. After 3 h the crude reaction mixture was filtered through a silica-celite plug, concentrated under reduced pressure and purified through column chromatography on silica gel (hexanes/ethyl acetate 99:5) to afford the product as a clear oil (4.38 g, 18.2 mmol, 57% yield).

**<sup>1</sup>H NMR (400 MHz, CDCl<sub>3</sub>):** δ = 8.66 (ddd, *J* = 4.8, 1.8, 0.9 Hz, 1H), 8.44 (dt, *J* = 8.0, 1.1 Hz, 1H), 8.18 (dd, *J* = 7.9, 1.0 Hz, 1H), 7.78 (td, *J* = 7.7, 1.8 Hz, 1H), 7.69 (t, *J* = 7.7 Hz, 1H), 7.26 (ddd, *J* = 7.5, 4.8, 1.2 Hz, 1H), 7.14 (dd, *J* = 7.7, 1.0 Hz, 1H), 2.89 – 2.81 (m, 2H), 1.86 – 1.72 (m, 2H), 1.45 – 1.25 (m, 6H), 0.93 – 0.84 (m, 3H) ppm.

**<sup>13</sup>C NMR (101 MHz, CDCl<sub>3</sub>):** δ = 162.1, 156.8, 155.6, 149.2, 137.1, 136.9, 123.5, 122.8, 121.3, 118.2, 38.5, 31.9, 29.8, 29.2, 22.7, 14.2 ppm.

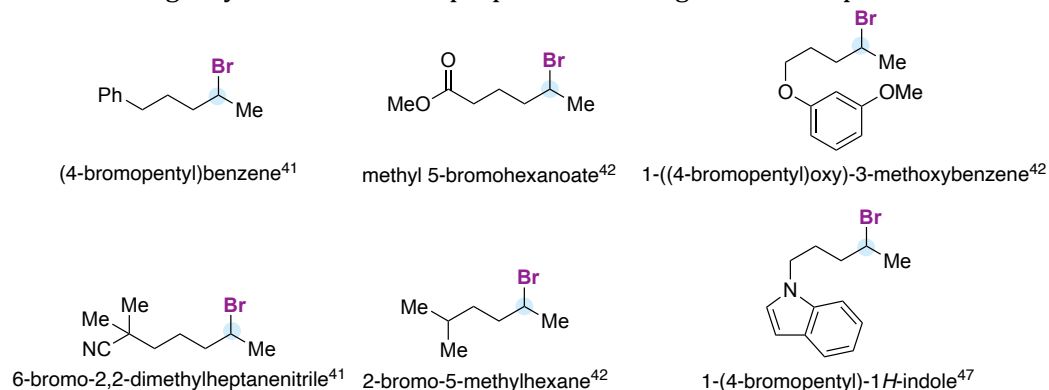
**IR (neat, cm<sup>-1</sup>):** 2925, 2855, 1581, 1563, 1458, 1428, 773.

**HRMS(ESI<sup>+</sup>):** [C<sub>16</sub>H<sub>21</sub>N<sub>2</sub>]<sup>+</sup> (M+H) calcd. 241.1699, found 241.1693.

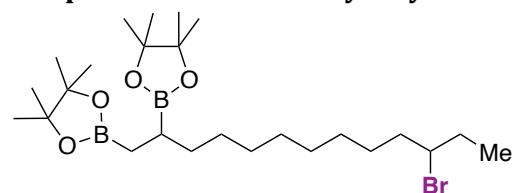
## Regiodivergent Ligand-Controlled Ni-Catalyzed Reductive Amidation of Unactivated Secondary Alkyl Bromides

### -Synthesis of secondary alkyl bromides.

The following alkyl bromides were prepared following a literature procedure:<sup>41,42,47</sup>



### -Preparation of secondary alkyl bromides from the corresponding alcohols:



**2,2'-(11-bromotridecane-1,2-diyl)bis(4,4,5,5-tetramethyl-1,3,2-dioxaborolane).** Adapting a literature procedure<sup>48</sup> in a round bottom flask, 4-cyanopyridine (104.1 mg, 1mmol, 0.2 equiv), NaBH<sub>4</sub> (94.6 mg, 2.5mmol, 0.5

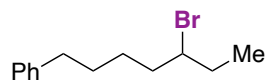
equiv) and B<sub>2</sub>pin<sub>2</sub> (2.54 g, 10 mmol, 2 equiv) were placed under inert atmosphere and tridec-12-en-3-ol<sup>49</sup> (1.00 g, 5 mmol) was added. MeOH (5 mL) was then added and the mixture was heated to 100 °C for 5 hours. The reaction mixture was cooled down to room temperature, brine was added, and the aqueous layer was then extracted with EtOAc. The combined organic phases were dried with anhydrous Na<sub>2</sub>SO<sub>4</sub> and the solvent was removed under reduced pressure. The crude mixture was dissolved in a 2:1 hexane:EtOAc mixture, filtered through a pad of silica and the solvent was removed under reduced pressure. The crude mixture obtained (1.60 g approximately) containing the alcohol was subjected to the general bromination conditions. Triphenylphosphine (1.15 g, 1.25 equiv.) was dissolved in dichloromethane (0.33 M based on alcohol). After cooling the solution to 0 °C, bromine (215 mL, 1.2 equiv) was added dropwise and allowed to stir for 10 min to obtain a suspension. Then pyridine (0.35 mL, 1.2 equiv.) and the alcohol (1.60 g, 1.0 equiv.) dissolved in dichloromethane (0.5 M) were added to the suspension. The reaction mixture was allowed to warm up to rt and stirred overnight. The resulting reaction mixture was quenched with aq. saturated NH<sub>4</sub>Cl and extracted with dichloromethane. The combined organic phases were washed with brine, dried over MgSO<sub>4</sub> and concentrated under reduced pressure. The crude mixture was purified by flash column chromatography through silica gel (hexane/ethyl acetate 100/0 to 95/5) to obtain the desired product as a colorless oil (966.7 mg, 38% yield).

**$^1\text{H}$  NMR (400 MHz,  $\text{CDCl}_3$ ):**  $\delta$  = 3.95 (tt,  $J$  = 7.8, 4.9 Hz, 1H), 1.88 – 1.71 (m, 4H), 1.54 – 1.33 (m, 4H), 1.27 – 1.22 (m, 10H), 1.20 (s, 24H), 1.11 – 1.04 (m, 1H), 1.00 (t,  $J$  = 7.2 Hz, 3H), 0.89 – 0.69 (m, 2H) ppm.

**$^{13}\text{C}$  NMR (101 MHz,  $\text{CDCl}_3$ ):**  $\delta$  = 82.8, 82.7, 60.6, 38.8, 33.8, 32.1, 29.8, 29.5, 29.4, 29.0, 28.8, 27.6, 24.9, 24.8, 24.8, 24.7, 18.4 (br), 12.7 (br), 12.0 ppm.

**IR (neat,  $\text{cm}^{-1}$ ):** 2976, 2924, 2854, 1462, 1369, 1310, 1214, 1140, 968, 846.

**HRMS (ESI+):** [ $\text{C}_{25}\text{H}_{49}\text{B}_2\text{BrNaO}_4$ ] $^+$  ( $\text{M}+\text{Na}$ ) calcd. 537.2893, found. 537.2897.



**(6-bromooctyl)benzene.** To a 250 mL round bottom flask containing a solution of triphenylphosphine (1.41g, 5,37 mmol) in DCM (30 mL) at 0 °C, bromine (858,6 mg, 5,37 mmol) was added dropwise and the mixture stirred for 30 min. Then, a solution of 7-phenylheptan-3-ol<sup>50</sup> (861 mg, 4,48 mmol) in DCM (20 mL) and pyridine (433,7 mL, 5,37 mmol) were subsequently added and the mixture was stirred for 4 h at room temperature. After completion, the mixture was partially concentrated and filtered through a plug of silica eluting with pentane. The filtrate was evaporated and the residue purified by flash column chromatography (EtOAc/Hexanes 5-10%) to afford the corresponding bromide as a colorless oil (900 mg, 3,53 mmol, 79% yield).

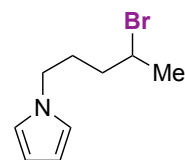
**$^1\text{H}$  NMR (400 MHz,  $\text{CDCl}_3$ ):**  $\delta$  = 7.33 – 7.24 (m, 2H), 7.23 – 7.14 (m, 3H), 3.98 (tt,  $J$  = 7.9, 5.0 Hz, 1H), 2.63 (t,  $J$  = 7.5 Hz, 2H), 1.95 – 1.74 (m, 4H), 1.71 – 1.56 (m, 3H), 1.52 – 1.41 (m, 1H), 1.04 (t,  $J$  = 7.3 Hz, 3H) ppm.

**$^{13}\text{C}$  NMR (101 MHz,  $\text{CDCl}_3$ ):**  $\delta$  = 142.6, 128.5, 128.4, 125.9, 60.5, 38.8, 35.9, 32.3, 31.1, 27.5, 12.2 ppm.

**IR (neat,  $\text{cm}^{-1}$ ):** 3062, 3026, 2966, 2934, 2858, 1603, 1496, 1453, 745, 697.

**HRMS (APCI+):** [ $\text{C}_{13}\text{H}_{19}$ ] $^+$  ( $\text{M}-\text{Br}$ ) $^+$  calcd. 175.1481, found. 175.1476.

### -Synthesis of secondary alkyl bromides from 1,4-dibromopentane:



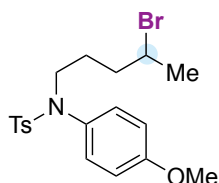
**1-(4-bromopentyl)-1H-pyrrole.** A solution of pyrrole (0.69 mL, 10 mmol; 1 equiv) in DMF (5 mL) was added slowly over a round bottom flask containing NaH (0.48 g of 60% NaH in mineral oil, 12 mmol; 1.2 equiv) in DMF (100 mL) and stirred at rt for 1h. Then, a solution of 1,4-dibromopentane (4 mL, 30 mmol; 3 equiv) in DMF (40 mL) was slowly added and the resulting mixture stirred for 48 h. The crude reaction mixture was evaporated under reduced pressure and the obtained oil purified through column chromatography to afford the title compound as a light-yellow oil (1.06 g, 4.9 mmol; 49% yield).

**$^1\text{H}$  NMR (500 MHz,  $\text{CDCl}_3$ ):**  $\delta$  = 6.65 (s, 2H), 6.15 (s, 2H), 4.12 – 4.05 (m, 1H), 3.92 (td,  $J$  = 6.9, 1.3 Hz, 2H), 2.08 – 2.00 (m, 1H), 1.97 – 1.84 (m, 1H), 1.84 – 1.71 (m, 2H), 1.69 (d,  $J$  = 6.7 Hz, 3H) ppm.

**<sup>13</sup>C NMR (126 MHz, CDCl<sub>3</sub>):**  $\delta$  = 120.6, 108.3, 50.9, 49.0, 38.2, 29.9, 26.6 ppm.

**IR (neat, cm<sup>-1</sup>):** 3099, 2924, 1684, 1499, 1445, 1280, 1088, 1066, 720, 617, 535.

**HRMS (APCI+):** [C<sub>9</sub>H<sub>15</sub>BrN]<sup>+</sup> (M+H) calcd. 216.0382, found. 216.0373.



***N*-(4-bromopentyl)-*N*-(4-methoxyphenyl)-4-methylbenzenesulfonamide.**

A solution of 1 g (3.61 mmol, 1.0 equiv) of *p*-MeO-Tosyl-aniline and K<sub>2</sub>CO<sub>3</sub> (598 mg, 4.33 mmol, 1.2 equiv.) in DMF (6 mL) was stirred for 1 h at room temperature. Then, the 1,4-dibromopentane (1.66 g, 7.21 mmol, 2.0 equiv) was subsequently added. The mixture was stirred at room temperature for 24-48 h. After completion, the mixture was extracted with EtOAc and washed with brine. The organic layer was dried over anhydrous MgSO<sub>4</sub> and concentrated. The residue was purified by flash column chromatography in silica gel with hexane/EtOAc, affording the desired compound as a yellowish viscous oil (800 mg, 1.88 mmol, 52% yield).

**<sup>1</sup>H NMR (400 MHz, CDCl<sub>3</sub>):**  $\delta$  = 7.50 – 7.45 (m, 2H), 7.30 – 7.21 (m, 2H), 6.98 – 6.91 (m, 2H), 6.86 – 6.79 (m, 2H), 4.12 (dq, *J* = 8.5, 6.5, 4.6 Hz, 1H), 3.81 (s, 3H), 3.58 (dt, *J* = 13.5, 6.9 Hz, 1H), 3.48 (dt, *J* = 13.0, 6.4 Hz, 1H), 2.43 (s, 3H), 1.98 – 1.73 (m, 2H), 1.69 (d, *J* = 6.6 Hz, 3H), 1.67 – 1.60 (m, 1H), 1.48 – 1.59 (m, 1H) ppm.

**<sup>13</sup>C NMR (100 MHz, CDCl<sub>3</sub>):**  $\delta$  = 159.1, 143.3, 135.2, 131.3, 129.9, 129.4, 127.7, 114.3, 55.4, 51.0, 49.8, 37.6, 26.6, 26.2, 21.6 ppm.

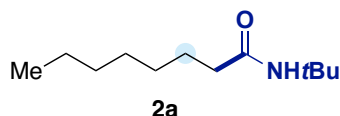
**IR (neat, cm<sup>-1</sup>):** 2925, 2838, 1605, 1506, 1443, 1343, 1246, 1158, 1089, 1030, 902, 814, 676, 579, 545.

**HRMS (ESI+):** [C<sub>19</sub>H<sub>24</sub>BrNNaO<sub>3</sub>S]<sup>+</sup> (M+Na) calcd. 448.0552, found. 448.0552.

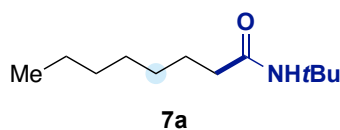
**Amidation of secondary alkyl bromides with isocyanates.**

**General Procedure A.** In a nitrogen-filled glovebox, an oven-dried screw-capped test tube containing a stirring bar was charged with  $\text{NiI}_2$  (3.9 mg, 0.013 mmol; 2.5 mol%), 6,6'-dimethyl-4,4'-diphenyl-2,2'-bipyridine (**L7**) (8.4 mg, 0.025, 5.0 mol%), Mn (68.7 mg, 1.25 mmol; 2.5 equiv) and NMP (1.0 mL). The obtained mixture was stirred until a deep purple color was observed (20-30 minutes). Subsequently, the corresponding alkyl bromide (0.5 mmol; 1 equiv) and isocyanate (0.75 mmol; 1.5 equiv) were added. The resulting mixture was stirred for 24 h, at 10 °C using a chiller. The crude reaction mixture was carefully quenched with 5% aq. HCl (1 mL) or saturated aq.  $\text{NH}_4\text{Cl}$  (2 mL) (when sensitive functional groups were present). Acid quench was followed by the addition of distilled water (*ca.* 10 mL) and by extraction with ethyl acetate ( $3 \times 15$  mL). The organic phase was washed with brine (40 mL), dried over  $\text{MgSO}_4$ , filtered and the solvent was evaporated under reduced pressure. The crude product was purified by column chromatography (hexanes/EtOAc or pentane/ $\text{Et}_2\text{O}$ ).

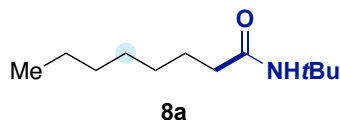
**General Procedure B.** In a nitrogen-filled glovebox, an oven-dried screw-capped test tube containing a stirring bar was charged with  $\text{NiBr}_2$  (2.7 mg, 0.013 mmol; 2.5 mol%), 6-hexyl-2,2'-bipyridine (**L13**) (6.0 mg, 0.025, 5.0 mol%), Mn (41.2 mg, 0.750 mmol; 1.5 equiv) and DMF (0.5 mL). The obtained mixture was stirred until a deep green color was observed (30-45 minutes). Subsequently, the corresponding alkyl bromide (0.5 mmol; 1 equiv) and isocyanate (0.75 mmol; 1.5 equiv) were added. The resulting mixture was stirred for 24 h, at 3 °C using a chiller. The crude reaction mixture was carefully quenched with 5% aq. HCl (1 mL) or saturated aq.  $\text{NH}_4\text{Cl}$  (2 mL) (when sensitive functional groups were present). Acid quench was followed by the addition of distilled water (*ca.* 10 mL) and by extraction with ethyl acetate ( $3 \times 15$  mL). The organic phase was washed with brine (40 mL), dried over  $\text{MgSO}_4$ , filtered and the solvent was evaporated under reduced pressure. The crude product was purified by column chromatography (hexanes/EtOAc or pentane/ $\text{Et}_2\text{O}$ ).



***N*-(*tert*-butyl)octanamide (2a)** Following procedure A, starting from 2-bromoheptane (89.6 mg, 0.500 mmol; 1 equiv) and *tert*-butyl isocyanate (86.0  $\mu$ L, 74.3 mg, 0.750 mmol; 1.50 equiv), compound **2a** was obtained as a 24:1 **2a:2b** by GC analysis of the crude. Chromatographic purification provided the compound as a pale-yellow oil (71.8 mg, 72% yield).



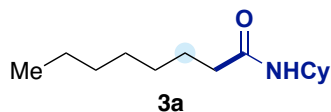
***N*-(*tert*-butyl)octanamide (7a)** Following procedure A, starting from 3-bromoheptane (89.6 mg, 0.500 mmol; 1 equiv) and *tert*-butyl isocyanate (86.0  $\mu$ L, 74.3 mg, 0.750 mmol; 1.50 equiv), compound **7a** was obtained as a 10:1 **7a:(2a+2b)** by GC analysis of the crude. Chromatographic purification provided the compound as a pale-yellow oil (56.9 mg, 57% yield).



***N*-(*tert*-butyl)octanamide (8a)** Following procedure A, starting from 4-bromoheptane (89.6 mg, 0.500 mmol; 1 equiv) and *tert*-butyl isocyanate (86.0  $\mu$ L, 74.3 mg, 0.750 mmol; 1.50 equiv), compound **8a** was obtained as a 8:1 **8a:(2a+2b+7b)** by GC analysis of the crude. Chromatographic purification provided the compound as a pale-yellow oil (66.1 mg, 66% yield).

**$^1\text{H}$  NMR (400 MHz,  $\text{CDCl}_3$ ):**  $\delta$  = 5.26 (s, 1H), 2.07 (d,  $J$  = 7.5 Hz, 2H), 1.58 (p,  $J$  = 7.0 Hz, 2H), 1.33 (s, 9H), 1.32 – 1.21 (m, 8H), 0.86 (t,  $J$  = 6.7 Hz, 3H) ppm.

**$^{13}\text{C}$  NMR (101 MHz,  $\text{CDCl}_3$ ):**  $\delta$  = 172.7, 51.2, 37.9, 31.8, 29.3, 29.2, 29.0, 25.9, 22.7, 14.2 ppm.



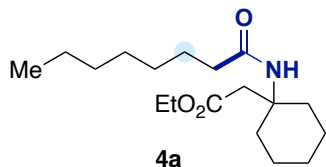
***N*-cyclohexyloctanamide (3a).** Following procedure A, starting from 2-bromoheptane (89.6 mg, 0.500 mmol; 1 equiv) and cyclohexyl isocyanate (93.9 mg, 0.750 mmol; 1.50 equiv), compound **3a** was obtained as an off-white solid (57.5 mg, 51% yield).

**$^1\text{H}$  NMR (400 MHz,  $\text{CDCl}_3$ ):**  $\delta$  = 5.47 (s, 1H), 3.80 – 3.67 (m, 1H), 2.14 – 2.06 (m, 2H), 1.87 (dd,  $J$  = 12.6, 4.0 Hz, 2H), 1.72 – 1.58 (m, 2H), 1.61 – 1.52 (m, 3H), 1.47 – 1.17 (m, 10H), 1.18 – 1.04 (m, 3H), 0.84 (t,  $J$  = 6.9 Hz, 3H) ppm.

**$^{13}\text{C}$  NMR (101 MHz,  $\text{CDCl}_3$ ):**  $\delta$  = 172.3, 48.1, 37.2, 33.3, 31.8, 29.3, 29.1, 26.0, 25.7, 25.0, 22.7, 14.1 ppm.

**mp:** 76 – 77  $^\circ\text{C}$ .

Spectroscopic data is in agreement with the literature.<sup>51</sup>

**Ethyl 2-(1-octanamidocyclohexyl)acetate (4a).**

Following procedure A, starting from 2-bromoheptane (132.9 mg, 0.500 mmol; 1 equiv) and ethyl 2-(1-isocyanatocyclohexyl)acetate (158.4 mg, 0.750 mmol; 1.50 equiv), compound **4a** was obtained as yellowish oil

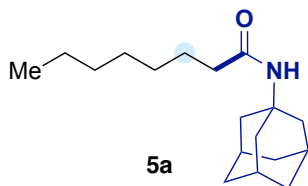
(78.0 mg, 50% yield).

**<sup>1</sup>H NMR (400 MHz, CDCl<sub>3</sub>):** δ = 5.33 (s, 1H), 4.05 (q, *J* = 7.1 Hz, 2H), 2.79 (s, 2H), 2.21 – 2.14 (m, 2H), 2.11 (t, *J* = 7.4 Hz, 2H), 1.62 – 1.36 (m, 9H), 1.30 – 1.21 (m, 9H), 1.20 (t, *J* = 7.1 Hz, 3H), 0.84 (t, *J* = 7.0 Hz, 3H) ppm.

**<sup>13</sup>C NMR (100 MHz, CDCl<sub>3</sub>):** δ = 173.1, 171.4, 60.1, 54.3, 41.9, 37.8, 34.9, 31.8, 29.3, 29.1, 25.8, 25.5, 22.7, 21.7, 14.3, 14.1 ppm.

**IR (neat, cm<sup>-1</sup>):** 3309, 2926, 2855, 1731, 1645, 1538, 1450, 1369, 1179, 1132, 1033.

**HRMS (ESI<sup>+</sup>):** [C<sub>18</sub>H<sub>34</sub>NO<sub>3</sub>]<sup>+</sup> (M+H) calcd. 312.2533, found 312.2541.

**N-(adamantan-1-yl)octanamide (5a).**

Following general procedure A, starting from 2-bromoheptane (89.6 mg, 0.500 mmol; 1 equiv) and 1-isocyanatoadamantane (133 mg, 0.750 mmol; 1.50 equiv), compound **5a** was obtained as a white solid (97 mg, 70% yield).

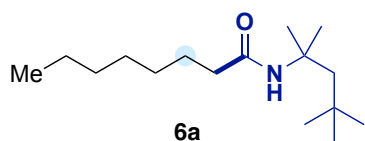
**<sup>1</sup>H NMR (400 MHz, CDCl<sub>3</sub>):** δ = 5.17 (s, 1H), 2.11 – 2.03 (m, 5H), 1.99 (d, *J* = 2.9 Hz, 6H), 1.67 (t, *J* = 3.1 Hz, 6H), 1.58 (p, *J* = 7.0 Hz, 2H), 1.33 – 1.21 (m, 8H), 0.92 – 0.82 (m, 3H) ppm.

**<sup>13</sup>C NMR (100 MHz, CDCl<sub>3</sub>):** δ = 172.4, 51.7, 41.7, 37.8, 36.4, 31.7, 29.5, 29.2, 29.1, 25.8, 22.6, 14.1 ppm.

**mp:** 69 – 71°C.

**IR (neat, cm<sup>-1</sup>):** 3297, 3073, 2902, 2846, 1635, 1546, 1467, 1453, 1359, 1293, 691, 647.

**HRMS (ESI<sup>+</sup>):** [C<sub>18</sub>H<sub>32</sub>NO]<sup>+</sup> (M+H) calcd. 278.2478, found 278.2478.

**N-(2,4,4-trimethylpentan-2-yl)octanamide (6a).**

Following general procedure A and starting from *tert*-octyl isocyanate (127 mg, 0.750 mmol; 1.50 equiv), compound **6a** was obtained as colorless oil

(104.7 mg, 82 % yield).

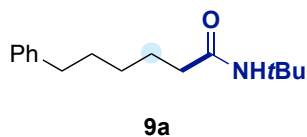
**<sup>1</sup>H NMR (400 MHz, CDCl<sub>3</sub>):** δ = 5.25 (s, 1H), 2.11 – 1.99 (m, 2H), 1.72 (s, 2H), 1.56 (q, *J* = 7.3 Hz, 2H), 1.37 (s, 6H), 1.34 – 1.17 (m, 8H), 0.98 (s, 9H), 0.91 – 0.76 (m, 3H).

**<sup>13</sup>C NMR (125 MHz, CDCl<sub>3</sub>):** δ = 172.5, 55.4, 51.9, 38.3, 32.1, 32.0, 31.9, 31.8, 29.7, 29.6, 29.4, 26.0, 23.0, 14.4 ppm.

**IR (neat, cm<sup>-1</sup>):** 3304, 2954, 2926, 2858, 1642, 1548, 1467, 1364, 1228.



**HRMS (ESI+):**  $[C_{16}H_{33}NNaO]^+$  (M+Na) calcd. 278.2454, found 278.2455.



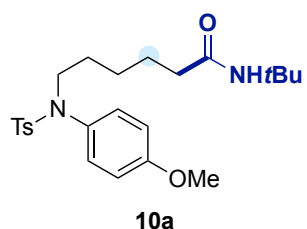
***N*-(*tert*-butyl)-6-phenylhexanamide (9a).** Following procedure A, starting from (4-bromopentyl)benzene (113.6 mg, 0.500 mmol; 1 equiv) and *tert*-butyl isocyanate (86.0  $\mu$ L, 74.3 mg, 0.750 mmol; 1.50 equiv), compound **9a** was obtained as a pale-yellow oil (61.1 mg, 50%).

**$^1H$  NMR (400 MHz,  $CDCl_3$ ):**  $\delta$  = 7.31 – 7.22 (m, 2H), 7.19 – 7.11 (m, 3H), 5.35 (s, 1H), 2.65 – 2.56 (m, 2H), 2.07 (t,  $J$  = 7.5 Hz, 2H), 1.69 – 1.57 (m, 2H), 1.41 – 1.34 (m, 2H), 1.33 (s, 9H) ppm.

**$^{13}C$  NMR (101 MHz,  $CDCl_3$ ):**  $\delta$  = 172.5, 142.6, 128.4, 128.3, 125.7, 51.1, 37.6, 35.8, 31.2, 29.7, 28.9, 28.8, 25.7 ppm.

**IR (neat,  $cm^{-1}$ ):** 3307, 2964, 2929, 2858, 1643, 1544, 1453, 1361, 1224, 745, 697.

**HRMS (ESI+):**  $[C_{16}H_{25}NNaO]^+$  (M+Na) calcd. 270.1828, found 270.1818.



***N*-(*tert*-butyl)-6-(*N*-(4-methoxyphenyl)-4-methylphenylsulfonamido)hexanamide (10a).**

Following general procedure A, starting from 213,18 mg (0,5 mmol) of *N*-(4-bromopentyl)-*N*-(4-methoxyphenyl)-4-methylbenzenesulfonamide which was added as an 0,7 mL solution in NMP to a 0,3 mL solution of reaction mixture (overall volume 1 mL). Compound **10a** was

obtained as an off white solid (112,10 mg, 0,25 mmol, 50% yield).

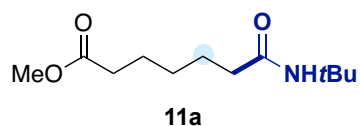
**$^1H$  NMR (400 MHz,  $CDCl_3$ ):**  $\delta$  = 7.43 (dd,  $J$  = 8.2, 1.6 Hz, 2H), 7.22 (d,  $J$  = 7.5 Hz, 2H), 6.93 – 6.85 (m, 2H), 6.82 – 6.74 (m, 2H), 5.35 (s, 1H), 3.77 (d,  $J$  = 1.6 Hz, 3H), 3.44 (td,  $J$  = 6.8, 1.5 Hz, 2H), 2.39 (d,  $J$  = 1.7 Hz, 3H), 2.02 (td,  $J$  = 7.5, 1.5 Hz, 2H), 1.53 (p,  $J$  = 7.6, 7.1 Hz, 2H), 1.45 – 1.26 (m, 12H) ppm.

**$^{13}C$  NMR (100 MHz,  $CDCl_3$ ):**  $\delta$  = 172.3, 159.1, 143.3, 135.4, 131.6, 130.0, 129.5, 129.4, 127.7, 127.7, 114.3, 114.2, 51.1, 50.5, 37.5, 28.9, 28.8, 27.9, 25.9, 25.2, 21.6 ppm.

**IR (neat,  $cm^{-1}$ ):** 3284, 3075, 2963, 2929, 2862, 1644, 1605, 1553, 1505, 1455, 1339, 1247, 1150, 1029, 832, 815, 683, 579, 559, 545.

**HRMS (ESI+):**  $[C_{24}H_{35}N_2O_4S]^+$  (M+H) calcd. 447.2312, found 447.2312.

**mp:** 119 – 121  $^{\circ}C$ .



**Methyl 7-(*tert*-butylamino)-7-oxoheptanoate (11a).**

Following procedure A and starting from methyl 5-bromohexanoate (104.5 mg, 0.500 mmol; 1 equiv) and *tert*-butyl isocyanate (86.0  $\mu$ L, 74.3 mg, 0.750 mmol; 1.50 equiv), compound **11a** was obtained as a yellow oil (65.0 mg, 57%)

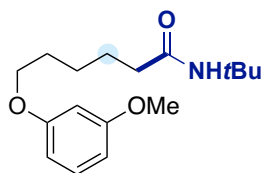
as an inseparable 11:1 mixture of terminal amidation : amidation next to the carbonyl group.

**<sup>1</sup>H NMR (500 MHz, CDCl<sub>3</sub>):**  $\delta$  = 5.25 (s, 1H), 3.65 (s, 3H), 2.30 (t,  $J$  = 7.5 Hz, 2H), 2.07 (t,  $J$  = 7.5 Hz, 2H), 1.68 – 1.53 (m, 4H), 1.38 – 1.26 (m, 2H), 1.33 (s, 9H) ppm.

**<sup>13</sup>C NMR (126 MHz, CDCl<sub>3</sub>):**  $\delta$  = 174.3, 172.3, 51.6, 51.2, 37.5, 34.0, 29.0, 28.7, 25.4, 24.7 ppm.

**IR (neat, cm<sup>-1</sup>):** 3315, 2957, 2865, 1737, 1645, 1542, 1454, 1362, 1223, 1172, 1088.

**HRMS (ESI+):** [C<sub>12</sub>H<sub>24</sub>NO<sub>3</sub>]<sup>+</sup> (M+H) calcd. 230.1751, found 230.1744.



**12a**

***N*-(*tert*-butyl)-6-(3-methoxyphenoxy)hexanamide**

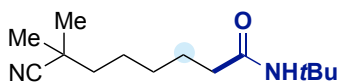
**(12a).** Following procedure A, starting from 1-((4-bromopentyl)oxy)-3-methoxybenzene (137 mg, 0.500 mmol; 1 equiv) and *tert*-butyl isocyanate (86.0  $\mu$ L, 74.3 mg, 0.750 mmol; 1.50 equiv), compound **12a** was obtained as a pale-yellow oil (83.6 mg, 57%).

**<sup>1</sup>H NMR (300 MHz, CDCl<sub>3</sub>):**  $\delta$  = 7.16 (t,  $J$  = 8.1 Hz, 1H), 6.53 – 6.41 (m, 3H), 5.29 (s, 1H), 3.94 (t,  $J$  = 6.4 Hz, 2H), 3.78 (s, 3H), 2.12 (t,  $J$  = 7.4 Hz, 2H), 1.85 – 1.61 (m, 4H), 1.56 – 1.42 (m, 2H), 1.34 (s, 9H) ppm.

**<sup>13</sup>C NMR (101 MHz, CDCl<sub>3</sub>):**  $\delta$  = 172.6, 161.0, 160.4, 130.0, 106.8, 106.3, 101.1, 67.8, 55.4, 51.4, 37.6, 29.2, 29.0, 25.8, 25.7 ppm.

**IR (neat, cm<sup>-1</sup>):** 3313, 29362, 2867, 1645, 1591, 1544, 1492, 1453, 1363, 1285, 1264, 1199, 1149, 1044, 761, 686.

**HRMS (ESI+):** [C<sub>17</sub>H<sub>27</sub>NNaO<sub>3</sub>]<sup>+</sup> (M+Na) calcd. 316.1883, found 316.1875.



**13a**

***N*-(*tert*-butyl)-7-cyano-7-methyloctanamide (13a).**

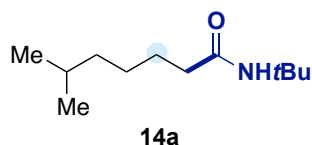
Following procedure A, starting from 6-bromo-2,2-dimethylheptanenitrile (109.1 mg, 0.500 mmol; 1 equiv) and *tert*-butyl isocyanate (86.0  $\mu$ L, 74.3 mg, 0.750 mmol; 1.50 equiv), compound **13a** was obtained as a yellow oil (69.1 mg, 58% yield).

**<sup>1</sup>H NMR (400 MHz, CDCl<sub>3</sub>):**  $\delta$  = 5.29 (s, 1H), 2.07 (t,  $J$  = 7.5 Hz, 2H), 1.68 – 1.56 (m, 2H), 1.55 – 1.40 (m, 4H), 1.32 (s, 9H), 1.31 (s, 6H) ppm.

**<sup>13</sup>C NMR (101 MHz, CDCl<sub>3</sub>):**  $\delta$  = 172.3, 125.3, 51.2, 41.0, 37.4, 32.5, 29.1, 28.9, 26.8, 25.4, 25.1 ppm.

**IR (neat, cm<sup>-1</sup>):** 3314, 2971, 2935, 2863, 2235, 1646, 1542, 1454, 1363, 1224.

**HRMS (ESI+):** [C<sub>14</sub>H<sub>26</sub>N<sub>2</sub>NaO]<sup>+</sup> (M+Na) calcd. 261.1937, found 261.1925.



***N*-(*tert*-butyl)-6-methylheptanamide (14a).**

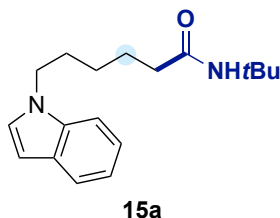
Following procedure A, starting from 2-bromo-5-methylhexane (90 mg, 0.500 mmol; 1 equiv) and *tert*-butyl isocyanate (86.0  $\mu$ L, 74.3 mg, 0.750 mmol; 1.50 equiv), compound **14a** was obtained as a pale-yellow oil (70.6 mg, 71%) as an inseparable mixture of 14:1 terminal amidation : retained amidation.

**$^1\text{H}$  NMR (400 MHz,  $\text{CDCl}_3$ ):**  $\delta$  = 5.46 (s, 1H), 2.05 (t,  $J$  = 7.6 Hz, 2H), 1.58 – 1.42 (m, 3H), 1.32 – 1.28 (m, 9H), 1.27 – 1.22 (m, 2H), 1.16 – 1.08 (m, 2H), 0.81 (d,  $J$  = 6.6 Hz, 6H) ppm.

**$^{13}\text{C}$  NMR (101 MHz,  $\text{CDCl}_3$ ):**  $\delta$  = 173.0, 51.1, 38.7, 37.7, 28.9, 28.9, 27.9, 27.0, 26.1, 22.6 ppm.

**IR (neat,  $\text{cm}^{-1}$ ):** 3307, 3077, 2957, 2929, 2869, 1644, 1546, 1454, 1391, 1363, 1225.

**HRMS (ESI+):** [ $\text{C}_{12}\text{H}_{26}\text{NO}$ ] $^+$  ( $M+H$ ) calcd. 200.2009, found 200.2005.



***N*-(*tert*-butyl)-6-(1*H*-indol-1-yl)hexanamide (15a).**

Following procedure A, starting from 1-(4-bromopentyl)-1*H*-indole (133 mg, 0.500 mmol; 1 equiv) and *tert*-butyl isocyanate (86.0  $\mu$ L, 74.3 mg, 0.750 mmol; 1.50 equiv), compound **15a** was obtained as a red solid (93.0 mg, 65%).

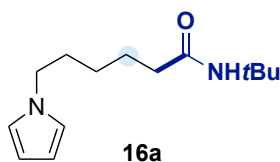
**$^1\text{H}$  NMR (300 MHz,  $\text{CDCl}_3$ ):**  $\delta$  = 7.62 (dt,  $J$  = 7.8, 0.9 Hz, 1H), 7.33 (dd,  $J$  = 8.2, 1.0 Hz, 1H), 7.19 (ddd,  $J$  = 8.2, 7.0, 1.2 Hz, 1H), 7.12 – 7.06 (m, 2H), 6.48 (dd,  $J$  = 3.1, 0.9 Hz, 1H), 5.13 (s, 1H), 4.13 (t,  $J$  = 7.0 Hz, 2H), 2.03 (t,  $J$  = 7.4 Hz, 2H), 1.92 – 1.79 (m, 2H), 1.69 – 1.56 (m, 2H), 1.39 – 1.27 (m, 11H) ppm.

**$^{13}\text{C}$  NMR (101 MHz,  $\text{CDCl}_3$ ):**  $\delta$  = 172.2, 136.0, 128.6, 127.9, 121.4, 121.0, 119.2, 109.4, 101.0, 51.1, 46.2, 37.3, 30.0, 28.9, 26.5, 25.3 ppm.

**IR (neat,  $\text{cm}^{-1}$ ):** 3276, 3080, 2959, 2935, 2857, 1366, 1555, 1455, 1164, 955, 787, 694.

**HRMS (ESI+):** [ $\text{C}_{18}\text{H}_{26}\text{N}_2\text{Na}$ ] $^+$  ( $M+Na$ ) calcd. 309.1937, found 309.1941.

**mp:** 71 – 73  $^\circ\text{C}$ .



***N*-(*tert*-butyl)-6-(1*H*-pyrrol-1-yl)hexanamide (16a).**

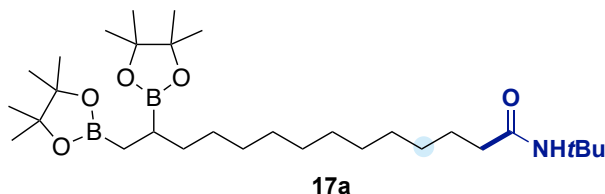
Following procedure A, starting from 1-(4-bromopentyl)-1*H*-pyrrole (108 mg, 0.500 mmol; 1 equiv) and *tert*-butyl isocyanate (86.0  $\mu$ L, 74.3 mg, 0.750 mmol; 1.50 equiv), compound **16a** was obtained as a pale-yellow oil (60.2 mg, 51%).

**$^1\text{H}$  NMR (400 MHz,  $\text{CDCl}_3$ ):**  $\delta$  = 6.63 (t,  $J$  = 2.1 Hz, 2H), 6.11 (t,  $J$  = 2.1 Hz, 2H), 5.27 (s, 1H), 3.86 (t,  $J$  = 7.1 Hz, 2H), 2.05 (t,  $J$  = 7.5 Hz, 2H), 1.81 – 1.71 (m, 2H), 1.66 – 1.54 (m, 2H), 1.32 (s, 9H), 1.30 – 1.21 (m, 2H) ppm.

$^{13}\text{C}$  NMR (101 MHz,  $\text{CDCl}_3$ ):  $\delta = 172.2, 120.6, 107.9, 51.2, 49.4, 37.5, 31.4, 28.9, 26.4, 25.3$  ppm.

IR (neat,  $\text{cm}^{-1}$ ): 3307, 2963, 2930, 2864, 1645, 1544, 1453, 1363, 1281, 1225, 1089, 722.

HRMS (ESI+):  $[\text{C}_{14}\text{H}_{24}\text{NNaO}]^+$  (M+Na) calcd. 259.1781, found 259.1776.



***N*-(*tert*-butyl)-13,14-bis(4,4,5,5-tetramethyl-1,3,2-dioxaborolan-2-yl)**

**tetradecanamide (17a).** Following procedure A using 5 mol% of  $\text{NiI}_2$  (7.8 mg), 10 mol% of **L7** (16.8 mg) and starting from 2,2'-(11-bromotridecane-1,2-diyl)bis(4,4,5,5-tetramethyl-1,3,2-dioxaborolane) (258.0 mg, 0.500 mmol; 1 equiv) and *tert*-butyl isocyanate (86.0  $\mu\text{L}$ , 74.3 mg, 0.750 mmol; 1.50 equiv), compound **17a** was obtained as a pale-yellow oil (117.8 mg, 44%).

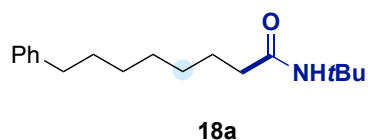
$^1\text{H}$  NMR (400 MHz,  $\text{CDCl}_3$ ):  $\delta = 5.28$  (s, 1H), 2.03 (t,  $J = 7.2$  Hz, 2H), 1.58 – 1.51 (m, 2H), 1.45 – 1.31 (m, 2H), 1.30 (s, 9H), 1.27 – 1.12 (m, 40H), 1.11 – 1.02 (m, 1H), 0.88 – 0.69 (m, 2H) ppm.

$^{13}\text{C}$  NMR (101 MHz,  $\text{CDCl}_3$ ):  $\delta = 172.6, 82.9, 82.8, 51.1, 37.8, 33.9, 29.9, 29.7, 29.7, 29.6, 29.5, 29.3, 29.0, 25.9, 25.0, 24.9, 24.9, 24.8, 18.5, 12.8$  ppm.

$^{11}\text{B}$  NMR (128 MHz,  $\text{CDCl}_3$ ):  $\delta = 32.8$  ppm.

IR (neat,  $\text{cm}^{-1}$ ): 3310, 2976, 2924, 2853, 1647, 1546, 1454, 1369, 1312, 1142, 968.

HRMS (ESI+):  $[\text{C}_{30}\text{H}_{60}\text{NB}_2\text{O}]^+$  (M+H) calcd. 536.4652, found 536.4645.



***N*-(*tert*-butyl)-8-phenyloctanamide (18a).**

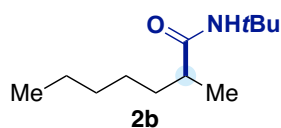
Following procedure A using 5 mol% of  $\text{NiI}_2$  (7.8 mg), 10 mol% of **L7** (16.8 mg) and starting from (5-bromoheptyl)benzene (127.6 mg, 0.500 mmol; 1 equiv) and *tert*-butyl isocyanate (86.0  $\mu\text{L}$ , 74.3 mg, 0.750 mmol; 1.50 equiv), compound **18a** was obtained as a pale-yellow oil (66.2 mg, 48%).

$^1\text{H}$  NMR (400 MHz,  $\text{CDCl}_3$ ):  $\delta = 7.29 - 7.22$  (m, 2H), 7.19 – 7.12 (m, 3H), 2.61 – 2.54 (m, 2H), 2.08 – 2.01 (m, 2H), 1.61 – 1.53 (m, 4H), 1.32 (s, 9H), 1.37 – 1.29 (m, 6H) ppm.

$^{13}\text{C}$  NMR (101 MHz,  $\text{CDCl}_3$ ):  $\delta = 172.6, 143.0, 128.5, 128.4, 125.7, 51.2, 37.9, 36.1, 31.6, 29.4, 29.3, 29.3, 29.0, 25.9$  ppm.

IR (neat,  $\text{cm}^{-1}$ ): 3307, 3026, 2964, 2927, 2855, 1644, 1545, 1453, 1391, 1362, 1224, 746, 697.

HRMS (ESI+):  $[\text{C}_{18}\text{H}_{29}\text{NNaO}]^+$  (M+Na) calcd. 298.2141, found 298.2146.



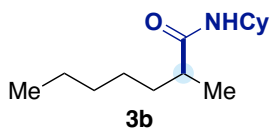
***N*-(*tert*-butyl)-2-methylheptanamide (2b).** Following general procedure B, starting from 4-bromoheptane (89.6 mg, 0.500 mmol; 1 equiv) and *tert*-butyl isocyanate (86.0  $\mu$ L, 74.3 mg, 0.750 mmol; 1.50 equiv), compound **2b** was obtained as a white solid (91.6 mg, 92% average yield).

**$^1\text{H}$  NMR (500 MHz,  $\text{CDCl}_3$ ):**  $\delta$  = 5.21 (s, 1H), 2.07 – 1.93 (m, 1H), 1.65 – 1.50 (m, 1H), 1.34 (s, 9H), 1.33 – 1.21 (m, 7H), 1.08 (d,  $J$  = 6.9 Hz, 3H), 0.87 (t,  $J$  = 6.9 Hz, 3H) ppm.  
 **$^{13}\text{C}$  NMR (126 MHz,  $\text{CDCl}_3$ ):**  $\delta$  = 176.1, 51.1, 42.5, 34.6, 32.0, 29.0, 27.3, 22.7, 18.1, 14.2 ppm.

**mp:** 58 – 60  $^\circ\text{C}$ .

**IR (neat,  $\text{cm}^{-1}$ ):** 3314, 2961, 2928, 2859, 1646, 1543, 1453, 1362, 1226.

**HRMS (ESI $^+$ ):** [ $\text{C}_{12}\text{H}_{25}\text{NNaO}$ ] $^+$  ( $M+\text{Na}$ ) calcd. 222.1828, found 222.1833.



***N*-cyclohexyl-2-methylheptanamide (3b)** Following procedure B and starting from 2-bromoheptane (89.6 mg, 0.500 mmol; 1 equiv) and cyclohexyl isocyanate (93.9 mg, 0.750 mmol; 1.50 equiv), compound **3b** was obtained as an off-white solid (47.3 mg, 42% yield).

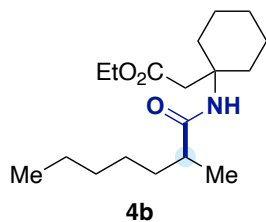
**$^1\text{H}$  NMR (400 MHz,  $\text{CDCl}_3$ ):**  $\delta$  = 5.36 (s, 1H), 3.88 – 3.55 (m, 1H), 2.17 – 2.00 (m, 1H), 1.95 – 1.83 (m, 2H), 1.75 – 1.54 (m, 4H), 1.42 – 1.20 (m, 10H), 1.12 – 1.05 (m, 2H), 1.09 (d,  $J$  = 6.9 Hz, 3H), 0.84 (t,  $J$  = 7.2 Hz, 3H) ppm.

**$^{13}\text{C}$  NMR (1001 MHz,  $\text{CDCl}_3$ ):**  $\delta$  = 175.7, 47.9, 41.9, 34.5, 33.5, 33.3, 31.9, 27.2, 25.7, 25.0, 25.0, 22.7, 18.1, 14.1 ppm.

**mp:** 85 – 87  $^\circ\text{C}$

**IR (neat,  $\text{cm}^{-1}$ ):** 3282, 3086, 2959, 2925, 2852, 1636, 1547, 1444, 1349, 1272, 1235, 1155, 1099, 892, 712.

**HRMS (ESI $^+$ ):** [ $\text{C}_{14}\text{H}_{28}\text{NO}$ ] $^+$  ( $M+\text{H}$ ) calcd. 226.2165, found 226.2161.



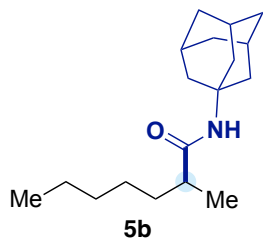
**Ethyl 2-(1-(2-methylheptanamido)cyclohexyl)acetate (4b)** Following procedure B, starting from 2-bromoheptane (132.9 mg, 0.500 mmol; 1 equiv) and ethyl 2-(1-isocyanatocyclohexyl)acetate (158.4 mg, 0.750 mmol; 1.50 equiv), compound **4b** was obtained as yellowish oil (70.1 mg, 45% yield).

**$^1\text{H}$  NMR (400 MHz,  $\text{CDCl}_3$ ):**  $\delta$  = 5.34 (s, 1H), 4.07 (q,  $J$  = 7.2 Hz, 2H), 2.87 (d,  $J$  = 15.0 Hz, 1H), 2.75 (d,  $J$  = 15.1 Hz, 1H), 2.33 – 2.15 (m, 2H), 2.15 – 2.02 (m, 1H), 1.68 – 1.39 (m, 9H), 1.32 – 1.23 (m, 7H), 1.21 (t,  $J$  = 7.1 Hz, 3H), 1.10 (d,  $J$  = 6.9 Hz, 3H), 0.86 (t,  $J$  = 6.7 Hz, 3H) ppm.

$^{13}\text{C}$  NMR (100 MHz,  $\text{CDCl}_3$ ):  $\delta = 176.5, 171.4, 60.1, 54.1, 42.6, 42.1, 34.9, 34.8, 34.3, 31.9, 27.3, 25.6, 22.6, 21.8, 21.6, 18.1, 14.3, 14.1$  ppm.

IR (neat,  $\text{cm}^{-1}$ ): 3338, 2928, 2857, 1730, 1650, 1529, 1450, 1369, 1249, 1214, 1133, 1032, 499, 469.

HRMS (ESI+):  $[\text{C}_{18}\text{H}_{34}\text{NO}_3]^+$  (M+H) calcd. 312.2533, found 312.2539.



***N*-(adamantan-1-yl)-2-methylheptanamide (5b).**

Following procedure B, starting from 2-bromoheptane (89.6 mg, 0.500 mmol; 1 equiv) and 1-isocyanatoadamantane (158.4 mg, 0.750 mmol; 1.50 equiv), compound **5b** was obtained as a white solid (111.8 mg, 80 % yield).

$^1\text{H}$  NMR (400 MHz,  $\text{CDCl}_3$ ):  $\delta = 5.08$  (s, 1H), 2.06 – 2.12 (m, 2H), 2.00 – 2.04 (m, 7H), 1.69 (t,  $J = 3.1$  Hz, 6H), 1.39 – 1.19

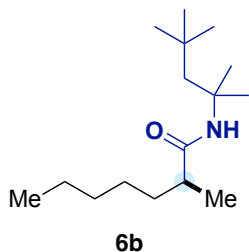
(m, 7H), 1.10 (d,  $J = 6.8$  Hz, 3H), 0.95 – 0.83 (m, 3H).

$^{13}\text{C}$  NMR (100 MHz,  $\text{CDCl}_3$ ):  $\delta = 175.8, 51.6, 42.4, 41.8, 41.8, 36.4, 36.3, 34.5, 31.9, 29.5, 27.1, 22.6, 18.1, 14.0$  ppm.

mp: 99 – 101 °C.

IR (neat,  $\text{cm}^{-1}$ ): 2399, 2959, 2904, 2849, 1641, 1542, 1451, 1360, 1236, 1102, 670.

HRMS (ESI+):  $[\text{C}_{18}\text{H}_{32}\text{NO}]^+$  (M+H) calcd. 278.2478, found 278.2470.



**2-methyl-*N*-(2,4,4-trimethylpentan-2-yl)heptanamide (6b).**

Following procedure B, starting from 2-bromoheptane (89.6 mg, 0.500 mmol; 1 equiv) and *tert*-octyl isocyanate (127.0 mg, 0.750 mmol; 1.50 equiv), compound **6b** was obtained as a colourless oil (106.6 mg, 79 % yield).

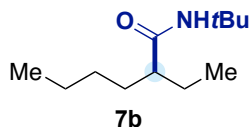
$^1\text{H}$  NMR (400 MHz,  $\text{CDCl}_3$ ):  $\delta = 5.30$  (s, 1H), 2.05 – 1.93 (m, 1H), 1.75 (d,  $J = 14.9$  Hz, 1H), 1.61 (d,  $J = 14.9$  Hz, 1H), 1.57 –

1.50 (m, 1H), 1.35 (d,  $J = 4.3$  Hz, 6H), 1.31 – 1.16 (m, 7H), 1.03 (d,  $J = 6.9$  Hz, 3H), 0.96 (s, 9H), 0.82 (t,  $J = 6.8$  Hz, 3H) ppm.

$^{13}\text{C}$  NMR (100 MHz,  $\text{CDCl}_3$ ):  $\delta = 175.6, 55.0, 52.1, 42.6, 34.4, 31.9, 31.7, 31.6, 29.3, 29.2, 27.2, 22.6, 17.9, 14.1$  ppm.

IR (neat,  $\text{cm}^{-1}$ ): 3325, 2956, 2930, 2872, 1644, 1541, 1458, 1387, 1364, 1253, 1227, 733.

HRMS (ESI+):  $[\text{C}_{16}\text{H}_{33}\text{NNaO}]^+$  (M+Na) calcd. 278.2454, found 278.2455.



***N*-(*tert*-butyl)-2-ethylhexanamide (7b).**

Following general procedure B and starting from 3-bromoheptane (89.6 mg, 0.500 mmol; 1 equiv), compound **7b** was obtained as a white solid (79.5 mg, 80% yield).

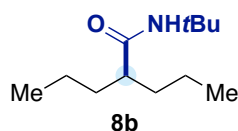
**<sup>1</sup>H NMR (300 MHz, CDCl<sub>3</sub>):**  $\delta$  = 5.21 (s, 1H), 1.78 – 1.70 (m, 1H), 1.63 – 1.50 (m, 2H), 1.35 (s, 9H), 1.32 – 1.20 (m, 6H), 0.88 (t,  $J$  = 7.2 Hz, 6H) ppm.

**<sup>13</sup>C NMR (75 MHz, CDCl<sub>3</sub>):**  $\delta$  = 175.3, 51.3, 50.7, 32.9, 30.0, 29.1, 26.4, 22.9, 14.2, 12.3 ppm.

**mp:** 78.2 – 80.0 °C.

**IR (neat, cm<sup>-1</sup>):** 3308, 2958, 2928, 2872, 2859, 1644, 1544, 1456, 1358, 1270, 1253, 1224, 905, 675.

**HRMS (ESI+):** [C<sub>12</sub>H<sub>26</sub>NO]<sup>+</sup> (M+H) calcd. 200.2009, found 200.2009.



***N*-(*tert*-butyl)-2-propylpentanamide (8b).** Following general procedure B and starting from 4-bromoheptane (89.6 mg, 0.500 mmol; 1 equiv), compound **8b** was obtained as a colorless solid (75.3 mg, 76% yield).

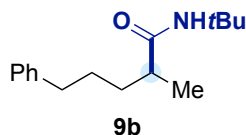
**<sup>1</sup>H NMR (400 MHz, CDCl<sub>3</sub>):**  $\delta$  = 5.31 (s, 1H), 1.91 – 1.77 (m, 1H), 1.59 – 1.43 (m, 2H), 1.29 (s, 9H), 1.26 – 1.13 (m, 6H), 0.83 (t,  $J$  = 7.2 Hz, 6H) ppm.

**<sup>13</sup>C NMR (101 MHz, CDCl<sub>3</sub>):**  $\delta$  = 175.4, 51.1, 48.4, 35.5, 28.9, 20.8, 14.2 ppm.

**mp:** 108.0 – 109.9 °C.

**IR (neat, cm<sup>-1</sup>):** 3294, 3076, 2956, 2929, 2872, 1638, 1549, 1448, 1360, 1266, 1228, 1121, 938, 754, 682.

**HRMS (ESI+):** [C<sub>12</sub>H<sub>25</sub>NNaO]<sup>+</sup> (M+Na) calcd. 222.1828, found 222.1823.



***N*-(*tert*-butyl)-2-methyl-5-phenylpentanamide (9b).** Following general procedure B starting from 4-bromopentyl]benzene (113.57 mg, 0.5 mmol), compound **9b** was obtained as a white solid (84.6 mg, 68% yield).

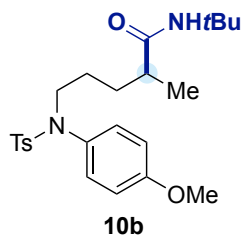
**<sup>1</sup>H NMR (400 MHz, CDCl<sub>3</sub>):**  $\delta$  = 7.36 – 7.26 (m, 2H), 7.20 (td,  $J$  = 7.2, 1.0 Hz, 2H), 5.24 (s, 1H), 2.72 – 2.50 (m, 2H), 2.13 – 1.95 (m, 1H), 1.78 – 1.55 (m, 3H), 1.48 – 1.39 (m, 10H), 1.35 (s, 9H), 1.11 (d,  $J$  = 6.8 Hz, 3H) ppm.

**<sup>13</sup>C NMR (101 MHz, CDCl<sub>3</sub>):**  $\delta$  175.9, 142.5, 128.5, 128.4, 125.8, 51.1, 42.3, 36.1, 34.2, 29.4, 29.0, 18.2 ppm.

**IR (neat, cm<sup>-1</sup>):** 3317, 3027, 2966, 2931, 2860, 1645, 1542, 1452, 1362, 1256, 1225, 747, 697.

**HRMS (ESI+):** [C<sub>16</sub>H<sub>25</sub>NNaO]<sup>+</sup> (M+H) calcd. 270.1828, found 270.1820.

**mp:** 75.1 – 77.0 °C.



***N*-(*tert*-butyl)-5-(*N*-(4-methoxyphenyl)-4-methylphenylsulfonamido)-2-methylpentanamide (10b).** Following procedure B, starting from *N*-(4-bromopentyl)-*N*-(4-methoxyphenyl)-4-methylbenzenesulfonamide (300 mg, 0.7 mmol) which was added as a 1 mL solution in DMF

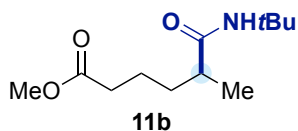
(prepared in a vial inside the glovebox) to a 0,4 mL solution of reaction mixture (overall volume 1,4 mL). Compound **10b** was obtained as a colorless viscous oil (196.7 mg, 0,44 mmol, 63% yield).

**<sup>1</sup>H NMR (400 MHz, CDCl<sub>3</sub>):**  $\delta$  = 7.46 – 7.32 (m, 2H), 7.22 – 7.13 (m, 2H), 6.90 – 6.82 (m, 2H), 6.78 – 6.69 (m, 2H), 5.53 (s, 1H), 3.72 (s, 3H), 3.50 (dt,  $J$  = 13.4, 6.9 Hz, 1H), 3.35 (dt,  $J$  = 13.0, 6.4 Hz, 1H), 2.35 (s, 3H), 2.14 – 1.99 (m, 1H), 1.68 – 1.52 (m, 1H), 1.40 – 1.28 (m, 3H), 1.23 (s, 9H), 0.98 (d,  $J$  = 6.8 Hz, 3H) ppm.

**<sup>13</sup>C NMR (101 MHz, CDCl<sub>3</sub>):**  $\delta$  = 175.6, 159.0, 143.3, 135.2, 131.3, 129.9, 129.4, 127.6, 114.2, 55.4, 50.8, 50.1, 40.7, 30.9, 28.7, 25.5, 21.5, 17.5 ppm.

**IR (neat, cm<sup>-1</sup>):** 3388, 3322, 2965, 2931, 2871, 1649, 1507, 1340, 1248, 1159, 1089, 1031, 913, 678, 581, 559, 546.

**HRMS (ESI+):** [C<sub>24</sub>H<sub>35</sub>N<sub>2</sub>O<sub>4</sub>S]<sup>+</sup> (M+H) calcd. 447.2312, found 447.2313.



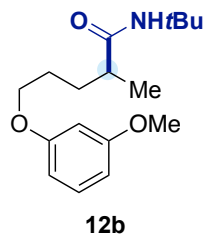
**Methyl 6-(*tert*-butylamino)-5-methyl-6-oxohexanoate (11b).** Following general procedure B with some modification, starting from methyl 5-bromohexanoate (104.5 mg, 0.500 mmol; 1 equiv), *tert*-butyl isocyanate (172  $\mu$ L, 149 mg, 1.5 mmol; 3 equiv) and Mn (55.0 mg, 1.0 mmol; 2 equiv), compound **11b** was obtained as a clear oil (87.7 mg, 76% average yield).

**<sup>1</sup>H NMR (500 MHz, CDCl<sub>3</sub>):**  $\delta$  = 5.32 (s, 1H), 3.65 (s, 3H), 2.37 – 2.22 (m, 2H), 2.10 – 1.98 (m, 1H), 1.68 – 1.52 (m, 3H), 1.39 – 1.34 (m, 1H), 1.33 (s, 9H), 1.09 (d,  $J$  = 6.8 Hz, 3H) ppm.

**<sup>13</sup>C NMR (126 MHz, CDCl<sub>3</sub>):**  $\delta$  = 175.6, 174.1, 51.6, 51.2, 42.2, 34.0, 33.9, 29.0, 22.9, 18.2 ppm.

**IR (neat, cm<sup>-1</sup>):** 3320, 2965, 2874, 1738, 1647, 1536, 1452, 1224.

**HRMS (ESI+):** [C<sub>12</sub>H<sub>23</sub>NNaO<sub>3</sub>]<sup>+</sup> (M+Na) calcd. 252.1570, found 252.1566.



***N*-(*tert*-butyl)-5-(3-methoxyphenoxy)-2-methylpentanamide (12b).** Following general procedure B, starting from 1-((4-bromopentyl)oxy)-3-methoxybenzene (136.6 mg, 0.500 mmol; 1 equiv) and *tert*-butyl isocyanate (86.0  $\mu$ L, 74.3 mg, 0.750 mmol; 1.50 equiv), compound **12b** was obtained as a colorless solid (110.1 mg, 75% average yield).

**<sup>1</sup>H NMR (500 MHz, CDCl<sub>3</sub>):**  $\delta$  = 7.17 (t,  $J$  = 8.2 Hz, 1H), 6.53 – 6.46 (m, 2H), 6.45 (t,  $J$  = 2.3 Hz, 1H), 5.31 (s, 1H), 4.02 – 3.95 (m, 1H), 3.95 – 3.88 (m, 1H), 3.79 (s, 3H), 2.16 – 2.10 (m, 1H), 1.82 – 1.72 (m, 3H), 1.59 – 1.50 (m, 1H), 1.35 (s, 9H), 1.13 (d,  $J$  = 6.8 Hz, 3H) ppm.

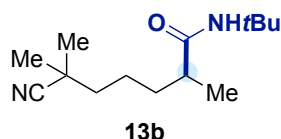
**<sup>13</sup>C NMR (126 MHz, CDCl<sub>3</sub>):**  $\delta$  = 175.7, 161.0, 160.3, 130.0, 106.8, 106.4, 101.1, 68.2, 55.4, 51.2, 42.1, 31.3, 29.0, 27.3, 18.3 ppm.

**IR (neat, cm<sup>-1</sup>):** 3322, 2964, 2873, 1649, 1594, 1493, 1453, 1151, 1046.



**HRMS (ESI+):**  $[\text{C}_{17}\text{H}_{27}\text{NNaO}_3]^+$  (M+Na) calcd. 316.1883, found 316.1870.

**mp:** 69.9 – 72.9 °C.



***N*-(*tert*-butyl)-6-cyano-2,6-dimethylheptanamide**

**(13b).** Following general procedure B, starting from 6-bromo-2,2-dimethylheptanenitrile (109.1 mg, 0.500 mmol; 1 equiv) and *tert*-butyl isocyanate (86.0  $\mu\text{L}$ , 74.3 mg, 0.750 mmol; 1.50 equiv), compound **13b** was obtained as an off white solid (100.6 mg, 87% yield).

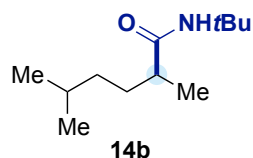
**$^1\text{H}$  NMR (400 MHz,  $\text{CDCl}_3$ ):**  $\delta$  = 5.33 (s, 1H), 2.12 – 1.98 (m, 1H), 1.70 – 1.56 (m, 1H), 1.52 – 1.42 (m, 5H), 1.32 (s, 9H), 1.30 (s, 3H), 1.28 (s, 3H), 1.08 (d,  $J$  = 6.8 Hz, 3H) ppm.

**$^{13}\text{C}$  NMR (101 MHz,  $\text{CDCl}_3$ ):**  $\delta$  = 175.6, 125.2, 51.1, 42.2, 41.0, 34.2, 32.5, 28.9, 27.0, 26.5, 23.4, 18.2 ppm.

**IR (neat,  $\text{cm}^{-1}$ ):** 3296, 3079, 2967, 2932, 2870, 2235, 1644, 1551, 1459, 1390, 1361, 1265, 1225, 687.

**HRMS (ESI+):**  $[\text{C}_{14}\text{H}_{27}\text{N}_2\text{O}]^+$  (M+H) calcd. 239.2118, found 239.2118.

**mp:** 86.1 – 88.4 °C.



***N*-(*tert*-butyl)-2,5-dimethylhexanamide (14b).** Following general procedure B and starting from 90 mg (0.5 mmol) of 2-bromo-5-methylhexane, compound **14b** was obtained as a white solid (56.5 mg, 0.28 mmol, 57% yield).

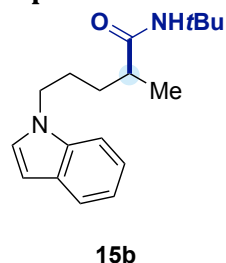
**$^1\text{H}$  NMR (400 MHz,  $\text{CDCl}_3$ ):**  $\delta$  = 5.24 (s, 1H), 2.07 – 1.86 (m, 1H), 1.63 – 1.40 (m, 2H), 1.37 – 1.25 (m, 10H), 1.19 – 1.09 (m, 2H), 1.07 (d,  $J$  = 6.8 Hz, 3H), 0.85 (dd,  $J$  = 6.7, 0.9 Hz, 6H). ppm.

**$^{13}\text{C}$  NMR (101 MHz,  $\text{CDCl}_3$ ):**  $\delta$  = 176.1, 51.0, 42.6, 36.8, 32.4, 29.0, 28.3, 28.2, 22.7, 22.7, 18.1 ppm.

**IR (neat,  $\text{cm}^{-1}$ ):** 3312, 3076, 2961, 2930, 2870, 1644, 1546, 1451, 1390, 1360, 1263, 1227, 672.

**HRMS (ESI+):**  $[\text{C}_{12}\text{H}_{26}\text{NO}]^+$  (M+H) calcd. 200.2009, found 200.2008.

**mp:** 52.2 – 54.0 °C.



***N*-(*tert*-butyl)-5-(1*H*-indol-1-yl)-2-methylpentanamide**

**(15b).** Following general procedure B, starting from 1-(4-bromopentyl)-1*H*-indole (133.1 mg, 0.500 mmol; 1 equiv) and *tert*-butyl isocyanate (86.0  $\mu\text{L}$ , 74.3 mg, 0.750 mmol; 1.50 equiv), compound **15b** was obtained as a yellow oil (134.7, 93% average yield).

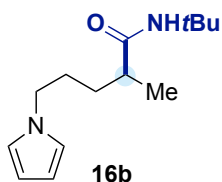
**$^1\text{H}$  NMR (400 MHz,  $\text{CDCl}_3$ ):**  $\delta$  = 7.63 (dt,  $J$  = 7.9, 0.9 Hz, 1H), 7.36 – 7.32 (m, 1H), 7.23 – 7.17 (m, 1H), 7.12 – 7.07 (m, 2H), 6.49 (dd,  $J$  = 3.1, 0.8 Hz, 1H),

5.07 (s, 1H), 4.21 – 4.03 (m, 2H), 1.93 – 1.87 (m, 1H), 1.87 – 1.78 (m, 2H), 1.72 – 1.61 (m, 1H), 1.40 – 1.31 (m, 1H), 1.29 (s, 9H), 1.05 (d,  $J = 6.8$  Hz, 3H) ppm.

$^{13}\text{C}$  NMR (101 MHz,  $\text{CDCl}_3$ ):  $\delta = 175.4, 136.0, 128.7, 127.9, 121.6, 121.1, 119.4, 109.5, 101.2, 51.2, 46.6, 42.0, 31.9, 28.9, 28.1, 18.4$  ppm.

IR (neat,  $\text{cm}^{-1}$ ): 3322, 2965, 2931, 2872, 1646, 1510, 1362, 1224, 737.

HRMS (ESI+):  $[\text{C}_{18}\text{H}_{26}\text{N}_2\text{NaO}]^+$  (M+Na) calcd. 309.1937, found 309.1943.



***N*-(*tert*-butyl)-2-methyl-5-(1*H*-pyrrol-1-yl)pentanamide (16b).** Following general procedure B, starting from 1-(4-bromopentyl)-1*H*-pyrrole (108.1 mg, 0.500 mmol; 1 equiv) and *tert*-butyl isocyanate (86.0  $\mu\text{L}$ , 74.3 mg, 0.750 mmol; 1.50 equiv), compound **16b** was obtained as a beige solid (106.0 mg, 90%

average yield).

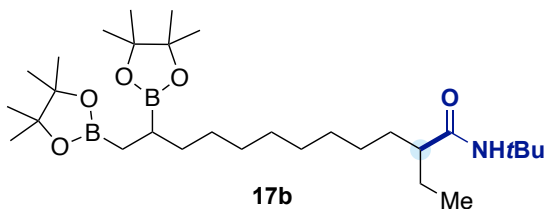
$^1\text{H}$  NMR (400 MHz,  $\text{CDCl}_3$ ):  $\delta = 6.64$  (s, 2H), 6.14 (s, 2H), 5.17 (s, 1H), 3.96 – 3.87 (m, 1H), 3.87 – 3.78 (m, 1H), 1.96 – 1.85 (m, 1H), 1.80 – 1.69 (m, 2H), 1.68 – 1.56 (m, 1H), 1.33 (s, 9H), 1.37 – 1.28 (m, 1H), 1.07 (d,  $J = 6.8$  Hz, 3H) ppm.

$^{13}\text{C}$  NMR (101 MHz,  $\text{CDCl}_3$ ):  $\delta = 175.5, 120.6, 108.1, 51.2, 49.8, 41.9, 31.8, 29.5, 29.0, 18.3$  ppm.

IR (neat,  $\text{cm}^{-1}$ ): 3320, 2965, 2931, 2873, 1645, 1541, 1452, 1088, 719.

HRMS (ESI+):  $[\text{C}_{14}\text{H}_{24}\text{N}_2\text{NaO}]^+$  (M+Na) calcd. 259.1781, found 259.1785.

mp: 59.5 – 61.9  $^\circ\text{C}$ .



***N*-(*tert*-butyl)-2-ethyl-12-(4,4,5,5-tetramethyl-1,3,2-dioxaborolan-2-yl)dodecanamide (17b).** Following general procedure B, starting from 2,2'-(11-bromotridecane-1,2-diyl)bis(4,4,5,5-tetramethyl-1,3,2-dioxaborolane) (258.0 mg, 0.500 mmol; 1 equiv) and *tert*-butyl isocyanate (86.0  $\mu\text{L}$ , 74.3 mg, 0.750 mmol; 1.50 equiv), compound **17b** was obtained as a yellow oil (242.7 mg, 91% average yield).

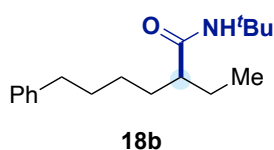
$^1\text{H}$  NMR (400 MHz,  $\text{CDCl}_3$ ):  $\delta = 5.25$  (s, 1H), 1.71 (dq,  $J = 9.5, 4.7$  Hz, 1H), 1.57 – 1.43 (m, 2H), 1.41 – 1.32 (m, 3H), 1.30 (s, 9H), 1.22 – 1.10 (m, 37H), 1.08 – 1.02 (m, 1H), 0.82 (t,  $J = 7.5$  Hz, 3H), 0.75 (d,  $J = 5.8$  Hz, 2H) ppm.

$^{13}\text{C}$  NMR (101 MHz,  $\text{CDCl}_3$ ):  $\delta = 175.2, 82.8, 82.7, 51.1, 50.4, 33.8, 33.0, 29.8, 29.7, 29.5, 29.5, 28.9, 28.8, 27.6, 26.2, 24.9, 24.8, 24.8, 24.7, 18.4, 12.7, 12.1$  ppm.

$^{11}\text{B}$  NMR (128 MHz,  $\text{CDCl}_3$ ):  $\delta = 33.1$  ppm.

IR (neat,  $\text{cm}^{-1}$ ): 3338, 2976, 2926, 2854, 2246, 1650, 1539, 1454, 1370, 1312, 1215, 1141, 968, 909, 846, 730.

**HRMS (ESI+):**  $[C_{30}H_{60}NB_2O]^+$  (M+H) calcd. 536.4644, found 536.4645.



***N*-(*tert*-butyl)-2-ethyl-6-phenylhexanamide (18b).**

Following general procedure B and starting from (5-bromoheptyl)benzene (127.6 mg, 0.500 mmol; 1 equiv) and *tert*-butyl isocyanate (86.0  $\mu$ L, 74.3 mg, 0.750 mmol; 1.50 equiv), compound **18b** was obtained as a white solid (113.0

mg, 82% average yield).

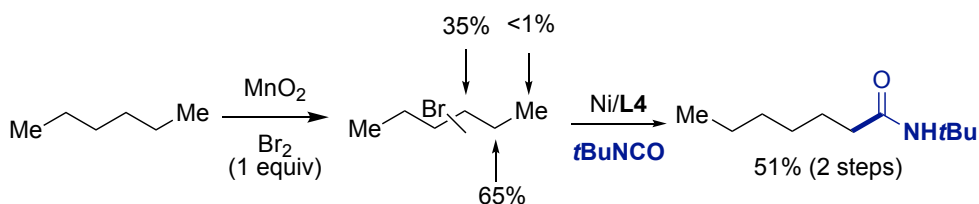
**$^1H$  NMR (400 MHz,  $CDCl_3$ ):**  $\delta$  = 7.33 – 7.24 (m, 2H), 7.22 – 7.14 (m, 3H), 5.29 (s, 1H), 2.61 (t,  $J$  = 7.3 Hz, 2H), 1.83 – 1.72 (m, 1H), 1.67 – 1.52 (m, 4H), 1.35 (s, 9H), 1.45 – 1.22 (m, 4H), 0.89 (t,  $J$  = 7.4 Hz, 3H) ppm.

**$^{13}C$  NMR (101 MHz,  $CDCl_3$ ):**  $\delta$  = 175.2, 142.7, 128.5, 128.4, 125.8, 51.3, 50.6, 36.0, 33.0, 31.6, 29.0, 27.4, 26.4, 12.2 ppm.

**IR (neat,  $cm^{-1}$ ):** 3320, 3026, 2962, 2930, 2858, 1644, 1540, 1453, 1391, 1361, 1225, 745, 697.

**HRMS (ESI+):**  $[C_{18}H_{29}NNaO]^+$  (M+Na) calcd. 298.2141, found 298.2140.

**mp:** 68.1 – 70.2  $^{\circ}C$ .



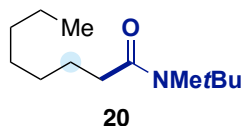
***N*-(*tert*-butyl)heptanamide (19).** 2.5 mL of HPLC grade *n*hexane were placed in a screw-capped vial with  $MnO_2$  (87.0 mg, 1.0 mmol).  $Br_2$  (79.9 mg, 25 mmol 0.500 mmol; 1 equiv) was added dropwise and stirred overnight. The resulting solution was filtered through a plug of  $SiO_2$  and the crude was partially evaporated at 300 mbar/40  $^{\circ}C$  to get approximately 300 mL of crude mixture. Following amidation procedure A using *tert*-butyl isocyanate (86.0  $\mu$ L, 74.3 mg, 0.750 mmol; 1.50 equiv) and the crude alkyl bromide obtained before, compound **19** was obtained as a pale light-yellow oil (47.4 mg, 51% yield).

**$^1H$  NMR (400 MHz,  $CDCl_3$ ):**  $\delta$  = 5.33 (s, 1H), 2.05 (t,  $J$  = 7.4 Hz, 2H), 1.55 (p,  $J$  = 7.7 Hz, 2H), 1.31 (s, 9H), 1.28 – 1.24 (m, 4H), 0.85 (t,  $J$  = 7.0 Hz, 3H) ppm.

**$^{13}C$  NMR (101 MHz,  $CDCl_3$ ):**  $\delta$  = 172.6, 51.1, 37.8, 31.7, 29.0, 28.9 (3C), 25.9, 22.6, 14.1 ppm.

**IR (neat,  $cm^{-1}$ ):** 3306, 3076, 2959, 2927, 2859, 1643, 1546, 1453, 1362, 1225.

**HRMS (ESI+):**  $[C_{11}H_{23}NNaO]^+$  (M+Na) calcd. 208.1672, found 208.1667.

***N*-(*tert*-butyl)-*N*-methyloctanamide (20).**

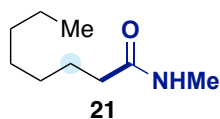
An oven-dried vial equipped with a stirring bar was directly transferred from the oven to the glovebox and charged with NiI<sub>2</sub> (3.91 mg, 0.012 mmol), Mn (68.67 mg, 1.25 mmol) and **L7** (8.41 mg, 0.025 mmol) and 1 mL of NMP. The suspension was left stirring time until its color turn to dark blue, moment in which the respective isocyanate (0.75 mmol) was added. The oven-dried screw-capped test was set in a temperature controlled (10 °C) reaction block outside the glovebox. The suspension was left to stir at this temperature for additional 15 min. Then, the alkyl bromide (0.5 mmol) was added dropwise. The reaction was left under stirring for additional 24 h at the same temperature, and after this period, it was treated with MeI and left to stir for 24h at 60 °C. It was quenched then with saturated NH<sub>4</sub>Cl solution and extracted with EtOAc. The organic phase was dried over MgSO<sub>4</sub> and concentrated under reduced pressure. The crude obtained was purified by flash chromatography (Hex/EtOAc 5%) to afford compound **20** as colorless oil (44 mg, 41% yield).

**<sup>1</sup>H NMR (400 MHz, CDCl<sub>3</sub>):** δ = 2.88 (s, 3H), 2.31 – 2.23 (m, 2H), 1.58 (p, *J* = 7.9, 7.4 Hz, 2H), 1.39 (s, 9H), 1.32 – 1.24 (m, 8H), 0.86 (t, *J* = 6.6 Hz, 3H) ppm.

**<sup>13</sup>C NMR (100 MHz, CDCl<sub>3</sub>):** δ = 174.0, 56.7, 37.0, 32.1, 31.9, 29.5, 29.3, 28.5, 25.5, 22.8, 14.2 ppm.

**IR (neat, cm<sup>-1</sup>):** 2957, 2924, 2855, 1647, 1456, 1386, 1362, 1217, 1126, 1097, 731.

**HRMS (ESI+):** [C<sub>13</sub>H<sub>27</sub>NNaO]<sup>+</sup> (M+Na) calcd. 236.19875, found 236.1982.

***N*-methyloctanamide (21).**

A schlenk tube was charged with the *N*-(*tert*-butyl)-*N*-methyloctanamide **20** (63 mg, 0,3 mmol), Cu(OTf)<sub>2</sub> (21 mg, 0,06 mmol, 2 mol%) and DCM. The system was stirred at 80 °C for 36 h, cooled down to room temperature and treated with water. The aqueous phase was extracted with DCM and the organic phases ware collected together, dried over MgSO<sub>4</sub> and concentrated. The crude was purified by chromatography to afford **21** as a white semi-solid (32 mg, 69% yield).

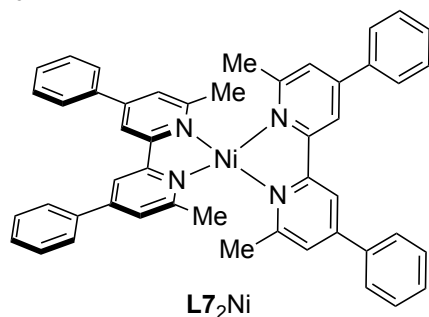
**<sup>1</sup>H NMR (400 MHz, CDCl<sub>3</sub>):** δ = 5.83 (s, 1H), 2.76 (d, *J* = 4.8 Hz, 3H), 2.24 – 1.97 (m, 2H), 1.58 (td, *J* = 8.5, 7.9, 4.5 Hz, 2H), 1.34 – 1.14 (m, 8H), 0.91 – 0.73 (m, 3H) ppm.

**<sup>13</sup>C NMR (100 MHz, CDCl<sub>3</sub>):** δ = 174.1, 36.8, 31.8, 29.4, 29.1, 26.3, 25.9, 22.7, 14.1 ppm.

**IR (neat, cm<sup>-1</sup>):** 3293, 2956, 2927, 2857, 1649, 1560, 1465, 1411.

**HRMS (ESI+):** [C<sub>9</sub>H<sub>20</sub>NO]<sup>+</sup> (M+H) calcd. 158.1539, found 158.1538.

Synthesis of **L7<sub>2</sub>Ni**:

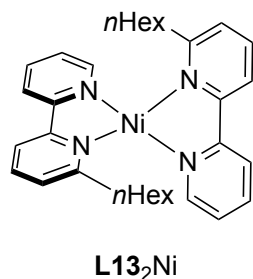


In the glovebox, **L7NiBr<sub>2</sub>** (383 mg, 0.29 mmol) was added to a 10 mL vial. A stirbar was added and it was charged with 3 mL of cold toluene (-36 °C), affording a pink suspension. **MgCl(CH<sub>2</sub>SiMe<sub>3</sub>)** in THF (730 uL 0.84M, 2.1 equiv) was then added dropwise turning the pink suspension into a brown solution which then turned red. After the addition of Grignard, **L7** (108 mg, 1.1 equiv) was added in 2 mL of

cold toluene (-36 °C) as a suspension where the solution turned purple. After 3 h the now blue solution was filtered through a pipette plug of celite with black solid being filtered off and a blue solution collected. The solvent was removed to afford a blue powder and washed with cold (-36 °C) pentane (1 mL x 3) to give **L7<sub>2</sub>Ni** (138 mg, 65 %) as a blue powder. Single crystals were obtained by cooling a saturated solution in pentanes.

**<sup>1</sup>H NMR (400 MHz, THF-*d*<sub>8</sub>)** δ = 8.20 (d, *J* = 1.7 Hz, 4H), 8.14 – 7.94 (m, 12H), 7.60 (t, *J* = 7.4 Hz, 4H), 7.31 (t, *J* = 7.8 Hz, 8H), 2.65 (s, 12H) ppm.

**<sup>13</sup>C NMR (101 MHz, THF-*d*<sub>8</sub>)** δ = 159.6, 144.6, 140.0, 131.0, 130.5, 126.0, 124.1, 122.9, 119.1, 28.2 ppm.



Synthesis of **L13<sub>2</sub>Ni**:

In the glovebox, **L13NiBr<sub>2</sub>** (92 mg, 0.21 mmol) was added to a 10 mL vial. A stirbar was added and it was charged with 2.5 mL of cold toluene (-36 °C) and **L13** (94 mg, 42 mmol) affording a pink suspension. **EtMgBr** in THF (150 mL, 3 M, 2.2 equiv) was then added dropwise turning the pink suspension, yellow and then blue. After 1 hour a black precipitate was filtered off through a celite plug and the blue filtrate was

concentrated to dryness. The solid was redissolved in pentane and filtered through a celite plug and concentrated to dryness affording **L13<sub>2</sub>Ni** (8 mg, 7 %) as a blue powder. Single crystals were obtained by cooling a saturated solution in pentanes.

**<sup>1</sup>H NMR (500 MHz, C<sub>6</sub>D<sub>6</sub>)** δ = 10.38 (dt, *J* = 5.9, 1.2 Hz, 2H), 8.29 – 8.03 (m, 4H), 7.63 (dd, *J* = 6.8, 1.1 Hz, 2H), 7.36 – 7.22 (m, 6H), 3.39 (dddd, *J* = 84.4, 13.6, 10.7, 5.4 Hz, 4H), 2.19 – 1.77 (m, 4H), 1.16 – 0.68 (m, 18H) ppm.

**<sup>13</sup>C NMR (126 MHz, C<sub>6</sub>D<sub>6</sub>)** δ = 149.1, 136.8, 136.2, 123.2, 122.9, 122.5, 121.7, 120.8, 119.6, 118.3, 42.3, 38.5, 31.9, 29.8, 29.5, 29.2, 28.8, 22.7, 14.0 ppm.

## Chapter 5

### Crystal data and structure refinement for $L7_2Ni$ .

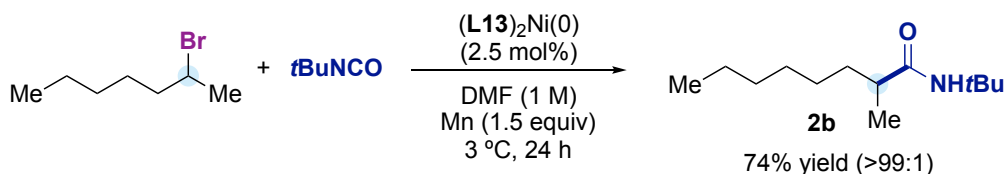
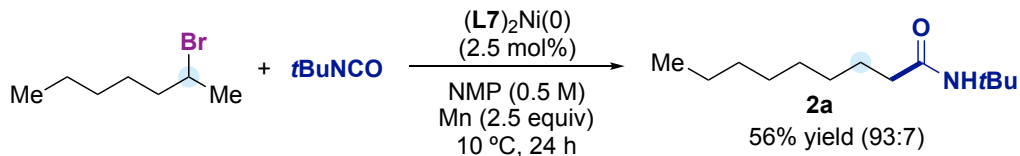
Empirical formula	C <sub>48</sub> H <sub>40</sub> N <sub>4</sub> Ni
Formula weight	731.55
Temperature	100(2)K
Wavelength	0.71073 Å
Crystal system	monoclinic
Space group	P 21/c
Unit cell dimensions	a = 18.259(3)Å      a = 90° b = 17.663(2)Å      b = 104.816(5)° c = 11.5624(13)Å    g = 90°.
Volume	3604.9(8) Å <sup>3</sup>
Z	4
Density (calculated)	1.348 Mg/m <sup>3</sup>
Absorption coefficient	0.580 mm <sup>-1</sup>
F(000)	1536
Crystal size	0.060 x 0.030 x 0.010 mm <sup>3</sup>
Theta range for data collection	2.156 to 25.713°.
Index ranges	-21 ≤ h ≤ 22, -21 ≤ k ≤ 14, -10 ≤ l ≤ 13
Reflections collected	21289
Independent reflections	6750 [R(int) = 0.1790]
Completeness to theta = 25.713°	98.3%
Absorption correction	Multi-scan
Max. and min. transmission	0.74 and 0.61
Refinement method	Full-matrix least-squares on F <sup>2</sup>
Data / restraints / parameters	6750 / 488 / 528
Goodness-of-fit on F <sup>2</sup>	0.970
Final R indices [I > 2σ(I)]	R1 = 0.0756, wR2 = 0.1124
R indices (all data)	R1 = 0.2162, wR2 = 0.1530
Largest diff. peak and hole	0.492 and -0.567 e.Å <sup>-3</sup>

Regiodivergent Ligand-Controlled Ni-Catalyzed Reductive Amidation of Unactivated  
Secondary Alkyl Bromides

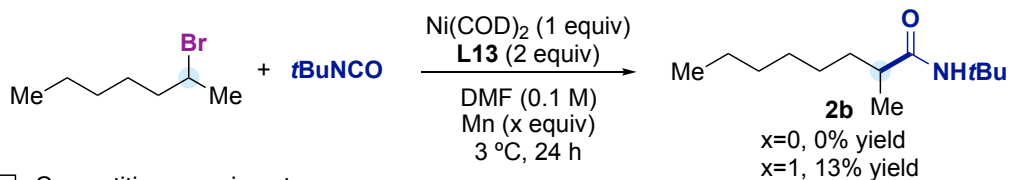
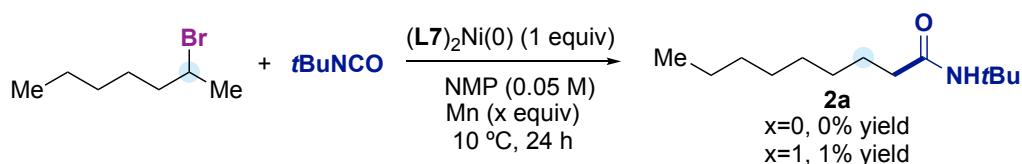
Crystal data and structure refinement for **L13<sub>2</sub>Ni**.

Empirical formula	C <sub>32</sub> H <sub>40</sub> N <sub>4</sub> Ni	
Formula weight	539.39	
Temperature	100(2)K	
Wavelength	0.71073 Å	
Crystal system	monoclinic	
Space group	P 2 <sub>1</sub> /n	
Unit cell dimensions	a = 17.2651(13)Å	a = 90°.
	b = 8.0978(6)Å	b = 102.933(2)°.
	c = 20.5663(16)Å	g = 90°.
Volume	2802.4(4) Å <sup>3</sup>	
Z	4	
Density (calculated)	1.278 Mg/m <sup>3</sup>	
Absorption coefficient	0.720 mm <sup>-1</sup>	
F(000)	1152	
Crystal size	0.500 x 0.200 x 0.030 mm <sup>3</sup>	
Theta range for data collection	2.032 to 33.945°.	
Index ranges	-26 ≤ h ≤ 26, -12 ≤ k ≤ 8, -32 ≤ l ≤ 32	
Reflections collected	58430	
Independent reflections	11254[R(int) = 0.0650]	
Completeness to theta = 33.945°	98.9%	
Absorption correction	Multi-scan	
Max. and min. transmission	0.74 and 0.64	
Refinement method	Full-matrix least-squares on F <sup>2</sup>	
Data / restraints / parameters	11254/ 246/ 392	
Goodness-of-fit on F <sup>2</sup>	1.028	
Final R indices [I > 2σ(I)]	R1 = 0.0468, wR2 = 0.0965	
R indices (all data)	R1 = 0.0863, wR2 = 0.1106	
Largest diff. peak and hole	0.567 and -0.336 e.Å <sup>-3</sup>	

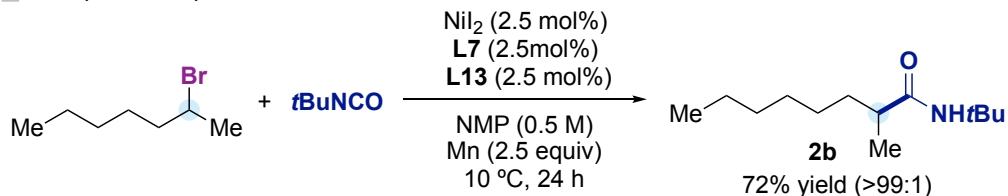
## Experiments for getting a mechanistic insight:

□ Activity of  $L_2Ni$  as catalyst

## □ Stoichiometric experiments



## □ Competitive experiment



In a nitrogen-filled glovebox, an oven-dried screw-capped test tube containing a stirring bar was charged with the nickel complex and ligand and/or Mn (if necessary). The obtained mixture was stirred at rt (*ca.* 1 min), after which *tert*-butyl isocyanate (0.75 mmol; 1.5 equiv) was added. Subsequently, the reaction mixture was cooled down to the desired temperature outside the glovebox, and 2-bromoheptane was added (0.5 mmol; 1 equiv). The resulting mixture was stirred for 24 h, at the desired temperature using a metallic block with a recirculating liquid refrigerated by a chiller. The crude reaction mixture was carefully quenched with 5% aq. HCl (1 mL) and extracted with ethyl acetate. A sample of the obtained solution was filtered through a silica-celite plug, eluted with ethyl acetate and analyzed by GC-FID using anisole as internal standard.



## References:

- (1) Ulrich, H. *Chemistry and Technology of Isocyanates*; Wiley, **1996**.
- (2) Villa, J. F.; Powell, H. B. Preparation, Characterization and Lewis Basicity of Some Copper(II) and Nickel(II) Adducts with Organic Isocyanates and Isothiocyanates. *Inorganica Chimica Acta* **1979**, *32*, 199–204. [https://doi.org/10.1016/S0020-1693\(00\)91661-X](https://doi.org/10.1016/S0020-1693(00)91661-X).
- (3) Braunstein, P.; Nobel, D. Transition-Metal-Mediated Reactions of Organic Isocyanates. *Chem. Rev.* **1989**, *89* (8), 1927–1945. <https://doi.org/10.1021/cr00098a013>.
- (4) Six, C.; Richter, F. Isocyanates, Organic. In *Ullmann's Encyclopedia of Industrial Chemistry*; American Cancer Society, 2003. [https://doi.org/10.1002/14356007.a14\\_611](https://doi.org/10.1002/14356007.a14_611).
- (5) Villa, J. F.; Powell, H. B. The Reaction of Some Inorganic Lewis Bases and Acids with Organic Isocyanates. *Synthesis and Reactivity in Inorganic and Metal-Organic Chemistry* **1976**, *6* (1), 59–63. <https://doi.org/10.1080/00945717608057340>.
- (6) Foley, S. R.; Yap, G. P. A.; Richeson, D. S. Formation of Novel Tetrasulfido Tin Complexes and Their Ability To Catalyze the Cyclotrimerization of Aryl Isocyanates. *Organometallics* **1999**, *18* (23), 4700–4705. <https://doi.org/10.1021/om990405w>.
- (7) Paul, F.; Moulin, S.; Piechaczyk, O.; Le Floch, P.; Osborn, J. A. Palladium(0)-Catalyzed Trimerization of Arylisocyanates into 1,3,5-Triarylisocyanurates in the Presence of Diimines: A Nonintuitive Mechanism. *J. Am. Chem. Soc.* **2007**, *129* (23), 7294–7304. <https://doi.org/10.1021/ja068291k>.
- (8) Blaise, E. E. Nouvelles Réactions de Dérivés Organométalliques. *Compt. rend* **1901**, *132*, 38–41.
- (9) Gilman, H.; Kinney, C. R. The Mechanism of the Reaction of Isocyanates and Isothiocyanates with the Grignard Reagent. *J. Am. Chem. Soc.* **1924**, *46* (2), 493–497. <https://doi.org/10.1021/ja01667a027>.
- (10) Gilman, H.; Furry, M. The Identification of Organomagnesium Halides by Crystalline Derivatives Prepared from  $\alpha$ -Naphthyl Isocyanate. *J. Am. Chem. Soc.* **1928**, *50* (4), 1214–1216. <https://doi.org/10.1021/ja01391a039>.
- (11) Gilman, H.; Breuer, F. The Mechanism of Reaction of Phenyl-Sodium and Phenyl-Lithium with Phenyl Isothiocyanate. *J. Am. Chem. Soc.* **1933**, *55* (3), 1262–1264. <https://doi.org/10.1021/ja01330a071>.
- (12) Coldham, I.; Dufour, S.; Haxell, T. F. N.; Vennall, G. P. Dynamic Resolution of N-Alkyl-2-Lithiopyrrolidines with the Chiral Ligand (–)-Sparteine. *Tetrahedron* **2005**, *61* (13), 3205–3220. <https://doi.org/10.1016/j.tet.2005.01.096>.
- (13) Schäfer, G.; Matthey, C.; Bode, J. W. Facile Synthesis of Sterically Hindered and Electron-Deficient Secondary Amides from Isocyanates. *Angew. Chem. Int. Ed.* **2012**, *51* (36), 9173–9175. <https://doi.org/10.1002/anie.201204481>.
- (14) Serrano, E.; Martin, R. Forging Amides Through Metal-Catalyzed C–C Coupling with Isocyanates. *Eur. J. Org. Chem.* **2018**, *2018* (24), 3051–3064. <https://doi.org/10.1002/ejoc.201800175>.
- (15) Correa, A.; Martin, R. Ni-Catalyzed Direct Reductive Amidation via C–O Bond Cleavage. *J. Am. Chem. Soc.* **2014**, *136* (20), 7253–7256. <https://doi.org/10.1021/ja5029793>.
- (16) Serrano, E.; Martin, R. Nickel-Catalyzed Reductive Amidation of Unactivated Alkyl Bromides. *Angew. Chem. Int. Ed.* **2016**, *55* (37), 11207–11211. <https://doi.org/10.1002/anie.201605162>.
- (17) Wang, X.; Nakajima, M.; Serrano, E.; Martin, R. Alkyl Bromides as Mild Hydride Sources in Ni-Catalyzed Hydroamidation of Alkynes with Isocyanates. *J. Am. Chem. Soc.* **2016**, *138* (48), 15531–15534. <https://doi.org/10.1021/jacs.6b10351>.
- (18) Ananikov, V. P.; Beletskaya, I. P. Alkyne and Alkene Insertion into Metal–Heteroatom and Metal–Hydrogen Bonds: The Key Stages of Hydrofunctionalization Process. In

*Hydrofunctionalization*; Ananikov, V. P., Tanaka, M., Eds.; Topics in Organometallic Chemistry; Springer Berlin Heidelberg: Berlin, Heidelberg, 2012; Vol. 43, pp 1–19. [https://doi.org/10.1007/3418\\_2012\\_54](https://doi.org/10.1007/3418_2012_54).

(19) Trost, B. M.; Ball, Z. T. Addition of Metalloid Hydrides to Alkynes: Hydrometallation with Boron, Silicon, and Tin. *Synthesis* **2005**, *2005* (6), 853–887. <https://doi.org/10.1055/s-2005-861874>.

(20) Zhou, J. (Steve); Fu, G. C. Cross-Couplings of Unactivated Secondary Alkyl Halides: Room-Temperature Nickel-Catalyzed Negishi Reactions of Alkyl Bromides and Iodides. *J. Am. Chem. Soc.* **2003**, *125* (48), 14726–14727. <https://doi.org/10.1021/ja0389366>.

(21) Rudolph, A.; Lautens, M. Secondary Alkyl Halides in Transition-Metal-Catalyzed Cross-Coupling Reactions. *Angew. Chem. Int. Ed.* **2009**, *48* (15), 2656–2670. <https://doi.org/10.1002/anie.200803611>.

(22) Hu, X. Nickel-Catalyzed Cross Coupling of Non-Activated Alkyl Halides: A Mechanistic Perspective. *Chem. Sci.* **2011**, *2* (10), 1867–1886. <https://doi.org/10.1039/C1SC00368B>.

(23) Weix, D. J. Methods and Mechanisms for Cross-Electrophile Coupling of Csp<sup>2</sup> Halides with Alkyl Electrophiles. *Acc. Chem. Res.* **2015**, *48* (6), 1767–1775. <https://doi.org/10.1021/acs.accounts.5b00057>.

(24) Richmond, E.; Moran, J. Recent Advances in Nickel Catalysis Enabled by Stoichiometric Metallic Reducing Agents. *Synthesis* **2018**, *50* (3), 499–513. <https://doi.org/10.1055/s-0036-1591853>.

(25) Duan, Z.; Li, W.; Lei, A. Nickel-Catalyzed Reductive Cross-Coupling of Aryl Bromides with Alkyl Bromides: Et<sub>3</sub>N as the Terminal Reductant. *Org. Lett.* **2016**, *18* (16), 4012–4015. <https://doi.org/10.1021/acs.orglett.6b01837>.

(26) McCallum, T.; Barriault, L. Direct Alkylation of Heteroarenes with Unactivated Bromoalkanes Using Photoredox Gold Catalysis. *Chem. Sci.* **2016**, *7* (7), 4754–4758. <https://doi.org/10.1039/C6SC00807K>.

(27) Zhang, P.; Le, C. “Chip”; MacMillan, D. W. C. Silyl Radical Activation of Alkyl Halides in Metallaphotoredox Catalysis: A Unique Pathway for Cross-Electrophile Coupling. *J. Am. Chem. Soc.* **2016**, *138* (26), 8084–8087. <https://doi.org/10.1021/jacs.6b04818>.

(28) Cherney, A. H.; Kadunce, N. T.; Reisman, S. E. Catalytic Asymmetric Reductive Acyl Cross-Coupling: Synthesis of Enantioenriched Acyclic  $\alpha,\alpha$ -Disubstituted Ketones. *J. Am. Chem. Soc.* **2013**, *135* (20), 7442–7445. <https://doi.org/10.1021/ja402922w>.

(29) Cherney, A. H.; Kadunce, N. T.; Reisman, S. E. Enantioselective and Enantiospecific Transition-Metal-Catalyzed Cross-Coupling Reactions of Organometallic Reagents To Construct C–C Bonds. *Chem. Rev.* **2015**, *115* (17), 9587–9652. <https://doi.org/10.1021/acs.chemrev.5b00162>.

(30) Xue, X.-S.; Ji, P.; Zhou, B.; Cheng, J.-P. The Essential Role of Bond Energetics in C–H Activation/Functionalization. *Chem. Rev.* **2017**, *117* (13), 8622–8648. <https://doi.org/10.1021/acs.chemrev.6b00664>.

(31) Jun, C.-H.; Park, Y. J.; Zhang, X.; Larock, R. C. C–H Transformation at Aldehydes and Imines. In *Handbook of C–H Transformations*; John Wiley & Sons, Ltd, 2008; pp 303–316. <https://doi.org/10.1002/9783527619450.ch7>.

(32) Hartwig, J. F.; Larsen, M. A. Undirected, Homogeneous C–H Bond Functionalization: Challenges and Opportunities. *ACS Cent. Sci.* **2016**, *2* (5), 281–292. <https://doi.org/10.1021/acscentsci.6b00032>.

(33) Perez-Rizquez, C.; Rodriguez-Otero, A.; Palomo, J. M. Combining Enzymes and Organometallic Complexes: Novel Artificial Metalloenzymes and Hybrid Systems for C–H Activation Chemistry. *Org. Biomol. Chem.* **2019**, *17* (30), 7114–7123.

<https://doi.org/10.1039/C9OB01091B>.

(34) Sommer, H.; Juliá-Hernández, F.; Martin, R.; Marek, I. Walking Metals for Remote Functionalization. *ACS Cent. Sci.* **2018**, *4* (2), 153–165. <https://doi.org/10.1021/acscentsci.8b00005>.

(35) Johnson, L. K.; Killian, C. M.; Brookhart, M. New Pd(II)- and Ni(II)-Based Catalysts for Polymerization of Ethylene and  $\alpha$ -Olefins. *J. Am. Chem. Soc.* **1995**, *117* (23), 6414–6415. <https://doi.org/10.1021/ja00128a054>.

(36) Vasseur, A.; Bruffaerts, J.; Marek, I. Remote Functionalization through Alkene Isomerization. *Nature Chem* **2016**, *8* (3), 209–219. <https://doi.org/10.1038/nchem.2445>.

(37) Keim, W. Oligomerization of Ethylene to  $\alpha$ -Olefins: Discovery and Development of the Shell Higher Olefin Process (SHOP). *Angew. Chem. Int. Ed.* **2013**, *52* (48), 12492–12496. <https://doi.org/10.1002/anie.201305308>.

(38) Bini, L.; Müller, C.; Vogt, D. Mechanistic Studies on Hydrocyanation Reactions. *ChemCatChem* **2010**, *2* (6), 590–608. <https://doi.org/10.1002/cctc.201000034>.

(39) Killian, C. M.; Tempel, D. J.; Johnson, L. K.; Brookhart, M. Living Polymerization of  $\alpha$ -Olefins Using Ni(II)- $\alpha$ -Diimine Catalysts. Synthesis of New Block Polymers Based on  $\alpha$ -Olefins. *J. Am. Chem. Soc.* **1996**, *118* (46), 11664–11665. <https://doi.org/10.1021/ja962516h>.

(40) Janssen-Müller, D.; Sahoo, B.; Sun, S.-Z.; Martin, R. Tackling Remote  $\text{Sp}^3$  C–H Functionalization via Ni-Catalyzed “Chain-Walking” Reactions. *Israel Journal of Chemistry* **2020**, *60* (3–4), 195–206. <https://doi.org/10.1002/ijch.201900072>.

(41) Juliá-Hernández, F.; Moragas, T.; Cornella, J.; Martin, R. Remote Carboxylation of Halogenated Aliphatic Hydrocarbons with Carbon Dioxide. *Nature* **2017**, *545* (7652), 84–88. <https://doi.org/10.1038/nature22316>.

(42) Sahoo, B.; Bellotti, P.; Juliá-Hernández, F.; Meng, Q.-Y.; Crespi, S.; König, B.; Martin, R. Site-Selective, Remote  $\text{Sp}^3$  C–H Carboxylation Enabled by the Merger of Photoredox and Nickel Catalysis. *Chem. Eur. J.* **2019**, *25* (38), 9001–9005. <https://doi.org/10.1002/chem.201902095>.

(43) Gaydou, M.; Moragas, T.; Juliá-Hernández, F.; Martin, R. Site-Selective Catalytic Carboxylation of Unsaturated Hydrocarbons with  $\text{CO}_2$  and Water. *J. Am. Chem. Soc.* **2017**, *139*(35), 12161–12164. <https://doi.org/10.1021/jacs.7b07637>.

(44) Sun, S.-Z.; Börjesson, M.; Martin-Montero, R.; Martin, R. Site-Selective Ni-Catalyzed Reductive Coupling of  $\alpha$ -Haloboranes with Unactivated Olefins. *J. Am. Chem. Soc.* **2018**, *140* (40), 12765–12769. <https://doi.org/10.1021/jacs.8b09425>.

(45) Sun, S.-Z.; Romano, C.; Martin, R. Site-Selective Catalytic Deaminative Alkylation of Unactivated Olefins. *J. Am. Chem. Soc.* **2019**, *141* (41), 16197–16201. <https://doi.org/10.1021/jacs.9b07489>.

(46) Mahatthananchai, J.; Dumas, A. M.; Bode, J. W. Catalytic Selective Synthesis. *Angew. Chem. Int. Ed.* **2012**, *51* (44), 10954–10990. <https://doi.org/10.1002/anie.201201787>.

(47) Kaldas, S. J.; Cannillo, A.; McCallum, T.; Barriault, L. Indole Functionalization via Photoredox Gold Catalysis. *Org. Lett.* **2015**, *17* (11), 2864–2866. <https://doi.org/10.1021/acs.orglett.5b01260>.

(48) Xu, R.; Lu, G.; Cai, C. 4-Cyanopyridine-Catalyzed Anti-Markovnikov Selective Hydroboration of Alkenes. *New J. Chem.* **2018**, *42* (20), 16456–16459. <https://doi.org/10.1039/C8NJ03222J>.

(49) Cryle, M. J.; Matovic, N. J.; De Voss, J. J. Products of Cytochrome P450<sub>Biol</sub> (CYP107H1)-Catalyzed Oxidation of Fatty Acids. *Org. Lett.* **2003**, *5* (18), 3341–3344. <https://doi.org/10.1021/ol035254e>.

(50) Tanaka, K.; Ewing, W. R.; Yu, J.-Q. Hemilabile Benzyl Ether Enables  $\gamma$ -C( $\text{Sp}^3$ )-H Carbonylation and Olefination of Alcohols. *J. Am. Chem. Soc.* **2019**, *141* (39), 15494–15497.

## Chapter 5

<https://doi.org/10.1021/jacs.9b08238>.

(51) Lücking, U.; Tucci, F. C.; Rudkevich, D. M.; Rebek, J. Self-Folding Cavitands of Nanoscale Dimensions. *J. Am. Chem. Soc.* **2000**, *122* (37), 8880–8889. <https://doi.org/10.1021/ja001562l>.

Regiodivergent Ligand-Controlled Ni-Catalyzed Reductive Amidation of Unactivated  
Secondary Alkyl Bromides

**$^1\text{H}$  NMR,  $^{13}\text{C}$  NMR and  $^{11}\text{B}$  NMR spectra**









Regiodivergent Ligand-Controlled Ni-Catalyzed Reductive Amidation of Unactivated Secondary Alkyl Bromides

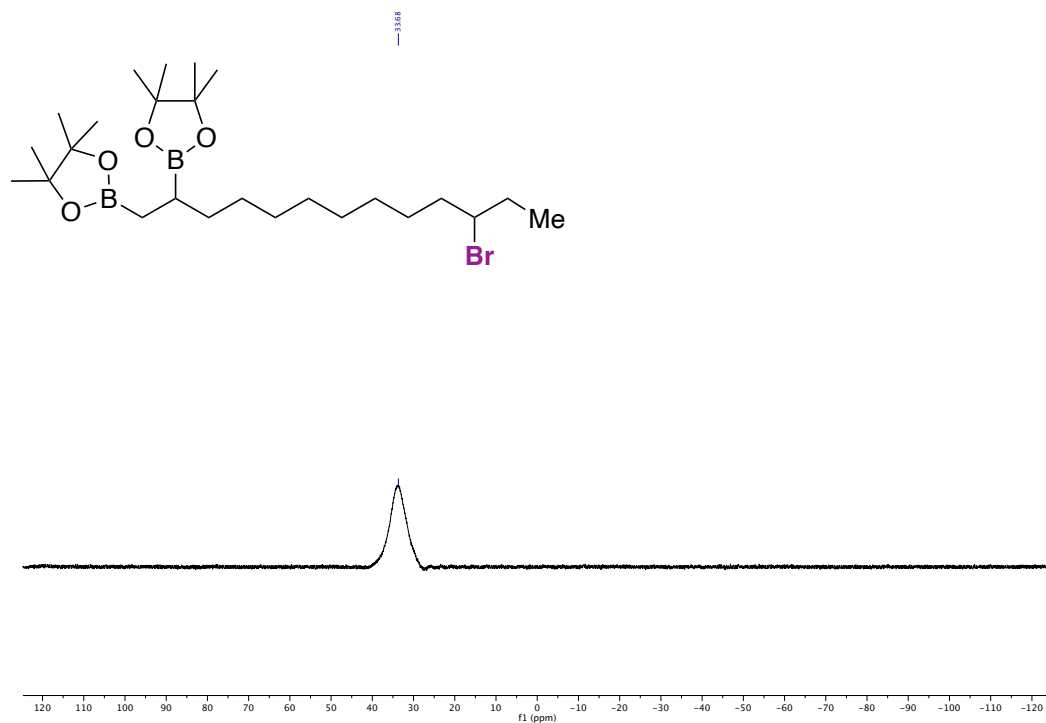


Figure 4.  $^1\text{H}$ ,  $^{13}\text{C}$  and  $^{11}\text{B}$  NMR spectra of 2-(11-bromotridecyl)-4,4,5,5-tetramethyl-1,3,2-dioxaborolane .

# Chapter 5

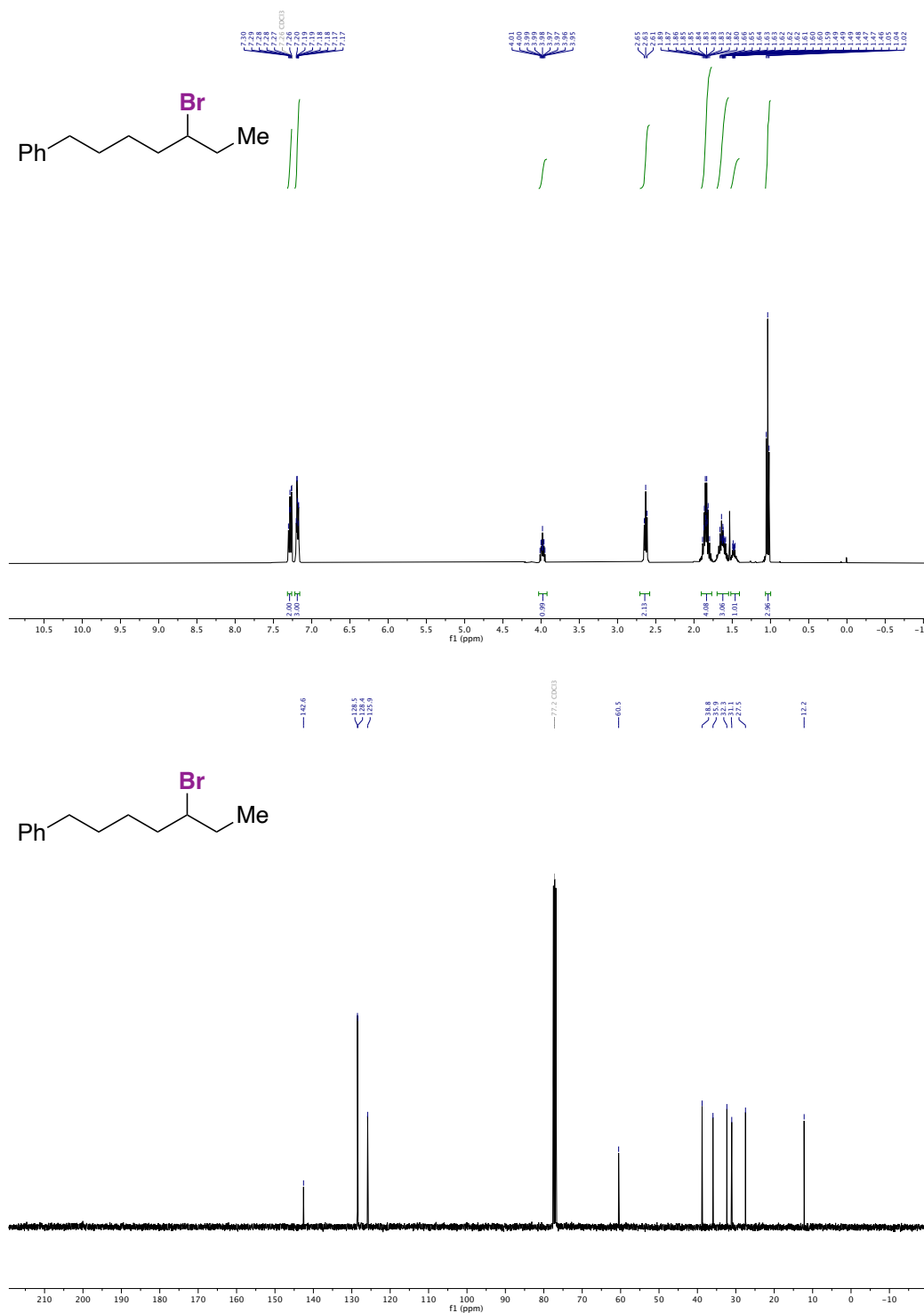


Figure 5. <sup>1</sup>H and <sup>13</sup>C NMR spectra of (6-bromooctyl)benzene.





# Regiodivergent Ligand-Controlled Ni-Catalyzed Reductive Amidation of Unactivated Secondary Alkyl Bromides

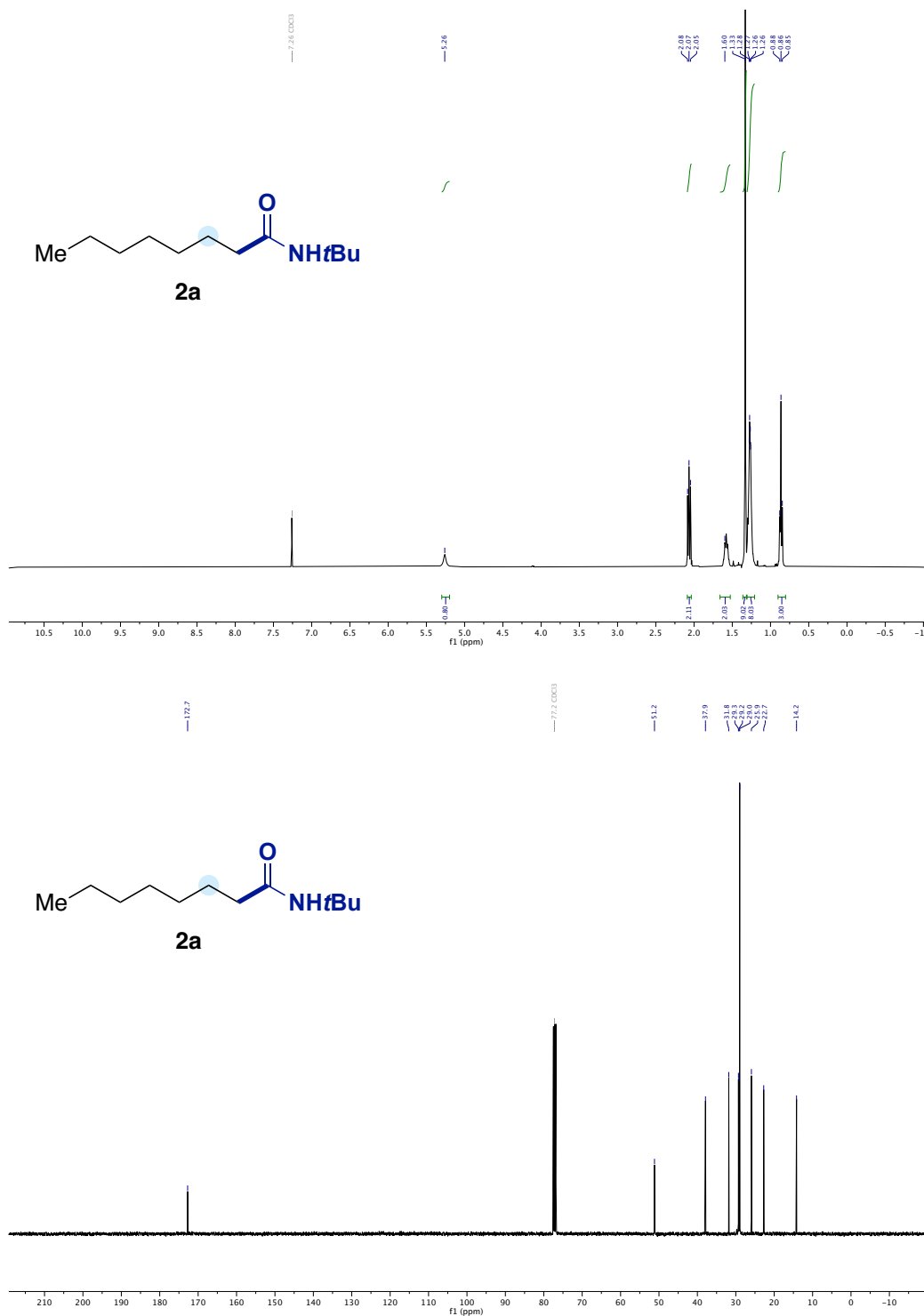


Figure 8. <sup>1</sup>H and <sup>13</sup>C NMR spectra of **2a**.

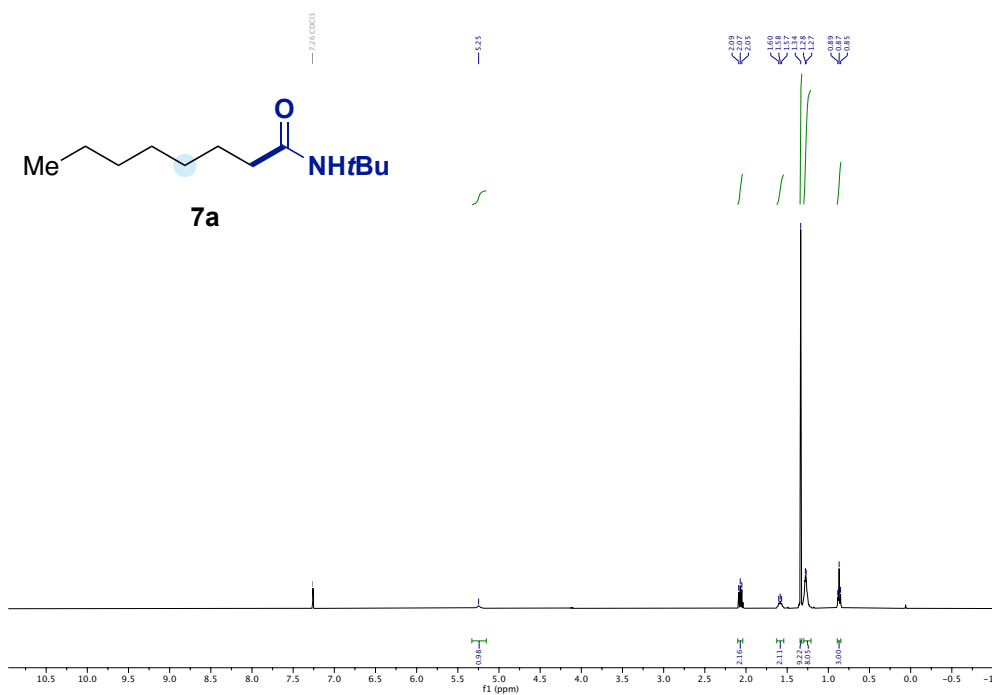


Figure 9. <sup>1</sup>H NMR spectrum of **7a** (Starting from 3-bromoheptane).

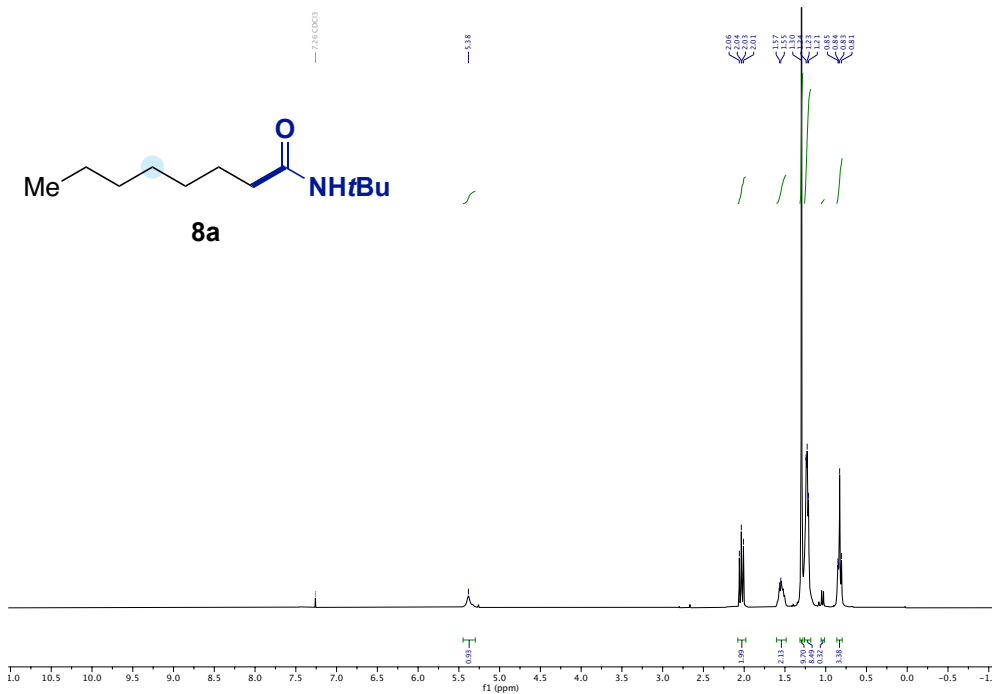
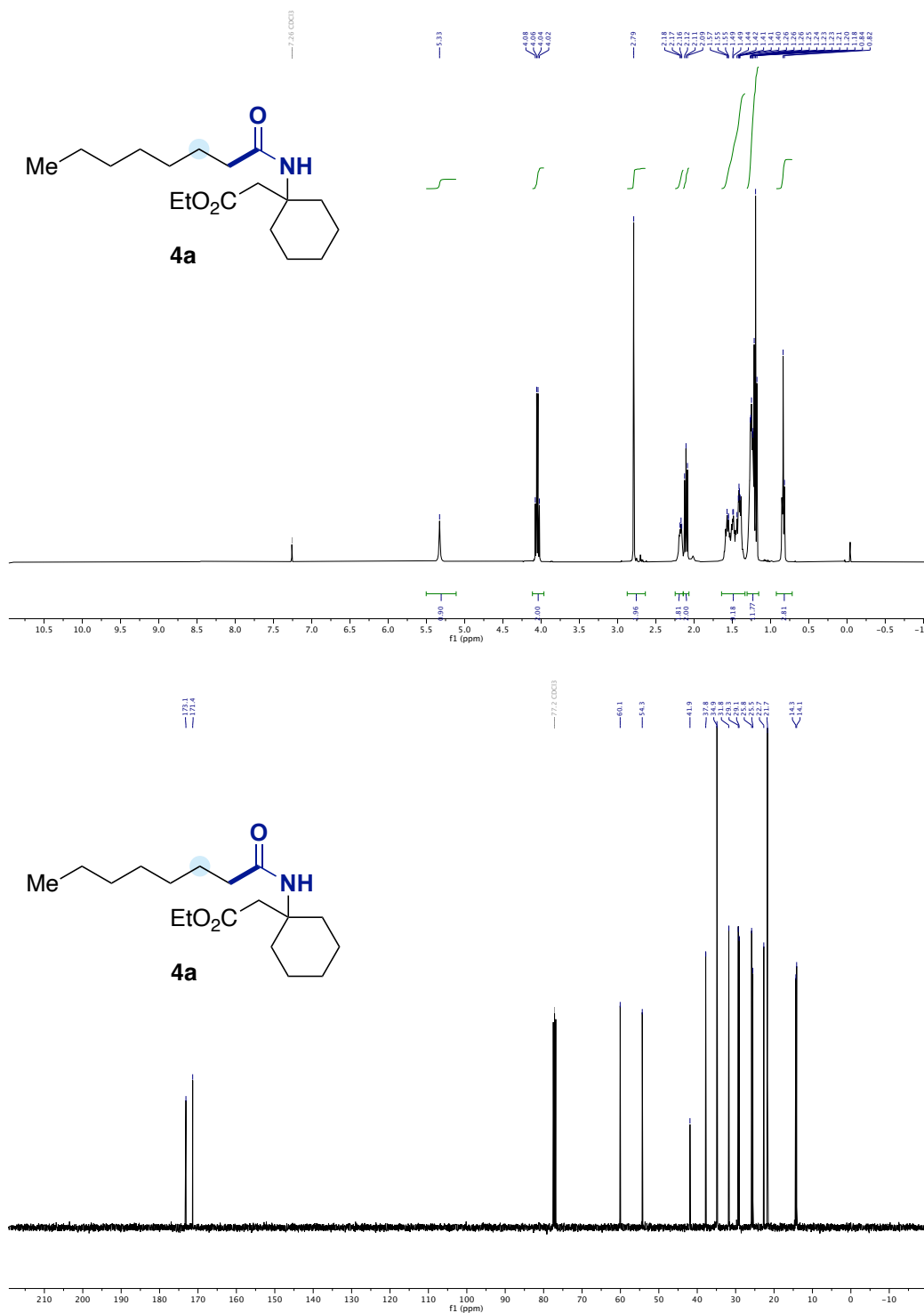


Figure 10. <sup>1</sup>H NMR spectrum of **8a** (Starting from 4-bromoheptane).



Figure 12. <sup>1</sup>H and <sup>13</sup>C NMR spectra of **4a**.



# Regiodivergent Ligand-Controlled Ni-Catalyzed Reductive Amidation of Unactivated Secondary Alkyl Bromides

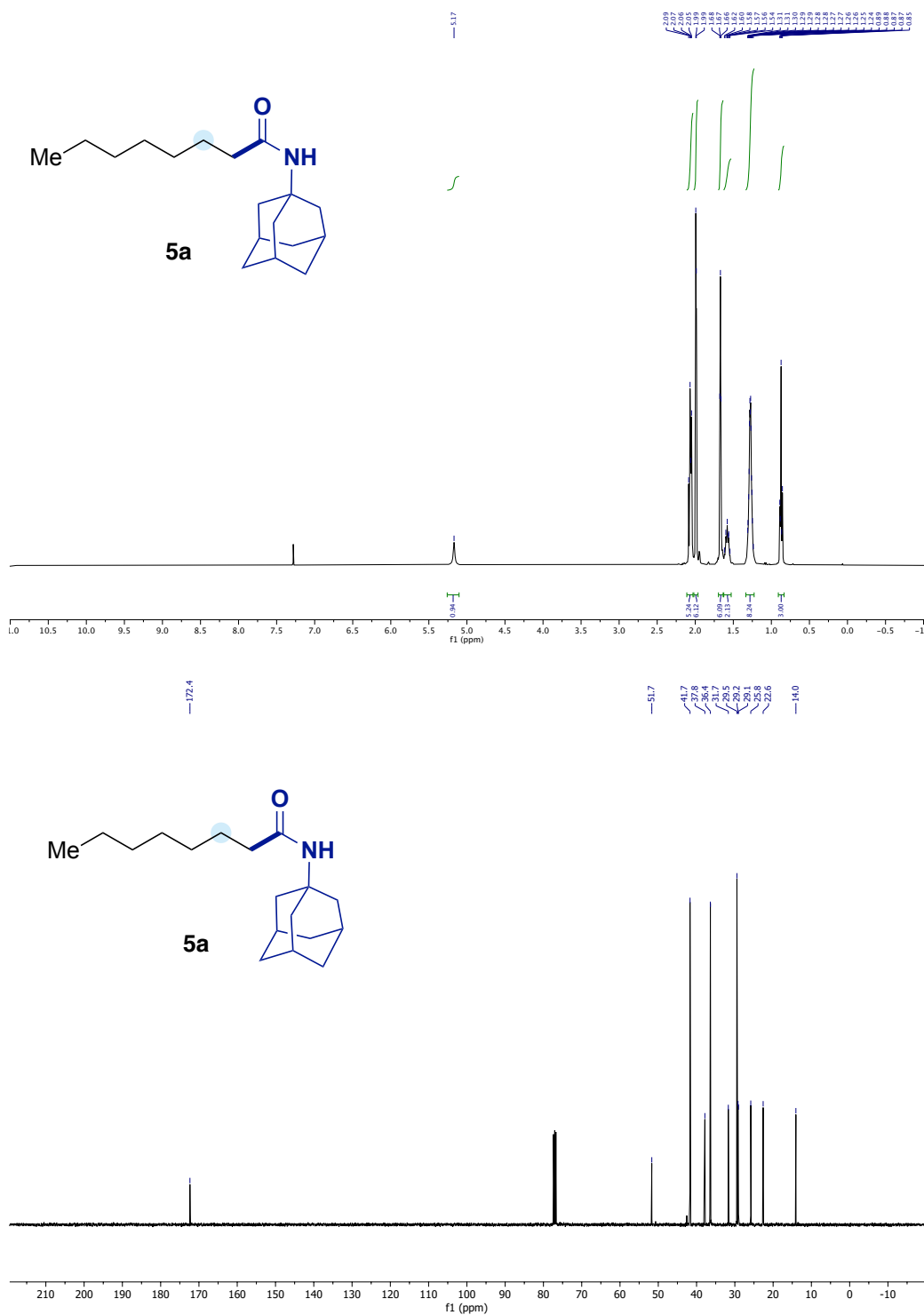


Figure 13. <sup>1</sup>H and <sup>13</sup>C NMR spectra of **5a**.

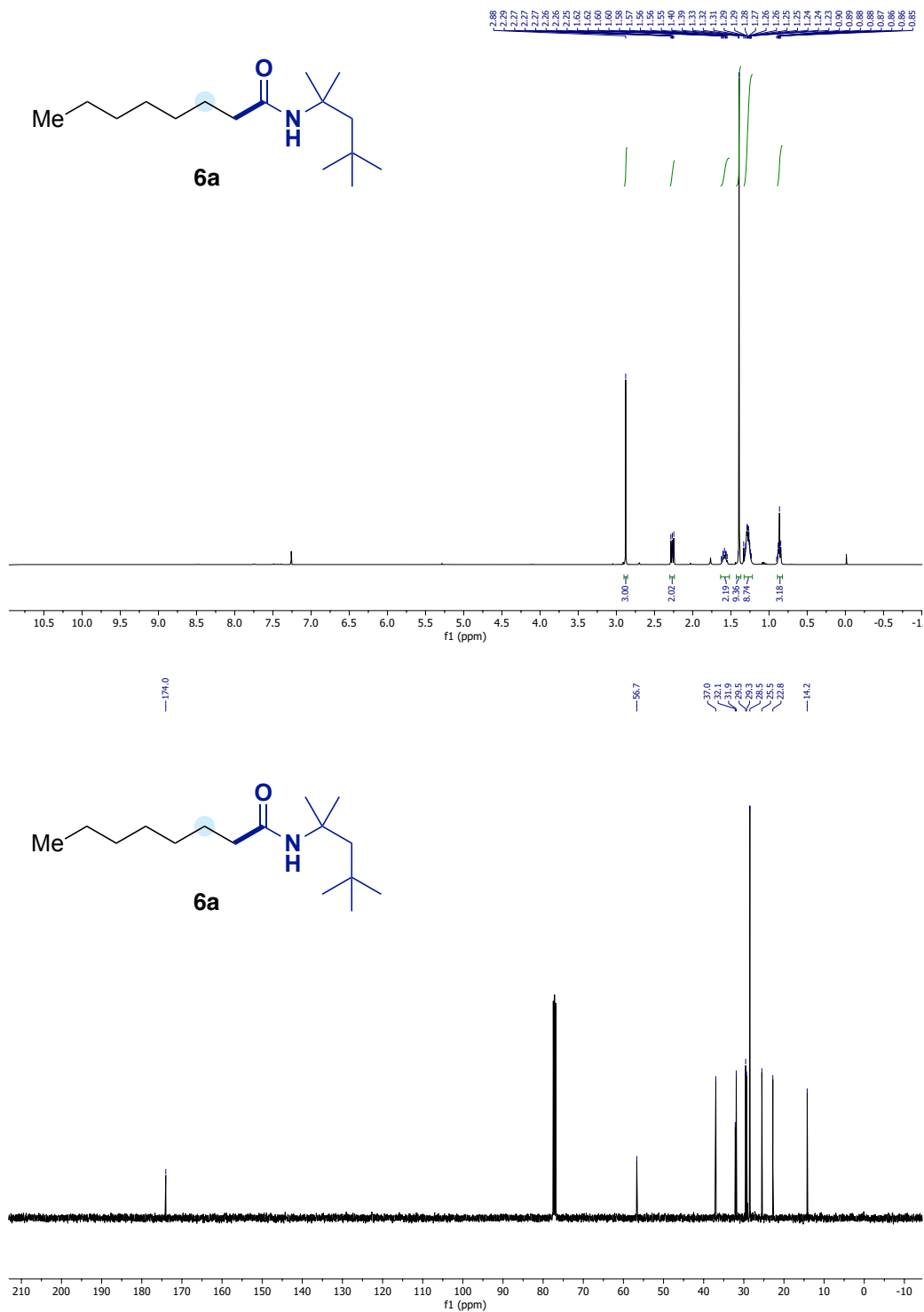
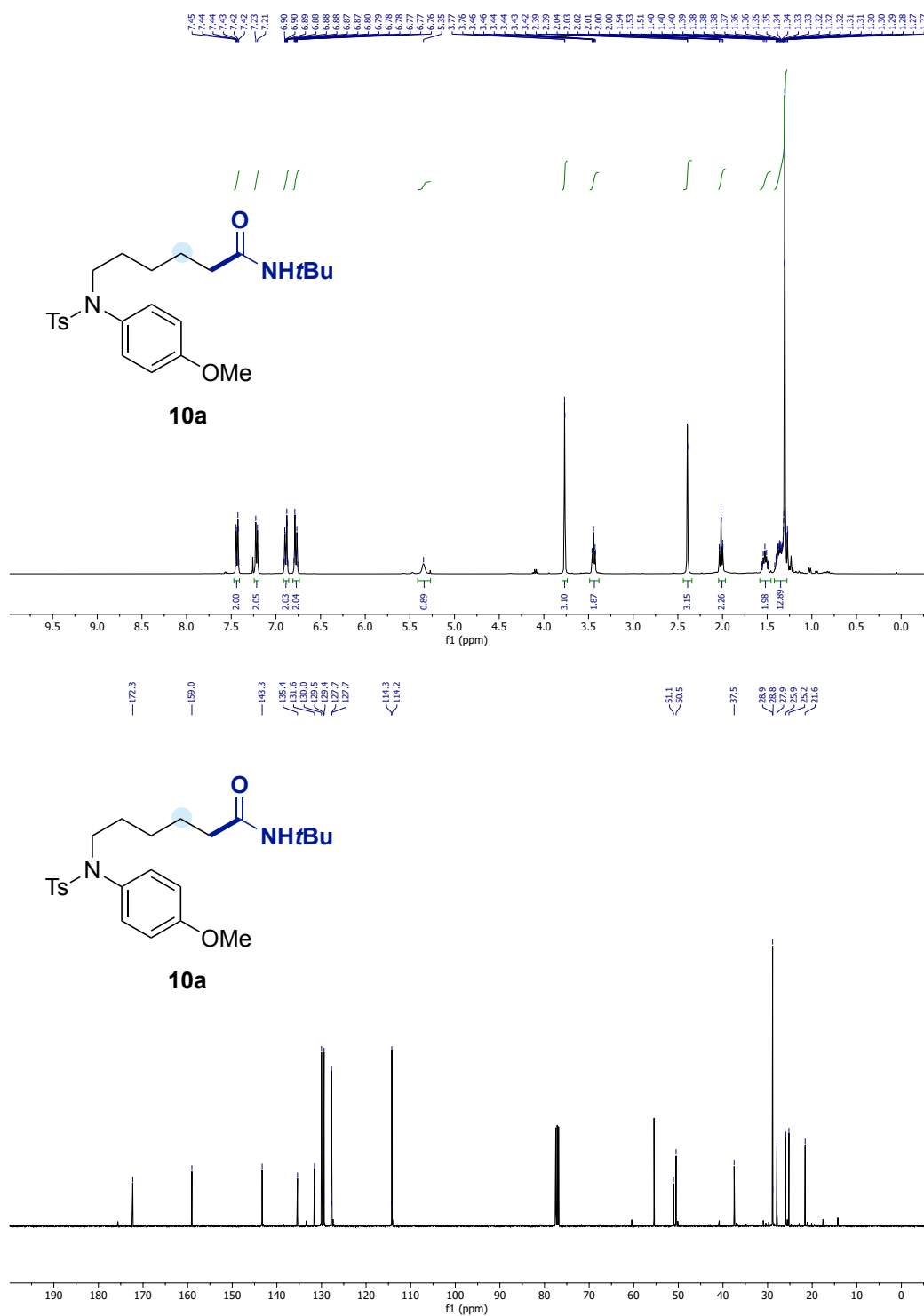


Figure 14. <sup>1</sup>H and <sup>13</sup>C NMR spectra of **6a**.



Figure 16. <sup>1</sup>H and <sup>13</sup>C NMR spectra of 10a.

Regiodivergent Ligand-Controlled Ni-Catalyzed Reductive Amidation of Unactivated Secondary Alkyl Bromides

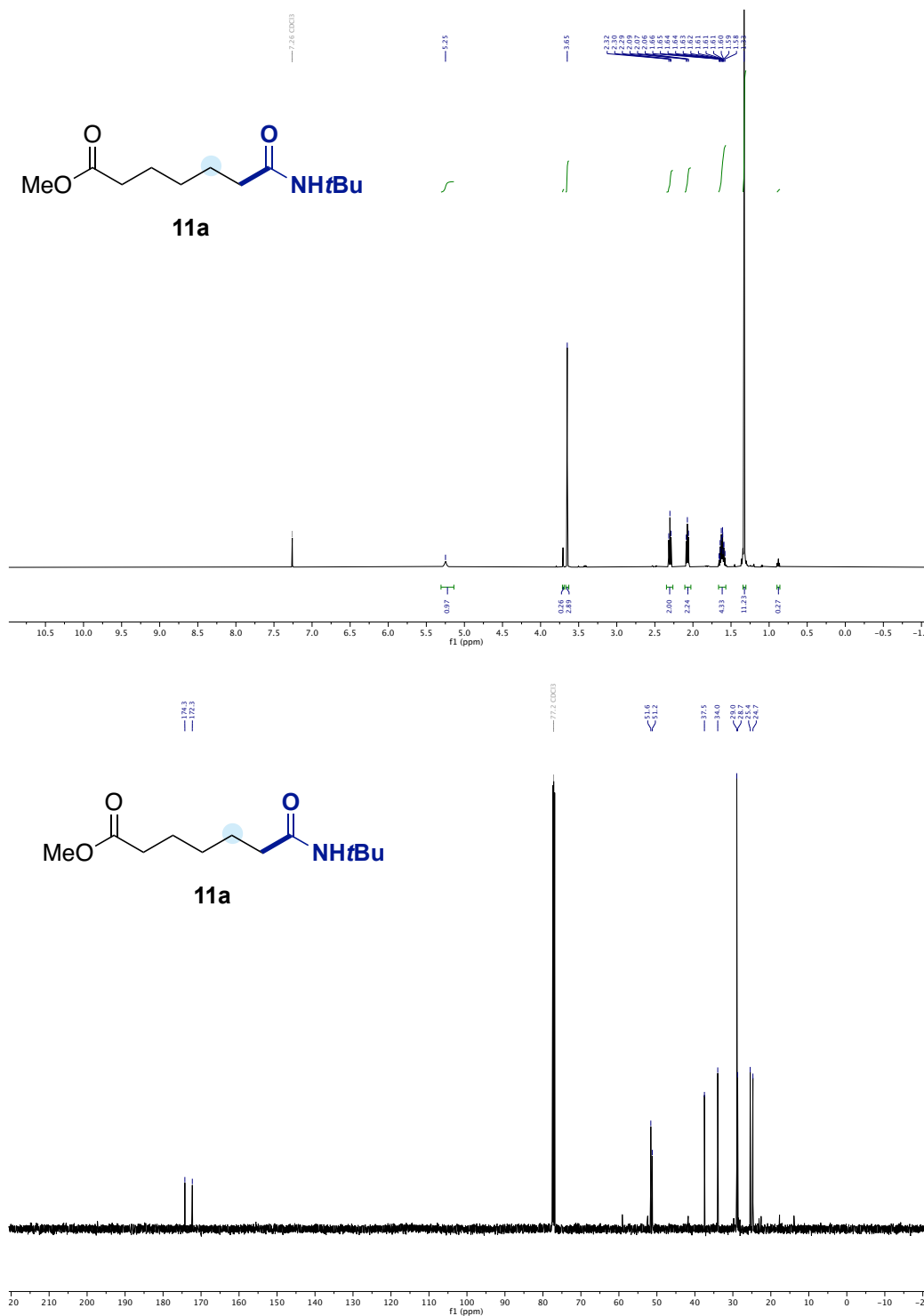
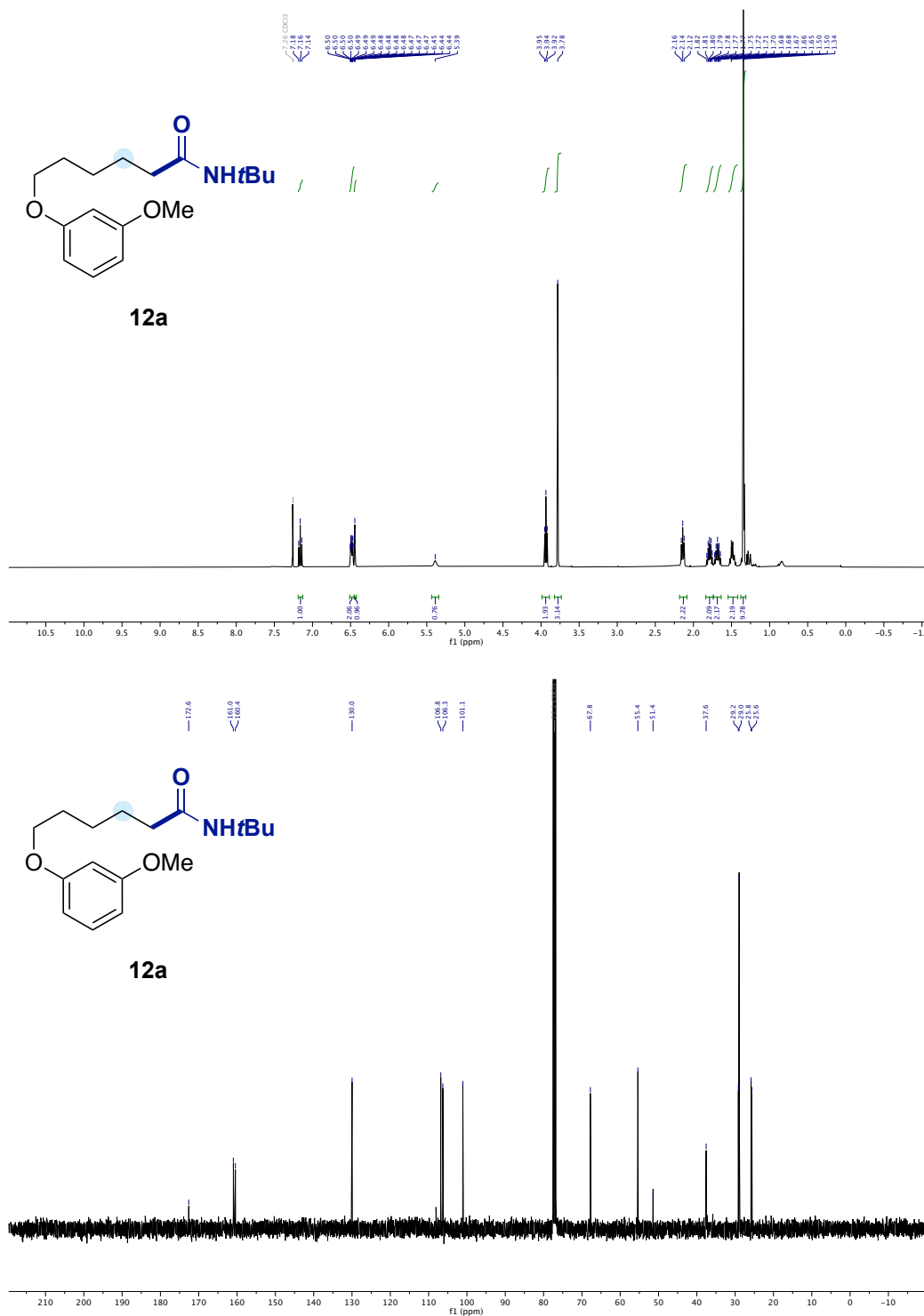


Figure 17. <sup>1</sup>H and <sup>13</sup>C NMR spectra of **11a**.

Figure 18.  $^1\text{H}$  and  $^{13}\text{C}$  NMR spectra of **12a**.

Regiodivergent Ligand-Controlled Ni-Catalyzed Reductive Amidation of Unactivated Secondary Alkyl Bromides

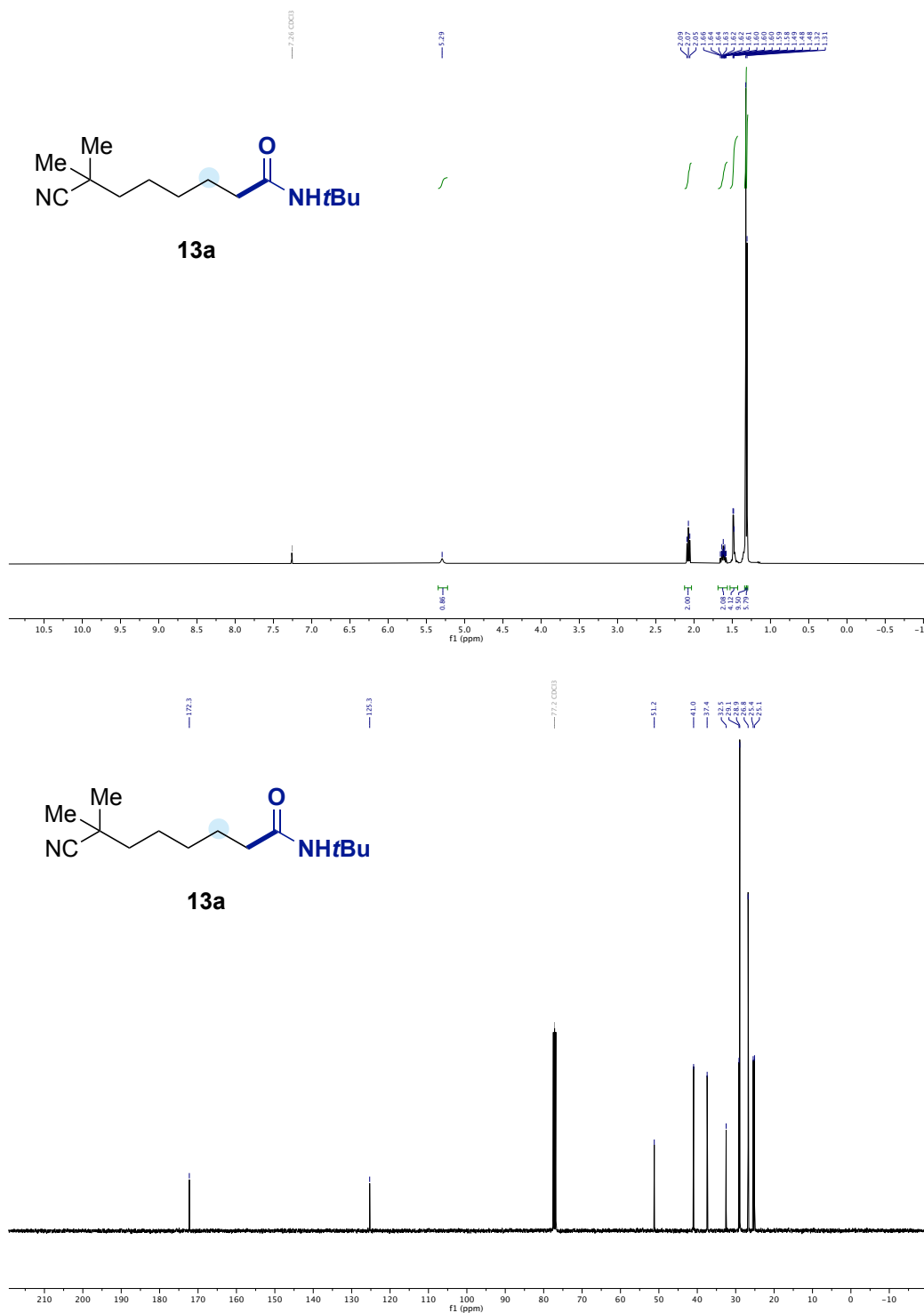
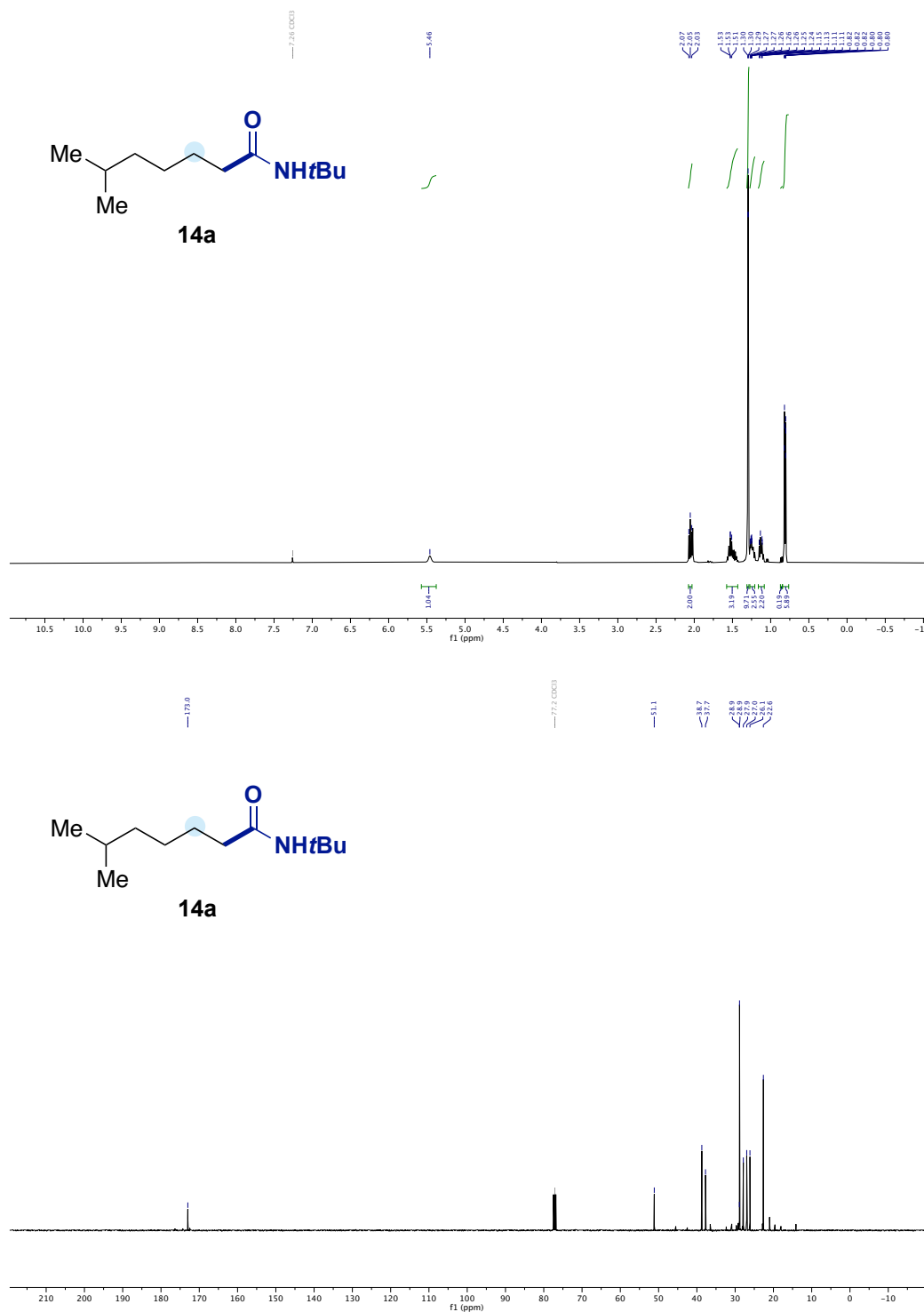


Figure 19. <sup>1</sup>H and <sup>13</sup>C NMR spectra of **13a**.

Figure 20.  $^1\text{H}$  and  $^{13}\text{C}$  NMR spectra of **14a**.



Regiodivergent Ligand-Controlled Ni-Catalyzed Reductive Amidation of Unactivated Secondary Alkyl Bromides

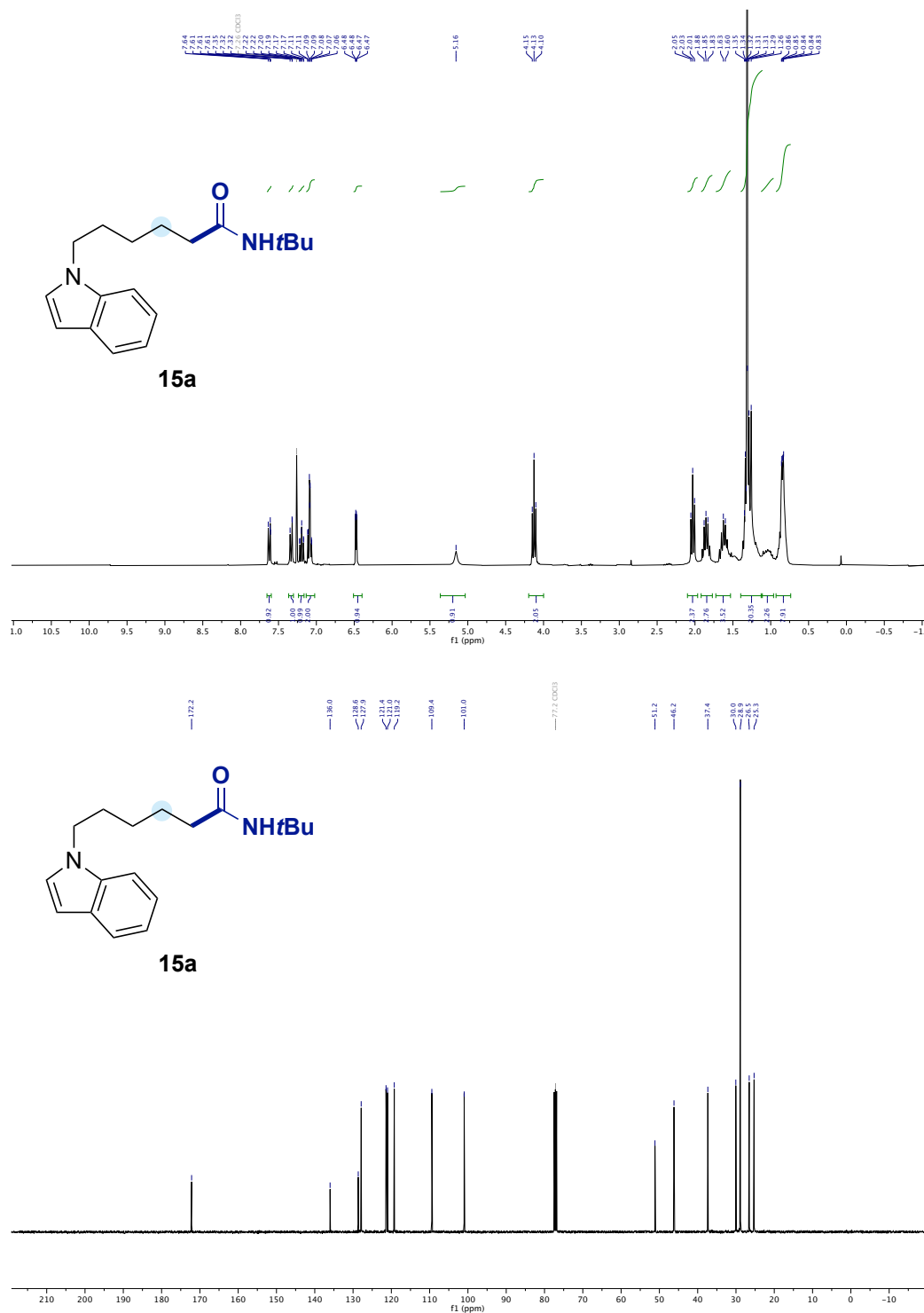
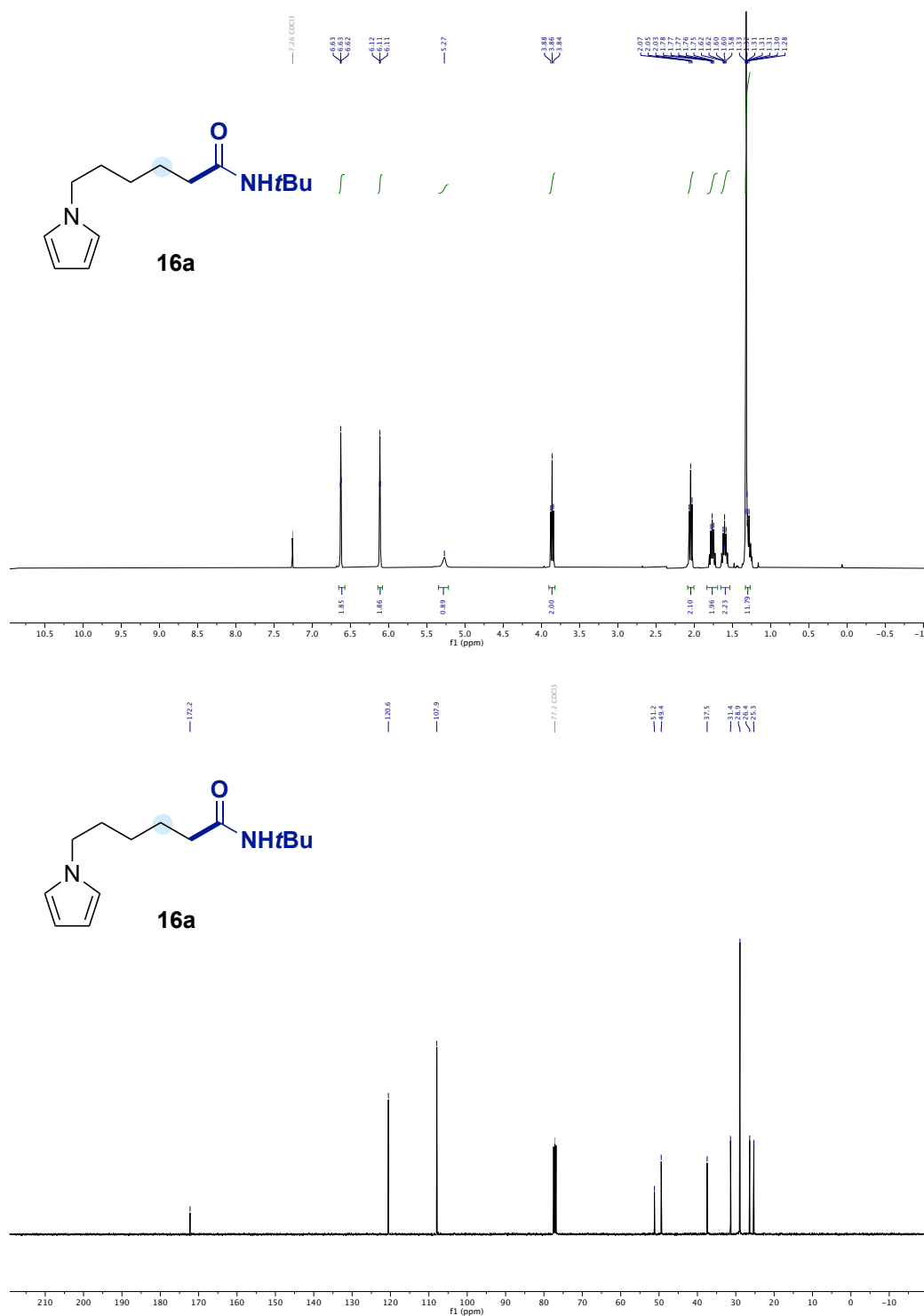


Figure 21. <sup>1</sup>H and <sup>13</sup>C NMR spectra of **15a**.

Figure 22. <sup>1</sup>H and <sup>13</sup>C NMR spectra of 16a.



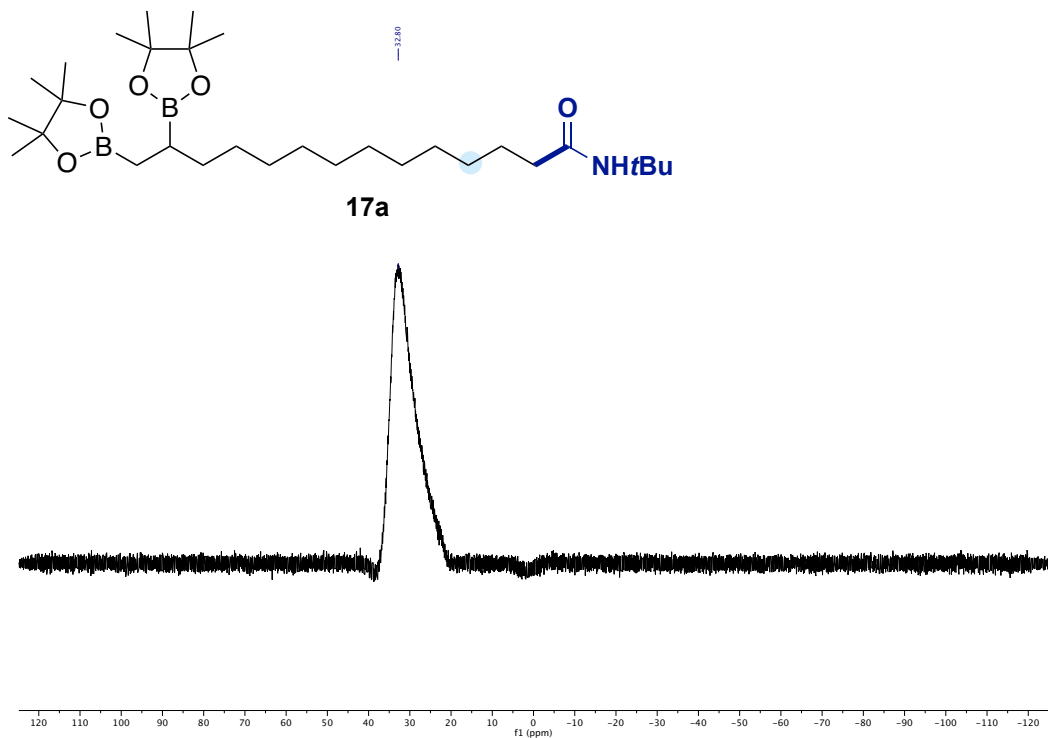


Figure 23.  $^1\text{H}$ ,  $^{13}\text{C}$  and  $^{11}\text{B}$  NMR spectra of **17a**.

# Regiodivergent Ligand-Controlled Ni-Catalyzed Reductive Amidation of Unactivated Secondary Alkyl Bromides

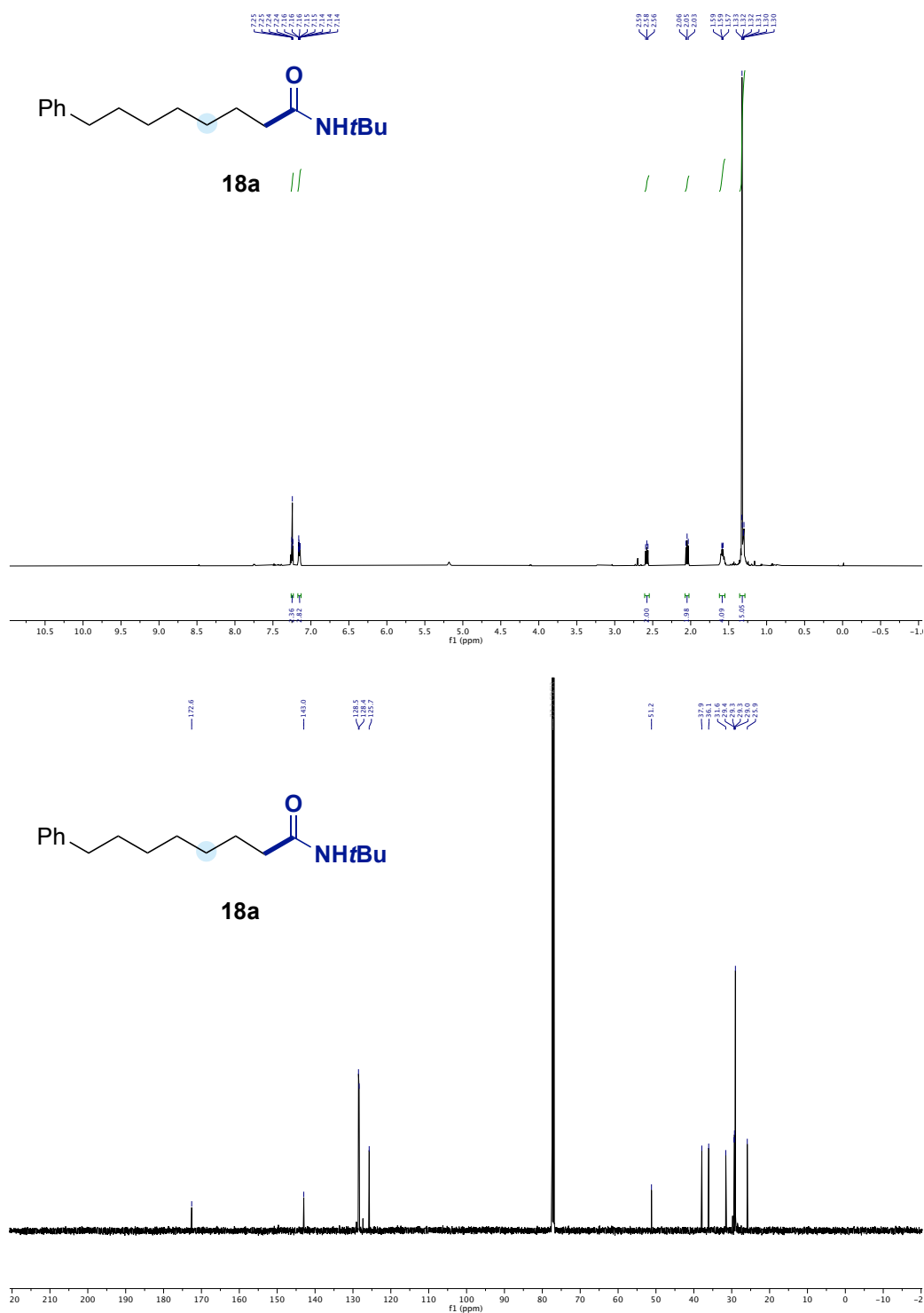


Figure 24. <sup>1</sup>H and <sup>13</sup>C NMR spectra of **18a**.



# Regiodivergent Ligand-Controlled Ni-Catalyzed Reductive Amidation of Unactivated Secondary Alkyl Bromides

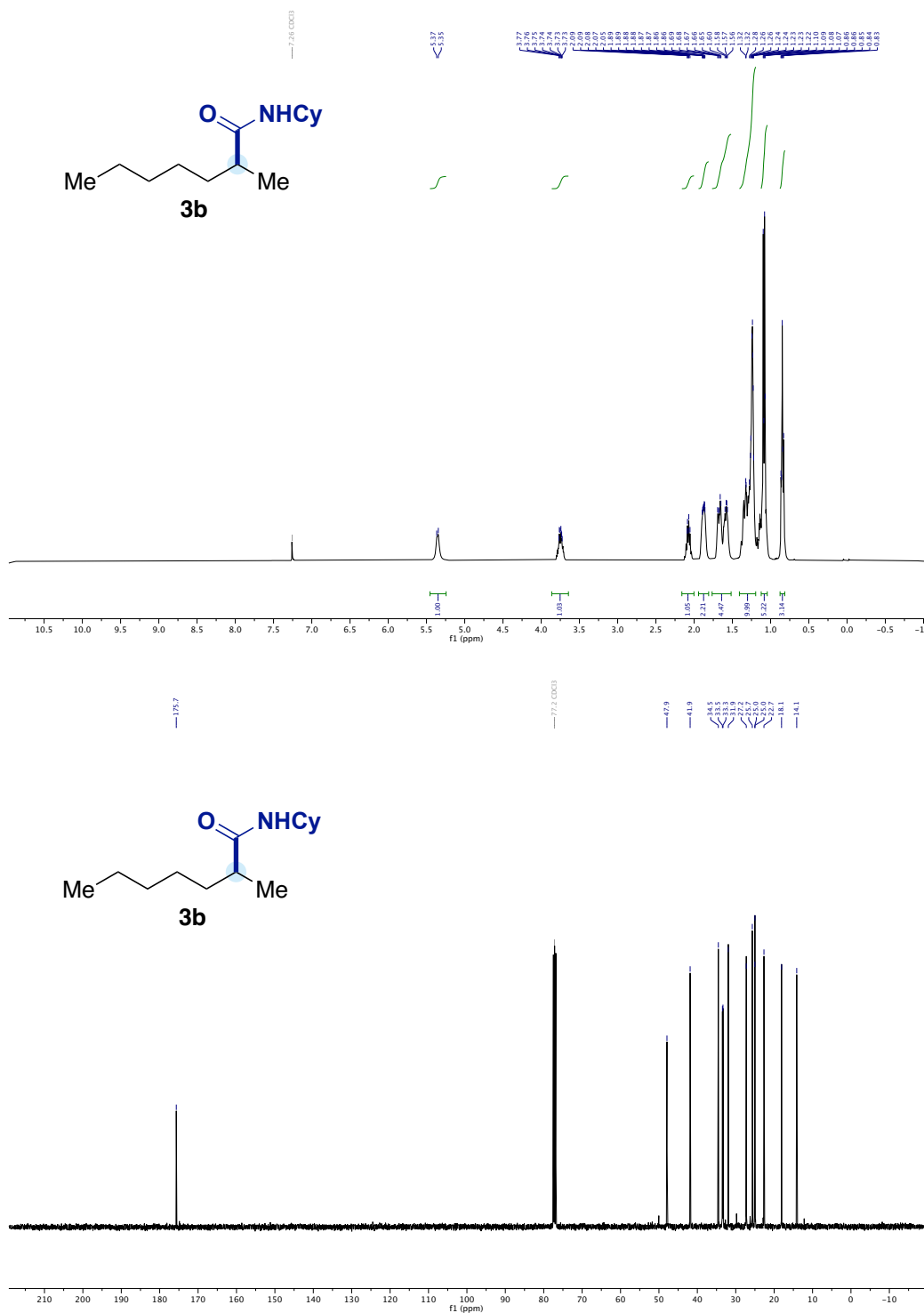
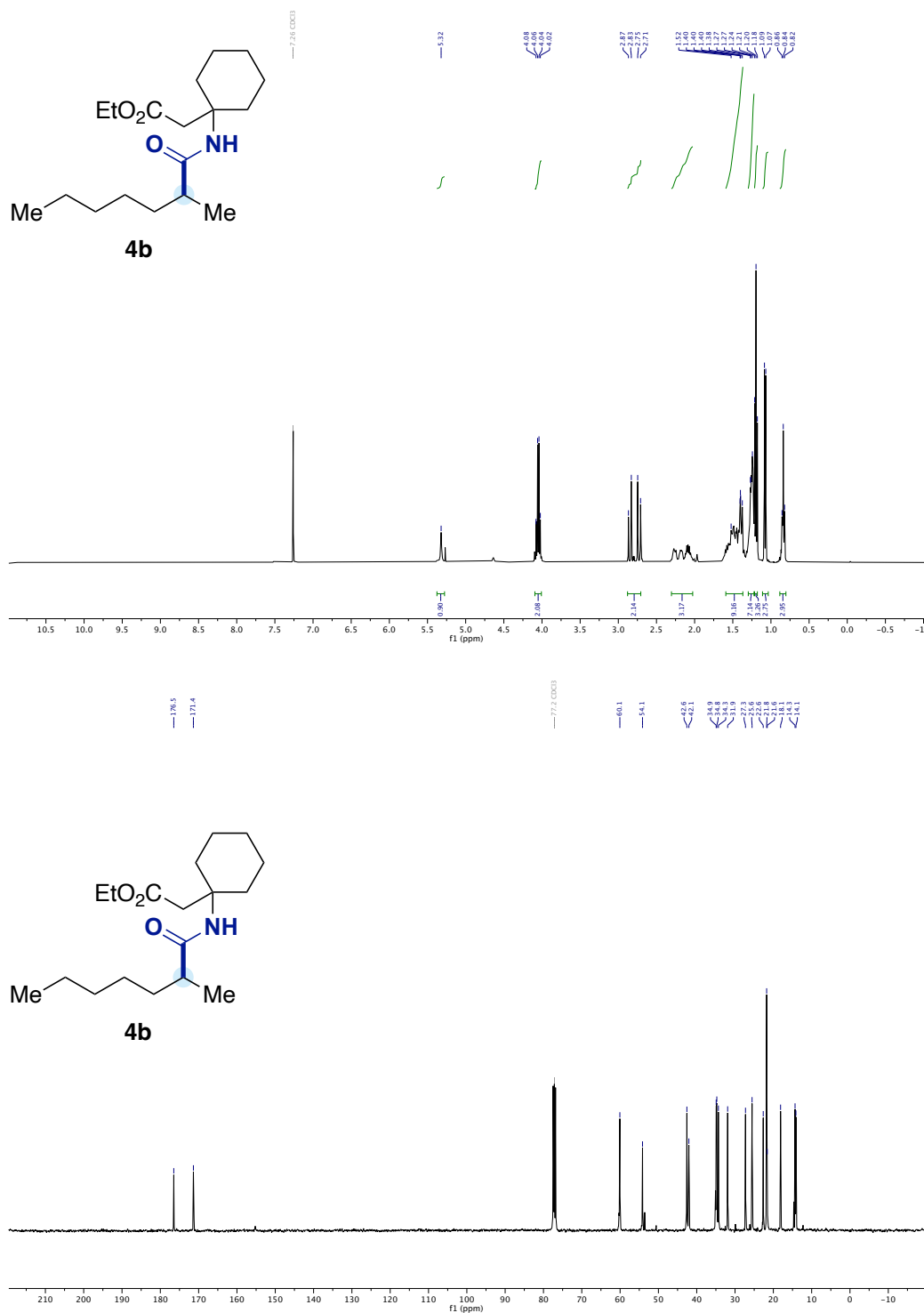


Figure 26. <sup>1</sup>H and <sup>13</sup>C NMR spectra of **3b**.

Figure 27. <sup>1</sup>H and <sup>13</sup>C NMR spectra of **4b**.



# Regiodivergent Ligand-Controlled Ni-Catalyzed Reductive Amidation of Unactivated Secondary Alkyl Bromides

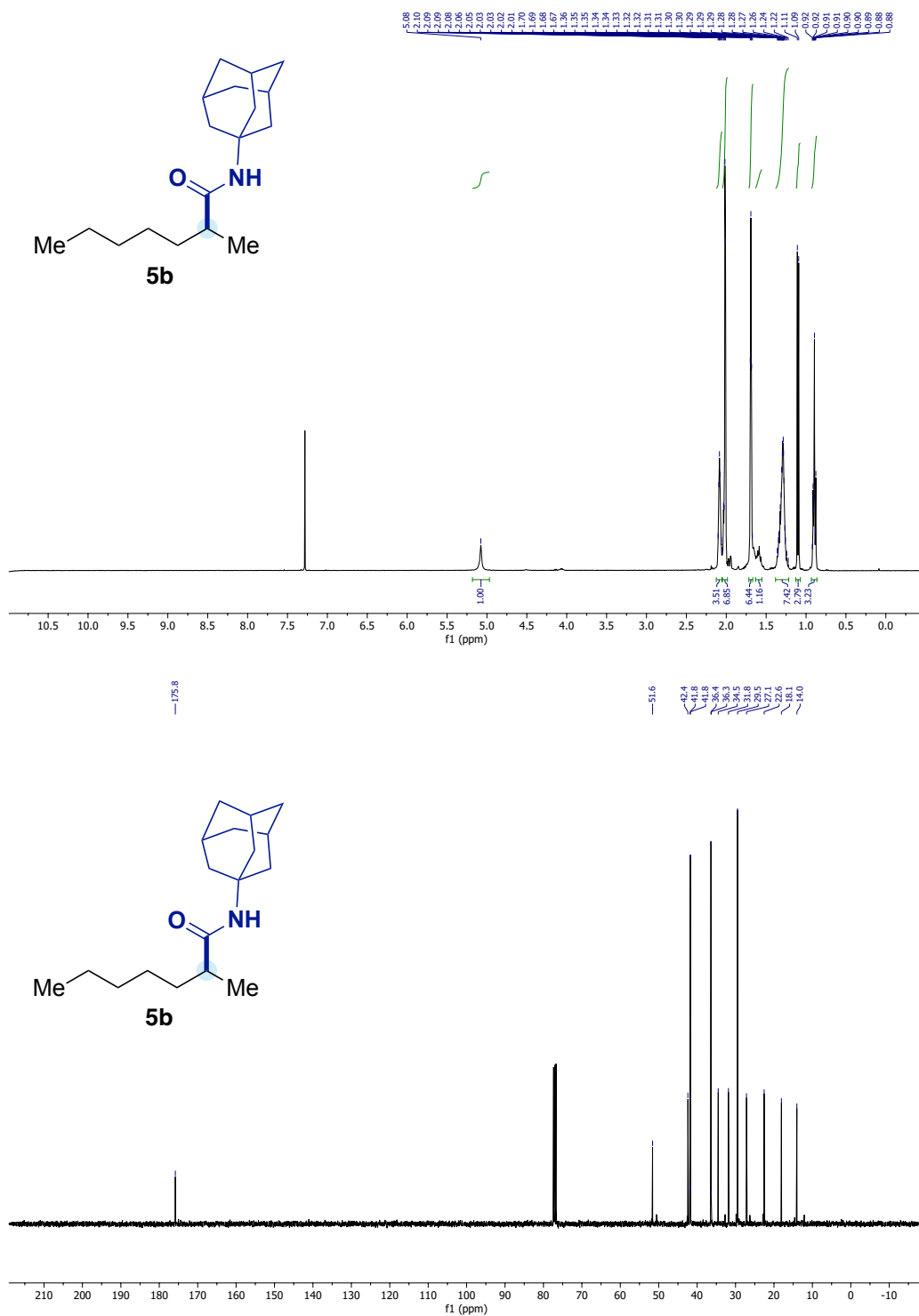
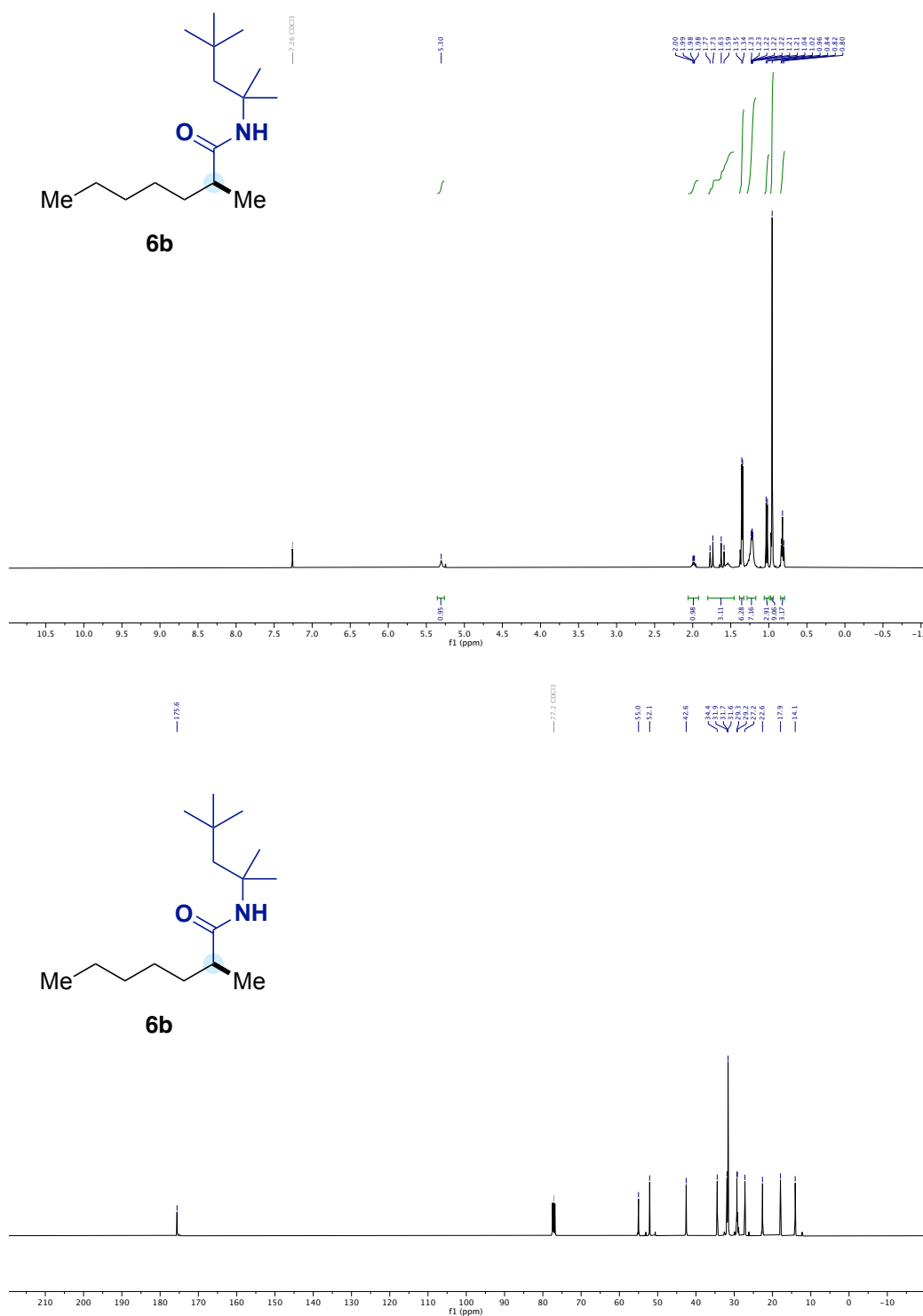


Figure 28.  $^1\text{H}$  and  $^{13}\text{C}$  NMR spectra of **5b**.

Figure 29. <sup>1</sup>H and <sup>13</sup>C NMR spectra of **6b**.

# Regiodivergent Ligand-Controlled Ni-Catalyzed Reductive Amidation of Unactivated Secondary Alkyl Bromides

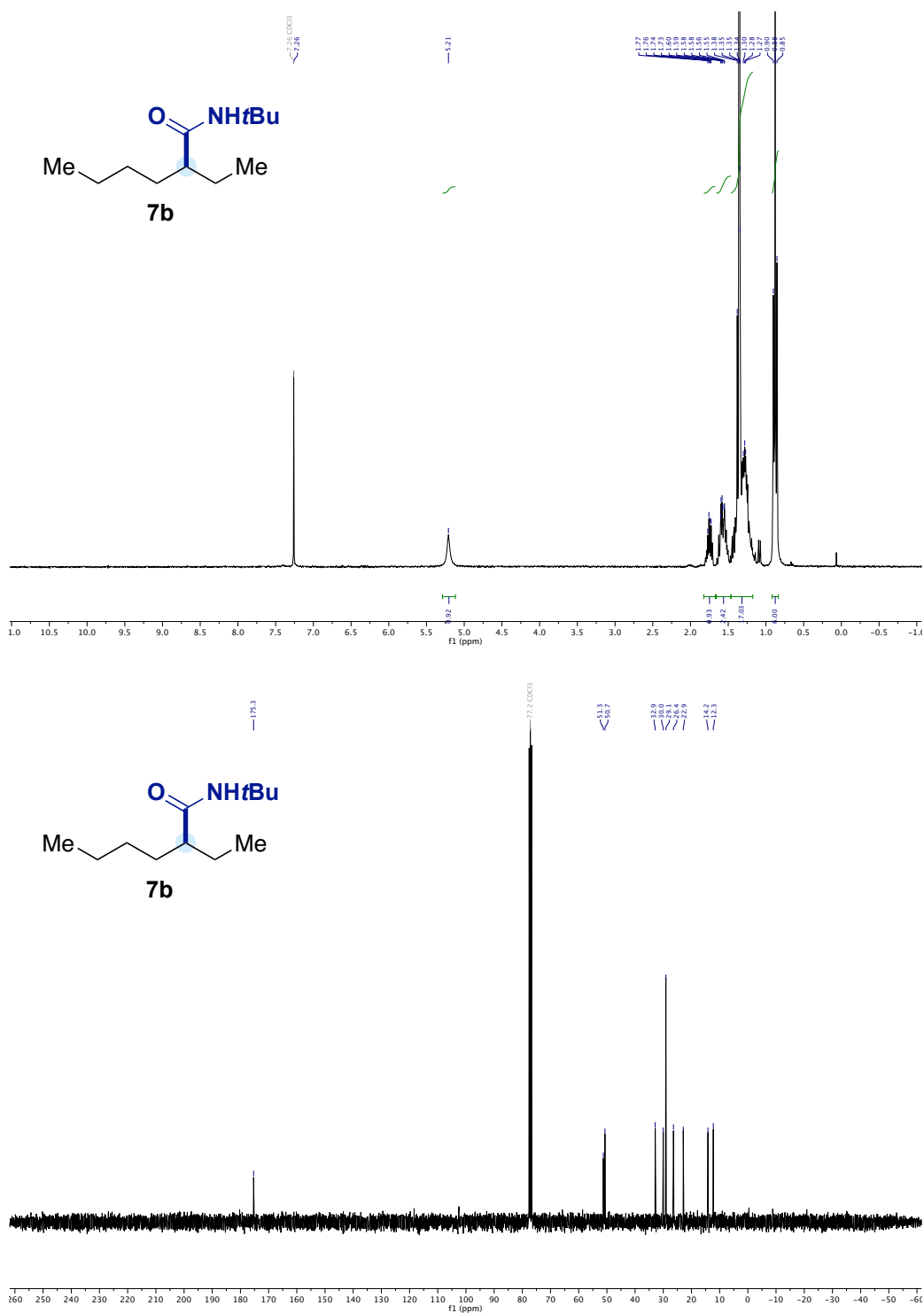
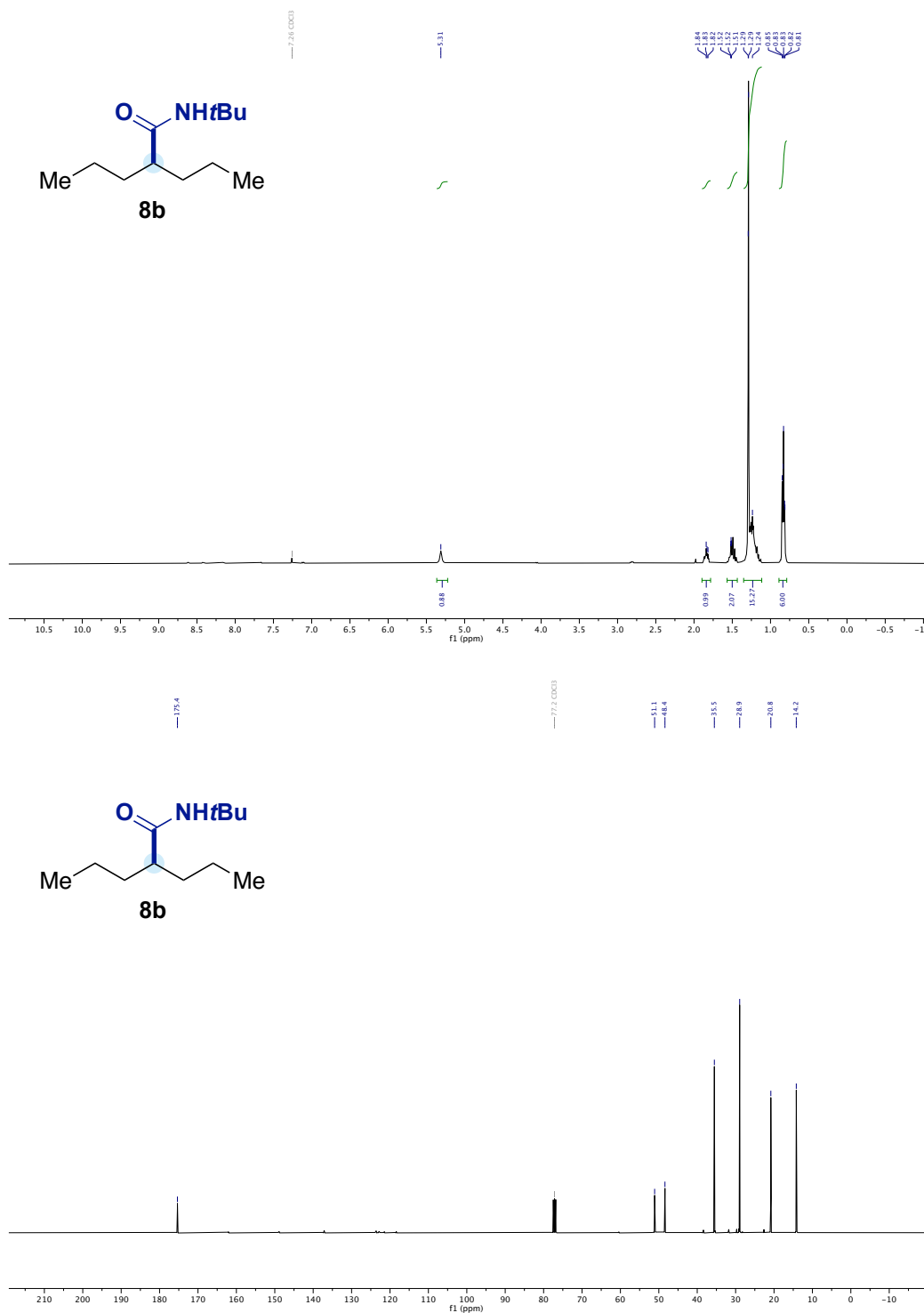


Figure 30. <sup>1</sup>H and <sup>13</sup>C NMR spectra of **7b**.

Figure 31.  $^1\text{H}$  and  $^{13}\text{C}$  NMR spectra of **8b**.

# Regiodivergent Ligand-Controlled Ni-Catalyzed Reductive Amidation of Unactivated Secondary Alkyl Bromides

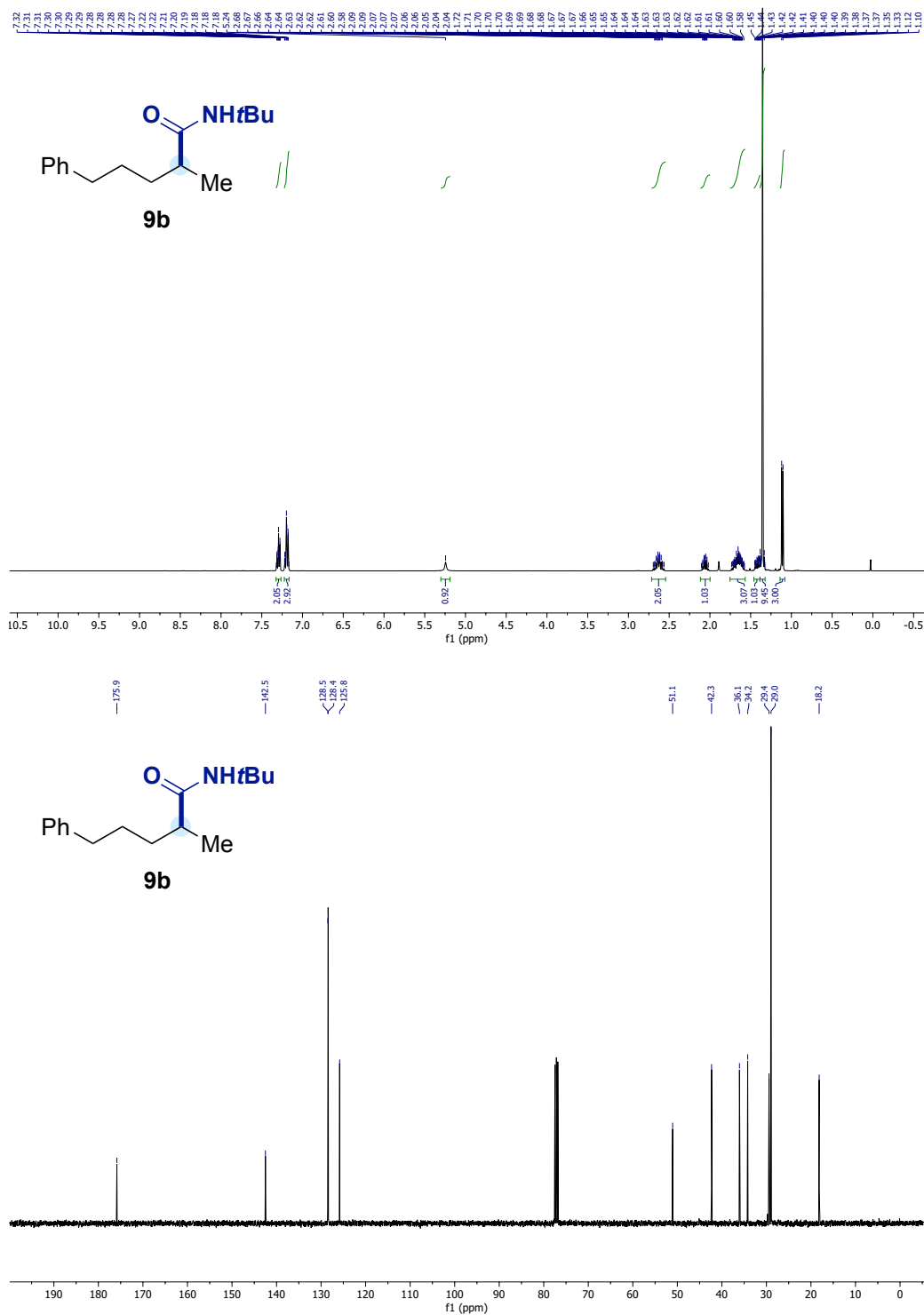


Figure 32. <sup>1</sup>H and <sup>13</sup>C NMR spectra of **9b**.

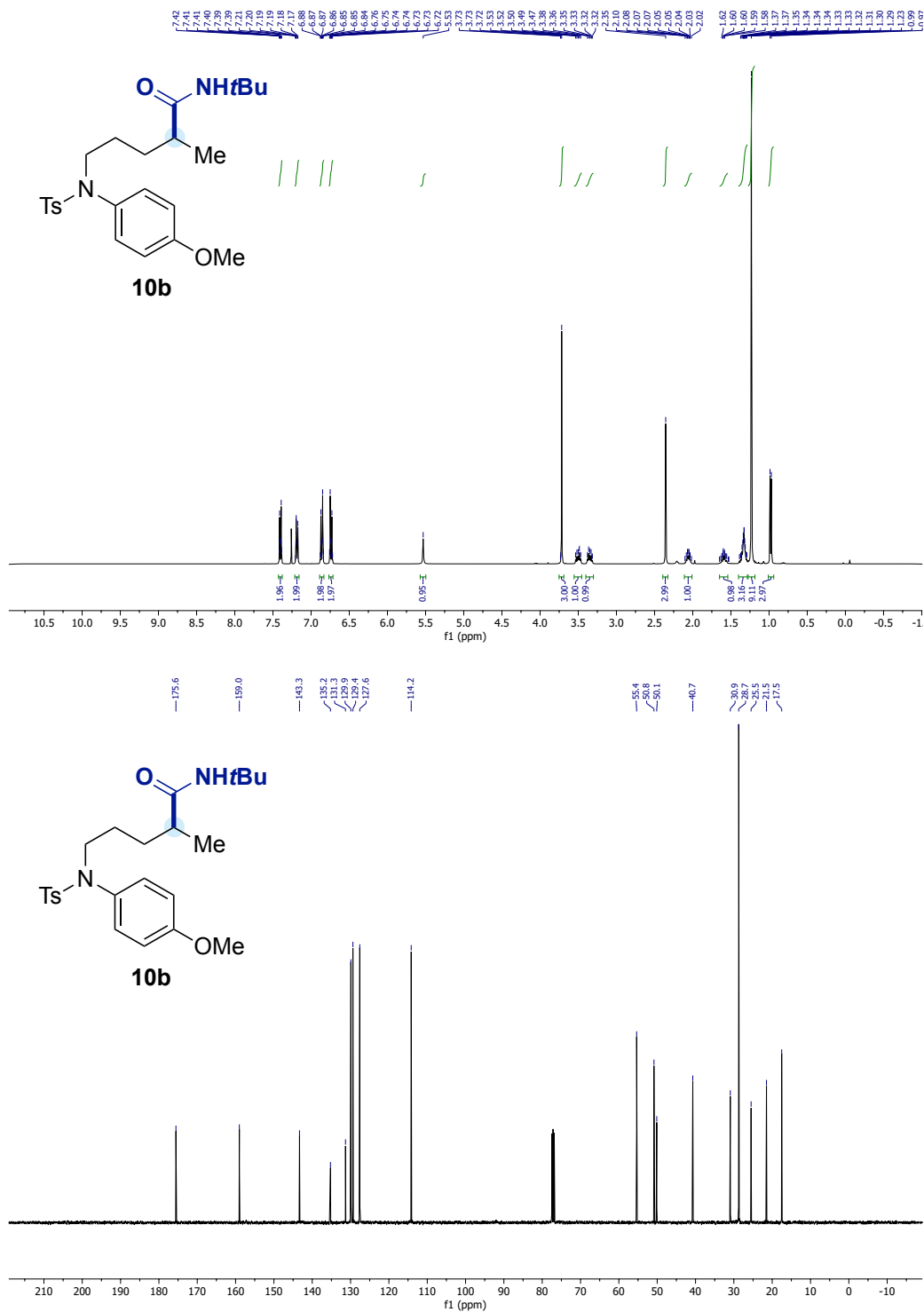


Figure 33. <sup>1</sup>H and <sup>13</sup>C NMR spectra of **10b**.

# Regiodivergent Ligand-Controlled Ni-Catalyzed Reductive Amidation of Unactivated Secondary Alkyl Bromides

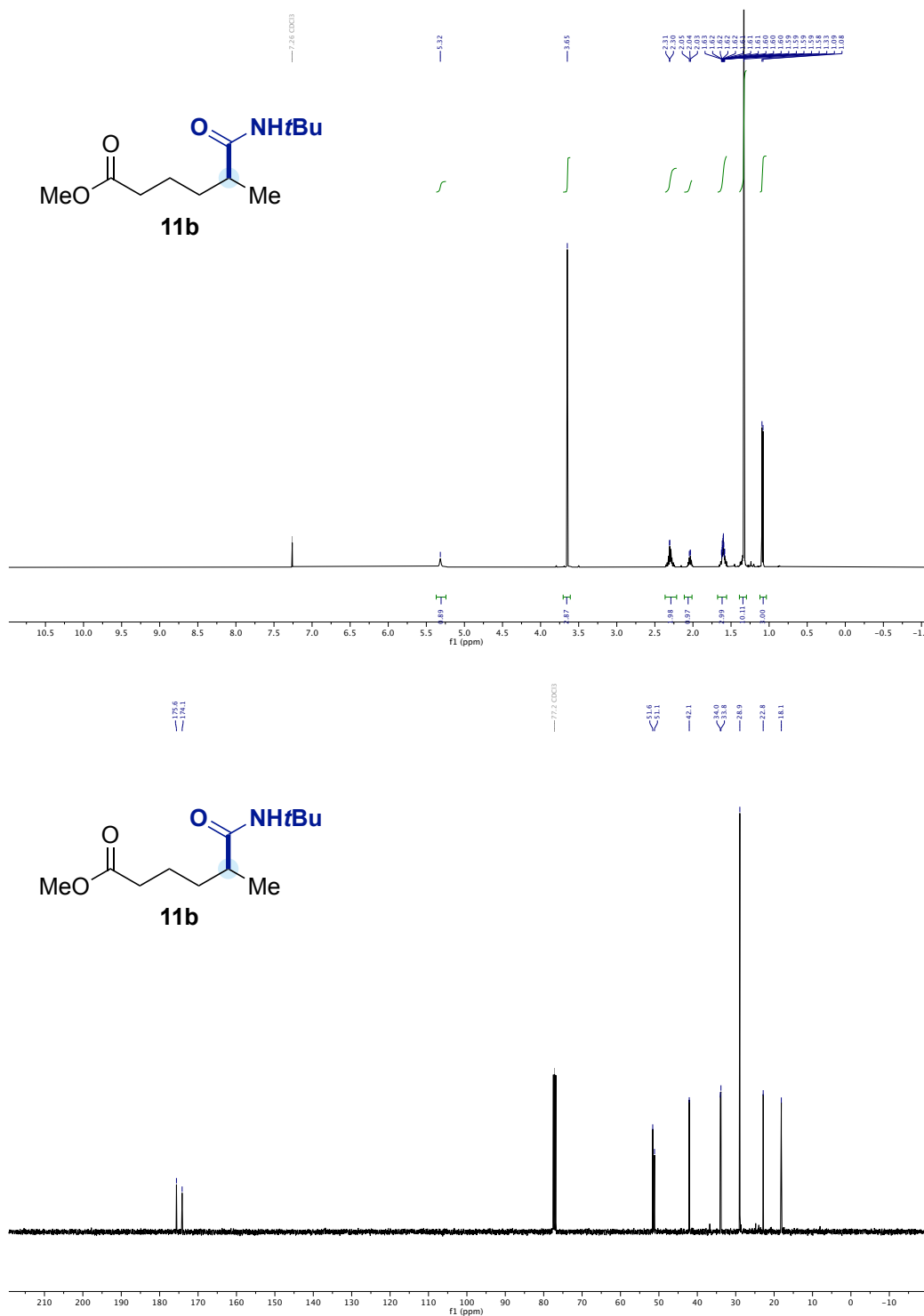
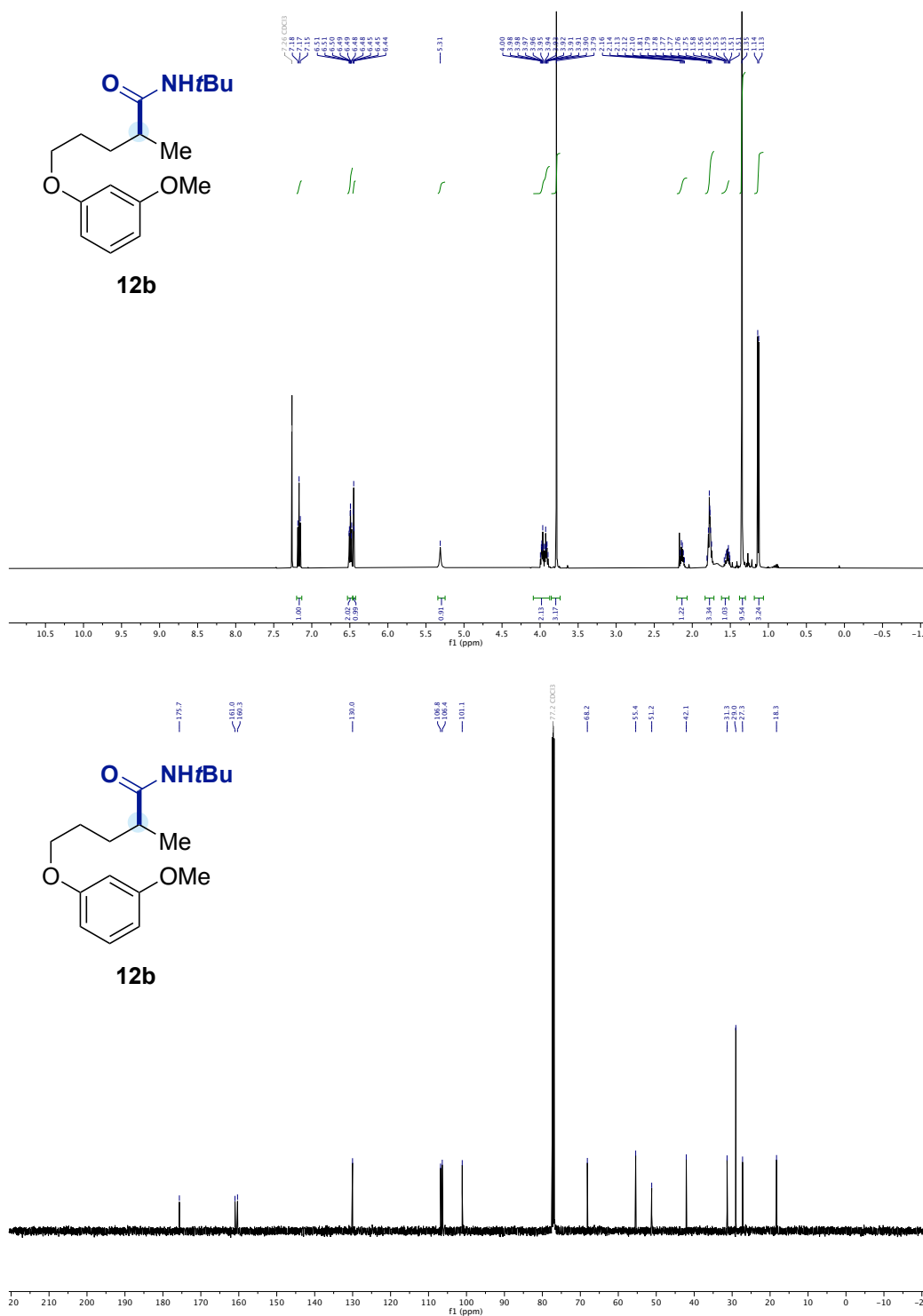


Figure 34. <sup>1</sup>H and <sup>13</sup>C NMR spectra of **11b**.

Figure 35.  $^1\text{H}$  and  $^{13}\text{C}$  NMR spectra of **12b**.



Regiodivergent Ligand-Controlled Ni-Catalyzed Reductive Amidation of Unactivated Secondary Alkyl Bromides

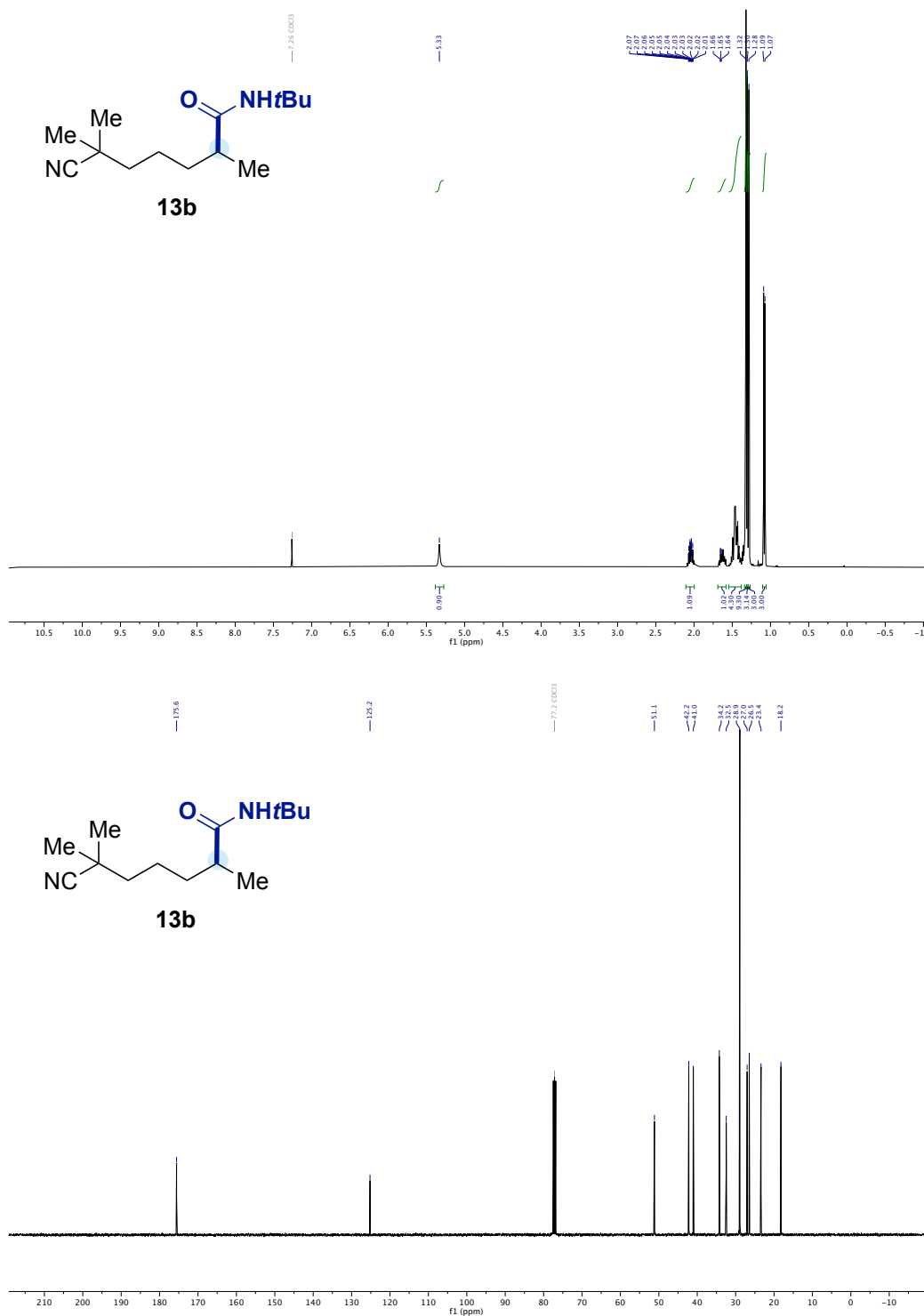


Figure 36. <sup>1</sup>H and <sup>13</sup>C NMR spectra of **13b**.

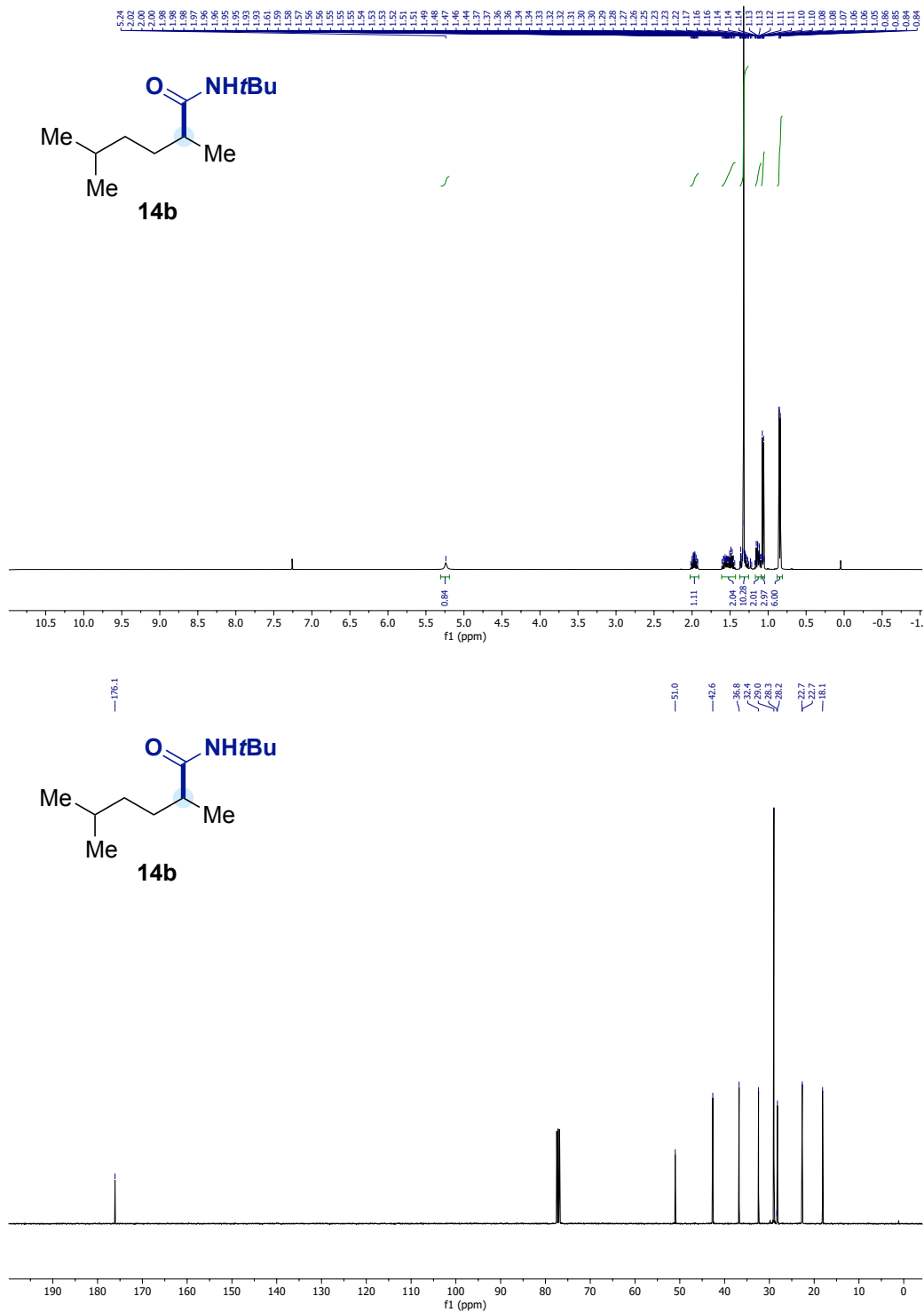


Figure 37. <sup>1</sup>H and <sup>13</sup>C NMR spectra of **14b**.

# Regiodivergent Ligand-Controlled Ni-Catalyzed Reductive Amidation of Unactivated Secondary Alkyl Bromides

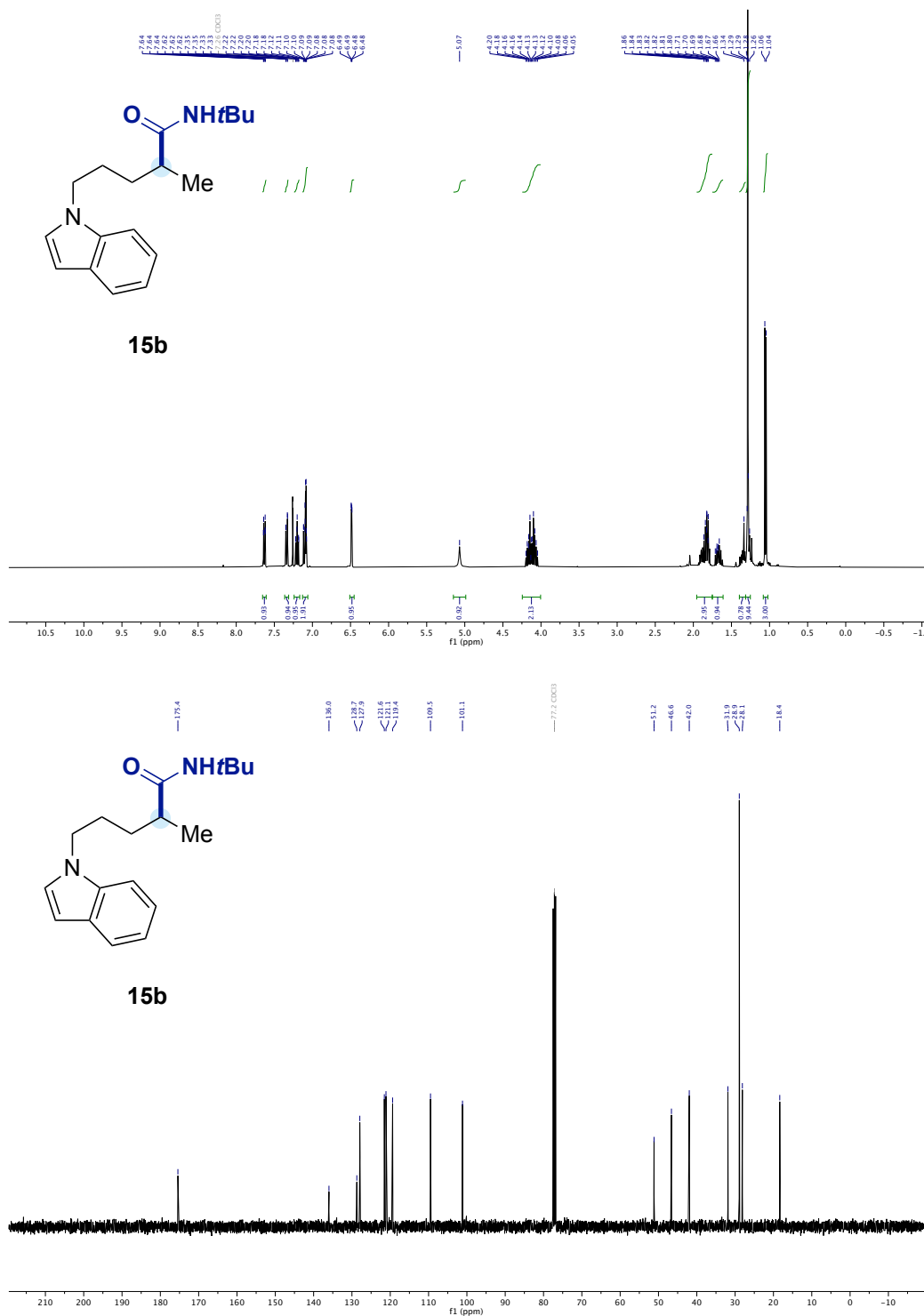
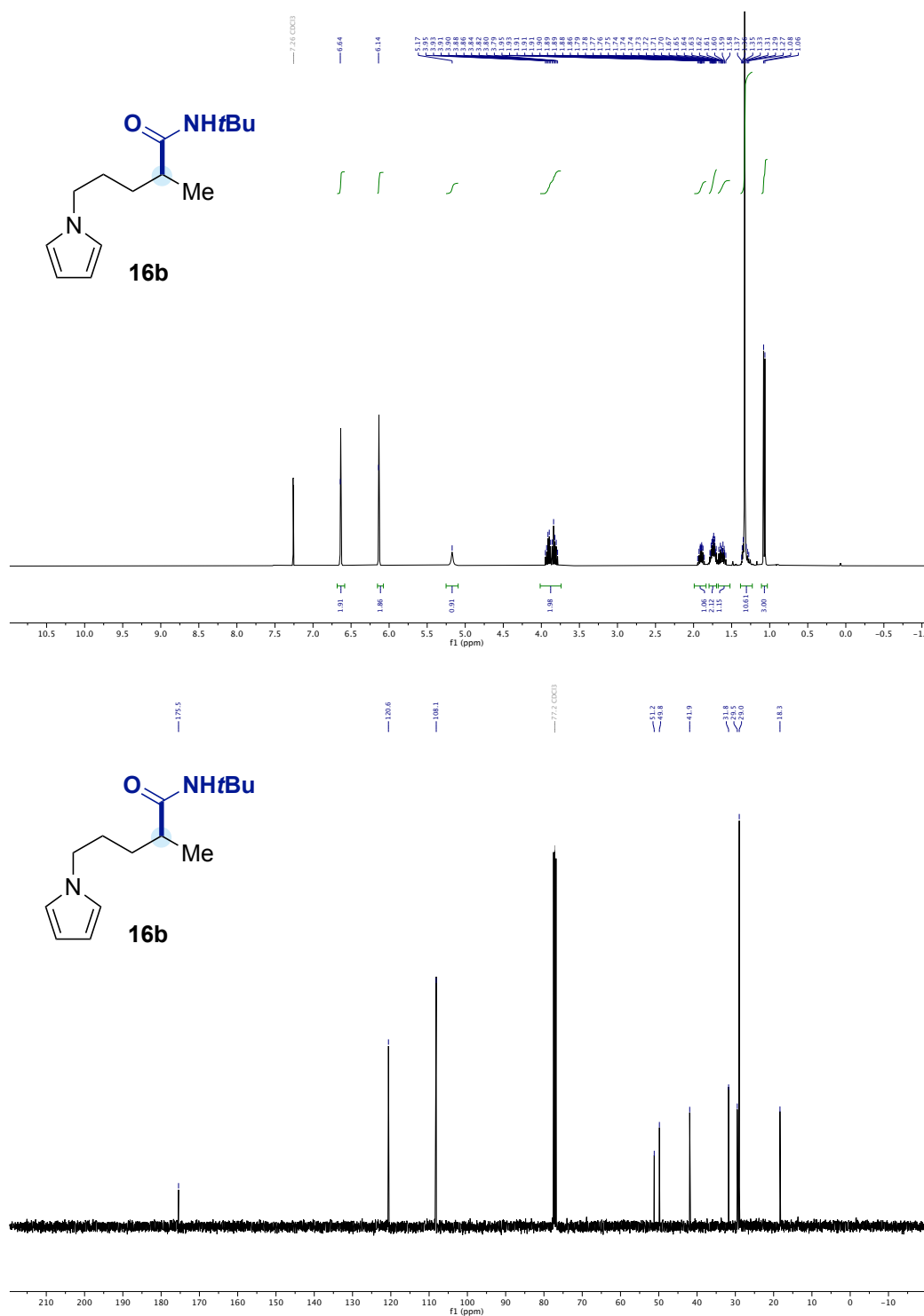
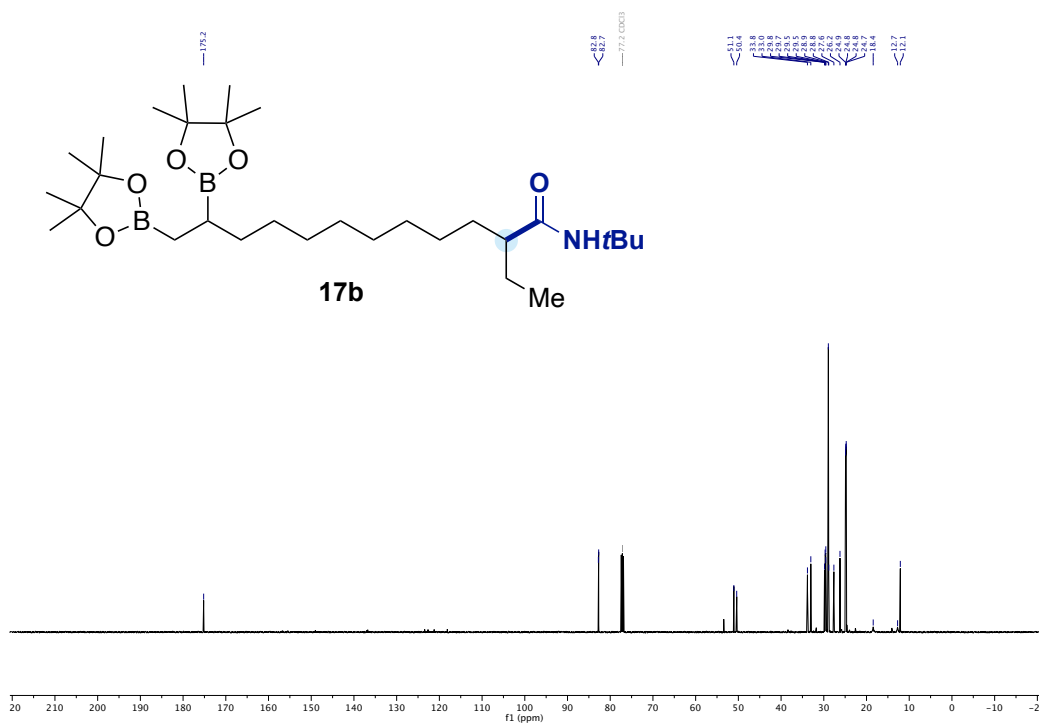
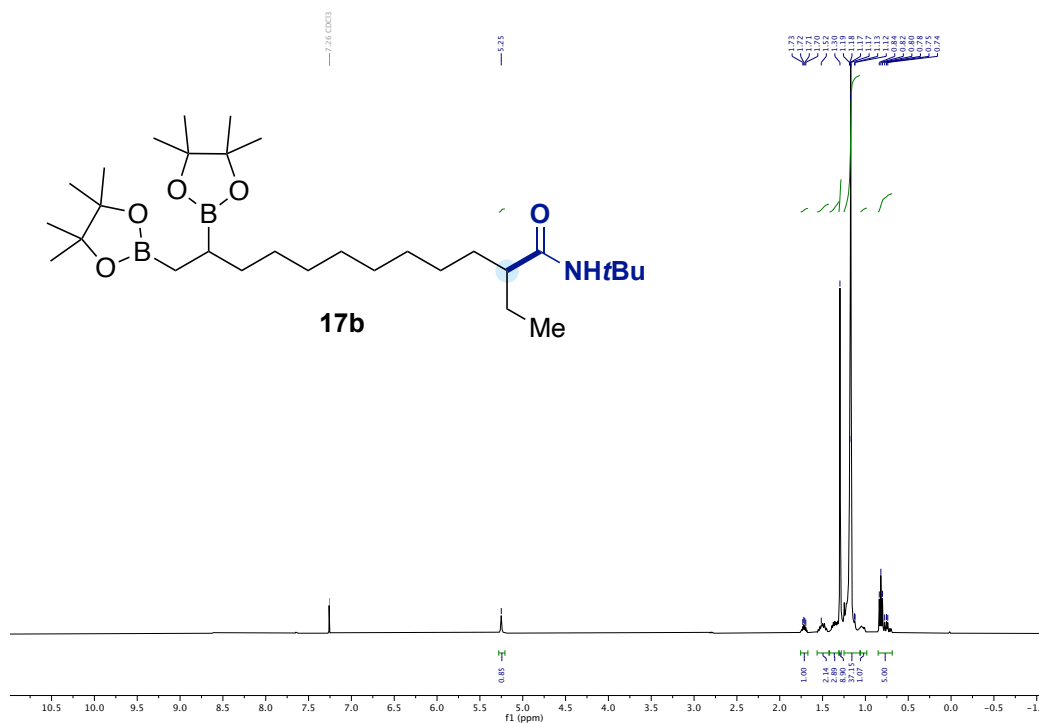


Figure 38. <sup>1</sup>H and <sup>13</sup>C NMR spectra of **15b**.

Figure 39. <sup>1</sup>H and <sup>13</sup>C NMR spectra of **16b**.

# Regiodivergent Ligand-Controlled Ni-Catalyzed Reductive Amidation of Unactivated Secondary Alkyl Bromides



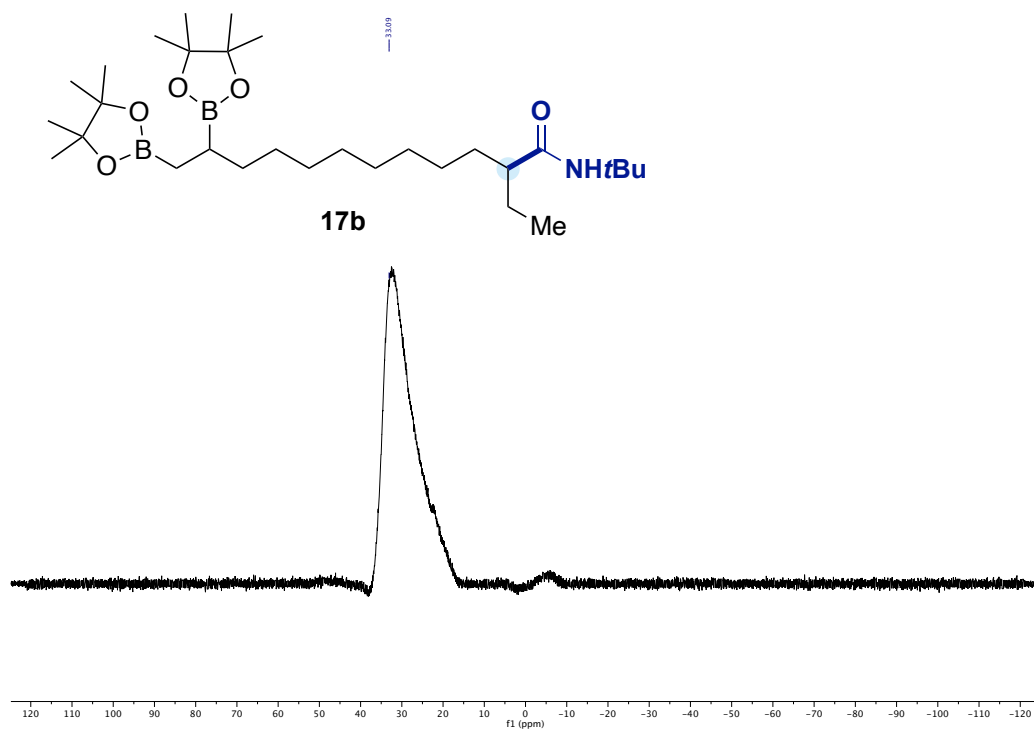
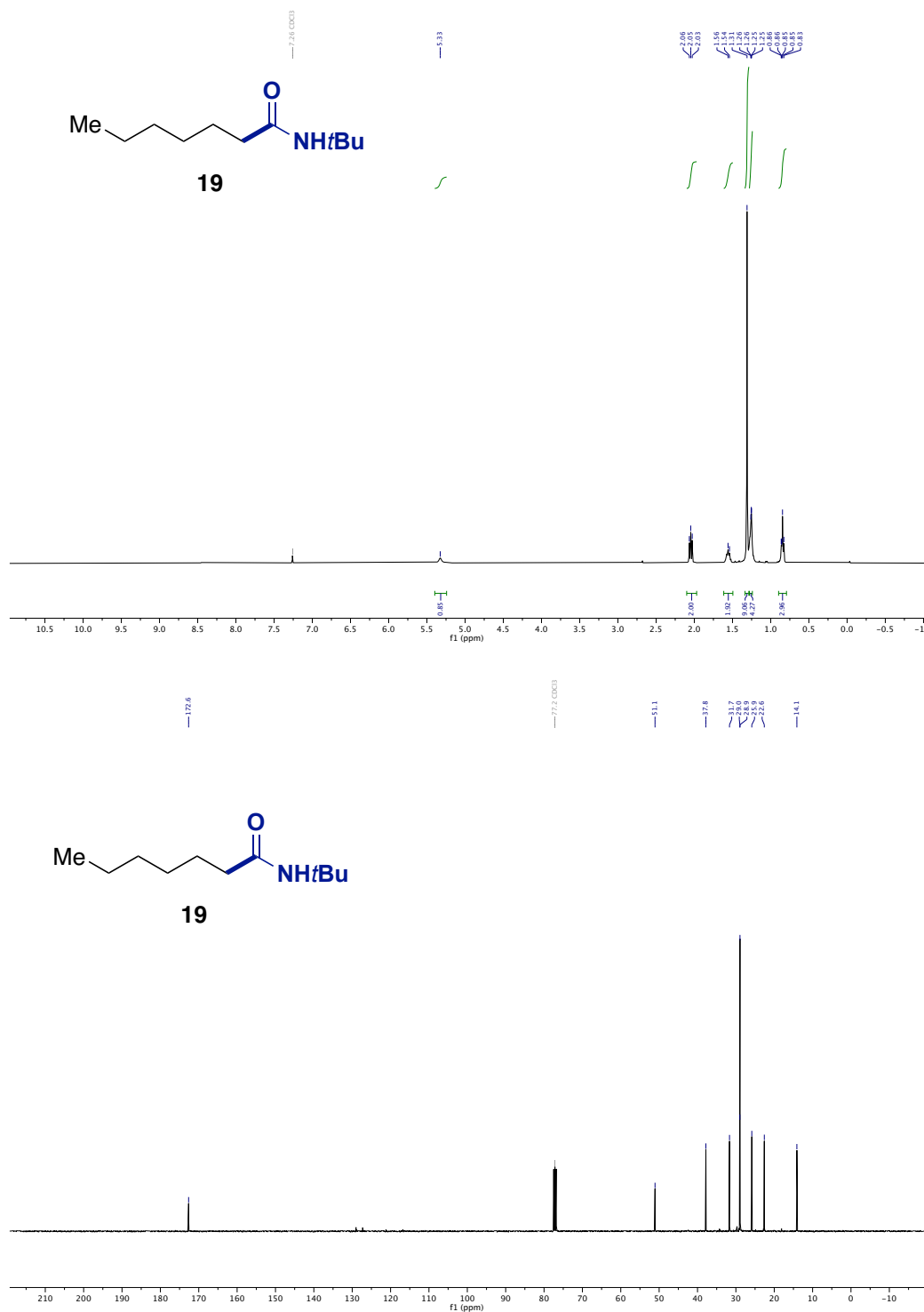


Figure 40.  $^1\text{H}$ ,  $^{13}\text{C}$  and  $^{11}\text{B}$  NMR spectra of **17b**.



Figure 42.  $^1\text{H}$  and  $^{13}\text{C}$  NMR spectra of **19**.



# Regiodivergent Ligand-Controlled Ni-Catalyzed Reductive Amidation of Unactivated Secondary Alkyl Bromides

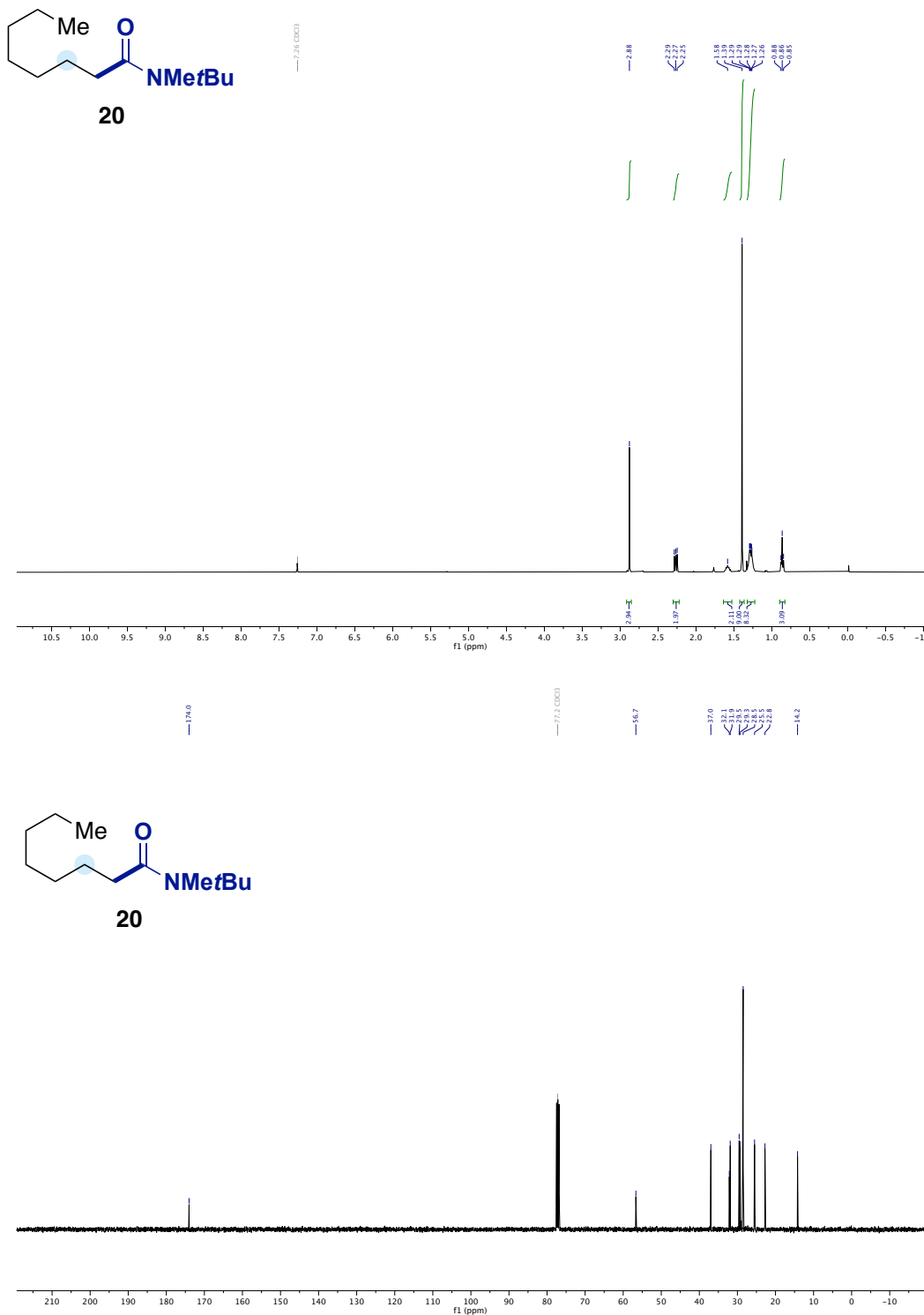


Figure 43. <sup>1</sup>H and <sup>13</sup>C NMR spectra of **20**.

Chapter 5

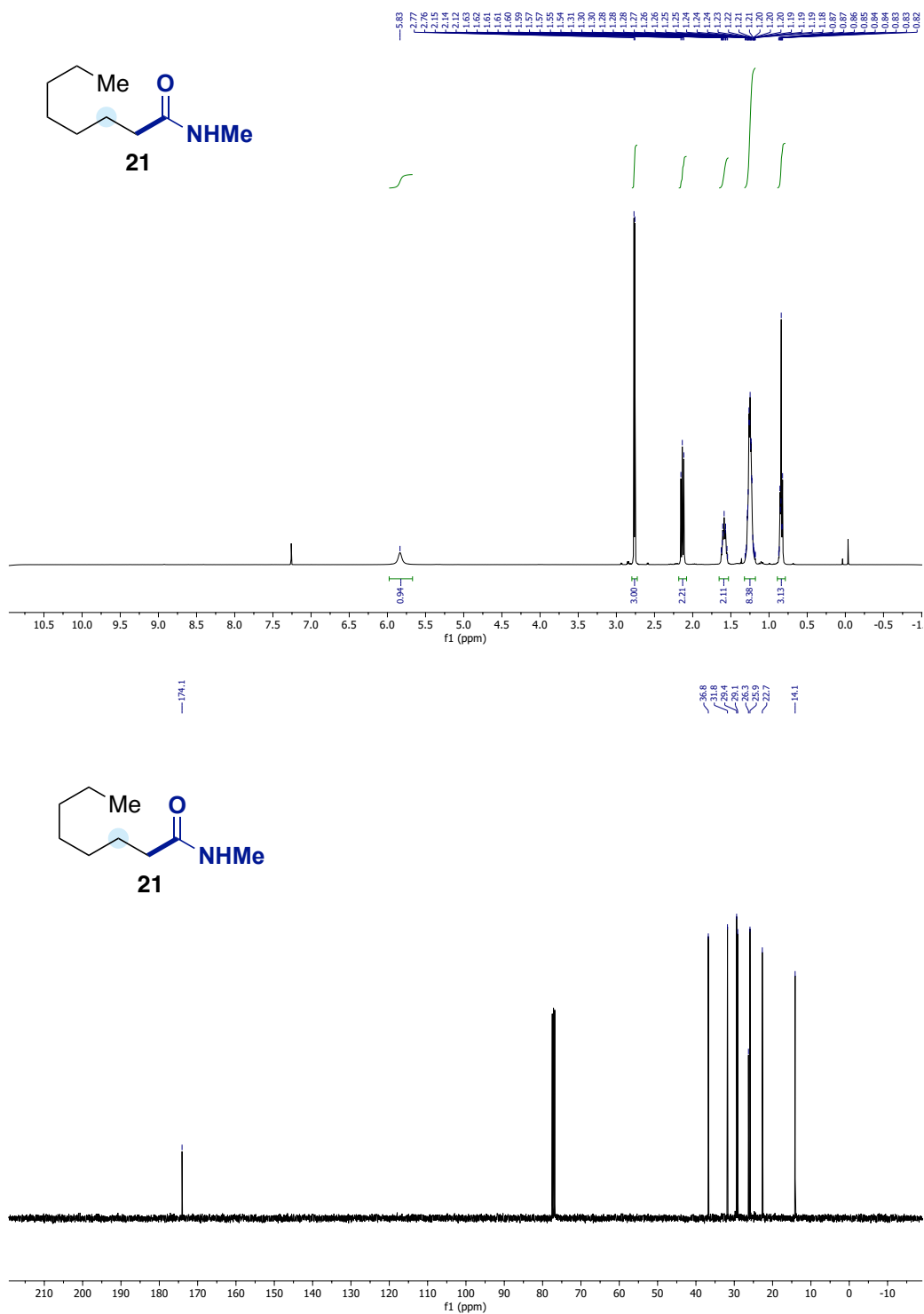


Figure 44. <sup>1</sup>H and <sup>13</sup>C NMR spectra of **21**.

# Regiodivergent Ligand-Controlled Ni-Catalyzed Reductive Amidation of Unactivated Secondary Alkyl Bromides

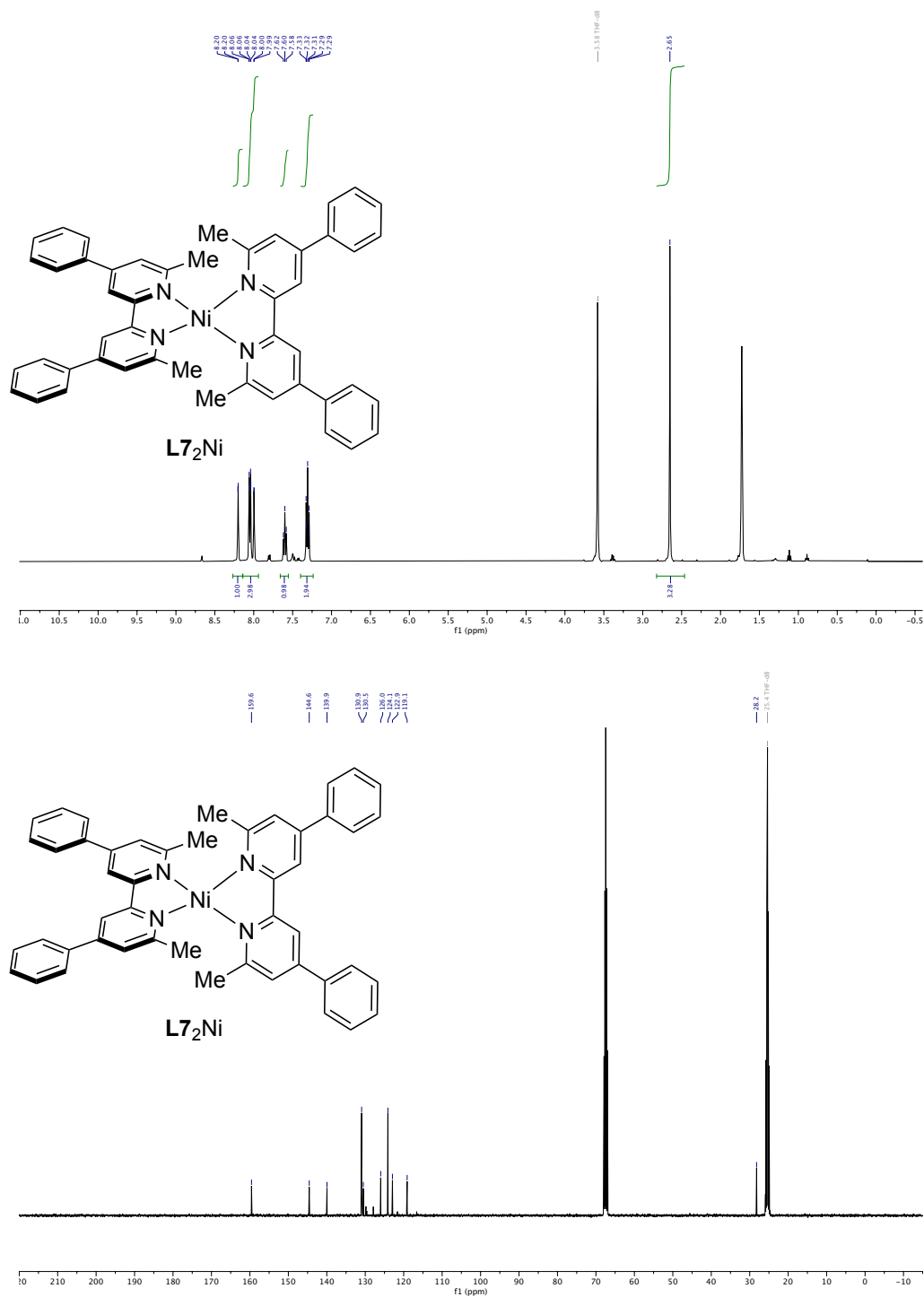


Figure 45.  $^1H$  and  $^{13}C$  NMR spectra of  $L_7_2Ni$ .



**Chapter 6:**  
***General Conclusions***



## Conclusions

The synthetic methods developed during this Doctoral Thesis have given access to a variety of carboxylic acids and amides via Ni-catalyzed reductive couplings using CO<sub>2</sub> or isocyanates as a carbonyl synthons. These reactions have all in common that are carried out under mild conditions using catalytic systems based on Ni(II) salts as precatalysts and bipyridine or phenanthroline type ligands, with Mn or Zn as a reducing agents in polar non-protic solvents (DMF, DMA or NMP). To conclude, we will analyze if our initial objectives have been successfully met:

### Chapter 2:

- A Ni-catalyzed switchable site-selective carboxylation of allylic alcohols with CO<sub>2</sub> has been described.
- This methodology provides a direct alternative for the preparation of linear or  $\alpha$ -branched  $\beta,\gamma$ -unsaturated carboxylic acids from naturally abundant allylic alcohols, while expanding our knowledge on C–OH bond activation assisted by CO<sub>2</sub>.
- Allylic alcohols have been employed within the context of cross-electrophile couplings on the absence of pyrophoric organometallic reagents for the first time.
- Although more rigorous mechanistic investigations must be carried out, our preliminary mechanistic studies helped us proposed a rationale based on Ni(I) carboxylation for the linear selectivity, and Ni(II) for the  $\alpha$ -branched selective process.

### Chapter 3:

- A protocol for the dicarboxylation of 1,3-dienes with CO<sub>2</sub> catalyzed by nickel has been developed.
- This transformation represents an alternative access to 1,6-dicarboxylic acids from 2 feedstock materials: CO<sub>2</sub> and 1,3-dienes.
- The applicability of the developed methodology has been demonstrated through the successful dicarboxylation of substrates with a variety of functional groups and industrially relevant 1,3-dienes.
- Based on the conducted mechanistic experiments, a Ni(II)/Ni(I)/Ni(0) catalytic cycle have been proposed, although further studies are necessary to fully understand it.

#### Chapter 4:

- A method for the *isotopic labeling of carboxylic acid with CO<sub>2</sub>* has been described.
- This approach represents a simple, efficient and highly versatile catalytic decarboxylation/carboxylation for carbon isotope exchange of carboxylic acids with <sup>13</sup>CO<sub>2</sub> or <sup>14</sup>CO<sub>2</sub>, enabling the access to labeled aliphatic or aromatic carboxylic acids, even at late stages, without changing the already established sequence *en route* to the parent compound.
- Different pharmaceutical and molecules with biological activity have been labelled, showcasing the applicability of this methodology to industrially relevant molecules.
- Even though <sup>13</sup>C and <sup>14</sup>C labeling has been successfully achieved, the use of <sup>11</sup>C (which require much shorter reactions) are not reached yet.

#### Chapter 5:

- A *Regiodivergent ligand-controlled Ni-catalyzed reductive amidation of unactivated secondary alkyl bromides* has been realized.
- This reaction proceeds with mild conditions and is able to access the amidation of alkyl bromides at the initial site or in remote positions depending on the ligand-structure used.
- The applicability of this methodology has been demonstrated through the preparation of primary/secondary or tertiary amides including bulky substituents in good yields, with a wide functional group tolerance.
- Mechanistic studies through the isolation and characterization of organometallic intermediates and experiments with these complexes helped us propose a catalytic cycle based on a Ni(0)/Ni(I)/Ni(II) regime.









UNIVERSITAT  
ROVIRA i VIRGILI



Institute  
of Chemical  
Research  
of Catalonia